The genomic and functional status of *TP53* in ovarian cancer: biomarker for chemotherapy outcome and determinant of response to MDM2 inhibitors

Maryam Zanjirband

Submitted to the Faculty of Medical Sciences, Newcastle University
In partial fulfilment of requirements for the degree of
Doctor of Philosophy

September 2016

Northern Institute for Cancer Research

Abstract

Background: Mutation and loss of *TP53* function is one of the most frequent genetic abnormalities in ovarian cancer. *TP53* genomic and functional status have been shown to provide potentially prognostic and predictive value in ovarian cancer; however, the results are controversial and evaluation in the context of a controlled clinical trial with single agent treatment have been lacking. Reactivation of p53 using MDM2-p53 antagonists is a promising therapeutic target for most patients with type I epithelial ovarian cancer and those left from type II harbouring wild-type *TP53*. *BRCA1/2* mutations are present in 70-85% of germline mutations in patients with inherited ovarian cancer, and deficiencies in homologous recombination repair (HRR) account for up to 50% of epithelial ovarian cancer, indicating the possible sensitivity of ovarian cancer patients to PARP inhibitors. MDM2-p53 antagonists and PARP inhibitors are now undergoing clinical trials as targeted therapy for different types of cancer. The effect of RG7388 on its own and in combination with cisplatin, and combined treatment between MDM2-p53 antagonists and PARP inhibitors have not been investigated in ovarian cancer.

Hypotheses: 1) Different genomic and functional status of p53 and some of its downstream targets such as $p21^{WAF1}$, MDM2 and WIP1 can be used as prognostic and predictive biomarkers for the outcome of chemotherapy and overall survival in ovarian cancer. 2) Reactivation of p53 by inhibition of its negative regulator MDM2, using the MDM2-p53 antagonists Nutlin-3 and RG7388, will result in p53-mediated growth arrest and apoptosis in wild-type *TP53* ovarian cancer cells, and combination of them with current therapeutic agents or rucaparib increases growth inhibition and/or apoptosis in ovarian cancer cell lines compared to either agent alone.

Methods: TP53 was sequenced in 260 ovarian cancer samples from the ICON3 trial using Sanger sequencing and Next Generation Sequencing (NGS) methods. The prognostic value of the expression levels of p53, $p21^{WAF1}$, MDM2 and WIP1 was investigated using immunohistochemistry (IHC). The effect of MDM2-p53 antagonists, Nutlin-3/RG7112/RG7388, and PARP inhibitor, rucaparib, as single agents and in combination with cisplatin or together were investigated on a panel of ovarian cancer cell lines. Sensitivity was measured by growth inhibition, clonogenic cell survival assay, apoptosis assays including caspase 3/7 activity and flow cytometry. The effect on the p53 molecular pathway and p53-regulated candidate gene expression were investigated by western blotting and Quantitative Reverse-Transcription Polymerase Chain Reaction (qRT-PCR) respectively.

Results: Patients from the ICON3 clinical trial treated with carboplatin whose tumours harbour wild-type *TP53* had a significantly better overall survival based on both univariate and multivariate analysis compared to those with mutant *TP53* regardless of sequencing method. Adding paclitaxel to the platinum-based treatment showed a trend in favour of greater benefit for those with mutant *TP53*, although this failed to reach statistical significance ($p>0.05$). Overexpression of p53 has potential prognostic value for overall survival of ovarian cancer patients.

Ovarian cancer cell lines with wild-type *TP53* were sensitive to MDM2-p53 antagonists, Nutlin-3/RG7112/RG7388, while those with mutant *TP53* were resistant to MDM2 inhibitors. Among the individual cell lines, A2780 and MDAH-2774 were sensitive and other cell lines (IGROV-1, OAW42, CP70, *MLH1*-corrected CP70+ and SKOV-3) were resistant to rucaparib regardless of *BRCA1/BRCA2* status or deficiencies in HRR reported for these cell lines.

Combination of Nutlin-3/RG7388 with cisplatin or rucaparib has synergistic and/or dose reduction potential dependent on cell genotype and the type of MDM2-p53 antagonist. Combined treatments using Nutlin-3/RG7388 and cisplatin led to greater levels of p53 stabilisation and upregulation of $p21^{WAF1}$ and MDM2, and higher expression of $p21^{WAF1}$ was associated with a greater synergistic effect for growth inhibition. In combination treatment with rucaparib and Nutlin-3/RG7388, rucaparib showed no increase in the effect of MDM2 inhibitors on the p53 pathway, indicating that the mechanism of observed synergy does not involve enhancement of p53 pathway activation by MDM2 inhibitors. Nutlin-3/RG7388 in combination with cisplatin or rucaparib resulted in changes in cell cycle distribution, SubG1 events and caspase 3/7 activity in a cell type, time and compound-dependent manner.

The fold changes in expression of candidate genes in response to MDM2 inhibitors were less in A2780 cells than IGROV-1 and OAW42. The balance of activity between growth inhibitory/pro-survival and pro-apoptotic genes dominates a small increase in the expression of several DNA repair genes as an explanation for the synergy observed for treatment with cisplatin and MDM2 inhibitors.

Conclusions: The genomic and functional status of *TP53* have potentially important prognostic and predictive values in ovarian cancer. Targeting the interaction between MDM2 and p53 using MDM2-p53 antagonists is a promising therapeutic strategy for ovarian cancer patients with wild-type *TP53* tumours, and combination treatment with them and cisplatin or rucaparib has synergistic and/or dose reduction potential dependent on cell genotype.

Declaration

I hereby declare that the work presented in this Ph.D. thesis entitled **"The genomic and functional status of *TP53* in ovarian cancer: biomarker for chemotherapy outcome and determinant of response to MDM2 inhibitors"** has been performed entirely by me and has not been submitted for any other degree or academic institution.

Signed:

Date: 23rd September 2016

Acknowledgments

I would like to extremely thank my supervisors Professor John Lunec, and Professor Richard Edmondson for their motivations and advice over the last 4 years as their student. In particular, I would like to appreciate Professor John Lunec for his patience, guidance and kindness throughout the time of my research and writing of this thesis.

I am very grateful to Professor Herbie Newell, Professor Nicola Curtin and members of Drug Development in NICR for kindly providing RG7112, RG7388 and rucaparib. The provision of the *MLH1*-corrected CP70+ cell line by Professor Nicola Curtin is gratefully acknowledged. I am also grateful to Dr. Arman Esfandiari, Dr. Claire Hutton, Dr. Jennifer Houniet, Dr. Laura Woodhouse, Dr. Peter Wu, Dr. Ahmed Mahdi, Dr. Carmela Ciardullo, Shirley Ho and all the other people in the NICR for their advice, teaching and assistance.

Thanks to Wendi Qian from the MRC Clinical Trials Unit for her assistance with statistical analysis relating to the ICON3 study, to Dr. Claire Hutton and Dr. Jennifer Houniet for their sample management, processing and analysis of Sanger DNA sequences relating to the ICON3 study. Thanks relating to the ICON3 study should also go to Professor Hilary Calvert, who had a major involvement in the original proposal and planning of the ICON3 *TP53* study and to Professor Ruth Plummer for her encouragement and support with Cancer Research UK financial resource for the next generation DNA sequencing. Dr. Paul Cross is gratefully acknowledged for his histopathological review of the ICON3 FFPE samples. A special thanks needs to go to the ovarian cancer patients, without whom none of the translational studies described in this thesis would be possible. I would also like to thank the BACR for the funding I have received to attend the Cancer Genomics international conference, July 2015. Funding and support for the ICON3 study from the Cancer Research UK BIDD Committee is gratefully acknowledged.

I would like to greatly appreciate my parents and my siblings for their encouragement. I am very much thankful to my beloved family, and do not know how to thank my dear husband, Mehrdad, and my lovely daughters, Pardis and Parnia. This work would have never been possible without their patience, encouragement and contribution. This study is dedicated to my family particularly my husband, who has always supported me emotionally and financially during the challenges of my education.

Last but not least, I would like to praise and thank my God for his blessings throughout my study to successfully complete my research.

Abbreviations

AEN	Apoptosis enhancing nuclease
ALL	Acute lymphoblastic leukaemia
AML	Acute myeloid leukaemia
ANOVA	Analysis of variance
APAF-1	Apoptotic protease activating factor 1
APST	Atypical proliferative serous tumour
AQP2/9	Aquaporin 2/9
ARF-BP1	ARF binding protein 1
Arg	Arginine
ATM	Ataxia telangiectasia mutated
ATR	Ataxia telangiectasia and Rad3-related protein
AUC	Area under the curve
AURKA	Aurora kinase A
AVA	Amplicon variant analysis
BAD	Bcl-2-associated death promoter
BAK	Bcl-2 homologous antagonist killer
BAX	B-cl-2-associated X
BBC3	Bcl2 binding component 3
BCA	Bicinchoninic acid assay
BCL-2	B-cell lymphoma 2
BH3-only	Bcl-2-homology domain 3 only
BID	BH3 interacting-domain death agonist
BIRC5	Baculoviral inhibitor of apoptosis repeat-containing 5
BMI	Body mass index
BRCA	Breast cancer susceptibility protein
BSA	Bovine serum albumin
C-terminus	Carboxyl-terminus
CA	Cancer antigen
CAP	Cyclophosphamide, doxorubicin and cisplatin
Caspase	Cysteine-dependent aspartate-directed proteases
CBP	Creb-binding protein
CCNG1	Cyclin-G1
CD95	Cluster of differentiation 95
Cdc	Cell division cycle
CDDP	Cis-diamino-dichloro-platinum
Cdk	Cyclin-dependent kinase
CDKI	Cyclin-dependent kinase inhibitor
CDKN1A	Cyclin-dependent kinase inhibitor 1 A
CDKN2A	Cyclin-dependent kinase inhibitor 2 A
cDNA	Complementary deoxyribonucleic acid
CEA	Serum carcinoembryonic antigen
Chk	Checkpoint kinase
CI	Combination index
COP1	Constitutive photomorphogenic 1
COSMIC	Catalogue of somatic mutations in cancer
CRUK	Cancer research United Kingdom
CT	Computerised tomography
CTR	Copper transporter

Cu	Copper
DAB	3, 3’ Diaminobenzidine
DBD	DNA binding domain
DDB2	Damage-specific DNA binding protein 2
ddNTP	Dideoxynucleotide triphosphate
DEC1	Deleted in esophageal cancer 1
DMEM	Dulbecco’s modified eagle medium
DMSO	Dimethyl sulfoxide
DNA	Deoxyribonucleic acid
dNTPs	Deoxynucleotide triphosphate
DPX	Distyrene, plasticizer and xylene
DR	Death receptor
DRI	Dose reduction index
ECL	Enhanced chemiluminescence
ED	Effective dose
EDTA	Ethylendiaminetetraacetic acid
EOC	Epithelial ovarian cancer
ETS	E26 transformation-specific
FA	Fanconi anemia
FACS	Fluorescence-activated cell sorting
FANC	Fanconi anemia complementation
FBS	Fetal bovine serum
FDA	Food and drug administration
FDXR	Ferredoxin reductase
FFPE	Formalin fixed paraffin embedded
FL2-A	FL2-Area
FL2-H	FL2-height
FL2-W	FL2-Width
FSC-H	Forward scatter-height
G0	Gap 0
G1	Gap 1
G2	Gap 2
GADD45	Growth arrest and DNA-damage-inducible 45
GAPDH	Glyceraldehyde-3-phosphate dehydrogenase
GI_{50}	Concentrations of drugs required to achieve 50% growth inhibition
HCC	Hepatocellular carcinoma
HDM2	Human double minute 2 homolog
HGPSC	High grade pelvic serous carcinoma
HGSC	High grade serous carcinoma
His	Histidine
HNPCC	Hereditary nonpolyposis colorectal cancer
HR	Hazard ratio
HRP	Horseradish peroxidase
HRR	Homologous recombination repair
IAP	Inhibitor of apoptosis
iASPP	Inhibitor of apoptosis-stimulating protein of p53
ICON3	International collaborative ovarian neoplasm 3
ICON4	International collaborative ovarian neoplasm 4
IgG	Immunoglobulin G
IHC	Immunohistochemistry

kDa	Kilodalton
LC_{50}	Lethal concentrations of drugs required to kill 50% of the population
Leu	Leucine
LGSC	Low grade serous carcinoma
M	Mitosis
MCL-1	Myeloid cell leukemia 1
MDM2	Mouse double minute 2
MDMX	Mouse double minute 4 homolog
MDR	Multiple drug resistance
miRNAs	MicroRNA
MLH1	MutL homolog 1
MLL	Mixed lineage leukaemia
MMR	Mismatch repair
MRC	Medical research council
MRI	Magnetic resonance imaging
MRP	Multidrug resistance protein
MSH2	MutS homolog 2
mTOR	Mammalian target of rapamycin
MW	Molecular weight
N-terminus	Amino-terminus
NEDD4	Neural precursor cell expressed developmentally down-regulated 4
NER	Nucleotide excision repair
NES	Nuclear export signal
NGS	Next generation sequencing
NOXA	NADPH oxidase activator
OS	Overall survival
OVCA	Ovarian cancer
p14ARF	p14 Alternative reading frame
$p21^{WAF1}$	p21 Wild-type activating fragment 1
p53BP	p53 binding protein
PAI1	Plasminogen activator inhibitor-1
PARP	Poly ADP ribose polymerase
PARPBP	Poly ADP ribose polymerase binding protein
PAX8	Paired box 8
PBS	Phosphate buffered saline
PCNA	Proliferating cell nuclear antigen
PCR	Polymerase chain reaction
PFS	Progression-free survival
Phe	Phenylalanine
PI	Propidium iodide
PI3K	Phosphoinositide 3-kinase,
Pirh2	p53-induced ubiquitin-protein ligase
PPM1D	Protein phosphatase Mg2+/Mn2+ dependent 1D
PRD	Proline- rich region
Pro	Proline
PTEN	Phosphatase and tensin homolog
PUMA	p53-upregulated modulator of apoptosis
PVDF	Polyvinylidene difluoride
qRT-PCR	Quantitative real-time polymerase chain reaction
Rb	Retinoblastoma

RBEL1A	Rab-like GTP-binding protein 1A
RNA	Ribonucleic acid
ROC	Receiver operating characteristic
RPMI	Roswell park memorial institute
RPS27L	Ribosomal protein S27 like
RQ	Relative quantities
RRM2B	Ribonucleotide reductase M2B
S-phase	Synthesis-phase
SDS-PAGE	Sodium dodecyl sulphate- polyacrylamide gel electrophoresis
SEM	Standard error of mean
SESN1	Sestrin 1
shRNA	Sort hairpin ribonucleic acid
siRNA	Small interfering ribonucleic acid
SNP	Single-nucleotide polymorphism
SPSS	Statistical package for the social sciences
SRB	Sulforhodamine B
SSC-H	Side scatter-height
SSCP	Single-strand conformation polymorphism
STICs	Serous tubal intraepithelial carcinomas
STR	Short tandem repeat
TAD	Transactivation domain
TAFs	TATA box binding protein associated factors
TBS	Tris buffered saline
TD	Tetramerization domain
TFID	Transcription initiation factor D
TFIH	Transcription initiation factor H
Thr	Threonine
TMA	Tissue microarray
TNFRSF10B	Tumour necrosis factor receptor superfamily 10B
TP53INP1	Tumour protein p53-inducible nuclear protein 1
Trp	Tryptophan
UTR	Untranslated region
UV	Ultraviolet
Val	Valine
WAF1	Wild-type p53 activated fragment 1
WIP1	Wild-type p53-induced phosphatase 1
WWP1	WW domain containing E3 ubiquitin ligase 1
XPC	Xeroderma pigmentosum, complementation group C
ZMAT3	Zinc finger matrin-type protein 3
ΔΔCt	ΔΔ Cycle threshold

Table of Contents

List of Figures

List of Tables

Chapter 1: Introduction

1.1 Ovarian cancer

1.1.1 Incidence and mortality

Ovarian cancer is the most lethal of all gynaecological malignancies and was reported to be responsible for approximately 152,000 death worldwide in 2012. "It is the seventh most common cancer worldwide for females, and the eighteenth most common cancer overall, with nearly 239,000 new cases diagnosed in 2012." (Ferlay J, 2013; Narod, 2016). In the UK, ovarian cancer is the sixth most common cancer in British women which accounts for 4% of all new cancer cases in females. The incidence rate is greatly influenced by age with the highest frequency in older females. More than half of the cases diagnosed in 2011-2013 in the UK were aged 65 and over (CRUK, 2016). With the exception of Japan, the highest incidence of ovarian cancer is found in developed countries, Europe, the USA and Israel (Hennessy *et al.*, 2009). The lifetime risk of developing ovarian cancer is one in fifty two for women in the UK (CRUK, 2016) and one in seventy two worldwide (Zhan *et al.*, 2013). In terms of ethnicity, rates for white females with ovarian cancer range from 17.4 to 18.1 per 100,000 which is significantly decreased for Asian, 9.2 to 15.5 per 100,000, and Black women, 6.6 to 12.1 per 100,000 (CRUK, 2016). Overall, the rate of ovarian cancer incidence has increased for most age categories in the UK since the late 1970s to 2013, with the exception of women aged 50-59 (Figure 1-1) (CRUK, 2016).

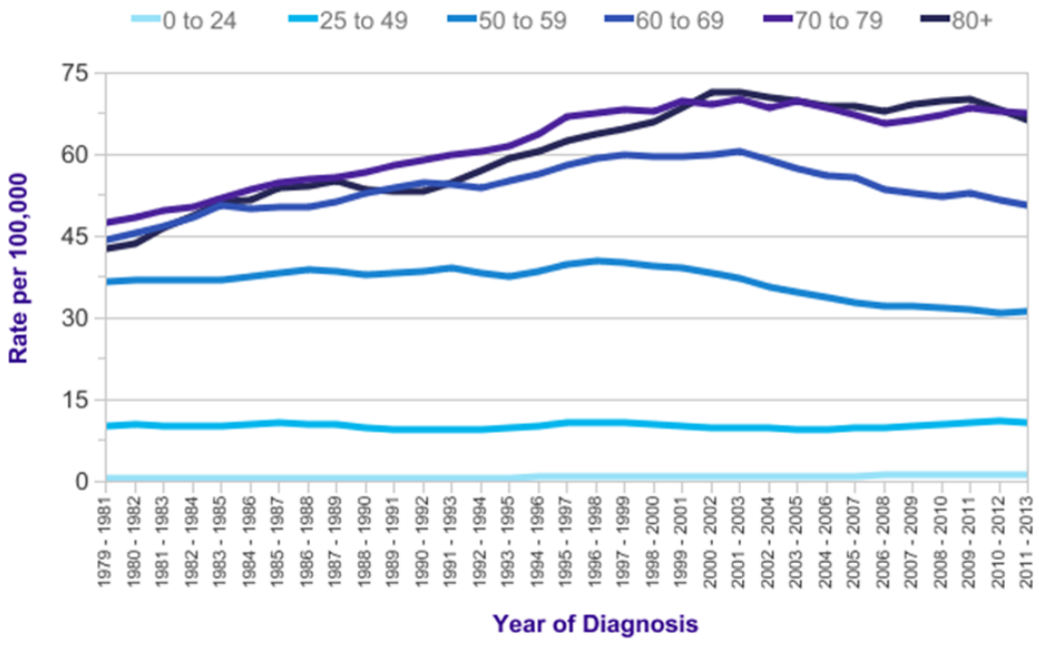

Figure 1-1: European Age-Standardised Incidence Rates per 100,000 Population, by Age, Females, Great Britain.

1.1.2 Symptoms and diagnosis

The symptoms of epithelial ovarian cancer are non-specific and early-stage disease is asymptomatic. The most common symptoms are increased abdominal size, persistent pelvic bloating, abdominal discomfort and pain, loss of appetite with low grade nausea, and inability to eat proper meals owing to feeling of fullness. Back pain, fatigue, irritable bowel syndrome, urinary burning, shortness of breath due to pleural effusion and menopausal symptoms are other clinical presentations of ovarian cancer (Bast *et al.*, 2009; Lokadasan *et al.*, 2016).

Diagnosis of ovarian cancer is challenging because of the similarity between its symptoms and many more prevalent gastrointestinal, genitourinary and other gynaecological conditions. Up until now, no diagnostic technique has been introduced in order to detect disease at initial stage. In most cases, the disease is diagnosed at advanced stage with metastasis beyond the ovary, at which point response to treatment is not favourable (Bast *et al.*, 2009; Bauerschlag *et al.*, 2010; Coleman, 2016; Lokadasan, *et al*., 2016). In order to detect ovarian cancer at early stages, use of multimodal screening including transvaginal sonography and serum CA125 measurement are likely to be effective. A combination of the two modalities has a higher specificity than either technique alone even though it is not considered as a gold standard for early detection (Bast *et al.*, 2009; Colombo *et al.*, 2010). CA125 is a glycoprotein which has been used as a biomarker for specific types of cancer, such as ovarian cancer due to its increased level in the blood of patients. The utility of serum CA125 to detect early disease is questionable due to its elevation only in about 50% of patients with FIGO stage I disease. It is also raised in about 85% of ovarian cancer patients with FIGO advanced stages. CEA (Serum carcinoembryonic antigen) and CA19-9 levels (Cancer antigen 19-9), CA125/CEA ratio and a number of morphological variables are sometimes used in specific situations. There are more tests which may be performed following the first diagnosis to determine how far the cancer has extended. Computerised tomography (CT) scans are used to evaluate the extent of disease and aid surgical planning, and chest CT or chest X-ray can be used to determine pleural effusion. Laparoscopy, laparotomy and removing abdominal fluid are other tests which may be performed. Magnetic Resonance Imaging (MRI) scan is not routinely used (Ledermann *et al.*, 2013; CRUK, 2016).

1.1.3 Risk factors

The identified risk factors can be divided into two categories, familial and non-familial. The former includes a history of ovarian or breast cancer in two or more first-degree relatives, which raises the risk of ovarian cancer. Acquiring mutated *BRCA1* or/and *BRCA2* leads to an increased risk of ovarian cancer, though germline mutations (*BRCA1*, *BRCA2*, and HNPCC) influence ovarian cancers in no more than 10%-15% of cases (Bast *et al.*, 2009; Ledermann *et al.*, 2013). More than 90% of ovarian cancers arise in the absence of germline mutations. The latter includes infertility, polycystic ovarian syndrome, raised body mass index (BMI) in premenopausal women, use of hormonal replacement treatment and talcum powder, having endometriosis, smoking and rising age (Ledermann *et al.*, 2013; CRUK, 2016). Older studies showed a link between using fertility drugs and an increased risk of ovarian cancer while more recent research found no strong evidence to support this (CRUK, 2016). Although some studies considered early menarche and late menopause as risk factors (Ledermann *et al.*, 2013), others found no significant association between those and risk of ovarian cancer (Modugno *et al.*, 2012).

In contrast, breastfeeding, pregnancy, multiparity, tubal ligation and oral contraceptives decrease the risk of ovarian cancer (Modugno *et al.*, 2012; Ledermann *et al.*, 2013). There is mounting evidence that steroid hormones have significant impact on the risk of ovarian cancer (Modugno *et al.*, 2012). Pregnancy and oral contraceptives protect against ovarian cancer by two mechanisms; induction of progestin-mediated apoptosis and association with anovulation. Progestins induce apoptosis, while androgens raise the level of risk by stimulatory effects on ovarian epithelium (Ho, 2003).

1.1.4 Histological subtypes

Ovarian cancer is a heterogeneous disease including different types of tumours. From the histological point of view, most tumours of the ovary are derived from one of three major cell types: surface epithelial cells, sex cord stromal cells (including granulose, theca, and hilus cells), and germ cells (oocytes). Since Epithelial Ovarian Carcinoma (EOC) is the major form of the disease, accounting for about 90% of ovarian tumours, it is a major focus of studies (Colombo *et al.*, 2010; Jelovac and Armstrong, 2011; Zhan *et al.*, 2013; CRUK, 2016). Based on the molecular genetic distinctive markers as well as morphologic and clinical differences, EOC can be categorised into two groups, type I and type II. Also, tumours in each cell type are subcategorized into benign, borderline and malignant groups. In clinical and molecular terms,

tumours presenting at low stage, are inactive, confined to the ovary and somewhat genetically stable are designated type I, including low grade serous carcinoma (LGSC), low-grade endometrioid, clear cell, mucinous and transitional carcinomas. Conversely, type II tumours are more aggressive and almost always present in advanced stage. Type II tumours include high-grade serous carcinoma (HGSC), high-grade endometrioid and undifferentiated carcinomas. Also, patients with type I disease present with different mutations to those suffering from type II tumours (Figure 1-2). For instance, *TP53* mutations, *CCNE1* (encoding cyclin E1) amplification, and mutation or promoter methylation of *BRCA1/2* are frequently been seen in type II tumours. On the other hand, type I tumours present with *KRAS, BRAF, ERBB2, PTEN, CTNNB1*, and *PIK3CA* gene abnormalities, which target specific cell signalling pathways (Kim *et al.*, 2012; Zhan *et al.*, 2013; Cobb *et al.*, 2015; Skirnisdottir *et al.*, 2015). Although clear cell and mucinous cancers are included in type I, they have a worse prognosis than type II when they are not detected early (Cobb *et al.*, 2015). The frequency distribution of HGSC is 60-80% of ovarian epithelial carcinoma (Li *et al.*, 2012). It is 10-20%, 3-10%% and 5-20% of epithelial ovarian cancers which are comprised of endometrioid, clear cell and mucinous tumours respectively (van Niekerk *et al.*, 2011). LGSC is uncommon and accounts for 3% of epithelial ovarian cancer (Chris M.J. Conklin, 2013).

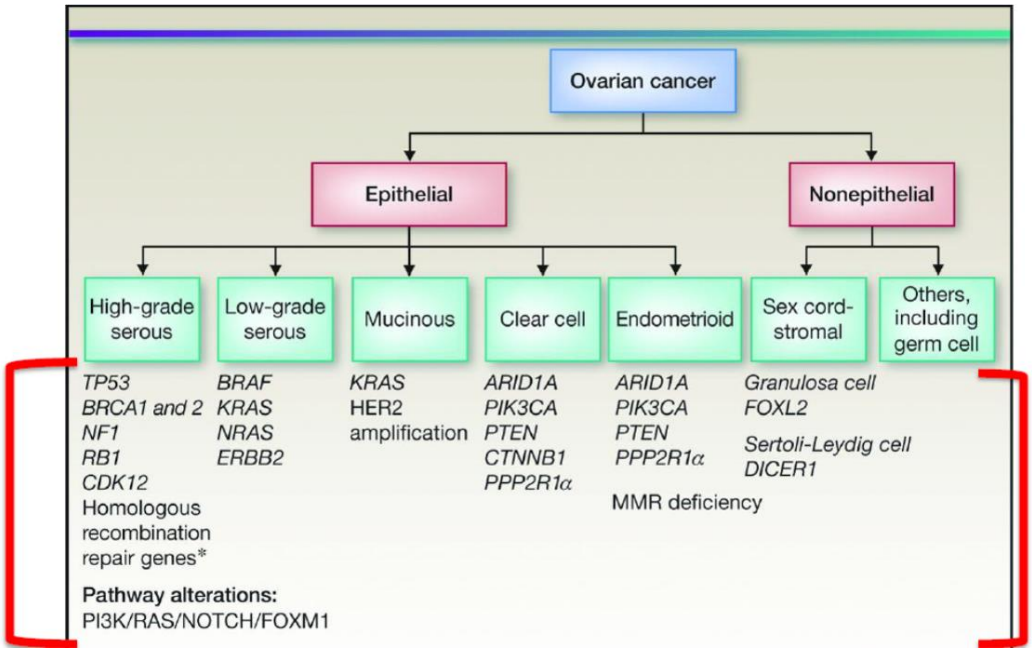

Figure 1-2: Histological subtypes of ovarian cancer and associated mutations/molecular alterations. MMR, Mismatch repair; *, *CHK2, BARD1, BRIP1, PALB2, RAD50, RAD51C, ATM, ATR, EMSY* and Fanconi anemia genes (Banerjee and Kaye, 2013).

1.1.5 Staging

According to the staging system called the FIGO (International Federation of Gynaecological Oncologists) system , ovarian cancer is distinguished into four categories at the time of surgery (Table 1-1). Due to current hypotheses that consider epithelial ovarian, peritoneal and tubal cancers represent a spectrum of disease originating in the Müllerian compartment, the FIGO staging classification was revised (Table 1-2) (Zeppernick and Meinhold-Heerlein, 2014; Cobb *et al.*, 2015).

Stage	Characteristics
I	Growth of tumour is limited to the ovary/ovaries
IA	Tumour influences in only one ovary; no tumour is distinguished on the exterior surfaces and malignant cells in ascites or peritoneal washings; the capsule of ovary is undamaged.
IB	Both ovaries are affected; no tumour is distinguished on the exterior surfaces and no malignant cells in ascites or peritoneal washings; ovary capsule is intact.
IC	Tumour is confined to one or both ovaries and is followed by one of these things: the ovary capsule is burst, the surface of ovary is affected by tumour or detection of cancerous cells in ascites or peritoneal washings is positive.
II	One or two ovaries are involved by tumour growth; pelvic extension is detected.
IIA	Tumour expansion or/and implantation into the uterus and/or the fallopian tubes is found but distinguish of cancerous cells in ascites or peritoneal washings is negative.
IIB	The tumour has stretched on another tissue in the pelvis; however, malignant cells are not detected in ascites or peritoneal washings.
IIC	Tumours are either stage IIA or IIB but malignant cells are detectable in the ascites or peritoneal washings.
III	One or both ovaries are influenced by tumour; peritoneal metastasis outside the pelvis and/or local lymph node metastasis Including liver capsule metastasis are distinguished.
IIIA	Tumour is confined to pelvis but there is microscopic peritoneal metastasis beyond the pelvis.
IIIB	Implantations of abdominal peritoneal surface can be detected, but not more than 2 cm in diameter. Nodes are negative.
IIIC	Abdominal implants are greater than 2 cm in diameter and/ or tumour metastases happens to local lymph nodes.
IV	Tumour is involved with distant metastases beyond the peritoneal cavity, and parenchymal liver metastases equals stage IV.
Source: Staging Announcement: FIGO Cancer Committee. Gynecol Oncol 25:383, 1986.	

Table 1-1: FIGO (1986) staging system for ovarian cancer.

Stage	Characteristics
I	`
IA	Tumour influences in only one ovary (capsule intact) or fallopian tube; no tumour is distinguished on ovarian or fallopian tube surface; and no malignant cells in ascites or peritoneal washings.
IB	Both ovaries (capsules intact); or fallopian tubes are affected; no tumour is distinguished on the ovarian or fallopian tube surface and no malignant cells in ascites or peritoneal washings.
IC	IC: Tumour is confined to one or both ovaries or fallopian tube(s) with any of the following:
	IC1: Surgical spill intraoperatively
	IC2: Capsule ruptured before surgery or tumor on ovarian or fallopian tube surface
	IC3: Malignant cells in the ascites or peritoneal washings
II	One or two ovaries or fallopian tubes are involved by tumour growth; pelvic extension or primary peritoneal cancer is detected.[2]
IIA	Tumour expansion or/and implantation into the uterus and/or the fallopian tubes and/or ovaries is found.
IIB	The tumour has stretched on other pelvic intra-peritoneal tissues.
III	One or both ovaries or fallopian tubes, or primary peritoneal cancer are influenced by tumour; peritoneal metastasis outside the pelvis and/or retroperitoneal lymph node metastasis.
IIIA	IIIA1: Positive retroperitoneal lymph nodes only (cytologically or histologically proven).
	IIIA1 (i): Metastasis up to 10 mm in greatest dimension.
	IIIA1 (ii): Metastasis more than 10 mm in greatest dimension.
	IIIA2: Microscopic extra-pelvic (above the pelvic brim) peritoneal involvement with or without positive retroperitoneal lymph nodes.
IIIB	Implantations of macroscopic peritoneal metastasis beyond the pelvis can be detected, but not more than 2 cm in diameter, with or without metastasis to the retro-peritoneal lymph nodes (includes extension of tumor to capsule of liver and spleen without parenchymal involvement of either organ).
IIIC	Implantations of macroscopic peritoneal metastasis beyond the pelvis can be detected, more than 2 cm in diameter, with or without metastasis to the retro-peritoneal lymph nodes (includes extension of tumor to capsule of liver and spleen without parenchymal involvement of either organ).
IV	IV: Distant metastasis excluding peritoneal metastases.
	IVA: Pleural effusion with positive cytology
	IVB: Parenchymal metastases and metastases to extra-abdominal organs (including inguinal lymph nodes and lymph nodes outside of the abdominal cavity).[3]
Source:	Staging Announcement: FIGO Cancer Committee Int J Gynaecol Obstet 124:1, 2014.

Table 1-2: FIGO (2013) staging system for ovarian cancer. 1, It is impossible to have stage I peritoneal cancer; 2, Dense adhesions with histologically proven tumour cells justify upgrading apparent stage I tumours to stage II; 3, Extra-abdominal metastases include transmural bowel infiltration and umbilical deposits.

1.1.6 Theories of ovarian carcinogenesis and molecular pathogenesis

It has been previously thought that epithelial ovarian tumour originates from ovarian surface epithelium, a single layer of epithelium covering the ovarian germ and stromal cells (Zeppernick *et al.*, 2015). Mounting evidence recently indicates that type I as well as type II epithelial ovarian tumours arise from outside the ovary, encompassing it secondarily. Furthermore, their development individually occurs as a result of alterations in various molecular pathways (Kurman and Shih, 2011; Tagawa *et al.*, 2012).

Ongoing investigations strongly indicate that the precursor of HGSC is fallopian tube epithelium rather than ovarian surface epithelium as formerly thought (Walton *et al.*, 2016). This hypothesis was suggested by a group of Dutch investigators in 2001. Piek *et al*. described existence of "serous tubal intraepithelial carcinomas (STICs)" and early invasive HGSC in the fallopian tube occurs in both familial and 50% to 60% of sporadic ovarian carcinoma (Kurman and Shih, 2011; Zeppernick *et al.*, 2015). STICs are also present in the majority of peritoneal (67%) and all tubal carcinomas (100%) (Cobb *et al.*, 2015). They are recognised by morphological characteristics such as disorganized, pleomorphic, hyperchromatic, and enlarged epithelial cells with highly atypical nuclei (Kurman and Shih, 2011; Zeppernick *et al.*, 2015). The lesions were almost always distinguished in the fimbria, suggesting that early malignant alterations initiate in secretory-type cells. There is some convincing evidence that supports this proposal. For example, the similarity of genes expressed in HGSC compared to fallopian tube is much more than to ovarian surface epithelium. Also, immunohistochemistry (IHC) staining shows expression of a Müllerian marker, PAX8, in HGSC which is different from Calretinin, a mesothelial marker (ovarian surface epithelium has a mesothelial not a Müllerian morphologic phenotype) (Figure 1-3). Moreover, coexpression of p53, p16, FAS, Ki-67 and cyclin E1 appear not only in STICs but also in HGSC. Lastly, some research has recently confirmed the existence of short telomeres in STIC lesions which is comparable with other precancerous lesions (Kurman and Shih, 2011; Zeppernick *et al.*, 2015). As previously mentioned, STICs are detectable in 50% to 60% of cases and there are other probabilities for remaining cases with no evidence of tubal involvement. Missing small STICs, disappearing STICs by overgrowth of invasive carcinoma and development from ovarian cortical inclusion cysts are other possibilities. The formation of these cysts occurs during ovulation while the fimbriae have close connections with the ovary and tubal epithelial cells become embedded within the disrupted ovarian surface (Figure 1-4). It seems that ovulation has a likely effect on

early ovarian carcinogenesis by the release of follicular fluid, producing free radicals and inflammation, which is consistent with the protective effects of pregnancy and the use of oral contraceptive pills (Kurman and Shih, 2011).

Endometriosis is the originator of endometrioid and clear cell carcinomas, but the origin of mucinous and transitional tumours is obscure. It seems that these arise from transitional epithelial nests placed in paraovarian locations at the tuboperitoneal junction. Confirmation of this concept would suggest that only gonadal stromal and germ cell tumours derive from ovaries (Kurman and Shih, 2010; Kurman and Shih, 2011; Cobb *et al.*, 2015). LGSC develops from spread of presumed fallopian tube epithelial stem cells into the ovulation site where those stem cells form surface inclusion cysts. Those cysts are likely to grow into serous cystadenomas and develop into serous borderline tumours representing the precursor lesions of LGSC (Figure 1-5) (Cobb *et al.*, 2015).

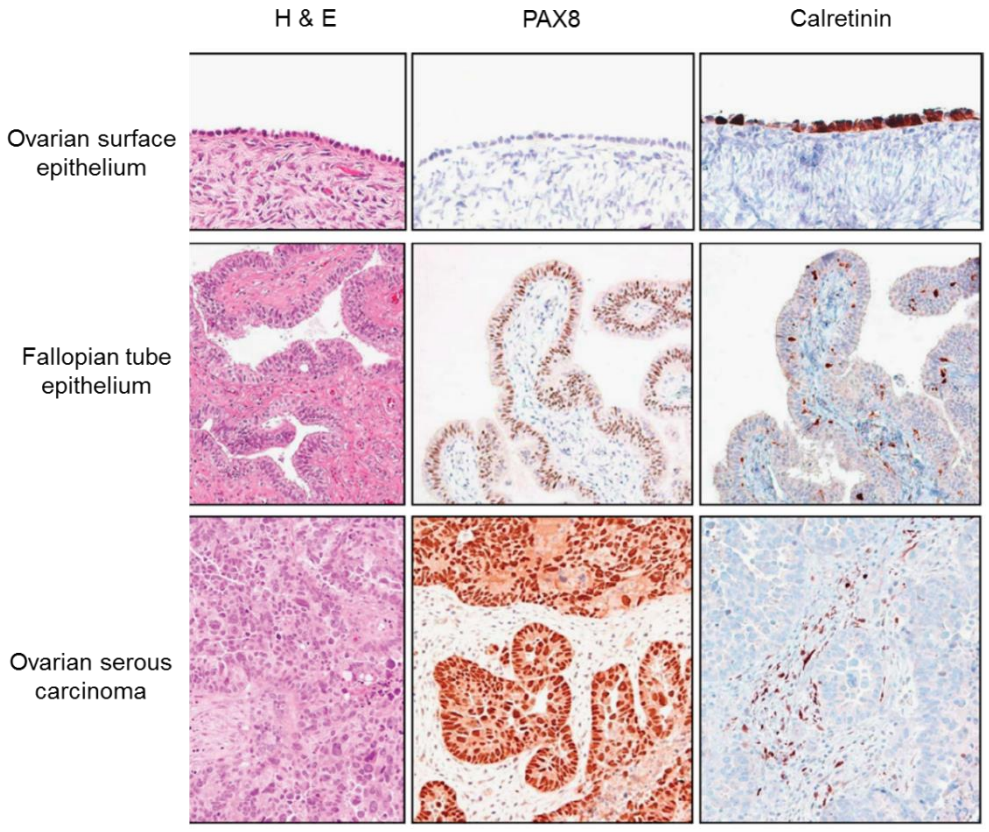

Figure 1-3: The comparison of IHC staining pattern for ovarian epithelium (mesothelium), normal fallopian tube epithelium, and HGSC. PAX8 is a marker of Müllerian-type epithelium, such as fallopian tube epithelium, and Calretinin is a marker of mesothelium (Kurman and Shih, 2010).

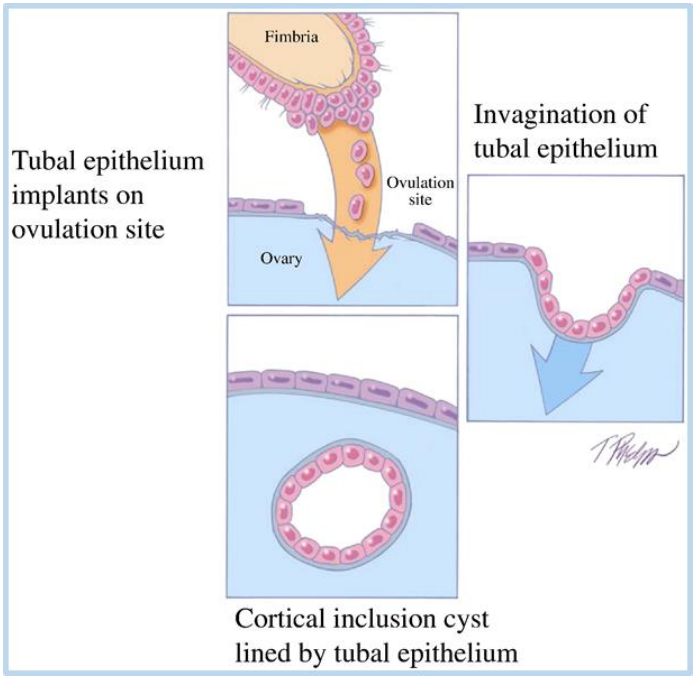

Figure 1-4: Development of a cortical inclusion cyst from tubal epithelium (Kurman and Shih, 2011).

A B

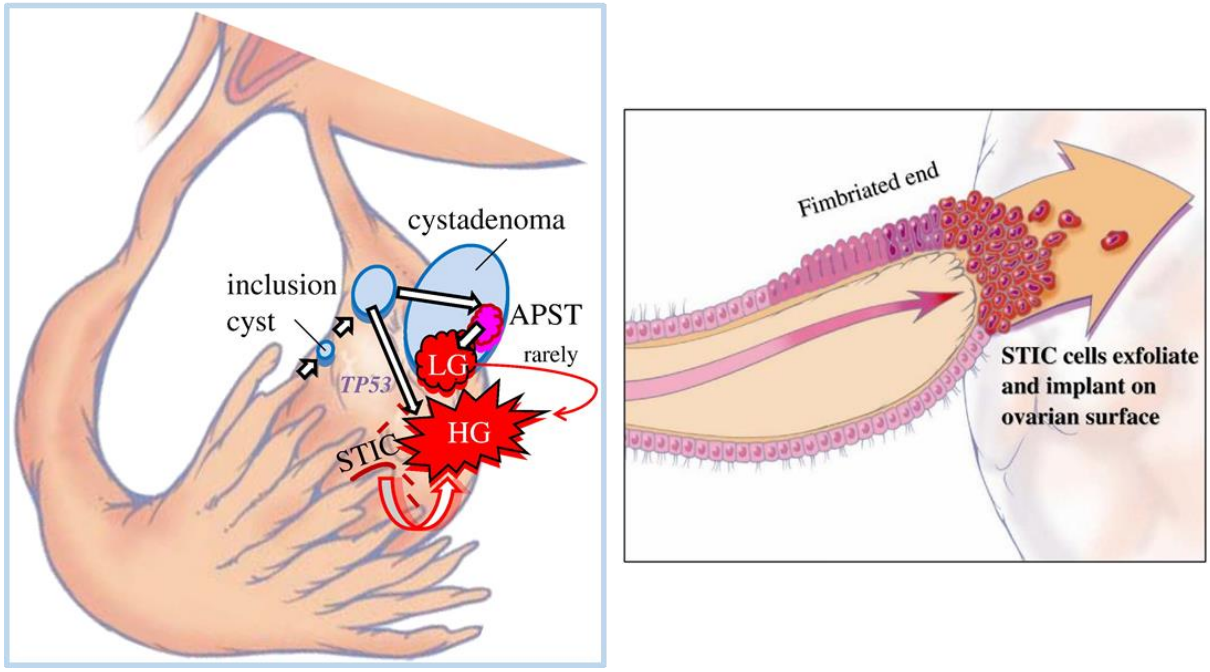

Figure 1-5: (A) Proposed development of LGSC and HGSC from tubal epithelium by way of a cortical inclusion cyst and cystadenoma or an intraepithelial carcinoma (STIC) implanting directly on the ovary developing into a HGSC. APST, atypical proliferative serous tumor. (B) A schematic representation of direct dissemination or shedding of STIC cells onto the ovarian surface (Kurman and Shih, 2011).

1.1.7 Survival

The rate of patient survival depends on many variables such as detection time, stage of disease, histological subtype, *TP53* status, effective surgery and response to treatment. Earlier diagnosis correlates with more survival; however, only about 20% of all recorded patients are diagnosed in the early stages. The overall 5-year survival is nearly 30% or less because of detection in advanced stages, which involve distant metastasis (Yasmeen *et al.*, 2011). The stage of disease has a huge impact on the survival as five-year relative survival ranges from 90% at stage I to 4% at stage IV (CRUK, 2016). Mutant and hence non-functional *TP53* is associated with resistance to present treatments and shorter survival. Complete cytoreduction where possible and treatment with optimized combinations of cytotoxic therapeutic drugs, greatly improve survival (Bast *et al.*, 2009; Kurman and Shih, 2010; Kim *et al.*, 2012).

1.2 Treatment of ovarian cancer

The treatment procedure is influenced by several issues, such as general health, fertility, type of ovarian cancer, disease stage and grade, and primary status or relapsed disease (CRUK, 2016). Nevertheless, standard therapy is cytoreductive surgery to remove the bulk of tumour, and a combination of platinum-and taxane-based chemotherapy (Banerjee and Kaye, 2013; CRUK, 2016).

1.2.1 Primary treatment

Combination of cytoreductive surgery and platinum-based chemotherapy is standard treatment for newly diagnosed disease. Debulking surgery decreases the size of tumour, which in theory results in having more access to the supply of oxygen and nutrient for the remained tumour cells and permits them to enter a proliferating phase and become much more sensitive to chemotherapy. Another advantage of surgical cytoreduction is eliminating or reducing existing resistant tumour cells, which may postpone the relapse. Due mainly to the fact that surgery alone is not completely curative, it must be followed by chemotherapy (Hennessy *et al.*, 2009; Colombo *et al.*, 2010; CRUK, 2016).

The aim of chemotherapy is to reduce the risk of relapse and/or to shrink the cancer. The chemotherapy may be performed before surgery if the tumour is large, in order to shrink the cancer and make it easier to remove. The surgery is likely to be curative for women who present

with borderline ovarian tumour or a very early cancer which is low stage (stage 1a) and grade (CRUK, 2016). In general, the treatment includes six cycles of platinum-based chemotherapy following primary debulking surgery or three cycles of neoadjuvant chemotherapy followed by interval debulking surgery and a further three cycles of chemotherapy.

1.2.2 Treatment of recurrent disease

Although up to 80% of patients with primary disease respond to first-line chemotherapy, relapse and resistance to treatment is prevalent, leading to lack of long-term benefit from treatment (Kim *et al.*, 2012). Platinum-based chemotherapy, platinum combinations, targeted therapies including angiogenesis inhibitors and poly-ADP ribose polymerase (PARP) inhibitors or addition of those to chemotherapy would be choices of treatment in relapsed platinum-sensitive ovarian cancer patients (defined as disease recurring ≥ 6 months) (Luvero *et al.*, 2014). The ICON4/OVAR 2.2 randomised trials showed significantly longer overall survival and progression free survival in combination of platinum and paclitaxel to platinum alone for platinum-sensitive patients with relapsed ovarian cancer (Parmar *et al.*, 2003). Platinum-resistant patients consist of different categories with various biological behaviour. Further treatment of a dose-dense schedule of platinum alone or in combination with etoposide or paclitaxel, paclitaxel, topotecan, gemcitabine or targeted therapy are the choices of treatment for platinum-resistant patients. Interval debulking surgery would be other choice of treatment in recurrent ovarian cancer (Luvero *et al.*, 2014).

1.2.3 The molecular mechanism of platinum-based treatment

Cisplatin (cis-diamminedichloroplatinum) was the first FDA-approved platinum compound for cancer treatment in 1978. Among several thousand analogues synthesised to enhance the therapeutic index, about 13 of those have been entered in clinical trials, with only carboplatin (1,1-cyclobutanecarboxylato) showing a definite advantage over cisplatin with reduced side effects (Figure 1-6) (Dasari and Tchounwou, 2014). Platinum drugs are used for treatment of different types of cancer including tumours of bone, blood vessels, and soft tissue and solid tumours such as ovarian cancer. They are genotoxic therapeutic agents interacting with DNA, RNA and protein. The uptake of platinum drugs occurs via passive diffusion and active transport through the copper transporters CTR1 and CTR2 (Johnstone *et al.*, 2014; Nasma *et al*., 2014). The efflux ATPases, MRPs and ATP7A/B, solute carrier importers, AQP2/9, and MDR1, the ATP-binding cassette transporter known as P-glycoprotein, are reported as transporters of platinum drugs as well (Dasari and Tchounwou, 2014). They are intracellularly

activated by a series of equation reactions including replacement of one or both cis-chloro groups with water molecules in the cytoplasm due to relatively low concentration of chloride ions. The hydrolysed products are potent electrophiles with the ability to react with any nucleophile compounds such as sulfhydryl groups on proteins or nitrogen donor atoms on nucleic acids (Galluzzi *et al.*, 2012; Dasari and Tchounwou, 2014). These drugs exert their cytotoxicity after their activation via interacting with N7-sites of purine residues in DNA, causing crosslinking of DNA as 1, 2-intrastrand (90%), 1, 3-intrastrand (5-10%), or interstrand (1-2%) crosslinks (Wang *et al.*, 2011). These adducts result in cessation of DNA replication and transcription, and are recognized by particular proteins involved in Nucleotide Excision Repair (NER) and Mismatch Repair (MMR) (Tanida *et al.*, 2012; Johnstone *et al.*, 2014). These DNA damage recognition proteins transmit DNA damage signals to downstream signalling pathways including p53, MAPK and p73 leading to induction of apoptosis (Figure 1-7). Platinum drugs also induce S- and G2/M phase arrest while their effect on the G0/G1 phase arrest is a later event and accumulation of cells in G0/G1 phase is rarely observed following platinum drug treatment (Tanida *et al.*, 2012). More than 90% of cisplatin-damaged DNA is repaired by the NER pathway associated with cisplatin resistance (Wang *et al.*, 2011), whereas apoptosis is triggered by the MMR pathway (Ataian and Krebs, 2006; Tanida *et al.*, 2012). The interstrand crosslinks induced by cisplatin are repaired via homologous recombination repair (HRR) (Wang *et al.*, 2011). In addition to DNA damage, oxidative stress is also induced after platinum-based treatment triggering cell death through apoptosis, necrosis and autophagy (Dasari and Tchounwou, 2014).

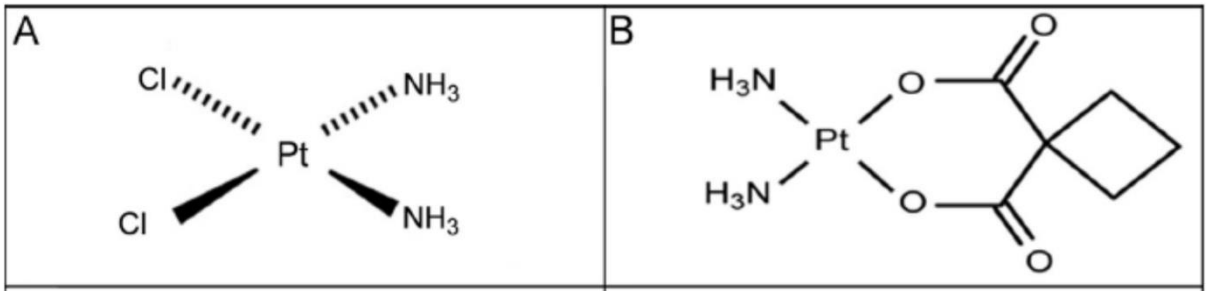

Figure 1-6: The chemical structure of (A) Cisplatin and (B) Carboplatin.

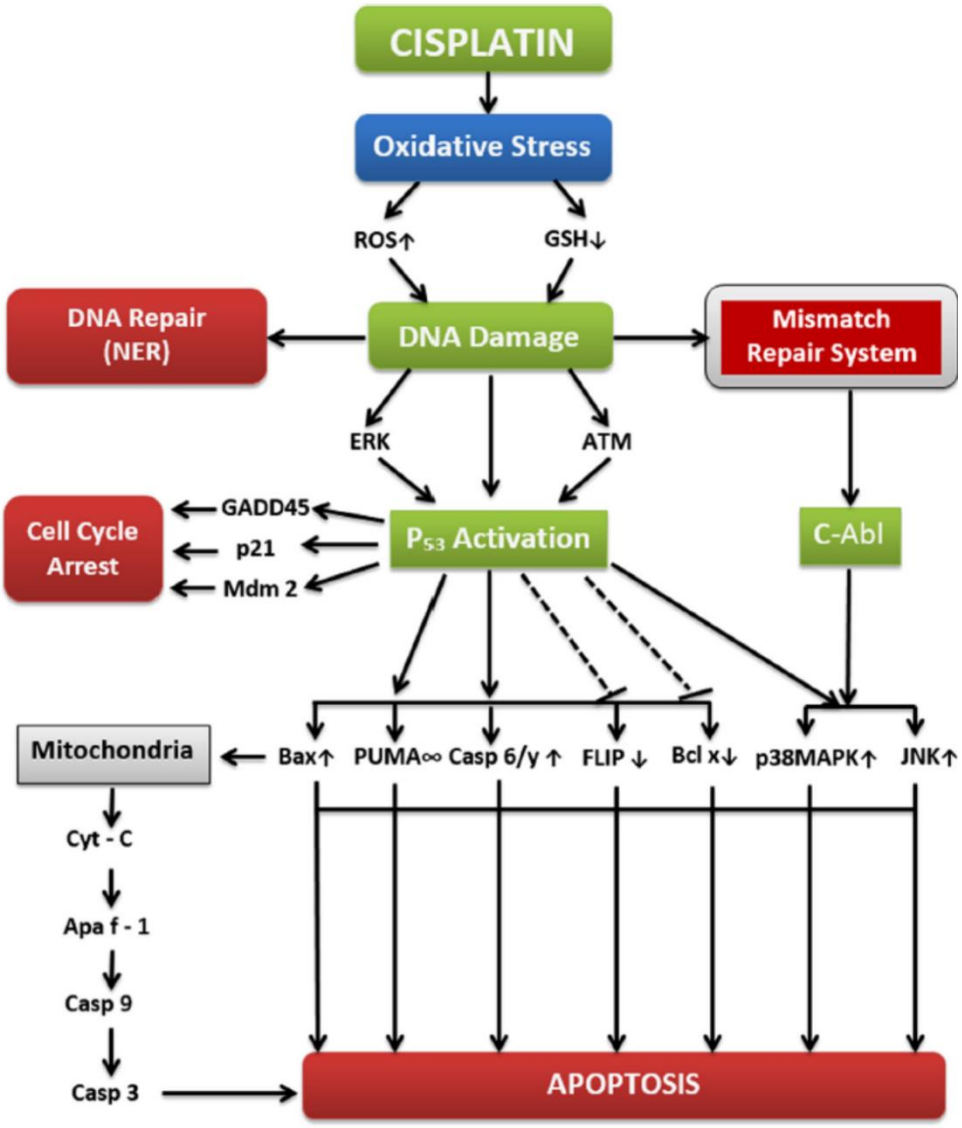

Figure 1-7: Overview of the molecular mechanisms of the platinum-based drug, cisplatin, in cancer treatment (Dasari and Tchounwou, 2014).

1.2.4 The p53 and DNA damage response to platinum-based treatment

Platinum-based drugs exert their cytotoxic effects by both p53-dependent and p53-independent pathways. Following exposure to platinum-based drugs, ATM and ATR phosphorylate several proteins including Chk1, Chk2 and p53. The phosphorylated Chk1 and Chk2 further phosphorylate p53 resulting in stabilisation and activation of p53. Activated p53 in turn trans-activates genes involved in cell cycle arrest, apoptosis and DNA repair (Tanida *et al.*, 2012; Wang, 2015).

1.2.5 The mechanisms of resistance to platinum-based chemotherapy

Different mechanisms are involved in resistance to cisplatin, referred to as pre-target or intrinsic resistance, on-target resistance, post-target resistance and off-target resistance (Galluzzi *et al.*, 2012). Increased drug efflux via multidrug resistance-associated proteins and copper transporting P-type ATPase protein, decreased drug uptake through inactivation or down regulation of uptake transporters and drug inactivation by thiol-containing molecules such as glutathione are examples of pre-target resistance. Enhanced DNA repair inhibits apoptosis progression because persistence of DNA adducts resulting from platinum treatment induces apoptosis. Therefore, NER and HRR proficiency result in on-target resistance to cisplatin (Galluzzi *et al.*, 2012; Tanida *et al.*, 2012; Nasma *et al*., 2014). Inhibition of the dissemination of DNA damage signals to apoptotic pathways or deficiency in genes in downstream pathways involved in response to platinum drugs such as *TP53, BIRC5* (Survivin), *BAX* and *BCL-2* can also confer resistance to platinum drugs (post-target resistance) (Galluzzi *et al.*, 2012; Tanida *et al.*, 2012). Cisplatin resistance can be induced by alterations in signalling pathways not directly targeted by cisplatin such as autophagy (Bao *et al.*, 2015) and heat shock proteins (off-target resistance) (Galluzzi *et al.*, 2012). It was also reported that BIN1, a tumour suppressor nucleocytoplasmic adaptor protein, directly interacts with the c-Myc oncoprotein and inhibits its transcriptional activity and cell transformation. It also sensitizes cells to cisplatin through directly interacting with PARP1 and inhibiting its activity. Deficiency in the *BIN1* gene, suppression of *BIN1* expression and restoration of PARP1 activity following overexpression of c-Myc are novel mechanisms reported to mediate cisplatin resistance (Tanida *et al.*, 2012).

1.3 Targeted therapy in ovarian cancer

The treatment of ovarian cancer remains a challenge in spite of advances in debulking surgery and changes in both chemotherapy schedules and routes of administration (Coward *et al.*, 2015). Platinum agents used to treat ovarian cancer have major adverse side effects including nephrotoxicity, ototoxicity, myelosuppression and gastrointestinal disorders (Pabla and Dong, 2012). Although chemotherapy prolongs survival, most patients with advanced disease experience relapse and eventually develop platinum resistance and die from treatment resistant progressive disease (Ledermann *et al.*, 2013; Luvero *et al.*, 2014). Cancer therapy has recently been improving with the introduction of targeted therapies to achieve greater specificity and less cytotoxicity (Yuan *et al.*, 2011).

The potential success of targeted therapy was first recognised in 1998 by FDA approval of a monoclonal antibody trastuzumab to treat breast cancer patients harbouring HER-2 positive metastasis. In contrast to chemotherapy affecting both cancer and normal rapidly dividing cells, targeted therapy has the potential for lower toxicity and greater selectivity by targeting molecular abnormalities specific to the cancer (Huang *et al.*, 2014).

Epithelial ovarian cancer is a heterogeneous disease with different histological subtypes representing distinct molecular aberrations, but are nonetheless all treated with the same conventional chemotherapy. The identification of deficiencies in distinct molecular pathways of individual subtypes and exploitation of them in targeted therapy offers the promise of improved clinical outcome in ovarian cancer (Banerjee and Kaye, 2013). Over the last few years, molecular targeted therapy of ovarian cancer as single agents or in combination with chemotherapy has been showing promising and encouraging results (Banerjee and Kaye, 2013; Luvero *et al.*, 2014). However, targeted therapy is challenged by identification of the correct population to treat, occurrence of drug resistance (Banerjee and Kaye, 2013; Huang *et al.*, 2014), marginal response rate across an unselected patient population (10-20%), short-lived clinical responders (6-12 months) and disease progression (Huang *et al.*, 2014). To overcome targeted therapy resistance, it is suggested that targeted therapies are likely to be most effective in combination with standard chemotherapeutic agents or other targeted therapeutic drugs.

1.4 Combined treatment

Intrinsic or acquired resistance is the major limitation of targeted cancer therapy. Design of strategies to overcome intrinsic resistance and delay acquired resistance to targeted therapy is crucial to benefit from the treatment. One strategy is use of more effective drug combinations to completely block the oncogenic signalling pathway or activate the tumour suppressor signalling pathways (Groenendijk and Bernards, 2014). Dose and toxicity reduction, resistance minimisation or delay, and achieving synergistic therapeutic effects are the main objectives of drug combination.This is because multiple drugs may affect various targets and/or subpopulations. Also, one single target may be targeted with different drugs with varied mechanisms of action (Chou, 2006; Chou, 2010; Foucquier and Guedj, 2015). Potentiation or enhancement are defined when in the combination of two drugs one has no effect and the effect of combination is greater than that of the effective drug. The effect of combination is defined as synergism, additive or antagonism if both drugs have an effect on their own, and can be defined by Combination Index (CI) values. The synergism and antagonism are defined as

greater or less effects than an additive effect. For cancer therapy, synergism at high effect levels (ED_{90}, ED_{95}) is more desirable than at low levels of effect (ED_{50}) (Chou, 2006).

1.5 The tumour suppressor *TP53* gene

The tumour suppressor *TP53* gene, discovered by David Lane in 1979, localized on chromosome 17p13.1 is referred to as the most often mutated or deleted gene in human cancers. It has been substantially established that p53, acting as a genome guardian, protects cells against environmental and intra-cellular stressful stimuli by playing important roles in regulating cell cycle control, differentiation, apoptosis, DNA repair and proliferation (Levine and Oren, 2009; Wade *et al.*, 2013).

1.5.1 The structure of p53

The p53 protein, a 53kDa nuclear phosphoprotein, contains five conserved domains (Figure 1-8) which are responsible for performing specific functions including:

1. A transcriptional activation domain (TAD) is located within the N-terminus portion (residues 1-42) required for transcriptional activity. It is also necessary for interaction with some proteins including transcription factors, and several TATA box binding protein associated factors (TAFs), and mediates interaction with the E3 ubiquitin ligase MDM2 and histone acetyltransferases CBP/P300 (Kamada *et al.*, 2015).
2. A proline- rich region (PRD) is located in the N-terminus region (residues 61-94) playing a role in p53 stability, transcriptional activity, and induction of transcription independent apoptosis (Kamada *et al.*, 2015).
3. The central DNA-binding domain (DBD) (residues 101-300) is targeted by 90% of p53 mutations in different cancers. It has sequence specific DNA binding activity within the nucleus and directly binds to a consensus DNA binding site (Kamada *et al.*, 2015).
4. The C-terminal tetramerization domain (TD) (residues 326-356) plays a role in reversible formation of p53 tetramers, regulates p53 oligomeric status and includes a Nuclear Export Signal (NES) as well (Kamada *et al.*, 2015).
5. An autoinhibitory domain (residues 364-393) is localized on the C-terminus of p53 which has been implicated in downregulation of the DNA binding domain (Kamada *et al.*, 2015).

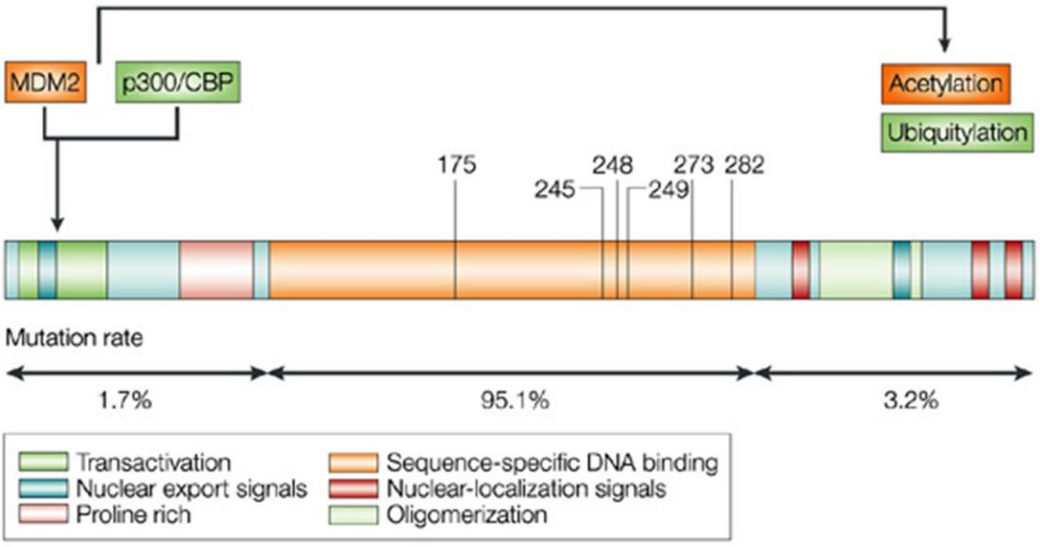

Figure 1-8: The p53 structure, its functional domains and location of tumour-associated mutation hotspots (Vousden and Lu, 2002).

1.5.2 Tetramer formation, post-translational modifications and functional regulation of p53

Formation of p53 tetramers is required for its site-specific DNA binding, post-translational modifications and protein-protein interactions. It also blocks the NES leading to inhibition of p53 nuclear export. The p53 response element consists of four pentanucleotide repeats and each repeat is recognised by one p53 DBD (Kamada *et al.*, 2015). In normal cells with wild-type p53, p53 is activated following a variety of stresses such as DNA damage, oncogene expression, starvation and oxidative stress. Stabilization and increased transcriptional activity of p53 result from diverse post-translational modifications, particularly phosphorylation, acetylation, and deubiquitination which are introduced into its N-terminus and C-terminal regulatory domains (Dai and Gu, 2010). The first crucial step of p53 stabilisation is phosphorylation of serine residues within the N-terminal p53 transactivation domain (Kruse and Gu, 2009; Cristiana, 2014). The tetrameric form of p53 is ubiquitinated and regulated by Pirh2 indicating regulation of the protein turnover of the p53 active form by Pirh2. The oligomeric status of p53 affects the MDM2-mediated poly-ubiquitylation of p53, whereas its proteasome degradation is only slightly affected by its tetramerization (Kamada *et al.*, 2015).

1.5.3 p53 function

The tumour suppressor protein p53, known as the guardian of genome, is located at the crossroad of a complex network of signalling pathways playing an essential role in cell growth regulation, senescence and apoptosis induced by genotoxic and non-genotoxic stresses (Figure 1-9) (Mandinova and Lee, 2011; Soussi, 2012; Kamada *et al.*, 2015; Su *et al.*, 2015). Other cellular processes of p53 are modulation of autophagy (Rosenfeldt *et al.*, 2013; Cristiana, 2014; Kamada *et al.*, 2015; Su *et al.*, 2015), inhibition of cell migration and metastasis (Kamada *et al.*, 2015; Su *et al.*, 2015), regulation of metabolism (Maddocks *et al.*, 2013; Cristiana, 2014; Kamada *et al.*, 2015) and angiogenesis (Cristiana, 2014), moderation of innate immune responses through its antagonism of nuclear factor κB signalling (Kamada *et al.*, 2015) and sensitisation of cells to ferroptosis (a non-apoptotic form of cell death) (Jiang *et al.*, 2015; Kamada *et al.*, 2015). It also targets and regulates the expression of specific microRNAs (miRNAs) such as miR-34a inducing cell cycle arrest, senescence and cell death, and miR-192 and miR-215 promoting $p21^{WAF1}$ expression (Cristiana, 2014).

In normal cells under normal conditions, the cellular levels of p53 are low due to a very short-life ranging from 5 to 30 minutes (Teoh and Chng, 2014). Following exposure to genotoxic or non-genotoxic stresses, upstream mediators distinguish and respond to the signals via stabilization of p53, as a result of posttranslational modifications of p53 and its regulators such as MDM2 and MDMX proteins. The downstream pathways involve p53 transcriptional transactivation events and interactions between proteins. The p53 protein regulates expression of its downstream transcriptional targets through both DNA binding and transactivation domains by binding to responsive DNA sequences and repressing or transactivating these target genes. The final outcome of p53 activation is either cell cycle arrest and DNA repair or apoptosis (Mandinova and Lee, 2011; Soussi, 2012).

The cellular reaction to different stresses is completely different based on the tissue and cell type, nature and strength of stress, genomic damage and the environment of the cell (Murray-Zmijewski *et al.*, 2008; Hanahan and Weinberg, 2011; Cristiana, 2014). Other variables affecting the p53 response to stress include p53 level, existence of p53 regulator and affinity of sites binding to p53. The promoters of genes halting proliferation and genes inducing apoptosis comprise high and low affinity sites respectively. The high affinity sites will be activated first and then at higher p53 concentrations the low affinity sites would become occupied. This would suggest the apoptosis sites should be of a lower affinity. Cell cycle arrest

and/or apoptosis are biological end-points of stress (Meek, 2004; Kitayner *et al.*, 2006; Hoe *et al.*, 2014). Induction of p53 expression at different levels using a doxycycline-regulated inducible p53 expression system in the hepatocellular carcinoma (HCC) cells showed that apoptosis and cell cycle arrest were induced at high and low levels of p53 expression respectively (Lai *et al.*, 2007). Furthermore, cell fate outcome after p53 activation is influenced by the expression levels of anti-apoptotic proteins in target cells, post-translational modification of p53 and its regulatory proteins, overexpression of iASPP (inhibitor of apoptosis-stimulating of p53 protein) (Hoe *et al.*, 2014), and the influence of other signalling pathways which are activated or inhibited (Valente *et al.*, 2013).

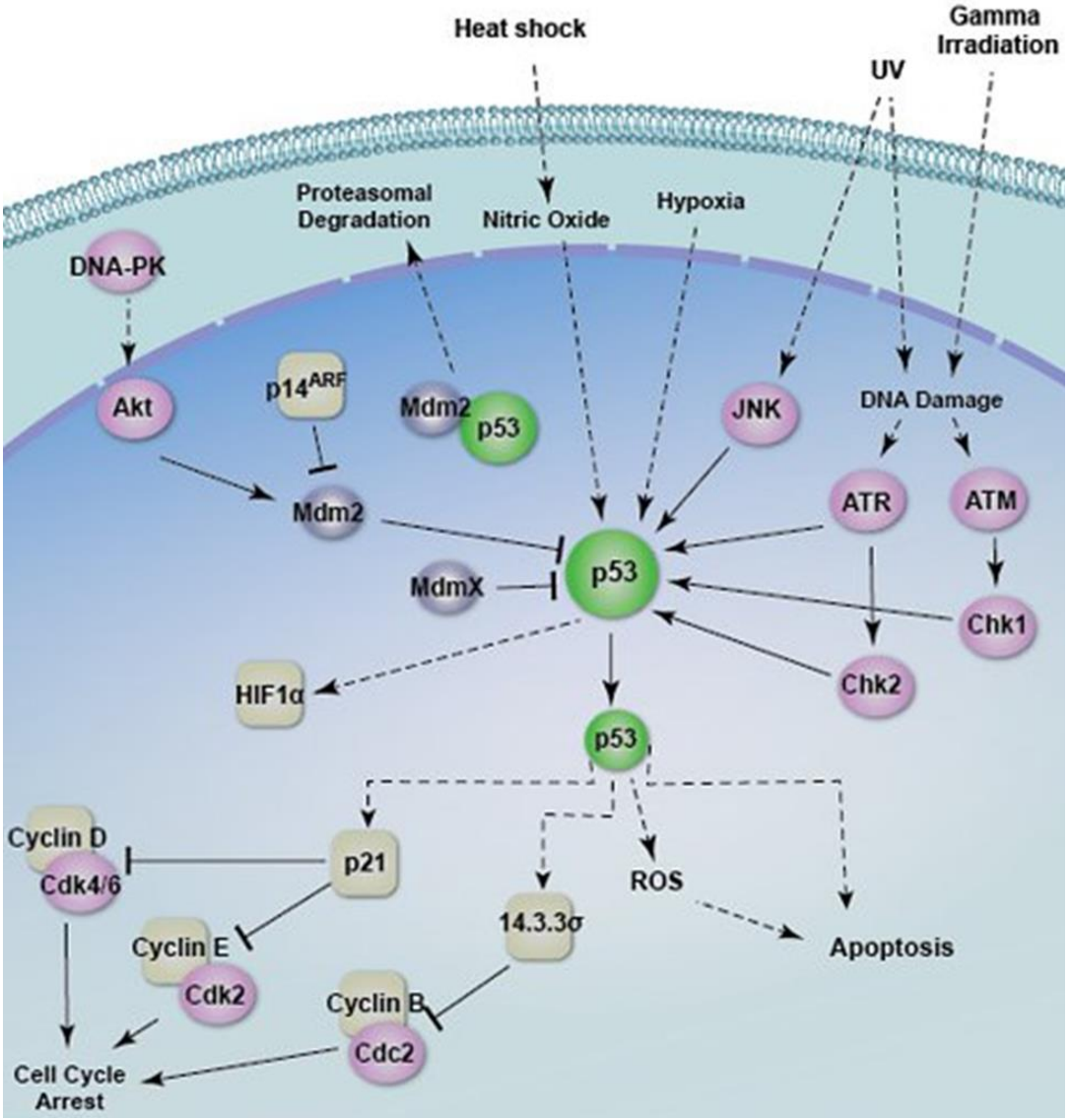

Figure 1-9: The p53 signalling pathway (www.tocris.com).

1.5.4 p53-mediated cell cycle arrest

p53-dependent cell cycle arrest in the G0/G1, G2/M, and S-phases occurs through transcriptional activation of the *CDKN1A* encoded cyclin-dependent kinase inhibitor $p21^{WAF1}$, *GADD45* (Growth arrest and DNA-damage-inducible 45) and *14-3-3σ* genes. The p53-induced cell cycle arrest at G0/G1 and G2/M phases is considered to allow time for the cells to repair genomic damage before entering the DNA synthesis and mitosis stages respectively (Zhu and Bai, 2006).

The $p21^{WAF1}$ protein, the best characterised mediator of p53-dependent cell cycle arrest, regulates both G1-S and G2-M checkpoints and prevents G1 to S and G2 to M progression leading to G0/G1 and G2/M cell cycle arrest. It directly binds to Cyclin/Cdk (Cyclin-dependent kinase) complexes such as Cyclin E/Cdk2 and Cyclin B/Cdk1 and induces G0/G1 and G2/M cell cycle arrest respectively. Induction of G0/G1 arrest via blockade of Cyclin E/Cdk2 is mediated by inhibition of Rb phosphorylation, a process required to release E2F transcription factor from Rb and promote expression of genes essential for progression from G1 to the S-phase (Zhu and Bai, 2006; Wang, 2007; Valente and Strasser, 2013). Furthermore, $p21^{WAF1}$ binds to proliferating-cell nuclear antigen (PCNA) which is required for DNA synthesis and DNA repair resulting in G2/M arrest (Wang, 2007; Piccolo and Crispy, 2012).

The *GADD45* and *14-3-3σ* genes are transcriptionally induced and upregulated by p53, and both proteins inhibit the G2/M transition and participate in G2/M arrest. GADD45 exerts its effect through binding to Cdc2 (cdk1) and subsequent inhibition of the cyclinB/Cdc2 interaction and kinase activity. The scaffold protein 14-3-3σ induces G2 arrest via sequestration of the cdk1 in the cytoplasm, blockade of cyclin B/cdk1 complex formation, and inhibition of Cdk1 activity (Zhu, 2006; Shulin Wang, 2007; Liz J Valente, 2013).

1.5.5 p53-mediated cellular senescence

Senescence, irreversible cell cycle arrest, is another mechanism by which p53 activation can result in removal of tumour cells, mediated by the promyelocytic leukemia (PML), plasminogen activator inhibitor-1 (PAI-1), deleted in esophageal cancer 1 (DEC1) and $p21^{WAF1}$ proteins (Qian and Chen, 2010; Valente and Strasser, 2013) and association of 'eat me' (opsonisation) signal leading to senescence-induced phagocytosis and killing of the senescent cells (Hoe *et al.*, 2014). PML, a direct p53 target, and p53 form a positive regulatory feedback loop during cellular senescence. PAI-1, is transcriptionally regulated by p53 and considered as

a marker of replicative senescence. It exerts its inhibitory effect on cell proliferation and induction of senescence through its physical association with uPA which is a promoter of G1/S transition. *DEC1* is a target gene of p53 implicated in cell cycle regulation, differentiation, apoptosis and p53-dependent cellular senescence. The cell cycle inhibitor $p21^{WAF1}$ plays an important role in p53-dependent cellular senescence; however, it is not essential and lack of $p21^{WAF1}$ reduces DNA damaged-induced premature senescence in tumour cells but does not abolish it (Qian and Chen, 2010). Due to the impact of mTOR (mammalian target of rapamycin) on the senescence program and inhibition of mTOR following p53 activation, it was reported that p53 acts as a suppressor of senescence and converts it into quiescence (reversible cell cycle arrest) (Demidenko *et al.*, 2010). However, more research indicated that the status of the mTOR pathway can partly determine the selection between senescence and quiescence in p53-activated cells (Lioubov G. Korotchkina, 2010; Liz J Valente, 2013).

1.5.6 p53-mediated apoptosis

There are two major pathways by which p53-regulated apoptosis is induced, named the intrinsic mitochondrial and extrinsic death receptor pathways. The intrinsic mitochondrial pathway is primarily used in p53-mediated apoptosis, while the extrinsic pathway is utilised to enhance the apoptosis response. The end point of both pathways is caspase activation and apoptosis (Zhu, 2006).

Following exposure to apoptotic stimuli and p53 activation, the intrinsic mitochondrial pathway is activated and dominated by BCL-2 family proteins, including anti-apoptotic proteins BCL-2 and MCL-1, multi-BH domain pro-apoptotic proteins BAX and BAK, and pro-apoptotic "BH3-only" proteins BID, BAD, NOXA and BBC3 (known as PUMA). PUMA has the ability to bind to anti-apoptotic proteins BCL-2, BCL-W, MCL-1, BCL-2A1 and BCL-X_L, whereas NOXA can only bind to MCL-1 and BCL-2A1 proteins (Zhu, 2006; Liz J Valente, 2013; Hoe *et al.*, 2014). Apoptotic stimuli are followed by transcriptional, post-transcriptional and/or post-translational activation of the pro-apoptotic BH3-only proteins. These activated proteins bind to anti-apoptotic BCL-2 proteins resulting in activation and formation of BAX and BAK homo-oligomers and their localisation on the mitochondria which induce production of mitochondrial outer membrane permeabilisation (MOMP) and subsequent cytochrome c release. Then, formation of the apoptosome complex is promoted by apoptotic protein activating factor-1 (Apaf-1) and caspase 9 (Zhu, 2006; Valente, 2013).

In the death receptor-mediated extrinsic pathway, another p53-regulated class of pro-apoptotic genes is upregulated including the death receptor gene products such as FAS/CD95, DR4 and DR5 located at the plasma membrane, and some other gene products implicated in this apoptotic pathway. These p53-upregulated receptors suppress Inhibitors of Apoptosis Proteins (IAPs) and induce caspase-mediated apoptosis (Zhu, 2006; Joana D, 2010; Valente, 2013).

Apoptosis may also be triggered by p53 through a non-transcriptional mechanism, an alternative cytosolic p53-mediated apoptosis. In this pathway, p53 can shuttle to the outer mitochondrial membrane where it directly interacts with the members of BCL-2 protein family such as BCL-X_L/BCL-2 to displace BAX or BH3 domain-only pro-apoptotic proteins, and induce their oligomerisation. The final outcome is production of MOMP, release of cytochrome c and consequently activation of the caspase cascade and apoptosis (Zhu, 2006; Kruse and Gu, 2009; Joana D, 2010; Liz J Valente, 2013; Hoe *et al.*, 2014).

1.5.7 Regulation of the p53 cellular levels

Tumour suppressor p53 has the potential to induce apoptosis and cell cycle arrest and that is why the cellular levels of this protein are maintained at a low level in normal cells (Teoh and Chng, 2014). Different mechanisms are involved in regulation of the cellular levels of p53.

The mouse double minute-2 homolog (MDM2) protein, also named HDM2 in human, is the main negative regulator of p53. The formation of an autoregulatory feedback loop between p53 and MDM2 regulates their cellular levels. MDM2 not only binds to the N-terminus domain of p53 to inhibit its transcriptional activity but also interacts with the DNA binding domain to promote its proteasomal degradation. The p53 protein is ubiquitylated by the MDM2 RING Finger and E3-ubiquitin ligase enzymatic activity of MDM2 to transfer the MDM2-p53 complex to the cytoplasm and target it for proteasome degradation in the cellular 26S proteasome (Figure 1-10) (Wade *et al.*, 2010; Pant *et al.*, 2011; Rew *et al.*, 2012; Rew and Sun, 2014; Teoh and Chng, 2014).

In line with the role of MDM2 as the main negative regulator of p53, MDM2 regulator proteins can indirectly regulate p53 cellular levels. For example, deregulation of p14ARF (Alternative Reading Frame, a negative regulator of MDM2) (Teoh and Chng, 2014), and WIP1 (wild-type p53-induced phosphatase, a protein which dephosphorylates MDM2) affects the stability and levels of MDM2 and consequently the stability and activity of p53 (Kruse and Gu, 2009). RBEL1A, a novel Rab-like GTP-binding protein, is predominantly GTP bound and functions

as a GTPase and is overexpressed in primary breast and colon cancer samples. Its direct interaction with both MDM2 and p53 proteins augments MDM2-dependent p53 ubiquitylation and degradation. RBELIA also exerts its inhibitory effect on p53 through inhibition of the transactivation potential of p53 and suppression of p53 activation (Lui *et al.*, 2013).

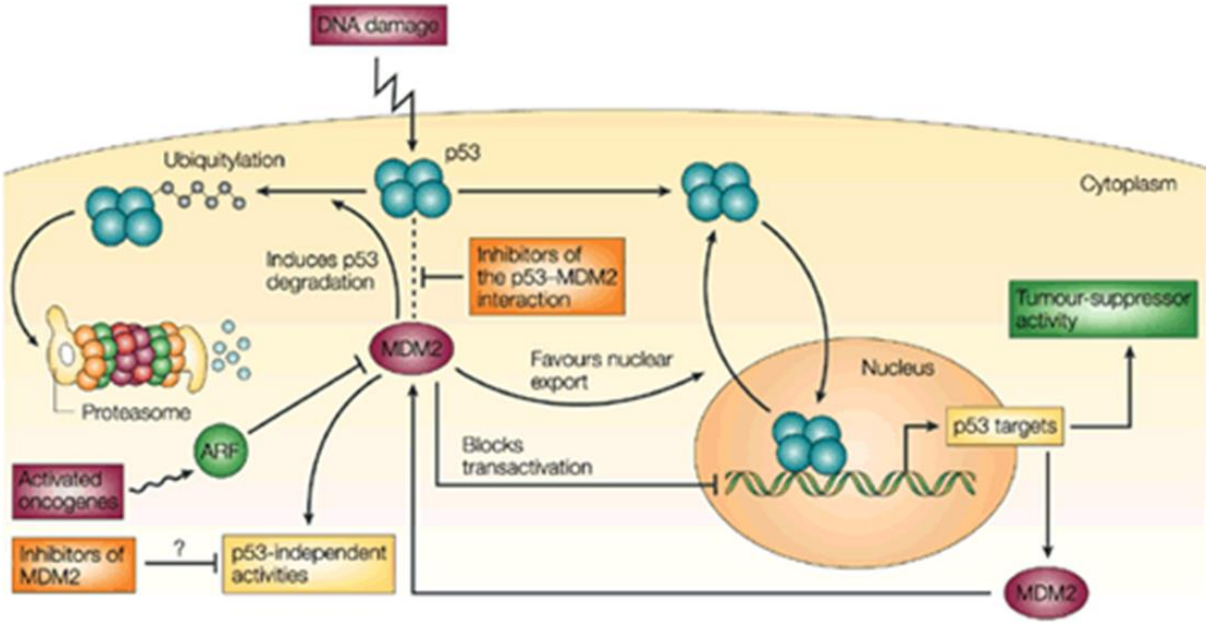

Figure 1-10: Regulation of p53 by MDM2 (Chene, 2003).

Another negative regulatory protein of p53 is MDMX which has a high sequence and structural similarity to MDM2. MDMX binds to p53 at the N-terminal transcriptional activation domain of p53 and inhibits its transactivation activity. MDMX has no intrinsic ubiquitination activity; however, interaction between MDMX and MDM2 via their C-terminal RING finger domains results in formation of an MDM2-MDMX heterodimer and subsequent activation of the E3 ligase activity of MDM2 in a dose-dependent manner (Pei *et al.*, 2012; Tollini and Zhang, 2012; Teoh and Chng, 2014).

Restoration of normal p53 levels after stress response is also induced by some ubiquitin E3-ligases other than MDM2 which promote p53 degradation including Pirh2, COP1 (Kruse and Gu, 2009; Collavin *et al.*, 2010) and Arf-BP1 (Kruse and Gu, 2009). WWP1, a member of NEDD4-like ubiquitin ligases, recognises proline-rich sequences on p53. WWP1 interacts with p53 producing a mono-ubiquitinated form of p53, retaining it in the cytoplasm and inhibiting its transcriptional activity (Collavin *et al.*, 2010).

Epigenetic regulation of TP53 can also regulate cellular levels of p53. One such mechanism is deregulation of miRNAs. miRNAs are a set of small noncoding RNA sequences of 19 to 25 nucleotides playing a critical role in regulating gene expression by binding to the 3'-untranslated regions (3'-UTR) of specific mRNAs. They degrade or destabilise the gene target coding mRNA and repress efficient translation of the mRNA into proteins. miR-125b and miR-504 are reported negative regulators of p53 in human cell lines (Teoh and Chng, 2014).

1.6 The role of p53 and its transcriptional targets in ovarian cancer

1.6.1 p53 and ovarian cancer

The frequency of *TP53* mutation in ovarian cancer is different based on the clinicopathological data, including stage of disease, histological subtype and grade of differentiation (Kmet *et al.*, 2003; Bauerschlag *et al.*, 2010; Rechsteiner *et al.*, 2013) ranging from 34% (Leitao *et al.*, 2004) for epithelial ovarian cancer regardless of histological subtype to (97%) for HGSC (Ahmed *et al.*, 2010). Accumulation of p53 is a frequent event in ovarian cancer occurring in 4% of borderline to 50% of advanced ovarian cancers. Inactivated p53 accumulates in either the nucleus or cytoplasm depending on the type of mutation even though the most common p53 abnormalities in ovarian cancer lead to nuclear accumulation of overexpressed p53 detectable by staining (M. Sharon Stack, 2009). In terms of correlation between *TP53* status/p53 overexpression and overall survival (OS) or progression free survival (PFS), the results are controversial and are explained in more detail later in chapter 3.5.2, 4.5.3 and 5.5.1.

1.6.2 $p21^{WAF1}$ and ovarian cancer

The $p21^{WAF1}$ protein, a member of the cyclin dependent kinase inhibitor (CDKI) superfamily, is encoded by the *CDKN1A* gene located on chromosome 6p21.2. It plays a dual role as a tumour suppressor through cell cycle arrest or oncogene via anti-apoptotic function based on its subcellular localisation cellular context and circumstances (Abbas and Dutta, 2009; Xia *et al.*, 2011; Maria Teresa Piccolo1, 2012). The $p21^{WAF1}$ has the ability to switch from a nuclear tumour suppressor to a cytoplasmic oncogene through the PI3K/Akt signalling pathway (Xia *et al.*, 2011; Lu, 2016). Post-translational modification of $p21^{WAF1}$ mediated by various kinases on its threonine and serine residues strongly impacts on its cellular localisation and its specific function as a negative regulator of cell cycle arrest. In fact, phosphorylation of $p21^{WAF1}$ on the specific residues Thr145 and Ser153, relocalizes $p21^{WAF1}$ to the cytoplasm inhibiting the interaction of $p21^{WAF1}$ with Cyclin/Cdk complexes or PCNA and induces its anti-apoptotic

function (Maria Teresa Piccolo1, 2012). The $p21^{WAF1}$ protein mediates its anti-apoptotic role through cell cycle arrest, suppression of pro-apoptotic genes regulated by E2F and its interaction with different pro-apoptotic proteins such as procaspase 3, caspase 8 and caspase 10 (Abbas and Dutta, 2009; Maria Teresa Piccolo1, 2012).

Recent studies indicated that cytoplasmic $p21^{WAF1}$ is significantly correlated with cisplatin resistance in ovarian cancer (Xia *et al.*, 2011; Lu, 2016). $p21^{WAF1}$ relocation from the nucleus to the cytoplasm is induced by Act-mediated phosphorylation. Transfection of cisplatin-resistant ovarian cancer cell lines with Act2 shRNA led to inhibition of cytoplasmic $p21^{WAF1}$ translocation and enhanced their sensitivity to cisplatin (Xia *et al.*, 2011).

Controversial results were reported in relation to the correlation between $p21^{WAF1}$ expression and overall or progression free survival in ovarian cancer, which is described in more detail later in chapter 3.5.3 and 5.5.4.

1.6.3 MDM2 and ovarian cancer

The MDM2 protein is encoded by the *MDM2* gene located on chromosome 12q14-15, which is amplified or overexpressed in many cancers (Forslund *et al.*, 2008). Due to the role of overexpressed and/or amplified *MDM2* as an alternative mechanism to inactivate p53, it is important to identify cancer types with overexpressed- or amplified-*MDM2*. The frequency of *MDM2* amplification in ovarian cancer is 3.1% (Mancini, 2012) and reported MDM2 overexpression varies from 17% to 47% (Foulkes *et al.*, 1995; Bast *et al.*, 2009; Mancini, 2012). Also, it was reported that different MDM2 polymorphisms affect the risk of ovarian cancer in *BRCA-1* related ovarian cancer. For example, *MDM2* SNP309 and SNP285C were reported to be associated with an increased and decreased the risk of ovarian cancer in *BRCA-1* related ovarian cancer respectively (Bjørnslett *et al.*, 2012). For the association between overexpression of MDM2 and overall or progression free survival, there is no consistency between reported results, and are explained in more detail later in chapter 3.5.6 and 3.5.7.

1.6.4 The PPM1D (WIP1) phosphatase and ovarian cancer

The protein phosphatase magnesium/manganese-dependent 1D (PPM1D), also known as wild-type p53 inducible phosphatase (WIP1), is a member of the type 2C phosphatase family encoded by the *PPM1D* gene located on chromosome 17q23.2. It preferentially dephosphorylates phosphoproteins containing SQ/TQ or TXY motifs (Ali *et al.*, 2012). WIP1 elicits its action through dephosphorylation of p53, ATM, Chk2 and γ-H2AX involved in DNA damage response, and leads to inactivation of these proteins (Han *et al.*, 2009; Yin *et al.*, 2016). *PPM1D* amplification and/or overexpression is correlated with poor prognosis, especially in hormone-regulated cancers including ovarian cancer. The oncogenic effect of WIP1 is due to dephosphorylation of p53, p38, Chk1 and Chk2 and subsequent inhibition of cellular G1-S and G2-M checkpoint activities in response to DNA damage (Han *et al.*, 2009). Amplification and/or overexpression of WIP1 was reported in ovarian clear cell adenocarcinoma (Hirasawa *et al.*, 2003; Tan *et al.*, 2009; Emelyanov and Bulavin, 2015) confering cisplatin resistance (Ali *et al.*, 2012). Despite the oncogenic role of WIP1 reported in many carcinomas, one recent study demonstrated an antitumour action of WIP1 by involving suppression of ovarian cancer metastasis in xenograft animal models mediated by regulation of the ATM/Akt/Snail signalling pathway (Yin *et al.*, 2016). No study has previously been published to evaluate the correlation between amplified/overexpressed WIP1 and overall or progression free survival in ovarian cancer patients.

1.7 p53 as a target for cancer therapy

1.7.1 p53 and cancer

Inactivation of the p53 tumour suppressor protein is a frequent event in the development of most human cancers with *TP53* mutation in more than 50% of many different cancers (Stegh, 2012). Most of *TP53* mutations occur within the DNA binding domain that result in disruption of p53 structure and/or abrogation of its DNA contact. The *TP53* mutations are usually followed by loss of heterozygosity (LOH) during tumour progression leading to inactivation of the remaining wild-type *TP53* allele (Bo Hong, 2014). Due to the crucial role of p53 in induction of cell cycle arrest, response to DNA repair and apoptosis, p53-deficient cells are prone to increased genomic instability, malignant transformation, metastasis, resistance to chemotherapy and radiotherapy, and poor survival (Lane *et al.*, 2010; Wade *et al.*, 2013; Bo Hong, 2014).

1.7.2 p53 and cancer therapy

The multi-functional transcription activity and anti-cancer effect of p53 in addition to frequent loss of its function in most types of tumour, motivated an enormous effort to develop new cancer treatments based on p53-targeted therapy (Lane *et al.*, 2010; Wang and Sun, 2010; Stegh, 2012; Hoe *et al.*, 2014). Numerous strategies and biologic approaches have been developed to correct p53 dysfunction and restore its activation, including gene therapy, development of oncolytic viruses and siRNA/antisense RNA against negative regulators of p53, p53-based vaccines, small molecules activating p53 (Lane *et al.*, 2010; Wang and Sun, 2010; Stegh, 2012; Bo Hong, 2014) and chaperone-like drugs binding to mutant p53 to restore its function (Stegh, 2012; Hoe *et al.*, 2014).

1.7.3 The pros and cons of p53-targeted cancer therapy

In spite of potential advantages of p53-targeted therapy including less harm to normal cells, fewer side effects, improved effectiveness and life quality, it has its potential drawbacks as well (di Iasio and Zauli, 2013). Over 65000 papers have been published on p53; however, none of those provide specific predictive biomarkers by which to identify cancer patients who are most likely to respond to p53-targeted cancer therapy with the best therapeutic index (di Iasio and Zauli, 2013). The therapeutic index is based on the relative sensitivity of both tumour and normal tissues towards p53 activating drugs. Resistance development and causing toxic on- or off-target side effects are other current challenges for p53-targeted cancer therapy. Another key issue in relation to p53 activation is the type of response, cell cycle arrest or cell death, and the magnitude of effect in tumour cells compared to normal cells. In terms of the cell fate after treatment, it is strongly dependent on the intrinsic properties and microenvironment of tumours (Hoe *et al.*, 2014). Furthermore, p53-targeted therapy may result in selection of p53-therapy resistant tumours and acquisition of somatic mutations in *TP53* gene (Aziz *et al.*, 2011; Bo Hong, 2014). Other biological processes influenced by activated p53 such as metabolism, angiogenesis, metastasis and age further complicate therapeutic targeting of the p53. However, development of predictive biomarkers in response to these therapeutic agents, combination therapy and optimisation of p53 restoration therapy (intermittent dosing regimens of drugs) are new opportunities to solve the challenges (Bo Hong, 2014).

1.8 Small molecule MDM2-p53 binding antagonists as p53-targeted therapeutic agents

Targeting interactions between MDM2 and p53 with small molecule inhibitors is an attractive strategy to activate wild-type *TP53* and its growth inhibitory and pro-apoptotic function.

1.8.1 MDM2-p53 binding antagonists as non-genotoxic activators of p53

Mutation of p53 occurs in about 50% of both sporadic and familial cancer cases. It seems that in the remaining malignancies, p53 function is inhibited through other mechanisms and reactivation of p53 is considered as a therapeutic target. When the *TP53* gene is not mutated, it may be possible to activate the growth inhibitory and pro-apoptotic functions of p53 by preventing the protein-protein binding interaction between p53 and its negative regulators MDM2 and MDMX. Recently, synthetic small molecule inhibitors have been developed which target a small hydrophobic pocket on MDM2 to which p53 normally binds (Rew and Sun, 2014).

One of the attractive features of these agents is their non-genotoxic mechanism of action compared with current chemotherapy (Aziz *et al.*, 2011; di Iasio and Zauli, 2013). Another potential use of MDM2-p53 binding antagonists is as probes for testing the functional status of p53 and its downstream signalling pathways, not only as potential biomarkers for response to MDM2-p53 antagonists, but also as indicators of responsiveness to established therapeutic agents that act through a p53-dependent mechanism. These compounds have shown promise as therapeutic agents in a number of preclinical studies and have entered early phase clinical trials.

1.8.2 The MDM2-p53 binding site

The MDM2-p53 interactions is primarily mediated by the N-terminus domains of both proteins (Michelsen *et al.*, 2012; Anil *et al.*, 2013). Recently, some studies indicate that it is likely parts of MDM2 outside the N-terminal domain (Arkin *et al.*, 2014) or alterations in the C-terminus of p53 (Nag *et al.*, 2013) also play a role in the binding interaction. 118 amino acids at the N-terminal transactivation domain of MDM2 and a 15-residue transactivation domain of p53 (residues 15-29) (Chene, 2003; Anil *et al.*, 2013) (residues 17-29) (Fu *et al.*, 2012) are involved in MDM2-p53 interaction. Based on genetic and biochemical studies as well as the crystal structure of the 109-residue amino-terminal domain of MDM2 bound to a 15-residue transactivation domain of p53, MDM-2 has three hydrophobic clefts (Rew *et al.*, 2012) binding to three critical amino acid residues of p53 namely Phe19, Trp23, and Leu26 (Figure 1-11A)

(Anil *et al.*, 2013; Tovar *et al*., 2013; Rew and Sun, 2014). Residues 19-25 of the p53 binding domain form an α-helix and residues 17, 18 and 26-29 take a more extended conformation. In addition, Thr18 plays an important role in the stability of the helix and regulation of the MDM2-p53 interaction via phosphorylation (Chene, 2003; Fu *et al.*, 2012). Both hydrogen bonds and van der Waals interactions are involved in the formation of the MDM2-p53 complex with Trp23 of p53 forming a strong hydrophobic interaction (Shangary and Wang, 2009; Fu *et al.*, 2012).

1.8.3 MDM2-p53 binding antagonists

Using small molecule inhibitors to target protein-protein interactions is challenging owing to the large and flat surfaces involved in these interactions causing difficulties for their disruption (Ding *et al.*, 2013; Nag *et al.*, 2013; Arkin *et al.*, 2014; Corbi-Verge and Kim, 2016). However, it is not a certain obstacle for the MDM2-p53 interaction due to the involvement of only three crucial amino acids for the binding of these proteins (Nag *et al.*, 2013). In the case of the MDM2-p53 interface, 70% of the atoms are non-polar resulting in a hydrophobic interface, and therefore having lipophilic groups is essential for MDM2-p53 inhibitors. Although the presence of lipophilic groups usually improves the binding energy, highly lipophilic inhibitors are poorly soluble and have limited bioavailability (Chene, 2003).

Different classes of small molecules inhibitors were designed mimicking the MDM2-p53 interaction (Figure 1-11B) and developed through combinatorial library screening such as Nutlins, Spiroxindoles, Isolindones and Chalcone derivatives with varied potency and selectivity (Nag *et al.*, 2013; Arkin *et al.*, 2014). The first published potent and selective MDM2-p53 antagonists were the cis-imidazoline compounds, named Nutlins, among which the most studied is Nutlin-3 (Shen and Maki, 2011; Ding *et al.*, 2013). RO5503781, SAR405838 and HDM201 are more potent and pharmacologically suitable MDM2 inhibitors subsequently developed and entered into clinical trials (Burgess *et al.*, 2016).

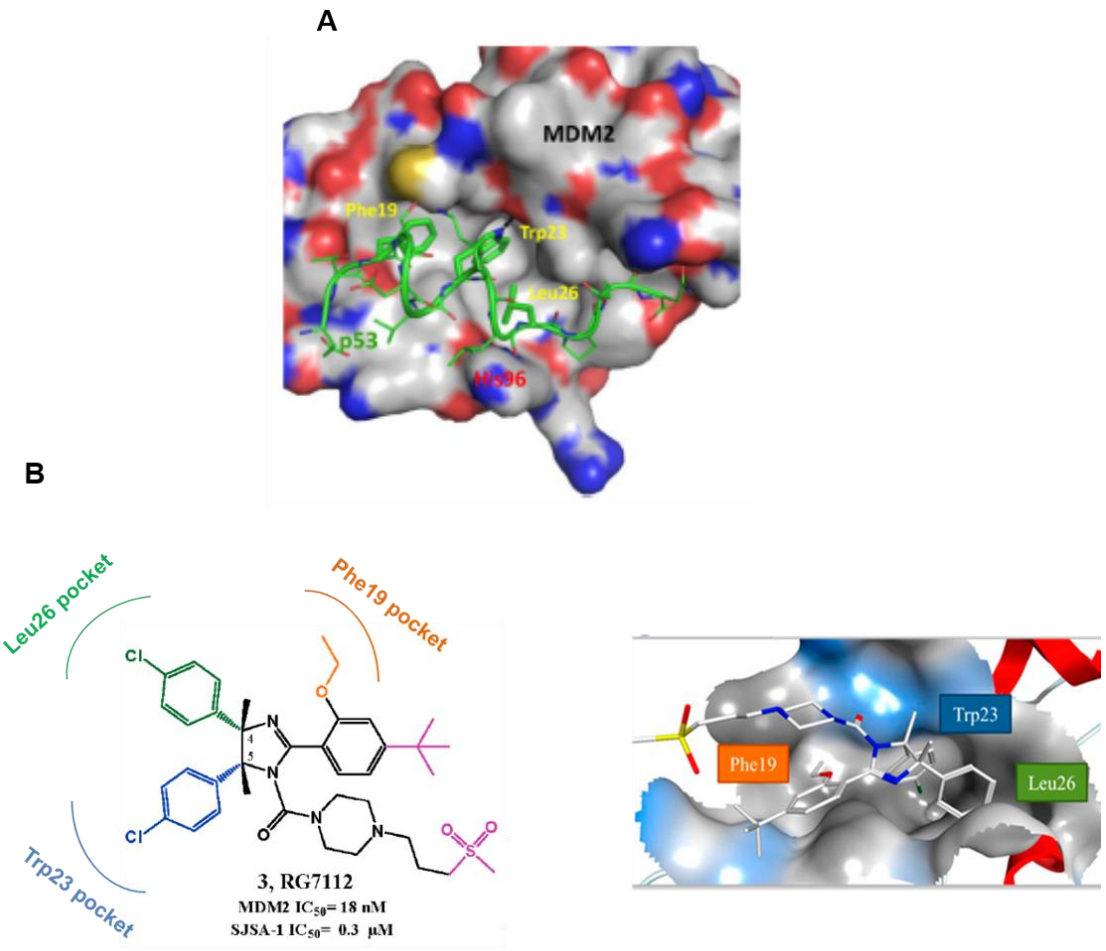

Figure 1-11: (A) MDM2-p53 complex and the three crucial amino acid residues of p53 at the MDM2-p53 binding site (Zhao *et al.*, 2015). (B) The MDM2 antagonists mimic the MDM2-p53 interaction. MDM2 surface is coloured in blue for hydrophilic areas and grey for hydrophobic areas (Ribeiro *et al.*, 2016).

1.8.4 Nutlins

Nutlins are analogues of cis-imidazoline including Nutlin-1, Nutlin-2 and Nutlin-3. They selectively target and bind a small hydrophobic pocket on MDM2, to which p53 normally binds, by competing with p53 and imitating the molecular interactions of the three crucial amino acid residues from p53 (Nag *et al.*, 2013). Disruption of the interaction between MDM2 and p53 inhibits ubiquitination and export of p53 by MDM2, leading to p53 stabilization, p53 nuclear accumulation and upregulation of p53 downstream transcriptional targets involved in cell cycle arrest and/or apoptosis, including genes encoding $p21^{WAF1}$, BAX and PUMA (Hu *et al.*, 2006; Mir *et al.*, 2013). Nutlin-1 and Nutlin-2 are racemic mixtures and Nutlin-3a (Figure 1-12) is the active enantiomer of Nutlin-3 disrupting the MDM2-p53 interaction with IC_{50} values of 260 nM, 140 nM and 90 nM respectively (Shangary and Wang, 2009; Zhao *et*

al., 2015). Nutlins have the ability to sensitise the cancer cells to conventional chemotherapies with the potential for synergistic effect (Mir *et al.*, 2013; Chen *et al.*, 2015). Nutlin-3 demonstrated the mechanistic proof-of-concept for inhibition of the MDM2-p53 interaction and continues to be a useful reference tool compound; however, its pharmacological properties are suboptimal for clinical use due to poor pharmacokinetic, bioavailability, solubility and permeability (Vu *et al.*, 2013; Ribeiro *et al.*, 2016).

1.8.5 RG7112

RG7112, an advanced member of the Nutlin family (Figure 1-12), is the first clinically tested small-molecule inhibitor of MDM2, with ability to displace p53 from the surface of MDM2 with an IC_{50} value of 18 nM (Tovar *et al*., 2013; Vu *et al.*, 2013). Its pharmacologic properties have been improved over the early Nutlins, with structural changes to prevent its oxidation, reduce molecular weight with the same efficacy, improve MDM2 binding (Yujun Zhao, 2013) and inhibit metabolic conversion to the inactive imidazole form (Tovar *et al*., 2013). RG7112 has been evaluated in early phase clinical trials as a single agent in adult advanced solid tumours, haematological neoplasms and liposarcomas and in combination with cytarabine in Acute Myeloid leukaemia (AML) or doxorubicin in soft tissue sarcoma (Hoe *et al.*, 2014). The results of the phase I trial of RG7112 in patients with relapsed/refractory Leukemia showed clinical activity in correlation with baseline expression levels of MDM2 and provided proof-of-concept that RG7112 can generate clinical response in hematologic malignancies (Andreeff *et al.*, 2016).

Initial testing of RG7112 by the Paediatric Preclinical Testing Program has confirmed tumour regression in wild-type *TP53* solid tumours, and showed strong antitumour activity against infant acute lymphoblastic leukaemia (ALL), including MLL-rearranged xenografts, encouraging further evaluation of RG7112 in both research and clinical trial in the paediatric setting (Carol *et al.*, 2013).

1.8.6 RG7388

RG7388, a Nutlin-3 analogue and a second generation MDM2 inhibitor (Figure 1-12) (Deben *et al.*, 2015), was subsequently developed with superior potency, selectivity and oral bioavailability suitable for clinical development with a cell-free IC_{50} value of 6 nM (Lu *et al.*, 2014). Initial studies have investigated the effect of RG7388 on neuroblastoma cell lines (Chen *et al.*, 2015; Lakoma *et al.*, 2015) and established human SJSA-1 osteosarcoma xenografts in nude mice (Ding *et al.*, 2013) and confirmed that RG7388 showed all the expected characteristics of a MDM2-p53 inhibitor with high affinity and specificity for activating the p53 signalling pathway. RG7388 has currently been used as a monotherapy or in combination with cytarabine in phase 1 clinical trial in patients with acute myelogenous leukemia, and in patients with refractory solid tumour malignancies in combination with posaconazole (Lakoma *et al.*, 2015). These studies support further research and clinical investigation of RG7388, which is ongoing.

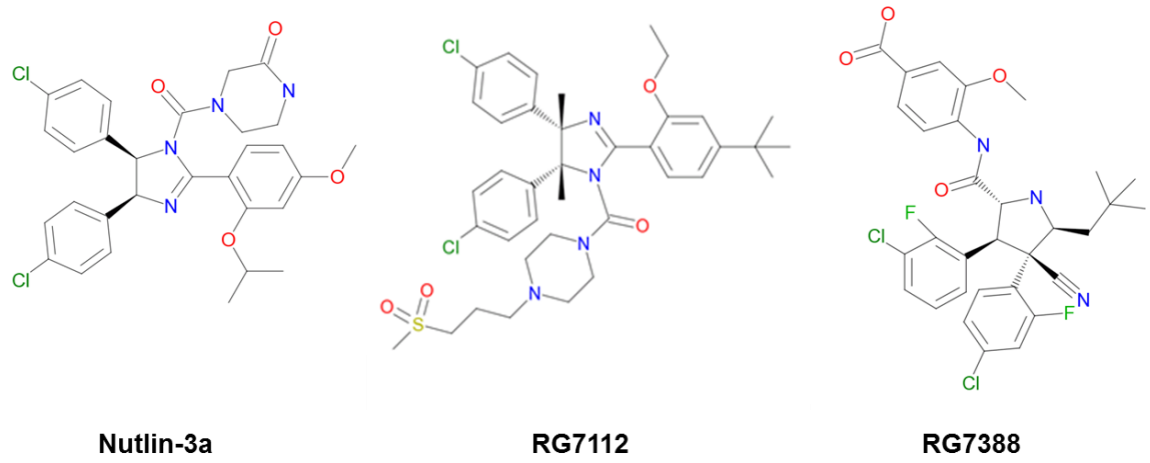

Figure 1-12: The chemical structures of Nutlin-3a, RG7112 and RG7388.

1.8.7 Adverse side effects of small molecule inhibitors of the MDM2-p53 interaction

A concern of p53 reactivating therapies is their effects on the normal cells. Cytotoxicity of MDM2 inhibitors to normal tissues was compared to radiotherapy in xenograft mice. Although both radiation and chemotherapy induced apoptosis in radiosensitive tissues such as small-intestine crypts and thymus, MI-219 caused no apoptosis or damage in normal mouse tissue. Furthermore, radiation and chemotherapy caused profound accumulation of p53 in intestinal crypts and thymus while MI-219 induced p53 activation in normal cells with minimal p53 accumulation (Shangary and Wang, 2009). However, such studies are flawed because the MDM2 inhibitors are optimised against human MDM2 and are much less potent against mouse MDM2 and mouse cell lines.

The most common side effects reported following use of RG7112 in clinical trials are gastrointestinal and haematological toxicities, including grade 3 and 4 febrile neutropenia and thrombocytopenia (Burgess *et al.*, 2016). Treatment with JNJ-26854165, an oral MDM2 inhibitor, was well tolerated in patients with advanced solid tumours even though frequent adverse grade 1-2events were observed, including nausea, vomiting, fatigue, insomnia, electrolyte imbalance and mild renal/liver function impairment (Yuan *et al.*, 2011). Due to ubiquitination of other proteins other than p53 such as steroid hormone receptors, androgen receptor and Rb via MDM2, other potential off-target effects of MDM2 inhibitors should be considered and may even be beneficial. However, no clinical relevance of these potential off-target effects have been reported in the current early phase trials (Burgess *et al.*, 2016). Overall, the most common side effect of small molecule inhibitors of MDM2 reported in clinical trials are dose-limiting haematological toxicities and thrombocytopenia (Ray-Coquard *et al.*, 2012; Zhao *et al.*, 2015; Andreeff *et al.*, 2016).

It has also been argued that inhibition of MDM2 may exert a selective pressure on small clonal subpopulations of cancer cells harbouring mutant *TP53*, leading to relapsed tumours resistant to p53-dependent chemotherapy and radiotherapy (Zhao *et al.*, 2015; Burgess *et al.*, 2016). This issue is discussed and explained in more detail later in general discussion, chapter 9.6.

1.8.8 Gene signatures to predict the response to MDM2-p53 inhibitors

As MDM2 inhibitors have recently entered into clinical trials, identification of genetic biomarkers to potentially predict sensitivity to these agents would be clinically beneficial. The main indicator for sensitivity to MDM2 inhibitors is wild-type *TP53* which is essential but not sufficient because not all wild-type *TP53* cells respond to these anti-cancer agents to the same extent. Therefore, prediction of sensitivity to MDM2 inhibitors via detection of a p53 target gene signature would be helpful to stratify patients who are likely to gain benefit from these therapeutic agents (Jeay *et al.*, 2015; Sonkin, 2015; Telfer, 2015).

A significant correlation was reported between high basal expression of *MDM2, XPC, PUMA* and low expression of *CDKN2A* genes, and sensitivity to MDM2 inhibitors (Telfer, 2015). In a separate study, the Novartis team compared basal levels of p53 downstream gene expression in a panel of cancer cell lines which were sensitive or insensitive to MDM2 inhibitor NVP-CFC218. They identified a minimal set of 13 known p53 target genes as a gene signature reflecting the presence of partially activated p53 pathway in the wild-type *TP53* sensitive cell lines. These genes are involved in negative (*MDM2*) or positive (*ZMAT3, RPS27L*) p53 regulation, cell cycle arrest (*CDKN1A, SESN1, CCNG1*), apoptosis (*AEN, BAX, FDXR, TNFRSF10B*), oxidative stress (*SESN1*) and DNA repair (*DDB2, RRM2B, XPC*) (Espinosa and Sullivan, 2015; Jeay *et al.*, 2015). However, another study (Sonkin, 2015) reanalysed the validation of *TP53* status in the same cell lines used by the Novartis team and found that nearly a quarter of them were mistakenly taken as wild-type *TP53* cell lines, thus calling into doubt their proposed gene signature as a predictive biomarker for response to MDM2 antagonists. Further research is required to define a gene signature set to predict which patients may benefit from MDM2 inhibitors.

1.8.9 The mechanisms of resistance to MDM2-p53 binding antagonists

Identification of intrinsic mechanisms of resistance towards MDM2 inhibitors is crucial to identify patients who are responsive to the treatment. The most important indicator of resistance to MDM2 inhibitors is mutant *TP53*, which is consistent with the mechanism of action (Long *et al.*, 2010; Shaomeng Wang, 2012; Hoe *et al.*, 2014). Strong induction of p53 with no response to MDM2 inhibitors is indicative of defective p53 protein function or deficiencies in other genes involved in the p53 pathway (Long *et al.*, 2010; Shaomeng Wang, 2012). Intrinsic resistance to apoptosis including mutation in pro-apoptotic genes or high cellular levels of anti-apoptotic genes may also play an important role in resistance to MDM2

inhibitors as well. *ARF* inactivation in a mouse model of glioblastoma resulted in development of resistance to p53-mediated growth inhibitory effect of Nutlin-3 (Hoe *et al.*, 2014). High cellular levels of MDMX have also been reported to render resistance to MDM2 inhibitors such as Nutlin-3 and MI drugs (Hoe *et al.*, 2014). However, sensitivity to Nutlin-3 was remained in AML cells with naturally high levels of MDMX (Tan *et al.*, 2014).

Persistent exposure to MDM2 inhibitors is likely to select for tumours with mutant *TP53* which are resistant to p53-dependent cancer therapies (Shaomeng Wang, 2012). However, *TP53* mutant cell lines are not resistant to a wide range of both targeted and non-targeted agents, apart from MDM2 inhibitors according to the COSMIC database (http://www.cancerrxgene.org). One study recently published showed that MDM2 inhibitors have the potential to select *TP53* mutations present in tumours at low frequency with resistance to MDM2 antagonists. Nevertheless, these tumours are responsive to ionising radiation (Drummond *et al.*, 2016). Overall, *TP53* mutant tumours selected following treatment with MDM2 inhibitors may remain responsive to alternative therapies.

1.8.10 MDM2-p53 antagonists in ovarian cancer

In comparison to type II epithelial ovarian cancer which presents with a high frequency of *TP53* mutation, type I tumours have mutations in genes other than *TP53* such as *KRAS*, *BRAF* and *PTEN* (Coward *et al.*, 2015). For most patients with type I epithelial ovarian cancer and those left from type II harbouring wild-type *TP53*, p53 targeted therapy such as MDM2 inhibitors are likely to be beneficial.

Limited previous studies have demonstrated that wild-type *TP53* ovarian cancer cell lines are sensitive to Nutlin-3 (Mir *et al.*, 2013; Erin K. Crane 2015). Nutlin-3 alone and in combination with resveratrol induced apoptosis in A2780 cells (Marimuthu *et al.*, 2011). Based on this limited prior research, the tool compound Nutlin-3 induces both cell proliferation and apoptosis in ovarian cancer cell lines encouraging further studies with clinically relevant inhibitors.

1.9 PARP inhibitors and their application in ovarian cancer

1.9.1 The Poly ADP Ribose Polymerase (PARP) enzymes and DNA repair

PARP, a family of nuclear enzymes, consists of 17 enzymes including PARP-1 and PARP-2 which play a critical role in DNA Base Excision Repair (BER) pathway. Following exposure to DNA damage, PARP-1 and PARP-2 are activated and catalyse the cleavage of Nicotinamide Adenine Dinucleotide (NAD^+) to form Poly ADP-Ribose (PAR) polymer. These PAR polymers are added to DNA, histones and DNA repair proteins including PARP, and recruit the repair machinery to repair DNA damage (Weil and Chen, 2011; Yuan *et al.*, 2011).

1.9.2 PARP inhibitors and synthetic lethality

Synthetic lethality is a cellular phenomenon in which the function of two different genes are simultaneously lost causing cell death, whereas cell death does not occur due to loss of either gene function alone. Dysfunctional HRR pathway and inhibition of PARP lead to synthetic lethality in cells (Weil and Chen, 2011; Yuan *et al.*, 2011; Curtin, 2013; Stordal *et al.*, 2013). Different types of PARP inhibitors such as olaparib, veliparib, niraparib and rucaparib inhibit PARP enzyme activity and hinder DNA repair via the BER pathway, resulting in multiple double-strand breaks normally repaired by the HRR pathway. The tumour cells with *BRCA1/2* mutation or BRCAness status cannot efficiently repair these double-strand breaks, leading to cell death (Figure 1-13) (Turner and Ashworth, 2011; Lupo and Trusolino, 2014; Michels *et al.*, 2014). Another mode of action for PARP inhibitors is to trap PARP proteins at sites of DNA damage, which is highly toxic to cells due to blockade of DNA replication and induction of a replication stress response. Research indicates that these trapped PARP-DNA complexes are more toxic than blocking PARP enzyme activity (Turner and Ashworth, 2011; Murai *et al.*, 2012; Lupo and Trusolino, 2014; Livraghi and Garber, 2015). PARP inhibitors are cytotoxic and proficiently result in synthetic lethality in tumour cells with *BRCA1/2* deficiencies or BRCAness more than normal cells (Underhill *et al.*, 2010; Weil and Chen, 2011).

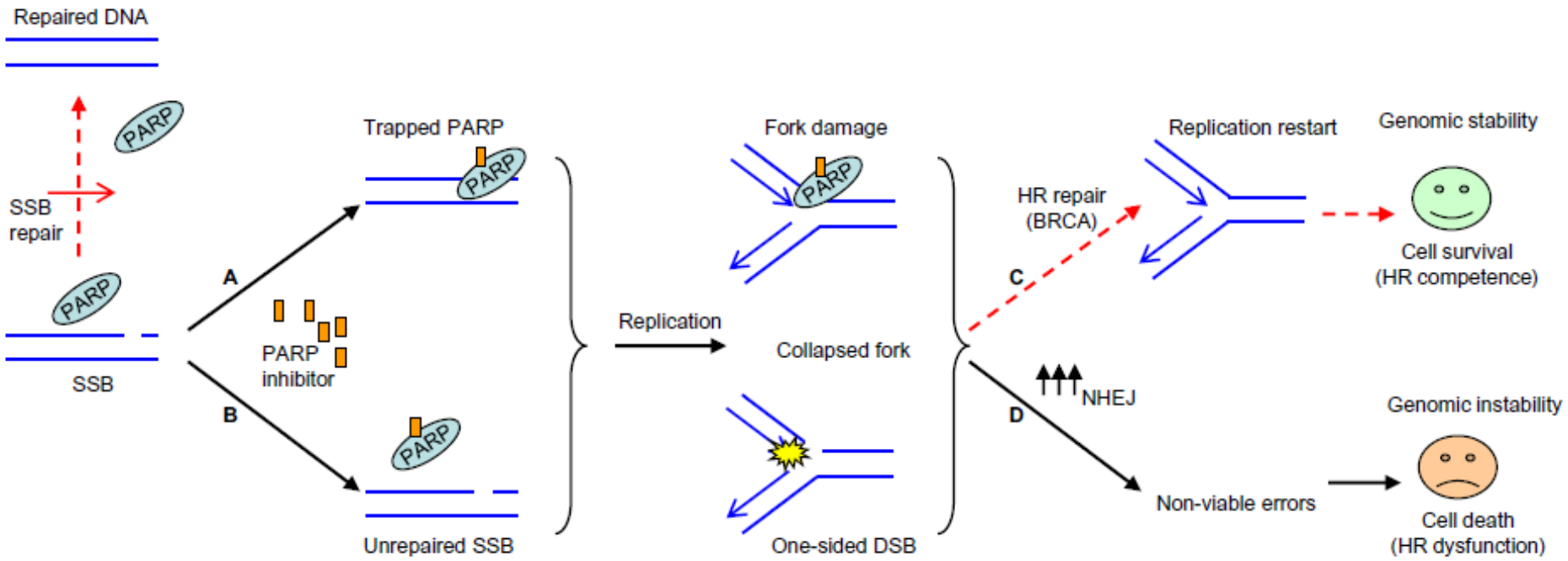

Figure 1-13: The role of PARP inhibitors in synthetic lethality. Molecular pathways underlying PARP/BRCA synthetic lethality. Red dotted lines indicate processes impaired by PARP blockade in HR-defective cells. In the presence of PARP inhibitors, SSB repair is precluded and either PARP is trapped onto DNA (A) or unrepaired SSBs are converted to DSBs by collision with the replication machinery (B). In both cases, resultant replication fork damage requires operational HR for efficient restart (C). HR-deficient *BRCA* mutant cells redirect to alternative, error-prone DNA repair pathways (D), undergoing genomic instability and cell death (Lupo and Trusolino, 2014).

1.9.3 Predictive biomarkers for response to PARP inhibitors

Up to now, several studies have investigated and highlighted the mutation and epigenetic modification of genes implicated in sensitivity to PARP inhibitors. Although germline mutations of *BRCA1*/*BRCA2* (Breast Cancer 1/2 tumour suppressor genes) were considered as robust predictive biomarkers of PARP inhibitor sensitivity, results of clinical trial have shown that the clinical efficacy of PARP inhibitors is not restricted to these genes (Yuan *et al.*, 2011; Brown *et al.*, 2016). A BRCAness phenotype, a biomarker of sensitivity to PARP inhibitors, is a defective HRR status due to epigenetic hypermethylation of the *BRCA1* promoter, somatic mutation of *BRCA1/2* or dysfunctional mutations in other HRR pathway genes (Konstantinopoulos *et al.*, 2010; Michels *et al.*, 2014; Bowtell *et al.*, 2015). Defects in *PTEN* (Turner and Ashworth, 2011; Stordal *et al.*, 2013), deficiency or low expression of *RAD51*, *ATM*, *ATR*, *EMSY* genes (Weil and Chen, 2011; Ihnen *et al.*, 2013) as well as mutation and reduced expression of $_{Y}$H2AX (Brown *et al.*, 2016) are proposed as markers of BRCAness status. Furthermore, amplification of *AURKA* and *EMCY* genes (Sourisseau *et al.*, 2010; Ihnen *et al.*, 2013), overexpression of Aurora kinase A and post-translational protein modification can also be considered as conferring a BRCAness phenotype (Michels *et al.*, 2014). Low expression of genes involved in HRR and response to platinum-based chemotherapy was also reported to be associated with sensitivity to rucaparib (Ihnen *et al.*, 2013).

In regard to *PTEN* gene, controversial results have been reported amongst which some demonstrated no statistically significant association between *PTEN* mutation and sensitivity to PARP inhibitors (Ihnen *et al.*, 2013), whereas others showed *PTEN* mutations sensitize tumour cells to PARP inhibitors through downregulation of *RAD51* and impaired HRR (Mendes-Pereira *et al.*, 2009; Turner and Ashworth, 2011; Weil and Chen, 2011; O'Sullivan *et al.*, 2014). The *EMCY* gene plays a role in HRR as a BRCA2-binding partner and its amplification may result in inactivation and silencing of the BRCA2 pathway in sporadic ovarian cancer (Ihnen *et al.*, 2013; Michels *et al.*, 2014). Furthermore, amplification or overexpression of the *AURKA* gene is implicated to be associated with sensitivity to rucaparib due to inhibition of RAD51 recruitment to DNA double-strand breaks (Ihnen *et al.*, 2013). Another protein reported to be involved in response to PARP inhibitors is FANCF protein which is an adaptor protein stabilising the interaction between FANCC/FANCE and FANCA/FANCG subcomplexes and plays a critical role in the correct assembly of Fanconi anemia, FA, core complex. The FA core complex is necessary for FANCD2 monoubiquitination localized with BRCA1, RAD51 and other DNA repair proteins (Taniguchi *et al.*, 2003). It was also suggested that aberrant

expression of ETS transcription factors shown in different cancers may repress *BRCA1/2*. Moreover, interaction of PARP1 binding protein PARPBP, known as PARI, with RAD51 at replication forks may result in inhibition of HRR (Michels *et al.*, 2014). Due to the greater toxicity of trapping PARP-DNA complexes compared to inhibition of PARP enzymatic activity and clinical importance of PARP trapping, PARP expression levels or baseline activity of PARP may be considered as a biomarker for PARP inhibition (Brown *et al.*, 2016).

1.9.4 Resistance to PARP inhibitors

Development of resistance to PARP inhibitors occurs through different mechanisms. Secondary mutations reversing the *BRCA* deficiency from a mutated reading frame to a normal sequence reading frame leads to resistance to PARP inhibitors. Reversion of mutation is a phenomenon occurring following selective pressure of drug treatment. Aberrant expression and activity of PARP, upregulation of efflux transporters such as p-glycoprotein, and loss of 53BP1 are other mechanisms implicated in resistance to PARP inhibitors (Weil and Chen, 2011; Lupo and Trusolino, 2014; Frey and Pothuri, 2015). Acquired resistance to PARP inhibitors resulting from a secondary mutation has been confirmed to occur in patients (Weil and Chen, 2011).

1.9.5 PARP inhibitors in ovarian cancer

Deficiencies in HRR occur in up to 50% of epithelial ovarian cancers (Mukhopadhyay *et al.*, 2012). *BRCA1/2* mutations are present in the germline of 70-85% of patients with inherited ovarian cancer regardless of histological subtypes, and account for 23% of HGSC. The rate of *BRCA1/2* mutation in sporadic ovarian cancer is low and low expression levels of BRCA1/2 is likely to be an important characteristic of non-inherited ovarian cancer (Weil and Chen, 2011). Some studies have identified impaired HRR pathway status in ovarian cancer cell lines, indicating the possible sensitivity of ovarian cancer patients bearing deficiencies in the HRR pathway other than only *BRCA1/2* mutation to PARP inhibitors (Weil and Chen, 2011; Yuan *et al.*, 2011; Rigakos and Razis, 2012; Ihnen *et al.*, 2013; Stordal *et al.*, 2013; Michels *et al.*, 2014). Amplification of the *EMSY* gene is present in about 20% of cases with HGSC and the *FANCF* methylation was reported in 21% of ovarian cancer (Rigakos and Razis, 2012).

PARP inhibitors are now undergoing clinical trials as targeted therapy for different types of cancer including ovarian cancer. Rucaparib is currently evaluated as a monotherapy in phase II clinical trials for patients with *BRCA*-associated ovarian cancer and in combination with chemotherapy for advanced solid tumours. The use of olaparib and veliparib as single agents

and in combination with chemotherapy is undergoing phases I and II clinical trials for patients with different types of cancer, including ovarian cancer (Anwar *et al.*, 2015; Frey and Pothuri, 2015). ARIEL2, a phase II trial of rucaparib in platinum sensitive, relapsed HGSC, and ARIEL3, a phase II clinical trials of rucaparib maintenance therapy following a platinum treatment in relapsed HGSC and endometrioid ovarian cancer, are ongoing to define a molecular signature of HR dysfunction in ovarian cancer patients (Frey and Pothuri, 2015). Niraparib, CEP-9722 and E7016 are other new PARP inhibitors currently undergoing clinical trials as single agents and in combination with chemotherapy in advanced solid tumours (Anwar *et al.*, 2015).

1.10 Hypothesis and Aims

Hypothesises:

1. The genomic and functional status of *TP53* are prognostic biomarkers in ovarian cancer patients.
2. The genomic status of *TP53* affects the response to MDM2-p53 antagonists, and MDM2-p53 binding antagonists have the potential for synergistic effects in combination with platinum drugs or PARP inhibitors in ovarian cancer.

Aims:

1. To establish whether immunohistochemical staining for p53, $p21^{WAF1}$, MDM2 and WIP1 provide additional predictive value for overall survival in the OVCA1-4 patient cohort.
2. To establish whether genomic status of *TP53*, and immunohistochemical staining for p53, and $p21^{WAF1}$ provide additional predictive value for chemotherapy outcome in the ICON3 patient clinical trial.
3. To test a panel of established ovarian carcinoma cell lines for their response to MDM2-p53 binding antagonists, and examine the relationship of this response to the genotype of the cells.
4. To assess the combined effect of MDM2-p53 antagonists with cisplatin.
5. To evaluate the combined effect of MDM2-p53 antagonists with the PARP inhibitor rucaparib.

Chapter 2: Materials and Methods

2.1 Tissue Microarray (TMA)

2.1.1 Tissue microarray (TMA)

TMA is a powerful molecular biology technique with the ability of arraying up to 1000 samples into a single paraffin block, which allows simultaneous assessment of gene product on a large number of specimens (Jawhar, 2009; Gately *et al.*, 2011). Several variables including antigen retrieval, incubation times, washing procedures and reagent concentration can also be standardized by TMA via analysing the whole cohort at the same time. One of the main drawbacks of TMA is that due to tumour heterogeneity one core may not be representative of the entire tumour (Jawhar, 2009; Barrette *et al.*, 2014). This problem can be overcome using IHC on more than one core, duplicate/triplicate, taken from different areas in the original samples. Efficient and useful application of IHC on TMA has been proven by a study showing good concordance between TMA core staining and whole-slide immunohistochemical data which is approximately 96% (Barrette *et al.*, 2014). Several studies also validated ovarian carcinoma tissue microarray as a reliable technique to analyse the expression of markers including p53 (Rosen *et al.*, 2004; Hecht *et al.*, 2008).

2.1.2 Development of TMA and collection of specimens

Ethical approval and specific consent were obtained for the collection and analysis of clinical material. Two sets of TMAs were used in this study. The first set consists of 167 patient samples assembled on TMA and labelled as OVCA 1 to OVCA 4. The second set collected and labelled as ICON3-1 to ICON3-6 consists of 260 patient samples. There are two cores from each tumour sample in the TMA to maximise the tumour area represented, and based on the reported studies indicating two cores are comparable to whole tissue section in the analysis of more than 95% of cases (Camp *et al.*, 2000) or in more than 96% of cases (Rosen *et al.*, 2004). The samples were in formalin fixed paraffin embedded (FFPE) blocks and cores taken only included tumour areas that were marked by a histopathologist. Histological analysis and grades of differentiation of the primary tumour specimens were determined according to the FIGO Cancer Committee.

2.1.3 TMA design

A TMA layout was designed and prepared for each set of TMAs. The TMA includes a marker, duplicates of the patient tissue samples and duplicates of normal human tissues such as prostate and spleen as control tissues. The cores were labelled with a number related to the patient

according to the numbers on the spreadsheet of patient data. The tissue core was taken from original histopathological blocks, known as donor blocks, and placed in an empty recipient block. The size of the cores was 1 mm in diameter and 4 mm in depth. A standard microtome and water bath were used to prepare paraffin sections.

2.2 Immunohistochemistry (IHC)

2.2.1 Principles and methods

Immunohistochemistry is the application of immunologic techniques to detect antigens in tissue sections using labelled antibodies. Cut sections of 3 to 4 micron thickness from paraffin-embedded blocks were used for immunohistochemistry analysis. Optimisations were performed using three different dilutions of primary anti-$p21^{WAF1}$ and anti-p53 antibodies (1:25, 1:50 and 1:100) and primary anti-MDM2 and anti-WIP1 antibodies (1:50, 1:100, 1:250 and 1:500), various incubation times (40, 50 and 60 minutes), different buffers including Citrate (10 mM Sodium citrate, 0.05% Tween 20, 1 litre deionized water, pH=6) and Tris (1M Tris, 1 litre deionized water, pH=9) and different antigen retrieval methods (microwave and decloaker). Finally, the best outcomes were used for experiments (Table 2-1). Slides were dewaxed in xylene for 5 minutes to remove paraffin and hydrated with graded ethanol (100%, 95%, and 75%) for 5 minutes. Antigen retrieval was performed as illustrated in Table 2-1. These antigen retrieval reagents break the protein cross-links formed by formalin fixation and uncover hidden antigenic sites, thereby enhancing staining intensity obtained with antibodies. To block endogenous peroxidase activity, sections were treated with 0.5% hydrogen peroxide (Fisher Scientific) for 10 minutes at room temperature. Slides were incubated at room temperature for primary antibodies. After rinsing in the 10X TBS Tween 20 buffer (0.5M Tris base, 9% NaCl, 1 litre deionized water, 0.5% Tween 20, pH=8.4) to wash away any unbound primary antibody, sections were exposed to the appropriate horseradish peroxidase (HRP) (MenaPath, UK) conjugated anti-rat/mouse/rabbit IgG secondary antibody for 30 minutes. This kit enhances signals produced by interaction between antigen and antibody for the detection of low concentrations of antigens, or for increased staining intensity in compensation for low titer primary antibodies. For primary mouse antibodies, universal probe (MenaPath, UK) was applied for 20 minutes before this stage, which increases staining sensitivity 10 to 40 times for mouse monoclonal antibodies. Then, they were rinsed in water to remove excess reagent and 3, 3’ diaminobenzidine (DAB, Sigma) was added, for 10 minutes for p53, MDM2, WIP1 and 5 minutes for $p21^{WAF1}$. This reagent is a precipitating substrate which produces a brown

formazan stain according to the amount of HRP activity and hence is indirectly a measure of the degree of primary antibody binding. This precipitate is insoluble in the presence of alcohol and xylene.

Dehydration of the sections was performed in graded alcohol and xylene, and distyrene, plasticizer and xylene (DPX) mounting (Sigma) used in order to preserve stain. Slides not incubated in primary antibody were used as an antibody negative control to test for specificity of staining.

Antigen	Antigen Retrieval	Buffer	Primary Antibody (Concentration)	Incubation Time
p53	Microwave	Citrate, PH.=6	DO-7, DaKO (1:100)	1 Hour
p21	Microwave	Tris, PH.=9	2947S, Cell Signaling (1:50)	1 Hour
MDM2	Decloaker	Citrate, PH.=6	OP46, MerkMillipore (1:50)	1 Hour
WIP1	Decloaker	Tris, PH.=9	F-10, Santa Cruz (1:500)	1 Hour

Table 2-1: The antigen retrieval method and antibody dilution used for different proteins.

2.2.2 Immunohistochemistry Scoring

Images of the stained slides were used for scoring and visualised via the Aperio ScanScope® CS, an automated digital scanner (Aperio Technologies, Bristol, UK) technology and Spectrum™ image management software. A modified H-Score was applied for immunoscoring, in which each specimen was scored by multiplying the intensity (no staining=0, weak=1, intermediate=2 and strong=3) by the proportion of staining (1=1-14%, 2=15-24%, 3=25-39%, 4=40-59%, 5=60-79% and 6=80-100%). Scores ranged from 0 up to 18. Score was considered 0, negative, where there was no staining and positive where there was nuclear or cytoplasmic staining. To consider the heterogeneity within the tumour and maximise the tumour area represented, 2 cores from different areas of tumour were scored,

which are comparable to whole tissue section in the analysis of more than 95% of cases (Camp *et al.*, 2000) or in more than 96% of cases (Rosen *et al.*, 2004). For each core with different intensity, several areas including 100 cells were chosen, scored and the average was calculated as the final score for each core. For example, if 20% of a core includes more cells stained weak, 60% includes more cells stained intermediate and 20% was negative, 1 part of area including weak and 3 parts of area including intermediate were chosen, scored and the average was considered as the final score for that core. A mean of two scores was used for the final score of duplicate TMA samples. The score of the remaining core was used where a core loss occurred. The samples were scored only by Maryam Zanjirband twice at two different times to avoid bias; however, it is a limitation of this study.

2.3 Tissue Culture

2.3.1 Characteristics of ovarian cancer cell lines investigated

The panel of ovarian cancer cell lines used in this study, is listed below and the histological subtype of the tumours from which they were derived and *TP53* status are summarised in Table 2-2.

A2780 cell line harbouring wild type *TP53* was derived from tumour tissue from an untreated patient. Cells grow as a monolayer including cell clusters of different sizes without any signs of differentiation (Pizao *et al.*, 1992).

IGROV-1 was established from tumour tissue from an untreated 47-year-old woman suffering from a stage III ovarian carcinoma. Histologically, this cell line was diagnosed with multiple differentiations with endometrioid for the major part of the tumour and some clear cells and undifferentiated foci. The IGROV-1 cells grow as a monolayer and indicate the presence of two cellular clones including one pseudodiploid with 46 chromosomes and the other hypotetraploid with 92 chromosomes with increased number of the tetraploid cells following increased number of subcultures (Bénard *et al.*, 1985). As information on the *TP53* status of IGROV-1 in the literature was contradictory, sequencing was performed and no mutation was detected.

OAW42 cell line with wild-type *TP53* was derived from an ascitic fluid sample of a 46-year-old woman with recurrent disease after a complete response to six courses of cis-platinum (Wilson *et al.*, 1996). The cell line was established from a serous cystadenocarcinoma. It grows

as a monolayer and cells have an intermediate morphology, neither as small round cells nor as large polygonal cells (Hills *et al.*, 1989).

CP70 is a resistant clone derived from A2780 by selection for growth in cisplatin. The CP70 cell line harbours a heterozygous *TP53* mutation (c.514 G->T, p.Val172Phe) (Lu *et al.*, 2001). The CP70 cell line is an MMR-deficient variant of the A2780 cell line with deficiency in the *MLH1* gene (Curtin *et al.*, 2004).

***MLH1*-corrected CP70+** is a chromosome 3 transferrant of the CP70 cells (Curtin *et al.*, 2004) and retains the heterozygous *TP53* mutation (c.514 G->T, p.Val172Phe) (Lu *et al.*, 2001).

MDAH-2774 was derived from a patient with endometrioid epithelial ovarian cancer growing as a monolayer (Dai *et al.*, 2009). MDAH-2774 harbours a *TP53* mutation located in exon 8 (c.818G->A, p.Arg273His). The mutant p53 is overexpressed and results in intense nuclear staining with p53 antibodies. This cell line also has a mutated *KRAS* gene, involving activation of the MAPK signalling pathway (Dai *et al.*, 2009).

SKOV-3 was stablished from an ascetic fluid sample from a patient with ovarian adenocarcinoma. It grows as a monolayer with colonies containing large polygonal cells. This cell line is one of the most resistant ovarian cancer cell lines to chemotherapy agents such as cisplatin and carboplatin (Hills *et al.*, 1989). Due to inconsistent information on the *TP53* status of SKOV-3 in the literature, sequencing was performed and a frame shift deletion (c.265delC, p.Pro89fsX33) was confirmed.

Cell Line	*TP53* Status	Histotype	Reference
A2780	Wild-type	Undifferentiated	(Pizao et al., 1992)
IGROV-1	Wild-type	Mixed, EC with CCC/UD	(Bénard et al., 1985)
OAW42	Wild-type	Serous Cystadenocarcinoma	(Hills et al., 1989; Wilson et al., 1996)
CP70	Mutant, Heterozygous (c.514 G->T; p.Val172Phe)	Undifferentiated	(Lu et al., 2001; Curtin et al., 2004))
***MLH1*-corrected CP70+**	Mutant, Heterozygous (c.514 G->T; p.Val172Phe)	Undifferentiated	(Lu et al., 2001; Curtin et al., 2004))
MDAH-2774	Mutant, Homozygous (c.818G->A; p.Arg273His)	Endometrioid	(Skilling et al., 1996; Dai et al., 2009)
SKOV-3	Mutant, Homozygous (265delC; p.Pro89fsX33)	Adenocarcinoma	(Hills et al., 1989)

Table 2-2: The ovarian cancer cell lines and their Histotype and mutational *TP53* status. EC, Endometrioid carcinomas; CCC, Clear cell carcinomas; UD, Undifferentiated.

2.3.2 Cell line authentication

The cell lines were authenticated by short tandem repeat (STR) DNA profiling using hypervariable DNA microsatellite regions, which are very small (3-6bp) long repeated DNA motifs (Dr. Claire Hutton) (McLaren *et al.*, 2013). All cell lines were regularly tested for Mycoplasma infection using a PCR based method by Elizabeth Matheson. The mutational status of *TP53* for IGROV-1, MDAH-2774 and SKOV-3 cell lines was analysed using a Sanger sequencing method and the results are presented in chapter 6.4.2.2. The *MLH1* status was tested for the *MLH1*-corrected CP70+ cell line using western blot and comparison with A2780 as a *MLH1*-proficient cells (positive control) and CP70 as a *MLH1*-deficient cell line (negative control) (Curtin *et al.*, 2004). The results are shown in chapter 6.4.1.

2.3.3 Cell culture

All cell lines were grown and maintained as monolayers. A2780, IGROV-1, OAW42 and CP70 were cultured in RPMI-1640 (Sigma) supplemented with 10% (volume/volume, v/v) Foetal Bovine Serum (FBS) (Gibco) and 5% (v/v) penicillin/streptomycin (Sigma). The *MLH1*-corrected CP70+ cell line was grown in RPMI-1640 supplemented with 10% (v/v) FBS and Hygromycin B (200 µg/ml: Life Technologies, Inc.) (Curtin *et al.*, 2004) for the selection and maintenance of the cells containing the Hygromycin resistance gene. MDAH-2774 and SKOV-3 cell lines were cultured in DMEM supplemented with 10% and 5% (v/v) FBS and penicillin/streptomycin respectively. All cells were routinely cultured in either 75 cm^2 or 25 cm^2 sterile tissue culture flasks and incubated at 37^0C in a humidified atmosphere of 5% carbon dioxide. To routinely passage adherent cells when they reached 70-80% confluence, culture medium from the flask was removed by aspiration; the monolayer was washed with 5-10 ml (according to the size of flask) phosphate buffered saline (PBS without cations and pH 7.2, Gibco) and cells were detached with 0.5-2 ml 1x (for OAW42 cells 1-3 ml 2.5x) trypsin/EDTA (10X, Sigma) in PBS. Trypsin enzymatically detaches adherent cells from tissue culture plates for passaging. Divalent cations such as calcium and magnesium, which are often present in the cell culture environment, inhibit this action. EDTA sequesters these ions and thus boosts the efficacy of trypsin. Then, cells were incubated at 37^0C for a few minutes until the cells lift off and 5-10 ml culture medium was added to neutralise the trypsin. Finally, an appropriate volume of cell suspension was dispensed into a fresh sterile flask. Due to use of concentrated trypsin/EDTA for OAW42 cells, the cells with medium was centrifuged, the medium removed and then the cells with fresh medium were split to sterile flasks. The cells were seeded at a low

density for routine cell culture and high density for an experiment within the next 3-4 days. All experimental cell manipulations and subculturings were performed using sterile equipment and reagents within a class II safety cabinet (Biomat, Medair Technologies, MA, USA) at all times.

2.3.4 Cryogenic storage of cell lines and revival of the cells

In order to store the cell lines, exponentially growing cells were detached, centrifuged, extra medium was aspirated and the pellet resuspended in freezing medium containing each cell line's appropriate growth media with 10% FBS (v/v) and 10% (v/v) DMSO (Sigma #276855). DMSO was added as a cryoprotectant to inhibit the formation of ice crystal within the cells at low temperature, which otherwise would disrupt the cell membrane. Aliquots of 1ml were retained in cryotubes (NUNC^{TM}, Rochester, NY, USA) and frozen slowly at -80^{0}C overnight. Cryotubes were then transferred to liquid nitrogen for long-term storage. To grow cells from stored liquid nitrogen stocks, the vials were quickly thawed in a water bath at 37^{0}C. Then, cells were suspended in growth media, centrifuged at 1000rpm to remove DMSO from the solution and resuspended in fresh medium for transfer into culture flasks or plates for growth.

2.4 Drugs and specificities

2.4.1 Cis-diamino-dichloro-platinum (CDDP or cisplatin)

Cisplatin (Cl2H6N2Pt^{+2}, MW=300.05104 g/mol), a DNA damaging agent, was purchased from Merck Millipore (Watford, UK). It was solubilised in distilled water at a final concentration of 2mM stocks and stored at -20ºC.

2.4.2 MDM2-p53 antagonists

Nutlin-3 (C30H30Cl2N4O4, MW=581.5 g/mol), a 1:1 racemic mixture of the active enantiomer Nutlin-3a and the inactive enantiomer Nutlin-3b, was purchased from NewChem Technologies Limited (#548472-68-0) in solid form (Newcastle, UK). DMSO was used as solvent to solubilise the powder at a final concentration of 10mM and smaller aliquots were stored at -20ºC. The interaction of MDM2 and p53 is inhibited by Nutlin-3 with cell free assay IC_{50} value of 90 nM.

RG7112 (C38H48Cl2N4O4S, MW= 727.78 g/mol), the first clinical small molecule inhibitor of MDM2-p53, and RG7388 (C31H29Cl2F2N3O4, MW= 616.48 g/mol), with more potency and selectivity, were kindly provided by Professor Herbie Newell and made available by the Newcastle Anticancer Drug Development Initiative. Both were dissolved in DMSO to a final

concentration of 1mM and the stocks stored as explained above. They inhibit the MDM2-p53 interaction with an IC_{50} value of 18 nM for RG7112 and 6 nM for RG7388.

2.4.3 Rucaparib

Rucaparib (C19H18FN3O.H3PO4, MW=421.36 g/mol) is the first PARP inhibitor that was entered into clinical trial as a chemopotentiator. It is one of a series of tricyclic benzimidazole carboxamide PARP inhibitors with Ki of 1.4 nM for PARP1 in a cell-free assay. It was kindly supplied by Professor Nicola Curtin, and prepared as described above in 10mM stocks solubilised in DMSO.

2.5 Cell counting

A Neubauer haemocytometer (Hawksley, Sussex, UK) was used to estimate cell densities. A 1:1 dilution of the suspension in 0.4% trypan blue dye (Biorad, #145-0021) or 10µl of cell suspension were added to each side of the haemocytometer, which was prepared based on the manufacturer's instructions. Each grid has a total volume of $0.1mm^3$ ($1mm^2$ (area) x 0.1 mm (depth)) and therefore n counts/grid are representative of $n\times10^4$ cells/ml. The average cell counts/grid of at least two grids on each side of the haemocytometer were calculated and multiplied by 10^4 or 2 x 10^4 in the case of 1:1 dilution with the 0.4% trypan blue before loading. Following exposure to trypan blue, dead/dying cells with damaged membrane integrity are stained blue whereas viable cells remain clear with intact plasma membrane. The absolute or proportion of viability can be measured by this method even though the cells must be counted quickly during 5 minutes after adding the dye, due to staining of viable cells after 5 minutes.

2.6 Sulforhodamine B (SRB) assay

2.6.1 Principles of SRB assay

SRB assay is a rapid, sensitive and inexpensive method to estimate the number of cells in 96-well microtiter plates for drug screening developed by Skehan *et al*. SRB is a purple anionic protein dye which binds to the basic amino acid residues in proteins under mild acidic conditions. The optical density of SRB is measured at 564nm with a signal to noise ratio of 1.5 with 1000 cells/well (Skehan *et al.*, 1990). The intensity of the staining depends on the amount of cellular protein and can be used as a measure of cell number and hence culture growth.

2.6.2 SRB assay method

The cells in 96-well plates were fixed by adding 25 µl Carnoy's fixative (three parts methanol plus one part concentrated acetic acid) at appropriate time-points, stored at 4^0C for at least 1 hour up to 2 weeks, washed 5 times in tap water and dried at 60^0C or room temperature. After fixation, adherent cells were stained with 0.4% (w/v) SRB dissolved in 1% (v/v) acetic acid for 30 minutes. The staining was followed by 5 washes with 1% (v/v) acetic acid to remove unbound stain, drying at 60^0C or room temperature, and solubilising the bound stain in 100µl/well of 10mM Tris buffer (pH 10.5) with gentle mixing for 20 minutes. Lastly, the absorbance of the redissolved stain was read at 570nm using a multi-well spectrophotometer (BioRad, Model 680).

2.7 Growth curves

Growth curves for all cell lines were established to measure the doubling times of the cell lines. Exponentially growing cells were detached, transferred to a sterile universal tube and centrifuged at 1000 rpm for 5 minutes. The supernatant was aspirated, the pellet was gently re-suspended in 10 ml of medium, and the cells were counted by a Haemocytometer. Five different dilutions of cells, (2.4×10^5, 1.2×10^5, 6×10^4, 3×10^4, and 1.5×10^4 ml^{-1}) were established and seeded into six 96-well plates by adding 100 µl of cells in each of 6 wells per plate for each density. To compensate for the edge effect due to evaporation, 100 µl medium was added to the outer rows and columns of the six 96-well plates. The cells were observed under a microscope to check their viability and confluence. One plate on each subsequent day after seeding was fixed by adding 25 µl Carnoy's fixative and stored at 4^0C. Then, the SRB assay was used as described above to estimate cell density in each well and growth curves were constructed by using GraphPad Prism statistical analysis software version 5.04.

2.8 Growth inhibition assay and calculation of GI_{50} values

Based on the growth curve previously done, a suitable seeding density of cells was chosen for plating which during the assay period resulted in growth of the culture which had negligible lag phase, a short doubling time, and did not reach plateau phase within the course of the experiment. This was then used for constructing growth inhibition curves and measuring concentrations of drugs required to achieve 50% growth inhibition (GI_{50}). The cell densities chosen were 4.5×10^4 (ml^{-1}) for A2780, 6×10^4 (ml^{-1}) for IGROV-1 and SKOV-3, 3×10^4 (ml^{-1}) for OAW42, CP70, and *MLH1*-corrected CP70+ and 2.25×10^4 (ml^{-1}) for MDAH-2774. The optimal number of exponentially growing cells were seeded in 96-well plates, and incubated at

37^0C for 24 hours to attach. Each column was then treated with a range of drug concentrations as detailed in the specific materials and methods section of the relevant chapters. For each treatment, the drug solvent was also used as a control. A Day 0 control was plated and immediately fixed by Carnoy's solution after 24 hours of attachment. The treatment plates were incubated with the mentioned concentration of drugs for 72 hours, fixed and were then stored at 4^0C for at least 1 hour. The relative amounts of cells were determined by SRB assay as described in 2.6.2. The SRB data from the spectrophotometer readings was transferred and interpreted by using Microsoft Excel software. The average plate Day 0 absorbance values were subtracted from the treatment plate values, and calculation of means and standard deviations of optical densities from $\geq$3 independent experiments were made. These figures were analysed and plotted by using GraphPad Prism 5.04 to plot the dose dependent growth inhibition curves and measure the interpolated GI_{50} values.

2.9 Clonogenic cell survival assay

To evaluate whether any of the treatment regimens led to reduction of colony formation ability of the cells, clonogenic assays were performed by the modified method in which the cells are not trypsinised after attachment. Based on the drug concentration and sensitivity of cell lines, 100 to 100,000 exponentially growing cells were seeded into triplicate six-well plates. After 24 hours, cells were treated with media, solvent and different concentrations of drugs for 48 hours. Then, the media including drug was removed and free-drug media was added. The cells were incubated for 1 to 3 weeks to form colony for counting (a colony was defined as a focus of $\geq$50 cells). After that, the plates were washed with PBS, fixed with Carnoy's fixative and stained with 0.4% (w/v) crystal violet for a few minutes. Plates were again washed and then left at room temperature to dry. The cloning efficiency in control samples treated with appropriate volumes of drug solvent alone, DMSO or distilled water, was calculated using cloning efficiency formula (colonies counted/cells seeded) x 100. The percentage survival at each data-point was calculated using the specific formula (drug treated cell cloning efficiency/control cell cloning efficiency) x 100. The LC_{50} values, the dose of drug leads to 50% loss of colony formation, were calculated using GraphPad Prism statistical analysis software version 5.04.

2.10 Combined treatment and median-effect analysis

2.10.1 Growth inhibition in response to combined treatment

For combination treatments, the appropriate densities of wild-type *TP53* cell lines were seeded for 24 hours and then treated for 72 hours with each agent alone and in combination simultaneously at constant 1:1 ratios of 0.25x, 0.5x, 1x, 2x, and 4x their respective GI_{50} concentrations. They were fixed and stained by SRB assay as outlined previously. The fraction of cells affected following treatment was calculated using GraphPad Prism 5.04. Median-effect analysis was used to calculate Combination Index (CI) and Dose Reduction Index (DRI) values using CalcuSyn software v2 (Biosoft, Cambridge, UK). The DRI values>1 are favourable and CI<1, CI=1 and CI>1 are indicators of synergism, additivity and antagonism respectively (Chou, 2006; Chou, 2010). More detail for interpretation of CI and DRI are described within the chapters where relevant.

2.10.1.1 Clonogenic cell killing assay in response to combined treatment

Based on the drug concentration and sensitivity of cell lines, appropriate numbers of exponentially growing cells were seeded into triplicate six-well plates. Cells were treated with each drug alone and in combination at constant 1:1 ratios of 0.25x, 0.5x, 1x, 2x and 4x or 0.25x, 0.5x and 1x their respective LC_{50} concentrations, depending on the cell line and its single agent LC_{50} values, for 48 hours. The colonies were fixed and stained as described in section 2.9. DRI and CI values were calculated and interpreted as explained above.

2.11 Western blotting

2.11.1 Principles of western blotting

Western blot analysis is a powerful technique applied to measure relative amounts of proteins in a sample of tissue homogenate or cell extract, according to the immunoreactivity between antigen and antibody. It is a practical method used to estimate protein sizes in kDa by directly comparing with a set of standard size marker proteins or ladder. Gel electrophoresis is used to separate denaturated proteins according to size. They are then transferred to a specific membrane (normally nitrocellulose or PVDF) to probe with antibodies to target specific proteins. Lastly, the labelled probes bound to the protein of interest are visualised by different methods including chemiluminescent detection. The technique contains several main stages as explained below.

2.11.2 Lysate (Cellular protein mixture) preparation

Exponentially growing cells were detached, counted and 3 mL of appropriate cell densities were used to seed into 70 mm tissue culture dishes as described in specific materials and methods where relevant. The cell cultures were incubated at 37^0C for 48 hours before drug treatment. After 48 hours, the medium was aspirated; 3ml medium, 3ml 1% solvent (Distilled water or DMSO), or 3ml of prepared drugs was added to the tissue culture dishes, which were then incubated at 37^0C for four hours before harvesting the cells and preparing lysates for Western blot analysis. At the end of each treatment the media was removed, the cells were washed with 4^0C PBS and 40µl of lysis buffer (0.0625M Tris-HCl pH 6.8, 2% w/v SDS (Sigma), 10% v/v Glycerol (Sigma)) was added to each well. The buffer contains SDS, which disrupts non-covalent bonds in the proteins and coats them with negative charge, denaturing them so that they migrate according to molecular weight during subsequent gel electrophoresis. Then, cells were scraped, the lysate was transferred into microfuge tubes (Eppendorfs), the samples were heated at 100^0C for 10 minutes and sonicated at 23KHz using a Soniprep 150 plus (MSE) for 10 sec (Amplitude set at 6.0) three times. A combination of sonication and lysis buffer was used to enhance protein extraction and reduce the viscosity of the samples by breaking up the DNA.

2.11.3 Measurement of protein concentration (bicinchoninic acid assay, BCA)

The concentration of protein in the cell lysates was estimated by using a bicinchoninic acid (BCA) assay to determine the volume of lysate that should be loaded on the gel for equal quantities of protein. BCA is a detergent containing two reagents A and B mixed with the ratio 50 portions of BCA reagent A to 1 part of BCA reagent B (Thermo Scientific; Prod. No: 23227) to produce a suitable dilution. Standard concentrations of 0.2, 0.4, 0.6, 0.8, 1.0, 1.2 mg/ml bovine serum albumin (BSA) and lysate sample dilutions of 1 in 10 were prepared. Aliquots of 10µl of standard or sample were added per well of a 96-well plate. Then, 190µl of the BCA mixture was added to each well and mixed up and down using a multi-channel pipette. The plate was wrapped in Clingfilm, incubated at 37^0C for 30 minutes and the absorbance read at 570nm using a spectrophotometer (Spectramax 250 Molecular Devices).

The BCA assay is a biochemical assay, indicating the protein concentration by changing colour of the sample solution from green to purple in proportion to protein concentration which can be measured by using colorimetric techniques. The A stock BCA solution contains sodium carbonate, sodium bicarbonate, sodium tartrate, bicinchoninic acid and cupric sulfate pentahydrate

in a highly alkaline solution with a pH 11.25. This method includes two reactions. In the first one, reduction of Cu^{2+} ions to Cu^{+}, which in the presence of proteins (a temperature dependent reaction) leads to chelation of copper with the protein and formation of a pale green complex. In the second one, two molecules of BCA react with Cu^{+} ions; to form a purple-coloured product that strongly absorbs light at a wavelength of 562 nm. It seems that formation of colour with BCA is influenced by protein structure, quantity of peptide bonds and existence of some specific amino acids such as cysteine, tryptophan and tyrosine. The protein concentration of the samples were calculated based on a BSA standard curve, and were multiplied by 10 to account for the dilution factor of the samples.

2.11.4 SDS polyacrylamide gel electrophoresis (SDS-PAGE)

Novex® 4-20% Tris-Glycine 12- or 15-well polyacrylamide gradient gels (Invitrogen) were used in the study. The polyacrylamide gels were placed in Invitrogen Mini-Cell gel electrophoresis tanks and filled with 1x electrode buffer (144g Glycine, 30g Tris base, 10g SDS, 800ml distilled water, the volume was brought to 1L).

According to the calculation from the protein estimation assay, a required volume of lysate was added to SDS loading buffer to achieve a final volume which contained 30µg of protein in 30µl. SDS loading buffer contains 0.4g SDS, 2ml glycerol, 1ml 0.1% bromophenol blue, 1ml ßeta-mercaptoethanol, 2.5ml 0.5M Tris/HCL and 13.5ml distilled water. The samples were heated at 100^{0}C for 10 minutes, loaded into the wells of the gel and electrophoresis carried out at 180V for 45 minutes to separate the proteins. SeeBlue® Plus2 Pre-Stained Standard molecular weight markers (Invitrogen) were used in the flanking wells of each gel.

2.11.5 Transfer

The separated proteins were transferred by perpendicular electrophoresis to a nitrocellulose Hybond^{TM} C membrane (Amersham, Buckinghamshire, UK). The transfer electrophoresis tank was set up according to the manufacturer's instructions and was filled with transfer buffer (3g Tris base, 14.14g glycine, 200ml methanol and distilled water was added to make the volume up to 1L). All Hybond™C membrane, filter paper and fibre pads were immersed for 10 minutes in transfer buffer. Cassettes were set up in this order: black side first, fibre pad, filter paper (Whatman 3MM, Kent UK), gel, HybondTMC membrane, filter paper, fibre pad. The cassettes were closed and placed in transfer tanks, with the black side of the cassette facing the black anode, and electrophoretic transfer performed at 100V for 30 minutes.

2.11.6 Blocking

The Hybond^{TM}C membrane now carrying the immobilised proteins was placed into a 50ml Falcon tube (BD Biosciences, San Jose, CA, USA) filled with 5% w/v non-fat milk or bovine serum albumin (BSA) dissolved in 1x TBS Tween-20 (Fisher BioReagents) pH 7.6 and washed by gentle shaking and rolling at room temperature for an hour. This step was carried out to block non-specific binding which otherwise produces a high background staining on the nitrocellulose membrane. The membrane was cut into strips according to molecular weight ranges estimated from the marker proteins in order to probe with appropriate antibodies.

2.11.7 Primary and secondary antibodies

The strips were incubated with specific primary antibodies added to 3 ml 5% w/v non-fat milk/1x TBS Tween or 5% BSA/1x TBS Tween according to specified antibody supplier guidelines as stated in Table 2-3. Then, the Falcon tubes were placed on the rolling mixer for 1 hour at room temperature or overnight at 4^0C. Finally, strips were washed three times with 1x TBS/Tween to remove unbound primary antibodies and to get ready for the next stage.

Horseradish peroxidase (HPR) conjugated goat anti-mouse IgG and goat anti-rabbit IgG secondary antibodies (1:1000) (DakO, Denmark) diluted in TBS Tween/5% milk or TBS Tween/5% BSA were applied for between 45 to 60 minutes at room temperature. Following that, the filter strips were washed for 4 minutes seven times in 1x TBS/Tween on the platform shaker.

2.11.8 Enhanced chemiluminescence protein detection

An Enhanced Chemiluminescence (ECL) kit (Amersham) was used for protein detection. Washed filters were exposed for 1 minute to a mixture of ECL1 and ECL2, which is a chemilominescent substrate used for chemilominescence-based immunodetection of HRP on western blot membranes. ECL contains two reagents; one is the luminol substrate and the other functions as an enhancer, used in equal volumes to attain the most intense light emission. The antibody-conjugated HRP converts the luminol substrate to triplet carbonyl and its decay to singlet carbonyl leads to emission of light. The membrane was covered by a clear film and placed in an autoradiography cassette (Genetic Research Instrumentation, Essex, UK). A sheet of X-ray film (Kodak) was placed on the membrane in the dark room and the exposed film was subsequently developed and fixed using a Mediphot 937 (Colenta, Austria) automated film processor.

Antibody	Migration at ≈ kDa	Cat No. (Company)	Raised in	Dilution	Blocking Reagent
Actin	42	A4700 (Sigma)	Mouse	1:3000	5% Milk
Bax	21	2772 (Cell signalling)	Rabbit	1;1000	5% BSA
MDM2	90	OP46 (Calbiochem)	Mouse	1:300	5% Milk
P21^{WAF1}	18	OP64 (Calbiochem)	Mouse	1:100	5% Milk
P53	53	NCL-L-p53-DO7 (Novocastra)	Mouse	1:500	5% Milk
Goat anti mouse HRP	N/A	PO447 (Dako)	Goat	1:1000	5% Milk
Goat anti rabbit HRP	N/A	PO448 (Dako)	Goat	1:1000	5% BSA

Note: All the solutions made up in TBS, 0.1% Tween 20 (pH=7.6). Incubation time for primary antibodies was 1 hour at room temperature or overnight at 4^0C

Table 2-3: The primary and secondary antibodies used for western blotting. HRP, Horseradish peroxidase.

2.12 Polymerase Chain Reaction (PCR)

PCR is an *in vitro* biochemical technique with the ability to rapidly and accurately amplify a few copies of specific sequences of DNA developed in 1983 by Kary Mullis and optimised in its present form by Saiki (Bartlett, 2003).

2.12.1 Principles of PCR

The PCR technique is based on thermal cycling, which typically includes 20-40 cycles of repeated heating and cooling of the reaction for DNA melting and DNA enzymatic replication. A variety of parameters including the concentration of divalent ions and deoxyribonucleic acids (dNTPs), melting temperature (Tm) of the primers and the DNA polymerase used for DNA synthesis impact the temperatures and the length of time they are applied in each cycle.

An initialisation step consisting of heating the reaction to a temperature of 94-96^{0}C held for 1-9 minutes is required for DNA polymerases. There are three steps after the initialisation step to a PCR reaction including denaturation, primer annealing and elongation. Denaturation at 94-980C for 20-30 seconds causes DNA melting of the DNA template by disrupting the hydrogen bonds between complementary bases, which produces single-stranded DNA. During the annealing step, specific primers (short complementary oligonucleotides of single stranded DNA about 20 base pairs long) flank the target region on the template DNA and serve as a starting point for DNA synthesis. Then, they prime a DNA polymerisation reaction in the presence of thermostable DNA polymerase (eg. from Thermus aquaticus or Pyrococcus furiosus), the deoxyribonucleic acids dATP, dTTP, dCTP and dGTP, an appropriate co-factor such as MgCl2, and buffer solution. Primer annealing occurs at a lower temperature (between 50-650C for 20-40 seconds) to allow specific hybridisation of primers to the complementary part of the template strand. Finally, there is an elongation step during which a new DNA strand complementary to the DNA template strand is synthesised in a 5' to 3' direction at 720C. A suitable chemical environment for optimum activity and stability of the DNA polymerase is essential and provided by the buffer solution. Magnesium acts as a cofactor and catalyser, increasing productivity of Taq DNA polymerase. Following the last PCR cycle, the final single elongation is performed at 70-74^{0}C for 5-15 minutes to fully extend any remaining single-stranded DNA.

2.12.2 DNA extraction

Genomic DNA was extracted using a QIAamp DNA Mini Kit (Qiagen, UK) as described by the manufacturer. The quality of DNA and its concentration were estimated using NanoDropTM ND-1000 Spectrophotometer and sample type DNA-50 (NanoDrop Technologies, Inc. Wilmington, DE, USA). A blank measurement of the appropriate solvent devoid of sample was used before sample measurement, and the pedestals were cleaned with distilled water between each measurement. The absorbance for nucleic acids is at 260nm, for protein or phenol contaminants at 280nm and for carbohydrate or solvent contamination at 230nm. Hence, the ratio of 260:280 or 260:230 can be used as a measure of sample purity. A ratio of 260:230 is higher than the ratio of 260:280 for a given sample, which normally is 1.8-2.2. The purity of DNA was determined by the ratio of 260nm:280nm, which is around 1.8 for good quality of DNA (Figure 2-1).

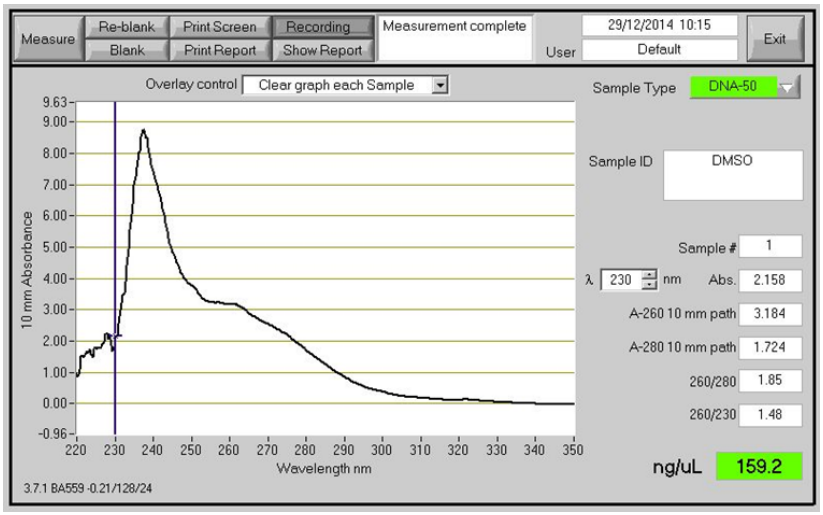

Figure 2-1: The absorbance spectra pertaining to a DNA sample

2.12.3 PCR protocol

All reagents needed for the PCR experiment were prepared at the appropriate concentration (the final concentration of DNA should be at least 100ng) and kept on the ice throughout the experiment (Table 2-4). The mixture of reagents was set up at the PCR station and the PCR tubes were placed into the thermal cycler (GeneAmp PCR Systems, AB Applied Biosystems) run based on the Touchdown programme (Table 2-5). The *TP53* exon 4 sequence was split into two partially overlapping amplicons due to its large size. The purification of PCR products was

carried out for subsequent analysis using the purelink PCR purification kit (Qiagen, UK) in accordance with the manufacturer's protocol.

Reagent	Concentration	Volume (µl)
PCR gold buffer	10X	2.5
MgCl2	25 mM	2
dNTP's	2.5 mM	2
Primer SN	10 µM	2
Primer ASN	10 µM	2
dH2O	-	To 25 total volume
Amplitaq Gold	2U/µl	0.4
DNA Template	*	**
Total	-	25

Table 2-4: The reagents and their volumes used for PCR. *, The concentration of DNA should be measured; **, the volume depends on the DNA concentration. SN, Sense; ASN, Antisense, dH2O, Distilled water.

PCR Programme	Hot Start	14 Cycles			26 Cycles			End
Temperature (° C)	94	94	62	72	94	55	72	72
Time (min/sec)	10 min	20 sec	1 * min	1 min	20 sec	1 min	1 min	5 min

Table 2-5: The PCR programme used to amplify exons 4.1, 4.2, 5, 8 & 9. *, The temperature decreases by 0.5^0C each cycle.

2.12.4 DNA gel electrophoresis

DNA gel electrophoresis was used to separate and identify DNA fragments based on the amplicon size. The loading buffer (G1881, Promega, UK) was added to the PCR products to visualize and load the samples into the wells, and to determine how far the samples have migrated during the run. The 100bp DNA Ladder (Life Technologies) was diluted in 1/10 with Tris 10mM and used as a DNA ladder. DNA gel electrophoresis was performed using 2%

agarose gel (Bp1356-500, Fisher Scientific) (w/v, 0.5x TBE) with 100 voltage for around 45 minutes. To prepare 0.5x TBE, 100 ml of 5x TBE (1.1M Tris; 900mM Borate; 25mM EDTA; pH 8.3) was added to 900mL of deionized water and mixed well. Then, DNA was visualised using Biorad image software under UV light on a transilluminator and digitally photographed (Figure 2-2). The length of amplicon was calculated applying the BioEdit v 7.2 software.

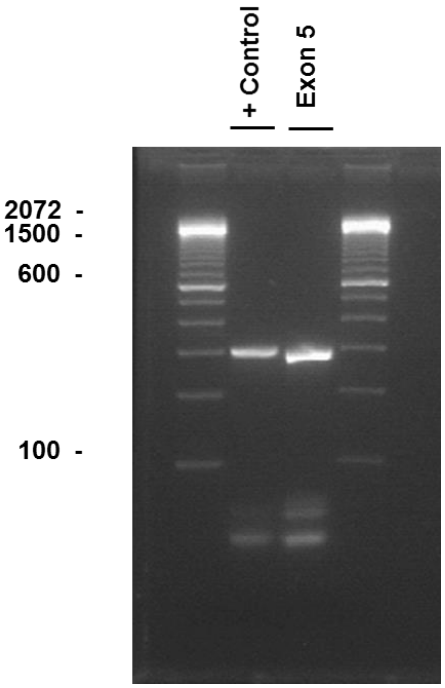

Figure 2-2: The PCR product for *TP53* exon 5 with the amplicon size of 294 bp (base pairs).

2.13 Quantitative real-time PCR

2.13.1 Principles of qRT-PCR

qRT-PCR is a molecular technique monitoring amplification of a targeted cDNA molecule during the PCR in real time. qRT-PCR was performed using SYBR® green RT-PCR master mix (Life technologies) on an ABI 7900HT sequence detection system. SYBR green is a fluorescent dye binding to the minor groove of double-stranded DNA, dsDNA, with an excitation wavelength of ~ 485nm and an emission wavelength of ~ 524nm. The intensity of fluorescent signal measured by a detector directly associates with double-stranded DNA quantity. Therefore, the amount of PCR double-stranded DNA products can be measured after

every elongation step in real time. The fold changes in the expression of the target gene in relation to internal reference genes is determined for relative quantification.

2.13.2 RNA extraction

Total RNA was extracted using an RNeasy Mini Kit (Qiagen, Germany) as described by the manufacturer. RNA purity and concentration were estimated with an ND-1000 spectrophotometer and sample type RNA-40 as stated in section 2.12.2 (NanoDrop Technologies, Thermo Scientific, UK). The purity of RNA was determined by the ratio of 260nm:280nm, which is approximately 2.0 for good quality of RNA.

2.13.3 cDNA synthesis

Total messenger RNA was converted to cDNA using the thermal cycler (GeneAmp PCR Systems, AB Applied Biosystems) in accordance with the manufacturer's guidelines (Table 2-6). PCR reactions were performed using cycling parameters (Stage 1: 42 ˚C for 1 hour, Stage 2: 95 ˚C for 5 min) for only 1 cycle.

2.13.4 Primer validation

All primers used were validated by preparing a serial dilution of the genomic DNA template and using SYBR Green Master Mix and SDS 2.3 software (Applied Biosystems) as described by the manufacturer (Figure 2-3). Validated primers used (Sigma-Aldrich UK) are listed in Table 2-7 and Table 2-8.

2.13.5 qRT-PCR protocol

PCR reactions with 50 ng/µl of the cDNA samples per 10µl final reaction volume, were performed using standard cycling parameters (Stage 1: 50˚C for 2min, Stage 2: 95˚C for 10min, then 40 cycles of 95˚C for 15 Sec and 60˚C for 1 min) on an ABI 7900HT sequence detection system. GAPDH was used as endogenous control due to its almost constant level of expression, and the DMSO solvent control sample used as the calibrator for each independent repeat. Data analysis using the ΔΔCt Method was carried out using SDS 2.3 software (Applied Biosystems). Data were presented as mean ± standard error of mean (SEM) relative quantities (RQ) of ≥3 independent repeats.

Reagent	Concentration	Volume (µl)
AMV Buffer	5X	2
MgCl2	25 mM	2
dNTP	10 mM	1
Rnasin Ribonuclease inhibitor	-	0.25
AMV RT	500 µg/ml	0.3
Oligo (dT) primers	-	0.5
Nuclease-free water	-	To 10 total volume
RNA	*	**
Total	-	10

Table 2-6: The reagents and their volumes used for q-RT-PCR. *, The concentration of RNA should be measured; **, the volume depends on the RNA concentration and the final concentration of RNA should be 500ng.

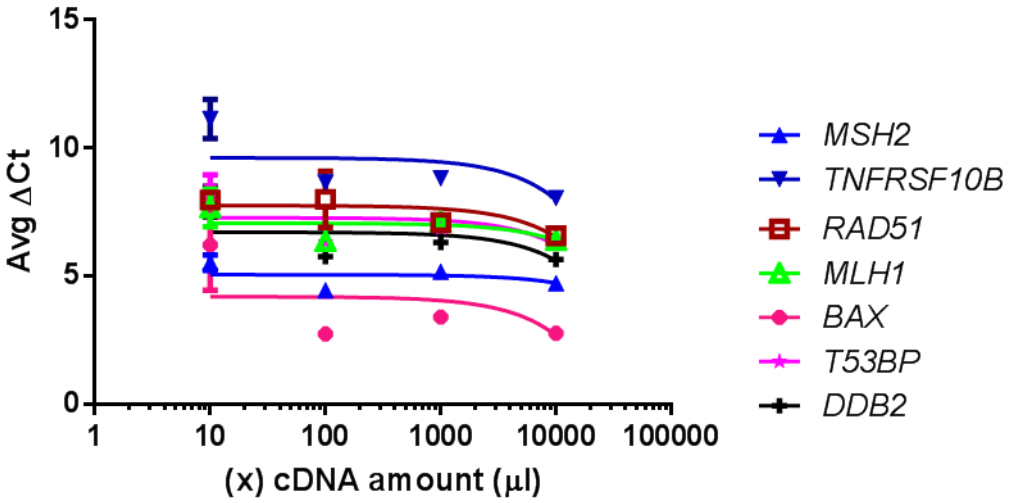

Figure 2-3: The results of primer validation.

Gene Symbol	Target Gene Product	Primer Sequence 5'-3'
DDB2	Damage-specific DNA binding protein2	F-ACCTCCGAGATTGTATTACGCC
		R-TCACATCTTCTGGTAGGAC
ERCC1	Excision repair cross-complementing rodent repair deficiency, complementation group 1	F-CTACGCCGAATATGCCATCTC
		R-GTACGGGATTGCCCCTCTG
MLH1	MutL homolog 1, colon cancer, nonpolyposis type 2 (E. coli)	F-GCAAACCCCTGTCCAGTCAG
		R-CTGGGAGTTCAAGCATCTCCT
MSH2	mutS homolog 2, colon cancer, nonpolyposis type 1 (E. coli)	F-CACTGTCTGCGGTAATCAAGT
		R-CTCTGACTGCTGCAATATCCAAT
RAD51	RAD51 homolog (S. cerevisiae)	F-CAACCCATTTCACGGTTAGAGC
		R-TTCTTTGGCGCATAGGCAACA
RRM2B	Ribonucleotide reductase M2B (*TP53* inducible)	F-ATTGGGCCTTGCGATGGATAG
		R-GAGTCCTGGCATAAGACCTCT
TP53BP1	Tumour protein p53 binding protein 1	F-TGAGCAGTTACCTCAGCCAAA
		R-AAGGGAATGTGTAGTATTGCCTG
XPC	xeroderma pigmentosum, complementation group C	F-CATCGTGGGAGCCATCGTAAG
		R-CTCACCATCGCTGCACATTTT

Table 2-7: The primers and their sequences used for qRT-PCR experiments for DNA repair genes. F, Forward; R, Reverse.

Gene Symbol	Target Gene Product	Primer sequence 5'-3'
AEN	Apoptosis enhancing nuclease	F-CTTCCAGGCGCTCAAGTATG
		R-GGGCCAGGTCCTTTAGAGAGA
BAX	BCL-2 associated X protein	F-CCCGAGAGGTCTTTTTCCGAG
		R-CCAGCCCATGATGGTTCTGAT
BBC3 (PUMA)	BCL2 binding component 3	F-GCCAGATTTGTGAGACAAGAGG
		R-CAGGCACCTAATTGGGCTC
TNFRSF10B	Tumor necrosis factor receptor superfamily, member 10b	F-ATGGAACAACGGGGACAGAAC
		R-CTGCTGGGGAGCTAGGTCT
TP53INP1	Tumor protein p53 inducible nuclear protein 1	F-TCTTGAGTGCTTGGCTGATACA
		R-GGTGGGGTGATAAACCAGCTC
MDM2	Mouse double minute 2 homolog	F-AGTAGCAGTGAATCTACAGGGA
		R-CTGATCCAACCAATCACCTGAAT
BCL-2	B-Cell CLL/Lymphoma 2	F-GGTGGGGTCATGTGTGTGG
		R-CGGTTCAGGTACTCAGTCATCC
BIRC5 (Survivin)	Baculoviral IAP Repeat-Containing 5	F-GGTGGGGTCATGTGTGTGG
		R-CGGTTCAGGTACTCAGTCATCC
MCL-1	Myeloid Cell Leukemia 1	F-GTGCCTTTGTGGCTAAACACT
		R-AGTCCCGTTTTGTCCTTACGA
CDKN1A	Cyclin-dependent kinase inhibitor 1A (p21, Cip1)	F-TGTCCGTCAGAACCCATGC
		R-AAAGTCGAAGTTCCATCGCTC
SESN1	Sestrin 1	F-TGCTTTGGGCCGTTTGGATAA
		R-TGTAGTGACGATAATGTAGGGGT
GADD45A	Growth Arrest And DNA-Damage-Inducible	F-GAGAGCAGAAGACCGAAAGGA
		R-CAGTGATCGTGCGCTGACT
GAPDH	Glyceraldehyde 3-phosphate dehydrogenase	F-CAATGACCCCTTCATTGACC
		R-GATCTCGCTCCTGGAAGAT

Table 2-8: The primers and their sequences used for qRT-PCR experiments for the pro-apoptotic, anti-apoptotic, cell cycle arrest and *GAPDH* genes. F, Forward; R, Reverse.

2.14 Analysis of cell cycle distribution and apoptosis via flow cytometry

The DNA content in the distinct cell cycle phases is different with diploid (2N) for G0/G1 phase cells, 2N>n<4N for the cells in S-phase and tetraploid (4N) for those in G2/M phases. The distribution of a population of cells into different phases of the cell cycle can be estimated through measuring the DNA concentration by Flow cytometry. Induced changes in the cell cycle distribution following exposure to drug may also provide information to understand underlying mechanisms of drug function.

2.14.1 The principles of FACS

For cell cycle analysis by flow cytometry, the plasma membrane of the cells must permeablised by using a buffer containing a detergent such as Triton-X. The cells should also be treated with RNase A to remove RNAs from the cells and eliminate artefacts distorting the results when the cells are stained with dyes binding to both DNA and RNA. The last step is quantitatively staining the DNA with a fluorescent dye such as propidium iodide (PI). PI is an intercalating dye binding to both double-stranded DNA and RNA with an excitation wavelength of ~ 535nm and an emission wavelength of ~ 617nm when bound to DNA. Following staining and putting the cell suspension through the FACSCalibur, the cells were sucked through a narrow sample injection tube by a vacuum. The cells and their PI stained nucleus intercept the 488-nm argon ion laser beam causing transmission and scattering of the light which is detectable via a forward-scattered (FSC) diode and a side-scattered (SSC) diode. FSC and SSC give information about the volume and granularity of cells respectively. The scattered light can be detected by photodetectors and fluorescent light emitted from PI is reflected on to the FL-2 585/42 detectors by dichromic mirrors at right angles to the beam of light whereas other wavelengths of light are transmitted for other detectors to pick up. Detectors are photomultipliers with the ability to amplify signals from single photons so that they can electronically be recorded.

2.14.2 FACSCalibur instrument setting and gating

The instrument settings have to be optimised to detect, record and analyse events with size and complexity characteristic of mammalian cells rather than other objects that intercept the light. To optimise instrument setting, the scatter plots of SSC-H vs. FSC-H and FL2-A vs. FL2-W were set up using CellQuest software (Beckton Dickinson) and an untreated control sample of each cell line. Furthermore, a histogram of counts vs. FL2-H was set up where the G0/G1 and G2/M peaks were set to 200 and 400 on a linear scale respectively. Therefore, the events which have a FL2-A intensity below diploid cells known as SubG1 events are detectable. For each sample, data acquisition was collected at 10000 events and saved.

2.14.3 Flow cytometry protocol

Based on the type of cells and their growth rate, the appropriate density of cells was seeded in a 6-well plates (Corning) or small cell culture flask (25 cm) and treated as described in specific materials and methods of the relevant chapters. Harvested cells, both floating and adherent, were washed with PBS and resuspended in 500 µL PBS and incubated at room temperature for around 20 minutes. Then, they were diluted 1:1 in a PI solution with 1mg/mL sodium citrate (Sigma, St Louis, MO), 100 µg/mL propidium iodide (Sigma), 200 µg/mL RNAse A (Sigma) and 0.3% Triton-X (Sigma) to stain. The samples were analysed on a FACSCalibur flow cytometer using CellQuest Pro software (Becton Dickinson, Oxford, UK) after three times syringing to remove any clumps of cells. It is an essential step because an aggregation of two G0/G1 cells can mistakenly be counted as a G2/M cell.

2.14.4 FACS data analysis

The CellQuest software was used to analyse acquired FACS files and generate representative 2D and 3D histograms of control and treated sample cell cycle distribution. The Cyflogic v 1.2.1 software (CyFlo Ltd, Turku, Finland) was applied to manually gate the population of events in different phases of cell cycle and gate-out the SubG1 events on the FL2-A histogram plots. The proportion of events in S-phase and the percentage of those in each of peaks corresponding to G0/G1 and G2/M was calculated and plotted on the grouped bar charts using GraphPad Prism 6 software. The proportion of SubG1 events, a surrogate marker of apoptosis, was calculated as a percentage of total events and represented as separate bar charts (Figure 2-4).

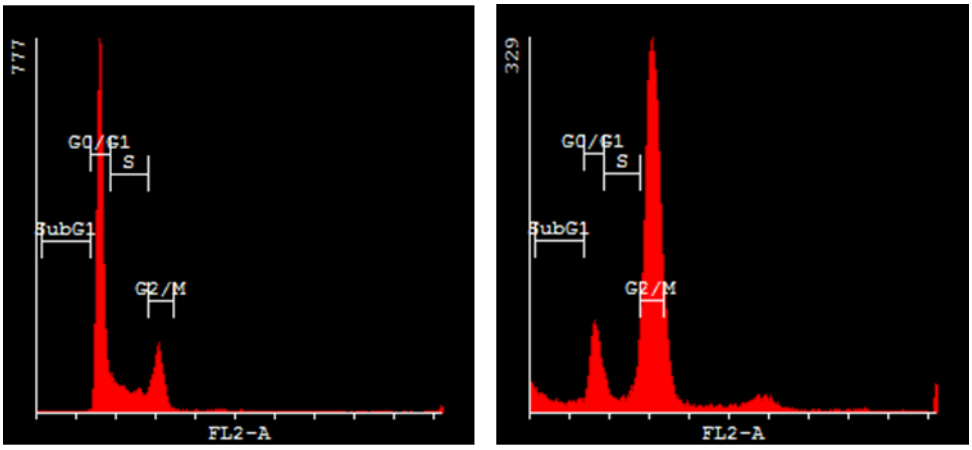

Figure 2-4: Cell cycle distribution and apoptotic endpoints of control (untreated) and treated samples in which the events were manually gated.

2.15 Caspase 3/7 activity

The Caspase-Glo® 3/7 Assay is a luminescent assay which includes a proluminescent caspase 3/7 substrate containing the tetrapeptide sequence DEVD. In the presence of caspase 3 and caspase 7 activities, the substrate is cleaved resulting in release of aminoluciferin which is a substrate of luciferase used in the production of luminescent light.

Caspase 3/7 activity was measured using a Caspase-Glo® 3/7 Assay (Promega, Southampton, UK) following the manufacturer's instructions. The cells were seeded at the appropriate densities and treated as outlined in specific materials and methods of the relevant chapters.The luminescence was measured using a Fluostar Omega Plate Reader (BMG LABTECH) and luminescence readings were normalized and plotted relative to the control.

2.16 Statistical analysis

All statistical tests presented were carried out using the SPSS 22.0 software package for windows (SPSS Inc., Chicago, USA) or GraphPad Prism version 5.04 software. The type of statistical tests used are specified in the individual materials and methods sections for each chapter. A p-value of <0.05 was considered to be statistically significant.

Chapter 3: An investigation of ovarian cancer tumour samples for p53, $p21^{WAF1}$, MDM2 and WIP1 expression using tissue microarrays (TMA) of OVCA1-4 cohort

3.1 Introduction

Mutation and overexpression of the *TP53* gene is one of the most frequent genetic abnormalities in ovarian cancer. Overexpression of p53 occurs in 51% of ovarian cancer, and the reported rate of *TP53* mutation ranges from 30% up to 80% (Reles *et al.*, 2001; Kmet *et al.*, 2003; Ling and Wei-Guo, 2006; Bast *et al.*, 2009). $p21^{WAF1}$, MDM2 and WIP1 are p53 downstream targets playing a critical role in cell cycle arrest, the p53 negative autoregulatory loop and dephosphorylation of p53 respectively (Abbas and Dutta, 2009; Le Guezennec and Bulavin, 2010; Wade *et al.*, 2013). Given the controversial results about the importance of p53, $p21^{WAF1}$ and MDM2 as prognostic biomarkers in ovarian cancer and the important role of WIP1 in dephosphorylation and inactivation of p53, this part of the study focussed on the investigation of the roles of these proteins as prognostic and predictive biomarkers in ovarian cancer (Sengupta *et al.*; Kmet *et al.*, 2003; Dogan *et al.*, 2005; Han *et al.*, 2009; Bauerschlag *et al.*, 2010; Le Guezennec and Bulavin, 2010; Ali *et al.*, 2012; Skirnisdottir and Seidal, 2013).

3.1.1 p53 as a guardian of the genome and cellular gatekeeper

The tumour suppressor p53 responds to intrinsic and extrinsic stress signals. Following exposure to stress, p53 stabilization, sequence-specific DNA binding, and transcriptional activation of target genes occur to protect cells against environmental and intra-cellular stress stimuli (Wade *et al.*, 2013). The p53 pathway can be divided into two parts; upstream pathway and downstream pathway. Upstream mediators distinguish and respond to stress signals to increase stabilisation of p53 largely as a result of post-translational modifications of p53 and its regulators such as the MDM2 and MDMX proteins. The downstream pathway involves p53 transcriptional transactivation events and interactions between proteins. The p53 protein regulates expression of its downstream transcriptional targets including upregulation of the growth inhibitory *WAF1* gene, proapoptotic genes such as *BAX* and *PUMA*, the *MDM2* autoregulatory p53 inhibitor, as well as inactivation of prosurvival *BCL2* family members. In summary, the final outcome of p53 activation is either cell cycle arrest and DNA repair, senescence or apoptosis (Vassilev, 2007; Mandinova and Lee, 2011). The role of $p21^{WAF1}$ in cell proliferation control, and the importance of MDM2 and WIP1 as negative regulators of p53 are described in chapter 1.5.4, 1.5.7 and 1.6.4 respectively.

Due to importance of p53 and its downstream targets, $p21^{WAF1}$, MDM2 and WIP1, it was set out to investigate the role of these proteins in ovarian cancer and their correlation with survival.

3.2 Hypothesis and Objectives

Hypothesis:

1. p53 and its downstream targets, $p21^{WAF1}$, MDM2 and WIP1 can be considered as prognostic biomarkers for overall survival in ovarian cancer.

Objectives:

1. To establish whether tumour sample immunohistochemical staining for p53, $p21^{WAF1}$ and MDM2 has prognostic value in the OVCA1-4 patient cohort.
2. To evaluate whether immunohistochemical staining for WIP1 provides additional predictive value for overall survival in the OVCA3-4 patient cohort.

3.3 Specific Materials and Methods

The first part of this study was performed using IHC on TMA samples collected from ovarian cancer patients from the North East of England, who had been referred to the Queen Elizabeth Hospital Gateshead Newcastle (QE).

3.3.1 TMA and patient characteristic

Ovarian cancer patients who underwent primary surgery between 1995 and 2000 were detected using the Queen Elizabeth Hospital pathology department database. Among the samples collected between these years, cases with minimum 5 years of clinical and survival data were selected and a collection of 167 of primary epithelial ovarian cancer was detected based on the all histology reports. All patient data including surgery, pathological and survival data were collected, entered into an anonymous databases and stored in a secure server in accordance to clinical laboratory practice guidelines.

3.3.2 Developing an ovarian cancer TMA

TMA design is described in chapter 2.1.3. All samples were immunostained with Cytokeratin to map the tumour areas which were determined by a pathologist (Dr Paul Cross). There was no pathology review to update the diagnosis of these archival samples. Sample cores were taken from individual tumour FFPE blocks to construct 4 TMA blocks representing all the patient's tumour specimens, with duplicate cores on each block. Four TMAs, OVCA1-4, were produced using a manual tissue microarray (TMA I, Beecher Instruments) by members of the ovarian cancer group, including Dr. Ali Kucukmentin, Dr. Ahmed Elattar and Dr. Richard Edmondson and with the help of Dr. Paul Cross (consultant pathologist at Queen Elizabeth Hospital, Gateshead).

As mentioned in most studies, a standard 1mm diameter core of tissue was taken from the marked area and used for these TMAs (Eckel-Passow *et al.*, 2010; Kim *et al.*, 2013). Following arraying of all the cores, the completed TMA block was incubated face down on to a normal glass slide at 37 ^{0}C for 30 minutes. This process was done to warm the paraffin which provides stability for the cores. Sections were cut from the TMA blocks and mounted on four slides labelled as OVCA1, OVCA2, OVCA3 and OVCA4. Immunohistochemical (IHC) staining was carried out on the TMA slides for p53, $p21^{WAF1}$, MDM2 and WIP1 proteins. There was appropriate ethical approval to analyse the samples and patient details obtained from hospital

records. Clinicopathological data had been recorded for histological subtype, stage, residual disease, CA125 and grade. Incomplete data were recorded as lost (Table 3-1).

3.3.3 Antibody specificity and optimization

Monoclonal Mouse Anti-Human p53 (Clone DO-7, Dako, 1:100), MDM2 (OP46, Calbiochem, 1:50), WIP1 (F-10, Santa Cruz Biotechnology, 1:500) and Monoclonal Rabbit Anti-Human $p21^{WAF1}$ (2947S, Cell Signalling, 1:50) proteins were used for IHC staining. Validation of MDM2 antibody was performed using paraffin-embedded pellets of MDM2 inhibitor treated (10 µM Nutlin-3) SJSA and its Nutlin-3 resistant daughter cell line SN40R2 (Bo *et al.*, 2014; Esfandiari *et al.*, 2016) as positive and negative control respectively. Due to cross reactivity between monoclonal anti-MDM2 clone SMP14 and cytokeratin 6, 14 or 16 causing a problem when working with epithelial cells (www.abcam.com/MDM2-antibody-SMP-14-ab3110; www.emdmillipore.com/.../Anti-MDM2-Antibody), we investigated the expression of these cytokeratins in the ovarian adenocarcinomas to be sure there is no cross-reactivity. Based on the literature, there is no expression of K6, K14 and K16 in ovarian carcinoma, whereas a $K7^{+}/K20^{-}$ expression is characteristic of ovarian adenocarcinomas (Karantza, 2011).

The paraffin-embedded pellets of MDM2 inhibitor treated (5 µM Nutlin-3) MCF7 cells was used as a positive control and DMSO treated SJSA cell line as a negative control to validate the WIP1 antibody (Figure 3-1). The SJSA and MCF7 cell lines are amplified for *MDM2* (Arkin et al., 2014) and *PPM1D* (Parssinen *et al.*, 2008) genes respectively. The antibodies were optimized as described in chapter 2.2.1 and the best outcomes were used for experiments (Figure 3-2).

3.3.4 Staining, scoring and categorising

IHC was carried out based on the details explained in section 2.2.1, and slides stained omitting the primary antibody were used for negative control (Burry, 2011). The H-score is a method to evaluate the extent of immunoreactivity, which is obtained according to the intensity of IHC staining and the percentage area stained. More detail for scoring is provided in section 2.2.2. Receiver Operating Characteristic (ROC) curve analysis was used to examine the relationship between sensitivity and specificity for immunohistochemical staining scores. The ROC curve (Cao *et al.*, 2014) or distribution of H-score values (Madjd *et al.*, 2011) were used to categorise the samples into two groups of high and low expression for p53, $p21^{WAF1}$, MDM2 and WIP1 proteins.

3.3.5 Statistical analysis

The statistical significance of observed differences in patient survival was analysed by the Kaplan-Meier method using a Log-rank test. For differences in the distribution of immunohistochemistry scores between subsets of patient samples an Analysis of variance (ANOVA) test was used. The Mann-Whitney and Kolmogorov-Smirnov tests were used to compare probability distribution in two samples. All statistical tests presented were carried out using the SPSS 22.0 software package for windows (SPSS Inc., Chicago, USA) or GraphPad Prism version 5.04 software. A p-value of <0.05 was considered to be statistically significant.

Variable	Number	Proportion %
Histological Subtype		
Adenocarcinoma	3	2
Clear Cell	16	10
Endometrioid	51	30
High Grade Serous	66	39
Low Grade Serous	13	8
Mucinous	18	11
Lost	0	0
Stage		
I	28	17
II	14	8
III	90	54
IV	18	11
Lost	17	10
Residual Disease		
Complete Cytoreduction (none)	54	32
Optimal Cytoreduction (≤1cm)	30	18
Suboptimal Cytoreduction (>1cm)	64	39
Lost	19	11
Grade		
Poorly Differentiated	80	48
Moderately Differentiated	45	27
Well Differentiated	42	25
Lost	0	0
CA125	139	83
Lost	28	17

Table 3-1: Clinicopathological data for 167 samples of ovarian cancer on TMA 1-4.

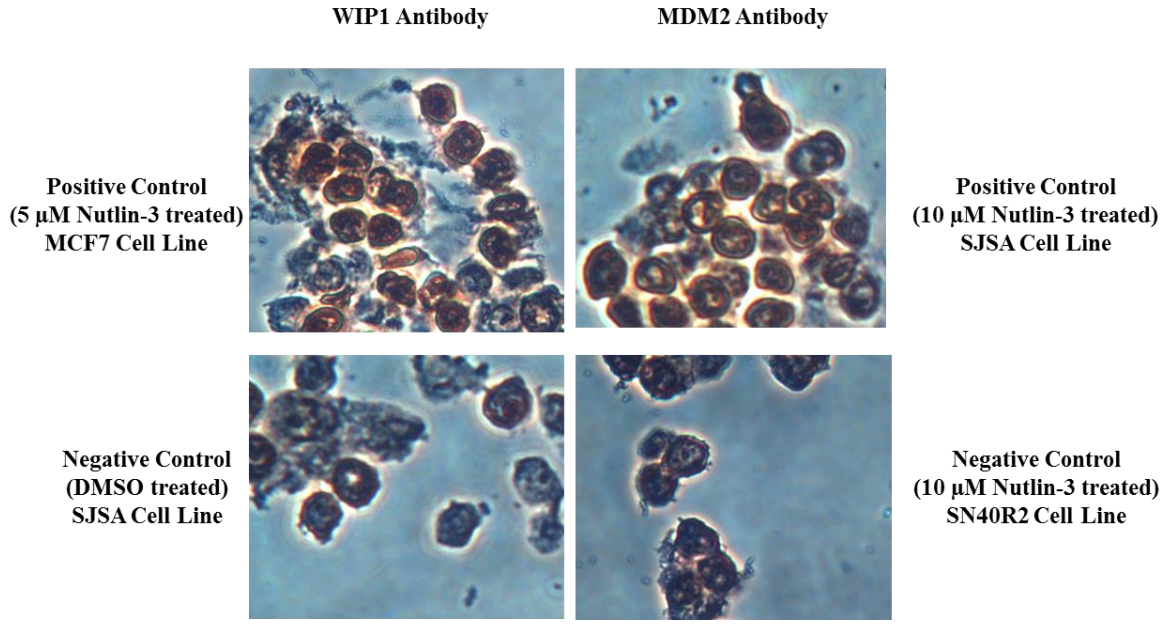

Figure 3-1: Image demonstrating validation of WIP1 (F-10, 1:500) and MDM2 (OP46, 1:1000) antibodies using FFPE pellets of MDM2 inhibitor or DMSO treated SJSA, MCF7 and SN40R2 cells.

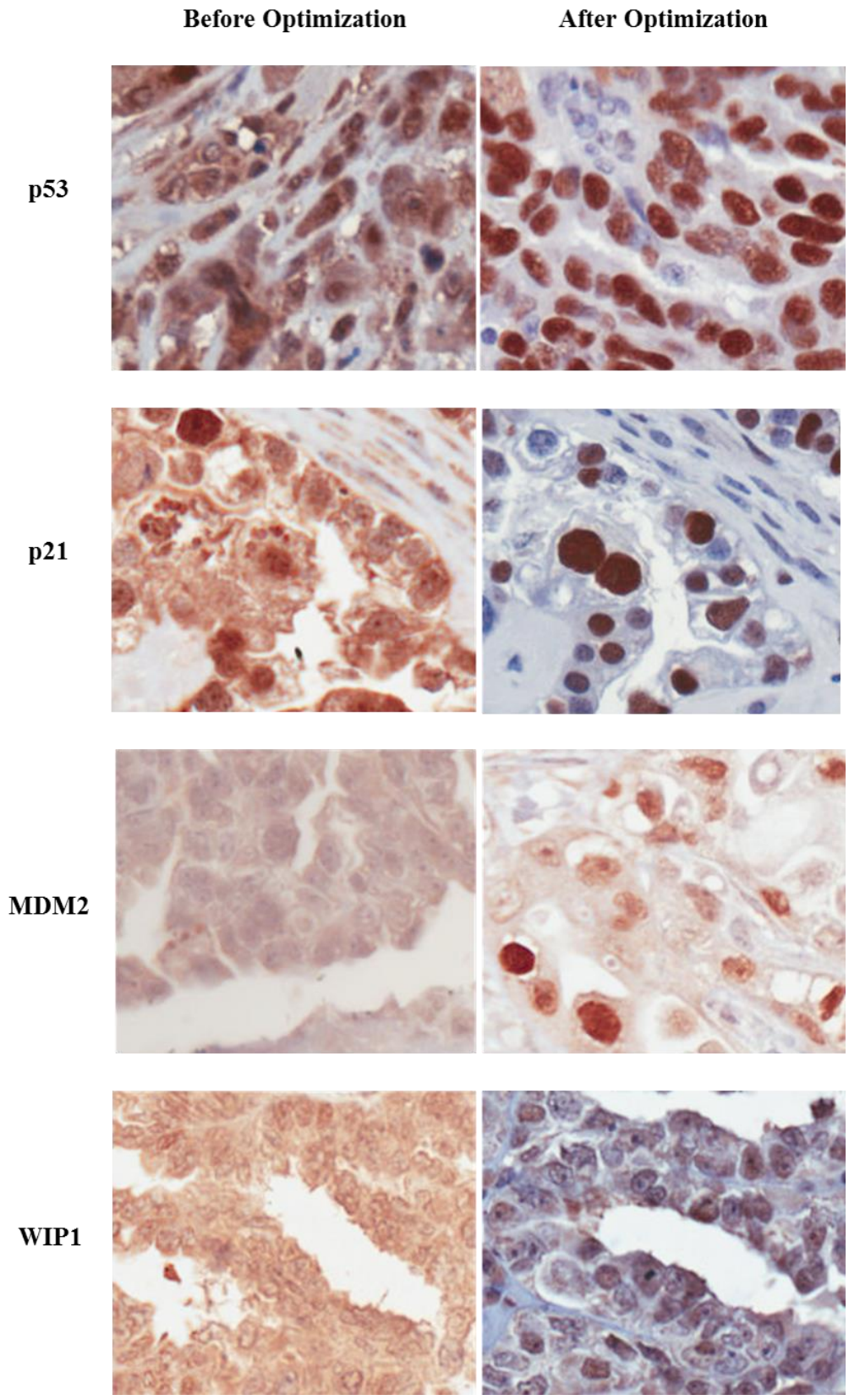

Figure 3-2: Image demonstrating optimization of p53, $p21^{WAF1}$, MDM2 and WIP1 antibodies on samples of tissue cores from the ovarian cancer TMA 1 to 4 slides. Images were captured and viewed by ScanScope® CS (Aperio Technologies, Bristol UK) at 10X magnification.

3.4 Results

3.4.1 Overall Survival (OS)

Overall disease related survival is the time for which people in a study or treatment category are alive, measured from date of diagnosis to the last time the patients were seen or their date of death as a result of disease, excluding deaths unrelated to disease (Bewick *et al.*, 2004). Kaplan-Meier analysis is a standard way to analyse survival when there is a variable follow-up time. This involves calculating the fraction of individuals surviving for a certain length of time after therapy in spite of variable follow-up times and loss to follow-up of some subjects (Rich *et al.*, 2010). Kaplan-Meier survival plots were applied to determine the relationship of variables to survival. Comparison between the survival curves was made by Log-rank test, employing logarithms of the ranks of the data and calculating a p-value to confirm whether or not the overall differences amongst survival curves are statistically significant.

In this cohort, 104 (62%) women died of ovarian cancer, 4 (2%) died because of other reasons, 10 (7%) were alive with disease recurrence, 38 (23%) were alive without disease and 11(6%) cases did not follow after surgery.

A Kaplan-Meier survival analysis was performed according to the clinicopathological data. The overall five year disease specific survival was 32% which is comparable to other studies with the overall 5-year survival about 30% (Agarwal and Kaye, 2003; Dogan *et al.*, 2005; Witham *et al.*, 2007; Corney *et al.*, 2008; Yasmeen *et al.*, 2011) (Figure 3-3). The median disease specific survival was 26.6 months in the range of 0-116 months (CI=95%).

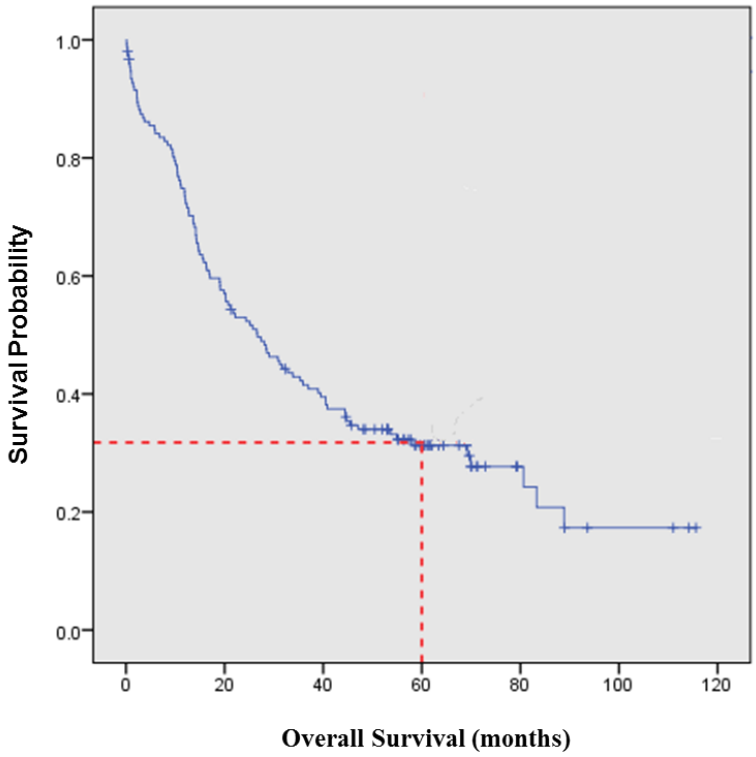

Figure 3-3: Kaplan-Meier graph showing 32% five-year overall survival for the TMA 1-4 patient cohort.

3.4.2 Histological tumour subtype and patient survival

The incidence in diverse histological subtypes was 66 cases (39%) HGSC, 51 cases (30%) endometrioid, 18 cases (11%) mucinous, 16 cases (10%) clear cell, 13 cases (8%) LGSC and 3 cases (2%) adenocarcinoma, with a total n=167. The observed differences among survival curves in relation to different histological subtypes were statistically significant X^2=14.61, *p=0.01*). None of the patients suffering from adenocarcinoma survived to 5 years, although the numbers were small. Individuals with clear cell (20%) and HGSC (20%) had the worst 5 year specific survival, whilst patients with endometrioid (46%), LGSC (45%) and mucinous (39%) tumour histologies were in a better prognosis group (Figure 3-4). These results were consistent with the fact that clear cell and HGSC are known to be more aggressive types of ovarian cancer and help to validate the cohort.

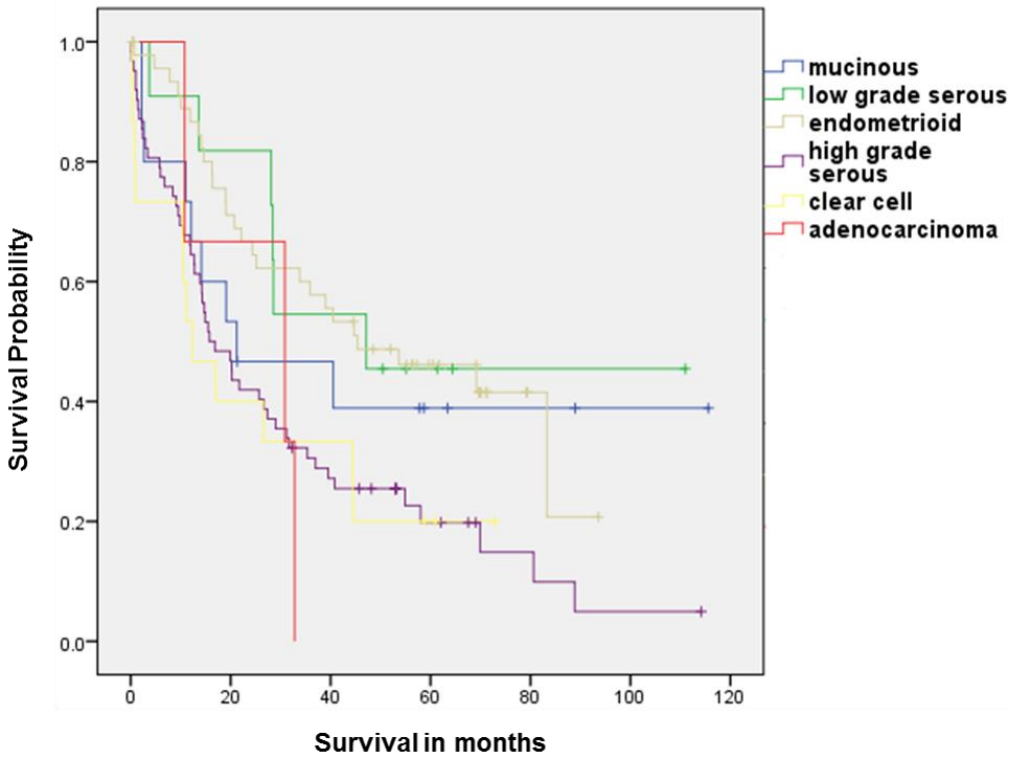

Figure 3-4: The survival times in relation to histological subtypes (*p=0.01*).

3.4.3 Stage and relationship with survival

The frequency distribution for different disease stages was 28 (17%), 14 (8%), 90 (54%) and 18 (11%) at I, II, III, IV stages respectively and 17 (10%) cases were missed, which give a total of n=150. Statistical analysis indicated that the stage of disease was a highly significant prognostic factor for survival (X^2=56.81, $p< 0.0001$). Diagnosis at an earlier stage of disease was associated with increased 5 year specific survival with 75%, 64%, 21%, and 0% for stages I, II, III and IV respectively (Figure 3-5).

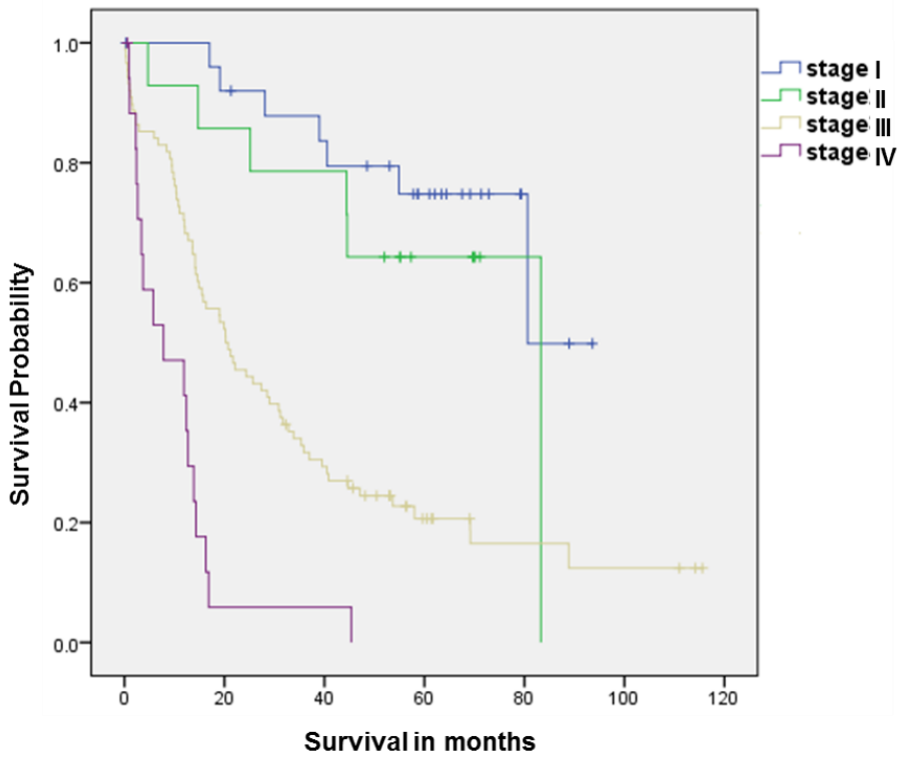

Figure 3-5: The survival times in relation to disease stage ($p< 0.0001$).

3.4.4 Tumour grade and patient survival

In the TMA 1-4 study cohort, 80 cases (48%) were recorded with grade III tumours (poorly differentiated), 45 cases (27%) were grade II (intermediate differentiation) and 42 (25%) were grade I (well differentiated) (n=167). Statistical analysis showed the grade to be a significant prognostic variable (X^2=6.93, $p=0.03$). The 5 year survival probability was 47%, 27% and 25% for well (I), intermediate (II) or poorly differentiated (III) tumours respectively (Figure 3-6).

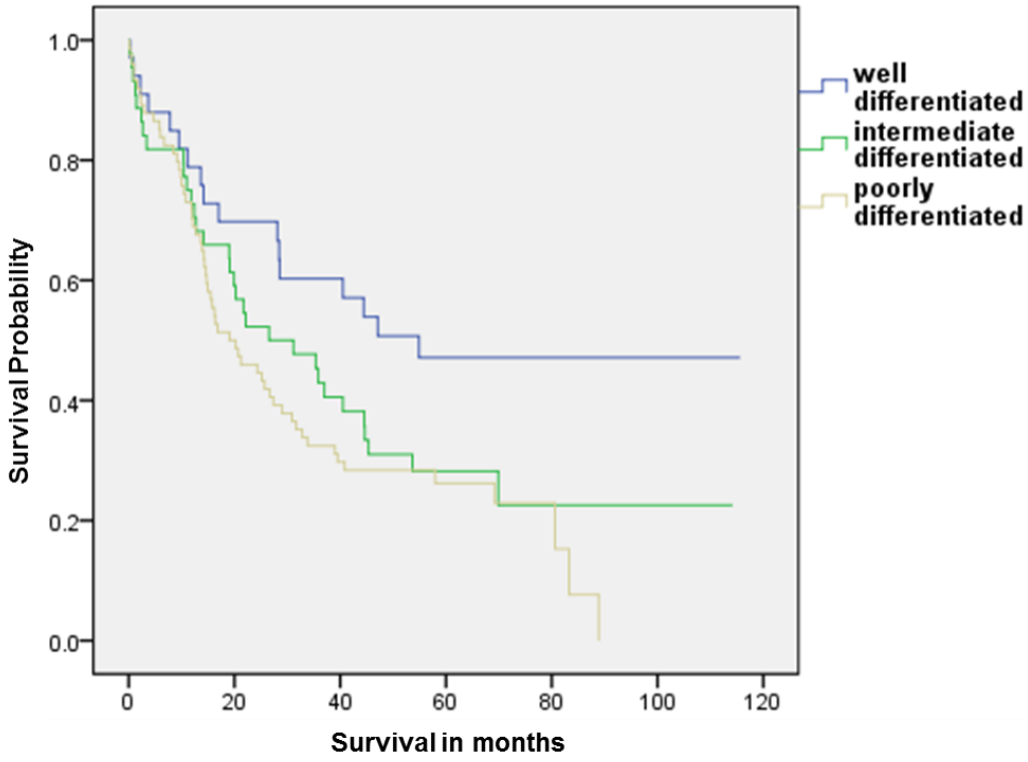

Figure 3-6: The survival times in relation to tumour grade (*p=0.03*).

3.4.5 Residual disease and patient survival

Malignant cells or neoplasia remaining after surgery is referred to as residual disease and the surgical outcome is categorised into three groups; complete, optimal and suboptimal. There is no remaining visually observable malignant tissue in the complete surgical cytoreduction category, whereas less and more than 1 centimetre nodules left at the end of surgery define optimal and suboptimal cytoreduction groups respectively.

54 (32%) of patients from the cohort had complete surgical removal of disease. 30 cases (18%) were grouped in the optimal and 64 (39%) in the suboptimal surgical cytoreduction categories (n=148) and 19 (11%) cases were lost. Residual disease was a highly significant prognostic factor (X^2=60.02, $p<0.0001$), and the 5 year survival probabilities were 66% for complete, 29% for optimal and less than 6% for suboptimal groups (Figure 3-7).

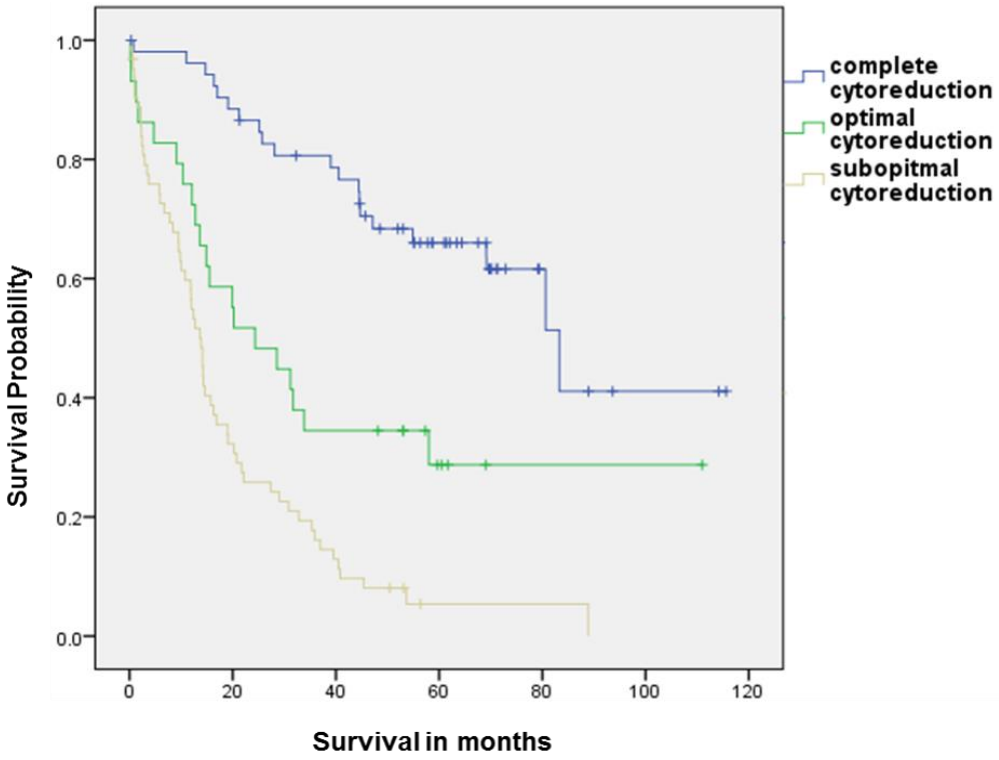

Figure 3-7: The survival times in relation to residual disease (*p<0.0001*).

3.4.6 CA125 and relationship with survival

CA125 is a glycoprotein, which has been used as a biomarker for specific types of cancer, such as ovarian cancer, due to increased level in the blood of patients. However, the role of it as a predictor is controversial because of lack of sensitivity and specificity.

In order to analyse the relationship of survival to available CA125 measurements on blood samples, the subjects were divided into two categories based on the median value of CA125 which was 480 within the range of 6 to 14465. Two groups were ≤ 480 CA125 level (71, 42%) and > 480 CA125 level (68, 41%), and data was missing for 28 (17%) cases with a total n=139.

As the graph shows, individuals with a low level of CA125 appeared to have improved survival in comparison with the high CA125 group, but the difference according to the Log-rank test (X^2=2.92, *p=0.08*) was not significant at the 95% confidence level (Figure 3-8).

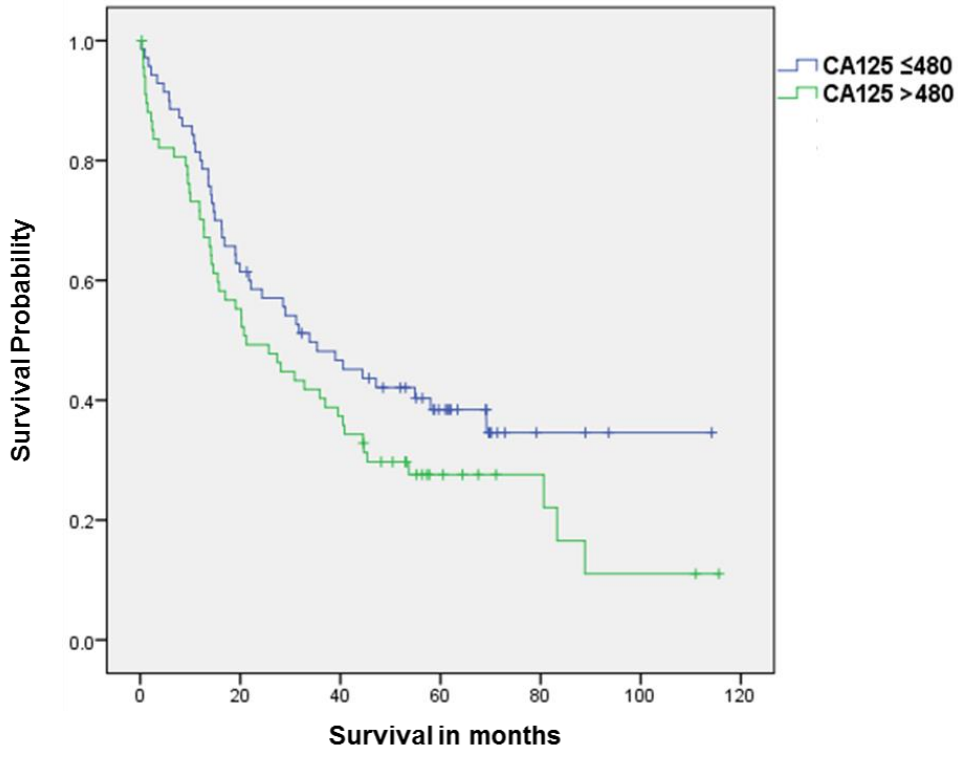

Figure 3-8: The survival times in relation to CA125 (*p=0.08*).

3.4.7 The p53 staining distribution, scores, categories and correlation with survival

From a total of 167 patients, 12 (7%) cores were lost because of processing or not having tumour cells. The staining was predominantly nuclear and ranged from negative to strongly positive (Figure 3-9). This observation is consistent with IHC results reporting nuclear staining of p53 in ovarian cancer tissue samples (Dogan *et al.*, 2005; Psyrri *et al.*, 2007; Corney *et al.*, 2008; Bauerschlag *et al.*, 2010). ROC curve analysis was used to determine a cut-off value and categorise the samples into high and low expression groups (Figure 3-10). The area under the ROC curve, AUC, showing the accuracy of the test was 0.66 and the p-value was 0.002. From a total of 155 samples, 2 (1%) were negative (H-score=0) and 153 (99%) of patients were positive (H-score>0) categorised as 95 (61%) low (H-score ≤9) and 60 (39%) high (10≤H-score≤18) (Figure 3-11).

The analysis of Kaplan-Meier survival in relation to p53 expression shown in Figure 3-12 indicates that the differences between two groups based on the H-score values of p53 expression are statistically significant. Individuals with tumours showing high staining for p53 had a worse survival probability compared with the low p53 staining groups (X^2=11.55, *p=0.001*) confirming p53 as a highly significant prognostic variable. The 5 year survival probabilities were 15% for high score, 43% for low score. The median disease specific survival was 37 months (in the range 0-116) for patients with tumour showing low expression of p53 compared to 19 months for those with tumour expressing high levels of p53.

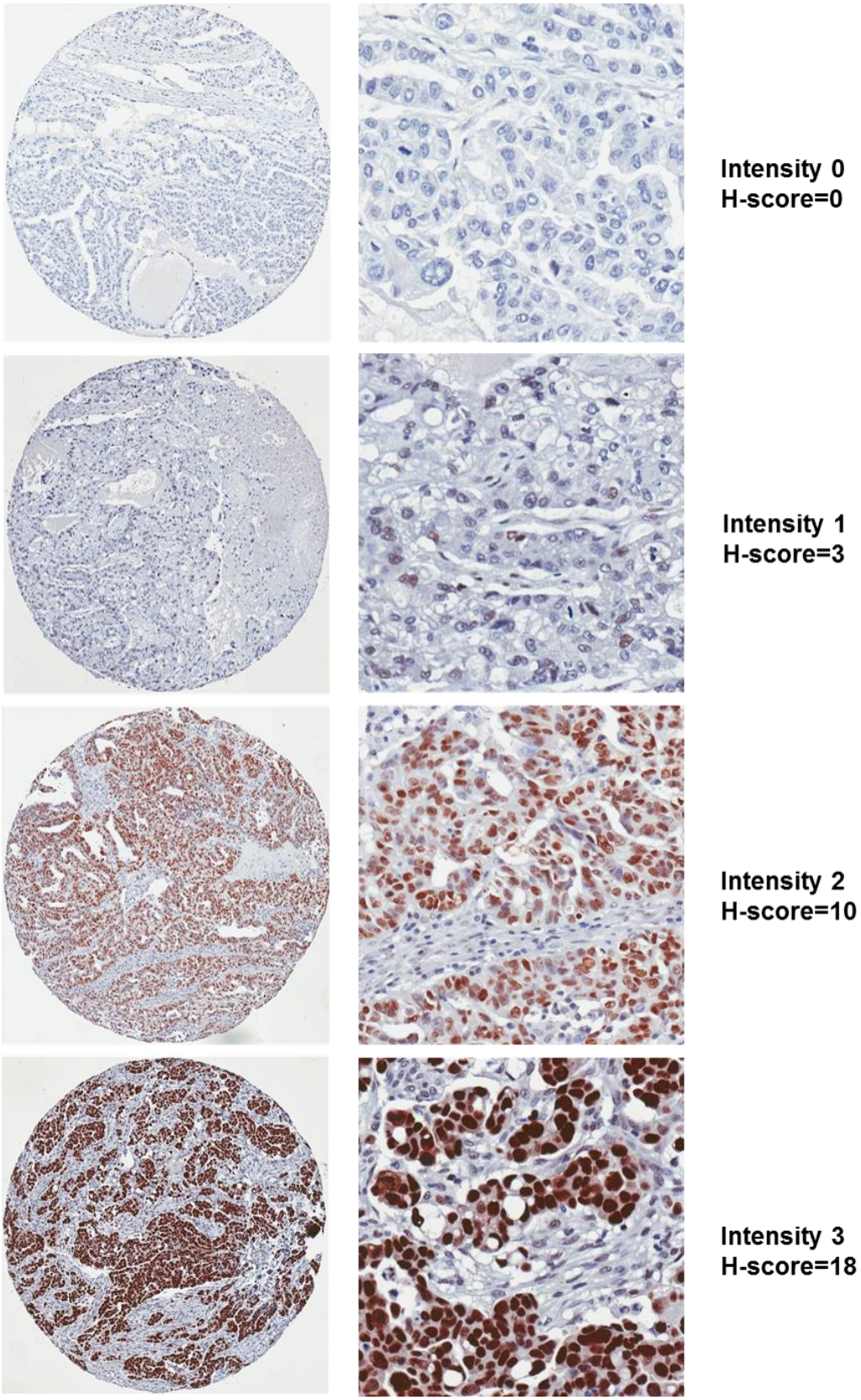

Figure 3-9: Image demonstrating p53-stained samples of tissue cores with different staining intensities and H-scores from the ovarian cancer TMA 1-4 slides.

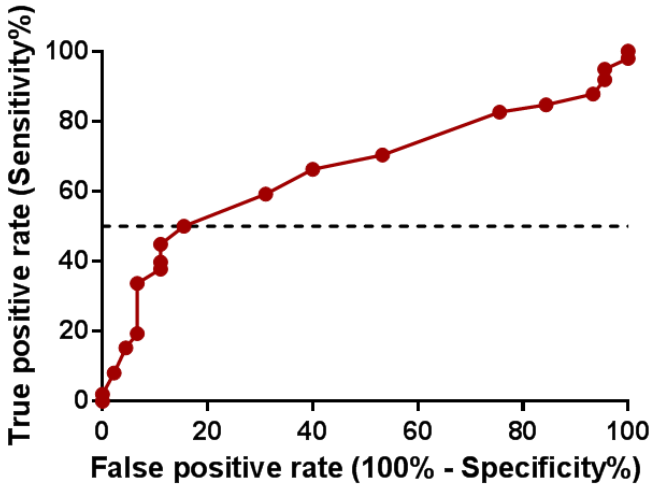

Figure 3-10: The ROC curve in relation to p53 expression demonstrating the area under the curve (AUC=0.66, *P=0.002*), and the optimal categorisation cut-off point for patient samples based on the p53 expression.

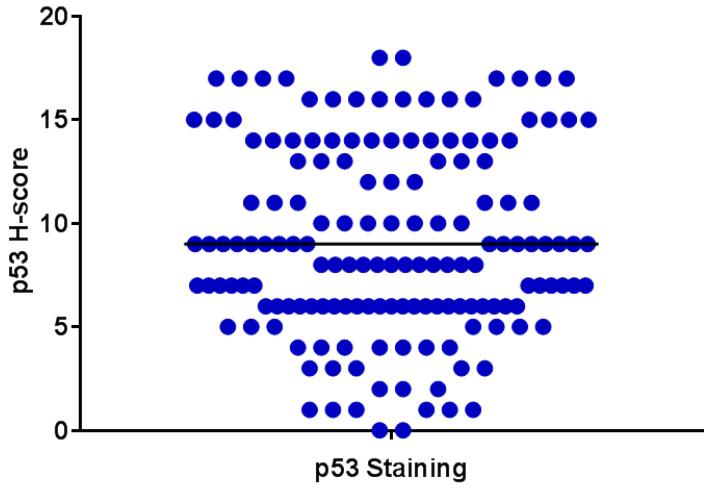

Figure 3-11: The p53 H-score distribution in samples from 155 patients. The horizontal black line represents the median, which equals to the optimal cut-point value gained by ROC curve.

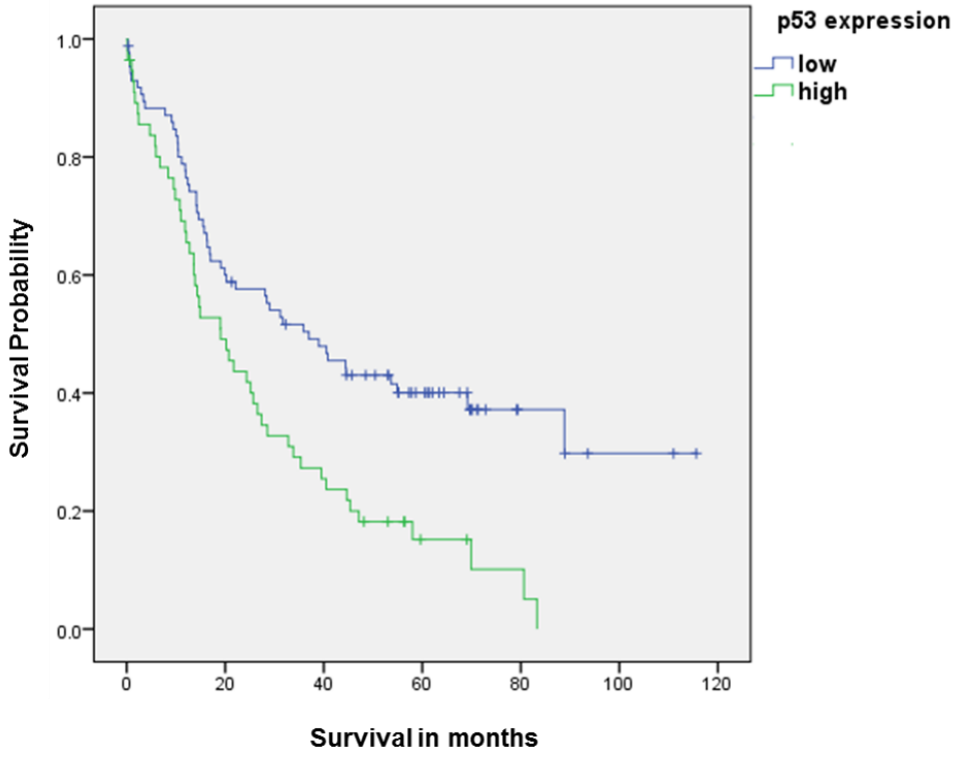

Figure 3-12: The survival times in relation to low (H-Score≤9) and high (10≤H-score≤18) expression of p53 (*p=0.001*).

3.4.8 Univariate analysis of p53 H-score and corresponding clinicopathological data

The Kruskal-Wallis one-way ANOVA test was used to determine whether there are any significant relationships between the level of p53 expression and prognostic variables shown in univariate analysis to be associated with poor survival, including grade, histological subtype, residual disease and stage (Figure 3-13). The results showed that generally p53 staining was higher in groups which are known to have a poor prognosis on the basis of other factors (Figure 3-13). The expression of p53 in patients at low stages of ovarian cancer (I & II) was lower than those at advanced stages (III & IV) (X^2=13.30, *p=0.004*). Both Mann-Witney and Kolmogorov-Smirnov tests are nonparametric tests which compare two unpaired groups of data. However, Mann-Whitney test is mostly sensitive to changes in the median. The Mann-Whitney (*p=0.0002*) and Kolmogorov-Smirnov (*p=0.0008*) tests both showed that the stage III p53 H-score was significantly higher than for stage I. However, there was no significant difference between stage I and stage II or IV. Also, on average individuals with complete debulking surgery had low expression of p53 compared to other groups (X^2=12.80, *p=0.002*). Based on the Mann-Whitney (*p=0.001*) and Kolmogorov-Smirnov (*p=0.005*) tests, p53 staining in patients with complete cytoreductive surgery was significantly lower compared to those with optimal cytoreduction. In comparison, only the Mann-Whitney test (*p=0.019*)

showed that individuals with completely cytoreductive surgery have lower expression of p53 compared to patients with suboptimal cytoreduction. Furthermore, well differentiated tumours had lower expression of p53 (X^2=20.13, *p<0.0001*). The Mann-Whitney (*p=0.0006*, *p<0.0001*) and Kolmogorov-Smirnov (*p=0.014*, *p=0.0006*) tests both indicated that the well differentiated tumours p53 H-score was significantly lower than for moderately and poorly differentiated tumours respectively. The p53 H-scores were also significantly different between histological subtypes (X^2=30.85, *p<0.0001*). The p53 immunostaining H-scores were significantly higher in HGSC than mucinous, (Man-Whitney *p=0.0003* and Kolmogorov-Smirnov *p=0.014*), clear cell (Man-Whitney *p=0.0001* and Kolmogorov-Smirnov *p=0.001*) and endometrioid (Man-Whitney *p=0.02*). The Mann-Whitney test also showed a statistically significant difference in p53 staining between mucinous and endometrioid (*p=0.018*) or LGSC (*p=0.035*) (Figure 3-13).

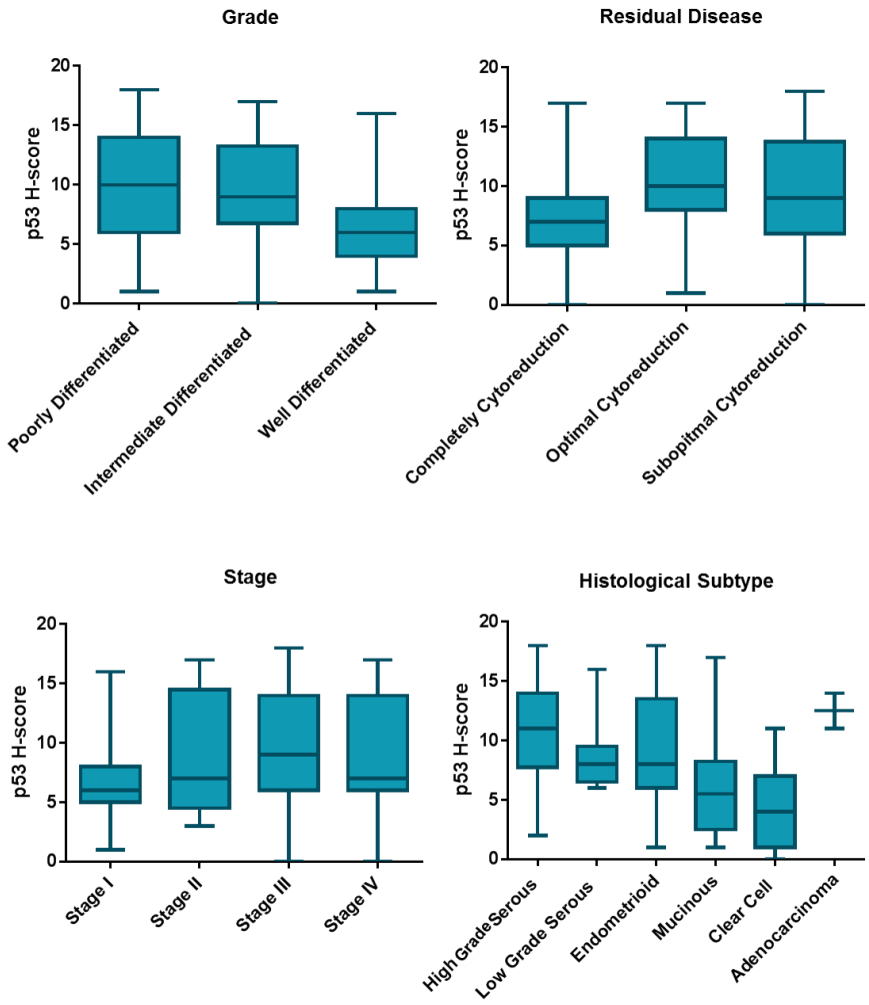

Figure 3-13: Statistical analysis of the relationship between p53 H-score and prognostic variables. Grade (*p<0.0001*), Residual disease (*p=0.002*), Stage (*p=0.004*) and Histological subtype (*p<0.0001*) (Kruskal-Wallis test).

Variable	Number (%)	Mean p53 H-score	P-Value	Median p53 H-score	P-Value
Histological Subtype			**<0.0001*** **		**<0.0001*** **
Adenocarcinoma	**2 (1)**	12.5		12.5	
Clear Cell	15 (9)	4.7		4	
Endometrioid	49 (30)	9.1		8	
High Grade Serous	62 (37)	10.9		11	
Low Grade Serous	13 (8)	8.8		8	
Mucinous	14 (8)	5.9		5.5	
Lost	12 (7)				
Stage			**0.004****		**0.007****
I	27 (16)	6.5		6	
II	13 (8)	8.8		7	
III	83 (50)	9.8		9	
IV	17 (10)	9.1		7	
Lost	27 (16)				
Residual Disease			**0.002****		**0.007****
Complete Cytoreduction (none)	51 (31)	7.6		7	
Optimal Cytoreduction (≤1cm)	27 (16)	10.7		10	
Suboptimal Cytoreduction (>1cm)	60 (36)	9.5		9	
Lost	29 (17)				
Grade			**<0.0001*** **		**<0.0001*** **
Poorly Differentiated	72 (43)	10.2		10	
Moderately Differentiated	42 (25)	9.7		9	
Well Differentiated	40 (24)	6.5		6	
Lost	13 (8)				

Table 3-2: Univariate analysis of p53 H-score and corresponding clinicopathological data. p53 H-score ranged from 0 to 18. Significant p-values are highlighted (Kruskal-Wallis test). *, *p<0.05*; **, *p<0.01*; *, *p<0.001*.**

3.4.9 The p21^{WAF1} staining distribution, scores, categories and relationship to survival

From a total of 167 patients, 11 (7%) cores were missing during processing and 156 (93%) remained to analyse. The staining was confined to the nucleus and ranged from negative to strong positive which is consistent with other IHC staining of p21^{WAF1} on ovarian cancer showing nuclear staining (Anttila *et al.*, 1999; Schmider *et al.*, 2000; Rose *et al.*, 2003a; Bali *et al.*, 2004; Skirnisdottir and Seidal, 2013) (Figure 3-14). To determine the cut-off value and categorise the samples based on the p21^{WAF1} expression, the ROC curve analysis was used. The AUC and p-value were 0.53 and 0.56 for p21^{WAF1} immunohistochemical staining indicating no significant relationship of p21^{WAF1} expression to survival (Figure 3-15). The frequency distribution for p21^{WAF1} staining was 13 (8%) negative and 143 (92%) positive with total cases N=156. Based on the frequency distribution of p21^{WAF1} scoring and the median, p21^{WAF1} scores were grouped as low (H-Score=0-2) and strong (H-Score=3-11) (Figure 3-16). These values were applied to determine relationship of p21^{WAF1} protein expression with survival.

The analysis of Kaplan-Meier survival in relation to p21^{WAF1} expression shown in Figure 3-17. The statistical analysis indicated that the p21^{WAF1} expression was not prognostic variable for survival (X^2=0.22, $p=0.64$).

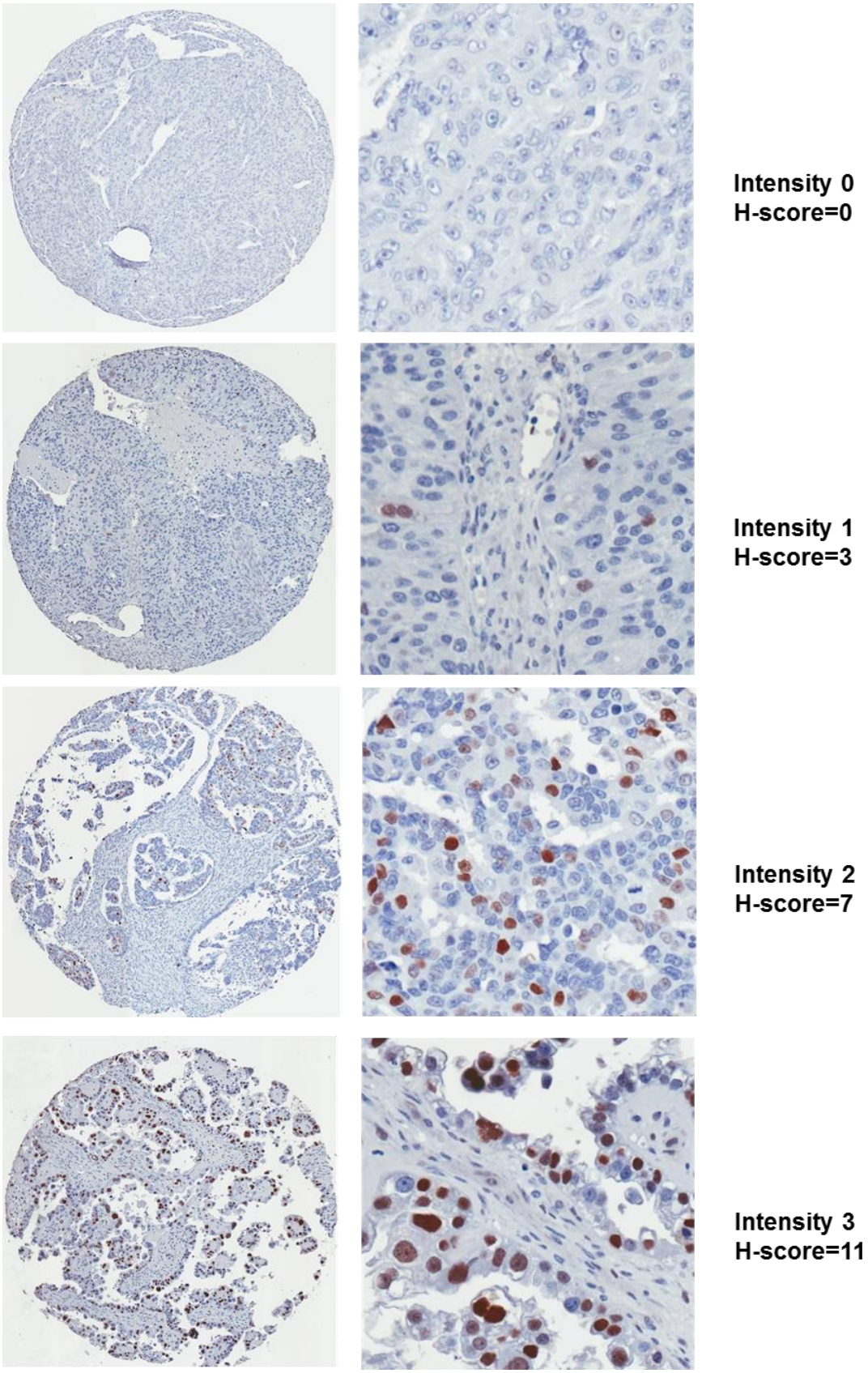

Figure 3-14: Example images of p21^{WAF1}-stained tissue cores from OVCA 1-4 slides. The images were captured using spectrumTM software.

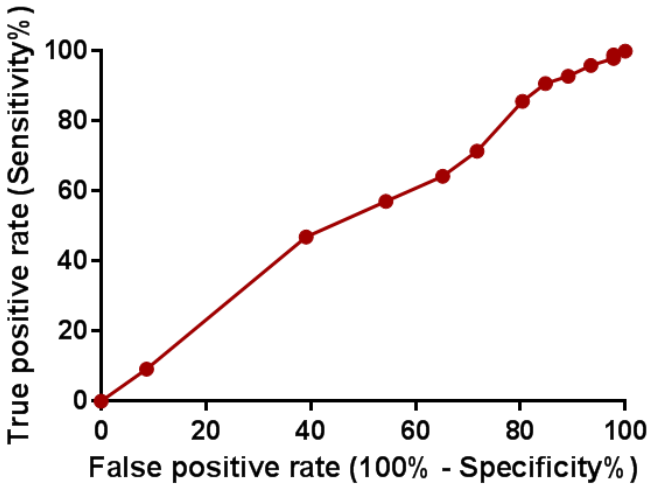

Figure 3-15: The ROC curve for p21^{WAF1} expression in relation to the prognostic value for patient survival (AUC=0.53, *p=0.56*). No clear optimal cut-point was evident.

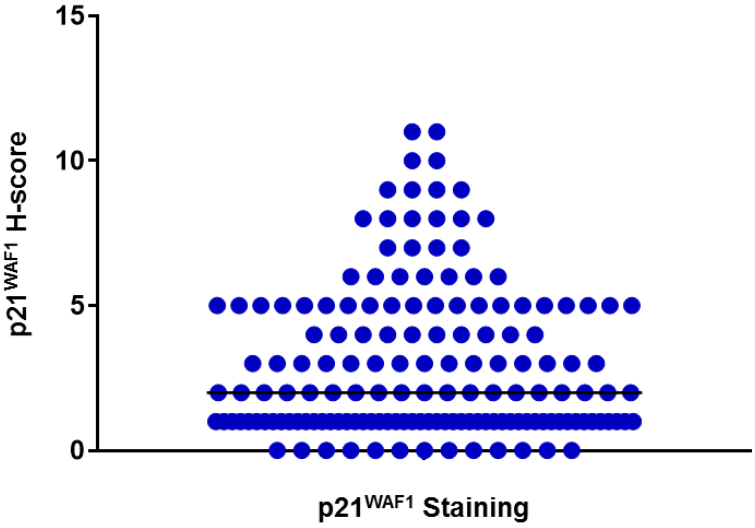

Figure 3-16: The p21^{WAF1} H-score distribution for tumour samples from 156 patients. The horizontal black line represents the median.

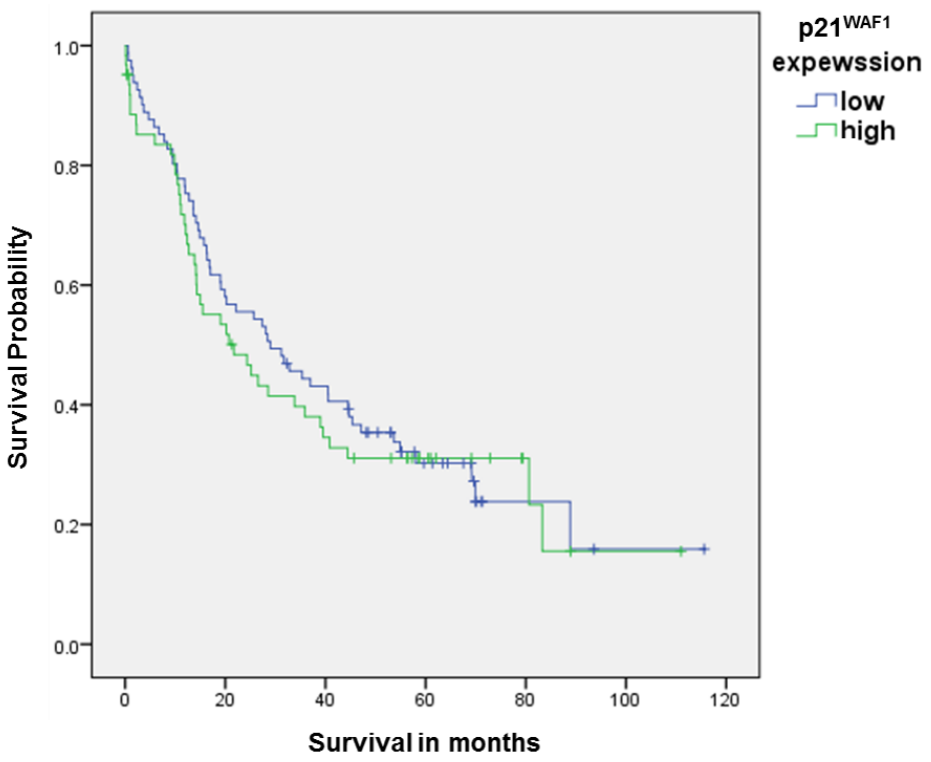

Figure 3-17: The survival times in relation to low (H-Score<2) and high (3≤H-score≤11) p21^{WAF1} expression (*p=0.64*).

3.4.10 Univariate analysis of p21^{WAF1} H-score and corresponding clinicopathological data

A scatter plot of the overall relationship between p53 and p21^{WAF1} expression, showed there was no overall inverse relationship between the expression of p53 and p21^{WAF1} in this dataset (Figure 3-18).

The relationship between p21^{WAF1} H-score and stabilised prognostic variables was examined by the Kruskal-Wallis test. The results showed no significant difference in p21^{WAF1} H-scores amongst the three grades (*p=0.8*). The p21^{WAF1} immunostaining H-scores were not significantly different between different histological subtypes (*p=0.07*) with one missing case (0.6%). No significant difference was observed between the three residual disease sub-groups (p=0.5) (with 18 lost cases, 11.5%) or for the four tumour stages (p=0.2) (with 15 missing cases, 9.6%) (Figure 3-19).

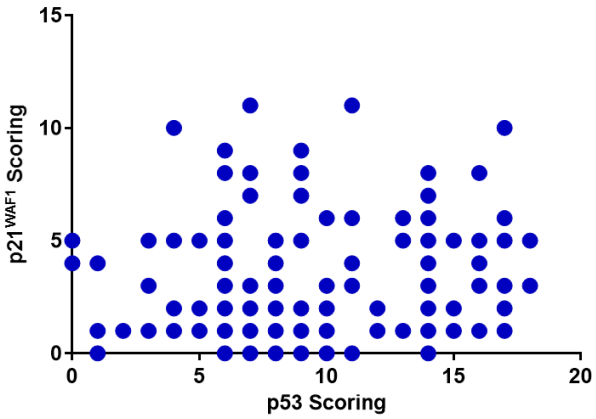

Figure 3-18: A scatter plot showing the lack of correlation between p53 and $p21^{WAF1}$ H-scores.

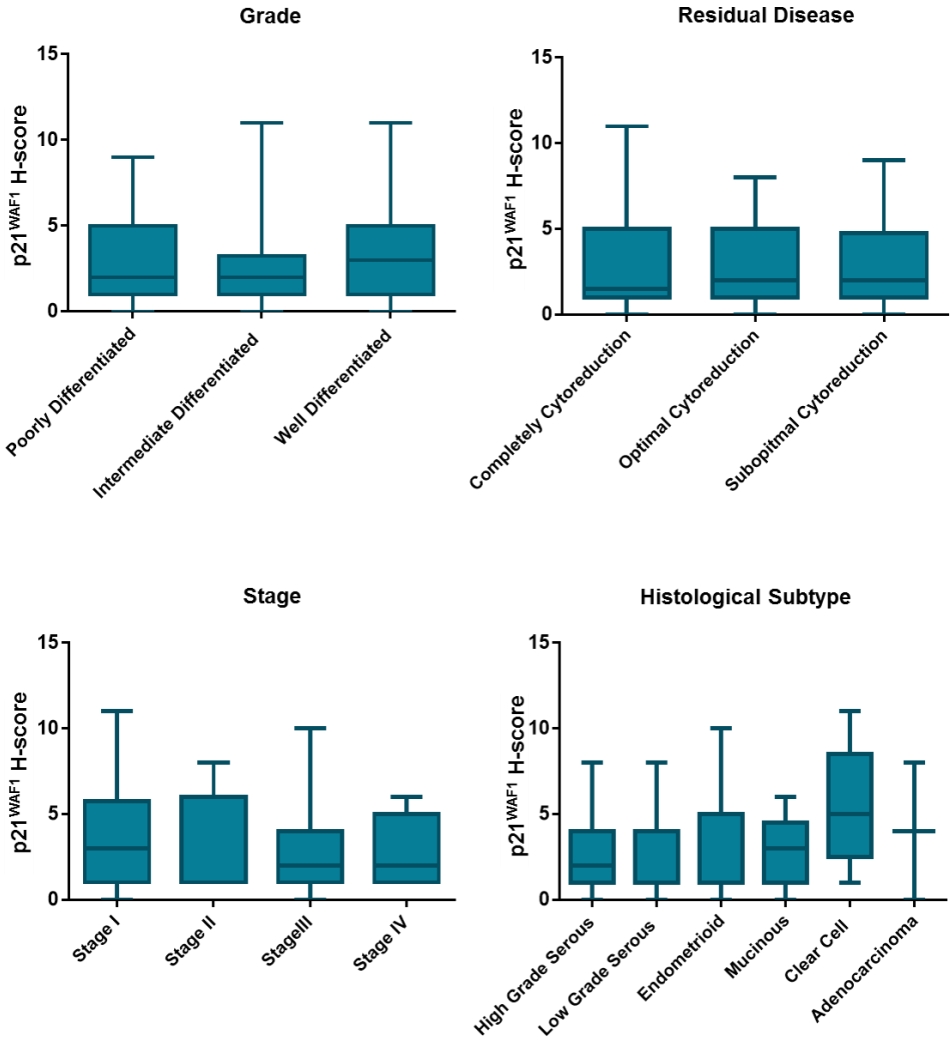

Figure 3-19: The statistical analysis of the relationship between $p21^{WAF1}$ H-score and prognostic variables. Grade (*p=0.80*), Residual disease (*p=0.57*), Stage (*p=0.21*) and Histological subtype (*p=0.07*) (Kruskal-Wallis test). For stage II, low grade serous and endometrioid, the median of H-scores is equal to 25% percentile.

3.4.11 Concomitant expression of p53 and p21^{WAF1} and correlation with survival

To study the relationship between concomitant expression of p53 and p21^{WAF1} and survival, the samples were grouped into four categories based on the level of H-scores for both proteins (Table 3-3). As shown in the Figure 3-20, there was a significant difference between the four categories based on the combination H-score values of p53 and p21^{WAF1} in relation to survival (X^2=11.92, *p=0.01*). However, the effect is related to the p53 expression levels not p21^{WAF1} status. No significant difference was observed between tumours with p53 high expression and p21^{WAF1} low expression compared to those with p53 high expression and p21^{WAF1} high expression (X^2=0.20, *p=0.66*). There was also no significant difference between patients with tumours expressing p53 low and p21^{WAF1} high or p53 low and p21^{WAF1} low (X^2=0.005, *p=0.94*). This indicates that the significant difference is related to the expression of p53, and p21^{WAF1} status does not add anything (Figure 3-20).

Group	p53 H-score	p21^{WAF1} H-score	Number (%)
I	Low (0-9)	Low (0-2)	52 (31)
II	Low (0-9)	High (3-11)	33 (20)
III	High (10-18)	Low (0-2)	30 (18)
IV	High (10-18)	High (3-11)	27 (16)
Lost			25 (15)

Table 3-3: Concomitant expression of p21^{WAF1} and p53 based on the H-score data.

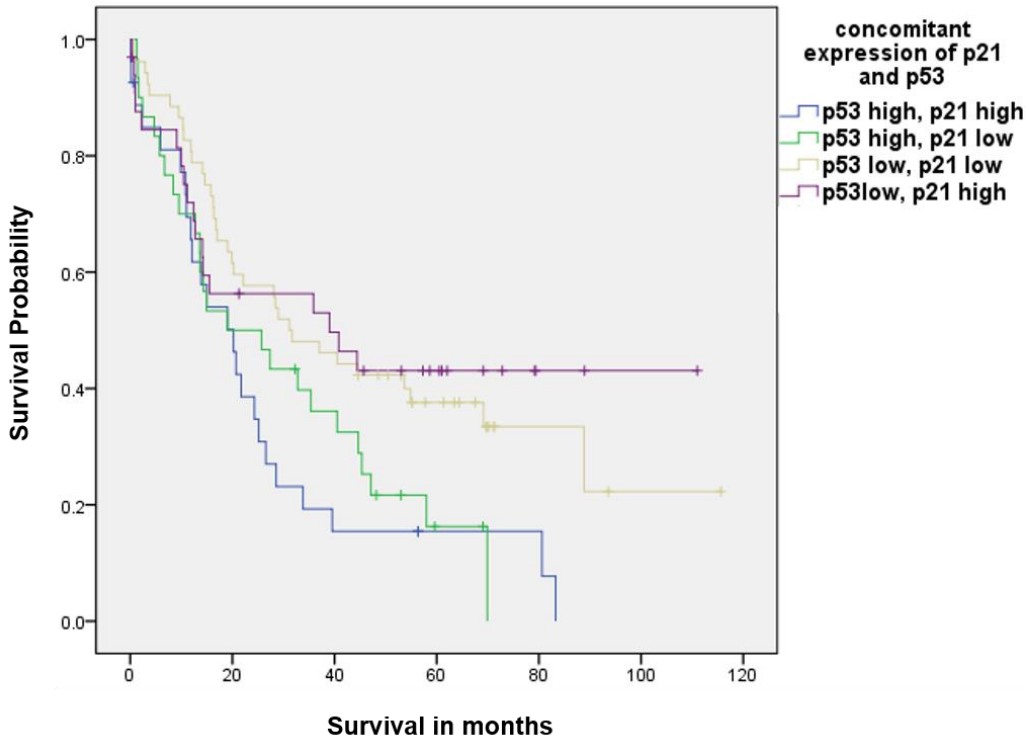

Figure 3-20: The survival times in relation to concomitant expression of p21^{WAF1} and p53 (*p=0.01*).

3.4.12 The MDM2 staining distribution, scores, categories and correlation to survival

The MDM2 IHC showed nuclear staining ranging from negative to strongly positive (Figure 3-21). This pattern of staining was consistent with other IHC findings for MDM2 on ovarian cancer tissue (Baekelandt *et al.*, 1999; Sengupta *et al.*, 2000; Dogan *et al.*, 2005). Of the 167 patients, 22 (13%) cases were lost because of processing or not having tumour cells. The ROC curve analysis gave an AUC=0.56 and *p=0.24*, which indicates no significant relationship between MDM2 expression and survival (Figure 3-22). Overall, 21 (14%) of patients had tumours that were negative and 124 (86%) were positive for MDM2 expression from a total of n=145 cases. The median H-score value was used to categorise the dataset into low (H-Score=0-2) and high (H-Score=3-11) groups to examine whether there was any relationship to patient survival (Figure 3-23).

The Kaplan-Meier survival analysis in relation to MDM2 expression (Figure 3-24) showed no significant correlation between MDM2 expression and survival times (X^2=0.94, *p=0.33*).

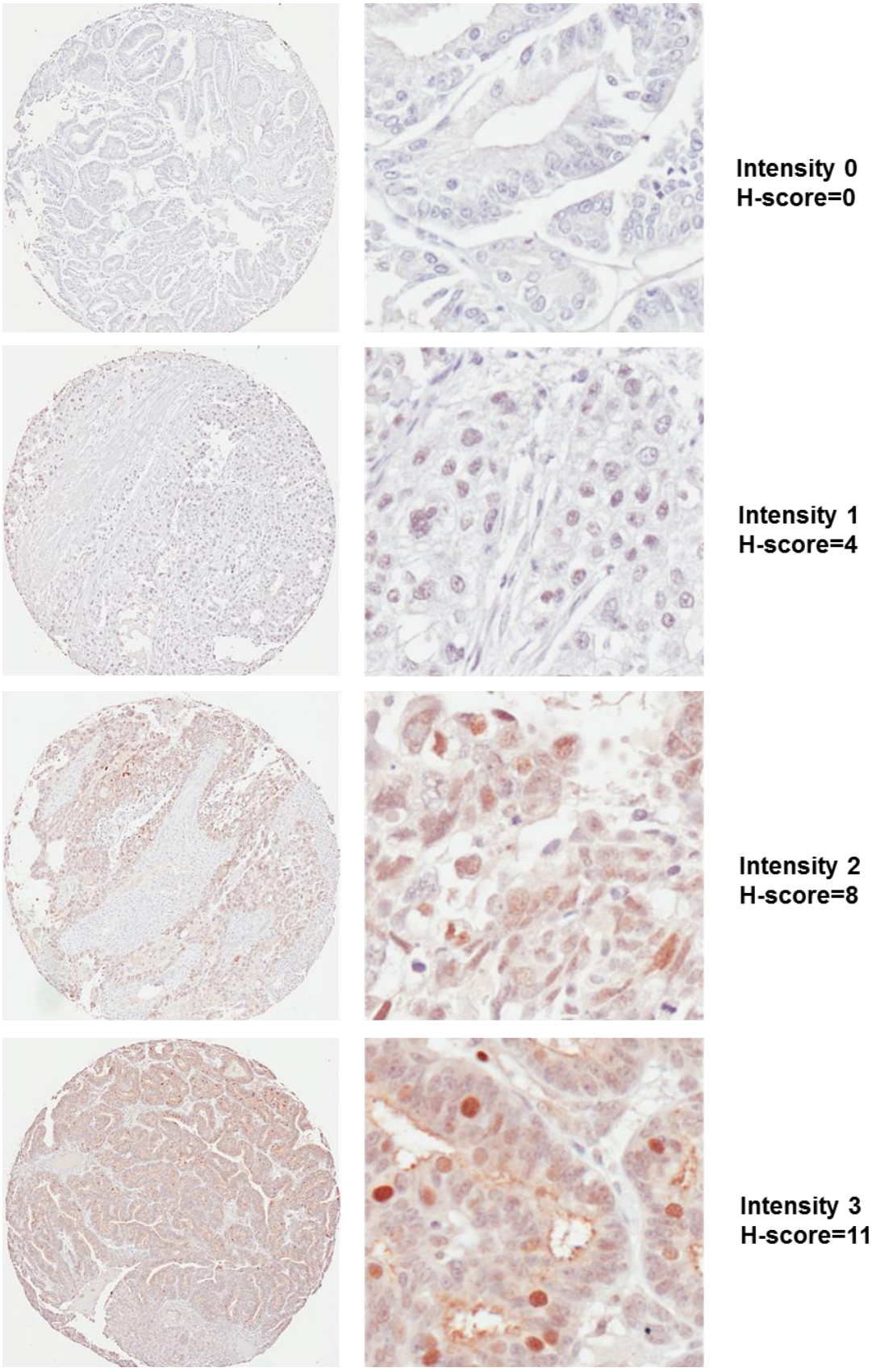

Figure 3-21: Example images of MDM2-stained tissue cores with different intensities from the OVCA1-4 microarray slides.

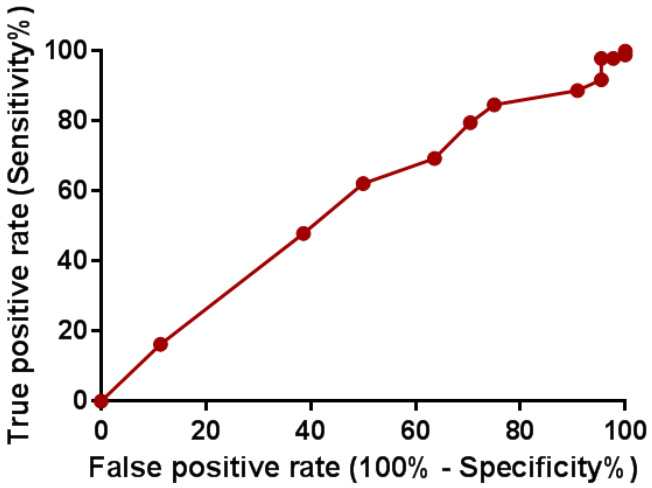

Figure 3-22: The ROC curve analysis for the survival prognostic value of MDM2 expression (AUC=0.56, *p =0.24*) showing no clear optimal cut-off level.

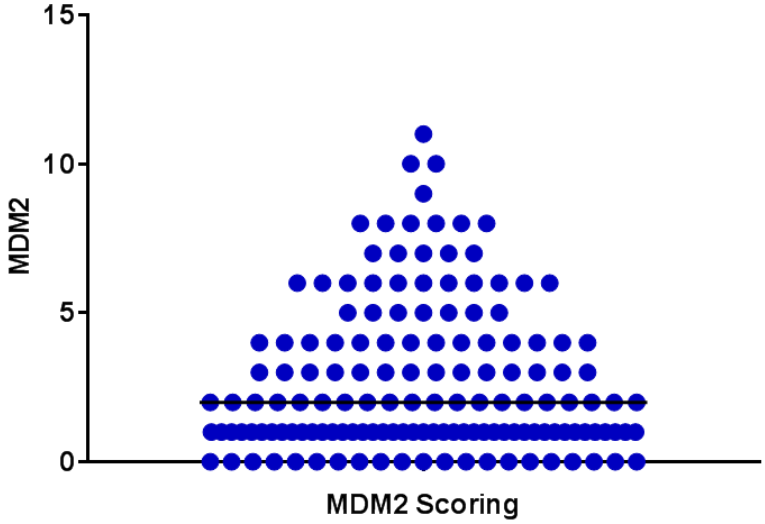

Figure 3-23: The frequency distribution of MDM2 H-score in samples from 145 patients. The horizontal black line represents the median.

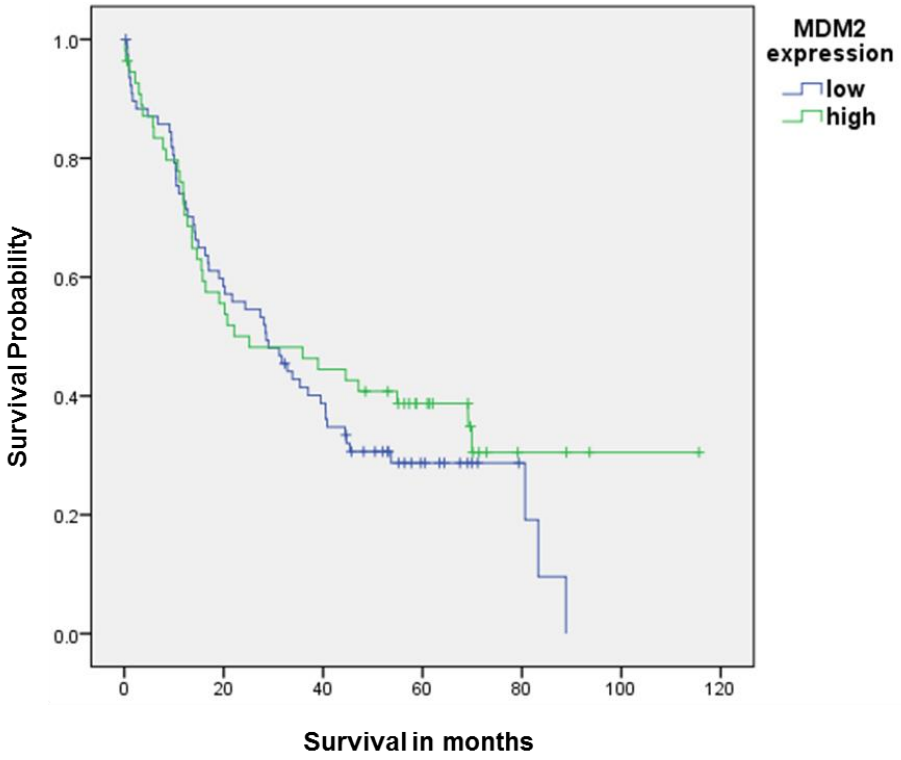

Figure 3-24: The survival times in relation to low (H-Score<2) and high (3≤H-score≤11) MDM2 expression (*p=0.33*).

3.4.13 Univariate analysis of MDM2 H-score and corresponding clinicopathological data

In the TMA data presented here, there was no significant difference in MDM2 H-scores amongst the six different histological subtypes (*p=0.59*), three grades (*p=0.63*), three residual disease groups (p=*0.18*) with 15 (10%) lost cases or the four stage groups (*p=0.36*) with 13 (9%) missing cases (Figure 3-25).

3.4.14 Concomitant expression of p53 and MDM2 and correlation to survival

To investigate the relationship of concomitant expression of p53 and MDM2 with survival, the samples were grouped into four categories based on the H-score data for both proteins. (Table 3-4). The Kaplan-Meier graph showed a significant difference among the four categories based on the combined H-score values of p53 and MDM2 in relation to survival (X^2=10.06, *p=0.018*) (Figure 3-26). The survival probability was significantly better in patients with low expression of p53 and high expression of MDM2 with the highest 5 year probability, 46%, and median disease free survival of 45 months versus individuals with high expression of both p53 and MDM2 who had the worst survival with a 19% 5 year survival probability and

median disease free survival of 14 months (*p=0.02*). Patients with low expression of both p53 and MDM2 had a significantly better overall survival than those with high expression of both p53 and MDM2 (*p=0.04*). There was also a significant difference in overall survival between individuals with low expression of p53 and high expression of MDM2 compared to patients with low expression of MDM2 and high expression of p53 (*p=0.02*).

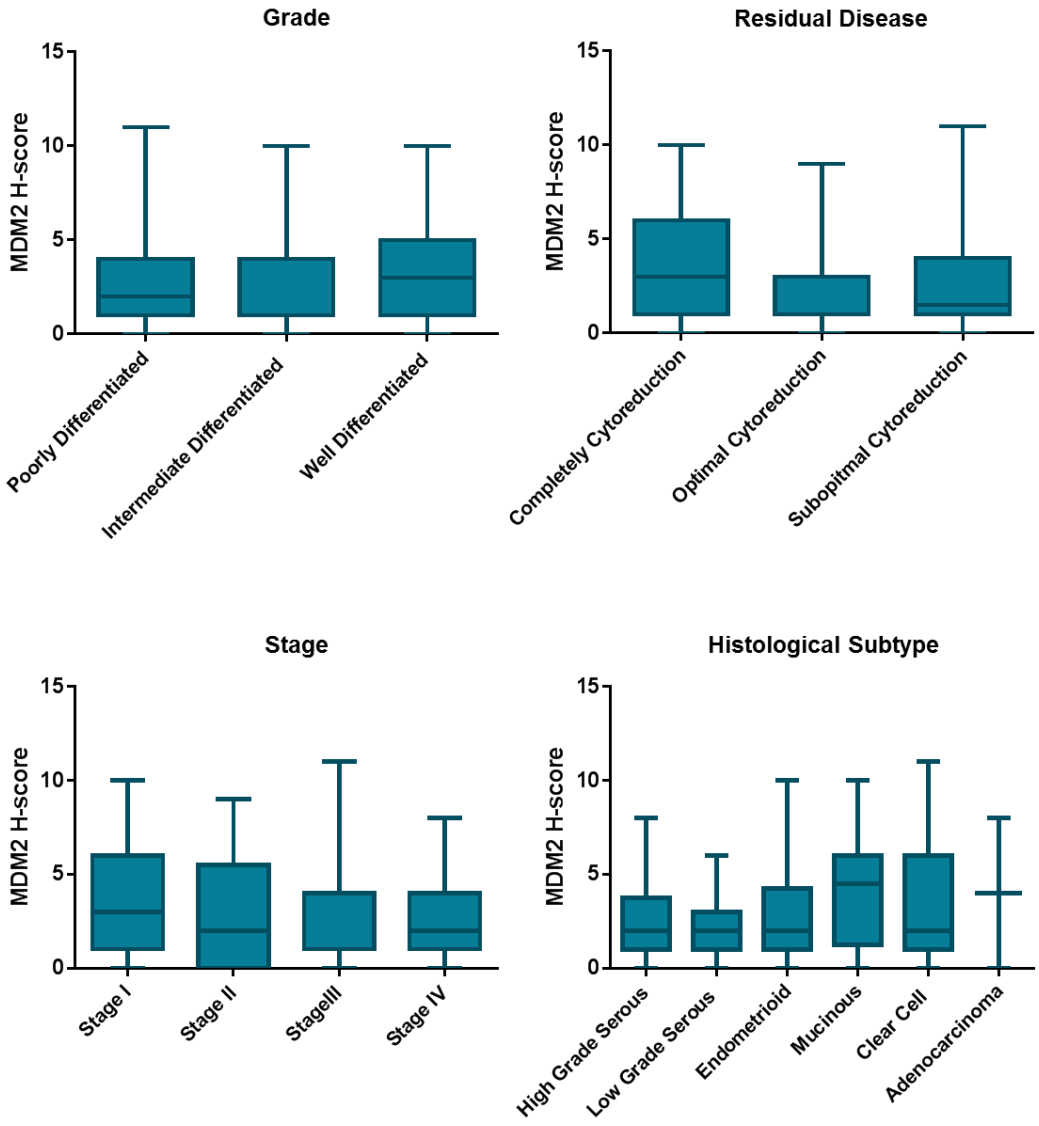

Figure 3-25: Statistical analysis of the relationship between MDM2 H-score and Grade (*p=0.63*), Residual disease (*p=0.19*), Stage (*p=0.36*) and Histological subtype (*p=0.59*) (Kruskal-Wallis test). For intermediate differentiated, optimal cytoreduction and stage III the median of H-scores is equal to 25% percentile.

Group	p53 H-score	MDM2 H-score	Number (%)
I	Low (0-9)	Low (0-2)	63 (38)
II	Low (0-9)	High (3-11)	21 (13)
III	High (10-18)	Low (0-2)	39 (23)
IV	High (10-18)	High (3-11)	10 (6)
Lost			34 (20)

Table 3-4: Concomitant expression of MDM2 and p53 based on the H-score data.

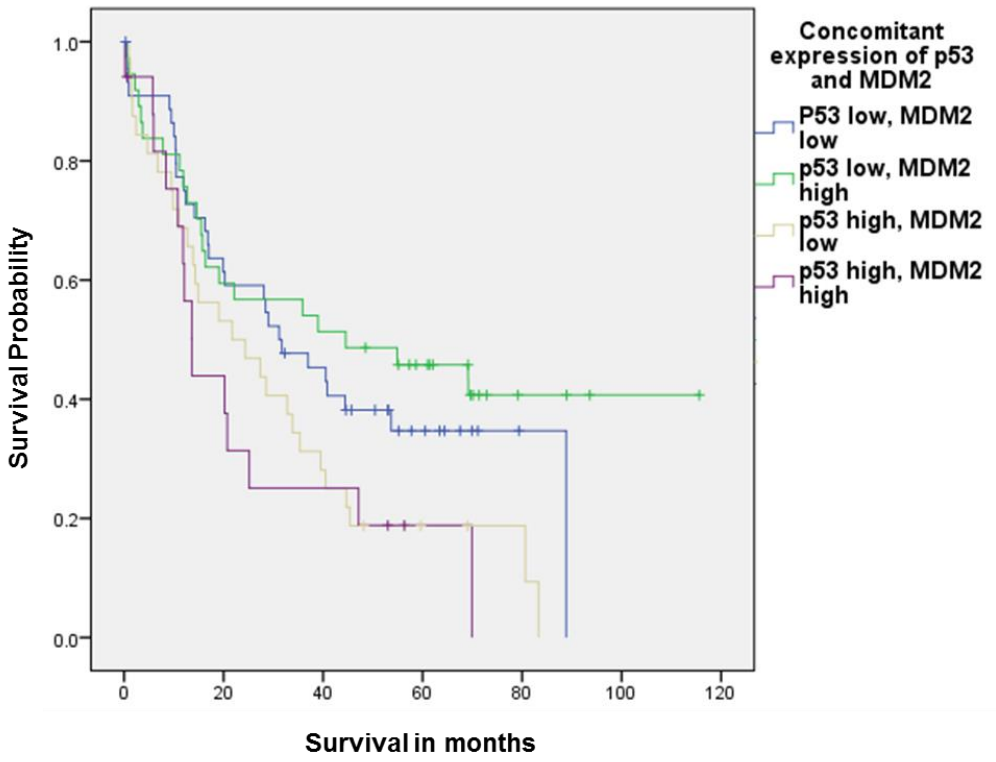

Figure 3-26: The survival times in relation to concomitant expression of MDM2 and p53 (*p=0.018*).

3.4.15 WIP1 staining, distributions, scores, categories and correlation to survival

The WIP1 IHC showed mostly nuclear and occasionally cytoplasmic staining on the OVCA3-4 slides, ranging from weak to strongly positive (Figure 3-27). From a total of 69 patients, 7 (10%) of WIP1 stained cores were lost due to processing or not having tumour cells. No significant correlation of WIP1 expression to survival was indicated by the ROC curve analysis (AUC=0.56, *p=0.48*) (Figure 3-28). WIP1 IHC positive staining was observed for all samples (n=62). The median WIP1 H-score was used to categorise samples as low (H-Score=4-8), and high (H-Score=9-13) (Figure 3-29). These values were applied to examine the relationship of WIP1 protein expression to patient survival.

The Kaplan-Meier graph showed no significant difference in survival between the two groups of individuals based on WIP1expression (X^2=0.47, *p=0.49*) (Figure 3-30). The 5 year survival was 35% for the high score group and 40% for the low score group, with a median disease specific survival of 31 months for both categories.

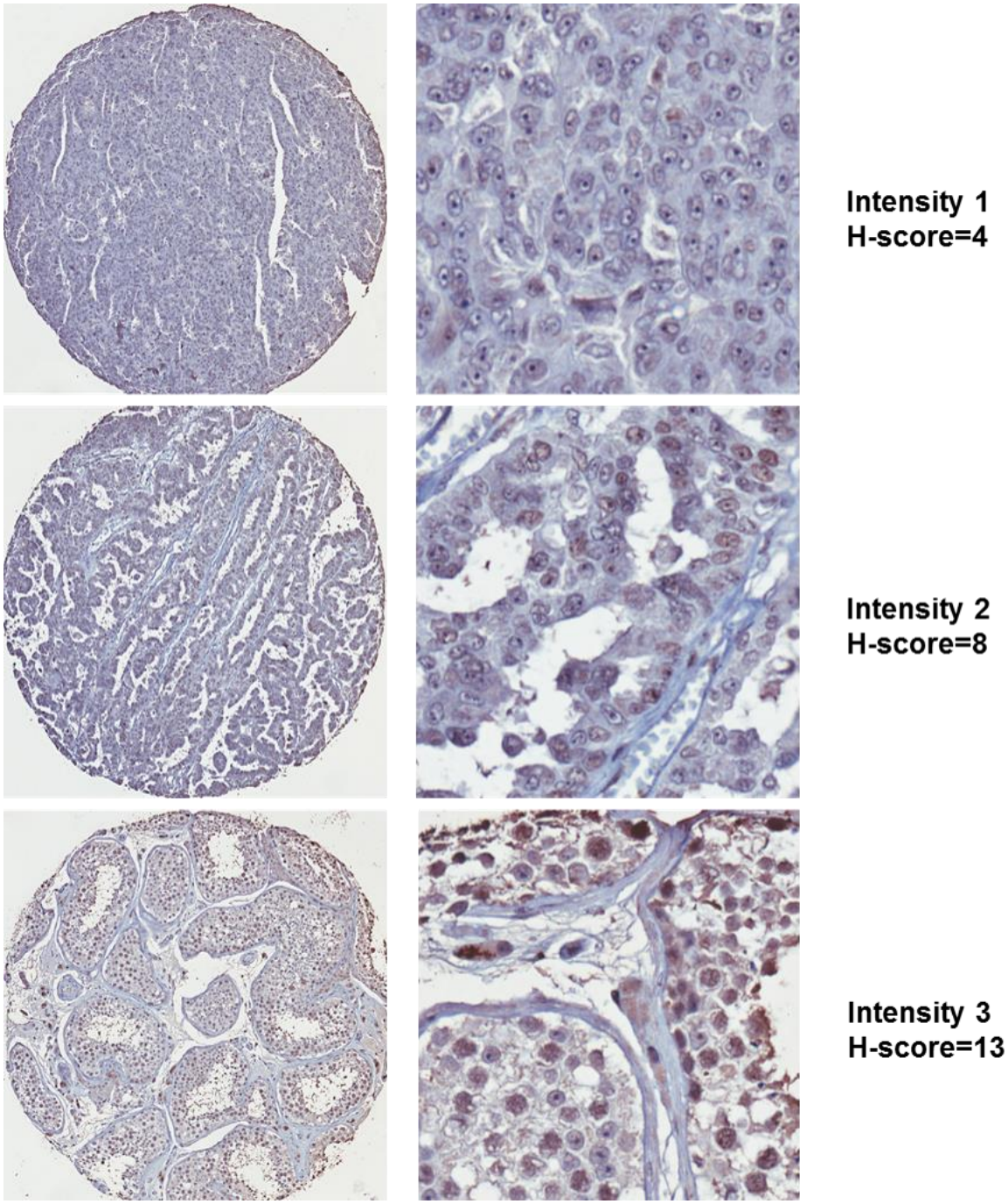

Figure 3-27: Example images showing WIP1-stained samples of tissue cores with different intensities from the OVCA3-4 TMA slides.

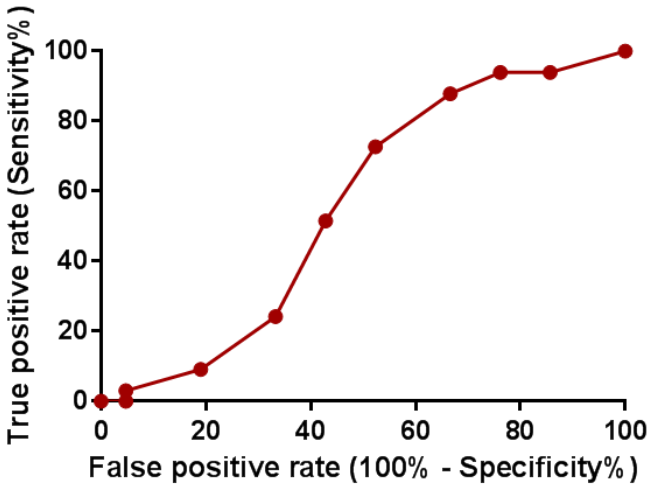

Figure 3-28: The ROC curve for the survival prognostic value of WIP1 expression (AUC=0.56, *p=0.48*) showing no clear optimal cut-off levels based on the WIP1 expression.

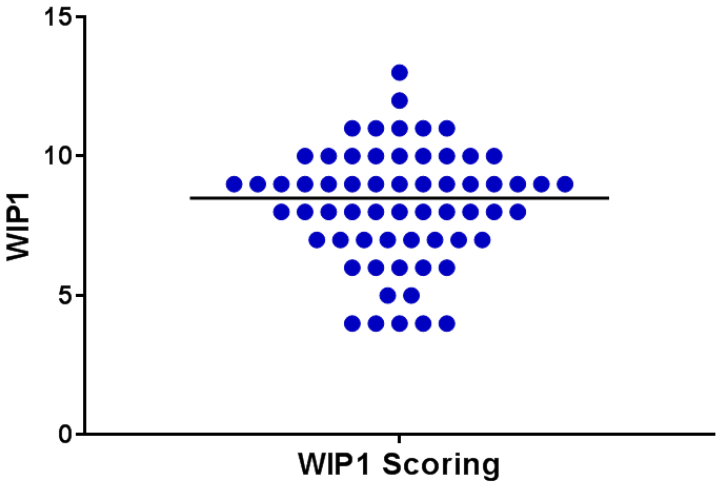

Figure 3-29: The frequency distribution of WIP1 H-score in samples from 62 patients. The horizontal black line represents the median.

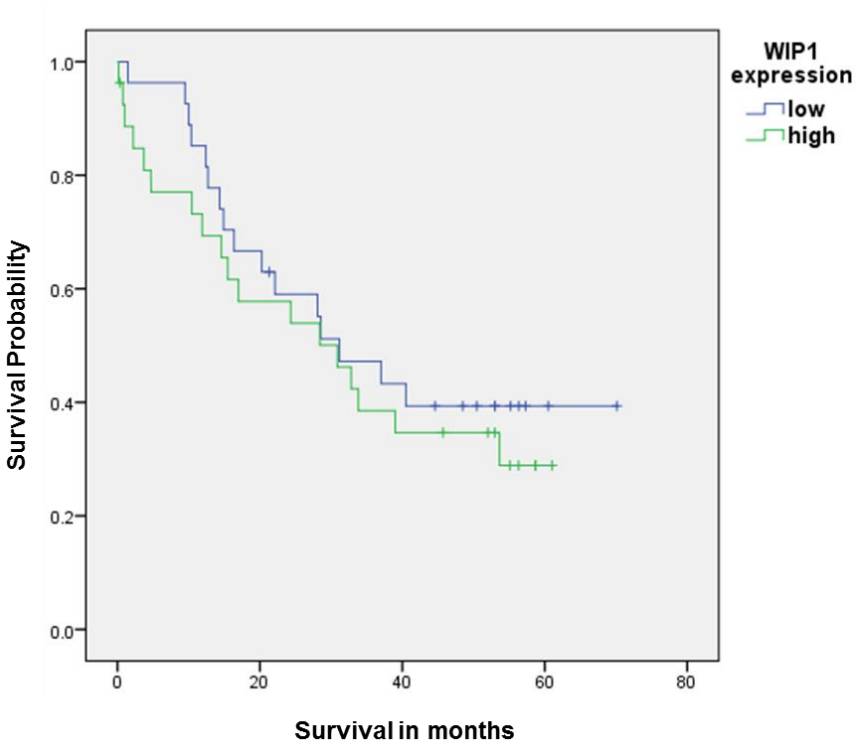

Figure 3-30: The survival times in relation to low (4≤H-score≤8) and high (9≤H-score≤13) WIP1 expression (*p=0.49*).

3.4.16 Univariate analysis of WIP1 H-score and corresponding clinicopathological data

No significant difference in WIP1 H-scores was observed between the six groups based on histological subtypes (*p=0.26*). A significant difference was shown neither for the four stage groups (*p=0.37*) with 6 missing cases (10%) nor for the three residual disease groups (*p=0.46*) with 8 lost cases (13%). The only significant difference in WIP1 IHC H-scores was amongst the three grades (X^2=6.61, *p=0.03*) with one missing case (2%). The Mann-Whitney test indicated that the well differentiated tumours WIP1 H-score was significantly higher than that of poorly differentiated tumours (*p=0.001*) while the difference between the well differentiated tumours WIP1 H-score and that of intermediately differentiate tumours was marginally significant *(p=0.05*) (Figure 3-31).

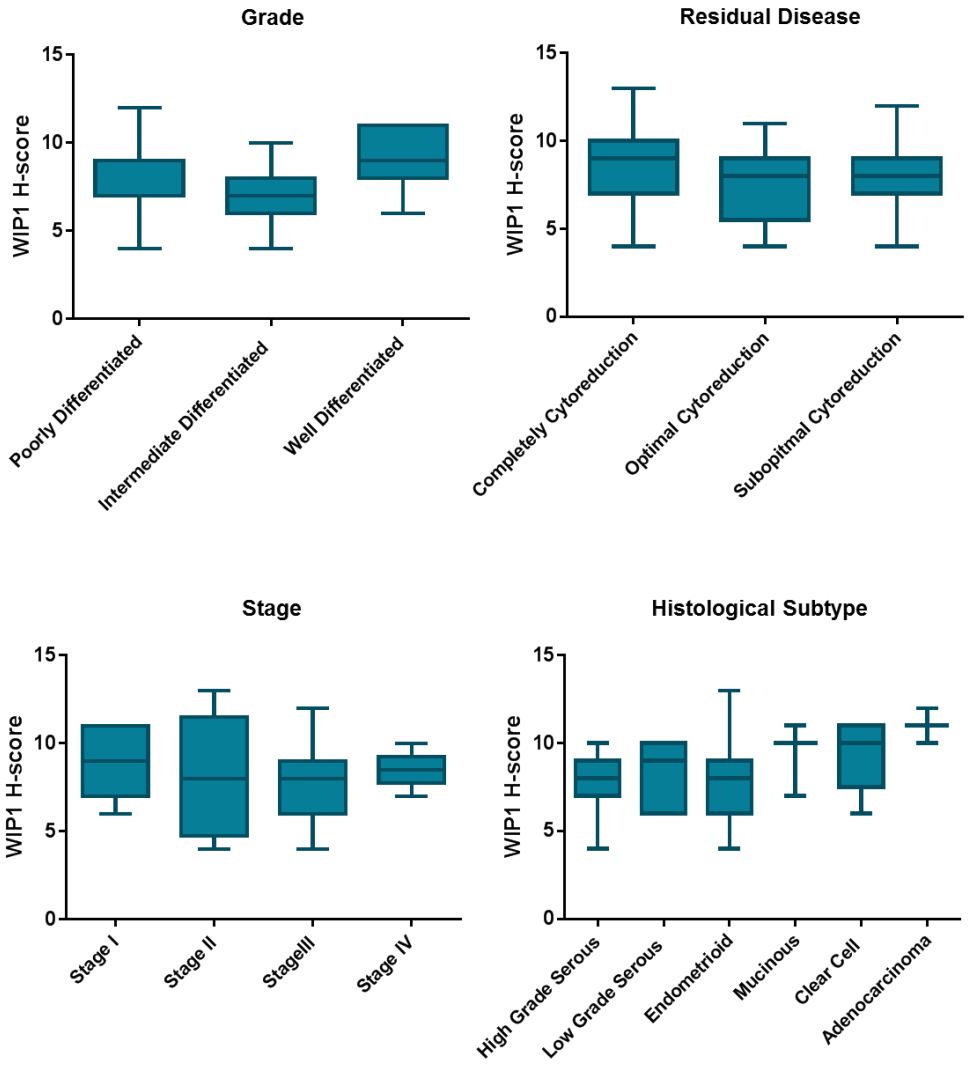

Figure 3-31: The statistical analysis of the relationship between WIP1 H-score and Grade (*p=0.03*), Residual disease (*p=0.46*), Stage (*p=0.37*) and Histological subtype (*p=0.12*) (Kruskal-Wallis test). For poorly differentiated, the median of H-scores is equal to 25% percentile.

3.4.1 Concomitant expression of p53 and WIP1 and relationship to survival

The H-scores for both proteins were categorised into four groups to study the relationship between concomitant expression of p53 and WIP1 with survival (Table 3-5). As shown in Figure 3-32, no significant differences were found among the four groups based on the H-score values of both proteins in relation to survival (X^2=1.78, *p=0.62*).

Group	p53 H-score	WIP1 H-score	Number (%)
I	Low (0-9)	Low (4-8)	20 (32)
II	Low (0-9)	High (9-13)	16 (26)
III	High (10-18)	Low (4-8)	6 (10)
IV	High (10-18)	High (9-13)	8 (13)
Lost			12 (19)

Table 3-5: Concomitant expression of p53 and WIP1 based on the H-score values.

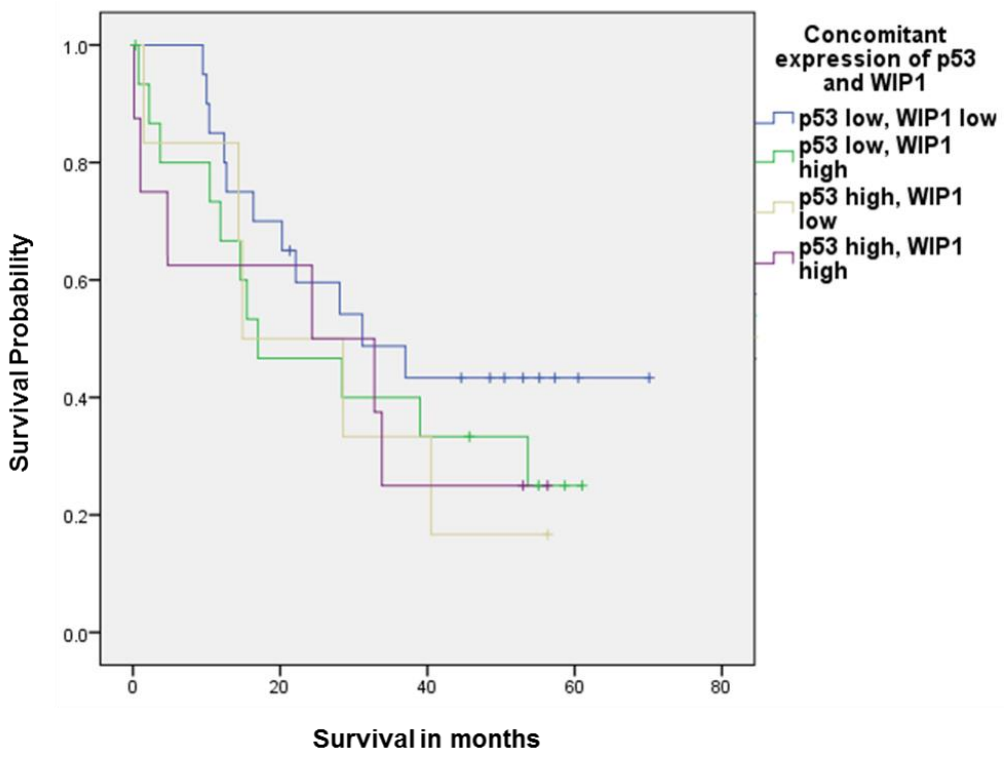

Figure 3-32: The survival times in relation to concomitant expression of p53 and WIP1 (*p=0.62*).

3.4.2 Multivariate cox regression analysis of survival

A forward stepwise multivariate analysis was then performed including variables shown to be significant predictors of survival difference on univariate analysis including grade, residual disease, stage, histological subtype, p53 and coexpression of p53 and $p21^{WAF1}$ or MDM2. In multivariate analysis, stage (*p=0.002*), histological subtype (*p=0.04*) and residual disease (*p=0.01*) were identified as independent prognostic variables for patients with ovarian cancer, with stage as the most significant indicator. In contrast grade (*p=0.47*), p53 (*p=0.23*), and concomitant expression of p53 and $p21^{WAF1}$ (*p=0.22*) or p53 and MDM2 (*p=0.06*) do not appear as independent prognostic variables in multivariate analysis (Table 3-6).

	Overall Survival	
Different variables	**Univariate analysis P-value**	**Multivariate analysis P-value**
Histological Subtype	0.01*	0.04*
Residual Disease	<0.0001***	0.01*
Stage	<0.0001***	0.002**
Grade	0.03*	0.47
CA125	0.08	
p53	0.001**	0.23
$p21^{WAF1}$	0.54	
MDM2	0.50	
WIP1	0.49	
Concomitant expression of p53 and $p21^{WAF1}$	0.01*	0.22
Concomitant expression of p53 and MDM2	0.02*	0.06
Concomitant expression of p53 and WIP1	0.62	

Table 3-6: Univariate and multivariate Cox regression analysis of p53/its downstream targets and survival. Histological subtype, stage and residual disease retain significance as independent prognostic variables for the OVCA 1-4 cohort. *, p<0.05; **, p<0.01; ***, p<0.001.

3.5 Discussion

Ovarian cancer is the fifth leading cause of cancer-related death in women (Zhan *et al.*, 2013). Although several prognostic variables including serum CA125 levels, stage, residual disease and histological subtype have been used to detect and define risk categories in ovarian cancer, identification of new prognostic markers is necessary to gain benefit from effective therapies (Dogan *et al.*, 2005; Huang *et al.*, 2010). A number of studies have examined the correlation between expression of p53, $p21^{WAF1}$, and MDM2 and survival in ovarian cancer; however, the findings are controversial (Anttila *et al.*, 1999; Baekelandt *et al.*, 1999; Schmider *et al.*, 2000; Harlozinska *et al.*, 2002; Dogan *et al.*, 2005; Psyrri *et al.*, 2007; Bartel *et al.*, 2008).

Given the central role of a functional p53 signalling pathway in cell cycle arrest, apoptosis, and response to chemotherapy and the previously reported controversial results, the first part of the study set out with the aim of assessing the importance of p53 and its downstream targets including $p21^{WAF1}$, MDM2 and WIP1 as biomarkers to forecast the likely overall survival. This is the first study to investigate WIP1 expression as a potential prognostic variable in ovarian cancer.

3.5.1 Overall survival and established prognostic variables

A comparison to previously published cohorts was performed to evaluate and validate the clinicopathological data for the cohort of patients used for the OVCA 1-4 TMA set. The five year overall survival was 32% for the cohort in this study which is in line with those of previous studies, 25% (Bartel *et al.*, 2008), 29% (Corney *et al.*, 2008), 30% (Agarwal and Kaye, 2003), 30.6% (Zhan *et al.*, 2013) and 35% (Dogan *et al.*, 2005). In terms of histological subtypes, serous is the most common subtype in ovarian cancer accounting for up to 80%, compared to 10-20% of endometrioid/mucinous and 5-10% of clear cell tumours (Colombo *et al.*, 2010; Wang *et al.*, 2012; Ledermann *et al.*, 2013; Sung *et al.*, 2014).

In the present study, the serous histological subtype (47%) represented the highest proportion of samples, whereas the adenocarcinoma (2%) were the lowest proportion of samples. The proportion of mucinous (11%) and clear cell (10%) was in accordance with other studies although the frequency of endometrioid (30%) was higher and HGSC was lower than previously reported studies. The frequency distribution of HGSC is 60-80% of ovarian epithelial carcinoma (van Niekerk *et al.*, 2011; Di Leva and Croce, 2013; Hua *et al.*, 2016) and it is 10-20% for endometrioid (Cho and Shih, 2009; Niekerk *et al.*, 2011). The higher frequency

of endometrioid and lower frequency of serous particularly for HGSC than what expected might be because of not performing pathology review to update the diagnoses of these archival samples. Another possible explanation is that the detection of HGSC from high grade endometrioid can be very difficult as some pathologists classify high grade endometrioid as HGSC with endometrioid features or as a mixture of HGSC and high grade endometrioid (Kurman and Shih, 2011). Therefore, it might be due to pathological misclassification.

Univariate analysis of overall survival indicated residual disease, FIGO stage, histological subtype and grade as significant prognostic factors ($p<0.05$). The subjects with HGSC and clear cell tumour had the worst 5-year specific survival, which is consistent with the established knowledge that these subtypes are more aggressive than others. Also, patients with advanced stages of disease, poorly differentiated tumour and incompletely resected residual disease had the worst 5-year specific survival, which is comparable to other studies (Reles *et al.*, 2001; Ding *et al.*, 2013). CA125 was not a significant prognostic variable in this study ($p>0.05$) consistent with data obtained by Osman (2008). The results of multivariate analysis confirmed stage, histological subtype and residual disease as independent prognostic variables while grade was not retained as an independent prognostic variable, as also found by other studies (Colombo *et al.*, 2010; Braicu *et al.*, 2011; Bamias *et al.*, 2012). The consistency with established observations serves to validate the clinicopathological data for the cohort of patients used for the OVCA 1-4 TMA set.

3.5.2 The p53 expression and relationship to survival and other prognostic variables

In this TMA study, the p53 H-scores were categorised into low and high groups based on the ROC curve analysis. From a total of 155 patients, 95 (61%) and 60 (39%) had low and high expression of p53 respectively. Interestingly, the observed differences in survival rates of patients with tumours showing low or high p53 expression was statistically significant (*$p=0.001$*), and supports p53 expression in univariate analysis as a prognostic factor in ovarian cancer. Individuals with tumours expressing a high level of p53 experience worse survival with 15% five year disease specific survival compared to patients with low p53 expression having a 44% rate of survival.

These results are in agreement with other studies which found a significant better overall survival (Schuyer *et al.*, 2001; Nakayama *et al.*, 2003; Dogan *et al.*, 2005; Bartel *et al.*, 2008; Leffers *et al.*, 2008; Vartiainen *et al.*, 2008; Skirnisdottir and Seidal, 2013) or marginally

significant better overall survival (Reles *et al.*, 2001; Darcy *et al.*, 2008) for patients whose tumours have low expression of p53 compared to those with high expression of p53.

In contrast, other studies indicated no significant association between p53 expression levels and overall survival (Shahin *et al.*, 2000; Sagarra *et al.*, 2002; Havrilesky *et al.*, 2003; Gadducci *et al.*, 2006; Green *et al.*, 2006; Tomsova *et al.*, 2008; Rechsteiner *et al.*, 2013). This inconsistency may be due to various options applied to classify the samples, sample size, type or histology of cancer and stage of disease. Darcy *et al*. (2008) investigated the prognostic value of p53 expression in two different cohorts named GOG-157 and GOG-111 including patients with high risk early stage or advanced stage epithelial ovarian cancer respectively. As the results of these cohorts illustrated in Table 3-7, advanced stages of disease decreased the significance of p53 expression.

The p53 Meta-analysis study was performed including 53 studies on the prognostic value of p53 expression. The results indicated that p53 protein expression have a modest effect on prognosis and overall survival despite the presence of heterogeneity between studies. Nevertheless p53 protein expression is unlikely to be useful as a predictive biomarker in clinical practice (de Graeff *et al.*, 2009). This study also showed that homogeneity patients in different subgroups such as patients with a particular differentiation grade or disease stage is important for biomarker analysis. For example, FIGO stage distribution affects study outcome using Meta-regression analysis. The p53 lost its significance prognostic value when the meta-analysis was limited to studies reporting results for stage III/IV tumours. In addition to this meta-analysis study, several studies performed on patients at advanced disease stages showed no significant association between p53 expression status and overall survival (Table 3-7). Antonia *et al*. (2002) stained ovarian carcinoma sections with three different primary antibodies against p53 protein (DO-7, PAb240, and PAb1620). The intensity of staining and percentage of reactive cells depended on the antibody used, and were higher with DO-7 antibody than other antibodies.

The observed differences between varying levels of p53 expression and clinicopathological prognostic indicators are very interesting. They demonstrate how p53 staining is higher in groups which are known to have a poor prognosis on the basis of other factors. Overall, the present findings indicate that the tumours with high p53 expression are more aggressive, thus tumours from patients with advanced stages of disease (III and IV), incompletely cytoreductive surgery, HGSC and poorly differentiated tumours are more likely to express high levels of p53.

It is somewhat surprising that there was no statistically significant difference between stage I and stage IV in relation to p53 expression. A possible explanation for this might be the small number of subjects in the stage IV group (17 out of 140, 12%).

Another interesting exception is the low level of p53 staining for the clear cell histological subtype, since this group was found to have a poor survival. This result is not surprising because clear cell morphology is known as an aggressive subtype of ovarian cancer with infrequent *TP53* mutation (Shih-Chu Ho *et al.*, 2001; Amikura *et al.*, 2006).

These observations are in accord with other studies showing a positive correlation between p53 high expression and established prognostic variables. Shahin *et al*. (2000), Sagarra *et al*. (2002) and Kmet *et al*. (2003) found that the incidence rates of p53 high expression among serous histological subtype, late stage and grade III differentiated tumours are clearly higher than other histological subtypes, early stage and grade I differentiated tumours. Another study by Reles *et al*. (2001) showed that high expression of p53 is associated with poor differentiation and late stage tumours. In another report in which clinicopathological correlations with p53 expression were examined, there was only a correlation between high level of p53 and loss of differentiation (Baekelandt *et al.*, 1999; Nakayama *et al.*, 2003). Moreover, Lihong *et al*. (2012) have demonstrated that there is a close relationship between the level of p53 protein and degree of malignancy (metastasis and recurrence) and prognosis of ovarian cancer. In contrast, Antonio *et al*. (2002) and Malamou *et al*. (2007) reported no significant correlation between p53 expression and histology, stage and grade of ovarian carcinoma ($p>0.05$). As explained above, the discrepancy observed between studies may be related to the type of antibody, the type of sample used for IHC staining, and how the samples were categorized.

Antibody	Sample Size/Type	Treatment	Type or Histology of Cancer	Cut-point Value	P-Value (OS)	Reference
DO-7	171, FFPE or frozen	Platinum-based or other	EOVCA	Negative vs positive	0.7	(Shahin *et al.*, 2000)
DO-7	178, Frozen	Platinum-based or other	OVCA	> 10% vs ≤ 10%*	0.06	(Reles *et al.*, 2001)
DO-7	78, FFPE	Platinum-based	OVCA	> 10% vs ≤ 10%*	0.03	(Schuyer *et al.*, 2001)
DO7-m7001	90, FFPE	Platinum-based	Invasive OVCA	> 10% vs ≤ 10%*	>0.05	(Sagarra *et al.*, 2002)
DO-7	134, FFPE	CAP	OVCA	> 10% vs ≤ 10%*	0.01	(Nakayama *et al.*, 2003)
DO-1	125, Frozen	Platinum-based	EOVCA, stage III & IV	> 30% vs ≤ 30%*	>0.05	(Havrilesky *et al.*, 2003)
NeoMarker	82, FFPE	Platinum-based	OVCA	≥10% vs <10%*	<0.05	(Dogan *et al.*, 2005)
DO-1	169, FFPE***	Platinum-based	EOVCA, stage IIb-IV	≥10% vs <10%*	0.8	(Green *et al.*, 2006)
Bp53-11	36, FFPE	Platinum-based	Advanced serous EOVCA	> 10% vs ≤ 10%*	>0.05	(Gadducci *et al.*, 2006)
DO-1	95, FFPE	Platinum-based	EOVCA stage IIc-IV	≥10% vs <10%*	0.04	(Malamou-Mitsi *et al.*, 2007)
DO-7	173, Not recorded	Platinum-based	Serous OVCA	≤ 10% vs aberrant (negative or >50%)*	<0.0001	(Vartiainen *et al.*, 2008)
DO-7	116, FFPE	Platinum-based	OVCA	Negative vs positive	0.1	(Tomsova *et al.*, 2008)
DO-7	108, FFPE	Not recorded	Invasive OVCA	> 10% vs ≤ 10%*	0.02	(Bartel *et al.*, 2008)
DO-7	143, FFPE***	Platinum-based	High risk early stage EOVCA	> 10% vs ≤ 10%*	0.06	(Darcy *et al.*, 2008)
DO-7	279, FFPE***	Platinum-based	Advanced stage EOVCA	> 10% vs ≤ 10%*	0.5	(Darcy *et al.*, 2008)
DO-7	329, FFPE	Platinum-based	OVCA	> 50% vs ≤ 50%**	<0.001	(Leffers *et al.*, 2008)
DO-7	142, FFPE	Platinum-based	EOVCA	> 60% vs ≤ 60%*	0.12	(Rechsteiner *et al.*, 2013)
DO-7	129, FFPE	Not recorded	EOVCA, stage I & II	Strong(+++) vs negative or weak (+,++)**	0.003	(Skirnisdottir and Seidal, 2013)

Table 3-7: The results of studies on the prognostic value of p53 expression. FFPE, Formalin fixed paraffin embedded; OVCA, Ovarian cancer; EOVCA, Epithelial ovarian cancer; Platinum-based, Platinum plus cyclophosphamide, paclitaxel, doxorubicin or etoposide; CAP, Cyclophosphamide, doxorubicin and cisplatin; *, Irrespective of intensity; **, In regard to intermediate or strong nuclear staining; *, Samples collected from a clinical trial.**

3.5.3 The p21^{WAF1} expression and its correlation with survival and prognostic indicators

According to the frequency distribution of p21^{WAF1} H-scores, the samples were grouped into low and high expression categories. The pattern of staining was quite different to that observed for p53 and generally the H-scores were much lower. No significant difference was observed in survival rates on a log-rank test for patients with tumours exhibiting low or high expression of p21^{WAF1}. These results support previous studies performed by Skirnisdottir *et al*. (2013) and Sengupta *et al*. (2000), but they are not consistent with those of Anttila *et al* (1999) and Rose *et al*. (2003) who observed that positive or high p21^{WAF1} expression conferred an overall survival advantage. Rose *et al*. (2003) used fresh, snap-frozen or paraffin-embedded samples, applied the WAF1/CIP1 monoclonal antibody, and categorised the samples into negative (54%) and positive (46%) groups. Anttila *et al*. (1999) observed negative p21^{WAF1} expression in 26%, low p21^{WAF1} expression (<10% of the tumour nuclei was positive) in 44% and high p21^{WAF1} expression (>10% of the tumour nuclei was positive) in 30% of FFPE samples with the p21^{WAF1}-specific mouse monoclonal antibody (NCL-WAF1). Different types of sample and antibody used may partly explain this inconsistency.

In terms of the relationship between p21^{WAF1} expression and clinicopathological data, the p21^{WAF1} immunostaining H-scores were not significantly different amongst various groups according to histological subtype, grade, stage and cytoreductive surgery ($p>0.05$). Another study by Harlozinska *et al*. (2002) found no significant correlation between p21^{WAF1} and histology, grade and stage, supporting the results in the current study. However, these findings differ from some published studies Anttila *et al* (1999) observed a significant statistical difference between low p21^{WAF1} expression and histological subtype ($p<0.00005$), high grade of tumour ($p=0.0005$), advanced stage ($p=0.001$) and primary residual tumour ($p=0.0001$). Rose *et al*. (2003) also indicated that positive p21^{WAF1} staining significantly correlated with lower stage tumours ($p=0.003$), tumours of clear cell histology ($p=0.001$) and those optimally cytoreduced ($p=0.02$); however, there was no relationship between positive p21^{WAF1} and tumour grade. Moreover, Skirnisdottir *et al*. (2013) found only a significant correlation between p21^{WAF1} status and histological subtype ($p=0.016$), not with grade, stage and cytoreductive surgery. As mentioned earlier, different types of antibody applied to stain and various techniques used to categorise data sets into two groups may explain discrepancies.

3.5.4 The correlation between p53 expression and $p21^{WAF1}$ expression

The present results showed no correlation between p53 and $p21^{WAF1}$ expression. Most studies have failed to observe a clear relationship between p53 and $p21^{WAF1}$ expression and concluded that $p21^{WAF1}$ is induced by both p53-dependent and p53-independent mechanisms. This has been concluded from frequently observed lack of inverse correlation between the expression of p53 and $p21^{WAF1}$. In particular, $p21^{WAF1}$ has been reported to be induced more by p53-independent mechanisms in ovarian cancer (Sengupta *et al.*; Phalke *et al.*, 2012).

3.5.5 The relationship of concomitant expression of p53 and $p21^{WAF1}$ with survival

In the present study, patients with p53 high expression and $p21^{WAF1}$ low expression had worse survival, with 14% five year disease specific survival, compared with individuals with p53 low expression and $p21^{WAF1}$ high expression, who had the best survival, with a 46% rate of survival. However, the significant difference was not better than on the basis of p53 IHC status alone and was completely similar with 15% five year disease specific survival for patients with high expression of p53 compared to 44% five year disease specific survival for individuals with low expression of p53. Therefore, the observed effect is related to p53 expression status other than $p21^{WAF1}$ expression status. Anttila *et al*. (1999) and Skirnisdottir *et al*. (2013) found a significant relationship between concomitant expression of p53 and $p21^{WAF1}$ and survival with a worse disease free survival for the subgroup of patients with concomitant p53 positive and $p21^{WAF1}$ negative tumours compared to other subgroups.

3.5.6 The MDM2 expression and its correlation with survival and prognostic indicators

The present findings indicated no significant difference in survival rates for patients with tumours showing high or low expression of MDM2. A number of studies have previously investigated the relationship of MDM2 expression to survival in patients with ovarian cancer (Baekelandt *et al.*, 1999; Sengupta *et al.*, 2000; Dogan *et al.*, 2005). Baekelandt *et al*. (1999) found no statistically significant difference between patients with tumours showing low or high expression of MDM2. Sengupta *et al*. (2000) categorised the samples two ways, including low, intermediate and high MDM2 expression or negative and positive MDM2 expression. In both cases, they did not observe any significant difference in survival rates for patients. They also used two different antibodies (clone SMP14 and clone IF2) for MDM2 protein staining. The pattern of staining was dependent on the antibody used, which was six times more positive when the clone IF2 was used. However, the study by Dogan *et al*. (2005) is in contrast with these findings. These authors used NeoMarker (291P906, USA) antibody for MDM2 protein

staining and observed patients with tumours positive for MDM2 expression (<1% indices were accepted as negative, and the remaining were accepted as positive) had worse survival compared to individuals with negative MDM2 expression ($p<0.01$). As mentioned earlier, various options used to categorise the samples and different types of antibodies applied may explain this inconsistency.

In the current study, the MDM2 immunostaining H-scores were not significantly different amongst different groups of histological subtype, grade, stage and cytoreductive surgery ($p>0.05$). These results support previous studies indicating no significant relationship of MDM2 expression to histological subtype, stage and residual disease while showing conflicting results in terms of the correlation between MDM2 expression and tumour grade. Sengupta *et al*. (2000) found an association between MDM2-positive tumours and whether the tumours were well differentiated ($p=0.022$) but not with other clinicopathological variables, whereas Dogan *et al*. (2005) observed a correlation between positivity for MDM2 expression and poor differentiation ($p<0.05$) but not to other prognostic variables.

3.5.7 The relationship between coexpression of MDM2 and p53 with survival

The relationship between coexpression of p53 and MDM2 and survival rates was statistically significant in this cohort (X^2=10.06, $p=0.018$). Across all four categories, patients with low expression of both p53 and MDM2 had a significantly better overall survival than those with high expression of both p53 and MDM2 ($p=0.04$). The survival probability was significantly better in patients with low expression of p53 and high expression of MDM2 versus individuals with high expression of both p53 and MDM2 ($p=0.02$). There was also a significant difference in overall survival between individuals with low expression of p53 and high expression of MDM2 compared to patients with low expression of MDM2 and high expression of p53 ($p=0.02$). Another study by Dogan *et al* (2005) categorised concomitant expression of p53 and MDM2 into two groups as positive or negative (cut-off levels were stratified at 10% for p53 and 1% for MDM2 indices) to examine the relationship to patient survival indicating coexpression of p53 and MDM2 was significantly related to poor outcome ($p<0.05$).

3.5.8 The WIP1 expression and its relationship with survival and prognostic indicators

This is the first study to investigate the correlation of WIP1 expression with survival using IHC in patients with ovarian cancer. A number of studies have recently investigated the mRNA expression levels of *PPM1D* (the gene for WIP1) in primary ovarian cancer tumours and/or a panel of established ovarian clear cell adenocarcinomas, confirming higher levels of *PPM1D* mRNA expression in the clear cell histological subtype (Hirasawa *et al.*, 2003; Tan *et al.*, 2009b; Ali *et al.*, 2012; Richter *et al.*, 2015). Contrary to expectations, this study did not find a significant difference in survival rates for patients with tumours showing low or high levels of WIP1 protein (*p=0.49*). A possible explanation for this unexpected result might be the relatively small number of clear cell adenocarcinoma samples in this study (6 out of 62, 9.6%).

In the present study, a significant relationship between WIP1 expression and tumour grade was observed with higher expression of WIP1 in well-differentiated tumours compared to poorly- and intermediately-differentiated tumours (*p=0.03*), but not with other prognostic indicators. Although no statistically significant difference was found between WIP1 expression and different histological subtypes (*p=0.26*), a higher number of clear cell adenocarcinomas tumours are needed for a stronger statistical comparison to be made.

3.5.9 The correlation between coexpression of p53 and WIP1 to survival

In this study, the observed differences amongst various categories of concomitant expression of p53 and WIP1 in relation to survival were not statistically significant (*p=0.62*). As shown in Table 3-5, the number of samples in each group is small and that limits the statistical analysis. Overall, a higher number of sample in each category, mainly in II, III and IV, is required to make a stronger statistical comparison.

3.5.10 Multivariate cox regression analysis of survival

A multivariate Cox regression analysis was applied to variables shown to be significant predictors of survival difference on univariate analysis, including grade, residual disease, stage, histological subtype, expression of p53, and coexpression of p53 and $p21^{WAF1}$, or p53 and MDM2 to compare survival rates. Stage, histological subtype and residual disease retained their significance in multivariate analysis as independent prognostic variables, while grade, p53, concomitant expression of p53 and $p21^{WAF1}$ or p53 and MDM2 did not retain significance as independent prognostic variables. Numerous studies have performed multivariate analysis based on the variables shown to be significant prognostic factors in univariate analysis.

Regardless of how many variables were used to perform multivariate analysis, stage retained significance as an independent prognostic and predictive factor for survival (Baekelandt *et al.*, 1999; Sengupta *et al.*, 2000; Reles *et al.*, 2001; Sagarra *et al.*, 2002; Dogan *et al.*, 2005; Zhang *et al.*, 2014).

3.6 Conclusion and further work

The frequency distribution of histological subtypes and prognostic indicators for survival validates the cohort in the present study as representative of ovarian cancer patient populations. The findings in this research confirm p53 as a potential prognostic marker of survival in patients with ovarian cancer, demonstrating that high expression of p53 is more prevalent in patients with more aggressive types of the disease at advanced stages (III/IV) with higher grade and serous histology subtype. These observations also indicate that coexpression of p53 and MDM2 has more potential as a prognostic factor compared to the expression of MDM2 alone. However, further work with larger sample sizes for high expression of both is needed to give a clear picture of MDM2 as a predictive marker of survival. Survival data show no significant correlation with WIP1 expression in two different categories though this requires further studies with a higher number of clear cell adenocarcinomas.

Although high expression of p53 is often considered as indicative of mutation, the expression may be elevated for other reasons, including increased transcription followed by translation, stabilization or resistance to degradation (Reles *et al.*, 2001; Havrilesky *et al.*, 2003; Bauerschlag *et al.*, 2010). To give a more accurate picture of p53 as a predictive marker in ovarian cancer, it is more pertinent to study the relationship between *TP53* gene status and p53 expression with survival in tumours from the same cohort of patients.

Chapter 4: *TP53* mutation analysis of ICON3 trial samples using Sanger and Next Generation Genomic DNA sequencing

4.1 Introduction

For ovarian cancer patients, earlier platinum-based chemotherapy has been superseded by a standard first-line treatment consisting of taxane-platinum based combination therapy. However, this is more costly, neurotoxic, and has no effect on 20 to 30% of patients (Kupryjanczyk *et al.*, 2008). Although most patients respond to the standard treatment, relapse with drug-resistant disease is prevalent. Given the critical role of the *TP53* gene in response to DNA damaging agents, a number of studies have explored the importance of *TP53* gene status in ovarian cancer (Canevari *et al.*, 2006; Gadducci *et al.*, 2006; Yang-Hartwich *et al.*, 2015). There is evidence supporting the hypothesis that patients harbouring wild-type *TP53* have a higher response rate to platinum-based chemotherapy and a better OS and/or PFS compared to those with mutant *TP53*. However, the role of *TP53* status in response to chemotherapy and determining resistance is controversial (Table 4-1). It is very important to improve the ability to predict and identify patients who are most likely to benefit from treatment. Our understanding of the role of *TP53* may help to predict sensitivity to chemotherapy and allow individualisation of treatment, thereby reducing morbidity and side effects whilst maintaining response rate in ovarian cancer.

Treatment	Association with OS	Association with PFS	Reference
Cisplatin+cyclophosphamide or carboplatin	No	No	(Fallows et al., 2001)
Cisplatin	ND	No	(Wang et al., 2004)
Platinum-based chemotherapy	No	ND	(Bauerschlag et al., 2009)
Cisplatin	Yes	ND	(Kigawa et al., 2001)
Platinum-based chemotherapy	Yes	Yes	(Reles et al., 2001)
Platinum-based chemotherapy	Yes	Yes	(Havrilesky et al., 2003)
Platinum-based chemotherapy	Yes	Yes	(Gadducci et al., 2006)

Table 4-1: Association between OS and/or PFS and *TP53* status according to treatment. OS, Overall survival; PFS, Progression-free survival; Platinum-based chemotherapy, Cisplatin or carboplatin plus cyclophosphamide or paclitaxel; ND, Not determined.

4.1.1 The rate of *TP53* mutation in ovarian cancer

A number of studies have reported the rate of *TP53* mutation in ovarian cancer to range from 34% to 96% (Table 4-2). This discrepancy amongst the results may be attributed to different techniques used to detect mutations and variation in the grades or stages of disease in the sample populations investigated. It may also be related to whether the most commonly mutated exons (exons 4-9), the entire coding region of *TP53* (exons 2-11) or the whole gene were sequenced. Furthermore, some confusion is based on whether *TP53* mutations are being reported in ovarian cancer generally, specifically epithelial ovarian cancer or for different histological subtypes, in particular serous or HGSC (de Graeff *et al.*, 2009; Ahmed *et al.*, 2010).

4.1.2 DNA sequencing as a gold standard method for mutation detection

There are different molecular methods used to identify mutations based on the type of nucleic acid and specimen, number of mutations and reliability of the method (Mahdieh and Rabbani, 2013). DNA sequencing is a powerful technique considered as a gold standard for mutation detection. Sanger sequencing and Next Generation Sequencing (NGS) represent the most extensively used techniques for DNA sequencing (Highsmith, 2006; Mahdieh and Rabbani, 2013). In some studies pre-screening by Single-strand conformation polymorphism (SSCP) was used and those DNA samples which showed mobility shifts on SSCP gels were sequenced.

4.1.2.1 Sanger sequencing

The dideoxynucleotide sequencing method, known as Sanger sequencing, is based on the selective incorporation of chain-terminating dideoxynucleotides by DNA polymerase during *in vitro* DNA replication and was introduced by Frederick Sanger and colleagues in 1977 (Highsmith, 2006; Hutchison, 2007). PCR-based Sanger sequencing is a multistep process starting with amplification of target DNA by PCR to increase sensitivity and specificity of the sequencing reaction. The next crucial step is removal of unused primers at the end of the amplification reaction to avoid noisy sequencing data (W. Edward Highsmthh, 2006; SenGupta and Cookson, 2010). Then, double stranded DNA is converted to single stranded DNA which is used for the sequencing reaction. We generated the exon PCR products here and sent the PCR samples off for sequencing. In the dye-terminator Sanger sequencing method used for this study, each of the four ddNTP chain terminators is labelled with a different fluorescent dye emitting light at different wavelengths in one reaction leading to greater efficiency and speed for automated sequencing. Different fluorescent colours are sequentially detected during

capillary electrophoresis to build up the sequence of the nucleotides as an chromatogram image (Highsmith, 2006).

4.1.2.2 Next Generation Sequencing (NGS)

The NGS techniques, known as high-throughput sequencing, include Roche 454, Illumina/Solexa, SOLiD, Ion Torrent, Pacific Biosciences/Single Molecule Sequencing and Intelligent Bio Systems improving both speed and cost at the expense of shorter read lengths compared to Sanger sequencing. They are capable of sequencing the whole genome, chromatin immunoprecipitation and genome wide RNA for mammalian and human tissue transcriptomes. A major development in NGS technology occurred with advances in library preparation methods. Large numbers of libraries can simultaneously be pooled and sequenced during a single sequencing run by multiplexing using bar-coding to sequence many samples for a given target sequence at the same time. It is hugely more efficient and for large numbers of samples can be more cost-effective. The high speed, high throughput, versatility and cost-effectiveness of NGS has resulted in NGS becoming the dominant genome sequencing technique. However, Sanger sequencing is considered as a "gold standard" technique to validate smaller studies and the only method widely used to sequence long read-lengths of DNA, up to 1,000 nucleotides in length (Ledergerber and Dessimoz, 2011; Mestan *et al.*, 2011).

Type or Histology of Cancer	*TP53* Mutation (Number) %	Sequenced Exons	Mutation Analysis	Treatment	P-Value (OS)	Reference
EOVCA	(23 of 43) 53	5-9	DNA sequencing	Paclitaxel-based chemotherapy	>0.05	(Laframboise S, 2000)
OVCA	(32 of 73) 44	5-8	SSCP & Sanger sequencing	Platinum-based chemotherapy	>0.05	(Fallows et al., 2001)
OVCA	(99 of 178) 56	2-11	SSCP & Sanger sequencing	Platinum-based or other chemotherapy regimens	0.01	(Reles et al., 2001)
Serous	(60 of 99) 61	2-11	SSCP & Sanger sequencing	Platinum-based or other chemotherapy regimens	ND	(Reles et al., 2001)
EOVCA	(32 of 82) 39	5-8	SSCP & DNA sequencing	Platinum-based chemotherapy	>0.05	(Schuyer *et al.*, 2001)
Serous	(56 of 74) 75	2-11	Sanger sequencing	Platinum-based chemotherapy	>0.05*	(Havrilesky et al., 2003)
OVCA	(125 of 267) 47	4-10	Sanger sequencing	Not available	ND	(Rose *et al.*, 2003)
EOVCA	(24 of 73) 34	2-11	Sanger sequencing	Not available	ND	(Leitao et al., 2004)
Serous	(14 of 21) 67	2-11	Sanger sequencing	Not available	ND	(Leitao et al., 2004)
HGSC	(30 of 59) 51	5-9	Sanger sequencing	Not available	ND	(Singer G1 et al., 2005)
Serous	(23 of 46) 50	5-9	Sanger sequencing	Platinum-based chemotherapy	0.10	(Gadducci et al., 2006)
EOVCA	(42 of 100) 42	5-8	Sanger sequencing	Platinum-based chemotherapy	0.03**	(Ueno *et al.*, 2006)
OVCA	(44 of 107) 41	5-8	Sanger sequencing	Platinum-based chemotherapy	0.86	(Bartel *et al.*, 2008)
EOVCA	(42 of 73) 58	5-8	SSCP & Sanger sequencing	Platinum-based chemotherapy	>0.05	(Bauerschlag *et al.*, 2009)

Table 4-2: The frequency of *TP53* mutation in ovarian cancer reported in different studies. OVCA, Ovarian cancer; EOVCA, Epithelial ovarian cancer; HGSC, High grade serous carcinoma; SSCP, Single-strand conformation polymorphism; Platinum-based chemotherapy, Cisplatin or carboplatin plus cyclophosphamide or paclitaxel; *, A mutation was associated with a short-term advantage in OS; however, there was no longer any improvement in survival for patients with mutant *TP53* tumours after 2.5 years from primary diagnosis; **, A mutation was associated with advantage in OS.

.

Type or Histology of Cancer	*TP53* Mutation (Number) %	Sequenced Exons	Mutation Analysis	Treatment	P-Value (OS)	Reference
HGPSC	(119 of 123) 97	2-11	NGS	Platinum-based chemotherapy	>0.05	(Ahmed et al., 2010)
Serous	(59 of 89) 66	2-11	NGS	Not recorded	ND	(Bernardini et al., 2010)
HGSC	(302 of 316) 96	2-11	NGS	Platinum-based chemotherapy	ND	(The Cancer Genome Atlas Research, 2011)
EOVCA	(108 of 190) 57	NM	SSCP & DNA sequencing	Platinum-based chemotherapy or other	0.03*	(Nadkarni *et al.*, 2013)
EOVCA	(73 of 142) 51	5-8	NGS, 454 (Roche)	Platinum-based chemotherapy	0.002	(Rechsteiner et al., 2013)
HGSC	(37 of 63*) 59	5-8	NGS, 454 (Roche)	Platinum-based chemotherapy	0.02	(Rechsteiner et al., 2013)
HGSC	(301 of 316) 95	2-11	NGS	Platinum-based chemotherapy	0.007**	(Wong *et al.*, 2013)

Table 4-2 (Continued): The frequency of *TP53* mutation in ovarian cancer reported in different studies. OVCA, Ovarian cancer; EOVCA, Epithelial ovarian cancer; HGSC, High grade serous carcinoma; HGPSC, High grade pelvic serous carcinoma; SSCP, Single-strand conformation polymorphism; Platinum-based chemotherapy, Cisplatin or carboplatin plus cyclophosphamide or paclitaxel; NGS, Next generation sequencing; *, Null mutation compared to wild-type *TP53*; **, A mutation was associated with advantage in OS. The Cancer Genomic Atlas Research (2011) and Wong *et al* (2013) used the same cohort.

4.2 Hypothesis and Objectives

Hypothesis:

1. Patients whose tumours have wild-type *TP53* are more sensitive to platinum-based chemotherapy than those with mutant *TP53,* therefore they survive longer as a result of response to treatment.
2. Patients with mutant *TP53* tumours gain benefit from addition of paclitaxel to treatment, while those with wild-type *TP53* do not benefit.

Objectives:

1. To study the role of *TP53* status as a prognostic factor for overall survival and progression-free survival in the ICON3 patient cohort.
2. To correlate *TP53* status with response to chemotherapy, and assess it as a predictive marker of disease outcome in the ICON3 patient cohort.
3. To evaluate the efficacy of paclitaxel plus carboplatin or CAP (cyclophosphamide, doxorubicin and cisplatin) with a control of either CAP or carboplatin alone with respect to *TP53* status.

4.3 Specific Materials and Methods

4.3.1 Patient characteristics

A total of 260 patient samples taken from ICON3 randomized clinical trial. The samples were collected at primary surgery between February, 1995, and October, 1998 with median follow-up of 11.9 years. From a total of 260 patient samples 207 samples were from UK and 53 were from Italy. There was a pathology review to update the diagnosis of these archival samples that was performed by Paul Cross, the pathologist at the Queen Elizabeth Hospital in Gateshead. The review was based on a single slide per case (as this was all we had) but at least that was taken from the exact block from which the DNA was extracted, which obviously minimises the effect of any heterogeneity. In fact, the review was limited to a single H&E slide but was carried out by an extremely experienced gynae pathologist. The pathologist was unable to perform any immunohistochemistry which is accepted as a part of the assessment of these tumours which is mentioned as a limitation of this study.

The aim of ICON3 was to compare the safety and efficacy of paclitaxel plus carboplatin with a control of either carboplatin alone or CAP. Patients had received no previous treatment likely to affect the outcomes, and patients requiring treatment were randomly assigned to paclitaxel plus carboplatin or control treatment, which was single agent carboplatin or CAP. The randomization was performed in a ratio of 2:1 in favour of the control group. Appropriate ethical approval was obtained to analyse the samples. Overall survival and progression-free survival were evaluated as primary and secondary outcomes. No evidence of a difference in OS between paclitaxel plus carboplatin and control was observed indicating single agent carboplatin and CAP are as effective as paclitaxel plus carboplatin as first line treatment.

The role of the TP53 gene in determining resistance remains controversial although there is increasing evidence to support the hypothesis that patients with wild-type TP53 tumours have high response rates to platinum-based treatment and may gain no benefit from addition of paclitaxel. Therefore, it was proposed to examine the samples for mutations of the TP53 gene and correlate this with subsequent outcome (Figure 4-1).

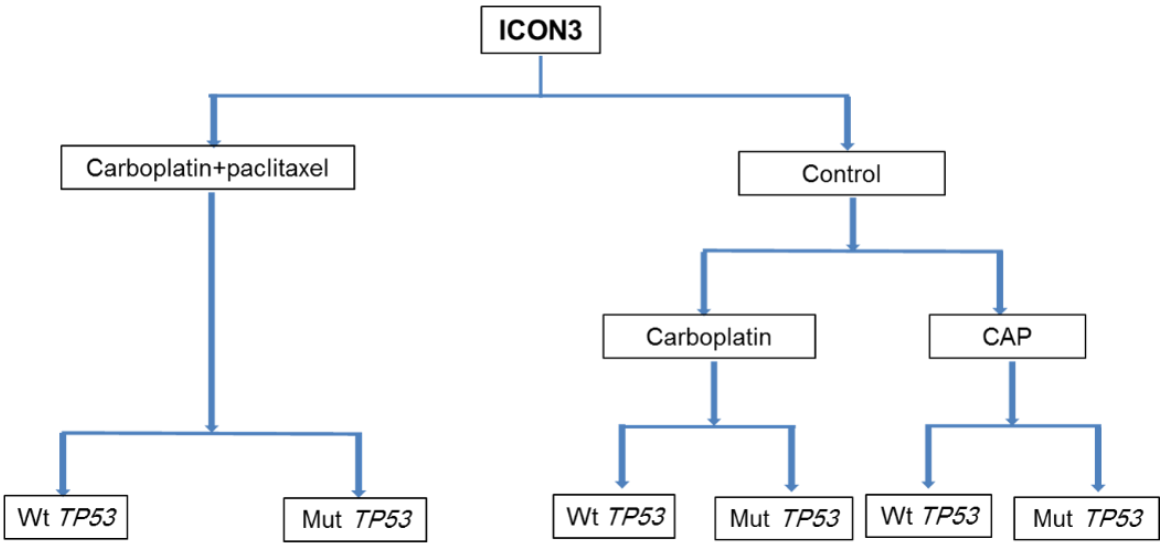

Figure 4-1: Diagram of the samples taken from ICON3 randomised clinical trial.

4.3.2 *TP53* mutation analysis

For the Sanger sequencing, the samples were macro-dissected using areas outlined by Paul Cross (a pathologist). The DNA extraction and exon PCR was performed in NICR (by Dr. Claire Hutton and Dr. Jennifer Houniet) and the PCR products were sent to DBS Genomics (Durham, UK) for sequencing. For the NGS, FFPE blocks were supplied to NewGene (Newcastle, UK) and whole tissue sections were used for DNA extraction and purified PCR products were used for sequencing. The proportion of tumour cells in the samples used for sequencing was around 90%. The general primer design rules or Primer 3Plus design (www.bioinformatics.nl/primer3plus) were used to design sequence specific PCR primers and https://secure.ngrl.org.uk/SNPCheck/ was applied to filter and check for the presence of SNPs. PCR primers used are presented in Table 4-3. The *TP53* exon 4 sequence was split into two partially overlapping amplicons due to its large size. Sequencing of all coding regions and adjacent splice sites (+/- 10bp) of the *TP53* gene (exon 2 to 11) was carried out using both Sanger sequencing and NGS.

NGS was performed using a Roche 454 system and was based on amplicon libraries. In total, the *TP53* region of interest was covered by 11 sequence specific primer pairs, each flanked by MID-labelled Primer A and Primer B sequences to barcode the samples. In each NGS experiment, a total of 88 amplicons, corresponding to the *TP53* region of interest of 8 distinct patients, were amplified from genomic DNA using a high fidelity Taq polymerase (FastStart High fidelity PCR System, Roche Diagnostics). The Agencourt AMPure XP beads (Beckman Coulter) and the Quant-iT PicoGreen dsDNA kit (Invitrogen) were used to individually

purified and quantified PCR products respectively. Each of the amplicons in combination with an equimolar ratio for each patient sample was applied to generate corresponding patient-specific amplicon pools.

The pools were diluted to a concentration of 1×10^6 molecules per µl and processed using the GS Junior Series Lib-A method (Roche Diagnostics). 5,000,000 beads per emulsion oil tube was used to perform forward (A beads) and reverse (B beads) reactions. The copy per bead ratio used was 1.1:1. The workflow recommended by the manufacturer was used to amplify reaction, break the emulsions and enrich the beads carrying amplified DNA. Lastly, the obtained amplicon library was loaded on a PicoTiterPlate (PTP) and subjected to NGS on the Genome Sequencers, GS-FLX or Junior instruments (454 Life Sciences).The commercially available software packages Amplicon Variant Analysis (AVA) (454 Life Sciences) and NextGene (Softgenetics) were used for data processing.

Amplicon coverage information was generated using AVA software by identifying primer sequences in de-multiplexed reads. Information on the forward and reverse reads was extracted using an in-house designed Perl program script for each barcode multiplex identifier (MID). The covered amplicons with less than 30 reads were insufficient, therefore they were re-amplified and sequenced in a separate run. Mapping to reference sequence NM_000546.5 and variant calling was performed by NextGene software v2.3.3 through to v2.3.4.4. The .sff files were converted to quality .fna files. Any reads with maximum number of uncalled bases >1, called base number of each read<100 and median score threshold <15 were rejected.

Based on the MID barcodes, all reads of adequate quality were sorted and assigned to a specific sample. To remove any artificial nucleotide strings (e.g. residual primer sequence in overlapping regions) that can interfere with the mapping process, the sequences were further trimmed by 27nt. Default settings for the Roche454 SNP/Indel discovery application were used for mapping with mutation filters, mutation percentage of 5%, SNP allele count of 3 and total coverage count of 5. It means that any variant with mutant allele frequency of at least 5% observed at least 3 times with at least 5 reads was retained in the filtered variant table. The average depth of sequencing of different amplicons was 265. Please see Appendix I for more information about the average depth of sequencing of each exon.

4.3.3 Statistical analysis

The sequencing and statistical analysis were performed independently, with the clinical data held by the MRC Clinical Trials Unit. The statistical analysis was carried out by Wendi Qian from the Medical Research Council (MRC) Clinical Trials Unit. The Kaplan-Meier method and log-rank test were used to analyse whether or not the observed differences in survival times were statistically significant. The clinical data with respect to *TP53* status were tested using a chi-squired test, Mann-Whitney test or t-test. The prognostic value of *TP53* status on platinum-based chemotherapy was evaluated by fitting Cox proportional hazards regression models or flexible models to PFS and OS. Both univariate and multivariate analyses were performed including *TP53* status and clinical baseline data. Analysis of the interaction between *TP53* status and addition of paclitaxel to platinum-based chemotherapy was performed in an exploratory manner due to small sample size and Cox proportional hazards regression models were used. All hypotheses were tested using two-sided p-values, and p-values of <0.05 were considered to be statistically significant.

Exon	Annealing Temperature (°C)	Primer Sequence 5'-3'
Exon 2	58	F-CGA GCT GTC TCA GAC ACT GG
		R-CCT TGT CCT TAC CAG AAC GTT G
Exon 3	55	F-CAT GGG ACT GAC TTT CTG CTC TTG
		R-CGG GGA CAG CAT CAA ATC ATC
Exon 4	55	F-GTT CTG GTA AGG ACA AGG GT
		R-ATA CGG CCA GGC ATT GAA GT
Exon 4.1	55	F-GTT CTG GTA AGG ACA AGG GT
		R-TGT AGG AGC TGC TGG TGC AG
Exon 4.2	55	F-AGC TCC CAG AAT GCC AGA GG
		R-ATA CGG CCA GGC ATT GAA GT
Exon 5	55	F-ATC TGT TCA CTT GTG CCC TG
		R-CAA CCA GCC CTG TCG TCT CTC
Exon 6	55	F-GCC TCT GAT TCC TCA CTG AT
		R-GGA GGG CCA CTG ACA ACC A
Exon 7	60	F-AAG GCG CAC TGG CCT CAT CTT
		R-CAG GGG TCA GCG GCA AGC AGA
Exon 8	60	F-GAG CCT GGT TTT TTA AAT GG
		R-TTT GGC TGG GGA GAG GAG CT
Exon 8 & 9	55	F-TTTAAATGGGACAGGTAGGAC
		R-GCCCCAATTGCAGGTAAAACAG
Exon 9	55	F-AGCGAGGTAAGCAAGCAGG
		R-GCCCCAATTGCAGGTAAAACAG
Exon 10	60	F-CTT CTC CCC CTC CTC TGT TGC
		R-GAA GGC AGG ATG AGA ATG GA
Exon 11	58	F-TGG TCA GGG AAA AGG GGC AC
		R-GAG AGA TGG GGG AGG GAG GC

Table 4-3: The primer sequences used for amplifying different exons of *TP53*. F, Forward; R, Reverse.

4.4 Results

4.4.1 Mutational analysis of *TP53*

The *TP53* sequence analysis was performed for exons 2-11 in a set of 260 FFPE ovarian cancer samples from the ICON3 cohort using both Sanger and NGS techniques. In addition, results are shown for analyses based on combined datasets; firstly in which a sample is registered as mutant if detected by either technique and secondly is only registered as mutant if detected by both techniques. The results showed differences between Sanger sequencing and NGS data. (Table 4-4).

Sanger sequencing data demonstrated that 131 tumour samples had mutations on a single exon, and fourteen samples had mutations on two different exons. Based on the NGS, 139 tumour samples exhibited mutations on one exon, 22, 4 and 1 samples showed mutations on two, three or four distinct exons respectively. The rate of *TP53* mutation was 72% based on the mutations detected by either Sanger or NGS method, and it was 47% according to the mutations detected by both methods. Both Sanger and NGS showed the majority of mutations occur in exons 5-8 of *TP53* (70%-80%) encoding the highly conserved DNA-binding domain.*TP53* mutations were detected in all exons by NGS; however, there were no *TP53* mutations in exon 2, 3 and 11 detected by the Sanger sequencing method. In addition, results are shown for analyses based on combined datasets; firstly in which a sample is registered as mutant if detected by either technique and secondly in which it is only registered as mutant if detected by both techniques.

Sequencing Method	Wild-Type *TP53* Number (%)	Mutant *TP53* Number (%)	Lost Number (%)	Total Number (%)
Sanger	115 (44)	145 (56)	0 (0)	260 (100)
NGS	92 (35)	166 (64)	2 (1)	260 (100)
Either	72 (28)	188 (72)	0 (0)	260 (100)
Both	135 (52)	123 (47)	2 (1)	260 (100)

Table 4-4: The frequency distribution of wild-type and mutant *TP53* based on the Sanger, NGS, either or both methods from 260 patients of ICON3 cohort. NGS, Next generation sequencing.

4.4.2 Results based on the Sanger sequencing

The *TP53* mutational status determined by Sanger sequencing was correlated with the clinicopathological data. The overall survival time of patients with wild-type *TP53* treated with single agent carboplatin or CAP was compared to those with mutant *TP53* treated with carboplatin or CAP. Also, additional analysis was carried out to analyse the efficacy of paclitaxel with carboplatin compared to a control of either CAP or carboplatin alone according to Sanger *TP53* status. The analyses were also performed for the subset of patients with serous histology. Lastly, a multivariate analysis was performed, which included Sanger *TP53* status and established clinicopathological prognostic variables known to be associated with OS in ovarian cancer.

4.4.2.1 Distribution of *TP53* status detected by Sanger sequencing

Data for a total of 253 tissue samples from patients was available, because seven patients received no chemotherapy treatment. *TP53* mutations were detected in 140 of the 253 samples (55%) and 113 tumour samples had wild-type *TP53* (45%). The frequencies of insertion, deletion, transversion and transition were 4%, 12%, 20% and 64% respectively. The highest frequency of substitution mutations was G>A (42%) (Figure 4-2A & B). The substitution mutations cover *TP53* hotspot mutations at codon 175, 237,248, 273 and 282, with a strong predominance at codon 237 (Figure 4-2C).

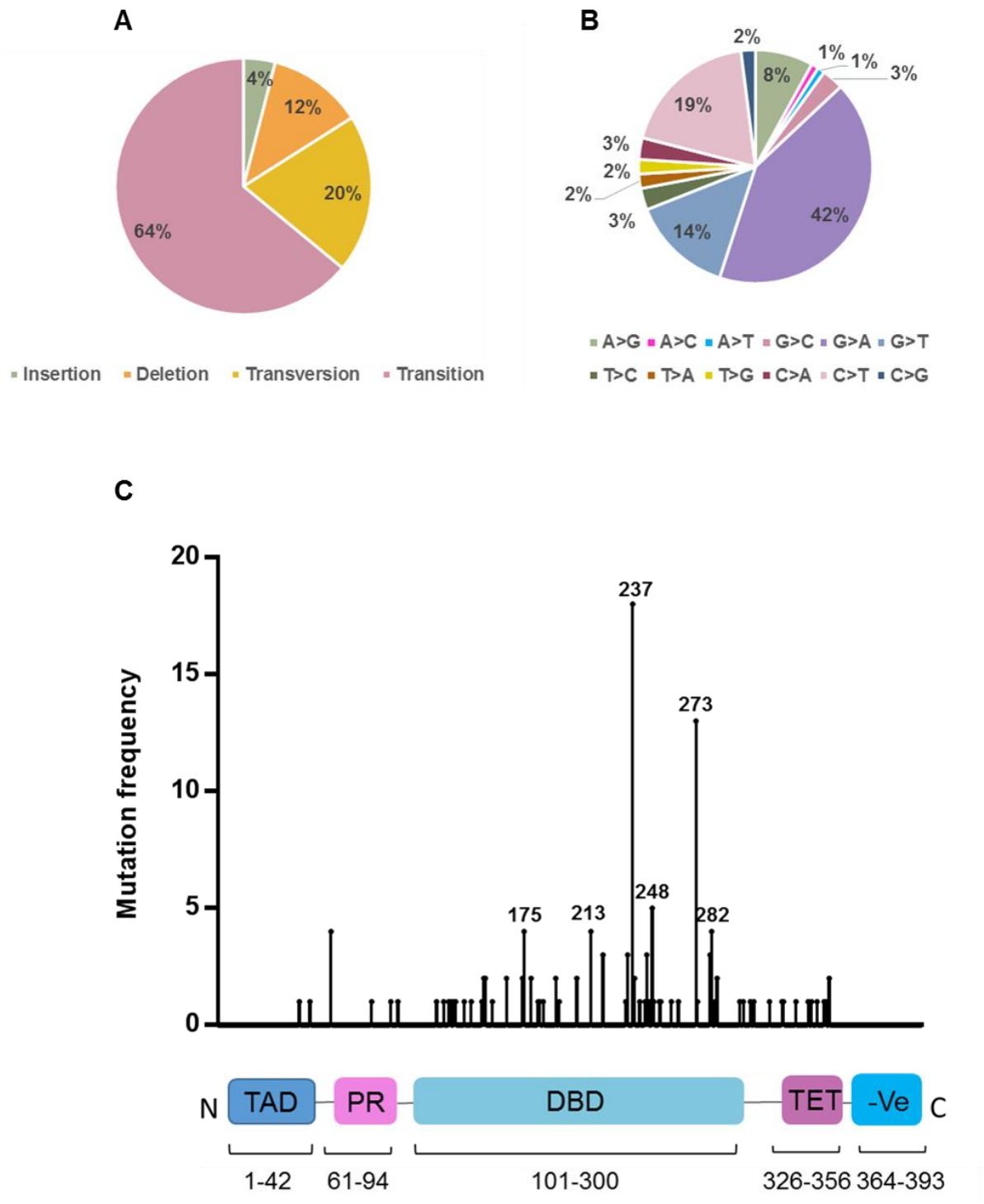

Figure 4-2: (A) Distribution of *TP53* mutations and (B) Distribution of *TP53* substitution mutations from 253 samples of the ICON3 cohort detected by Sanger sequencing. (C) Distribution of the *TP53* mutations in p53 residues from 253 samples of the ICON3 cohort detected by Sanger sequencing.

4.4.2.2 Distribution of clinicopathological variables according to Sanger *TP53* status

Table 4-5 summarizes the characteristics of both wild-type and mutant *TP53* groups for 253 patients with respect to histological subtypes, FIGO stage, residual disease and differentiation grade.

The largest histological group was recorded as HGSC, with a distribution of 159 (63%). Lower frequencies were observed for LGSC with 26 cases (10%), clear cell with 25 cases (10%), endometrioid with 21 cases (8%), undifferentiated with 17 (7%) and mucinous with 5 cases (2%). HGSC was the major histological subtype in both categories with 53% for wild-type *TP53* tumours and 71% for mutant *TP53* tumours (Table 4-5). Distribution of histological subtypes was different in regard to the mutational status of *TP53*, and the rate of *TP53* mutation was significantly higher for patients with HGSC than those with LGSC ($p=0.03$) or other histological subtypes (clear cell, endometrioid, mucinous and undifferentiated) ($p=0.03$).

From a total of 253 patients, there were 42 (17%) with FIGO disease stage I/II, 169 (66%) with stage III and 42 (17%) with stage IV (Table 4-5). There was no significant difference in the proportion of tumours from patients within each FIGO stage between those with wild-type *TP53* compared to those with mutant *TP53* (X^2=1.31, $p=0.52$).

60 (24%) of individuals from the cohort had complete cytoreductive surgery, 51 (20%); and 142 (56%) had <2 cm and ≥2 cm residual bulk disease respectively. Statistical analysis showed no significant difference in the frequency of residual bulk disease between the two *TP53* status groups (X^2=1.03, $p=0.60$) (Table 4-5).

The frequency distribution for differentiation grade was 155 cases (62%) grade 3 (poorly differentiated), 76 cases (30%) grade 2 (intermediate differentiation) and 20 cases (8%) grade 1 (well differentiated) (Table 4-5). The presence of mutant *TP53* was significantly associated with poor differentiation (X^2=13.22, $p=0.001$).

Variable	Wild-Type *TP53* Number (%)	Mutant *TP53* Number (%)	Total Number (%)
Histological Subtype			
Clear Cell	15 (13)	10 (7)	25 (10)
Endometrioid	12 (11)	9 (7)	21 (8)
High Grade Serous	60 (53)	99 (71)	159 (63)
Low Grade Serous	16 (14)	10 (7)	26 (10)
Mucinous	3 (3)	2 (1)	5 (2)
Undifferentiated	7 (6)	10 (7)	17 (7)
Total	113 (100)	140 (100)	253 (100)
Stage			
I/II	22 (19)	20 (14)	42 (17)
III	72 (64)	97 (69)	169 (66)
IV	19 (17)	23 (17)	42 (17)
Total	113 (100)	140 (100)	253 (100)
Residual Disease			
Complete Cytoreduction (none)	30 (27)	30 (21)	60 (24)
< 2cm	23 (20)	28 (20)	51 (20)
≥ 2cm)	60 (53)	82 (59)	142 (56)
Total	113 (100)	140 (100)	253 (100)
Grade			
Poorly Differentiated	56 (50)	99 (71)	155 (61)
Moderately Differentiated	42 (37)	34 (24)	76 (30)
Well Differentiated	14 (12)	6 (4)	20 (8)
Lost	1 (1)	1 (1)	2 (1)
Total	113 (100)	140 (100)	253 (100)

Table 4-5: Distribution of clinicopathological data with respect to Sanger *TP53* status for 253 samples from patients in the ICON3 cohort.

4.4.2.3 Sanger *TP53* status and Overall Survival/Progression-Free Survival

Survival curves were constructed based on the mutational status of *TP53* using the Kaplan-Meier analysis method. The log-rank test was applied to compare the differences between survival curves to establish whether or not the observed differences are statistically significant. As shown in Figure 4-3, there was a significant difference in survival time between patients whose tumours have wild-type *TP53* and those harbouring mutant *TP53* (X^2=6.91, *p=0.008*).

PFS was defined as the length of time between the first day of treatment and the date of recurrence, last follow-up, or death. The Kaplan-Meier plot showed that the PFS probability was significantly better in individuals with wild-type *TP53* compared to patients with mutant *TP53* (X^2=4.20, *p=0.04*) (Figure 4-4).

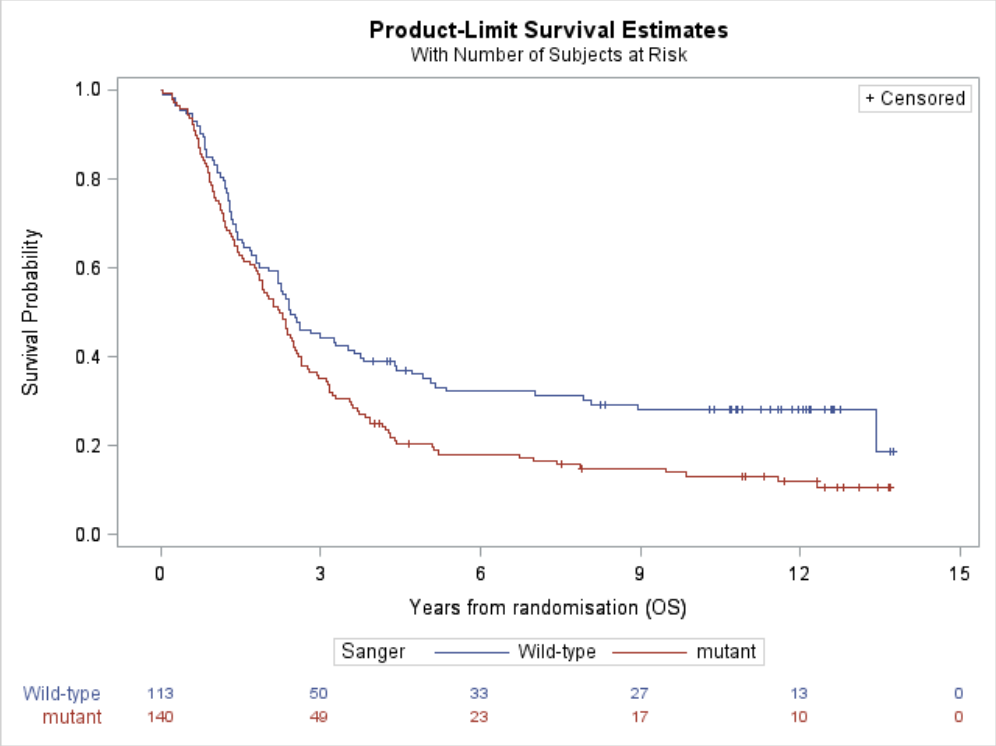

Figure 4-3: Overall survival for all patients in relation to Sanger *TP53* status (*p=0.008*).

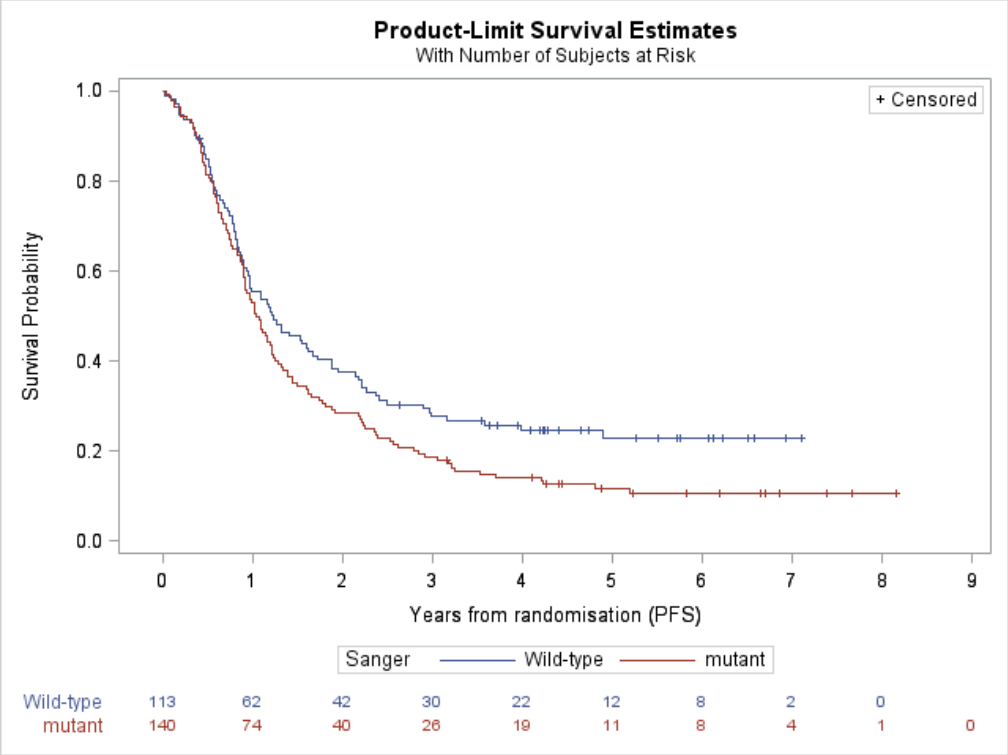

Figure 4-4: Progression-free survival for all patients in relation to Sanger *TP53* status (*p=0.04*).

4.4.2.4 Survival following treatment with carboplatin alone in relation to Sanger *TP53* status

The Kaplan-Meier plot and univariate analysis showed the presence of wild-type *TP53* was significantly correlated with better survival probability for patients treated with single agent carboplatin (X^2=6.32, *p=0.01*) (Figure 4-5). For multivariate analysis of overall survival for patients treated with single agent carboplatin, the mutational status of *TP53* (*p=0.0007*), stage III (*p=0.04*), residual bulk ≥2 cm (*p=0.003*) and endometrial histology (*p=0.01*) were all retained as independent prognostic variables with the most significant variable being the *TP53* status (Table 4-6).

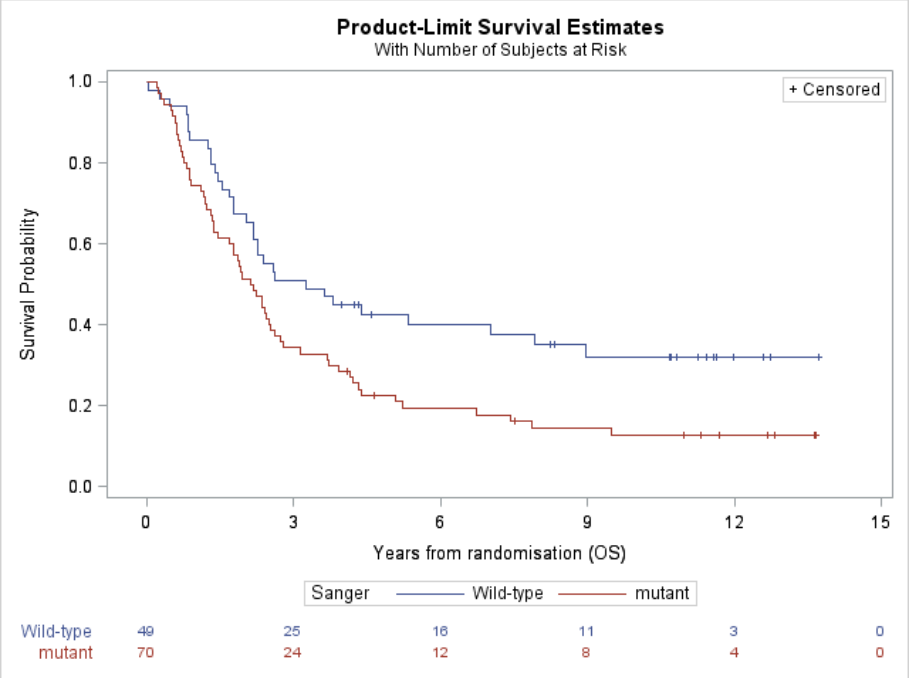

Figure 4-5: Overall survival for patients treated with carboplatin alone in relation to Sanger *TP53* status (*p=0.01*).

Overall Survival			
Variable	**HR**	**95% CI**	**p value**
Sanger *TP53* status	2.43	1.46-4.04	**0.0007*** **
Age	1.01	0.99-1.03	0.35
Stage I/II	0.38	0.12-1.23	0.10
Stage III	0.47	0.23-0.98	**0.04***
Residual bulk < 2	2.56	0.98-6.71	0.06
Residual bulk ≥ 2	4.24	1.61-11.17	**0.003****
Intermediate differentiation	0.76	0.20-2.98	0.70
Poor differentiation	0.37	0.09-1.56	0.18
Clear cell	5.22	0.62-43.98	0.13
Endometrioid	19.03	1.98-182.61	**0.01***
High grade serous	5.12	0.66-39.70	0.12
Low grade serous	3.34	0.35-31.95	0.30
Mucinous	4.77	0.37-60.96	0.23

Table 4-6: Multivariate analysis of overall survival for patients treated with carboplatin alone. *, *p<0.05*; **, *p<0.01*; *, *p<0.001*. Significant p-values are highlighted.**

4.4.2.5 Survival following treatment with either single agent carboplatin or CAP in relation to Sanger *TP53* status

In the case of individuals treated with either single agent carboplatin or CAP, there was a significant difference in median survival time between women with wild-type and mutant *TP53* tumours (X^2=5.99, *p=0.01*) (Figure 4-6). The multivariate analysis for the group of patients who received either carboplatin or CAP demonstrated that *TP53* mutational status (*p=0.002),* residual disease <2 cm (*p=0.04)* and residual disease ≥2 cm (*p=0.002)* retained prognostic significance (Table 4-7). These results demonstrate that *TP53* mutational status defined by Sanger sequencing is an independent prognostic variable and individuals with wild-type *TP53* tumours survive longer as a result of this treatment.

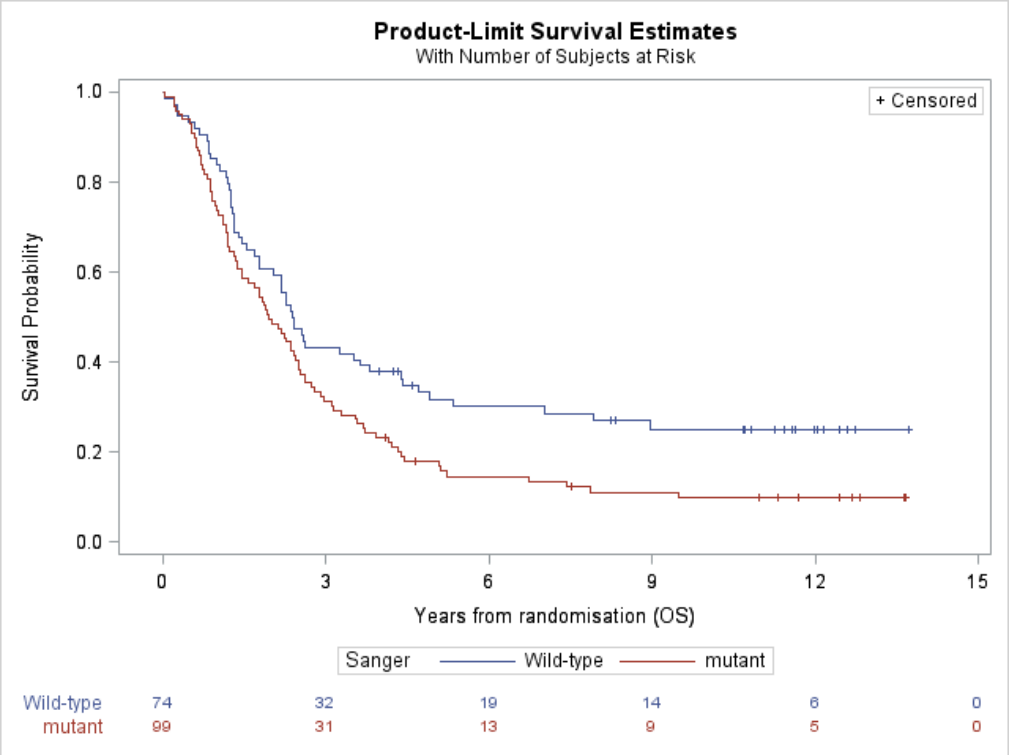

Figure 4-6: Overall survival for patients treated with either carboplatin or CAP in relation to Sanger *TP53* status (*p=0.01*).

Overall Survival			
Variable	**HR**	**95% CI**	**p value**
Sanger *TP53* status	1.79	1.24-2.59	**0.002****
Age	1.02	1.0-1.04	0.07
Stage I/II	0.48	0.19-1.17	0.11
Stage III	0.79	0.49-1.28	0.33
Residual bulk < 2	2.09	1.03-4.24	**0.04***
Residual bulk ≥ 2	2.83	1.47-5.44	**0.002****
Intermediate differentiation	1.46	0.65-3.29	0.36
Poor differentiation	0.85	0.37-1.95	0.71
Clear cell	1.20	0.49-2.90	0.69
Endometrioid	2.05	0.82-5.09	0.12
High grade serous	0.96	0.48-1.94	0.92
Low grade serous	0.78	0.32-1.89	0.58
Mucinous	0.97	0.19-5.02	0.97

Table 4-7: Multivariate analysis of overall survival for patients treated with either carboplatin or CAP. *, *p<0.05*; **, *p<0.01*. Significant p-values are highlighted.

4.4.2.6 Analysis of survival for patients with serous histology tumours following treatment with carboplatin alone in relation to Sanger *TP53* status

Due to the previously reported high proportion of *TP53* mutations in HGSC (Ahmed *et al.*, 2010; Kurman, 2013), the most aggressive histological subtype of ovarian cancer, subgroup survival analysis was performed in relation to *TP53* status and treatment options for 90 patients with serous histology. The Kaplan-Meier analysis showed a highly significant association between the mutational status of *TP53* and OS (X^2=8.59, *p=0.003*) (Figure 4-7). Based on the multivariate analysis for this subgroup, *TP53* (*p=0.0002*), stage III (*p=0.03*), residual disease <2 cm (*p=0.02*) and residual disease ≥2 cm (*p=0.005*) were retained as independent prognostic variables (Table 4-8).

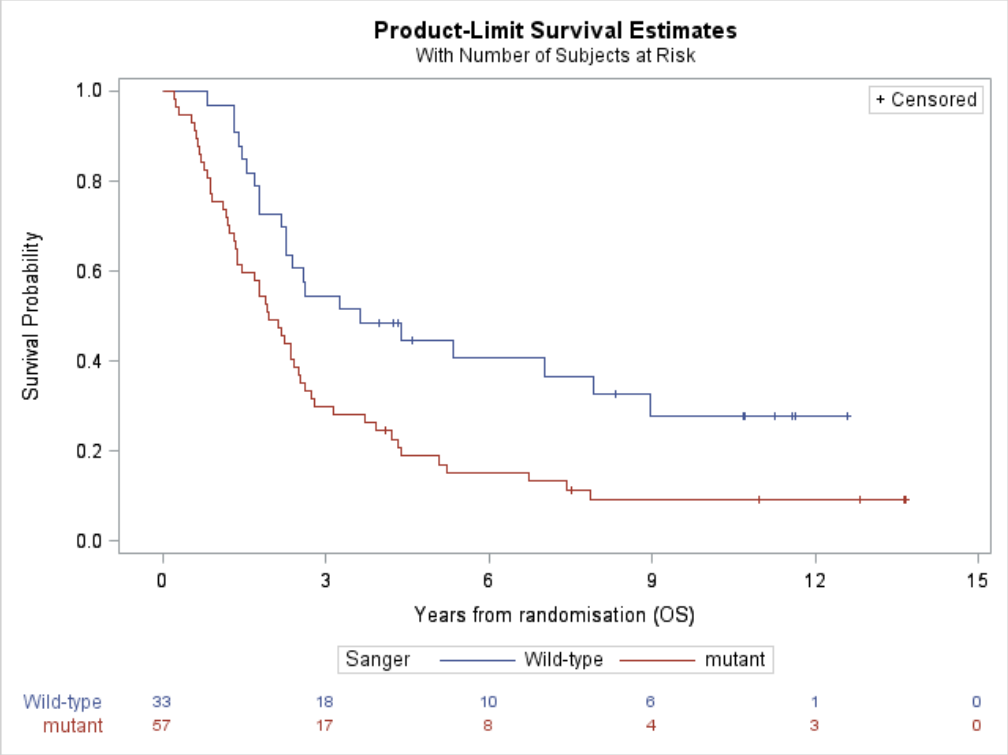

Figure 4-7: Overall survival for treatment with carboplatin alone for patients with serous histology tumours in relation to Sanger *TP53* status (*p=0.003*).

Overall Survival			
Variable	**HR**	**95% CI**	**p value**
Sanger *TP53* status	3.07	1.72-5.49	**0.0002*** **
Age	1.02	0.99-1.04	0.16
Stage I/II	0.44	0.12-1.59	0.21
Stage III	0.39	0.171-0.90	**0.03***
Residual bulk < 2	3.73	1.23-11.32	**0.02***
Residual bulk ≥ 2	4.71	1.60-13.81	**0.005****
Intermediate differentiation	1.66	0.18-15.53	0.66
Poor differentiation	0.81	0.08-8.21	0.86
High grade serous	1.25	0.49-3.21	0.64

Table 4-8: Multivariate analysis for overall survival following treatment with carboplatin alone for patients with serous histology tumours. *, *p<0.05*; **, *p<0.01*; *, *p<0.001*. Significant p-values are highlighted.**

4.4.2.7 Analysis of survival for patients with serous histology tumours following treatment with either carboplatin or CAP in relation to Sanger *TP53* status

As shown in Figure 4-8, the women with serous histology and wild-type *TP53* tumours who received carboplatin or CAP had significantly better survival times compared to those with mutated *TP53* (X^2=8.84, *p=0.003*). Also, mutational status of *TP53* (*p=0.0001*), residual disease <2 cm (*p=0.03*) and residual disease ≥2 cm (*p=0.001*) retained their significance as independent prognostic variables on multivariate analysis (Table 4-9).

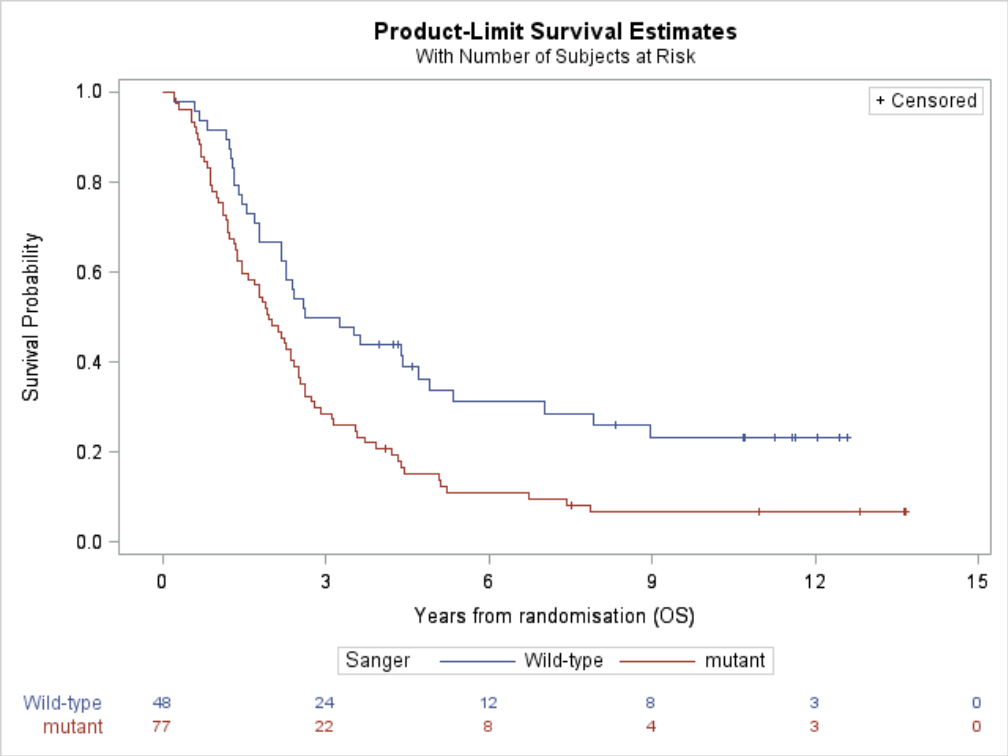

Figure 4-8: Overall survival following treatment with either carboplatin or CAP, for patients with serous histology tumours in relation to Sanger *TP53* status (*p=0.003*).

Overall Survival			
Variable	**HR**	**95% CI**	**p value**
Sanger *TP53* status	2.43	1.55-3.82	**0.0001*** **
Age	1.01	0.99-1.03	0.29
Stage I/II	0.65	0.21-2.05	0.47
Stage III	0.70	0.39-1.25	0.23
Residual bulk < 2	2.65	1.13-6.23	**0.03***
Residual bulk ≥ 2	3.60	1.65-7.83	**0.001****
Intermediate differentiation	1.76	0.62-4.93	0.29
Poor differentiation	1.10	0.39-3.12	0.85
High grade serous	1.01	0.53-1.92	0.97

Table 4-9: Multivariate analysis for overall survival following treatment with carboplatin or CAP, for patients with serous histology tumours. *, *p<0.05*; **, *p<0.01*; *, *p<0.001*. Significant p-values are highlighted.**

4.4.2.8 The effect of paclitaxel addition on overall survival for treatment with either carboplatin or CAP, according to tumour Sanger *TP53* status

The survival times for patients treated with platinum-based chemotherapy versus those additionally treated with paclitaxel, were analysed by *TP53* status. As can be seen in Figure 4-9, addition of paclitaxel showed a trend for improved overall survival, which was greater in the *TP53* mutated subgroup, particularly for patients with serous tumours, however this did not reach statistical significance (*p=0.11*).

4.4.2.9 The effect of paclitaxel addition on overall survival for treatment with CAP alone, according to tumour Sanger *TP53* status

To study whether women whose tumours have wild-type *TP53* gain benefit from addition of paclitaxel to carboplatin compared to CAP, the survival times were analysed in relation to *TP53* status. There was no significant difference in survival between patients treated with CAP compared to those received carboplatin and paclitaxel by *TP53* status (*p=0.08*) (Figure 4-9).

4.4.2.10 The effect of paclitaxel addition on overall survival for treatment with carboplatin alone, according to tumour Sanger *TP53* status

As shown in Figure 4-9, no significant difference was observed in survival for patients treated with carboplatin compared to those treated with addition of paclitaxel to carboplatin in respect to *TP53* status (*p=0.57*).

4.4.2.11 The effect of paclitaxel addition on survival for treatment with carboplatin or CAP for patients with serous histology tumours, according to tumour Sanger *TP53* status

In terms of patients with serous histological subtype, women treated with addition of paclitaxel appeared to be associated with better overall survival compared to individuals treated with either carboplatin or CAP, in particular for those with mutant *TP53*, nevertheless this difference was marginally significant (*p=0.06*) with an odds ratio of 0.66 (0.44-1.00) (Figure 4-9).

4.4.2.12 The effect of paclitaxel addition on survival for treatment with CAP alone for patients with serous histology tumours, according to tumour Sanger *TP53* status

In the case of individuals with serous histology tumours who received addition of paclitaxel, no significant difference in survival was observed irrespective of *TP53* status (*p=0.12*) (Figure 4-9).

4.4.2.13 The effect of paclitaxel addition on survival for treatment with carboplatin alone for patients with serous histology tumours, according to tumour Sanger *TP53* status

As can be seen in Figure 4-9, patients with serous histology tumours gain no benefit from addition of paclitaxel to carboplatin (*p=0.28*) (Figure 4-9).

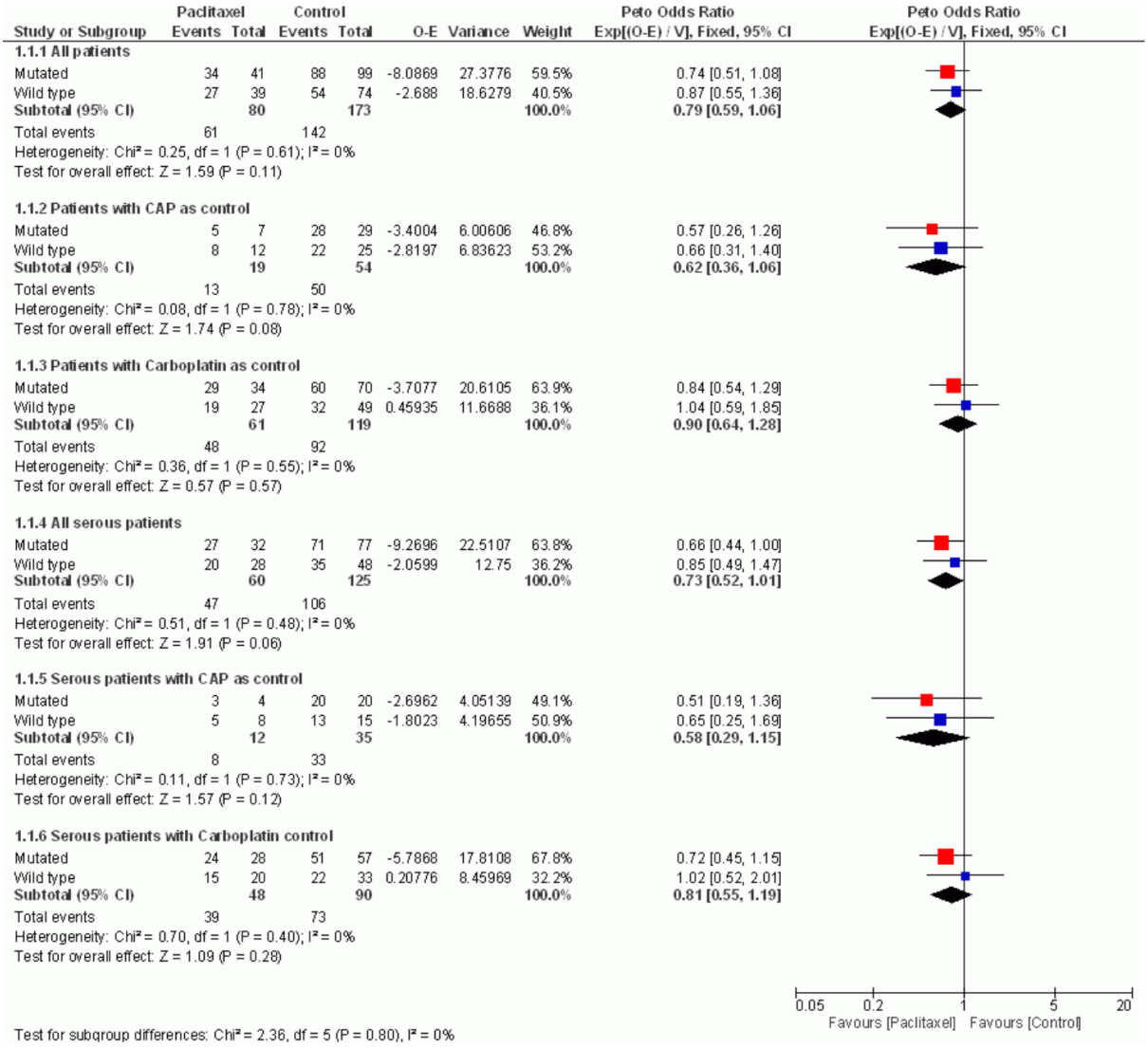

Figure 4-9: The effect of paclitaxel addition on overall survival for patients treated with platinum-based chemotherapy, in relation to Sanger *TP53* status (*p>0.05*). All patients in this context refers to CAP or carboplatin as control.

4.4.3 Results based on the Next Generation Sequencing (NGS)

4.4.3.1 Distribution of *TP53* status detected by NGS

162 (64%) out of 253 patients had tumours with mutant *TP53*, 89 (35%) showed wild-type *TP53* and 2 cases (1%) were lost. NGS detected a higher incidence of mutant *TP53* cases compared to Sanger sequencing, 64% versus 55%. The frequencies of insertion, deletion, transversion and transition mutations were 7%, 14%, 14% and 65% respectively. The highest frequency of substitution mutations was C>T (37%) (Figure 4-10A & B). The substitution mutations cover *TP53* hotspot mutations at codon 175, 237, 248, 273 and 282, with a predominance in codon 273 (Figure 4-10C). This difference compared to the Sanger sequencing (Figure 4-2C) could be due to the low success rate for exon 7 sequencing by NGS.

4.4.3.2 Distribution of clinicopathological variables according to NGS *TP53* status

Table 4-10 illustrates the frequency distribution of *TP53* mutations in regard to clinicopathological data including histological subtypes, residual disease, FIGO stage and differentiation grade. The overall differences between the frequency distribution of different histological subtypes with respect to mutational status of *TP53* was statistically significant (X^2=24.06, *p=0.0002*).

The distribution of different disease stages was associated with genomic status of *TP53* (X^2=11.03, *p=0.004*), which is in contrast with Sanger sequencing data (X^2=1.31, *p=0.52*). Consistent with Sanger sequencing data, there was no significant difference in the frequency distribution for each category of residual disease based on the mutational status of *TP53* (X^2=4.10, *p=0.13*). Furthermore, the presence of mutant *TP53* was significantly associated with poor differentiation (X^2=17.75, *p=0.0001*) (Table 4-10).

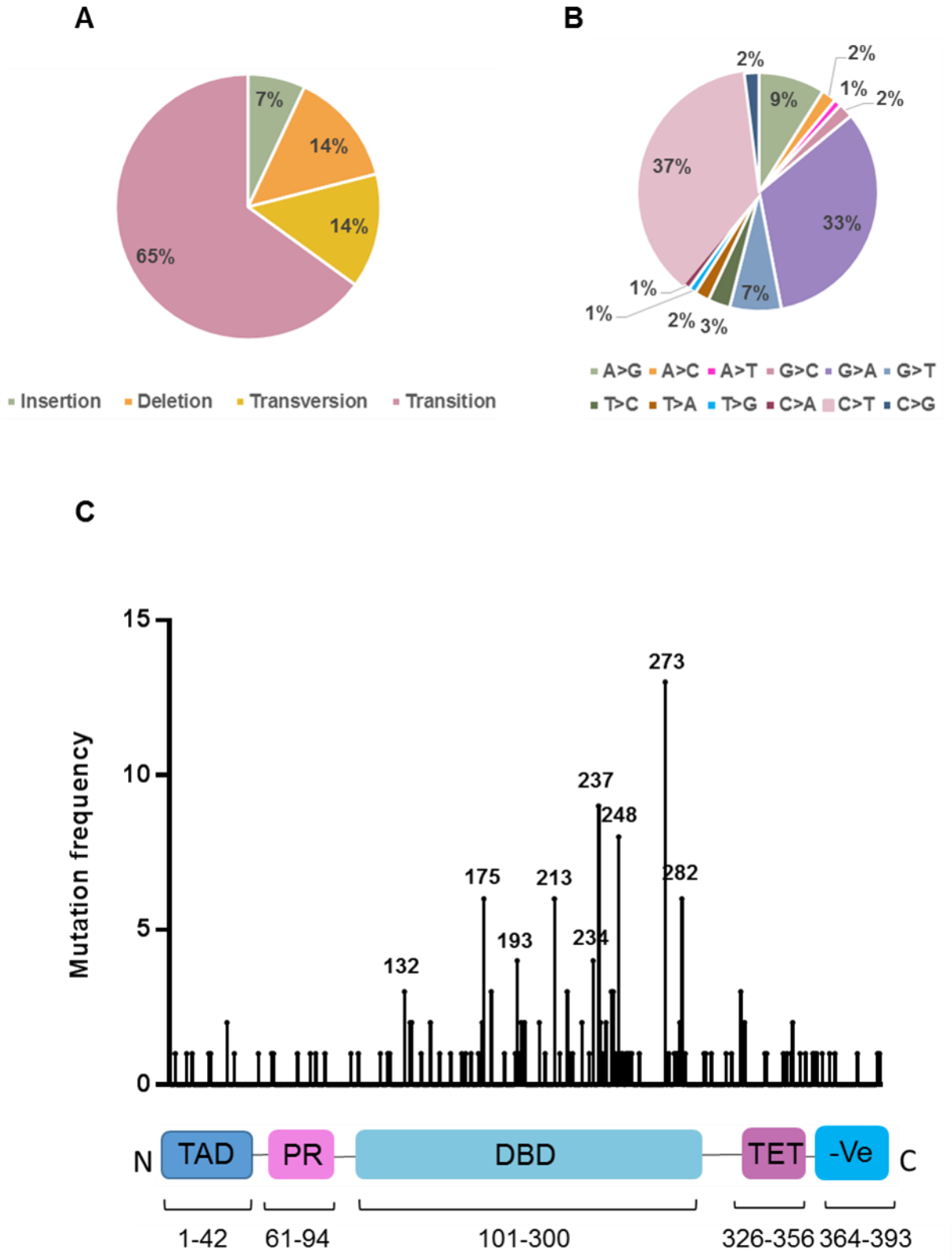

Figure 4-10: (A) Distribution of *TP53* mutations and (B) Distribution of *TP53* substitution mutations from 253 samples of the ICON3 cohort detected by NGS. (C) Distribution of the *TP53* mutations in p53 residues from 253 samples of the ICON3 cohort detected by NGS.

Variable	Wild-Type *TP53* Number (%)	Mutant *TP53* Number (%)	Total Number (%)
Histological Subtype			
Clear Cell	18 (20)	7 (4)	25 (10)
Endometrioid	11 (12)	10 (6)	21 (8)
High Grade Serous	45 (51)	112 (69)	157 (62)
Low Grade Serous	9 (10)	17 (10)	26 (10)
Mucinous	3 (3)	2 (1)	5 (2)
Undifferentiated	3 (3)	14 (9)	17 (7)
No result	-	-	2 (1)
Total	89 (100)	162 (100)	253 (100)
Stage			
I/II	24 (27)	18 (11)	42 (17)
III	50 (56)	118 (73)	168 (66)
IV	15 (17)	26 (16)	41 (16)
No result	-	-	2 (1)
Total	89 (100)	162 (100)	253 (100)
Residual Disease			
Complete Cytoreduction (none)	27 (30)	31 (19)	58 (23)
< 2cm	17(19)	34 (21)	51 (20)
≥ 2cm	45 (51)	97 (60)	142 (56)
No result	-	-	2 (1)
Total	89 (100)	162 (100)	253 (100)
Grade			
Poorly Differentiated	39 (44)	115 (71)	154 (61)
Moderately Differentiated	39 (44)	36 (22)	75 (29)
Well Differentiated	10 (11)	10 (6)	20 (8)
Lost	1 (1)	1 (1)	2 (1)
No result	-	-	2 (1)
Total	89 (100)	162 (100)	253 (100)

Table 4-10: Distribution of clinicopathological data with respect to NGS *TP53* status for 253 samples from patients in the ICON3 cohort.

4.4.3.3 NGS *TP53* status and Overall Survival/Progression-Free Survival

The Kaplan-Meier analysis method was used to construct survival curves based on the NGS *TP53* status. In contrast with the Sanger sequencing data, there was no significant difference in OS (X^2=2.14, *p=0.14*) and PFS (X^2=1.08, *p=0.30*) times between patients with wild-type *TP53* compared to individuals with mutant *TP53* tumours (Figure 4-12 & Figure 4-12).

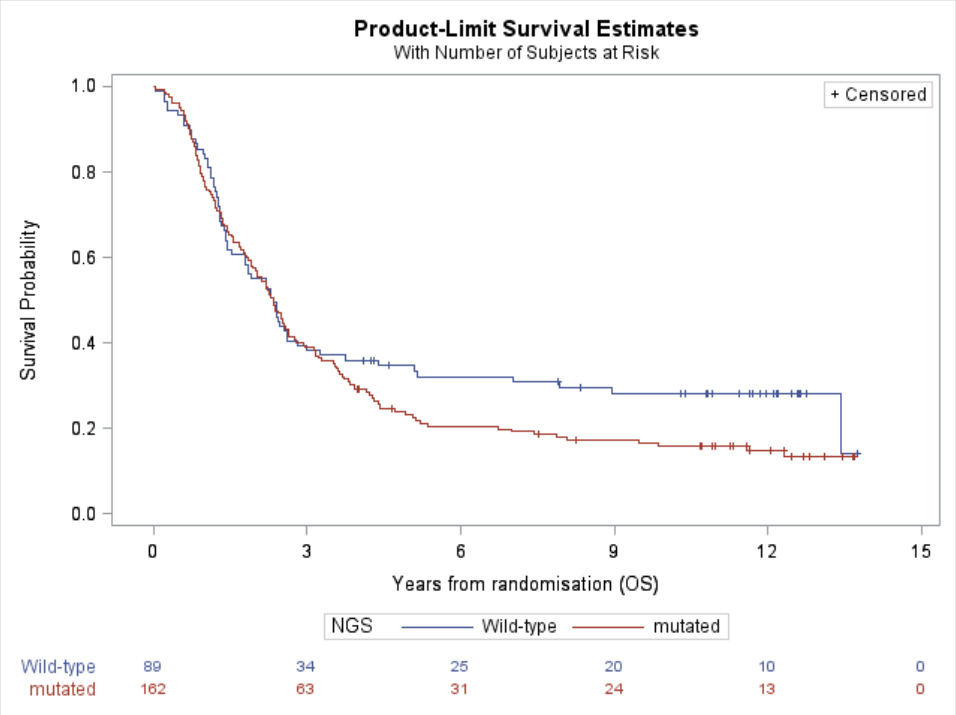

Figure 4-11: Overall survival for all patients in relation to NGS *TP53* status (*p=0.14*).

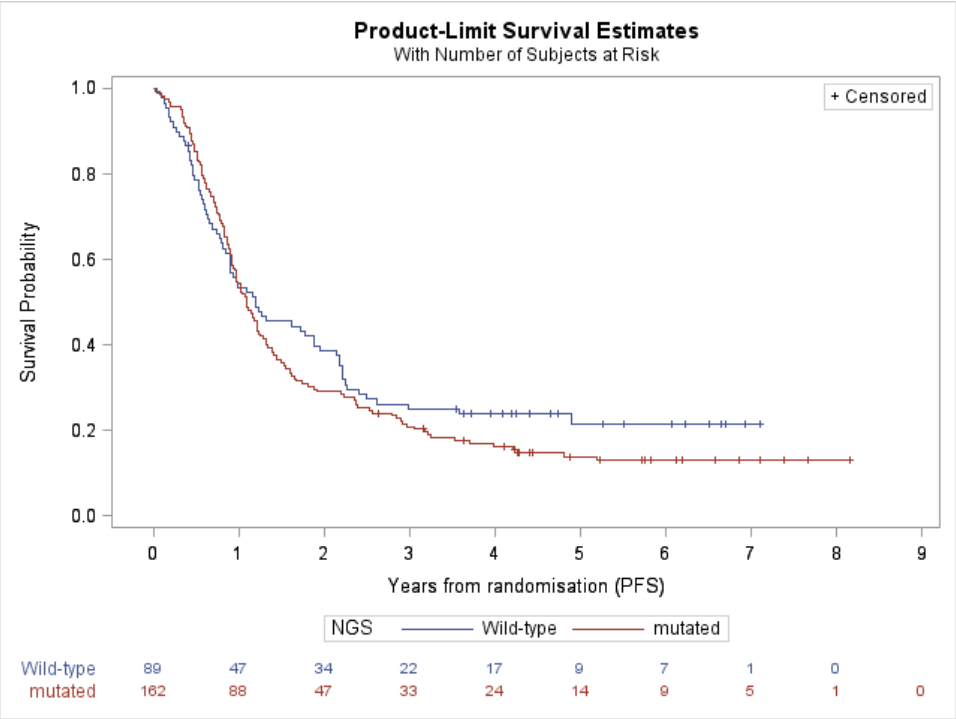

Figure 4-12: Progression-free survival for all patients in relation to NGS *TP53* status (*p=0.30*).

4.4.3.4 Survival following treatment with carboplatin alone in relation to NGS *TP53* status

As shown in Figure 4-13, the survival probability was significantly better for patients with wild-type *TP53* tumours who received carboplatin than those with mutant *TP53* tumours (X^2=3.98, *p=0.04*). The *TP53* (*p=0.003*), residual bulk ≥2 cm (*p=0.004*) and endometrioid histology (*p=0.02*) were all retained as independent prognostic variables on multivariate analysis, with the most significant variable being the *TP53* mutational status (Table 4-11).

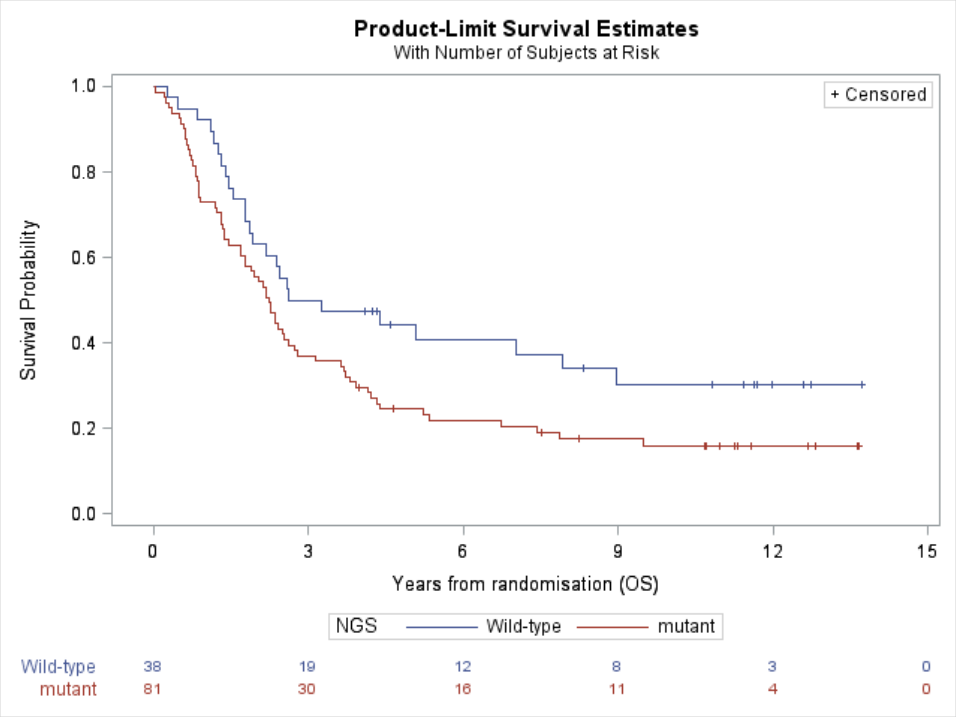

Figure 4-13: Overall survival for patients treated with carboplatin alone in relation to NGS *TP53* status (*p=0.04*).

Overall Survival			
Variable	**HR**	**95% CI**	**p value**
NGS *TP53* status	2.25	1.31-3.85	**0.003****
Age	1.00	0.98-1.03	0.65
Stage I/II	0.50	0.16-1.58	0.24
Stage III	0.58	0.29-1.16	0.12
Residual bulk < 2	2.25	0.90-5.63	0.08
Residual bulk ≥ 2	3.96	1.54-10.19	**0.004****
Intermediate differentiation	0.96	0.25-3.71	0.95
Poor differentiation	0.39	0.09-1.60	0.19
Clear cell	5.30	0.64-48.88	0.12
Endometrioid	12.48	1.41-110.72	**0.02***
High grade serous	4.78	0.64-35.85	0.13
Low grade serous	2.37	0.26-21.52	0.44
Mucinous	4.46	0.37-54.33	0.24

Table 4-11: Multivariate analysis of overall survival for patients treated with carboplatin alone. *, *p<0.05*; **, *p<0.01*. Significant p-values are highlighted.

4.4.3.5 Survival following treatment with either carboplatin or CAP in relation to NGS *TP53* status

In contrast with the Sanger sequencing data, survival times were not significantly different between women treated with either single agent carboplatin or CAP with respect to NGS *TP53* status (X^2=1.62, *p=0.20*) (Figure 4-14). The only significant predictor of survival which was retained as an independent variable on multivariate analysis was residual disease ≥2 cm (*p=0.004*) (Table 4-12).

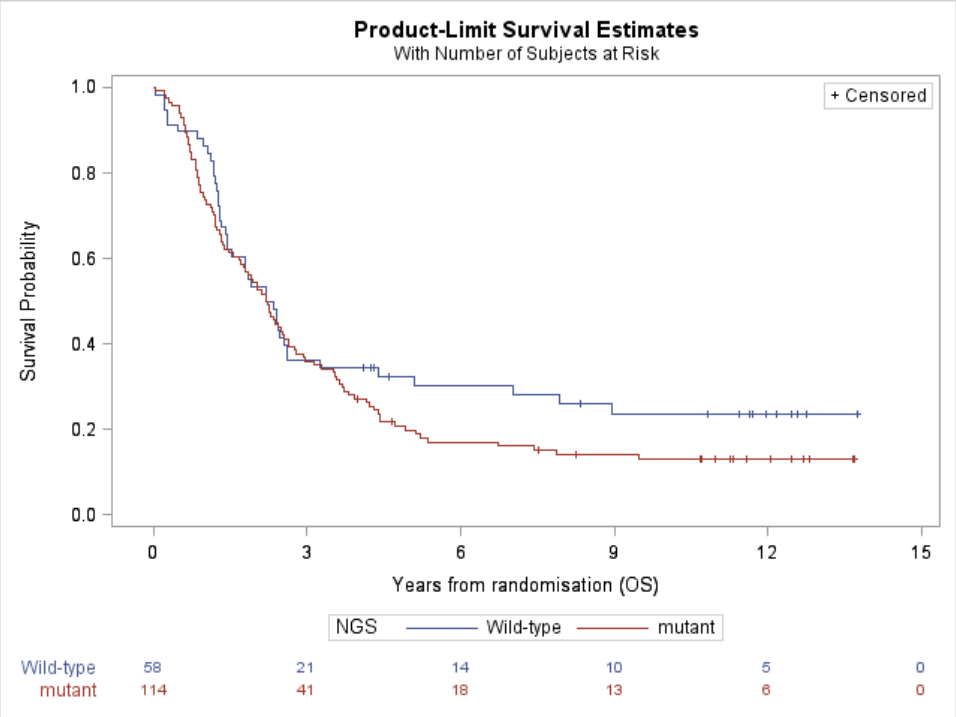

Figure 4-14: Overall survival for patients treated with either carboplatin or CAP in relation to NGS *TP53* status (*p=0.20*).

Overall Survival			
Variable	**HR**	**95% CI**	**P-value**
NGS *TP53* status	1.22	0.82-1.83	0.32
Age	1.02	0.98-1.03	0.11
Stage I/II	0.49	0.20-1.23	0.13
Stage III	0.86	0.53-1.39	0.53
Residual bulk ≤ 2	1.93	0.95-3.93	0.07
Residual bulk > 2	2.70	1.37-5.29	**0.004****
Intermediate differentiation	1.56	0.69-3.52	0.28
Poor differentiation	1.00	0.44-2.33	0.99
Clear cell	1.33	0.55-3.21	0.53
Endometrioid	1.97	0.79-4.91	0.14
High grade serous	0.97	0.48-1.94	0.93
Low grade serous	0.71	0.29-1.74	0.45
Mucinous	1.09	0.21-5.59	0.92

Table 4-12: Multivariate analysis of overall survival for patients treated with either carboplatin or CAP. **, *p<0.01*. Significant p-values are highlighted.

4.4.3.6 Analysis of survival for patients with serous histology tumours following treatment with carboplatin alone in relation to NGS *TP53* status

As can be seen in Figure 4-15, survival times were not associated with *TP53* status for patients with serous histology tumours treated with carboplatin alone (X^2=2.01, *p=0.16*). Cox regression multivariate analysis identified the *TP53* status (*p=0.006*), residual bulk <2 cm (*p=0.04*) and residual disease ≥2 cm (*p=0.009*) as independent prognostic factors (Table 4-13).

4.4.3.7 Analysis of survival for patients with serous histology tumours following treatment with either carboplatin or CAP in relation to NGS *TP53* status

No significant difference was observed in survival time between patients with serous histology and wild-type *TP53* tumours treated with carboplatin or CAP compared to those with mutant *TP53* (.X^2=0.55, *p=0.46*) (Figure 4-16). The only variable which retained its significance as an independent prognostic factor on multivariate analysis was residual disease ≥2 cm (.X^2=6.84, *p=0.009*) (Table 4-14).

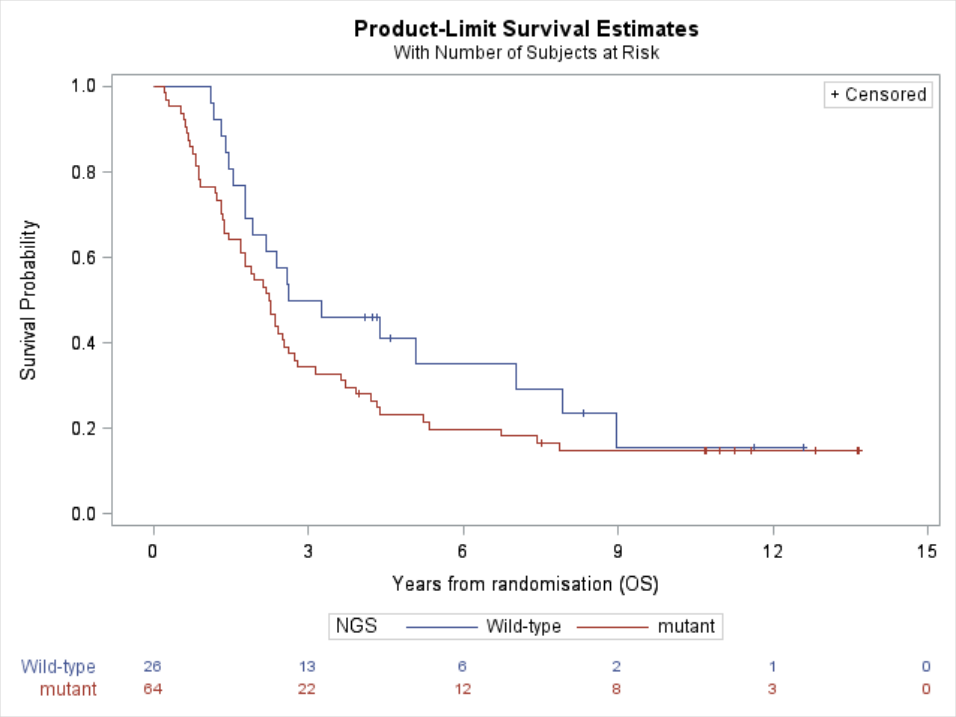

Figure 4-15: Overall survival for treatment with carboplatin alone, for patients with serous histology tumours in relation to NGS *TP53* status (*p=0.16*).

Overall Survival			
Variable	**HR**	**95% CI**	**P-value**
NGS *TP53* status	2.33	1.28-4.23	**0.006****
Age	1.01	0.99-1.04	0.30
Stage I/II	0.55	0.15-2.00	0.36
Stage III	0.59	0.27-1.30	0.19
Residual bulk < 2	3.22	1.08-9.64	**0.04***
Residual bulk ≥ 2	4.20	1.43-12.30	**0.009****
Intermediate differentiation	1.95	0.20-18.76	0.56
Poor differentiation	0.77	0.07-8.21	0.83
High grade serous	1.84	0.72-4.72	0.21

Table 4-13: Multivariate analysis for overall survival following treatment with carboplatin alone for patients with serous histology tumours. *, *p<0.05*; **, *p<0.01*. Significant p-values are highlighted.

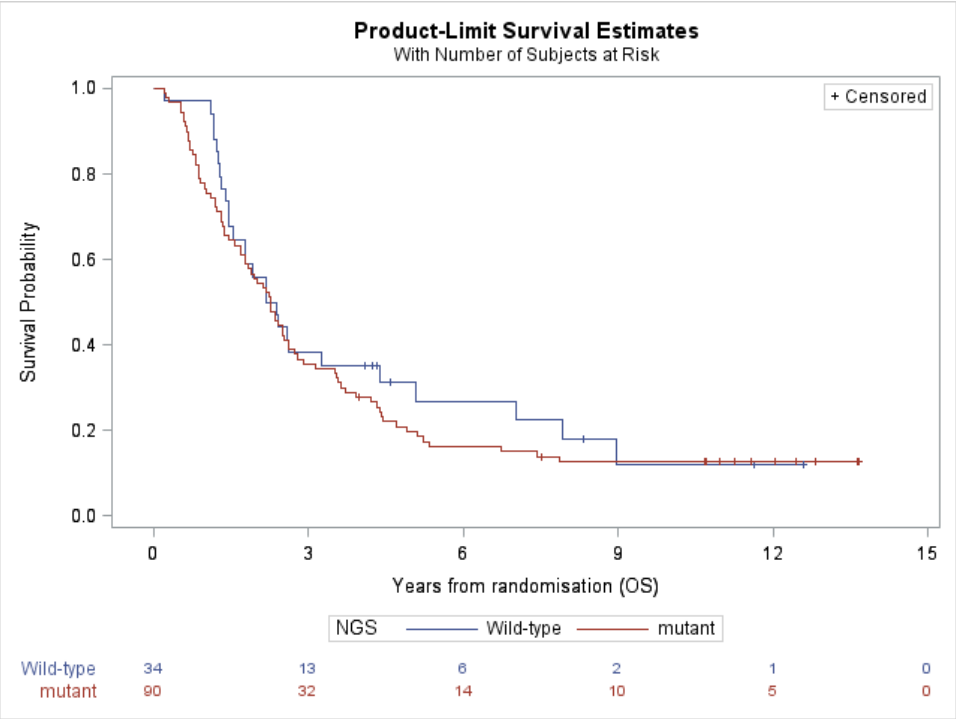

Figure 4-16: Overall survival following treatment with either carboplatin or CAP, for patients with serous histology tumours in relation to NGS *TP53* status (*p=0.46*).

Overall Survival			
Variable	**HR**	**95% CI**	**P-value**
NGS *TP53* status	1.28	0.80-2.00	0.30
Age	1.01	0.99-1.03	0.37
Stage I/II	0.63	0.20-1.98	0.43
Stage III	0.81	0.45-1.43	0.46
Residual bulk < 2	2.27	0.93-5.51	0.07
Residual bulk ≥ 2	3.03	1.32-6.94	**0.009****
Intermediate differentiation	1.90	0.67-5.36	0.23
Poor differentiation	1.44	0.50-4.18	0.50
High grade serous	1.18	0.60-2.30	0.63

Table 4-14: Multivariate analysis for overall survival following treatment with either carboplatin or CAP for patients with serous histology tumours. **, *p<0.01*.

4.4.3.8 The effect of paclitaxel addition on overall survival for treatment with either carboplatin or CAP, according to tumour NGS *TP53* status

The overall survival was analysed for patients treated with either carboplatin or CAP compared to those who received paclitaxel plus carboplatin in relation to NGS *TP53* status. As shown in Figure 4-17, no significant impact on survival was observed by addition of paclitaxel (*p=0.12*).

4.4.3.9 The effect of paclitaxel addition on overall survival for treatment with CAP alone, according to tumour NGS *TP53* status

Individuals treated with a combination of carboplatin and paclitaxel appeared to be associated with better long-term survival compared to those received CAP alone, in particular for patients with mutant *TP53* tumours even though this difference did not reach statistical significance (*p=0.07*) (Figure 4-17)

4.4.3.10 The effect of paclitaxel addition on overall survival for treatment with carboplatin alone, according to tumour NGS *TP53* status

As can be seen in Figure 4-17, paclitaxel addition had no significant impact on survival for patients who received single agent carboplatin, irrespective of mutational status of *TP53* (*p=0.62*).

4.4.3.11 The effect of paclitaxel addition on survival for treatment with either carboplatin or CAP for patients with serous histology tumours, according to tumour NGS *TP53* status

For patients with serous histology tumours, there was no significant difference in survival time between women treated with either carboplatin or CAP compared to those treated with an addition of paclitaxel to carboplatin irrespective of *TP53* status (*p=0.07*) (Figure 4-17).

4.4.3.12 The effect of paclitaxel addition on survival for treatment with CAP alone for patients with serous histology tumours, according to tumour NGS *TP53* status

The statistical analysis showed no significant difference in survival between patients with serous histology tumours treated with CAP alone compared to those who received carboplatin and paclitaxel, regardless of *TP53* status (*p=0.11*) (Figure 4-17).

4.4.3.13 The effect of paclitaxel addition on survival for treatment with carboplatin alone for patients with serous histology tumours, according to tumour NGS *TP53* status

No significant difference in survival was observed between patients with serous histology tumours treated with carboplatin alone versus those treated with a combination of carboplatin and paclitaxel by *TP53* mutational status (*p=0.28*) (Figure 4-17).

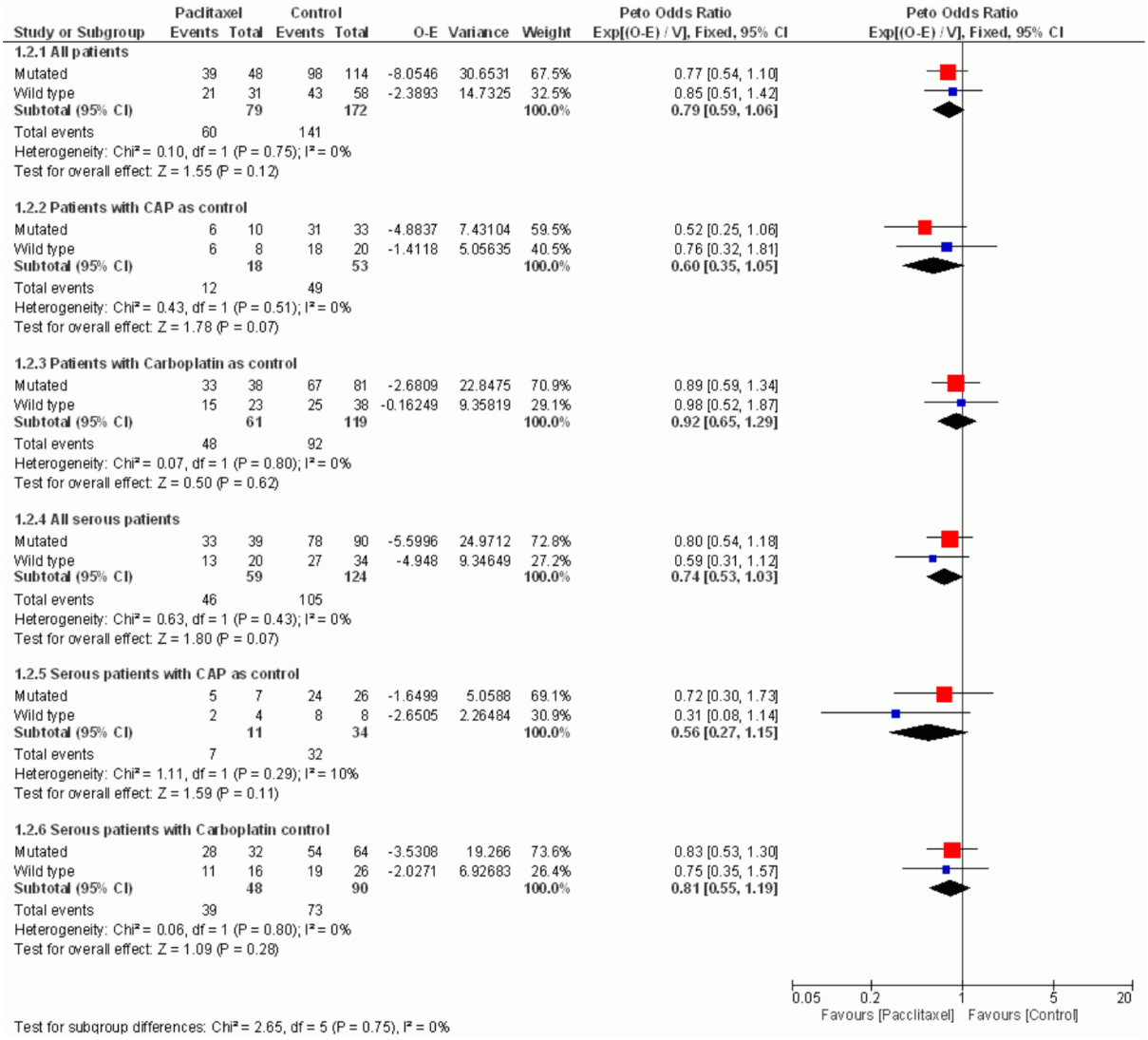

Figure 4-17: The effect of paclitaxel addition on overall survival for patients who treated with platinum-based chemotherapy, in relation to NGS *TP53* status (*p>0.05*). All patients in this context refers to CAP or carboplatin as control.

4.4.4 Analysis of hypotheses in regard to Sanger sequencing, NGS, either Sanger or NGS, and both techniques

4.4.4.1 Overall survival and progression-free survival

Table 4-15 summarises the log-rank test p-values for the observed differences between OS or PFS times in relation to *TP53* mutational status. The results for patients with serous histology are also summarised. The summary results are shown for individual analyses using *TP53* mutation data detected by Sanger sequencing, NGS, either Sanger or NGS, and both techniques. The analysis based on the Sanger sequencing indicated that mutational status of *TP53* is a significant prognostic biomarker for all patients and for the subgroup with serous histology tumours. The *TP53* status retained its significance for overall survival when the data were analysed based on detection by both techniques. However, for PFS, significant differences in survival were only observed according to *TP53* status detected using Sanger sequencing.

Overall Survival and Progression Free Survival			
Patients	***TP53* Sequencing Technique**	**Overall Survival**	**Progression Free Survival**
All patients	Sanger	**0.009****	**0.04***
	NGS	0.14	0.30
	Either	0.06	0.09
	Both	**0.02***	0.13
All serous patients	Sanger	**0.002****	**0.03***
	NGS	0.13	0.25
	Either	0.08	0.11
	Both	**0.004****	0.06

Table 4-15: Summary overall survival and progression-free survival for all patients and patients with serous histology tumours in relation to *TP53* mutational status detected by different techniques. *, *p< 0.05*; **, *p< 0.01*. NGS, Next generation sequencing. Significant p-values are highlighted.

4.4.4.2 Analysis of the first hypothesis for all patients

We hypothesised that patients with wild-type *TP53* are more sensitive to carboplatin than those with mutant *TP53* and survive longer as a result of this treatment.

Regardless of the sequencing method or combinations of datasets (Either or Both), patients whose tumours harboured wild-type *TP53* were more sensitive to single agent carboplatin than those with mutant *TP53* ($p < 0.05$). Furthermore, *TP53* genomic status was also retained as an independent predictive variable in multivariate analysis including age, disease stage (I/II and III), residual disease, grade of differentiation (poor and intermediate differentiation), histology and *TP53* mutational status ($p<0.01$) (Table 4-16).

TP53 mutational status detected by Sanger sequencing or defined by the combination of both Sanger and NGS had prognostic significance in both univariate and multivariate analyses for all patients who received either single agent carboplatin or CAP (Table 4-16).

For PFS, the *TP53* status was not significantly associated with survival for patients in response to all treatment options with the exception of those treated with carboplatin, in relation to mutational status of *TP53* detected by either Sanger sequencing or NGS. Interestingly, *TP53* status was an independent prognostic factor in multivariate analysis for patients treated with carboplatin irrespective of sequencing method or *TP53* status dataset combination (Table 4-17).

4.4.4.3 Analysis of the first hypothesis for patients with serous histology tumours

For patients with serous histology tumours treated with single agent carboplatin, individuals with wild-type *TP53* detected by Sanger sequencing and by both sequencing techniques had a better OS compared to those with mutant *TP53*. The *TP53* status was significant as a prognostic biomarker in multivariate analysis irrespective of sequencing technique. Furthermore, the prognostic value of *TP53* retained significance for patients with serous histology tumours treated with carboplatin or CAP for both univariate and multivariate analysis based on the Sanger sequencing and on detection by both sequencing methods (Table 4-18).

No significant difference was observed in PFS for patients with serous histology tumours by *TP53* status irrespective of sequencing method. However, the *TP53* status was significant in the Cox multivariate regression analysis model for treatment with carboplatin alone (Table 4-19).

Overall Survival, All Patients					
Treatment Option	***TP53* Sequencing Technique**	**Univariate Analysis**		**Multivariate Analysis**	
		P-value	**HR**	**P-value**	**HR**
Carboplatin	Sanger	**0.01***	1.73	**0.0007*****	2.43
	NGS	**0.048***	1.59	**0.003****	2.25
	Either	**0.02***	1.85	**0.001****	2.67
	Both	**0.02***	1.63	**0.0009*****	2.29
Carboplatin or CAP	Sanger	**0.02***	1.53	**0.002****	1.79
	NGS	0.20	1.26	0.32	1.22
	Either	0.15	1.34	0.12	1.40
	Both	**0.02***	1.50	**0.007****	1.66

Table 4-16: Univariate and Multivariate Cox regression analysis of overall survival for patients treated with carboplatin alone, either carboplatin or CAP in relation to *TP53* status. *, *p< 0.05*; **, *p< 0.01*; *, *p< 0.001*; NGS, Next generation sequencing. Significant p-values are highlighted.**

Progression Free Survival, All Patients					
Treatment Option	***TP53* Sequencing Technique**	**Univariate Analysis**		**Multivariate Analysis**	
		P-value	**HR**	**P-value**	**HR**
Carboplatin	Sanger	0.1	1.40	**0.01***	1.87
	NGS	0.07	1.49	**0.004****	2.10
	Either	**0.04***	1.69	**0.004****	2.28
	Both	0.14	1.35	**0.009****	1.85
Carboplatin or CAP	Sanger	0.09	1.33	**0.03***	1.49
	NGS	0.23	1.24	0.33	1.21
	Either	0.18	1.30	0.20	1.31
	Both	0.10	1.31	0.06	1.42

Table 4-17: Univariate and Multivariate Cox regression analysis of progression-free survival for patients treated with carboplatin alone, either carboplatin or CAP in relation to *TP53* status. *, *p< 0.05*; **, *p< 0.01*; NGS, Next generation sequencing. Significant p-values are highlighted.

Overall Survival, Patients with serous histology					
Treatment Option	***TP53* Sequencing Technique**	**Univariate Analysis**		**Multivariate Analysis**	
		P-value	**HR**	**P-value**	**HR**
Carboplatin	Sanger	**0.004****	2.09	**0.0002*****	3.07
	NGS	0.15	1.46	**0.006****	2.33
	Either	0.056	1.80	**0.003****	2.84
	Both	**0.01***	1.83	**0.0002*****	2.77
Carboplatin or CAP	Sanger	**0.003****	1.86	**0.0001*****	2.43
	NGS	0.46	1.18	0.30	1.29
	Either	0.24	1.34	0.15	1.47
	Both	**0.008****	1.70	**0.0003*****	2.23

Table 4-18: Univariate and Multivariate Cox regression analysis of overall survival following treatment with carboplatin alone, either carboplatin or CAP for patients with serous histology tumours in relation to *TP53* status. *, *p< 0.05*; **, *p< 0.01*; *, *p< 0.001*; NGS, Next generation sequencing. Significant p-values are highlighted.**

Progression Free Survival, Patients with serous histology					
Treatment Option	***TP53* Sequencing Technique**	**Univariate Analysis**		**Multivariate Analysis**	
		P-value	**HR**	**P-value**	**HR**
Carboplatin	Sanger	0.14	1.42	**0.01***	2.02
	NGS	0.28	1.31	**0.006****	2.17
	Either	0.16	1.50	**0.008****	2.44
	Both	0.22	1.32	**0.01***	1.97
Carboplatin or CAP	Sanger	0.12	1.36	**0.02***	1.66
	NGS	0.72	1.08	0.40	1.22
	Either	0.53	1.16	0.35	1.27
	Both	0.19	1.29	**0.03***	1.60

Table 4-19: Univariate and Multivariate Cox regression analysis of progression-free survival following treatment with carboplatin alone, either carboplatin or CAP for patients with serous histology tumours in relation to *TP53* status. *, *p< 0.05*; **, *p< 0.01*; NGS, Next generation sequencing. Significant p-values are highlighted.

4.4.4.4 Analysis of the second hypothesis, patients whose tumours have mutant *TP53* may benefit from the addition of paclitaxel to carboplatin while those with wild-type *TP53* do not benefit

Overall, at the 95% confidence level, addition of paclitaxel had no statistically significant benefit for ovarian cancer patients irrespective of *TP53* genomic status and sequencing techniques or combination datasets used, with a few exceptions listed in Table 4-20 & Table 4-21.

Overall Survival						
Treatment Option	**Sequencing Technique**	***TP53* Status**	**All Patients**		**Patients With Serous Histology**	
			P-value	**HR**	**P-value**	**HR**
Carboplatin versus Carboplatin+ Paclitaxel	Sanger	Mutant	0.41	0.83	0.17	0.71
		Wild-type	0.89	1.04	0.9	1.03
	NGS	Mutant	0.57	0.89	0.42	0.83
		Wild-type	0.96	0.98	0.44	0.74
	Either	Mutant	0.55	0.89	0.28	0.78
		Wild-type	0.81	1.09	0.87	0.93
	Both	Mutant	0.42	0.83	0.27	0.75
		Wild-type	0.96	0.99	0.67	0.87
CAP versus Carboplatin +Paclitaxel	Sanger	Mutant	0.16	0.51	0.18	0.44
		Wild-type	0.28	0.64	0.38	0.63
	NGS	Mutant	0.07	0.45	0.46	0.70
		Wild-type	0.53	0.74	0.07	0.26
	Either	Mutant	0.17	0.59	0.43	0.68
		Wild-type	0.18	0.50	**0.04***	0.20
	Both	Mutant	**0.03***	0.28	0.19	0.45
		Wild-type	0.43	0.74	0.30	0.56

Table 4-20: Kaplan-Meier and Log-rank test analysis of overall survival for patients treated with platinum-based versus addition of paclitaxel to carboplatin in regard to *TP53* mutational status.*, *$p<0.05$*. Significant p-values are highlighted.

Progression-Free Survival						
Treatment Option	**Sequencing Technique**	***TP53* Status**	**All Patients**		**Patients With Serous Histology**	
			P-value	**HR**	**P-value**	**HR**
Carboplatin versus Carboplatin+ Paclitaxel	Sanger	Mutant	0.40	0.83	0.23	0.74
		Wild-type	0.59	0.86	0.26	0.69
	NGS	Mutant	0.25	0.78	0.15	0.71
		Wild-type	0.89	0.96	0.30	0.68
	Either	Mutant	0.29	0.80	0.14	0.72
		Wild-type	0.95	0.98	0.43	0.72
	Both	Mutant	0.33	0.79	0.24	0.73
		Wild-type	0.58	0.87	0.19	0.67
CAP versus Carboplatin +Paclitaxel	Sanger	Mutant	0.24	0.56	0.26	0.50
		Wild-type	0.21	0.60	0.18	0.49
	NGS	Mutant	0.10	0.49	0.48	0.71
		Wild-type	0.47	0.71	**0.03***	0.13
	Either	Mutant	0.23	0.62	0.41	0.67
		Wild-type	0.14	0.47	**0.01***	0.10
	Both	Mutant	0.06	0.33	0.30	0.53
		Wild-type	0.44	0.74	0.21	0.49

Table 4-21: Kaplan-Meier and Log-rank test analysis of progression-free survival for patients treated with platinum-based versus addition of paclitaxel to carboplatin in regard to *TP53* mutational status.*, *$p<0.05$*. Significant p-values are highlighted.

4.5 Discussion

The optimum treatment for ovarian cancer still remains challenging despite large and well-designed clinical trials. One of the major determinants of outcome in ovarian cancer is sensitivity and response to chemotherapy. The role of the *TP53* gene in resistance to treatment is controversial even though many studies show the mutational status of *TP53* is a significant determinant of response to chemotherapy (Havrilesky *et al.*, 2003; Canevari *et al.*, 2006; Gadducci *et al.*, 2006; Bast *et al.*, 2009; Gadducci *et al.*, 2009). A body of experimental evidence suggests the hypothesis that patients with wild-type *TP53* are more sensitive to platinum-based chemotherapy than those with mutant *TP53*, and that patients with mutant *TP53* tumours may gain greater benefit from a combination treatment of platinum-based chemotherapy and paclitaxel. The identification of determinants of tumour response to chemotherapy and development of laboratory techniques to determine sensitivity to chemotherapy prior to treatment help physicians to optimise and individualise patients' treatment and avoid more normal tissue toxicity.

4.5.1 Limitations of FFPE tissues for DNA sequencing

Recently, cancer therapy has been improved by using molecularly targeted therapies which have greatly increased the clinical request for detection of actionable mutations (A subset of driver mutations that have significant diagnostic, prognostic, or therapeutic implications in subsets of cancer patients and for specific therapies) in cancer patients. In fact, precision medicine depends on accurate detection of these actionable mutations (Do and Dobrovic, 2015).

FFPE tissue is one of the most widely used methods to preserve nucleic acid and protein for disease diagnosis and research although use of FFPE tissue for detection of actionable mutations is challenging (Do and Dobrovic, 2015; Gagan and Van Allen, 2015; Arreaza *et al.*, 2016). The FFPE process results in different types of DNA damage including DNA fragmentation because of hydrolysis of phosphodiester bounds, formaldehyde-induced crosslinks, generation of a basic sites and deamination of cytosine base leading to C-> T mutations which can be considered as direct or indirect sources of sequence artifacts. The amount of amplifiable templates available for PCR amplification is significantly reduced by extensive fragmentation of DNA. Another issue for working with FFPE tissue is insufficient and limited quantity of DNA extracted from FFPE samples which results in poor uniformity sequencing data and inhibits the power of mutation detection (Munchel *et al.*, 2015). Despite

these limitations, the results of DNA sequencing data sets from 13 pairs of matched FFPE and fresh-frozen tissue samples indicated high rate of concordant calls between those at reference and variant position in three commonly used sequencing approaches including whole genome, whole exome and targeted exon sequencing. Furthermore, statistical approaches and bioinformatics have been developing to decrease the background mutations, improve the sensitivity of sequencing and eliminate false-positive calls (Munchel *et al.*, 2015).

4.5.2 Analysis of *TP53* mutation

In this study, 260 tumour samples were examined for *TP53* status by genomic DNA sequencing of the coding exons, 2-11, using Sanger sequencing and NGS techniques. The prevalence of *TP53* mutations wad 47%, 56%, 64% and 72% according to the mutations detected by both techniques, Sanger, NGS and either Sanger or NGS respectively. The results from Sanger and NGS are comparable to most previous studies that have sequenced the full coding exons of *TP53* in ovarian cancer (Wen *et al.*, 1999; Shahin *et al.*, 2000; Reles *et al.*, 2001) or in the serous histological subtype of ovarian cancer (Bernardini *et al.*, 2010). However, it was lower than the rate of *TP53* mutation in exons 2-11 for patients with serous ovarian cancer reported by Havrilesky *et al*. (2003) (75%), women with high grade pelvic serous ovarian cancer reported by Ahmed *et al*. (2010) (97%), or those with HGSC reported by The Cancer Genomic Atlas Research (2011) (96%).

Also, the frequency of ovarian cancer *TP53* mutation was higher than other studies which sequenced only exons 5-8 (Fallows *et al.*, 2001; Schuyer *et al.*, 2001; Amikura *et al.*, 2006; Bartel *et al.*, 2008; Rechsteiner *et al.*, 2013). These results indicate that sequencing only exons 5-8 misses some mutations located in exons 2-4 and 9-11. Both Sanger and NGS identified the majority of *TP53* mutations to be located in exons 5-8 which is consistent with other studies (Fallows *et al.*, 2001; Reles *et al.*, 2001; Havrilesky *et al.*, 2003; Ahmed *et al.*, 2010). From a total of 159 patients with HGSC, 99 (62%) and 112 (71%) had mutant *TP53* by Sanger status and NGS status respectively. These results differ from two published studies which reported a very high frequency of *TP53* mutation in HGSC (>95%) (Ahmed *et al.*, 2010; The Cancer Genome Atlas Research, 2011; Wong *et al.*, 2013). Given the fact that exons 2-11 of *TP53* was sequenced by NGS in above studies, this inconsistency is not due to different techniques used or exons sequenced in these studies. From a total of 25 patients with clear cell ovarian cancer, 10 (40%) and 7 (28%) had mutant *TP53* by Sanger and NGS status respectively. This is unlikely that the lower frequency of *TP53* mutation in HGSC and higher frequency of *TP53*

mutation in clear cell and endometrioid histological subtypes is due to misclassification of the samples. Diagnoses from the historical ICON3 clinical trial were reviewed and updated in early 2012 by an extremely experienced gynae pathologist. when the classification changed the percentages in each group also changed and the up to date classification correlates with the current publications representing 60-80% of epithelial ovarian cancer as HGSC (Li *et al.*, 2012; Devouassoux-Shisheboran and Genestie, 2015; McCluggage *et al.*, 2015) and 5-10% as clear cell ovarian cancer (Devouassoux-Shisheboran and Genestie, 2015; Levitan, 2016). However, the frequency of LGSC (10%) was slightly higher than previously reported studies, 3% (Chris M.J. Conklin, 2013) and 6-8% (Rachel N. Grisham, 2016). Moreover, if the proportion of HGSC is considered as the percentage reported by more currently published studies (70%) (Devouassoux-Shisheboran and Genestie, 2015; McCluggage *et al*., 2015) which is 8% higher than the presented results in this study (62%), the *TP53* mutation rate of HGSC would be 70% (62% + 8%) and 79% (71% + 8%) by Sanger status and NGS status respectively. Furthermore, low rates of allele frequency may be responsible in some way for the observed differences in the rate of *TP53* mutation in our study compared to others. An interesting paper indicates that p53 mutations can be found in anyone (including women without cancer) if you look hard enough (Krimmel *et al*., 2016)

The most prominent mutations were substitution/missense, which is consistent with other studies (Reles *et al.*, 2001; Schuyer *et al.*, 2001; Yemelyanova *et al.*, 2011; Rechsteiner *et al.*, 2013).

4.5.3 Relationship of *TP53* status to clinicopathological variables

In the current study, analysis of the relationship between clinicopathological variables and Sanger *TP53* status did not show significant differences amongst different disease stages and residual bulk groups in regard to Sanger *TP53* status. In contrast, the presence of mutant *TP53* was significantly correlated with poor differentiation and high grade serous histology. These results are in accord with other studies that found no association between *TP53* status and disease stage (Bauerschlag *et al.*, 2010; Kim *et al.*, 2014) and other findings that patients with mutant *TP53* are more likely to be associated with increasing tumour grade (Kmet *et al.*, 2003; Bauerschlag *et al.*, 2010; Rechsteiner *et al.*, 2013).

TP53 status by NGS indicated that *TP53* mutations were significantly associated with histological subtype, advanced FIGO stage and poor differentiation, while no association between residual disease and NGS *TP53* status was shown. Two previous studies by Kemet et al. (2003) and Rechsteiner *et al*. (2013) also reported significant associations between *TP53* status and clinicopathological data. However, some other studies reported no significant association between the presence of *TP53* mutation and some clinical pathological data (Fallows *et al.*, 2001; Rose *et al.*, 2003). Literature differences can be explained in part bydifferent sequencing methods, different sequenced exons, study design and size of samples in various studies.

4.5.4 The relationship between *TP53* status and overall survival or progression-free survival regardless of treatment in the ICON3 study

The data from Sanger sequencing for all patients and the subgroup of patients with serous ovarian cancer showed *TP53* mutational status as a significant prognostic factor for OS and/or PFS. Mutational status defined by detection using both sequencing techniques also indicated a significant association between *TP53* mutation and OS but not with PFS. Several studies support these results and found a clear trend with longer OS and/or PFS for patients with wild-type *TP53 t*umour compared to those harbouring mutant *TP53* tumour (Reles *et al.*, 2001; Schuyer *et al.*, 2001; Nadkarni *et al.*, 2013; Rechsteiner *et al.*, 2013). Gadducci *et al*. (2006) found a clear trend for better OS and PFS for ovarian cancer patients with wild-type *TP53* tumour compared to those with mutant *TP53*, although the observed differences did not reach statistical significance. Some other studies have reported no significant association between *TP53* mutation and OS and/PFS (Laframboise S, 2000; Fallows *et al.*, 2001; Bartel *et al.*, 2008;

Ahmed *et al.*, 2010; Bauerschlag *et al.*, 2010). However, HGSC cases with a high rate of *TP53* mutation, 96.7%, were used in the study performed by Ahmed *et al*.

In contrast, no significant correlation was observed in OS and PFS with respect to NGS *TP53* status and mutations defined in a combination dataset by the detection by either Sanger or NGS methods. In fact, the increased frequency of mutations in the combined dataset led to a decrease in the prognostic value of *TP53*. These results indicate that the inclusion of samples with a low percentage of mutant reads, because of the higher sensitivity and lower accuracy of the NGS method, may lead to the inclusion of samples as mutant when only small *TP53* mutant subclones are present, which are likely not to have the same impact on response to treatment and patient survival time. This suggests it would be interesting to perform a ROC curve analysis based on the percentage of mutant allele reads to see if it is possible to define an optimal cut-point for what is a prognostically significant percentage of mutant reads. This might explain the difference between the Sanger and NGS results. The potential for FFPE-induced artefacts such as cytosine deamination which induce C>T changes can be considered as another possible explanation for the observed differences in Sanger sequencing and NGS data. Another reason for these differences may be due to the issues related to exon 7 sequencing by NGS. As illustrated above and in Table 4-2, the frequency distribution of *TP53* mutation and its correlation with survival in patients with ovarian cancer have been the subject of several studies even though the results are inconsistent. This inconsistency in findings might be related to different DNA sequencing techniques, the number of exons sequenced, various sample sizes and study design, diverse chemotherapy treatment options and dose. The significance of *TP53* status as a prognostic biomarker in the present study was dependent on the sequencing methods used to detect mutation.

It has been suggested that the classification of mutations based on their impact on p53 structure and function could further refine the prognostic accuracy of *TP53* mutational status, with distinct types of mutations resulting in differing impact on patient survival (Canevari *et al.*, 2006; Liu *et al.*, 2010; Brachova *et al.*, 2015). Several studies analysed correlation between *TP53* status and OS and/or PFS in regard to type of mutation. Shahin *et al.* (2000), Rose *et al.* (2003) and Nadkarni *et al*. (2013) analysed the impact of *TP53* status on overall survival according to the type of *TP53* mutation, demonstrating a significant association between null *TP53* and OS, while the presence of missense mutant *TP53* was not significantly correlated with OS. Another study investigated the association between *TP53* mutation and survival in patients diagnosed with advanced serous ovarian cancer and reported significantly worse PFS

in patients with "oncomorphic" *TP53* mutation, in which the mutations lead to both the elimination of wild-type *TP53* function and conferment of dominant oncogenic function, compared to patients with tumours harbouring mutations not categorised as oncomorphic (Brachova *et al.*, 2015). An additional study demonstrated that patients with HGSC grouped according to structural classes of *TP53* mutations have different survival outcomes for OS and PFS (Seagle *et al.*, 2015). In contrast, Ahmed *et al*. (2010) and Wang *et al.* (2004) reported no indication of significant association between the type of *TP53* mutation (missense versus non-missense) and OS or PFS. This is a possible avenue to explore in further analysis of the current study dataset.

Surprisingly, a few studies have reported that patients with advanced HGSC and mutant *TP53* had significantly better OS and/or PFS than those with wild-type *TP53* tumour (Ueno *et al.*, 2006; Wong *et al.*, 2013).

4.5.5 Patients from the ICON3 study with wild-type *TP53* tumours treated with single agent carboplatin have better overall survival than those with mutant *TP53*

This is the first time that carboplatin single agent is compared with combination plus paclitaxel by *TP53* mutational status in a randomized controlled clinical trial. For the primary objective in the present study, *TP53* mutational status was a significant predictor of OS following treatment with single agent carboplatin, regardless of the sequencing method, and retained independent prognostic significance on multivariate analysis alongside established clinicopathological prognostic factors. For PFS and treatment groups other than single agent carboplatin, the significance of *TP53* status as a predictive biomarker in the present study was dependent on the sequencing methods used to detect mutation.

For patients with serous histology, *TP53* retained its significance in response to treatment according to the data collected by Sanger or both sequencing methods in univariate analysis, but in multivariate analysis based on all sequencing data, Sanger sequencing, NGS, either Sanger or NGS, and both Sager and NGS data. A possible explanation for decreased predictive significance of *TP53* for patients with serous histology might be that the rate of *TP53* mutation is higher in serous ovarian cancer compared to other histological subtypes (Ahmed *et al.*, 2010).

These results are consistent with other studies which described a better response to platinum-based chemotherapy and longer OS for patients whose tumours have wild-type *TP53* than individuals harbouring mutant *TP53* (Reles *et al.*, 2001; Gadducci *et al.*, 2006). However, they

are not part of a controlled clinical trial and not testing carboplatin as a single agent versus carboplatin plus paclitaxel.

Reles *et al*. (2001) investigated the relationship between *TP53* genomic status and OS for patients who received cisplatin plus cyclophosphamide, carboplatin plus cyclophosphamide or other chemotherapy regimens. They reported a better OS for patients whose tumours harbour wild-type *TP53* than those with mutant *TP53* tumours. Gadducci *et al*. (2006) found a clear trend for longer OS and PFS for ovarian cancer patients with wild-type *TP53* tumours who received paclitaxel plus carboplatin-based chemotherapy compared to those with mutant *TP53* tumours. A significant association between *TP53* mutational status and OS was shown for patients with advanced epithelial ovarian cancer who received platinum-based chemotherapy (Havrilesky *et al*., 2003).

In contrast, other authors reported no significant relationship between *TP53* genomic status and response to platinum-based chemotherapy and overall survival (Fallows *et al*., 2001; Wang *et al*., 2004; Bauerschlag *et al*., 2010). As mentioned above, none of these studies are part of a controlled clinical trial.

4.5.6 Patients from the ICON3 study whose tumours have mutant *TP53* gain benefit from addition of paclitaxel to carboplatin, while those with wild-type *TP53* do not benefit

Overall, for the current cohort taken from the ICON3 trial, the whole patient group did not gain statistically significant benefit from a combined treatment with paclitaxel and carboplatin compared to those treated with carboplatin alone or CAP alone irrespective of *TP53* status and serous histology. However, there was a statistical trend for the inclusion of paclitaxel to confer greater survival benefit for the *TP53* mutant subgroup compared with patients who had wild-type *TP53* tumours.

These results differ from a few previous studies which have been previously performed to evaluate the efficacy of taxane-platinum versus platinum-based therapy in regard to *TP53* status in ovarian cancer (Smith-Sørensen *et al*., 1998; Kupryjanczyk *et al*., 2008). Smith *et al*. (1998) assessed the effect of paclitaxel and cisplatin versus cyclophosphamide and cisplatin in tumours from 45 randomized patients with ovarian cancer in relation to *TP53* status detected by direct DNA sequencing. In terms of relapse free survival, patients with mutant *TP53* treated with paclitaxel plus cisplatin had a significantly better survival than those with mutated *TP53* treated with cyclophosphamide and cisplatin (p=0.002). Kupryjanczyk *et al*. (2008) assessed

effectiveness of taxane-platinum therapy compared to platinum-based therapy with respect to *TP53* status estimated by immunohistochemistry in non-randomized ovarian cancer patients with stage IIB-IV. 10% staining was considered as the optimal cut-off value for separation of tumours with or without a missense mutation in *TP53* gene. The results showed that OS and PFS were not affected by the type of treatment in patients whose tumours stained by less than 10%. In contrast, individuals with tumours stained more than 10% gained benefit from addition of paclitaxel to platinum-based chemotherapy and survived longer ($p=0.008$). As explained before, these differences can partly be explained by the size, study design, mixed histological subtypes, grades and stages, and different methods used to identified the genomic status of *TP53* gene of the various studies.

4.5.7 Conclusion and further work

This study evaluates for the first time the effect of *TP53* genomic status on OS or PFS for ovarian cancer patients from a controlled clinical trial, ICON3, who received single agent carboplatin or CAP as a control versus those treated with a combination of paclitaxel with carboplatin. The results of current study clearly show predictive value of *TP53* genomic status in response to single agent carboplatin for ovarian cancer patients regardless of sequencing method. Using ROC curve analysis to determine the optimal cut-off value for the number of reads in NGS may give a better result in relation to mutational status of *TP53* as predictive and prognostic biomarker in ovarian cancer.

Studies have clearly indicated that ovarian cancer is a complex series of distinctly different diseases with different aetiologies and heterogeneity at the molecular level (Wang *et al.*, 2004; Bast *et al.*, 2009; Ahmed *et al.*, 2010; Le Page *et al.*, 2010; Prat, 2012). This suggests that development of reliable and consistent prognostic biomarkers must be specific to histopathological subtype and in the case of *TP53* mutation should investigate differences between mutation subclasses. Also, functional evaluation of the p53 pathway may provide added value, rather than looking at *TP53* mutation alone in order to predict response to chemotherapy, individualisation of treatment and survival outcome in patients with ovarian cancer.

Chapter 5: An investigation of ovarian cancer tumour samples for p53 and $p21^{WAF1}$ expression using tissue microarrays (TMA) from the ICON3 cohort

5.1 Introduction

The most frequent genetic event in ovarian cancer is alteration of the *TP53* gene, involving mutation and either absence of expression or overexpression due to stabilisation of mutant forms. Although numerous studies have previously been performed to evaluate the predictive value of *TP53* alterations in ovarian cancer, the outcomes are ambiguous.

Truncating mutations such as nonsense mutations, deletions and insertions are missed by immunohistochemistry staining, and overexpression of *TP53* is not necessarily a signature of mutation. Several studies have assessed both *TP53* gene status and its protein expression status together as predictive biomarkers in relation to survival outcomes (Reles *et al.*, 2001; Schuyer *et al.*, 2001; Wang *et al.*, 2004; Gadducci *et al.*, 2006; Bartel *et al.*, 2008; Rechsteiner *et al.*, 2013) and a few have correlated the combined status of *TP53* alteration with both response to chemotherapy and survival (Shahin *et al.*, 2000; Bartel *et al.*, 2008). Assessing the expression and functional status of p53 as well as *TP53* genomic status may be more informative for predicting response to treatment.

5.2 Hypothesis and Objectives

Hypothesis:

1. There is an association between the presence of *TP53* mutation and immunohistochemistry staining results.
2. The expression and functional status of the *TP53* gene can add prognostic value to predict survival outcomes in ovarian cancer patients.

Objectives:

1. To establish whether immunohistochemical staining for p53 can be considered as an additional prognostic variable in the ICON3 patient cohort.
2. To correlate immunohistochemical staining patterns of p53 expression with *TP53* mutational status.
3. To evaluate the role of combined status of *TP53* genomic alterations, p53 expression and functional status for their combined prognostic value in ovarian cancer.

5.3 Specific Materials and Methods

5.3.1 TMA and patient characteristic

The patient cohort characteristics were described in chapter 4.3.1. The tumour FFPE blocks were used to take sample cores and construct 6 TMA blocks which represented all patients tumour specimens with duplicate cores on each block. Six TMAs, ICON3-1 to ICON3-6 were produced by Dr. Jennifer Houniet with a standard 1 mm diameter core as suggested by other researchers (Eckel-Passow *et al.*, 2010; Kim *et al.*, 2013). Then, sections were cut from the TMA blocks and mounted on six slides labelled as ICON3-1 to ICON3-6. The slides were used to perform immunohistochemistry staining for p53, and $p21^{WAF1}$ as a downstream transcriptional target of p53.

5.3.2 Antibody specificity and optimization

The antibodies used, their dilution and optimisation are provided in section 2.2.1 and 3.3.2.

5.3.3 Staining, scoring and categorising

The slides were stained and the samples scored and categorised as described in section 3.3.3.

5.3.4 DNA sequencing

The *TP53* gene, exons 2-11, was sequenced as explained in section 4.3.2.

5.3.5 Statistical analysis

The Kaplan-Meier method and log-rank test were used to analyse the statistical significance of observed differences in patient survival. The relationship between *TP53* mutational status and p53 H-scores was analysed using the Mann-Whitney and Kolmogorov-Smirnov tests. The LIFETEST Procedure was applied to compute the homogeneity of strata due to the importance of biomarker analysis in homogeneous sub-groups of patients. The Chi-square test was used to analyse differences on a contingency table with 2 columns and 3 or more rows. All statistical tests presented were performed using the GraphPad Prism version 5.04 software and a p-value of <0.05 was considered to be statistically significant.

5.4 Results

5.4.1 The p53 staining distribution, scores, categories and correlation with survival

A total of 253 tissue samples from the 260 patients were used; seven patients with no treatment cycles were omitted. 22 (9%) cores were lost due to processing or no tumour cells in the patient sample. The p53 staining pattern was nuclear, ranging from negative to strongly positive. The distributions of immunohistochemical staining found are shown in Figure 5-1. ROC curve analysis was used to identify whether there was an optimal prognostic cut-off point to categorise the samples for subsequent Kaplan-Meier analysis; however, the area under the ROC curve, AUC, was 0.53 and no clear cut-point was evident (data not shown). From a total of 231 samples, 30 (13%) were negative (H-score=0), and 201 (87%) of patients were positive (H-score>0). The samples were categorised based on the LIFETEST procedure in three groups including 82 (35%) tumour samples having low expression of p53 (0≤H-score≤3), 64 (28%) tumour samples with an intermediate level of p53 (4≤H-score≤7), and 85 (37%) of tumours expressing high level of p53 (8≤H-score≤16). The Kaplan-Meier survival curves in relation to these three categories of p53 expression are shown in Figure 5-2. Although intermediate expression of p53 appeared to be associated with better overall survival compared to other two groups, this difference did not reach statistical significance on a log-rank test (X^2=5.66, *p=0.06*).

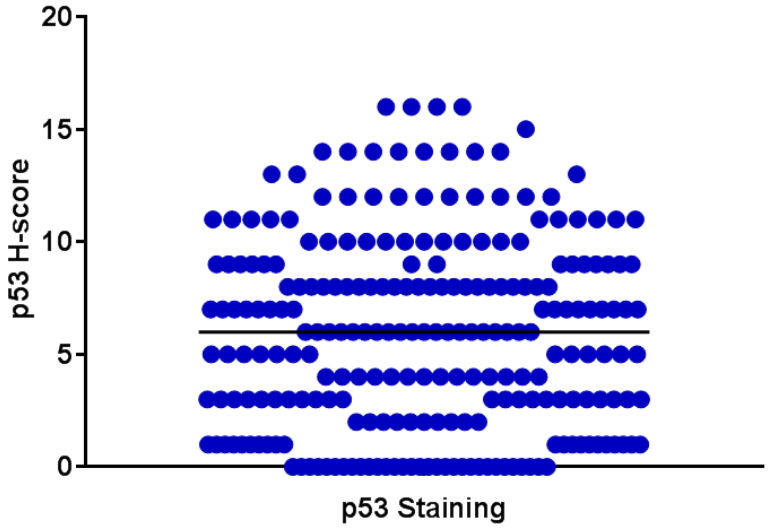

Figure 5-1: The p53 H-score distribution in samples from 231 patients. The horizontal black line represents the median.

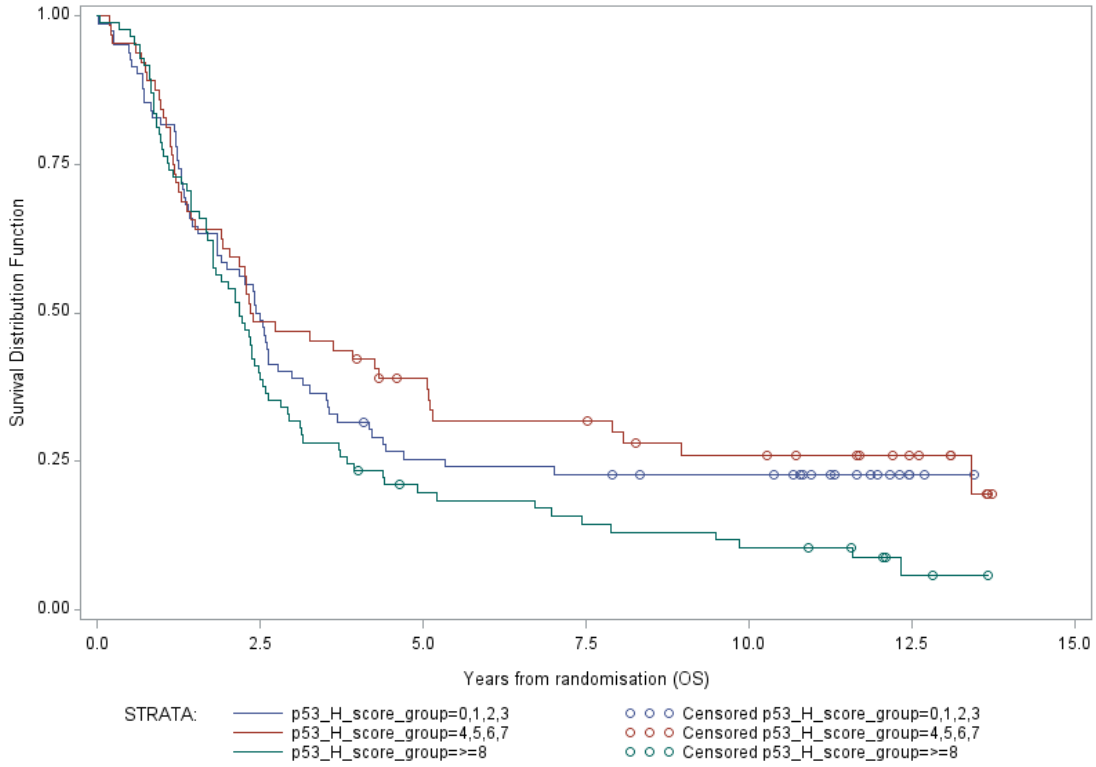

Figure 5-2: The survival times in relation to low (0≤H-score≤3), intermediate (4≤H-score≤7), and high expression (8≤H-score≤16) of p53 (*p= 0.06*).

5.4.2 Correlation of *TP53* status and p53 protein expression

This part of the study set out to investigate whether p53 immunohistochemical analysis can be used as a robust method for inferring the presence of *TP53* mutation in ovarian carcinoma. Overall, there was a significant correlation between strong immunohistochemical staining for p53 and *TP53* mutation detected by Sanger sequencing and NGS.

5.4.2.1 Results based on the Sanger *TP53* status

A scatter plot comparison of the p53 immunohistochemistry H-score between *TP53* wild-type (N=100) and mutant (N=131) sample sub-groups was constructed based on the Sanger sequencing data (Figure 5-3). The Mann-Whitney (*p=0.01*) and Kolmogorov-Smirnov (*p=0.009*) tests both showed that the distributions are significantly different in shape and median. The Mann-Whitney test confirmed that the median H-score is significantly higher for the *TP53* mutant group (Median of H-score=7) than the *TP53* wild-type category (Median of H-score=4) (Figure 5-3). A ROC curve analysis showed the sensitivity and specificity of 34% and 81% respectively for optimal predictive values of p53 immunohistochemistry as a surrogate for *TP53* mutation (AUC=0.6, *P=0.04*).

From a total of 131 *TP53*-mutated samples, 110 cases (84%) were positive and 21 cases (16%) were completely negative for p53 staining. In the wild-type *TP53* sub-group, 91 cases (91%) were positive and 9 cases (9%) were negative for p53 staining (Table 5-1). The distributions of negative and strong expression of p53 was higher in tumours with mutant *TP53* compared to those with wild-type *TP53*. Conversely, there was a higher proportion of samples with low expression of wild-type *TP53* compared to those with low expression of mutant *TP53* (Figure 5-4). The observed differences between different groups are statistically significant (X^2=4.67, *p=0.03*) based on a Chi-square test.

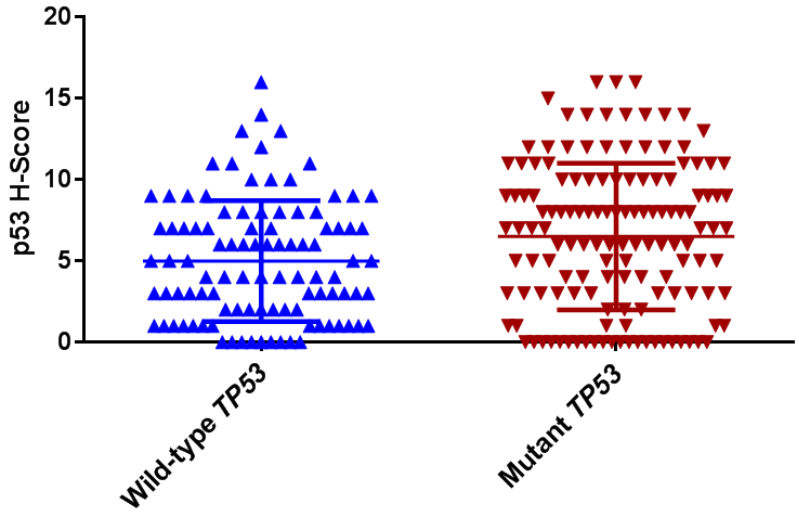

Figure 5-3: The distribution of p53 H-scores in relation to Sanger *TP53* status. The horizontal line represents the median (Mann-Whitney (*p=0.01*), Kolmogorov-Smirnov (*p=0.009*).

p53 IHC Staining Pattern	Sanger Sequencing Method	
	Wild-type *TP53* No (%)	Mutant *TP53* No (%)
Negative (H-score=0)	9 (9)	21 (16)
Low (1≤H-score≤3)	32 (32)	20 (15)
Intermediate (4≤H-score≤7)	33 (33)	31 (24)
High (8≤H-score≤16)	26 (26)	59 (45)
Total	100 (100)	131 (100)

Table 5-1: The frequency distribution of p53 H-scores in relation to Sanger *TP53* status (X^2 = 4.67, *p=0.03*). IHC, Immunohistochemical staining; No, Number.

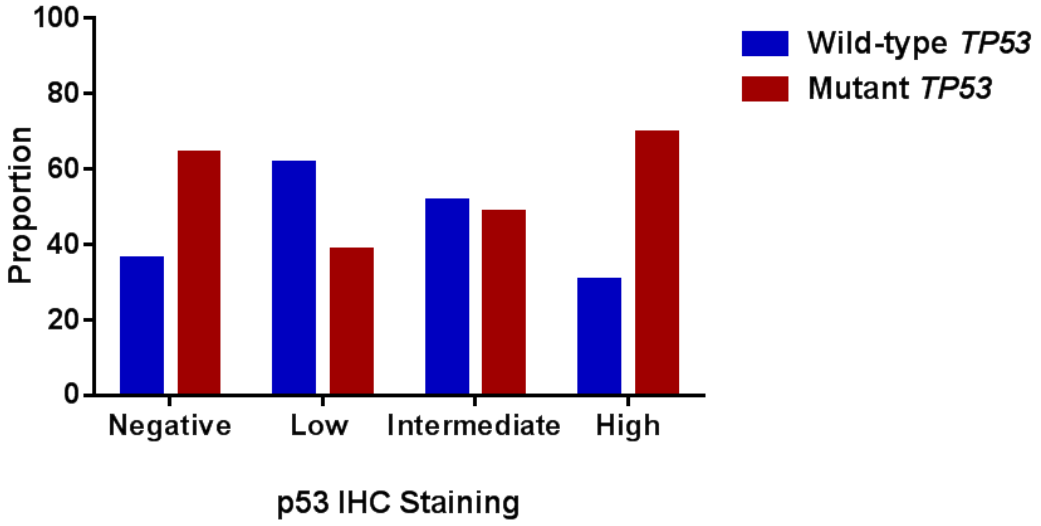

Figure 5-4: The proportion of p53 H-score in different categories in regard to Sanger *TP53* status. Low (0≤H-score≤3); Intermediate (4≤H-score≤7); High expression (8≤H-score≤16) (X^2=4.67, *p=0.03*).

5.4.2.2 The association between p53 immunohistochemistry staining and type of Sanger *TP53* mutation

Immunohistochemical analysis of p53 was evaluated in relation to the type of *TP53* mutation (missense or nonsense/frameshift) based on the Sanger data. The most common type of mutations were missense mutations affecting 95 (73%) cases included, and this group included the highest proportion of high p53 expression cases. From a total of 36 tumour samples with nonsense, deletion or insertion mutation, 10 samples were negative for IHC staining. (Table 5-2). A Chi-square test confirmed that the observed differences in the frequency of p53 IHC staining with respect to type of *TP53* mutation was statistically significant (X^2=14.02, *p=0.003*) (Figure 5-5). More statistical analysis using the Poisson distribution test indicated that accumulation of p53, high expression of p53, is significantly higher for patients whose tumours harbour missense mutation compared to those with nonsense or frameshift mutation (*p<0.0001*, Poisson distribution test). Furthermore, no significant difference was observed in the proportion of negatively stained tumours between missense and nonsense or frameshift mutation groups (*p=0.1*, Poisson distribution test).

p53 IHC Pattern / Type of *TP53* Mutation	Negative No (%)	Low No (%)	Intermediate No (%)	High No (%)	Total No (%)
Missense	11(52)	13 (65)	19 (61)	52 (88)	95 (73)
Nonsense/ Deletion/Insertion	10 (48)	7(35)	12 (39)	7 (12)	36 (27)
Total	21 (100)	20 (100)	31 (100)	59 (100)	131 (100)

Table 5-2: The frequency distribution of p53 immunohistochemistry staining in relation to the type of Sanger *TP53* mutation. Negative (H-score=0); Low (1≤H-score≤3); Intermediate (4≤H-score≤7); High expression (8≤H-score≤16) (X^2=14.02, *p=0.003*); No, Number.

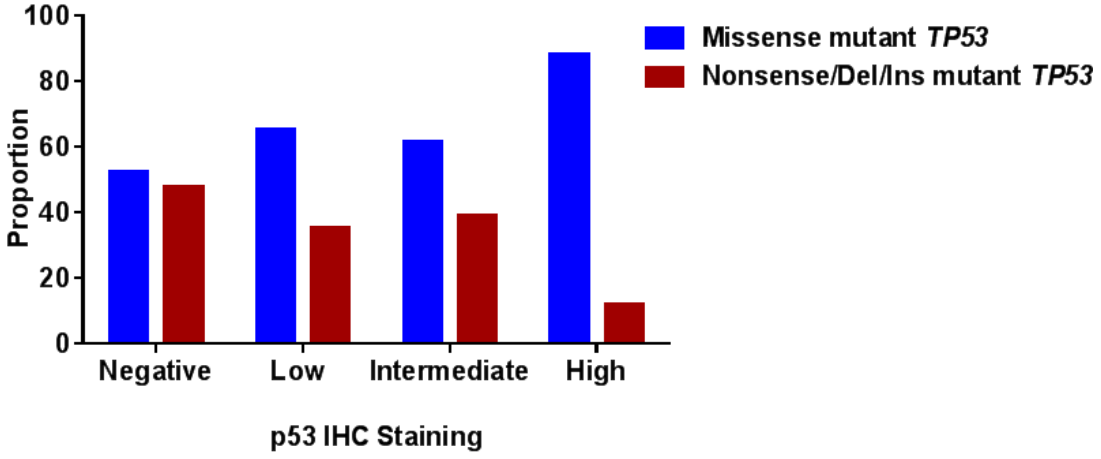

Figure 5-5: The frequency distribution of p53 immunohistochemistry staining in relation to the type of Sanger *TP53* mutation. Negative (H-score=0); Low (1≤H-score≤3); Intermediate (4≤H-score≤7); High expression (8≤H-score≤16) (X^2=14.02, *p=0.003*). Del, deletion; Ins, insertion.

5.4.2.3 Results based on the NGS *TP53* status

The frequency distribution of p53 immunohistochemistry H-score between wild-type *TP53* (N=80) and mutant (N=150) sample sub-groups was compared based on the NGS results (no result for one tumour sample) (Figure 5-6). The frequency distribution of p53 H-scores in relation to *TP53* status was significantly different according to both Mann-Whitney (*p=0.005*) and Kolmogorov-Smirnov (*p=0.003*) tests. The median H-score is significantly higher for the *TP53* mutant group (Median of H-score=7) than the *TP53* wild-type category (Median of H-score=4) (Figure 5-6). The sensitivity and specificity of predictive values of p53 immunohistochemistry as a surrogate for *TP53* mutation were 35% and 88% respectively based on the ROC curve analysis (AUC=0.61, *P=0.04*). Of the cases with mutant TP53, 24 (16%) showed negative staining for p53 and 126 (84%) showed positive staining. Of tumours with wild-type *TP53*, 6 cases (7%) and 74 cases (93%) were negative and positive for p53 staining respectively (Table 5-3). Figure 5-7 shows that the distributions of tumours with negative and high expression of mutant *TP53* was higher than those with negative and high expression of wild-type *TP53* demonstrating the relationship between *TP53* mutation and no expression or high expression of p53. . In contrast, the frequency distribution of samples with low expression of wild-type *TP53* was higher than those with low expression of mutant *TP53*. The Chi-Square test analysis confirmed that the observed differences between different categories are statistically significant (X^2=5.82, *p=0.01*).

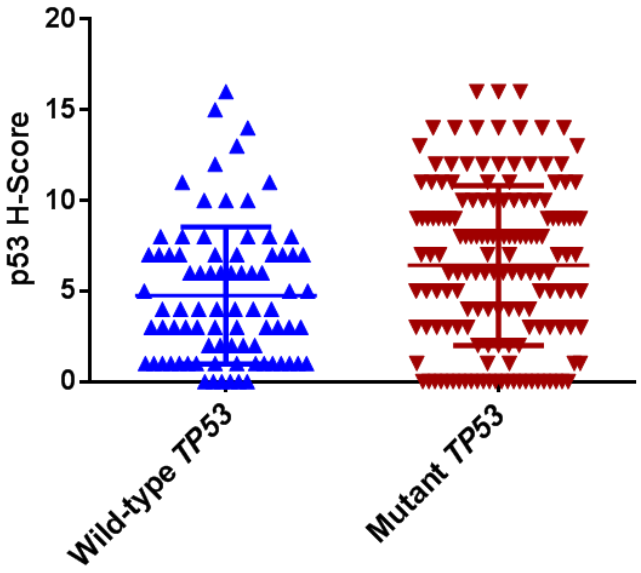

Figure 5-6: The distribution of p53 H-scores in relation to NGS *TP53* status. The horizontal line represents the median (Mann-Whitney (*p=0.005*), Kolmogorov-Smirnov (*p=0.003*)).

p53 IHC Staining Pattern	NGS Method	
	Wild-type *TP53* No (%)	Mutant *TP53* No (%)
Negative (H-score=0)	6 (7)	24 (16)
Low (1≤H-score≤3)	31 (39)	21 (14)
Intermediate (4≤H-score≤7)	28 (35)	36 (24)
High (8≤H-score≤16)	15 (19)	69 (46)
Total	80 (100)	150 (100)

Table 5-3: The frequency distribution of p53 H-scores in relation to NGS *TP53* status (X^2=5.82, *p=0.01*). IHC, Immunohistochemical staining; No, Number.

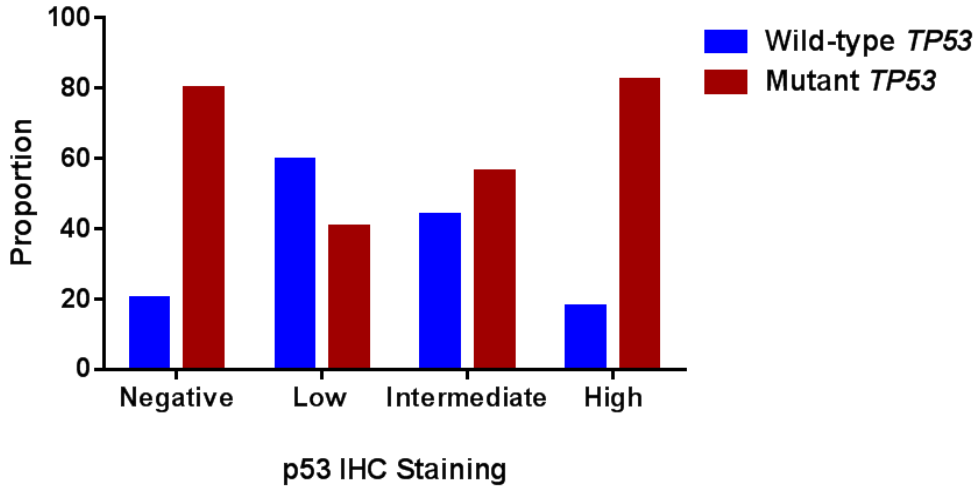

Figure 5-7: The proportion of p53 H-score in different categories in regard to NGS *TP53* status. Negative (H-score=0); Low (1≤H-score≤3); Intermediate (4≤H-score≤7); High expression (8≤H-score≤16) (X^2=5.82, *p=0.01*).

5.4.2.4 The association between p53 immunohistochemistry staining and type of *TP53* mutation

Immunohistochemical analysis of p53 was evaluated in relation to the type of *TP53* mutation (missense or truncated) based on the NGS data. Missense mutations were the most common, with 128 (85%) cases included, and this group included the highest proportion of high p53 expression cases. From a total of 22 tumour samples with nonsense, deletion or insertion mutation, negative staining was the predominant pattern of IHC staining (Table 5-4). A Chi-

square test confirmed that the observed differences in the frequency of p53 IHC staining with respect to type of *TP53* mutation was statistically significant (X^2=29.96, $p<0.0001$) (Figure 5-8). More statistical analysis using the Poisson distribution test indicated that accumulation of p53, high expression of p53, is significantly higher for patients whose tumours harbour missense mutation compared to those with truncating mutation ($p<0.0001$, Poisson distribution test). Furthermore, no significant difference was observed in the proportion of negatively stained tumours between missense and nonsense/frame shift mutation groups ($p=0.1$, Poisson distribution test).

p53 IHC Pattern / Type of *TP53* Mutation	Negative No (%)	Low No (%)	Intermediate No (%)	High No (%)	Total No (%)
Missense	12 (52)	13 (72)	34 (89)	69 (97)	128 (85)
Nonsense/Deletion /Insertion	11 (48)	5 (28)	4 (11)	2 (3)	22 (15)
Total	23 (100)	18 (100)	38 (100)	71 (100)	150 (100)

Table 5-4: The frequency distribution of p53 immunohistochemistry staining in relation to the type of NGS *TP53* mutation. Negative (H-score=0); Low (1≤H-score≤3); Intermediate (4≤H-score≤7); High expression (8≤H-score≤16) (X^2=29.96, $p<0.0001$); No, Number.

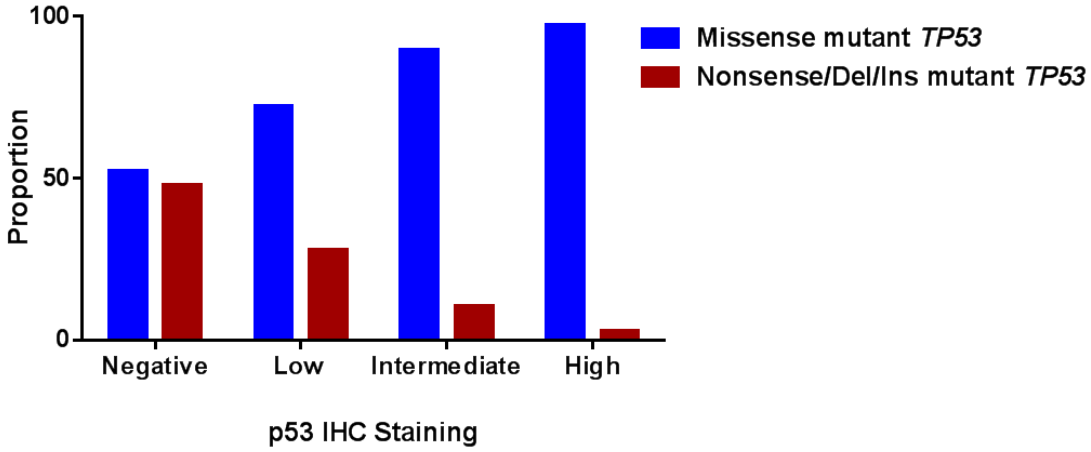

Figure 5-8: The frequency distribution of p53 immunohistochemistry staining in relation to the type of NGS *TP53* mutation. Negative (H-score=0); Low (1≤H-score≤3); Intermediate (4≤H-score≤7); High expression (8≤H-score≤16) (X^2=29.96, $p<0.0001$). Del, deletion; Ins, insertion.

5.4.3 Combined status based on *TP53* mutation and p53 protein expression: correlation with survival

To study the association between combined status of *TP53* alterations and survival outcomes, 231 patient samples were categorised according to their combined *TP53* mutational and protein expression status into six groups. In terms of p53 protein expression, each sub-group of wild-type *TP53* or mutant *TP53* was divided into three categories as low expression (0≤H-score≤3), intermediate (4≤H-score≤7) and high expression (8≤H-score≤16).

5.4.3.1 Results based on the Sanger *TP53* status

231 samples were grouped into six categories including mutant and low expression (39, 17%), mutant and intermediate expression (31, 14%), mutant and high expression (61, 26%), wild-type and low expression (43, 19%), wild-type and intermediate expression (33, 14%) and wild-type and high expression (24, 10%). Kaplan-Meier survival analysis represented in Figure 5-9 shows a significant difference in patient survival across the sub-groups. The survival probability was significantly better in patients with intermediate p53 expression and wild-type *TP53* genomic status compared to other groups (X^2=11.67, $p=0.04$).

Further analysis was separately carried out for sub-groups of patients whose tumours had wild-type or mutant *TP53*. From a total of 100 patients whose tumours harboured wild-type *TP53*, 43 cases (43%), 33 cases (33%) and 24 cases (24%) were categorised as low, intermediate and high expression respectively. There was again a significant difference in survival, and patients with intermediate expression and wild-type *TP53* genomic status had a longer survival time compared to those with low or high expression and wild-type *TP53* (X^2=7.26, $p=0.03$) (Figure 5-10). In contrast, when patients with mutant *TP53* were categorised into three groups based on the levels of p53 expression as low (39, 30%), intermediate (31, 24%) and high expression (61, 46%), no significant difference in survival time was observed in the analysis between patients with mutant *TP53* with respect to p53 protein expression status (X^2=1.20, $p=0.5$) (Figure 5-11).

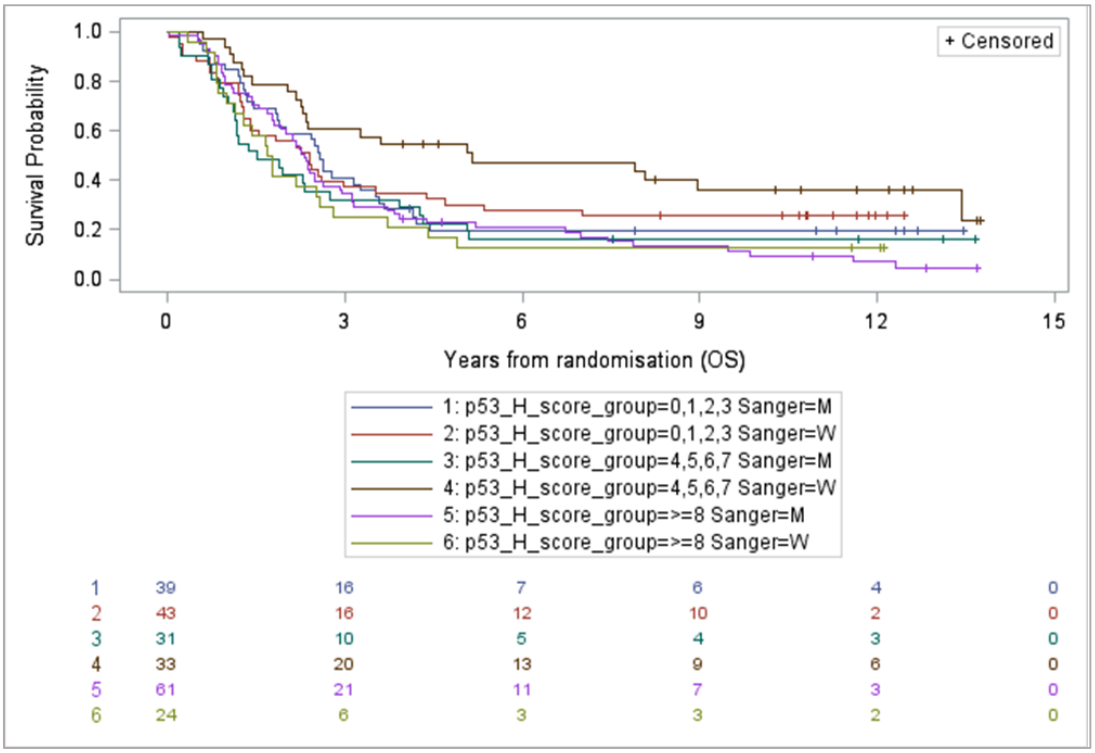

Figure 5-9: The survival times in relation to combined Sanger *TP53* tumour mutational and p53 protein expression status (*p=0.04*).

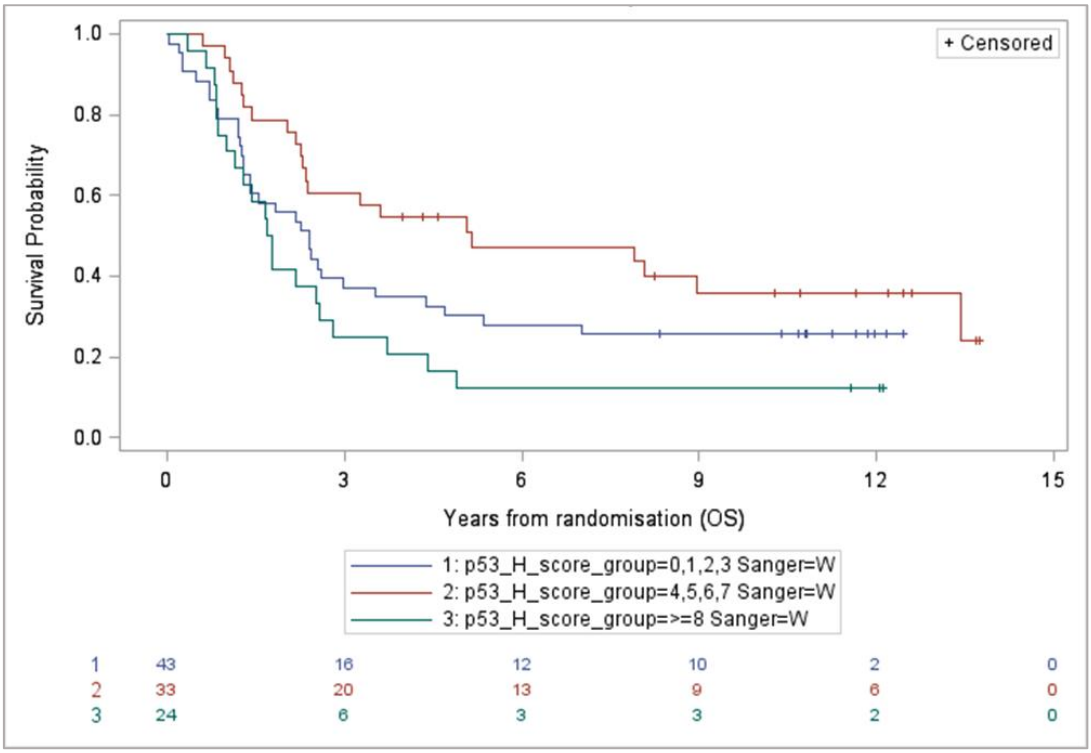

Figure 5-10: The survival times in relation to tumour p53 protein expression status for the wild-type Sanger *TP53* tumour genomic status sub-group (*p=0.03*).

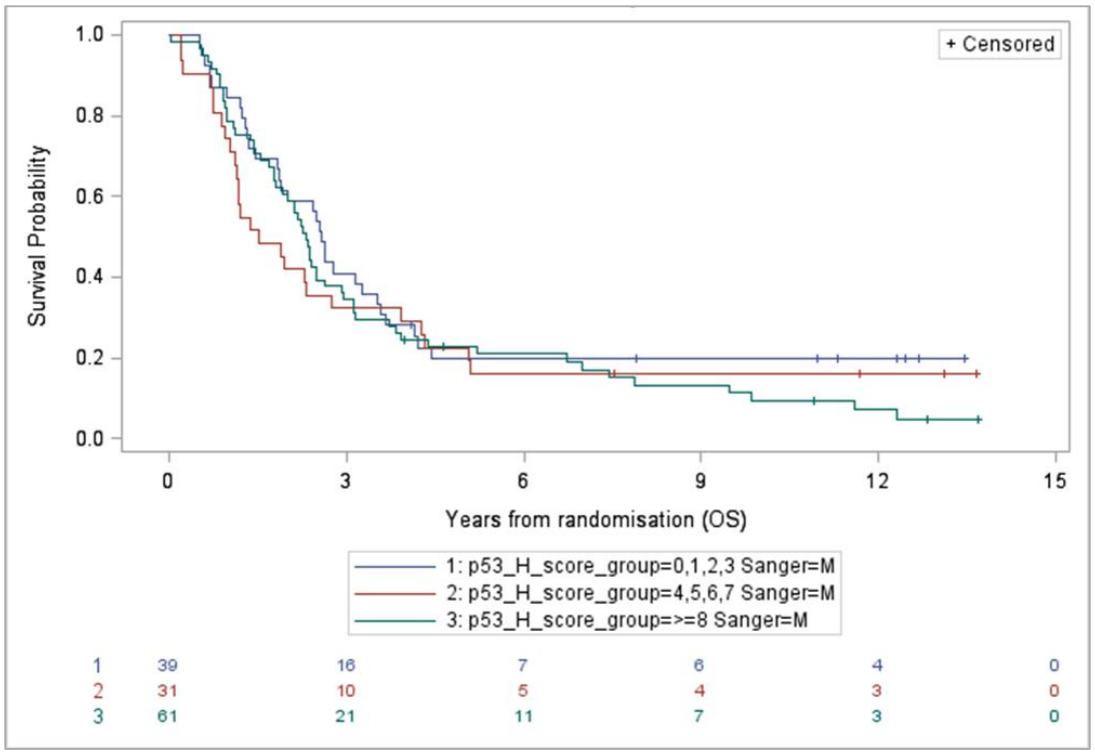

Figure 5-11: The survival times in relation to tumour p53 protein expression status for the mutant Sanger *TP53* tumour genomic status sub-group (*p=0.5*).

5.4.3.2 Results based on the NGS *TP53* status

A majority of women had tumours with mutant *TP53* (150, 65%) with a distribution of 45 (19.5%) low expression, 36 (16%) intermediate expression and 69 (30%) high expression. The frequency distribution for expression levels of wild-type *TP53* (80, 34.5%) was 37 cases (16%) low expression, 28 cases (12%) intermediate expression and 15 cases (6%) high expression. Also, there was 1 (0.5%) missing case with no result for NGS *TP53* status, which gives a total of n=231. As shown in Figure 5-12, there was no significant difference in survival between patients in relation to combining the NGS *TP53* mutational and protein expression status (X^2=8.13, *p=0.3*). When the data were separately analysed for patients with wild-type or mutant *TP53*, no significant difference was observed in relation to p53 protein expression levels. In the wild-type NGS *TP53* sub-group, although high p53 immunostaining appeared to be associated with worse patient survival compared to those with intermediate or low tumour p53 immunostaining, this difference did not reach statistical significance on a Log-rank test (X^2=4.43, *p=0.1*) (Figure 5-13). The Kaplan-Meier analysis in Figure 5-14 shows no significant relationship between survival time and p53 immunostaining in the mutant NGS *TP53* sub-group (X^2=2.58, *p=0.3*).

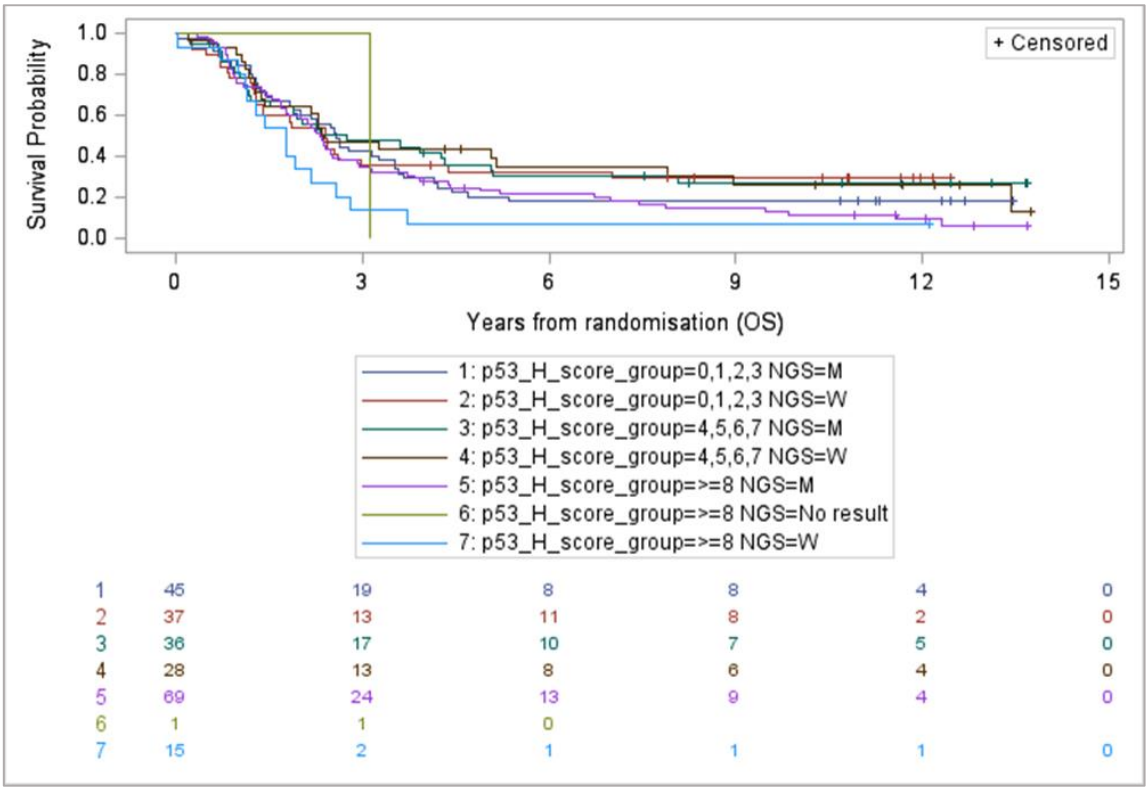

Figure 5-12: The survival times in relation to combining the NGS *TP53* mutational and p53 protein expression status (*p=0.2*).

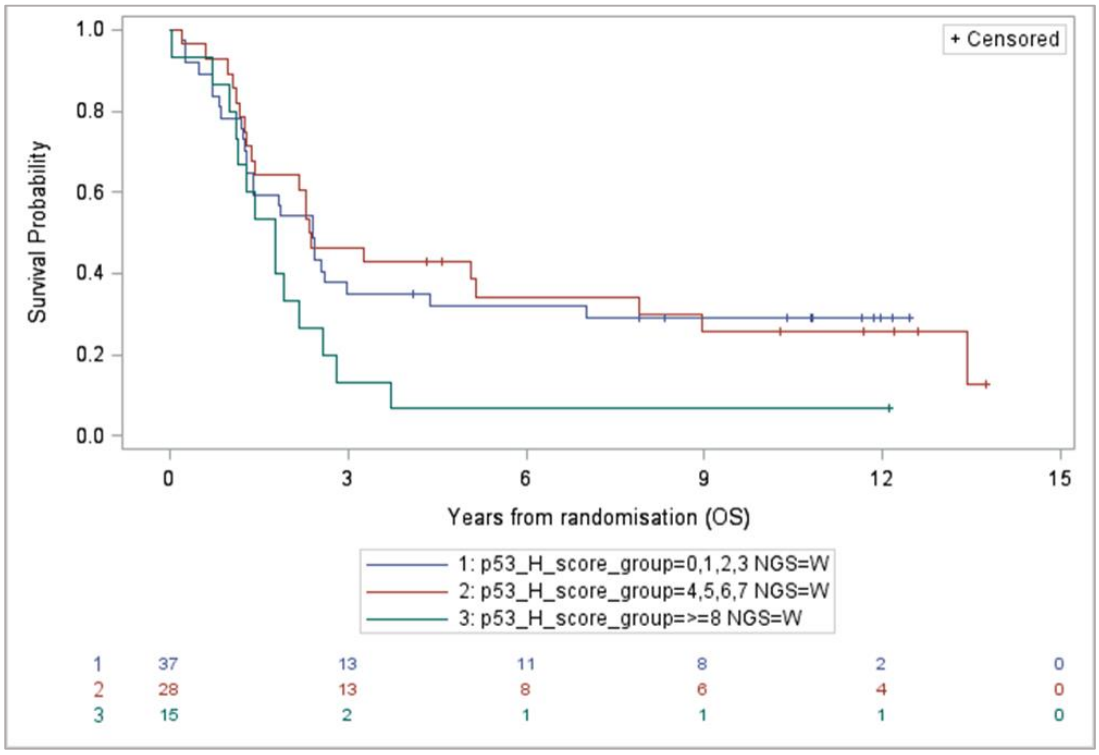

Figure 5-13: The survival times in relation to p53 IHC score in the wild-type NGS *TP53* sub-group (*p=0.1*).

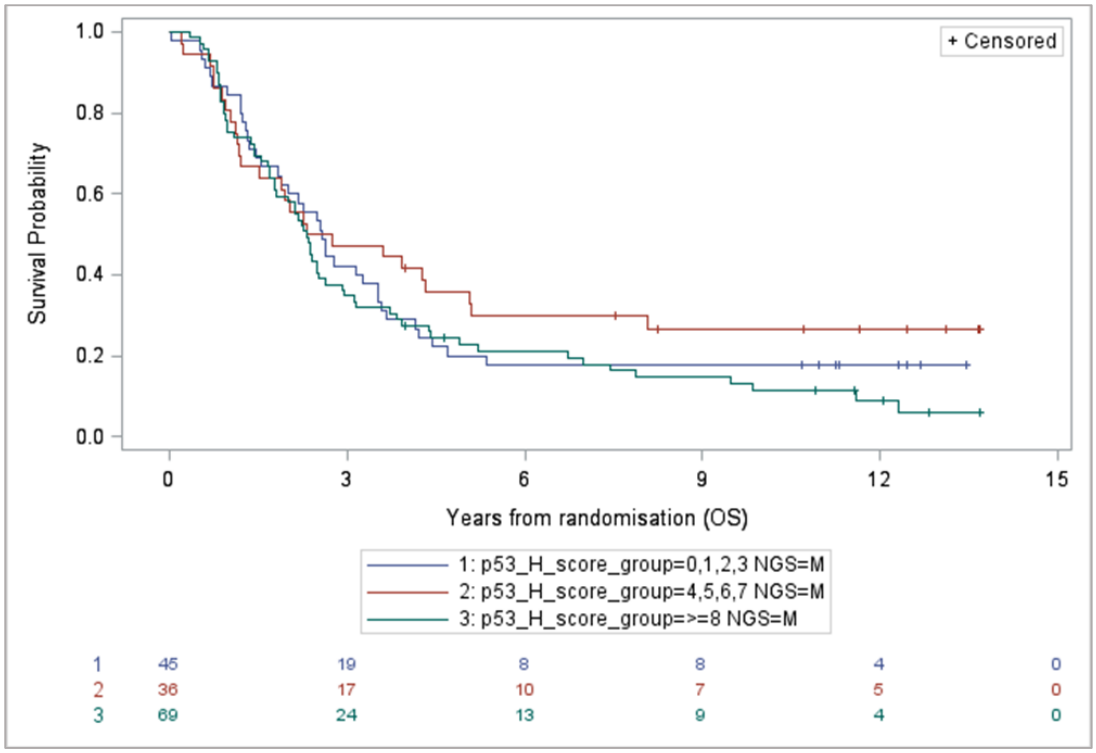

Figure 5-14: The survival times in relation to p53 IHC score in the mutant NGS *TP53* sub-group (*p=0.3*).

5.4.4 The p21^{WAF1} staining distribution, scores, categories and correlation with survival

From a total of 253 samples, 21 (8%) cores were missing during processing or contained no tumour cells in the patient sample, and 232 (92%) remained to analyse. The staining was limited to nuclei and ranged from negative (H-score=0) to positive (1≤H-score≤10) (Figure 5-15). The area under the curve from ROC curve analysis for p21^{WAF1} IHC staining was 0.52 demonstrating the correlation of p21^{WAF1} expression to survival was weak. The frequency distribution for p21^{WAF1} staining was 52 (22%) negative and 180 (78%) positive. Fifty-two samples (22%) were negative (H score = 0), 121 samples (52%) showed low expression (H score = 1), and 59 samples (26%) showed intermediate or high expression (H score between 1 and 10). As shown in Figure 5-16, the p21^{WAF1} expression was not a prognostic variable for survival (X^2=0.49, *p=0.8*).

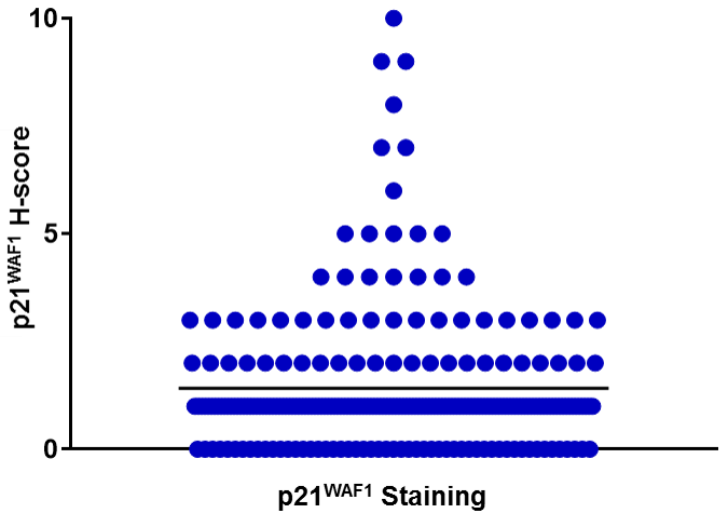

Figure 5-15: The p21^{WAF1} H-score distribution in samples from 232 patients. The horizontal black line represents the median.

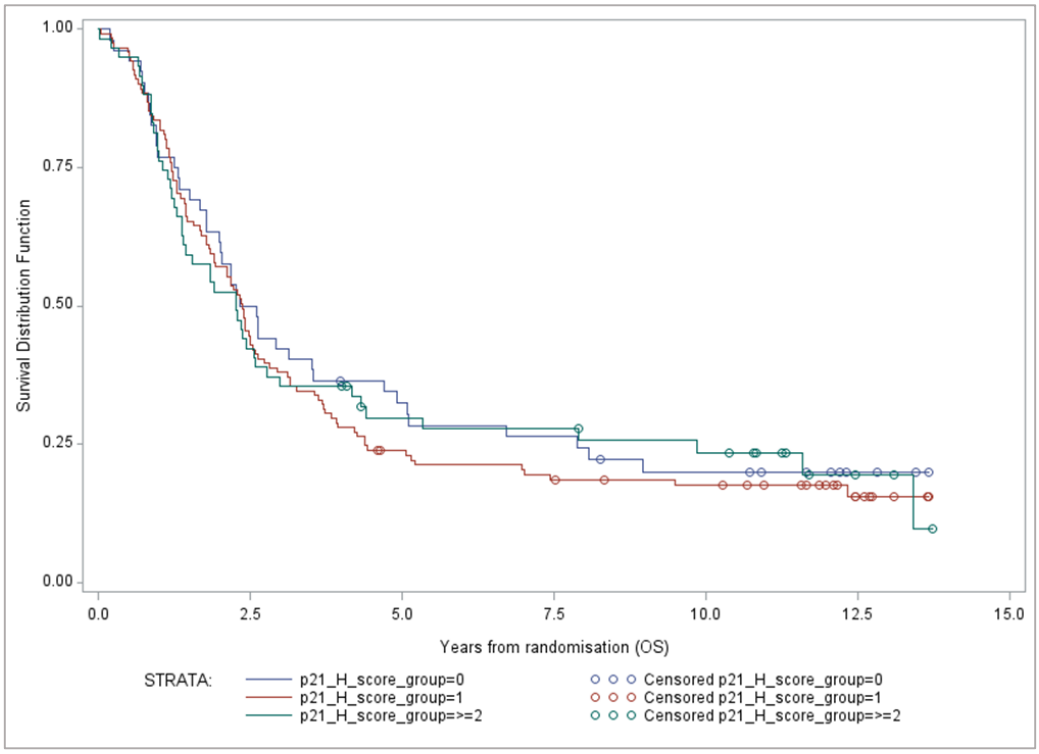

Figure 5-16: The survival time in relation to p21^{WAF1} expression (*p=0.8*).

5.4.5 Relationship between of *TP53* status and p21^{WAF1} protein expression

The *CDKN1A* gene encoding p21^{WAF1} is a downstream transcriptional target of p53, but can also be upregulated by p53-independent pathways. To study the relationship between p21^{WAF1} expression and mutational status of *TP53*, a scatter plot was constructed indicating the frequency distribution of p21^{WAF1} immunostaining H-scores in relation to *TP53* mutational status.

5.4.5.1 Results based on the Sanger *TP53* status

The expression levels of p21^{WAF1} were compared between wild-type *TP53* (N=100) and mutant (N=132) sample sub-groups according to the Sanger sequencing results (Figure 5-17). Neither Mann-Whitney ($p=0.9$) nor Kolmogorov-Smirnov ($p=0.99$) tests showed a significant difference in the distributions of p21^{WAF1} H-scores in relation to Sanger *TP53* status. For the mutant *TP53* sub-group, most of the samples were categorised as low expression with a distribution of 73 (55%). Lower frequencies were observed for tumour samples grouped as negative with 29 cases (22%) and intermediate or high expression with 30 cases (23%). In comparison, 23 (23%) of patients with wild-type *TP53* had no p21^{WAF1} expression, 48 (48%) and 29 (29%) of those were grouped as low and intermediate or high expression respectively (Table 5-5) (Figure 5-18). The Chi-square test confirmed no significant difference between various categories (X^2=0.32, $p=0.6$).

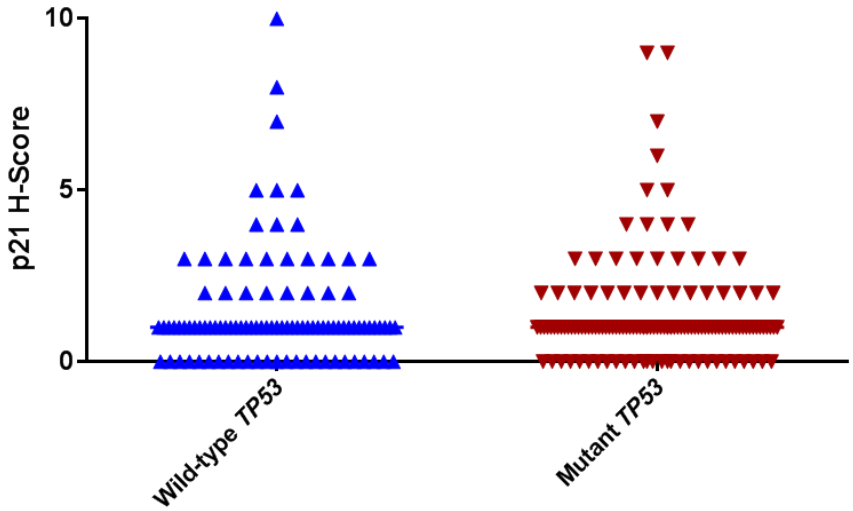

Figure 5-17: The frequency distribution of p21^{WAF1} H-scores in relation to Sanger *TP53* status (Mann-Whitney ($p=0.9$), Kolmogorov-Smirnov ($p=0.99$)). The horizontal line represents the median.

P21^{WAF1} IHC Staining Pattern	Sanger Sequencing Method	
	Wild-type *TP53* No (%)	Mutant *TP53* No (%)
Negative (H-score=0)	23 (23)	29 (22)
Low (H-score=1)	48 (48)	73 (55)
Intermediate+high (2≤H-score≤10)	29 (29)	30 (23)
Total	100 (100)	132 (100)

Table 5-5: The frequency distribution of p21^{WAF1} H-score in relation to Sanger *TP53* status (X^2=0.32, *p=0.6*). IHC, Immunohistochemical staining; No, Number.

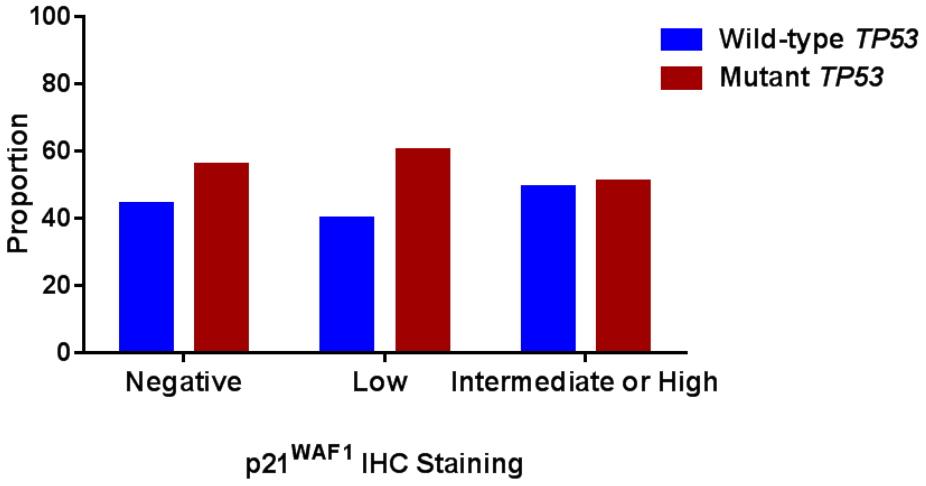

Figure 5-18: The proportion of p21^{WAF1} H-score in different categories in regard to Sanger *TP53* status. Negative (H-score=0); Low (H-score=1); Intermediate or high (2≤H-score≤10) (X^2=0.32, *p=0.6*).

5.4.5.2 Results based on the NGS *TP53* status

Figure 5-19 compares the distributions of $p21^{WAF1}$ immunohistochemistry H-score between wild-type *TP53* and mutant sub-categories based on the NGS results. Neither Mann-Whitney (*p=0.05*) nor Kolmogorov-Smirnov (*p=0.31*) tests showed a significant difference in the distributions of $p21^{WAF1}$ H-scores in relation to NGS *TP53* status. From a total of 151 patients with mutant *TP53*, 40 (26%) of tumour samples had no expression of $p21^{WAF1}$, 78 (52%) of those were grouped with low expression and 33 (22%) had intermediate or high expression. For patients with *TP53* wild-type tumour, 12 (15%) were categorised as negative, 42 (53%) had low expression and 26 (32%) were grouped as intermediate or high expression (Table 5-6) (Figure 5-20). One sample had no NGS result (H-score=1). Consistent with the Sanger sequencing data, the Chi-square test indicated no significant difference in the proportion of *TP53* mutant cases between different $p21^{WAF1}$ H-score sub-groups (*p=0.07*).

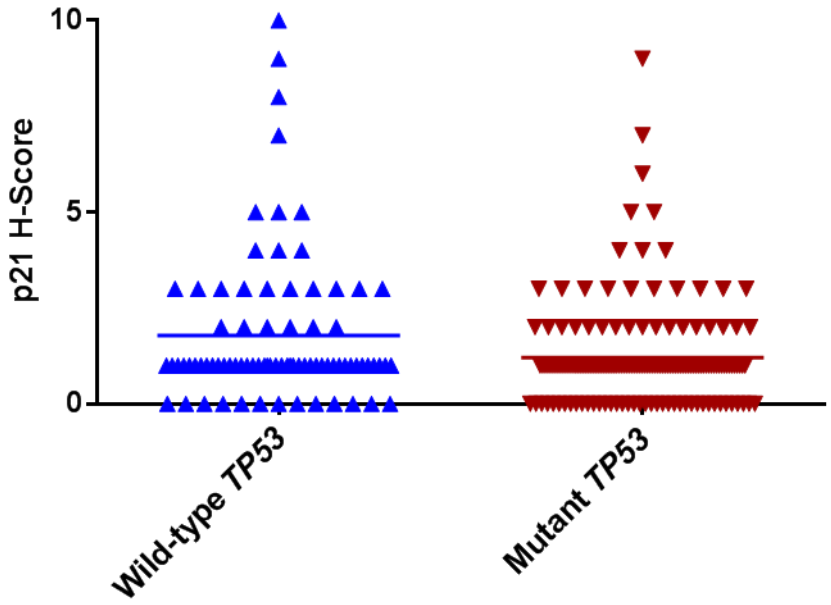

Figure 5-19: The frequency distribution of $p21^{WAF1}$ H-scores in relation to NGS *TP53* status (Mann-Whitney (*p=0.05*), Kolmogorov-Smirnov (*p=0.31*). The horizontal line represents the median.

p21^{WAF1} IHC Staining Pattern	NGS Method	
	Wild-type *TP53* No (%)	Mutant *TP53* No (%)
Negative (H-score=0)	12 (15)	40 (26)
Low (H-score=1)	42 (53)	78 (52)
Intermediate+high (2≤H-score≤10)	26 (32)	33 (22)
Total	80 (100)	151 (100)

Table 5-6: The frequency distribution of p21^{WAF1} H-score in relation to NGS *TP53* status (X^2=5.40, *p=0.07*). IHC, Immunohistochemical staining; No, Number.

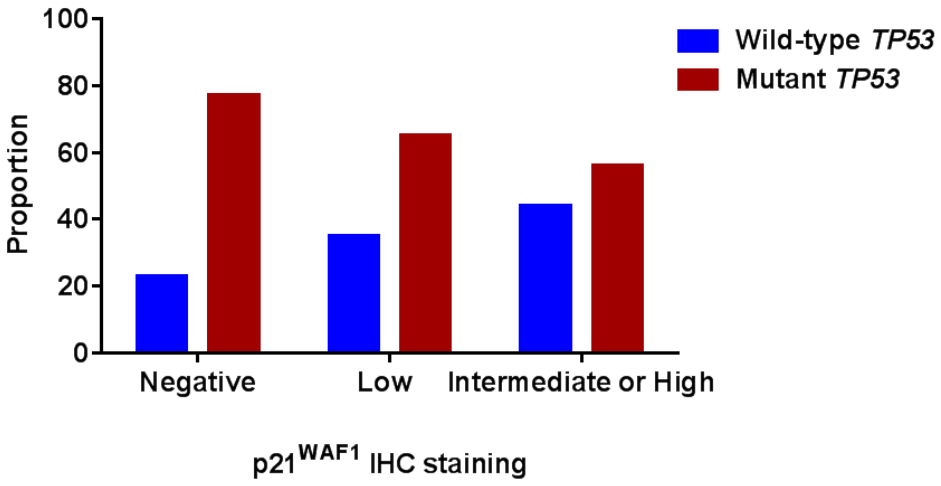

Figure 5-20: The proportion of p21^{WAF1} H-score in different categories in regard to NGS *TP53* status. Negative (H-score=0); Low (H-score=1); Intermediate or high (2≤H-score≤10) (X^2=5.40, *p=0.07*).

5.4.6 The relationship between p21^{WAF1} expression and survival in regard to *TP53* mutational status

232 patient samples were categorised according to their combined *TP53* mutation and p21^{WAF1} protein expression status into six groups. Each sub-group of wild-type *TP53* or mutant was divided into three categories as negative (H-score=0), low expression (H-score=1), and intermediate or high expression (2≤H-score≤10). The data was also analysed separately in regard to either wild-type *TP53* or mutant *TP53* group.

5.4.6.1 Results based on the Sanger *TP53* status

232 tumour samples were grouped into six categories with respect to p21^{WAF1} H-score and Sanger *TP53* status, and association between the groups with survival was studied. The Kaplan-Meier survival analysis represented in Figure 5-21 shows no significant difference in survival times between different categories (X^2=4.4, p=*0.5*). Further analysis was performed to evaluate the relationship between p21^{WAF1} expression and survival in relation to either wild-type *TP53* or mutant *TP53* (Figure 5-22 & Figure 5-23). The Kaplan-Meier plots and statistical analysis showed that survival data were not correlated with changes in p21^{WAF1} staining with respect to wild-type *TP53* (X^2=0.57, p=*0.8*) or mutant *TP53* (X^2=0.03, p=*1.0*).

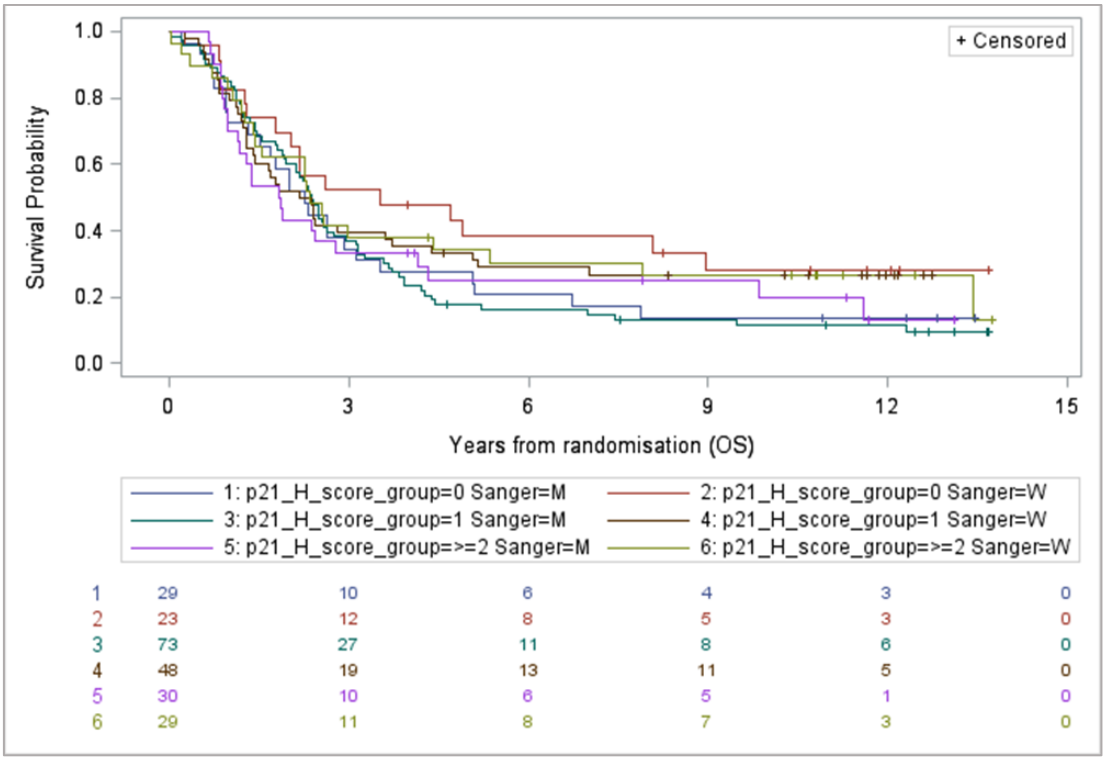

Figure 5-21: The survival times in relation to combining the Sanger *TP53* status and p21^{WAF1} expression (*p=0.5*).

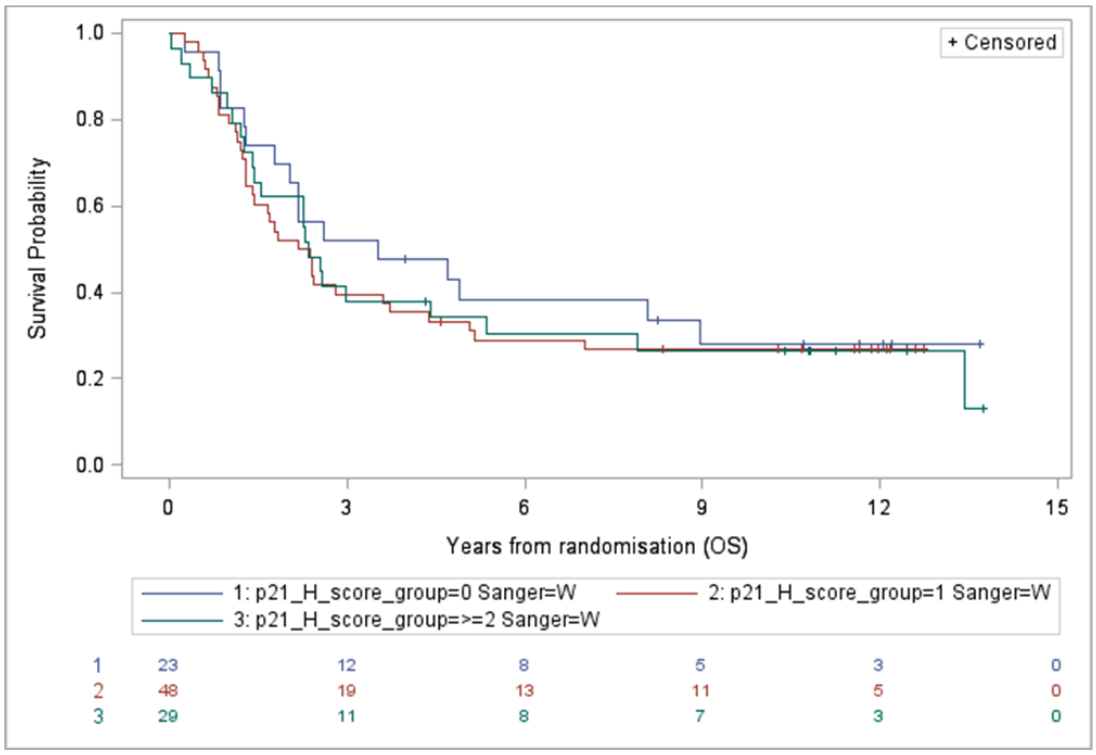

Figure 5-22: The survival times in patients with wild-type Sanger *TP53* tumour in relation to p21^{WAF1} expression (*p=0.8*).

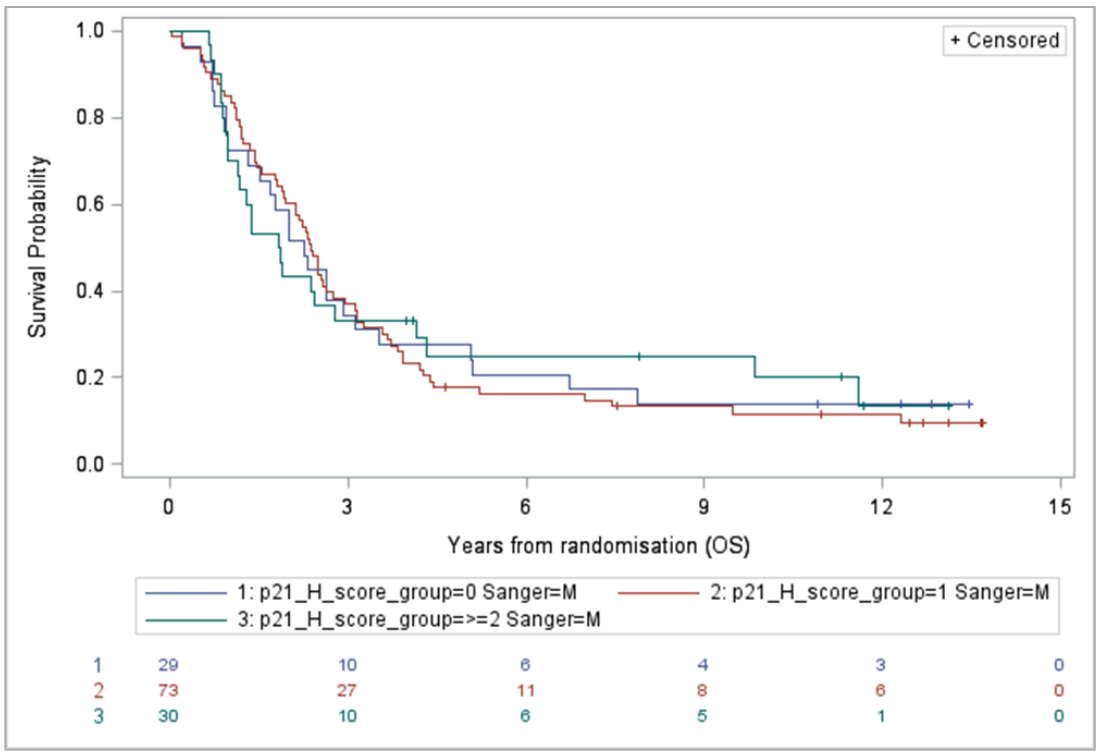

Figure 5-23: The survival times in patients with mutant Sanger *TP53* tumour in relation to p21^{WAF1} expression (*p=1.0*).

5.4.6.2 Results based on the NGS *TP53* status

231 tumour samples were categorised into six categories with respect to $p21^{WAF1}$ expression and NGS *TP53* status, and relationship between the groups with survival was studied. Overall, no significant difference was observed in survival rate for patients with tumours showing different levels of $p21^{WAF1}$ expression in relation to NGS *TP53* status (Figure 5-24) (X^2=6.16, $p=0.4$). Of patients with wild-type *TP53* tumour, survival data were not correlated with changes in $p21^{WAF1}$ expression in three different groups (Figure 5-25) (X^2=2.90, $p=0.2$). For individuals with mutant *TP53* tumours, there was no significant difference in survival amongst different groups in relation to $p21^{WAF1}$ expression (Figure 5-26) (X^2=2.88, $p=0.2$).

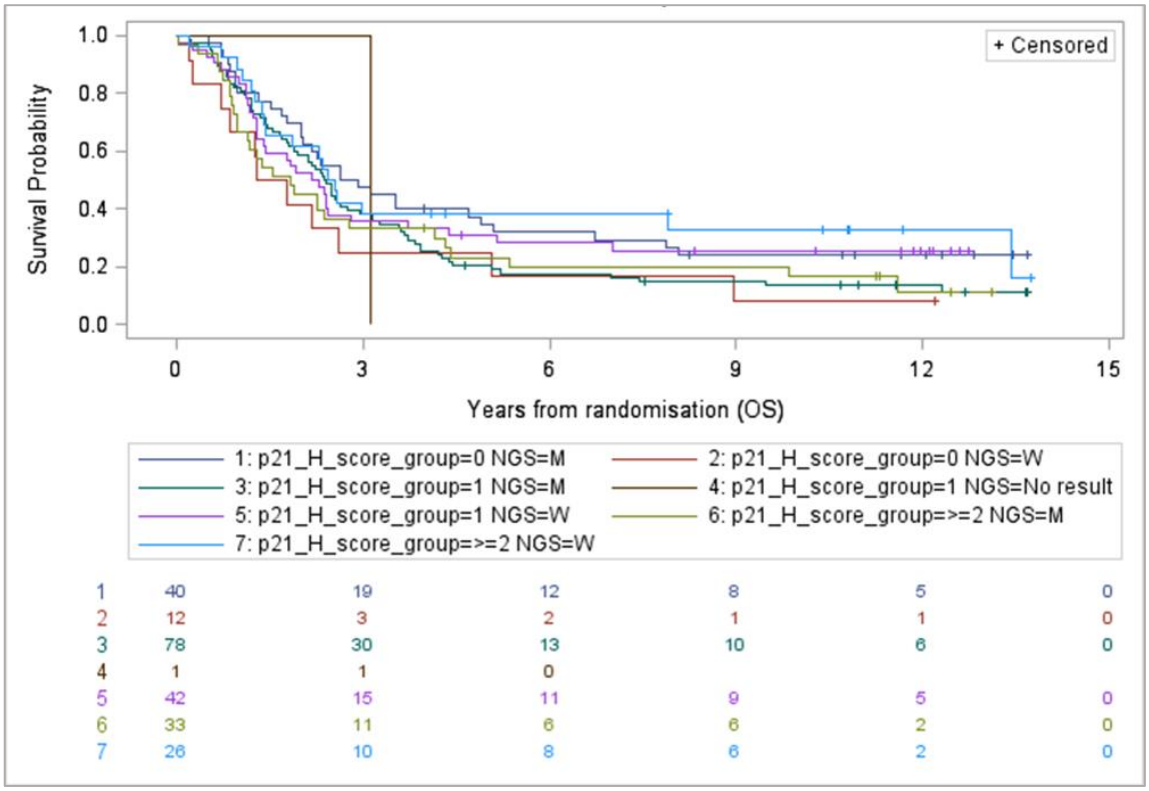

Figure 5-24: The survival times in relation to combining the NGS *TP53* status and $p21^{WAF1}$ expression ($p=0.4$).

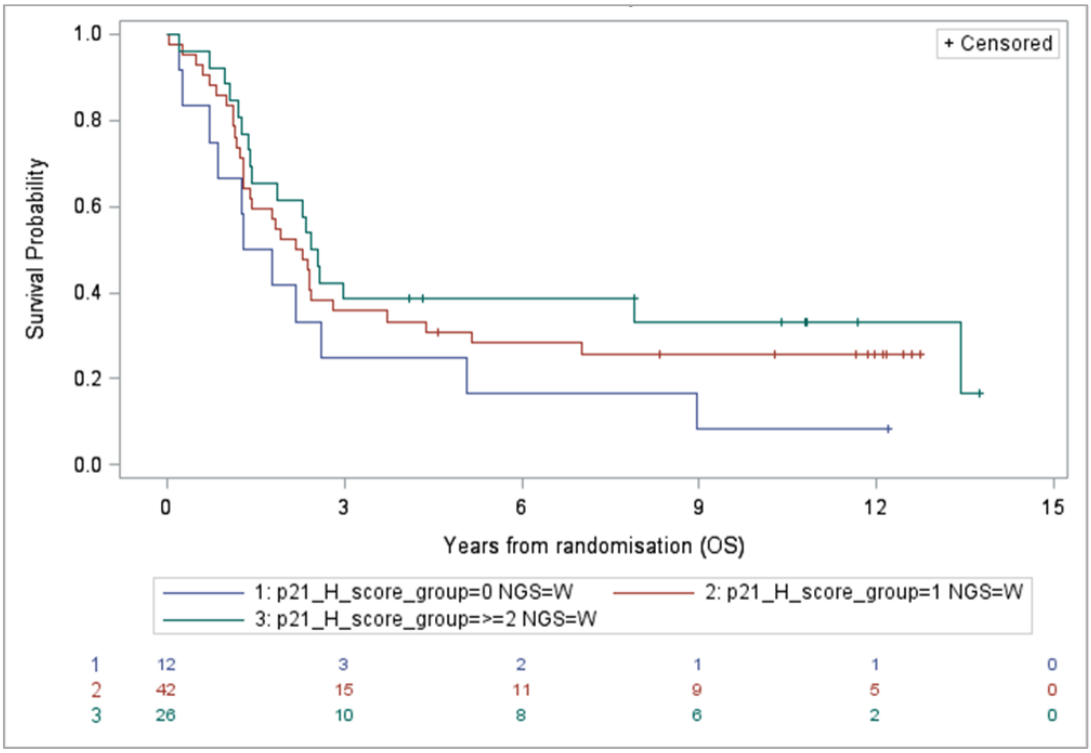

Figure 5-25: The survival times in patients with wild-type NGS *TP53* tumour in relation to p21^{WAF1} expression (*p=0.2*).

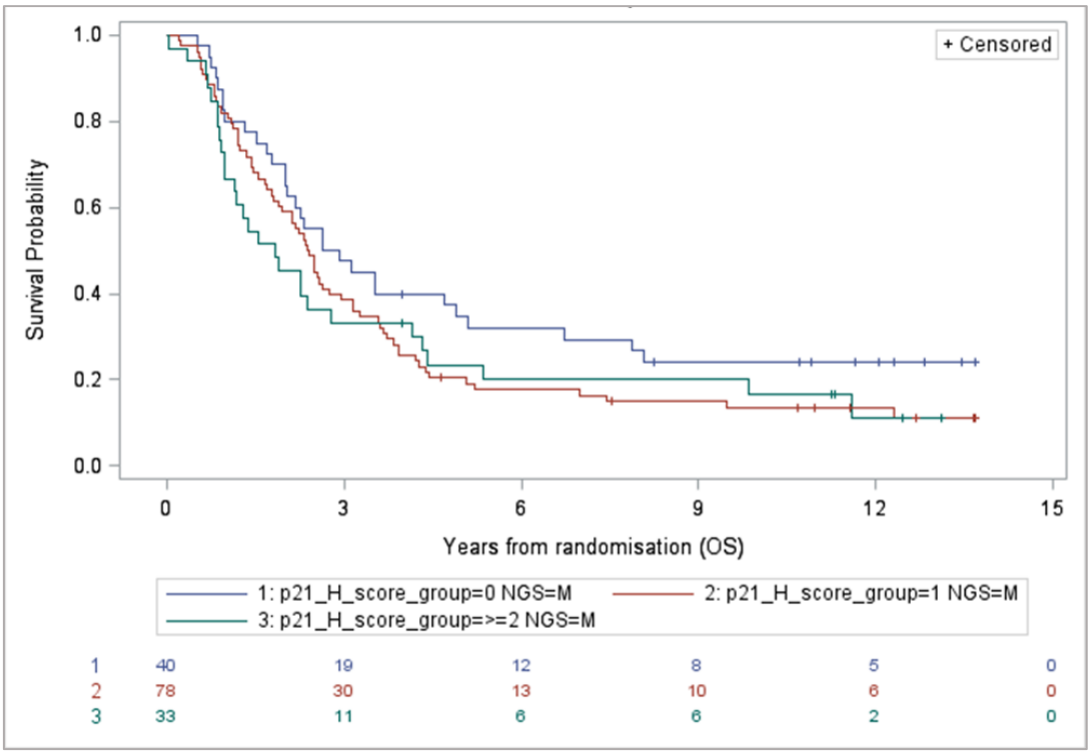

Figure 5-26: The survival times in patients with mutant NGS *TP53* tumour in relation to p21^{WAF1} expression (*p=0.2*).

5.5 Discussion

Although there are established prognostic variables in ovarian cancer, including stage of disease, histological subtype, residual disease and tumour differentiation, more additional predictive biomarkers are necessary to further refine the predicted efficacy of response to treatment and survival outcomes (Schuyer *et al.*, 2001). Prior studies which have evaluated the association between p53 protein expression levels and/or *TP53* mutational status with survival outcomes have found inconsistent results on whether *TP53* status or p53 protein expression can be considered as significant predictive and prognostic variable for ovarian cancer patients. It is suggested that the status of p53 alterations (combining the mutational and protein expression status) might be more helpful than either gene status or protein status alone (Shahin *et al.*, 2000; Bartel *et al.*, 2008). Therefore, this part of the study concentrated on evaluation of combined mutational and protein expression status of p53 as a prognostic biomarker in ovarian cancer.

5.5.1 The p53 staining distribution and correlation with overall survival

In the current study, 87% (201 of 231) of patients were positive for p53 expression, which is nearly in keeping with the finding of other studies which also categorised tumours with no p53 protein expression as a negative staining (66% in Havrilesky *et al*. (2003); 70% in Yemelyanova *et al*. (2011)). However, it is higher than the 45% of tumours with positive p53 expression reported by Leitao *et al*. (2004). Most studies have categorised tumours with >10% stained cells as positive and those with ≤10% stained cells as negative.

The p53 H-scores were categorised into low, intermediate and high expression groups, and the difference in survival time between all groups was only marginally significant (X^2=5.66, p= *0.06*). Although these results differ from some published studies which indicated a worse survival time for patients with high expression of p53 protein (Schuyer *et al.*, 2001; Nakayama *et al.*, 2003; Bartel *et al.*, 2008), they are consistent with other reported studies which showed no significant association between p53 protein expression and survival outcome (Shahin *et al.*, 2000; Reles *et al.*, 2001; Havrilesky *et al.*, 2003; Gadducci *et al.*, 2006; Rechsteiner *et al.*, 2013). A meta-analysis of 53 studies on the prognostic value of p53 expression indicated that p53 protein expression has a modest effect on prognosis and overall survival despite the presence of heterogeneity between studies, but nevertheless it is unlikely to be useful as a predictive biomarker in clinical practice (de Graeff *et al.*, 2009).

This limitation, as described in section 3.5.2, can be explained in part by small sample size, sub-optimal design of some studies, different antibodies and cut-offs, alterations of other genes encoding proteins associated with p53 protein expression or regulation (Shahin *et al.*, 2000; Canevari *et al.*, 2006). It may also be due to the different treatment options (Levesque *et al.*, 2000), immunohistochemical methods (de Graeff *et al.*, 2009; Rechsteiner *et al.*, 2013), time of follow-up and histological subtypes of the tumours analysed in diverse series (Havrilesky *et al.*, 2003; Gadducci *et al.*, 2006). Also, Graeff *et al*. (2009) found FIGO stage distribution affects study outcome using meta-regression analysis.

5.5.2 *TP53* gene mutation and relationship with immunohistochemical staining

In this study, a significant correlation between the *TP53* mutational status and protein expression of p53 was found regardless of sequencing technique used ($p \leq 0.01$). The results showed higher incidence of high p53 protein accumulation as well as cases of no p53 expression in tumours with mutant *TP53* compared to those with wild-type *TP53*. One mechanism through which p53 protein accumulates at high levels in the presence of *TP53* mutation is the inability of mutant p53 protein to transactivate wild-type *TP53* target genes including *MDM2*. Therefore, reduced MDM2 protein levels result in decreased p53 degradation (Wiman, 2007; Oren and Rotter, 2010). Also, *PTEN* expression increases mutant p53 protein levels through MDM2 inactivation or possibly direct binding to mutant p53 protein (Li *et al.*, 2008). Stabilisation of mutant p53 protein can also probably occur via contribution of heat-shock proteins (Wiman, 2007). The mechanisms involved in accumulation of wild-type *TP53* are not completely understood (Leitao *et al.*, 2004) but nonetheless there are some possible explanations for this abnormal stability. Deregulation of MDM2 and p14ARF, high expression of p14ARF and low expression of MDM2, could result in the accumulation and stability of p53 protein. It is also suggested that the expression of MDM2 splice variants which are short variants of MDM2 protein acting as dominant negative inhibitors to the activity of full-length MDM2 or those variants lacking the p53 binding domain may affect the stability of wild-type p53 protein (Wang *et al.*, 2005; Bartel *et al.*, 2008). Furthermore, PTEN confers p53 protection from MDM2 degradation via inhibition of P13K/AKt signalling enhancing MDM2 nuclear translocation (Vlachostergios *et al.*, 2012). Negative immunohistochemistry staining results from nonsense mutations, deletions and insertions (Nakayama *et al.*, 2003; Bartel *et al.*, 2008; Yemelyanova *et al.*, 2011) or through MDM2 degradation (Oren and Rotter, 2010). The results of this study are consistent with other research which found a significant association between *TP53* mutation and the pattern of immunohistochemical detection of p53 expression

(Lavarino *et al.*, 2000; Reles *et al.*, 2001; Schuyer *et al.*, 2001; Wang *et al.*, 2004; Yemelyanova *et al.*, 2011; Rechsteiner *et al.*, 2013). Leitao *et al*. (2004) found a relationship between p53 expression and *TP53* mutation and suggested that sensitivity, specificity and predictive values of p53 immunoreactivity can be used modestly as an approximate surrogate indication of *TP53* mutation. In contrast to these findings; however, no evidence of sufficient specificity and sensitivity of immunohistochemistry data for surrogate detection of *TP53* mutation was concluded by Singer *et al*. (2005), Gadducci *et al*. (2006) and Bartel *et al*. (2008).

In terms of correlation between p53 expression and type of *TP53* mutation, our results showed a significant relationship between different patterns of p53 expression and the type of *TP53* mutation, which was mainly an association of p53 high expression with missense mutation (88% based on the Sanger sequencing and 97% according to NGS). In comparison, only 48% of protein-truncating *TP53* mutations were reflected by negative immunohistochemistry staining and this did not significantly differ from the percentage of negative p53 staining identified in the missense *TP53* mutation group (52%). These results support previous research into this area which link missense mutations in the *TP53* gene with stable p53 protein resulting in high p53 expression. In fact, optimised p53 IHC assay interpreted correctly can be used as a surrogate for the *TP53* mutational status, and use of both IHC and sequencing techniques can be considered as a gold standard to predict the functional status of p53 (Kobel *et al.*, 2016) Leitao *et al*. (2004) found positive p53 expression in 72% of tumours with missense *TP53* mutation. Reles *et al*. (2001), Schuyer *et al*. (2001) and Rechsteiner *et al*. (2013) also reported that missense *TP53* mutations were significantly associated with high expression of p53 in epithelial ovarian cancer. Moreover, Yemelyanova *et al*. (2011) found overexpression or complete absence of p53 was closely correlated with a *TP53* mutation.

5.5.3 The functionality of *TP53* and correlation with survival

It can be argued that combining *TP53* mutational status and p53-dependent protein expression as an indication of the functional status of p53 may have greater prognostic value than either *TP53* gene status or p53 protein expression alone. This part of study set out to investigate the relationship between functionality of *TP53* and overall survival.

The results based on the Sanger *TP53* status showed that patients with wild-type *TP53* and intermediate levels of p53 protein expression have a better OS compared to other groups with altered *TP53* ($p=0.04$). For patients with wild-type *TP53* tumours, p53 protein expression retained its significance and patients with intermediate p53 protein expression showed a longer

OS than those with low or high p53 protein expression (*p=0.03*). In contrast, for patients with mutant *TP53* tumours p53 protein expression was not significantly associated with differences in survival (*p=0.5*).

According to NGS *TP53* data, no significant association was observed in survival time between patients categorised based on combining the *TP53* mutational and protein expression status (*p=0.2*). p53 expression levels had no significant relationship to survival for patients with either wild-type (*p=0.1*) or mutant (*p=0.3*) *TP53* tumours.

A few studies have evaluated the correlation of *TP53* functionality with survival outcome. One of these studies indicated that a combination of both *TP53* mutations and overexpression of p53 is a stronger predictive biomarker than either alone (Wen *et al.*, 1999). Shahin *et al*. (2000) found wild-type *TP53* immunonegative groups had a slightly worse survival than those with wild-type *TP53* immunopositive tumours. Bartel *et al*. (2008) categorised the patient samples into four groups including patients with overexpressed (>10 % p53 staining) or not expressed (≤10% p53 staining) wild-type *TP53* and those with overexpressed or no expressed mutant *TP53*. They found individuals with overexpression of wild-type *TP53* had the worst survival time compared to other groups; however, the difference was only marginally significant (*p=0.08*). When p53 protein expression levels were compared between patients with wild-type *TP53*, the difference in survival time reached statistical significance (*p=0.02*).

5.5.4 The p21^{WAF1} staining distribution and correlation with survival

The samples were categorised into three groups including 52 (22%) cases negative, 121 (52%) cases with low expression (H-score=1) and 59 (26%) with intermediate or high expression (2≤H-score≤10). No significant difference in survival was observed in analysis between patients whose tumours had no p21^{WAF1} expression, low p21^{WAF1} expression or intermediate/high expression of p21^{WAF1} (*p= 0.8*). Prior studies which evaluated the correlation of p21^{WAF1} protein expression with survival time have found inconsistent results. Green *et al*. (2006) grouped 169 tumour samples into two low (p21^{WAF1} staining<3%) and high expression (3%≤ p21^{WAF1} staining) categories. Survival data were correlated with changes in p21^{WAF1} staining in two different groups and patients with low p21^{WAF1} expression had a median survival time less than those with high p21^{WAF1} expression (*p= 0.03*). Rose *et al*. (2003) categorised 267 tumour samples into two groups with negative (<2%) and positive (≥2%) staining There was a significant difference in OS between patients with positive and negative p21^{WAF1} staining, with an OS advantage for patients whose tumours had positive p21^{WAF1}

staining (*p= 0.02*). Two further studies categorised patients into groups with negative ($p21^{WAF1}$ staining<10%) and positive (10%≤ $p21^{WAF1}$ staining) $p21^{WAF1}$ expression and found significant difference in survival between two categories (Bali *et al.*, 2004; Terauchi *et al.*, 2005). In contrast to these previous studies, some published studies which are consistent with our results indicated that the survival probability was not significantly better in patients with positive or high expression of $p21^{WAF1}$ compared to those with negative or low expression of $p21^{WAF1}$ (Levesque *et al.*, 2000; Geisler *et al.*, 2001; Skirnisdottir and Seidal, 2013). As previously mentioned in part 5.5.1, this discrepancy may partly be explained by different sample size, sub-optimal design of some studies, different antibodies and cut-off values, different treatment options and immunohistochemical methods used in various studies.

5.5.5 Correlation of *TP53* status and $p21^{WAF1}$ protein expression

The correlation between frequency distribution of $p21^{WAF1}$ H-scores and *TP53* mutational status was examined using Mann-Whitney and Kolmogorov-Smirnov statistical tests. No significant association was observed in distribution of $p21^{WAF1}$ H-scores in regard to either Sanger *TP53* status or NGS *TP53* status (*p≥0.05*).

Some studies have included $p21^{WAF1}$ protein expression with p53 protein expression, some of which found no statistically significant associations between p53 protein expression and $p21^{WAF1}$ protein expression (Levesque *et al.*, 2000; Harlozinska *et al.*, 2002; Skirnisdottir and Seidal, 2013). In contrast, other researchers found a significant inverse relationship between p53 and $p21^{WAF1}$ expression (Anttila *et al.*, 1999; Geisler *et al.*, 2001; Bali *et al.*, 2004). A possible explanation for this inconsistency might be no uniform definition of how to describe and categorise immunohistochemistry stained samples as negative and positive p53/ $p21^{WAF1}$ staining (Rose *et al.*, 2003).

A few studies have investigated the association between *TP53* mutational status and $p21^{WAF1}$ protein expression. Rose *et al*. (2003) evaluated $p21^{WAF1}$ expression as a function of sequenced *TP53* gene mutation (exons 4-10, Sanger technique). The frequency distribution of positive $p21^{WAF1}$ nuclear staining (2%≤$p21^{WAF1}$ staining) in wild-type *TP53* ovarian tumours was significantly higher than tumours with either missense or null *TP53* mutations (*p=0.04*). One more study has noted an inverse correlation between $p21^{WAF1}$ expression and overexpression of mutant *TP53* (Bowtell, 2003).

5.5.6 The correlation of $p21^{WAF1}$ expression to survival in regard to *TP53* mutational status

In this study, tumour samples were split into 6 categories based on the both $p21^{WAF1}$ expression levels and *TP53* mutational status, and the differences in survival time between different groups were analysed. Overall, the difference in survival time between various sub-groups did not reach statistical significance on a log-rank test irrespective of the techniques for sequencing *TP53* ($p>0.05$).

Rose *et al*. (2003) categorised 267 tumours based on the $p21^{WAF1}$ expression and *TP53* mutational status (Sanger sequencing method). There was a trend toward a survival advantage for patients with $p21^{WAF1}$-positive tumours when only wild-type *TP53* tumours were assessed ($p=0.06$). For patients whose tumours had missense mutant *TP53*, survival data were not correlated with changes in $p21^{WAF1}$ staining in different groups. However, significant difference in survival was detected in the analysis between individuals with *TP53*-null and $p21^{WAF1}$-negative stained tumours and those with *TP53*-null and $p21^{WAF1}$-positive stained tumour, with a survival advantage for the former group ($p=0.005$). The difference between our results and this study can be explained in part by use of different cut-off value and consideration of the type of *TP53* mutation in the analysis by Rose *et al*. (2003).

5.5.7 Conclusion and further work

In summary, the combined evaluation of *TP53* mutation and protein expression provides additional information compared to either *TP53* mutation or p53 protein expression alone, particularly in those patients with wild-type *TP53*. As explained in chapter 4, using ROC curve analysis to determine the optimal cut-off value for the number of reads in NGS may give a better result in relation to mutational status of *TP53* as predictive and prognostic biomarker in ovarian cancer. Generally speaking, p53 immunohistochemistry staining can be informative as a surrogate indication for *TP53* mutation, especially with high expression of p53 for missense *TP53* mutation, but it is unlikely to be accurate enough on its own for clinical practice. Also, evaluation of other genes/proteins involving in the p53 pathway may be more informative compared to *TP53* mutational and/or protein expression status alone and can provide functional insight.

Chapter 6: An investigation of the effect of MDM2-p53 binding antagonists as single agents on ovarian cancer cell lines

6.1 Introduction

The treatment of ovarian cancer remains challenging due to relapse and resistance to chemotherapy, leading to lack of long-term benefit from treatment. For this reason, molecular alterations in tumours, particularly those involved in growth signalling pathways, cell cycle progression and apoptosis are being investigated to potentially exploit for targeted therapy (Agarwal and Kaye, 2003; Bast *et al.*, 2009; Huang *et al.*, 2010). This chapter set out to investigate the role of p53 in response to MDM2-p53 antagonists Nutlin-3, RG7112 and RG7388 as single agents in a panel of ovarian cancer cell lines. The chemical structures of MDM2-p53 antagonists and their mechanism of action are described in chapter 1.8.

6.1.1 Inactivation of p53 in ovarian cancer

TP53 mutation is the most common cause of p53 inactivation in ovarian cancer occurring in 30% up to 80% of cases (Reles *et al.*, 2001; Kmet *et al.*, 2003; Ling and Wei-Guo, 2006; Metindir *et al.*, 2008; Bast *et al.*, 2009). In the remaining malignancies, p53 function is held in check through other mechanisms and reactivation of p53 is a potential therapeutic strategy (Ling and Wei-Guo, 2006). Other mechanisms of p53 inactivation in ovarian cancer include *MDM2* amplification/overexpression and p14ARF deficiency. A few reports indicated negative expression or genetic alterations of p14ARF (Havrilesky *et al.*, 2003; Nam and Kim, 2008) in epithelial ovarian cancer. The p14ARF protein is a negative regulator of MDM2, binding to MDM2 and sequestering it into the nucleus resulting in activation of p53 (Nam and Kim, 2008; Creighton *et al.*, 2010). There is a lack of evidence to confirm significant association of p14ARF expression and survival or clinicopathological features in epithelial ovarian cancer (Nam and Kim, 2008).

Regulation of the p53 cellular level is discussed in detail in chapter 1.5.7. Given the important role of MDM2 in degradation and inactivation of p53, inhibition of the MDM2-p53 binding interaction has been considered as a promising therapeutic target for malignancy with wild-type *TP53*.

6.2 Hypothesis and Objectives

Hypothesis:

1. Wild-type *TP53* ovarian cancer cell lines are sensitive to the growth inhibitory and/or apoptotic effects of the MDM2-p53 antagonists Nutlin-3, RG7112 and RG7388, whereas mutant *TP53* cell lines are resistant.

Objectives:

1. To test a panel of established ovarian carcinoma cell lines for their response to MDM2-p53 antagonists Nutlin-3, RG7112 and RG7388, and evaluate the relationship of this response to the genotype of the cells.

6.3 Specific Materials and Methods

6.3.1 Cell lines

Three wild-type *TP53* and four mutant *TP53* epithelial ovarian carcinoma cell lines used in this study were sourced from the NICR authenticated cell bank and regularly tested for mycoplasma. The wild-type *TP53* cell lines used were A2780, IGROV-1, OAW42 and the mutant *TP53* cell lines were CP70, *MLH1*-corrected CP70+, MDAH-2774 and SKOV-3. More details of these cell lines and their cell culture are provided in chapter 2.3.1, 2.3.2 and 2.3.3.

6.3.2 Growth curves and growth inhibition assays

The SRB assay was used to generate growth curves, growth inhibition curves for 72 hours, and calculate GI_{50} values as described in chapter 2.7 and 2.8. Based on the growth curves, the appropriate cell densities were chosen for cells to be in the exponential phase of growth.

6.3.3 PCR

Genomic DNA was extracted from a pellet of IGROV-1, MDAH-2774, or SKOV-3 including 1 x 10^6 cells, using a QIAamp DNA Mini Kit (Qiagen, UK) as described in general materials and methods (2.12.2). The quality of the DNA and its concentration were estimated using a NanoDrop ND-1000 Spectrophotometer (NanoDrop Technologies, Inc. Wilmington, DE, USA). The purity of DNA was determined by the ratio of 260nm:280nm, which is around 1.8 for good quality of DNA. The DNA extracted from IGROV-1 was amplified for *TP53* exon 5, from MDAH-2774 for *TP53* exon 8 and from SKOV-3 for *TP53* exon 4 and exon 5 (Table 6-1). Purification of PCR products was carried out for subsequent analysis using the Purelink PCR purification kit (Qiagen, UK) in accordance with the manufacturer's protocol previously explained (2.12.3). Agarose gel electrophoresis was performed using a 2% agarose gel with 100 volts for approximately 45 minutes. Then, DNA was visualised using a Biorad Gel Documentation System under UV light trans-illumination and digitally photographed. The purified DNA was sent to DBS Genomics (Durham, UK) for Sanger Dideoxy DNA sequencing.

Target Exon	Primer Sequence 5'-3'
Exon 4.1	F-GTTCTGGTAAGGACAAGGGT
	R-TGTAGGAGCTGCTGGTGCAG
Exon 4.2	F-AGCTCCCAGAATGCCAGAGG
	R-ATACGGCCAGGCATTGAAGT
Exon 5	F-GCTGCCGTCTTCCAGTTGCT
	R-CCAGCCCTGTCGTCTCTCCA
Exon 8 & 9	F-TTTAAATGGGACAGGTAGGAC
	R-GCCCCAATTGCAGGTAAAACAG

Table 6-1: The primers and their sequences used for PCR-based sequencing for different exons of *TP53* gene. F, Forward; R, Reverse.

6.3.4 Western blot

2 x 10^5 cells were seeded per 35mm diameter well in 6-well tissue culture plates (Corning Corp) for western blot analysis and left for 48 hours to adhere and grow. To study the effect of Nutlin-3/RG7388 on the functional p53 pathway, cells were treated with 0.2, 1 and 5 µM Nutlin-3 or 0.02, 0.1 and 0.5 µM RG7388 and lysates were extracted after 4 hours. For time course analysis, the cells were treated with 2x GI_{50} Nutlin-3, RG7388 or cisplatin and lysates were prepared after 0.5, 1, 2, 4, 6, 8 and 24 hours. Medium, distilled water and DMSO treated cells were used as control. The antibodies used and their details are provided in chapter 2.11.7.

6.3.5 Flow cytometry

Flow cytometry was performed to analyse cell cycle distribution changes and induced apoptosis over 24 hours treatment, as described in chapter 2.14.3. The A2780 and IGROV-1 cell lines were seeded at 1.7 x 10^5 cells/well in 6-well plates and the OAW42 cell line at 1.3 x 10^5 per small flask. Cells were treated with cisplatin, Nutlin-3, and RG7388 at 1x GI_{50} concentration for 24 hours. Adherent and non-adherent cells were harvested to analyse the cell cycle distribution and SubG1 apoptotic cells by propidium iodide (PI) staining. Harvested cells were washed with PBS and re-suspended in 500 µL PBS with 1mg/mL sodium citrate (Sigma, St Louis, MO), 100 µg/mL propidium iodide (Sigma), 200 µg/mL RNAse A (Sigma)

and 0.3% Triton-X (Sigma). Samples were analysed on a FACSCalibur^{TM} flow cytometer using CellQuest Pro software (Becton Dickinson, Oxford, UK). Cell cycle distribution was determined using Cyflogic (CyFlo Ltd, Turku, Finland).

6.3.6 Clonogenic cell survival assay

Clonogenic survival assays were performed for the panel of 6 ovarian cancer cell lines as described in chapter 2.9.

6.3.7 Caspase 3/7 activity assay

The Caspase-Glo® Assay (Promega, Southampton, UK) was used to measure the caspase-3 and -7 activities in cultures of cells. The A2780 and IGROV-1 cell lines were seeded at 4.5 x 10^4 cells/well and OAW42 cell line at 3 x 10^4 cells/well in white-welled 96-well plates (Corning, UK) for 24 hours. The cells were treated with 1x GI_{50} concentration of cisplatin, Nutlin-3 and RG7388 for 24 hours. The Caspase 3/7 kit was defrosted, the buffer was added and allowed to reach room temperature. A 1:1 volume of caspase reagent was added to each well and the plates covered with aluminum foil and incubated for 1 hour at room temperature. Following exposure to caspase reagent, cells lyse and release activated caspase to cleave the substrate resulting in a ‘glow-type ‘luminescence. The resulting lysates were analyzed on a microplate luminometer (Berthold Technologies, Herefordshire, UK) after the incubation period. Luminescence readings were normalized and plotted relative to the control.

6.3.8 Statistical analysis

The statistical paired t-test was used to compare the mean of 3 or more paired biological repeats and p-values <0.05 were considered statistically significant.

6.4 Results

6.4.1 Determination of the growth characteristics of 7 ovarian cancer cell lines

Growth curves were constructed for A2780, IGROV-1, OAW42, CP70, *MLH1*-corrected CP70+, MDAH-2774 and SKOV-3 cell lines, as described in chapter 2.7 (Figure 6-1). The cell densities and doubling time for each cell line were determined based on the growth curves as described in section 2.7 (Table 6-2). Overall, all cell lines used in this study grow well with the exception of SKOV-3 which grows relatively slowly. There was difficulty detaching OAW42 cells, which was solved by using 2.5x Trypsin/EDTA and 10 minutes incubation time. To validate the *MLH1*-corrected CP70+ cell line by western blot analysis, A2780, the MMR-proficient cell line, and CP70, its *MLH1*-deficient variant, were used as positive and negative controls respectively (Curtin *et al.*, 2004) (Figure 6-2)

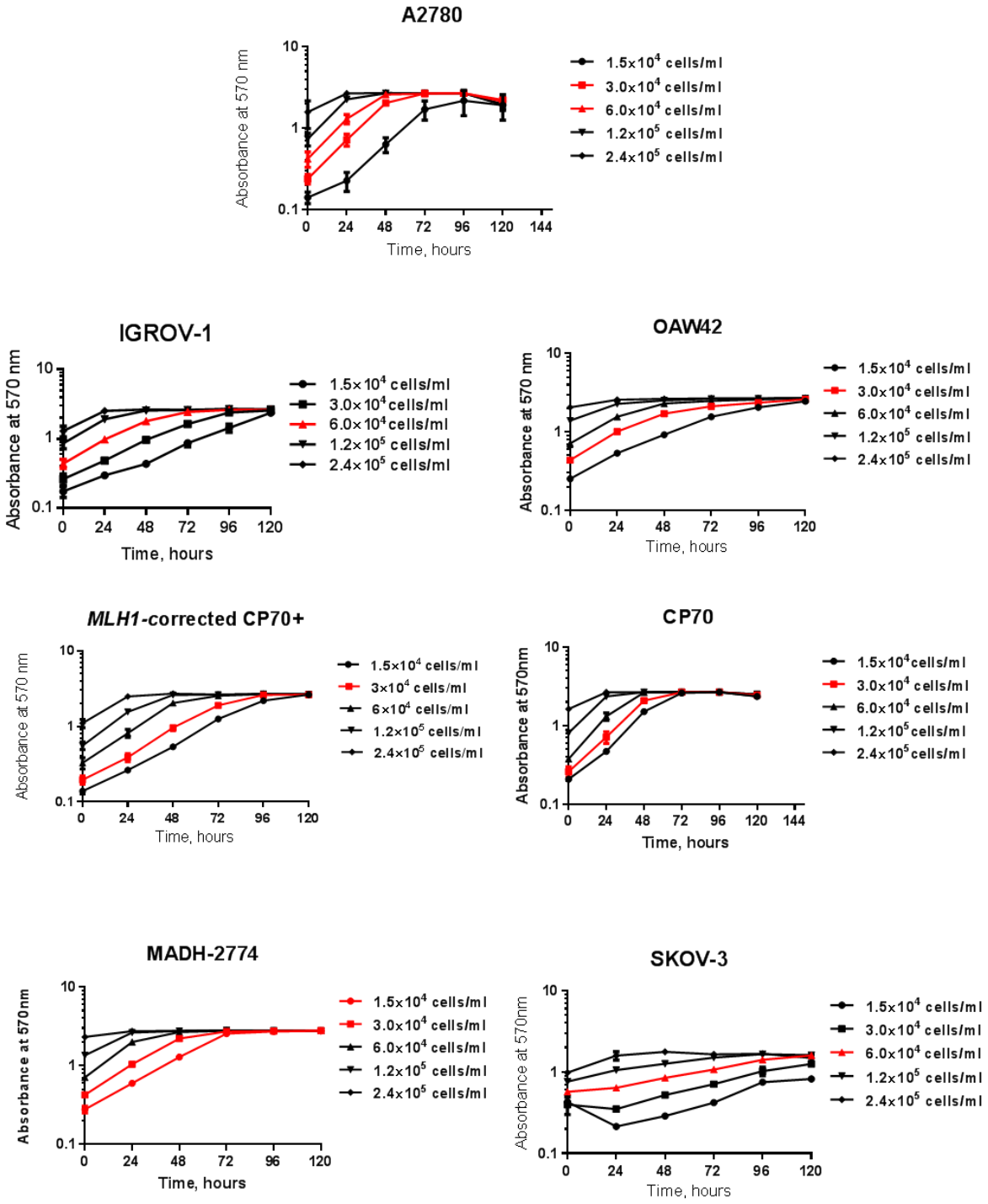

Figure 6-1: Growth curves to determine the cell density used for growth inhibition assays. The curves and seeding densities chosen for growth inhibition assays are shown as red lines. For A2780 and MDAH-2774, the average of two densities was used.

Cell Line	Cell Density (cells/ml)	Doubling Time (hours)
A2780	4.5×10^4	18.43
IGROV-1	6.0×10^4	25.21
OAW42	3.0×10^4	18.88
CP70	3.0×10^4	15.72
***MLH1*-corrected CP70$^+$**	3.0×10^4	22.44
SKOV-3	6.0×10^4	45.23
MHAD-2774	2.25×10^4	22.25

Table 6-2: The seeding densities of cells used for growth inhibition assays and doubling time calculated for each cell line.

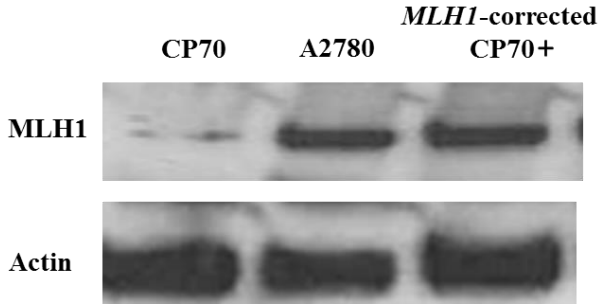

Figure 6-2: Western blot analysis showed the expression of MLH1 protein in the *MLH1*-corrected CP70+ cell line. A2780, the MMR-proficient cell line, and CP70, its *MLH1*-deficient variant, were used as a positive and negative control respectively.

6.4.2 Sequencing of *TP53* exon 5 in the IGROV-1, *TP53* exon 8 & 9 in the MDAH-2774 and *TP53* exon 4 and 5 in the SKOV-3 cell lines

Due to contradictory information on the *TP53* status of IGROV-1 and SKOV-3 cell lines in the literature and to check the reported *TP53* mutation for MDAH-2774 cell line, DNA was extracted and PCR-based sequencing of the *TP53* gene in these cell lines was carried out. Based on the Sanger website Cosmic database, there are an insertion (c.267_268insC) and a substitution mutation (c.377 A->G) in the IGROV-1 cell line. However, some studies cited

IGROV-1 as a wild-type *TP53* cell line (Le Moguen *et al.*, 2006). A frame shift deletion (c.267delC) based on the Sanger website and a substitution mutation (c.179 A->G) (O'Connor *et al.*, 1997) were reported in the SKOV-3 cell line. Furthermore, a substitution mutation (c.818G->A) was reported in MDAH-2774 (Dai *et al.*, 2009).

6.4.2.1 Determination of extracted DNA concentration and PCR amplification

DNA purity and concentration were estimated and good quality DNA was used for PCR amplification of *TP53* exon 5 for IGROV-1, *TP5*3 exon 8 for MDAH-2774 and *TP53* exon 4 and exon 5 for SKOV-3 cell lines. The 2% agarose gel electrophoresis showed the amplification of the expected amplicons, which were 261 bp for exon 4.1, and 241 bp for exon 4.2, 294 bp for exon 5, and 443 bp for exon 8 & 9.

6.4.2.2 Sequencing results

The results of PCR-based Sanger sequencing of the *TP53* exon 5 confirmed the wild-type *TP53* status of the IGROV-1 cell line (Figure 6-3). The results also indicated that MDAH-2774 harbours a *TP53* mutation located in exon 8 (c.818G->A, p.Arg273His) (Figure 6-4). A frame shift deletion (c.265delC, p.Pro89fsX33) (Figure 6-5) was confirmed in *TP53* exon 4 and no substitution mutation (c.179 A->G) was detected in *TP53* exon 5 for the SKOV-3 cell line (Figure 6-6). This frameshift deletion results in premature termination and dysfunctional p53 protein.

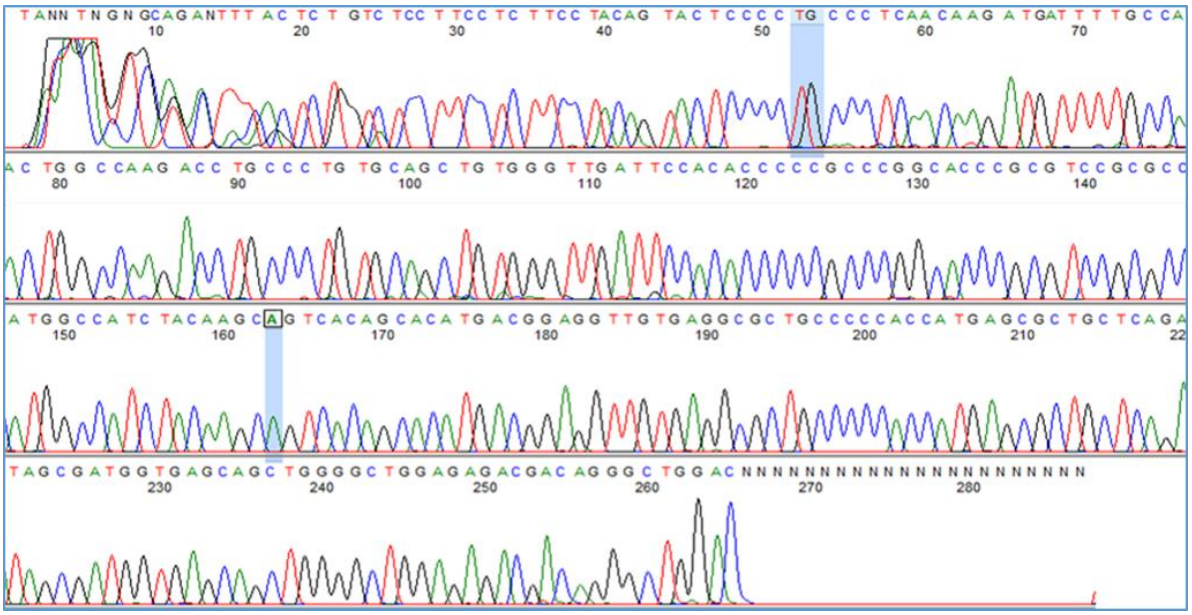

Figure 6-3: Exon 5 DNA sequencing of the IGROV-1 cell line. Neither an insertion (c.267_268insC) nor a substitution mutation (c.377 A->G) was confirmed by Sanger sequencing.

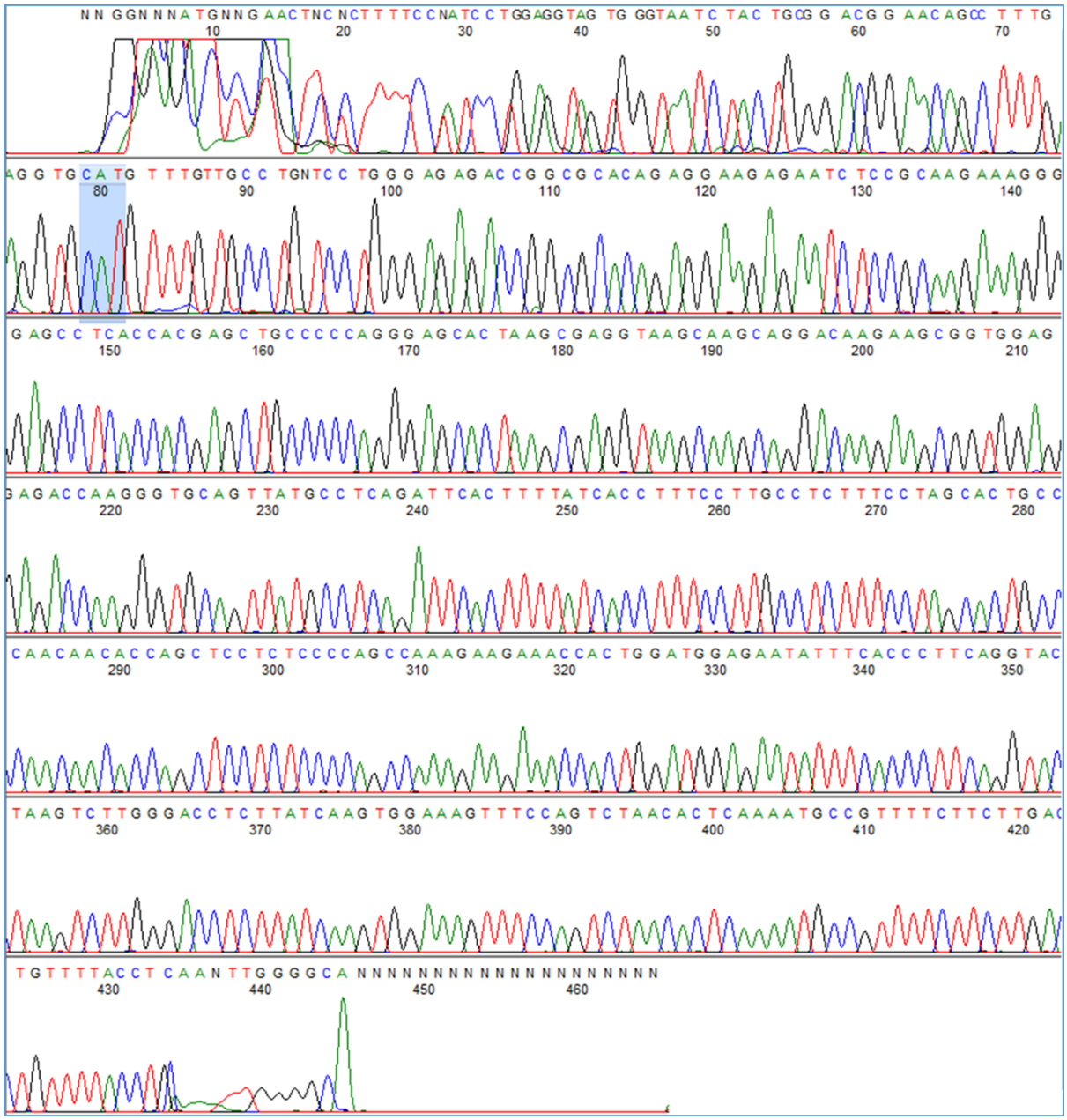

Figure 6-4: Exon 8 & 9 DNA sequencing of the MDAH-2774 cell line. A substitution mutation (c.818 G->A, p.Arg273His) in exon 8 of *TP53* was detected by Sanger sequencing.

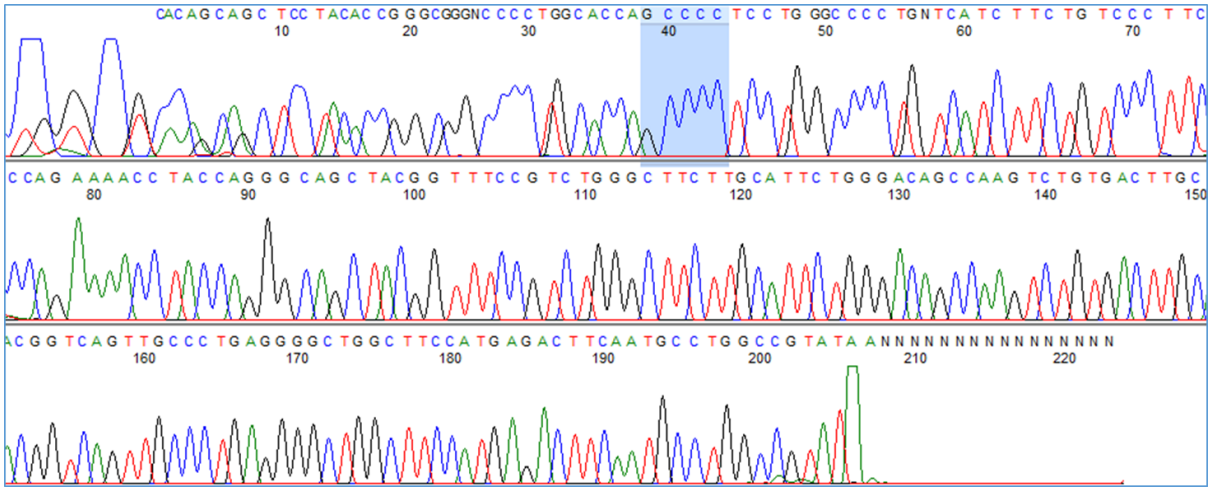

Figure 6-5: Exon 4 DNA sequencing of SKOV-3 cell line. A frame shift deletion (c.265delC, P.pro89fsX33) was detected by Sanger sequencing.

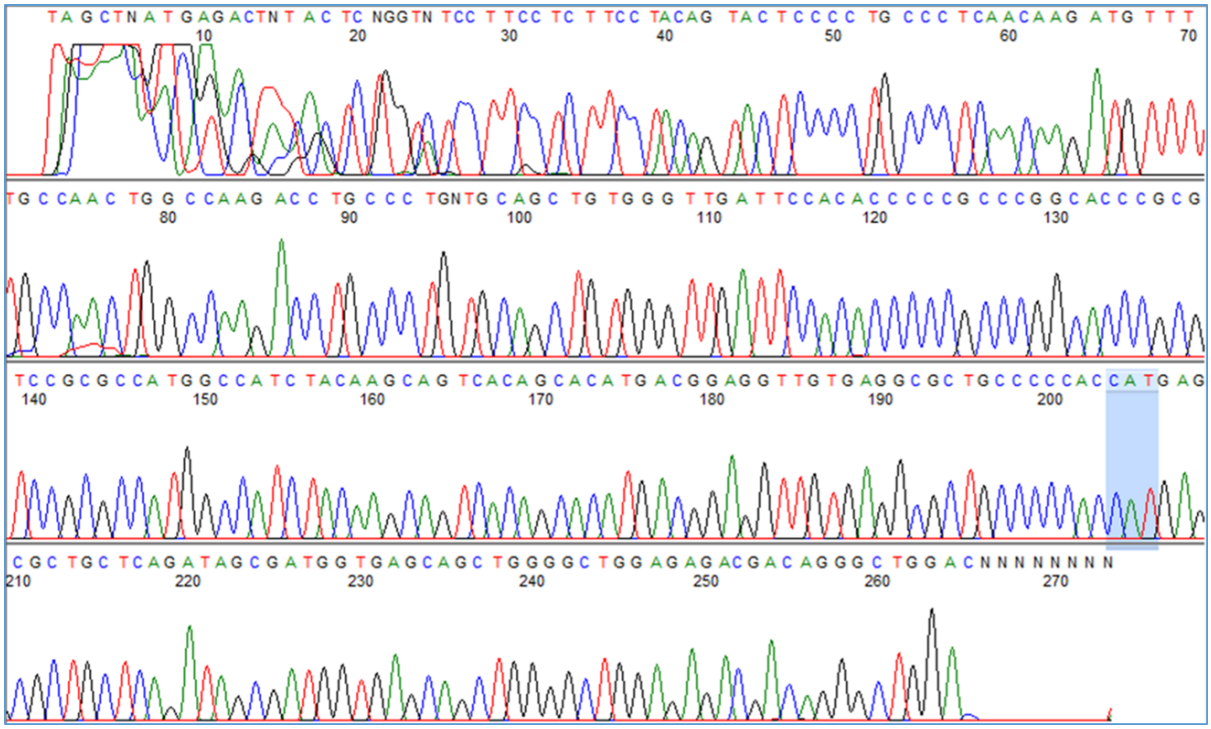

Figure 6-6: Exon 5 DNA sequencing of the SKOV-3 cell line. No substitution mutation (c.179 A->G) was detected by Sanger sequencing.

6.4.3 Wild-type *TP53* ovarian cancer cell lines are sensitive to the growth inhibitory effect of MDM2-p53 antagonists, Nutlin-3, RG7112 and RG7388

Both wild-type and mutant *TP53* cell lines were treated with different concentrations of cisplatin (0-16 μM) and Nutlin-3 (0-30 μM). Wild-type *TP53* cells were treated with lower concentrations of RG7112 or RG7388 (0-5 μM) and mutant cells treated with higher concentrations of RG7112 or RG7388 (0-30 μM). Growth inhibition assays and the GI_{50} values were calculated following 72 hours exposure to drugs (Table 6-3). The results (Figure 6.7 and 6.8) show clear resistance to MDM2-p53 antagonists in mutant *TP53* cell lines. The GI_{50} values were significantly lower in wild-type *TP53* cell lines compared to mutant, which is consistent with their mechanism of action. Both Mann-Whitney ($p<0.0001$) and Kolmogorov-Smirnov ($p<0.0001$) tests showed the observed differences are highly statistically significant (Table 6-3 and Figure 6.8). The GI_{50} values for wild-type *TP53* cell lines for RG7112 (716.7±165.9 (SEM) nM) and RG7388 (253.3±73.1 (SEM) nM) were in the nanomolar range, while for Nutlin-3 they were in the micromolar range (1.76±0.51 (SEM) μM). In contrast, mutant *TP53* cell lines had GI_{50} values greater than 10 μM: 19.7 ± 1.3 μM for RG7112, 17.8 ± 2.9 μM) for RG7388 and 21.2->30 μM for Nutlin-3. Due to the greater potency of RG7388 compared to RG7112 and clinical interest, other experiments were carried out with Nutlin-3 and RG7388.

Cell line	*TP53* Status	Cisplatin (μM)	Nutlin-3 (μM)	RG7112 (μM)	RG7388 (μM)
A2780	Wild-type	0.82 ± 0.17	1.23 ± 0.23	0.41 ± 0.09	0.11 ± 0.01
IGROV-1	Wild-type	0.85 ± 0.04	2.8 ± 0.48	0.98 ± 0.06	0.35 ± 0.04
OAW42	Wild-type	0.73 ± 0.02	1.3 ± 0.1	0.76 ± 0.323	0.31 ± 0.04
CP70	Mutant	5.8 ± 1.1	21.2 ± 2.5	22.0 ± 0.57	11.7 ± 1.81
***MLH1*-corrected CP70+**	Mutant	2.4 ± 0.25	21.2 ± 1.22	21.8 ± 0.29	14.5 ± 1.09
MDAH-2774	Mutant	1.11± 0.14	21.4 ± 0.9	16.7 ± 1.6	20.7 ± 1.43
SKOV-3	Mutant	8.8 ± 0.49	> 30	18.37 ± 0.93	24.6 ± 1.54

Table 6-3: GI_{50} concentrations of cisplatin, Nutlin-3, RG7112 and RG7388 for the panel of ovarian cancer cell lines of varying *TP53* status. Data represent the mean of at least 3 independent experiments ± SEM.

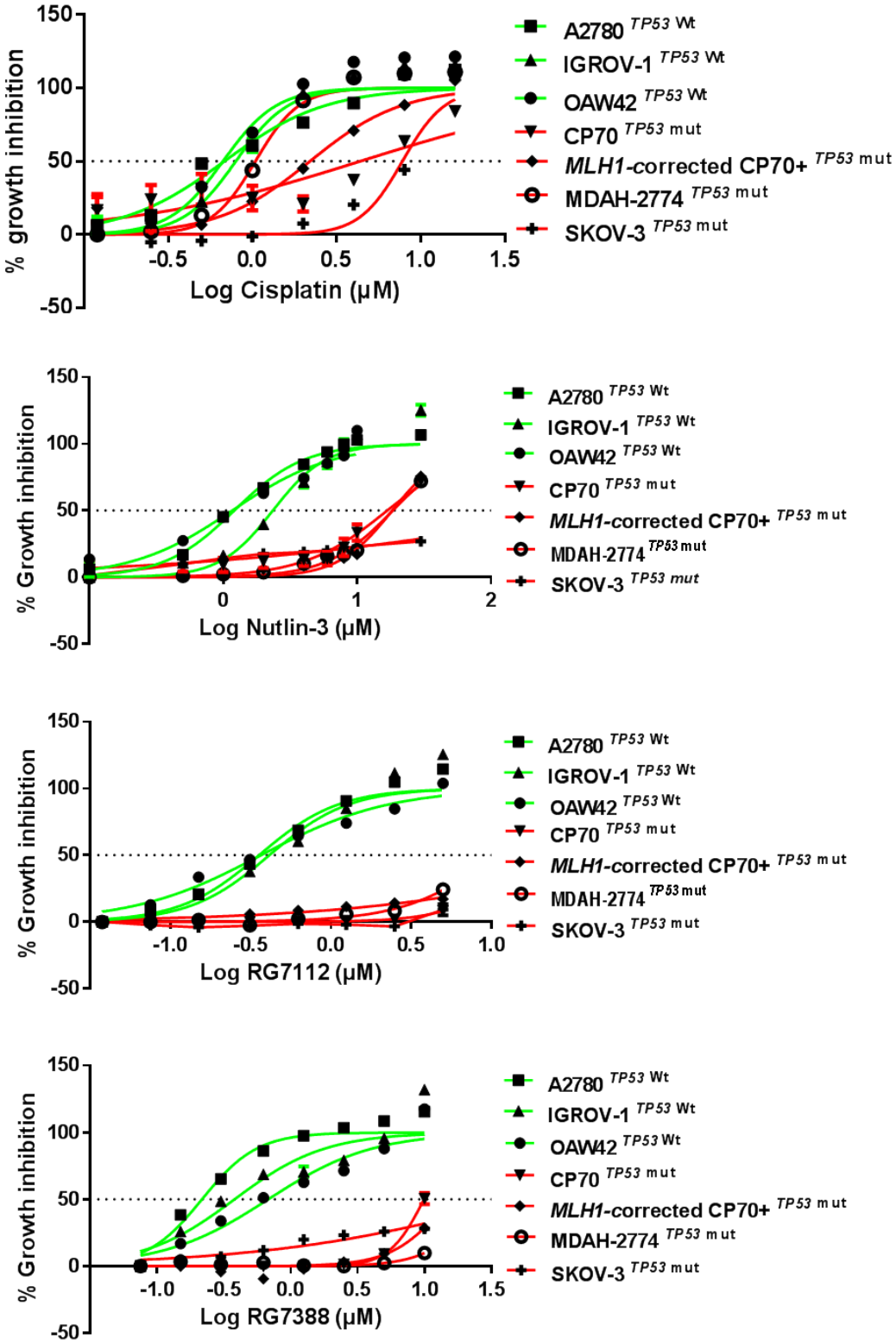

Figure 6-7: Growth inhibition curves demonstrating the effect of MDM2-p53 antagonists compared to cisplatin in a panel of ovarian cancer cell lines. The results clearly show the effect of MDM2-p53 antagonists is *TP53* dependent. Data represent the mean of at least 3 independent experiments.

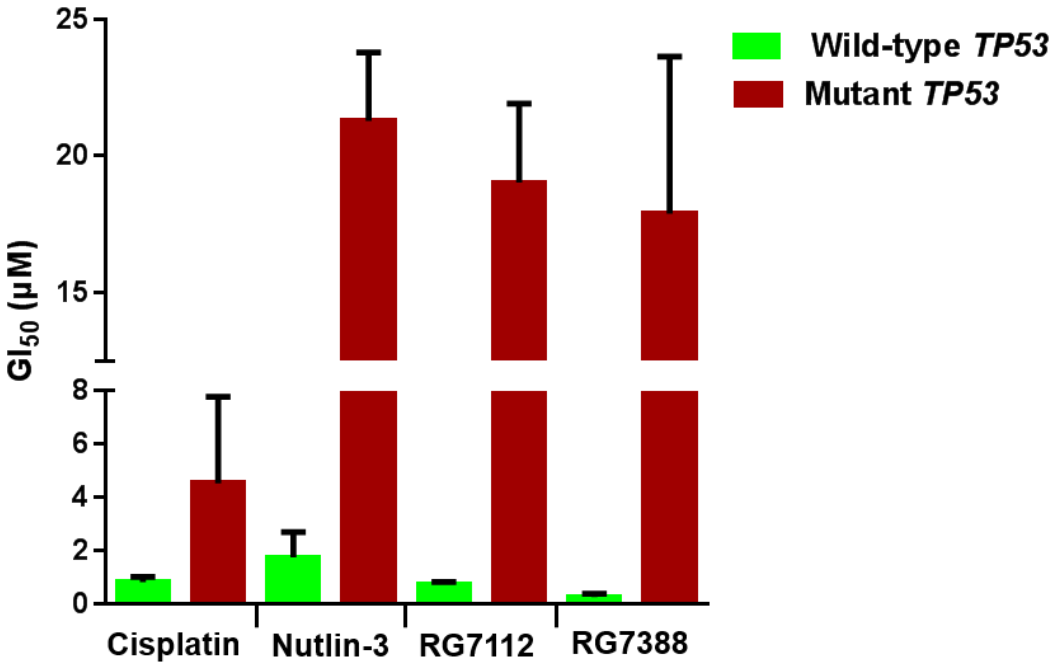

Figure 6-8: The sensitivity to cisplatin and MDM2 antagonists, Nutlin-3, RG7112 and RG7388, in a panel of wild-type and mutant *TP53* ovarian cancer cell lines. Wild-type *TP53* cell lines are significantly more sensitive to growth inhibition by cisplatin (Mann Whitney test, p< 0.0001 and Kolmogorov-Smirnov test p=0.001), Nutlin-3, RG7112 and RG7388 (Mann Whitney and Kolmogorov-Smirnov tests, p< 0.0001) treatment for 72 hours compared to mutant *TP53* cell lines. Data shown are the average of at least three independent experiments and error bars represent SEM.

6.4.4 Functional activation of the p53 pathway in wild-type *TP53* cell lines in response to Nutlin-3/RG7388

The p53-dependent response to Nutlin-3/RG7388 assessed by western blotting showed that Nutlin-3/RG7388 induced stabilization of p53 and upregulation of $p21^{WAF1}$ and MDM2 protein levels four hours after the commencement of treatment in a concentration-dependent manner and confirmed functional activation of wild-type p53 by release from MDM2. However, as anticipated, it had no effect on p53-dependent gene expression in the *TP53*-mutant cell lines with the delivered dose range of Nutlin-3/RG7388 (Figure 6-9). Interestingly this was despite a small increase in stabilization of mutant p53 in response to RG7388 at the doses of 0.1 and 0.5 µM with the CP70 and *MLH1*-corrected CP70+ cell lines. This result indicates that some forms of mutant p53 are still targeted for degradation by MDM2 even though they have lost their transcriptional function. Also, there is a frame-shift deletion in the SKOV-3 cell line leading to an absence of detectable p53, $p21^{WAF1}$ and MDM2 expression.

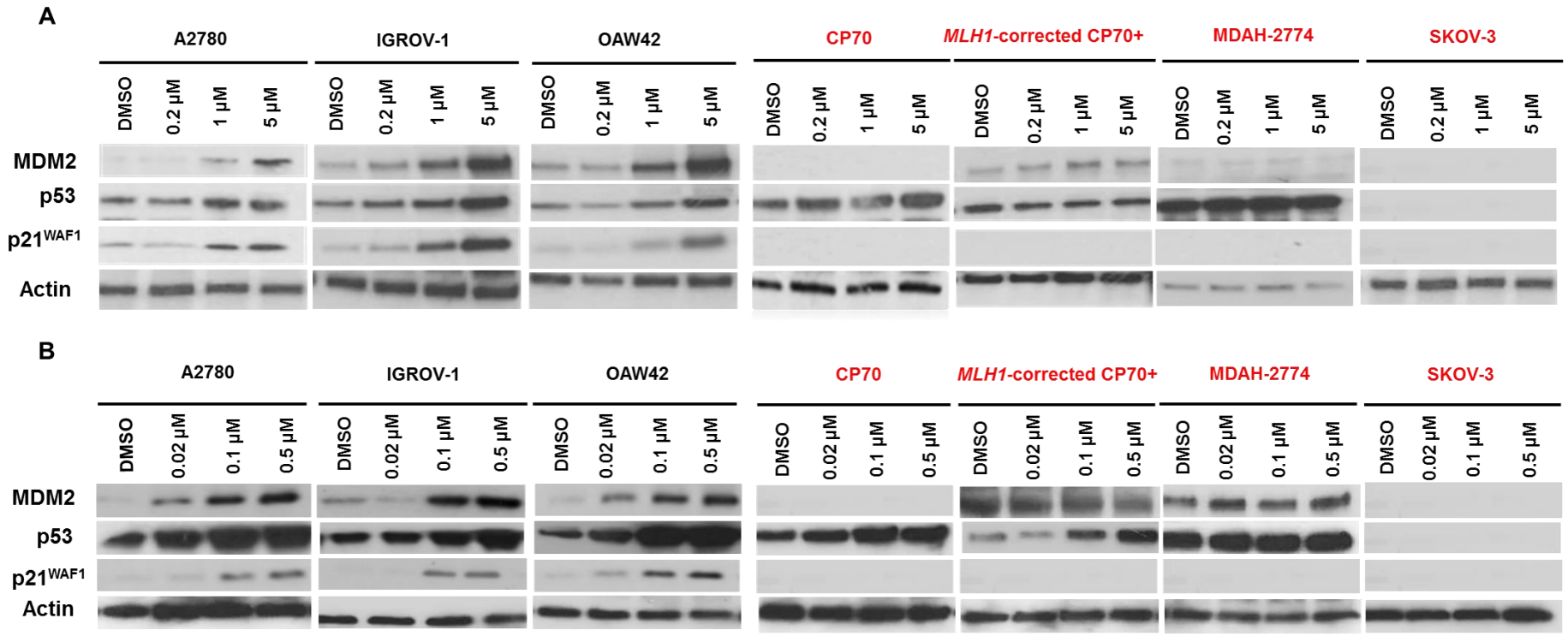

Figure 6-9: Western blot analysis for (A) Nutlin-3 and (B) RG7388 showed stabilization of p53 and upregulation of p53 transcriptional target gene protein levels, MDM2 and p21^{WAF1}, four hours after the commencement of treatment in wild-type *TP53* cell lines with the indicated doses (µM); however, they had no effect on downstream transcriptional targets of p53 in mutant *TP53* ovarian cancer cell lines with the delivered dose range of MDM2 antagonists despite stabilization of the mutant p53 in the CP70 and *MLH1*-corrected CP70+ cells. *TP53* mutant cell lines are highlighted in red colour.

6.4.1 Time course western blot analysis of p53, $p21^{WAF1}$ and MDM2 expression in wild-type *TP53* cell lines treated with cisplatin or Nutlin-3/RG7388

Time course analysis for the expression of p53, $p21^{WAF1}$ and MDM2 was carried out using three wild-type *TP53* cell lines treated with cisplatin, Nutlin-3 or RG7388 at 2x their respective GI_{50} concentrations. Lysates were extracted after 0.5, 1, 2, 4, 6, 8, and 24 hours. What is interesting in this data is that MDM2-p53 antagonists, Nutlin-3/RG7388, induced $p21^{WAF1}$ upregulation more than cisplatin. The highest levels of induced p53 were 4 hours after commencement of Nutlin-3/RG7388 treatment in A2780 and OAW42 compared to 8 and 24 hours post-treatment of cisplatin in A2780 and OAW42 respectively (Figure 6-10 & Figure 6-11). Unexpectedly, no significant upregulation of $p21^{WAF1}$ was detected in these cell lines following cisplatin treatment. With the IGROV-1 cell line, cisplatin and Nutlin-3/RG7388 treatment increased induction and stabilisation of p53 at the highest levels after 8 and 6 to 8 hours post-treatment respectively (Figure 6-11). These results indicated that MDM2-p53 antagonists are more effective at inducing p53 and upregulating its downstream targets, $p21^{WAF1}$ and MDM2, compared to cisplatin in ovarian cancer cell lines; however, the effect is cell type and time dependent.

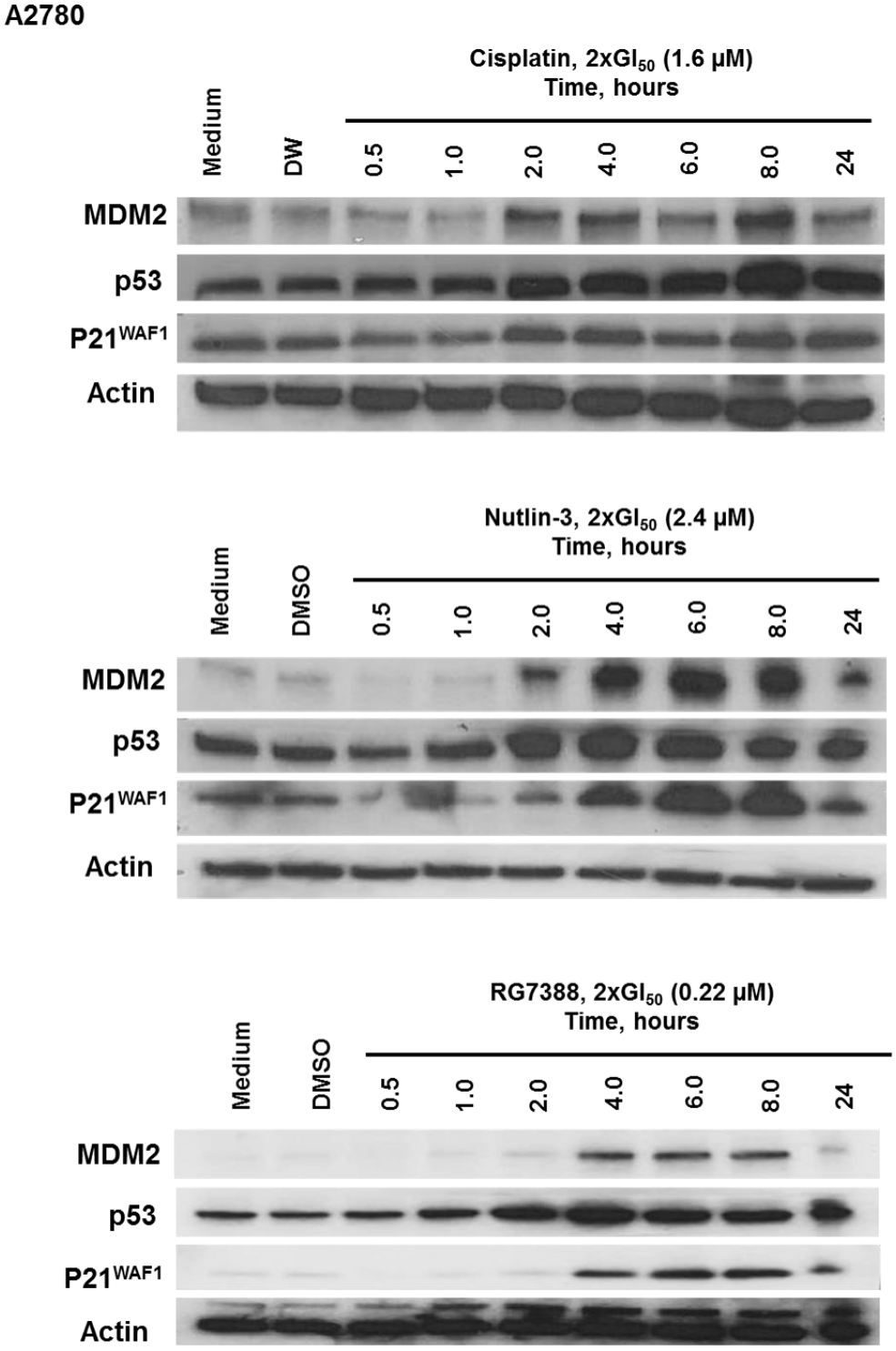

Figure 6-10: Western blot analysis showing time course analysis of the p53, p21^{WAF1} and MDM2 expression in the A2780 cell line treated with 2x GI_{50} concentrations of cisplatin, Nutlin-3 or RG7388. Actin was used as a loading control.

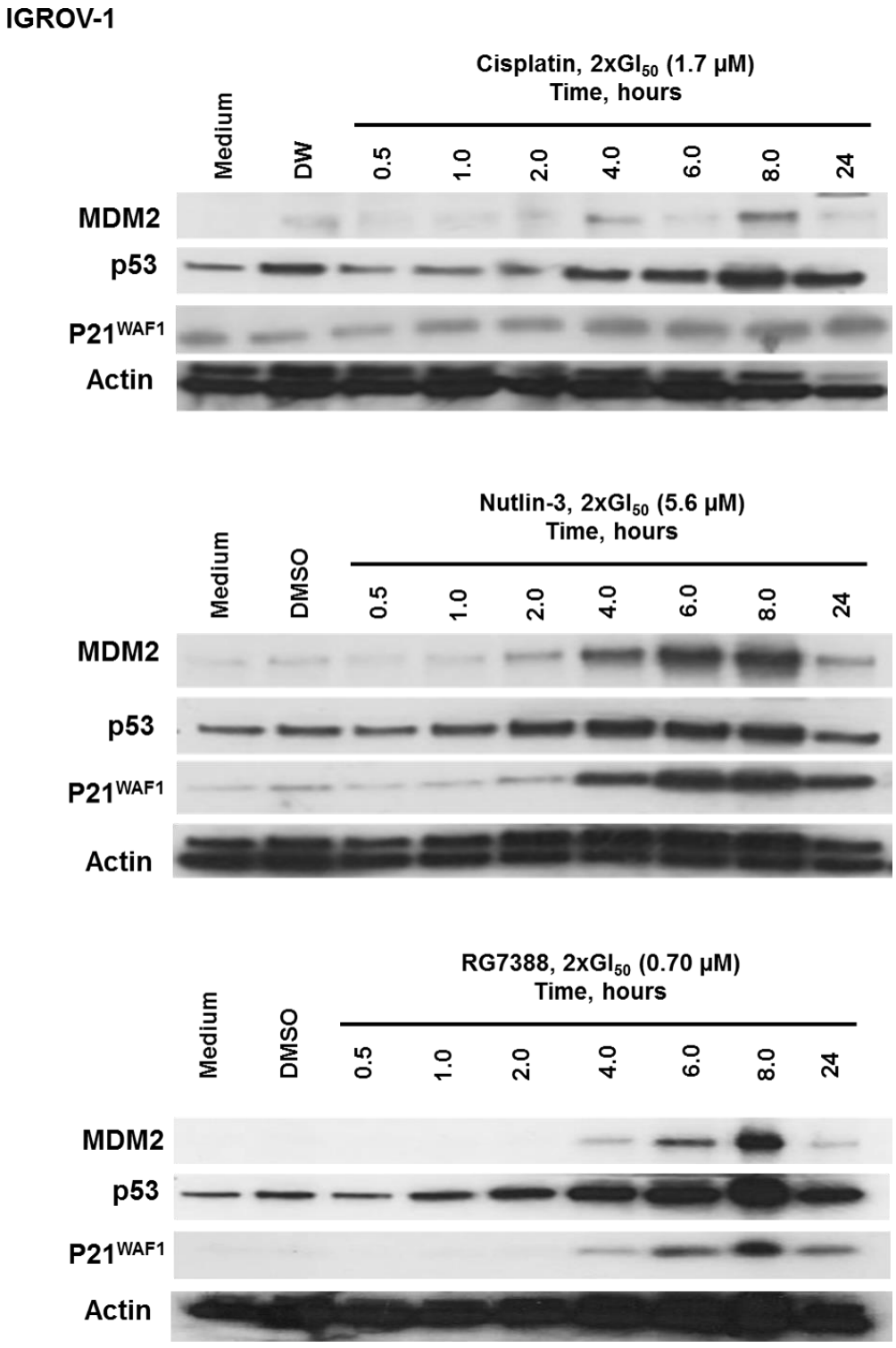

Figure 6-11: Western blot analysis showing time course analysis of the p53, p21^{WAF1} and MDM2 expression in the IGROV-1 cell line treated with 2x GI_{50} concentrations of cisplatin, Nutlin-3 or RG7388. Actin was used as a loading control.

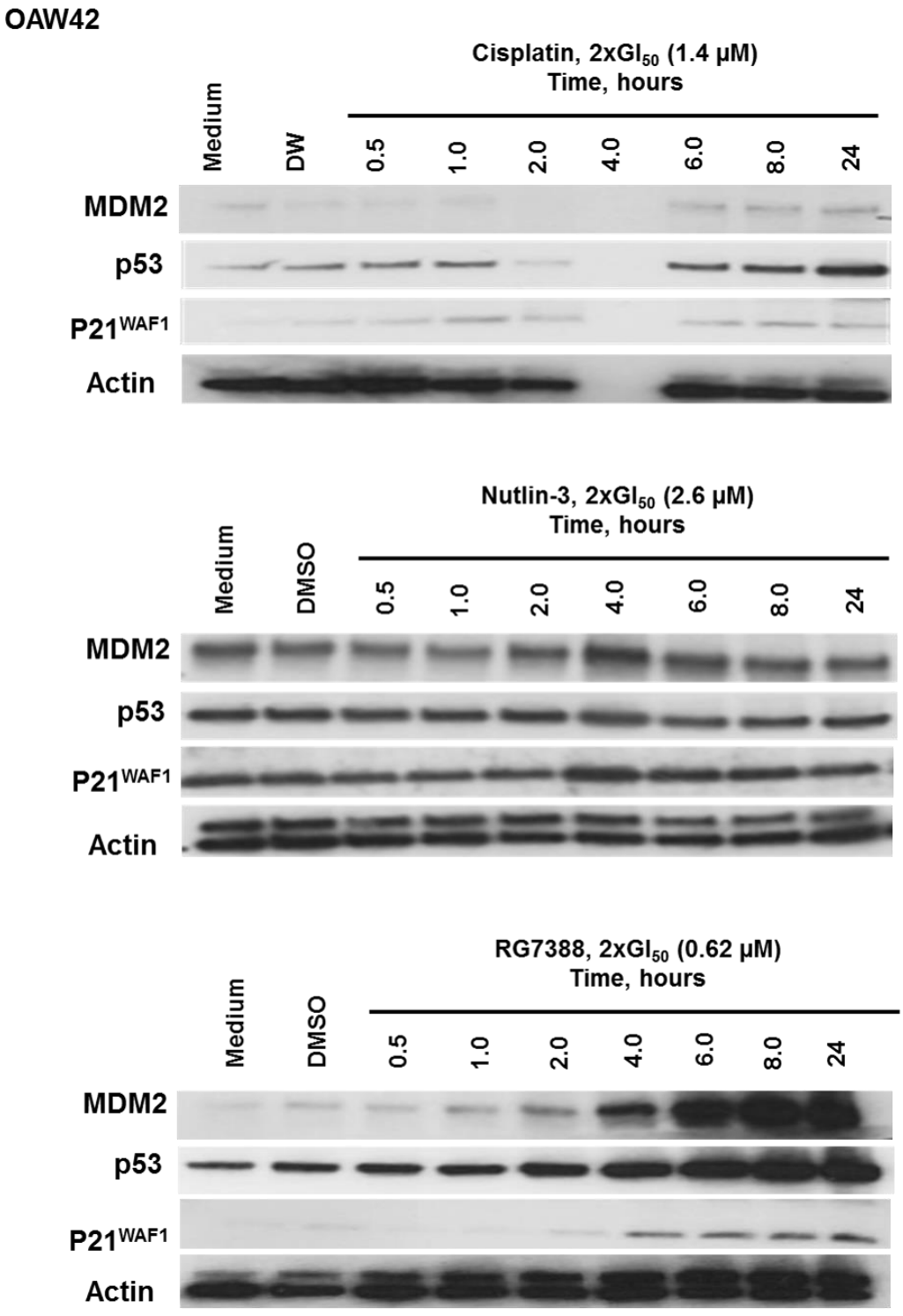

Figure 6-12: Western blot analysis showing time course analysis of the p53, p21^{WAF1} and MDM2 expression in the OAW42 cell line treated with 2x GI$_{50}$ concentrations of cisplatin, Nutlin-3 or RG7388. Actin was used as a loading control.

6.4.2 The effect of Nutlin-3/RG7388 on cell cycle distribution changes and/or apoptosis in wild-type *TP53* ovarian cancer cell lines

Wild-type *TP53* cell lines were analysed for their cell cycle response to Nutlin-3/RG7388 as a single agent compared to DMSO control. Cells were treated with Nutlin-3/RG7388 at 1x their respective GI_{50} concentrations for 24 hours. They were then analysed by flow cytometry for cell cycle phase distribution changes and evidence of apoptosis in response to treatment. Nutlin-3 increased slightly the proportion of cells in G0/G1 phase. Nutlin-3 also increased the percentage of SubG1 events, a surrogate marker of apoptosis, across three cell lines. RG7388 after 24 hours treatment led to a substantial increase in the proportion of cells in the G0/G1 phase of the cell cycle across all cell lines compared to Nutlin-3 at the same GI_{50} doses. RG7388 induced SubG1 events in all cases, which was more significant in the IGROV-1 ovarian cancer cell line (Figure 6-13A & B).

6.4.3 The effect of Nutlin-3/RG7388 as a single agent on the Caspase 3/7 activity in wild – type *TP53* ovarian cancer cell lines

The induction of apoptosis was also evaluated by caspase 3/7 enzymatic assay, which is a sensitive and specific indicator of apoptosis (Chen *et al.*, 2015). Wild-type *TP53* ovarian cancer cell lines were treated for 24 hours with 1x their respective Nutlin-3/RG7388 GI_{50} concentrations. No significant increase in the caspase 3/7 activity in response to Nutlin-3/RG7388 was detected in the A2780 and OAW42 cell lines. With IGROV-1, a significant increase in caspase 3/7 activity in response to Nutlin-3/RG7388 compared to DMSO control was observed (Figure 6-13C).

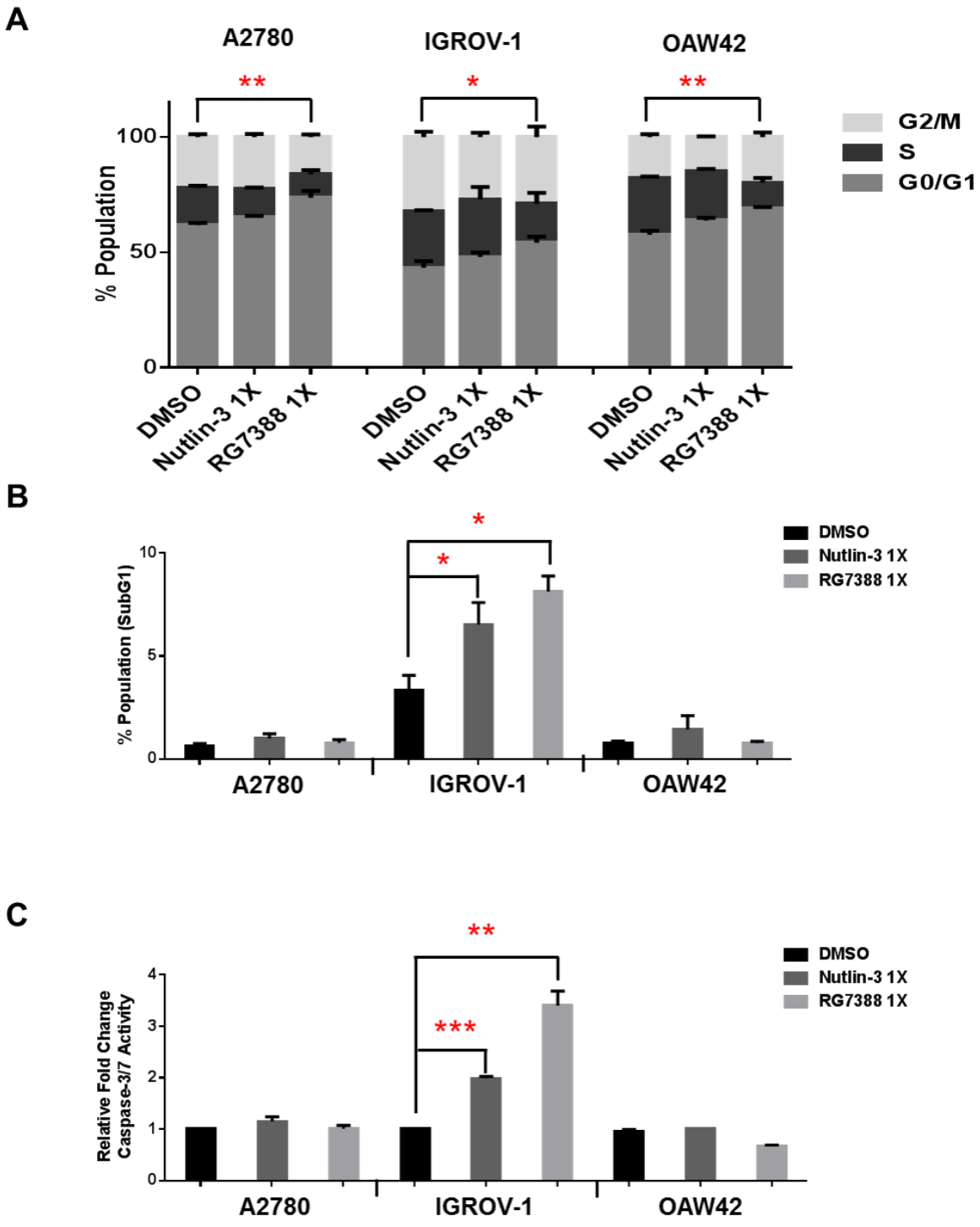

Figure 6-13: Nutlin-3/RG7388 affects the cell cycle distribution and apoptotic endpoints. (A) Nutlin-3/RG7388 increased the proportion of cells in G0/G1 phase compared to DMSO control. (B) Flow cytometry for SubG1 events and (C) Caspase 3/7 activity is represented as fold change relative to DMSO solvent control. *, p < 0.05; **, P < 0.01; ***, P < 0.001. Data are shown as the average of at least 3 independent experiments and error bars represent SEM.

6.4.4 Nutlin-3/RG7388 alone results in clonogenic cell death in a p53-dependent manner

Clonogenic survival assays were performed for the panel of six ovarian cancer cell lines. Exponentially proliferating cell cultures were counted and seeded at appropriate densities for colony formation and treated with different concentrations of cisplatin or Nutlin-3/RG7388. The results showed *TP53* mutant cell lines were significantly more resistant to Nutlin-3/ RG7388, but also demonstrated a wide range of responses for the wild-type *TP53* cell lines (Figure 6-14 & Table 6-4). Nutlin-3 markedly decreased the clonogenic survival of A2780 cells (LC_{50}=1.65±0.7 (SEM) µM); however, IGROV-1 (LC_{50}=11±2.1 (SEM) µM) and OAW42 (LC_{50}=6.25±0.50 (SEM) µM) were substantially less sensitive to Nutlin-3 (Figure 6-14B).

RG7388 was much more potent than Nutlin-3, and decreased the clonogenic survival of all the wild-type *TP53* ovarian cancer cell lines. Consistent with the mechanism of action for MDM2 antagonists, RG7388 had little or no effect on mutant *TP53* cell lines in the 0-2 µM dose range (Figure 6-14C). Interestingly, although all three cell lines were sensitive to RG7388, the relative sensitivity of the wild-type *TP53* cell lines to Nutlin-3 and RG7388 was very different. The clonogenic cell survival responses to RG7388 for A2780 and OAW42 were similar, whereas for Nutlin-3 their relative responses were quite different, with only A2780 showing sensitivity to Nutlin-3. Overall, the clonogenic cell survival assays showed not only that mutant *TP53* genomic status was a major determinant of resistance to Nutlin-3 and RG7388, but also that the relative response of the wild-type *TP53* cell lines differed for the two MDM2 inhibitors in a way that was not explicable simply by the relative potency of the compounds in cell-free MDM2-p53 binding assays. Consistent with growth inhibition assays, MDM2 antagonists showed a clearer and more effective p53-dependent response compared to cisplatin.

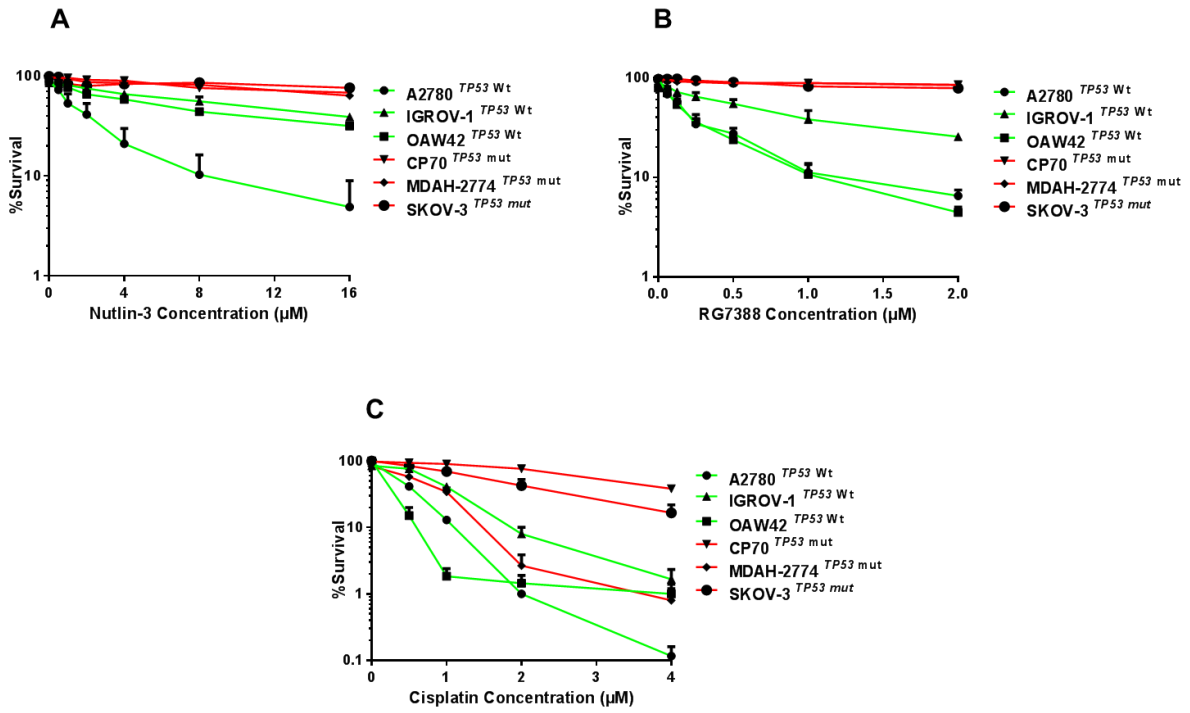

Figure 6-14: Clonogenic survival for the panel of ovarian cancer cell lines. Treatment with (A) Nutlin-3 (B) RG7388 and (C) Cisplatin. Clonogenic cell survival LC_{50} values were dependent on the *TP53* genomic status. Data are shown as the average of at least 3 independent experiments and error bars represent SEM.

Cell line	*TP53* Status	Cisplatin (μM)	Nutlin-3 (μM)	RG7388 (μM)
A2780	Wild-type	0.42 ± 0.0003	1.65 ± 0.71	0.14 ± 0.03
IGROV-1	Wild-type	0.82 ± 0.06	11 ± 2.08	0.67 ± 0.15
OAW42	Wild-type	0.28 ± 0.01	6.25 ± 0.50	0.15 ± 0.04
CP70	Mutant	3.39 ± 0.05	> 16	>2
MDAH-2774	Mutant	0.67 ± 0.08	> 16	>2
SKOV-3	Mutant	1.87 ± 0.42	> 16	>2

Table 6-4: LC_{50} concentrations for cisplatin, Nutlin-3 and RG7388 for the panel of ovarian cancer cell lines of varying *TP53* status. Data represent the mean of at least 3 independent experiments ± SEM.

6.5 Discussion

Ovarian cancer is the most lethal gynaecological malignancy and in most cases it is diagnosed at advanced stage with metastasis beyond the ovary, at which point treatment is not favourable (Bauerschlag *et al.*, 2010; Qinglei Zhan *et al.*, 2013). Advanced ovarian cancer treatment usually involves a combination of debulking surgery and platinum-based chemotherapy, alone or with addition of paclitaxel. Although chemotherapy prolongs survival, most patients with advanced disease die from treatment resistant progressive disease (Kim *et al.*, 2012; Ledermann *et al.*, 2013). Cancer therapy has recently been improving with the introduction of targeted therapies to achieve greater specificity and less cytotoxicity (Munagala *et al.*, 2011; Yuan *et al.*, 2011; Nicolas Andre *et al.*, 2012). Due to the crucial role of p53 in tumour suppression, it is an attractive target for cancer therapy. Different strategies have been developed to restore p53 function including inhibition of the MDM2-p53 interaction as a promising therapeutic target for cancer therapy (Wang and Sun, 2010; Hong B *et al.*, 2014).

This study evaluates for the first time the effect of the MDM2-p53 binding antagonist RG7112 and RG7388, as a single agent in a panel of ovarian cancer cell lines of defined *TP53* genomic status.

6.5.1 Ovarian cancer cell lines and response to MDM2-p53 antagonists, Nutlin-3/RG7122/RG7388

To evaluate the effect of Nutlin-3, RG7122 and RG7388 in *TP53* wild-type compared to mutant cell lines, growth inhibition assays were performed. Although there is uncertainly underlying the subtype classification of some commonly used ovarian cancer cell lines, (Domcke 2013) these results need to be discussed. Domcke *et al*. (2013) analysed a panel of 47 ovarian cancer cell lines to identify those that have highest genetic similarity to ovarian tumour according to the copy-number changing, mutations and mRNA expression profiles. They reported that A2780, SKOV-3 and IGROV-1 cell lines are poorly suited as models for HGSC because of having a flat copy-number profile, and A2780 and SKOV-3 have no *TP53* mutation. They reported IGROV-1 cell line as endometrioid or clear cell rather than HGSC origin. It is confusing because many published literatures including the original one reported A2780, SKOV-3 and IGROV-1 as undifferentiated, adenocarcinoma and a mixture of endometrioid and clear cell lines respectively rather than HGSC (Bénard *et al.*, 1985; Hills *et al.*, 1989; Pizao *et al.*, 1992; Anglesio *et al.*, 2013; Stordal *et al.*, 2013). Moreover, SKOV-3 was reported as an ovarian cancer cell line with mutant *TP53*, homozygous deletion (Sonego *et al.*, 2013;

Mullany *et al.*, 2015; Zanjirband *et al.*, 2016) rather than an ovarian cancer cell line with wild-type *TP53*.

Within the panel of ovarian cancer cell lines studied, wild-type *TP53* cell lines were significantly more sensitive to Nutlin-3, RG7112 and the more potent RG7388 compared to mutant *TP53* cell lines, which is consistent with their mechanism of action. Use of cell lines from different subtypes had no impact on the conclusion drawn about the influence of *TP53* status on the biological phenotypes studied. These results are consistent with limited previous studies demonstrating that wild-type*TP53* ovarian cancer cell lines are responsive to Nutlin-3 and extends observations to the second generation MDM2 inhibitor RG7388 currently in early phase clinical trials (Mir *et al.*, 2013; Erin K. Crane 2015).

6.5.2 Functional activation of the p53 pathway in response to MDM2-p53 antagonists, Nutlin-3/RG7388, in *TP53* wild-type ovarian cancer

Nutlin-3 and RG7388 treatment led to more p53 stabilization and induction of $p21^{WAF1}$ and MDM2 in the wild-type *TP53* ovarian cancer cell lines. There was no upregulation of p53 downstream target genes in *TP53* mutant ovarian cancer cell lines in response to Nutlin-3 and RG7388 treatment. Interestingly, despite the lack of downstream function, there was some evidence of mutant p53 stabilization in response to treatment with MDM2 inhibitors in the *TP53* mutant CP70 and *MLH1*-corrected CP70+ cell lines. This suggests some mutant forms of p53 still show evidence of degradation by MDM2 (Oren and Rotter, 2010) which is prevented by the MDM2 inhibitors. For the SKOV-3 cell line, no expression of p53 was observed due to a frame shift deletion at codon 89 (c.265delC, P.pro89fsX33) which results in production of an undetectable level of truncated protein. These results are in accord with two limited recent ovarian cancer cell line studies indicating that Nutlin-3a increased stabilisation and induction of $p21^{WAF1}$ in a wild-type *TP53*-dependent manner (Mir *et al.*, 2013; Erin K. Crane 2015).

6.5.3 Time course western blot analysis of the p53, $p21^{WAF1}$ and MDM2 expression in the wild-type *TP53* cell lines treated with cisplatin or Nutlin-3/RG7388

The results of this part of the study demonstrated earlier and stronger response of the p53 pathway to Nutlin-3/RG7388 treatment compared to cisplatin, indicating that MDM2-p53 antagonists act in a more specifically p53-dependent manner than cisplatin. These results also give some information on how to schedule the order of drugs in sequential combined treatment

to gain more p53 stabilisation and $p21^{WAF1}$ upregulation. Overall, it is expected that treatment with cisplatin followed with Nutlin-3/RG7388 four hours after cisplatin treatment might result in more synergistic effect.

6.5.4 Nutlin-3/RG7388 affects cell cycle arrest and/or apoptosis in wild-type *TP53* ovarian cancer cell lines

Nutlin-3 and RG7388 induced cell cycle arrest and/or apoptosis in wild-type *TP53* ovarian cancer cell lines in a cell-type dependent manner. When cells were treated with the GI_{50} isoeffect doses of RG7388 or Nutlin-3, RG7388 had a greater effect on the cell cycle distribution, with increased accumulation of cells in G0/G1. There is a consistency between Flow cytometry results and the growth inhibitory effect of Nutlin-3/RG7388. The GI_{50} values for RG7388 were lower than those for Nutlin-3 across all wild-type *TP53* cell lines which is supported by the higher proportion of G0/G1 phase arrest for the cells treated with RG3788 compared to Nutlin-3. These results are in agreement with those of Mir *et al*. (2013) who found G0/G1 cell cycle phase arrest in *TP53* wild-type ovarian cancer treated with Nutlin-3a , and Chen *et al*. (2015) who reported G0/G1 phase arrest in *TP53* wild-type neuroblastoma cell lines treated with RG7388.

To further investigate the effect of Nutlin-3/RG7388 on the induction of apoptosis, caspase 3/7 activity was analysed in wild–type *TP53* ovarian cancer cell lines. Significantly increased levels of caspase3/7 activity in IGROV-1 cells treated with Nutlin-3/RG7388 compared to DMSO control was in agreement with the increased proportion of SubG1 events in Nutlin-3/RG7388 treated IGROV-1 cells. Furthermore, the lack of a significant increase in caspase3/7 activity in A2780 and OAW42 cell lines following Nutlin-3/RG7388 treatment is consistent with no significant change in the percentage of SubG1 events in these cell lines after treatment. Overall, there was a consistent relationship between the detection of SubG1 events on Flow cytometry and caspase 3/7 activity; however, cell cycle arrest is not always accompanied by the induction of apoptosis (Weng *et al.*, 2001) as seen for OAW42 cells in this study. These results are in agreement with those obtained by Chen *et al*. (2015) that also indicated a consistency between increased SubG1 events and higher caspase 3/7 activity in neuroblastoma cell lines treated with RG7388.

6.5.5 Nutlin-3/RG7388 alone results in clonogenic cell death in a p53-dependent manner

The clonogenic cell survival assays also showed *TP53* mutant cell lines were much more resistant to Nutlin-3 & RG7388, but nevertheless also demonstrated a range of different relative single agent responses for the wild-type *TP53* cell lines. A possible explanation for this range of responses between the wild-type *TP53* cell lines might be differences in drug uptake (Chen *et al.*, 2014), deficiencies or variation in the expression of p53 target genes involved in apoptosis and other mechanisms of cell death, including the pro-apoptotic proteins BAX and PUMA and anti-apoptotic proteins BCL-2 and MCL-1 (Haupt *et al.*, 2003; Jeffers *et al.*, 2003).

6.5.6 Conclusion and further work

In conclusion, the present study demonstrates that MDM2-p53 antagonists are potent anti-cancer compounds *in vitro* leading to cell cycle arrest and/or apoptosis of wild-type *TP53* ovarian cancer cell lines as a single agent. The findings show that following exposure to MDM2-p53 antagonists, different outcomes are obtained due to various downstream alterations of the p53 pathway. They clearly indicate that the presence of wild-type *TP53* remains the main predictive biomarker of response to MDM2 inhibitors; however, more research is needed to identify other genes and signalling pathways involved as determinants of response to MDM2-p53 antagonists in wild-type *TP53* tumour cells.

Using MDM2-p53 antagonists as single-agent therapy has been suggested to be potentially limited due to acquisition of resistance through continuous exposure to MDM2 inhibitors followed by *de novo* mutations (Wei *et al.*, 2013; Khoo *et al.*, 2014). It is therefore logical to consider using MDM2 antagonists in combination with established therapeutic agents to improve treatment, with the possibility of dose reduction and less normal tissue cytotoxicity and genotoxicity. In the context of ovarian cancer it is of interest to investigate the combination of cisplatin and MDM2 inhibitors, particularly as individually these agents have different dose limiting toxicities.

Chapter 7: An investigation of the effect of MDM2-p53 antagonists in combined treatment with cisplatin on ovarian cancer cell lines

7.1 Introduction

Targeted therapies in ovarian cancer have been investigated to overcome relapse and chemoresistance, which is the main challenge for treatment. Different strategies have been developed to reactivate p53 in tumours with dysfunctional p53 including inhibition of the p53-MDM2 interaction. However, some concerns have been expressed that resistance to MDM2-p53 antagonists may be acquired following repeated treatment with MDM2 inhibitors (Bo *et al.*, 2014). For this reason, targeting more than one signalling pathway by combination therapy may be a useful approach and is a widely accepted concept in cancer therapy. This study evaluates for the first time the effect of the MDM2-p53 binding antagonist RG7388 in combination with cisplatin in a panel of wild-type *TP53* ovarian cancer cell lines and compares this to the combination of Nutlin-3 with cisplatin in the same cell line panel.

7.1.1 Combination therapy

Combination treatment is an approach to improve therapeutic effect, reduce dose and toxicity, and minimise and/or delay drug resistance. This is because multiple drugs may affect various targets and/or subpopulations. Also, one single target may be targeted with different drugs with varied mechanisms of action (Chou, 2006; Chou, 2010). Induction of cell cycle arrest and apoptosis following treatment with many types of chemotherapeutic drugs occur through activation of the p53 pathway. Therefore, reactivation of the p53 pathway may supplement and increase the sensitivity of tumours to a range of conventional chemotherapeutic agents (Almazov *et al.*, 2007; Wang and Sun, 2010; Bo *et al.*, 2014). This part of the study was designed to investigate the combined effect of Nutlin-3/RG7388 with cisplatin on a panel of wild-type *TP53* established ovarian cancer cell lines to identify potential improvements in the efficacy of therapy for ovarian cancer patients.

7.2 Hypothesis and Objectives

Hypothesis:

1. The combination of MDM2-p53 antagonists with cisplatin has synergistic potential for the treatment of ovarian cancer.
2. The MDM2-p53 antagonists decrease the expression of DNA repair genes implicated in response to cisplatin and capacity for repair of cisplatin induced DNA damage leading to a synergistic effect in combined treatment with Nutlin-3/RG7388 and cisplatin.

Objectives:

1. To investigate the effect of combined treatment of Nutlin-3/RG7388 with cisplatin on a panel of wild-type *TP53* ovarian cancer cell lines and determine the synergistic, additive or antagonistic effect of combination.
2. To investigate possible induced changes in the mRNA expression levels of p53-regulated genes involved in growth arrest, apoptosis and DNA repair in response to cisplatin following exposure to Nutlin-3/RG7388 as a single agent.

7.3 Specific Materials and Methods

7.3.1 Cell lines

Three wild-type *TP53* ovarian carcinoma cell lines, A2780, IGROV-1 and OAW42 were used in this study. More details of these cell lines are provided in chapter 2.3.1 and 2.3.2.

7.3.2 Combined treatment of Nutlin-3/RG7388 with cisplatin, SRB assay

For combination treatment of Nutlin-3 or RG7388 with cisplatin, the wild-type *TP53* cell lines were treated for 72 hours with each agent alone and in combination simultaneously at constant 1:1 ratios of 0.25x, 0.5x, 1x, 2x, and 4x their respective GI_{50} concentrations. Median-effect analysis was used to calculate Combination Index (CI) and Dose Reduction Index (DRI) values (Chou, 2006) using CalcuSyn software v2 (Biosoft, Cambridge, UK).

7.3.3 Western blot

2×10^5 cells were seeded per 35mm well of a 6-well plate for western blot analysis and left for 48 hours to adhere and grow. To investigate the effect of combined treatment of Nutlin-3/RG7388 with cisplatin on the functional p53 pathway, cells were treated with each agent alone and in simultaneous combination at constant 1:1 ratios of 1x and 2x their respective GI_{50} concentrations. Lysates were extracted following 4 hours treatment. The antibodies used and their details are found in chapter 2.11.7.

7.3.4 Flow cytometry

Flow cytometry was performed to analyse cell cycle distribution changes and induced apoptosis over 24, 48 and 72 hours after treatment as described in chapter 2.14.3 and 6.3.5. The A2780 and IGROV-1 cell lines were seeded at 1.7×10^5 cells/well in 6-well plates and the OAW42 cell line at 1.3×10^5 per small flask, T25. Cells were treated with cisplatin, Nutlin-3, and RG7388 alone and with a combination of Nutlin-3 or RG7388 with cisplatin simultaneously at constant 1:1 ratios of 1x and 2x (A2780 and IGROV-1) or 0.5x and 1x (OAW42) their respective GI_{50} concentrations for 24, 48 and 72 hours. The samples were analysed as described in chapter 6.3.5.

7.3.5 Combined treatment of Nutlin-3/RG7388 with cisplatin, clonogenic cell survival assay

To study the effect of combined treatment on clonogenic cell survival, cells were treated with Nutlin-3, RG7388 and cisplatin alone and in combination at constant 1:1 ratios of 0.25x, 0.5x, 1x, 2x and 4x or 0.25x, 0.5x and 1x their respective LC_{50} concentrations, depending on the cell line and its single agent LC_{50} values, for 48 hours. More details are described in chapter 2.9. DRI and CI values were calculated using CalcuSyn software v2 (Biosoft, Cambridge, UK). (Chou, 2006).

7.3.6 Caspase 3/7 activity assay

The Caspase-Glo® Assay (Promega, Southampton, UK) was used to measure the caspase-3 and -7 activities in the cultures of cells. The A2780 and IGROV-1 cell lines were seeded at 4.5 x 10^4 cells/well and OAW42 cell line at 3 x 10^4 cells/well in white-welled 96-well plates for 24 hours. Then, cells were treated with Nutlin-3, RG7388 and cisplatin alone and in combination at constant 1:1 ratios of 1x and 2x their respective GI_{50} concentrations for 24 and 48 hours. The caspase 3/7 activity assay was performed as described in chapter 6.3.7.

7.3.7 Quantitative Reverse-Transcription Polymerase Chain Reaction (qRT-PCR)

Total RNA was extracted using an RNeasy Mini Kit (Qiagen, Germany). RNA purity and concentration were estimated with an ND-1000 spectrophotometer (NanoDrop Technologies, Thermo Scientific, UK). The purity of RNA was determined by the ratio of 260nm:280nm, which is around 2 for pure RNA. Total messenger RNA was converted to cDNA using the Promega Reverse Transcription System (A3500, Promega) as described in chapter 2.12.2. More details of validated primers used and qRT-PCR protocol are provided in chapter 2.13.4 and 2.13.5.

7.3.8 Statistical analysis

The statistical paired t-test was used to compare the mean of 3 or more paired biological repeats and the p-values <0.05 were considered statistically significant.

7.4 Results

7.4.1 Nutlin-3/RG7388 synergise with cisplatin for growth inhibition of wild-type *TP53* ovarian cancer cell lines

The effect of Nutlin-3/RG7388 in combination with cisplatin was investigated for 3 wild-type *TP53* ovarian cancer cell lines using median-effect analysis. The sensitivity of these *TP53* wild-type cell lines to growth inhibition during 72 hours exposure to Nutlin-3, RG7388 and cisplatin was determined as single agents, and in combination at 5 equipotent concentrations between 0.25× and 4× their respective GI_{50} concentrations. The effect of combined treatment was cell type and compound dependent. Combination of Nutlin-3/RG7388 with cisplatin at all concentrations led to greater growth inhibition compared to either agent alone for the A2780 cell line. From the data in Figure 7-1, it is apparent that combination treatment of Nutlin-3 with cisplatin at concentrations lower than the individual 1x GI_{50} dose resulted in more growth arrest compared to higher than 1x GI_{50} dose. Combination treatment of OAW42 and IGROV-1 cell lines also produced more growth arrest at concentrations equal to or lower than the individual 1x GI_{50} dose (Figure 7-1 & Figure 7-2).

To determine whether the observed differences in growth inhibition were additive or synergistic, the data were analysed using median-effect analysis and CI and DRI values calculated. CI values for each constant ratio combination and at effect levels of ED_{50}, ED_{75} and ED_{90} were computed. Also, the average of CI values at ED_{50}, ED_{75} and ED_{90} was determined (Figure 7-3 & Table 7-1). Across all cell lines, the effect of combination treatment of Nutlin-3/RG7388 with cisplatin ranged from additive to synergistic based on the CI at ED_{50}. Although the effect of combined treatment based on overall CI was synergism for A2780, it was antagonism for IGROV-1 and OAW42 (Table 7-1 & Figure 7-3). The data analysis showed there was a favourable DRI, which demonstrates how many-fold the dose of each drug in a combination treatment may be reduced to achieve a given effect level compared with the doses of each drug alone. Both Nutlin-3, and RG7388 had favourable DRI values for combined treatment with cisplatin, with most experimental values ranging from 1.1-fold to 6.9-fold dose reduction (Table 7-2). These DRI values have clinical implications, demonstrating a significant individual drug dose reduction may be achieved for a given combination therapeutic effect, compared with the dose of either drug alone as a single agent to obtain the same therapeutic effect.

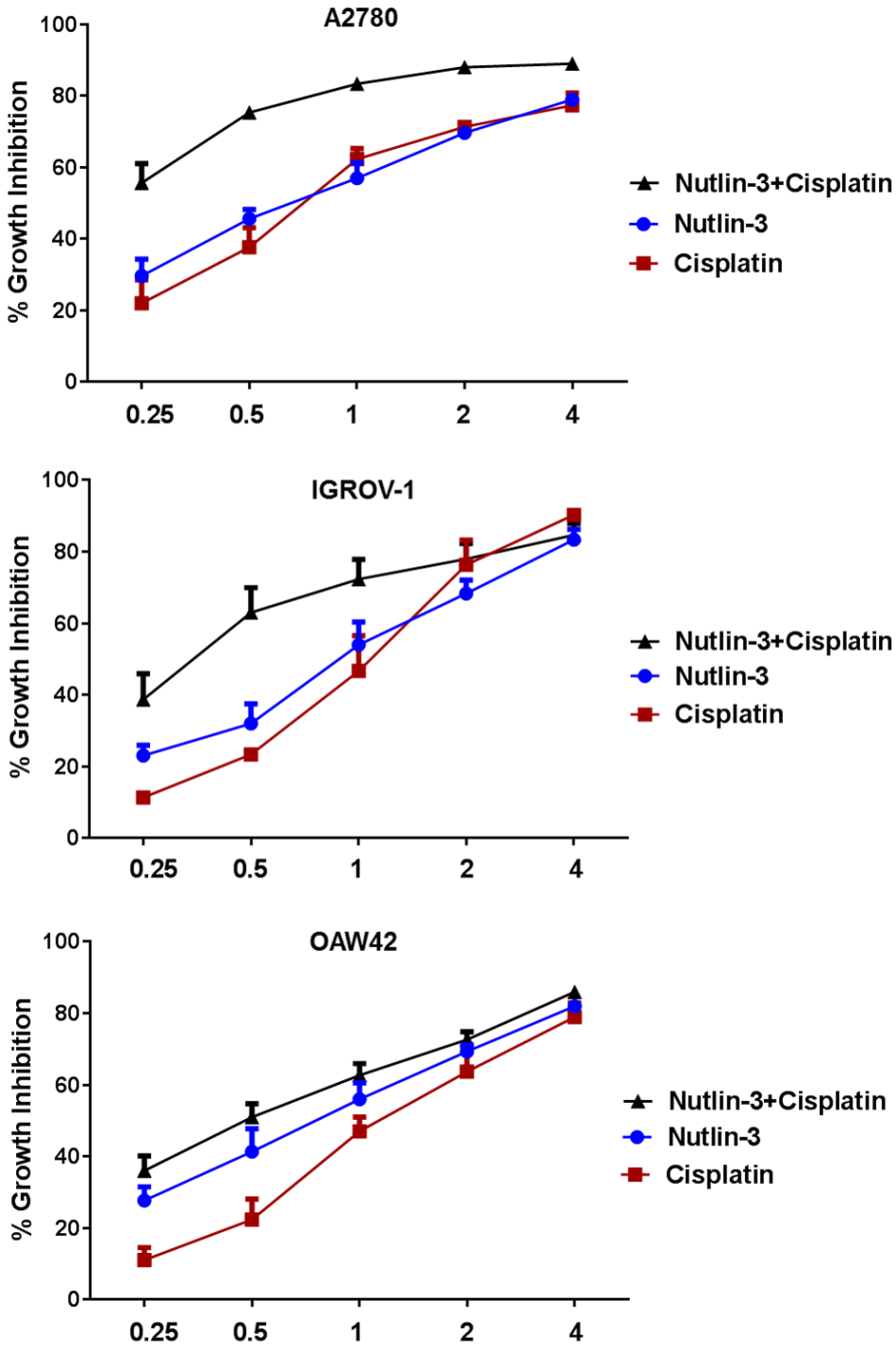

Figure 7-1: Growth inhibition curves of three wild-type *TP53* cell lines exposed to Nutlin-3 and cisplatin alone, and in combination at constant 1:1 ratios of 0.25x, 0.5x, 1x, 2x and 4x their respective GI_{50} concentrations for 72 hours. Data are shown as the average of at least 3 independent experiments and error bars represent SEM.

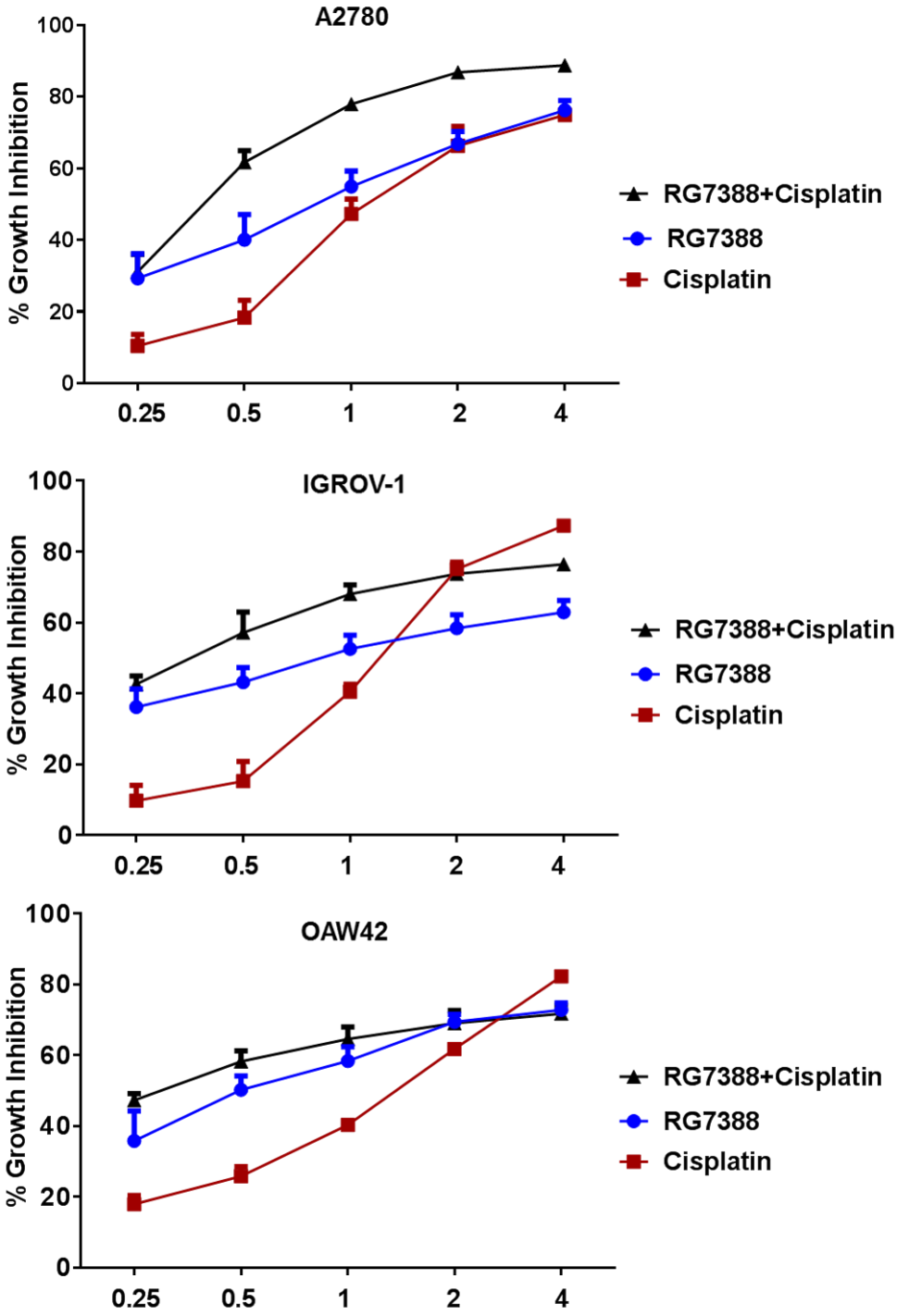

Figure 7-2: Growth inhibition curves of three wild-type *TP53* cell lines exposed to RG7388 and cisplatin alone, and in combination at constant 1:1 ratios of 0.25x, 0.5x, 1x, 2x and 4x their respective GI_{50} concentrations for 72 hours. Data are shown as the average of at least 3 independent experiments and error bars represent SEM.

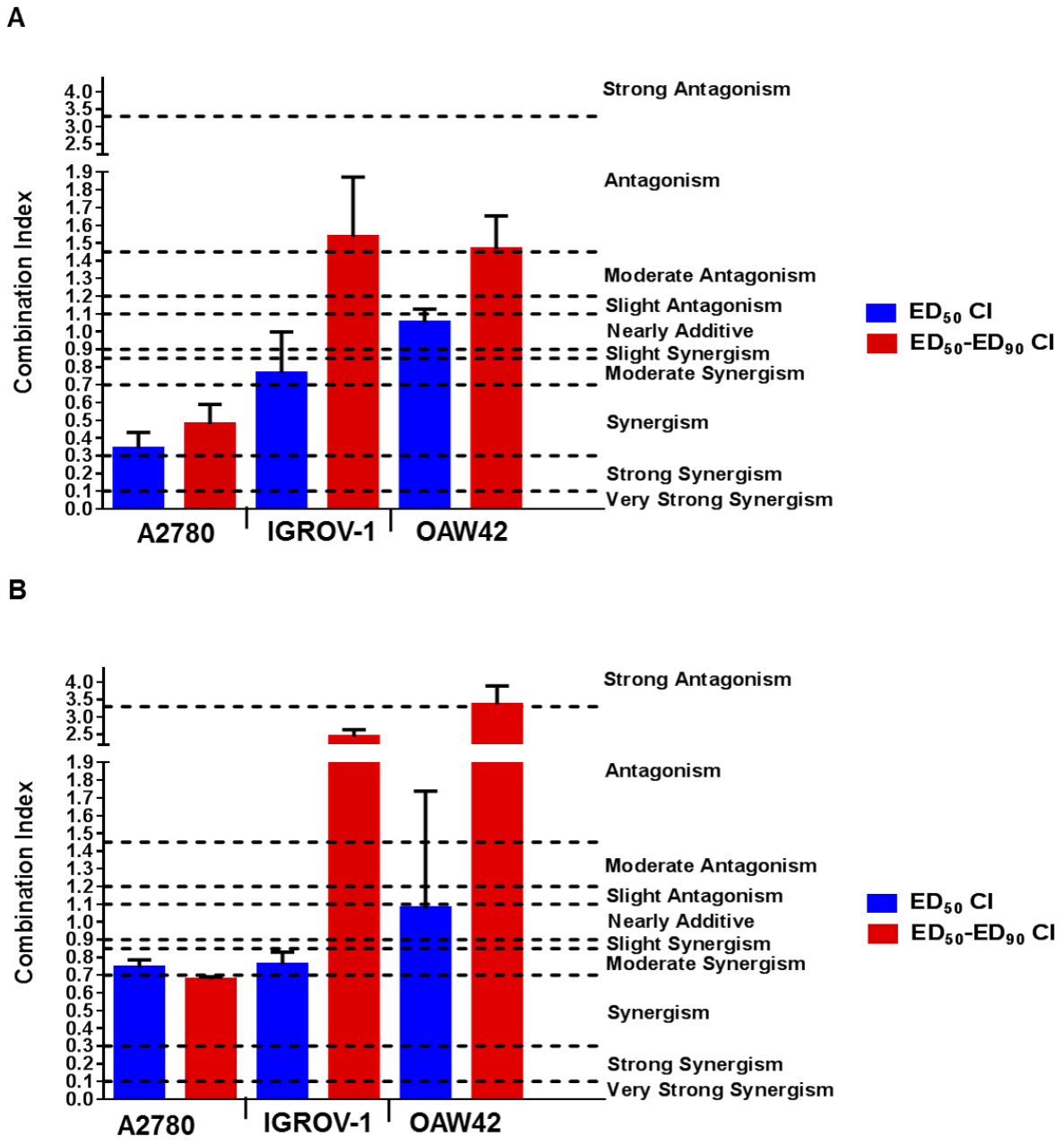

Figure 7-3: The growth inhibition combination index (CI) values for Nutlin-3/RG7388 in combination with cisplatin at ED_{50} and the average of CI values at effect levels ED_{50}, ED_{75} and ED_{90} in three wild-type *TP53* ovarian cancer cell lines. (A) CI values for Nutlin-3 in combination with cisplatin. (B) CI values for RG7388 in combination with cisplatin. Data are shown as the average of at least 3 independent experiments and error bars represent SEM. CI, Combination Index; ED, Effective dose.

Cell Line	Combination	CI					CI ED_{50}	CI ED_{75}	CI ED_{90}	CI Average ED_{50-90}
		XGI_{50}								
		0.25	0.5	1	2	4				
A2780	Nutlin-3+Cisplatin	**0.5**	**0.4**	**0.4**	**0.6**	1.0	**0.3**	**0.5**	**0.8**	**0.5**
	RG7388+Cisplatin	1.2	**0.5**	**0.5**	**0.5**	**0.9**	**0.7**	**0.7**	**0.6**	**0.7**
IGROV-1	Nutlin-3+Cisplatin	**0.8**	**0.7**	1.0	1.6	2.2	**0.8**	1.4	2.5	1.5
	RG7388+Cisplatin	**0.8**	**0.8**	**0.7**	1.1	1.9	**0.8**	1.5	5.1	2.4
OAW42	Nutlin-3+Cisplatin	1.0	1.1	1.3	1.7	1.5	1.1	1.4	1.9	1.5
	RG7388+Cisplatin	1.3	1.2	1.5	2.1	3.1	1.1	3.5	5.6	3.4

243

Table 7-1: Growth inhibition CI values for Nutlin-3/RG7388 in combination with cisplatin for the wild-type *TP53* ovarian cancer cell lines. The combined treatment was performed at the indicated fixed 1:1 ratios relative to their respective GI_{50} concentrations. CI values were calculated for each constant ratio combination and at effect levels ED_{50}, ED_{75} and ED_{90} from the average of at least three independent experiments. CI Ave ED_{50-90} represents the average of CI values at effect levels of ED_{50}, ED_{75} and ED_{90}. CI range: < 0.1 very strong synergism; 0.1-0.3 strong synergism; 0.3-0.7 synergism; 0.7-0.85 moderate synergism; 0.85-0.9 slight synergism; 0.9-1.1 nearly additive; 1.1-1.2 slight antagonism; 1.2-1.45 moderate antagonism; 1.45-3.3 antagonism; 3.3-10 strong antagonism; > 10 very strong antagonism. Synergistic combinations are highlighted in bold font. CI, Combination Index; ED, Effective dose.

Cell Line	Combination	Compound	DRI				
			XGI_{50}				
			0.25	0.5	1	2	4
A2780	Nutlin-3+Cisplatin	Nutlin-3	**2.6**	**5.7**	**5.5**	**4.3**	**2.6**
		Cisplatin	**4.3**	**6.9**	**6.4**	**5.2**	**3.2**
	RG7388+Cisplatin	RG7388	**1.2**	**3.3**	**4.3**	**5.0**	**3.2**
		Cisplatin	**3.3**	**4.53**	**3.7**	**3.0**	**1.7**
IGROV-1	Nutlin-3+Cisplatin	Nutlin-3	**2.3**	**3.2**	**2.5**	**1.6**	**1.2**
		Cisplatin	**2.9**	**2.8**	**1.8**	**1.1**	0.7
	RG7388+Cisplatin	RG7388	**1.8**	**2.5**	**5.5**	**6.2**	**4.5**
		Cisplatin	**3.6**	**2.43**	**1.8**	**1.1**	**0.6**
OAW42	Nutlin-3+Cisplatin	Nutlin-3	**1.5**	**1.6**	**1.4**	**1.1**	**1.5**
		Cisplatin	**3.6**	**2.9**	**2.0**	**1.4**	**1.3**
	RG7388+Cisplatin	RG7388	**2.2**	**2.1**	**1.6**	**1.1**	0.72
		Cisplatin	**4.5**	**3.2**	**2.0**	**1.2**	0.7

Table 7-2: DRI values for growth inhibition by RG7388/Nutlin-3 in combination with cisplatin for the wild-type *TP53* ovarian cancer cell lines. The combined treatment was performed at the indicated fixed 1:1 ratios relative to their respective GI_{50} concentrations. DRI values were calculated for each constant ratio combination from the average of at least three independent experiments. Favourable DRI values are highlighted in bold font. DRI, Dose reduction index.

7.4.2 The effect of combination treatment with Nutlin-3/RG7388 and cisplatin on activation of the p53 pathway

Further analysis was performed to investigate the effect of combination treatment on the p53 molecular pathway using western blotting. Wild-type *TP53* cell lines were treated with Nutlin-3/RG7388 and cisplatin alone, and in combination at constant 1:1 ratios of 1x and 2x their respective GI_{50} concentrations for 4 hours. Western analysis showed that treatment with Nutlin-3/RG7388 and cisplatin as a single agent and in combination with cisplatin induced p53 stabilization and upregulation of $p21^{WAF1}$ and MDM2, confirming functional activation of wild-type *TP53* (Figure 7-4). Moreover, combination treatment in all cases led to greater levels of p53 stabilization, $p21^{WAF1}$ and MDM2 upregulation compared to cisplatin on its own, and in most cases these were greater than those induced or upregulated by Nutlin-3/RG7388 alone. Higher expression of $p21^{WAF1}$ for combined treatment was associated with a greater synergistic effect for growth inhibition. However, Nutlin-3 and RG7388 led to little change of BAX expression compared to DMSO control, and their combination with cisplatin showed only a small increase in the expression of BAX compared to cisplatin on its own. Interestingly, cisplatin alone at a GI_{50} or 2x GI_{50} dose showed much less p53 pathway induction than Nutlin-3 or RG7388 alone.

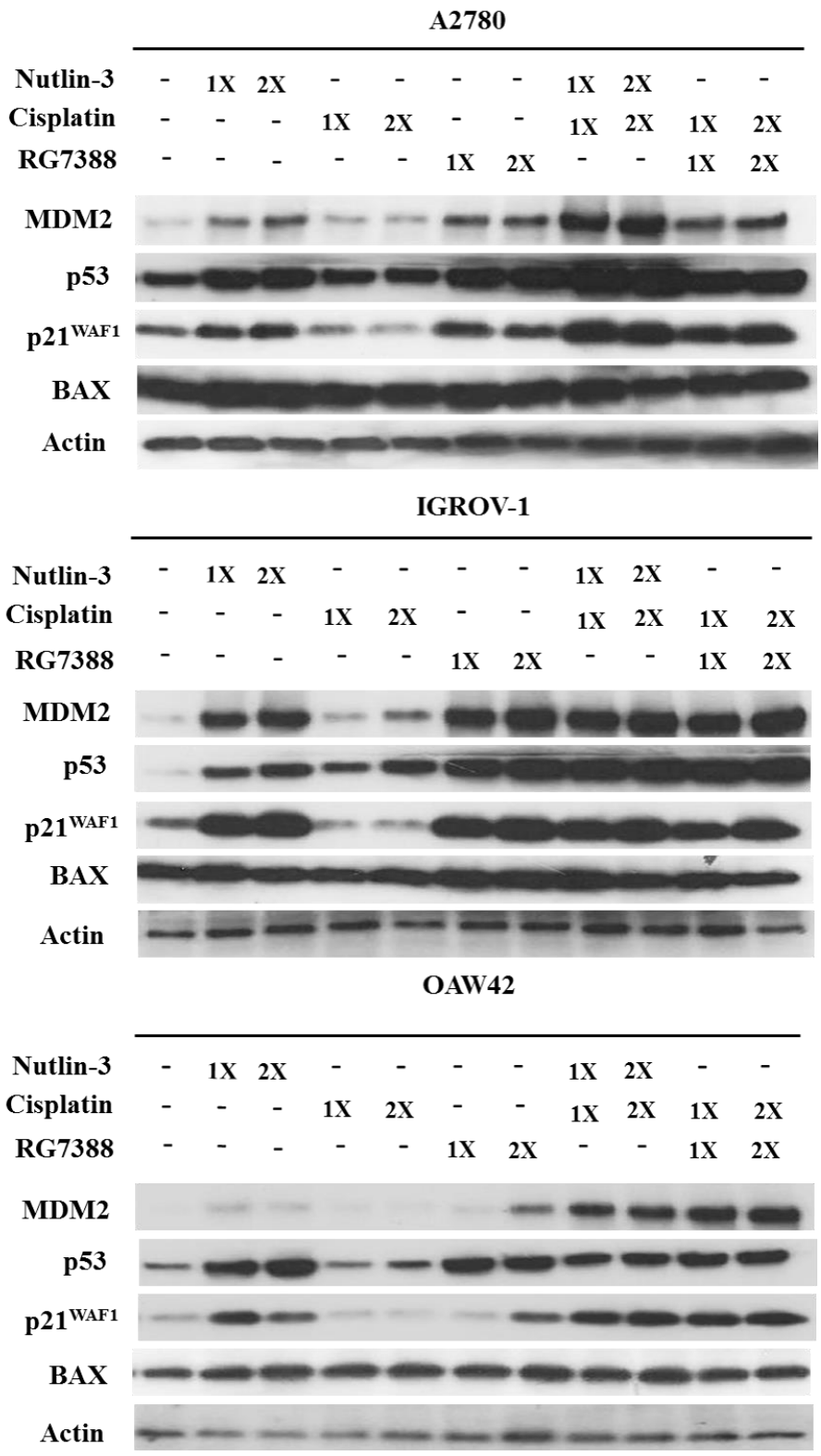

Figure 7-4: Combination of Nutlin-3/RG7388 with cisplatin increased stabilization of p53 and upregulation of its downstream targets, MDM2 and $p21^{WAF1}$ compared to cisplatin on its own. Total levels of p53, $p21^{WAF1}$, MDM2 (4 hours) and BAX (8 hours) after the commencement of treatment with Nutlin-3 and RG7388 alone, and in combination with cisplatin at constant 1:1 ratios of 1x and 2x their respective GI_{50} concentrations analysed by western blot in three wild-type *TP53* ovarian cancer cell lines.

7.4.3 Nutlin-3/RG7388 in combination with cisplatin induces cell cycle distribution changes and/or apoptosis in wild-type *TP53* ovarian cancer cell lines

Wild-type *TP53* cell lines were treated with Nutlin-3/RG7388 and cisplatin, alone and in simultaneous combination at constant 1:1 ratios of 1x and 2x (1/2 x & 1x for OAW42) their respective GI_{50} concentrations for 24, 48 and 72 hours. They were then analysed by flow cytometry for cell cycle phase distribution changes and evidence of apoptosis in response to treatment.

7.4.3.1 The effect of Nutlin-3 in combination with cisplatin on cell cycle distribution and SubG1 events in wild-type *TP53* ovarian cancer cell lines

Nutlin-3 only showed a modest increase in the proportion of cells in G0/G1 phase in a dose and time-dependent manner (Figure 7-5A, Figure 7-6A & Figure 7-7A). Nutlin-3 also increased the percentage of SubG1 events, a surrogate marker of apoptosis, in A2780 and IGROV-1 cell lines in a treatment time and dose-dependent manner (Figure 7-5B & Figure 7-6B). For A2780 and IGROV-1 cells, combination treatment of Nutlin-3 with cisplatin led to a dose and time-dependent increase in the proportion of cells in G2/M phase and the proportion of SubG1 events compared to cisplatin on its own, particularly for A2780 cells (Figure 7-5 & Figure 7-6). Interestingly, combination of Nutlin-3 with cisplatin at 1x GI_{50} concentrations led to a significantly increase in G2/M cell cycle arrest compared to cisplatin on its own at both 1x and 2x GI_{50} concentrations after 48 and 72 hours for A2780 and IGROV-1 cell lines. In terms of OAW42 cell line, combined treatment of Nutlin-3 with cisplatin resulted in a decrease in cells in G2/M phase compared to cisplatin on its own (Figure 7-7A). Furthermore, combined treatments decreased the proportion of SubG1 events compared to cisplatin on its own demonstrating the protective effect of Nutlin-3 against cisplatin in OAW42 cell line (Figure 7-7B).

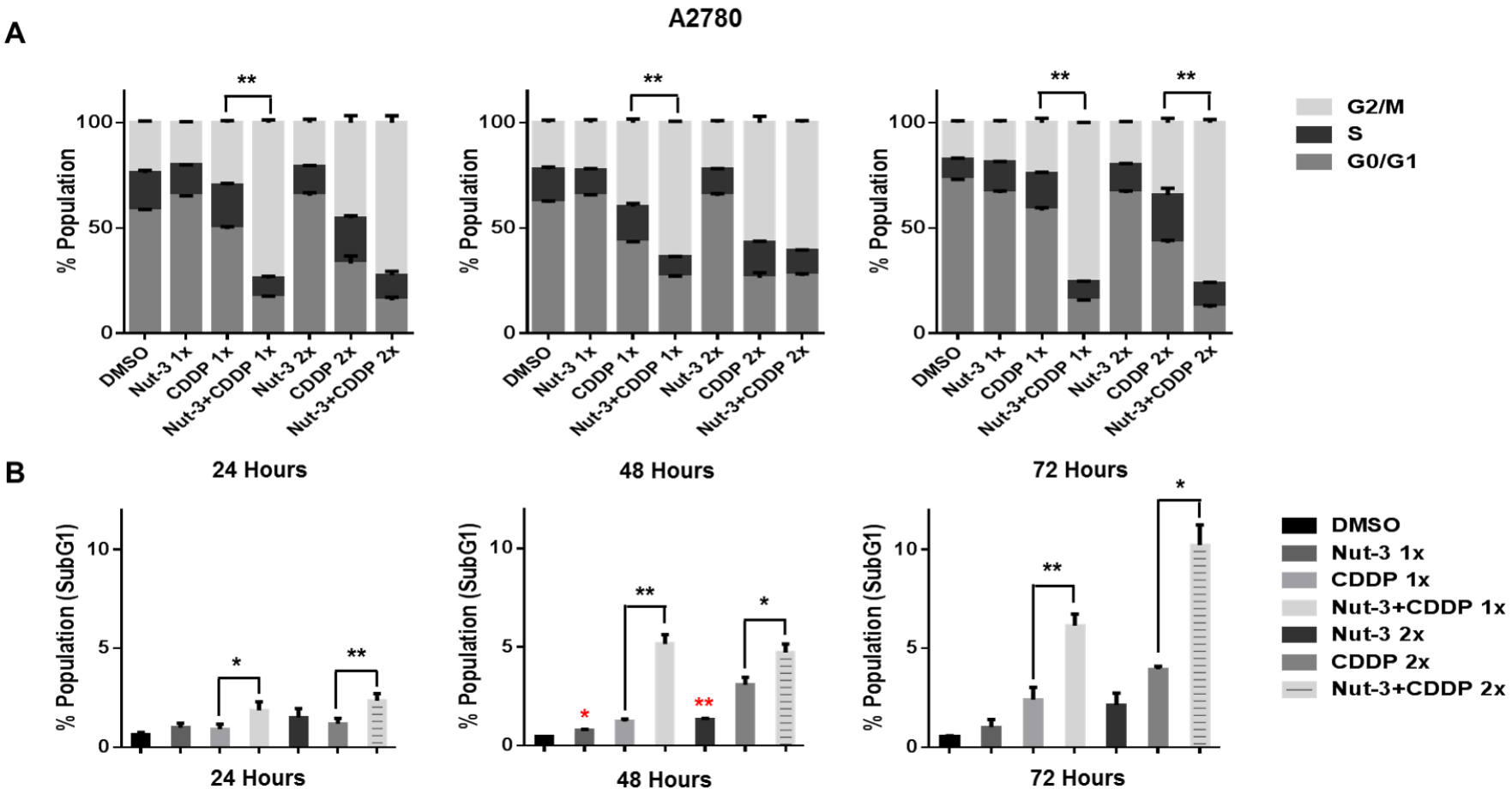

Figure 7-5: Combination of Nutlin-3 with cisplatin affects the cell cycle distribution and apoptotic endpoints. A2780 cell line was treated for 24, 48 and 72 hours with Nutlin-3 or cisplatin alone and at constant 1:1 ratios of 1x and 2x their respective GI_{50} concentrations. Combination of Nutlin-3 with cisplatin led to an increased proportion of cells in G2/M phase (A) and SubG1 events (B) compared to either agent alone in a time and concentration-dependent manner. Nut-3, Nutlin-3; CDDP, Cisplatin; *, *p<0.05*; **, *p<0.01*. The red stars represent significant increase in SubG1 events compared to DMSO control. Data are shown as the average of at least 3 independent experiments and error bars represent SEM.

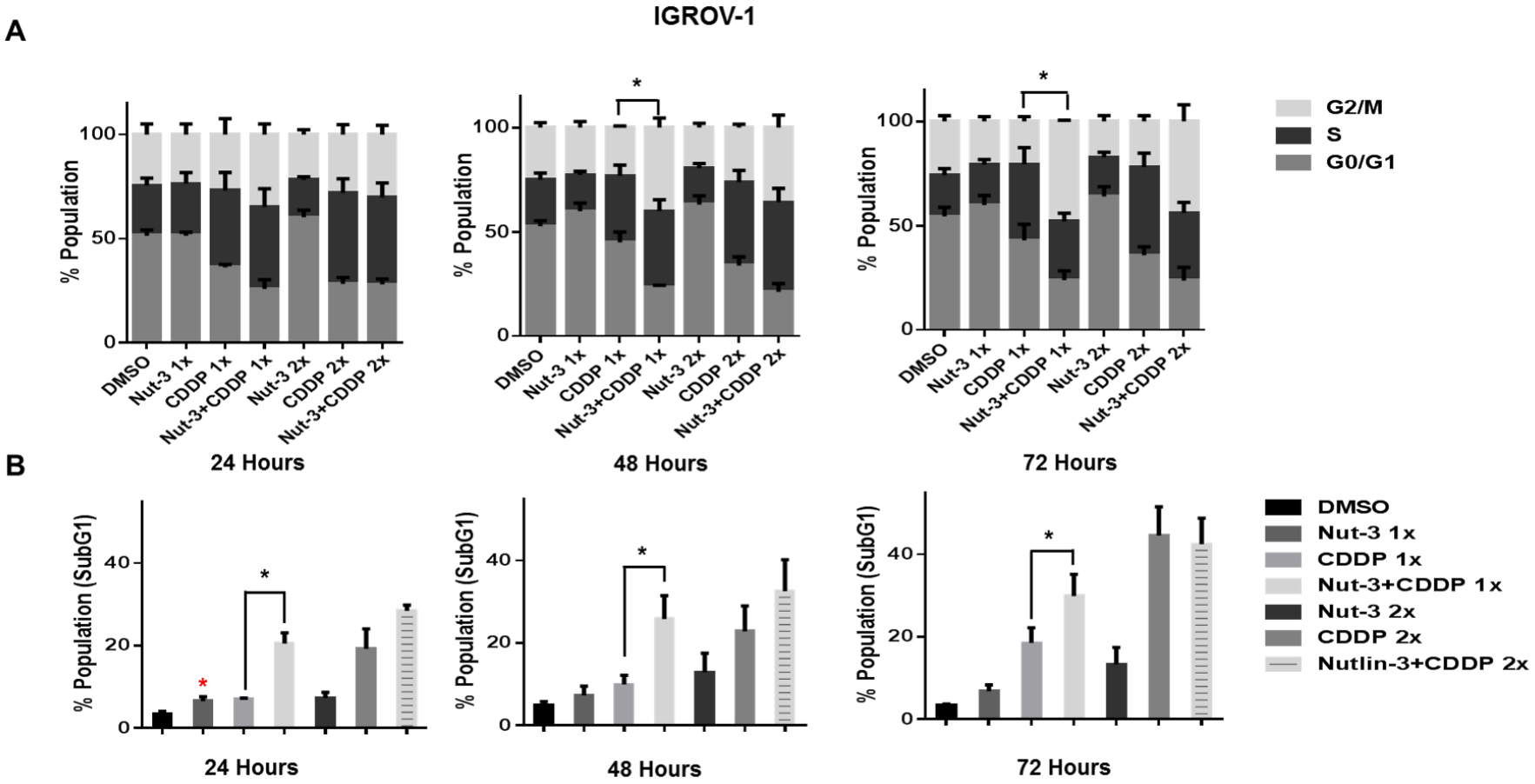

Figure 7-6: Combination of Nutlin-3 with cisplatin affects the cell cycle distribution and apoptotic endpoints. IGROV-1 cell line was treated for 24, 48 and 72 hours with Nutlin-3 or cisplatin alone and at constant 1:1 ratios of 1x and 2x their respective GI_{50} concentrations. Combination of Nutlin-3 with cisplatin led to an increased proportion of cells in G2/M phase (A) and SubG1 events, with the exception of SubG1 events after 72 hours at 2x GI_{50} concentration (B) compared to either agent alone in a time and concentration-dependent manner. Nut-3, Nutlin-3; CDDP, Cisplatin; *, *$p<0.05$*. The red stars represent significant increase in SubG1 events compared to DMSO control. Data are shown as the average of at least 3 independent experiments and error bars represent SEM.

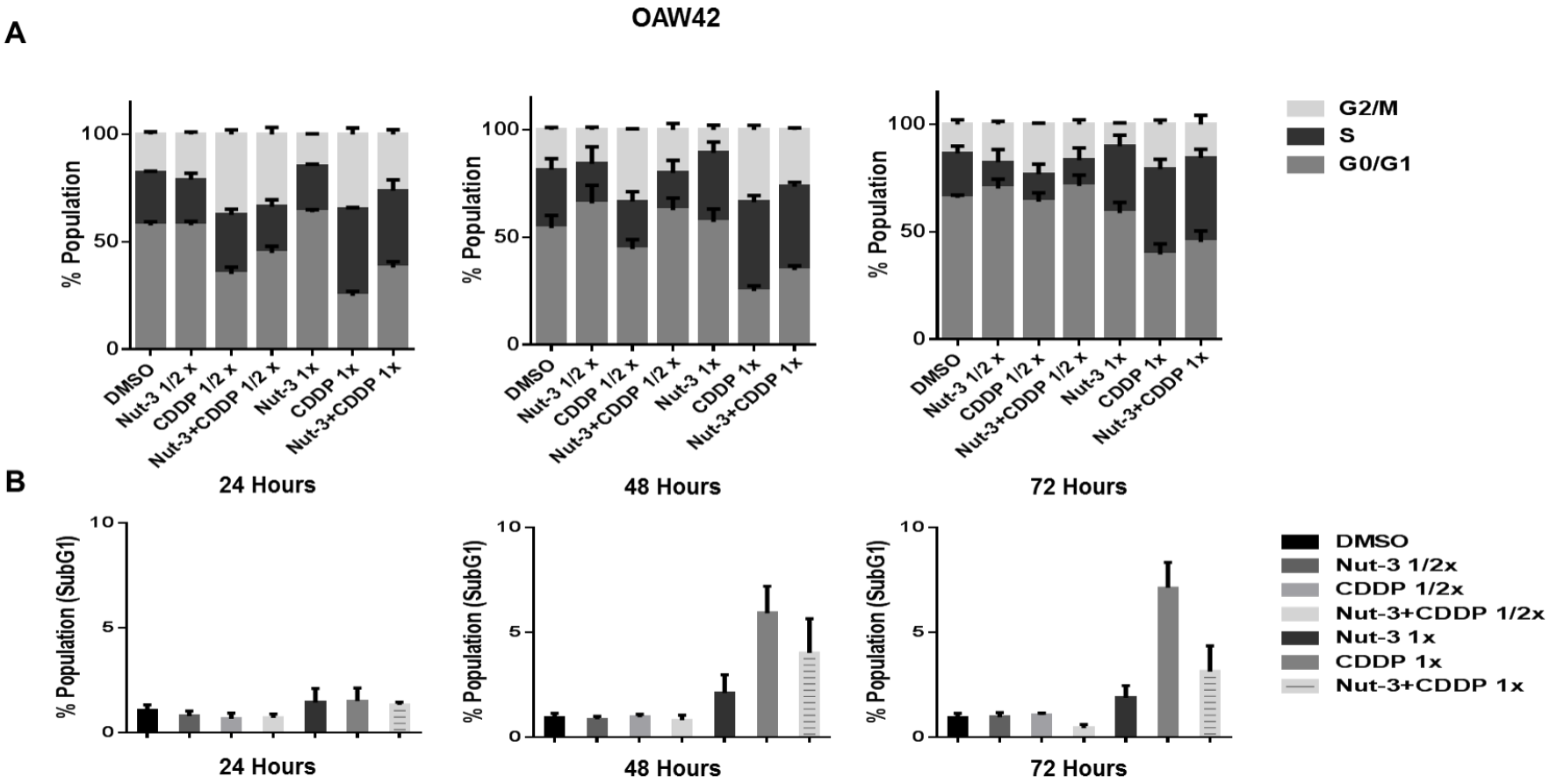

Figure 7-7: Combination of Nutlin-3 with cisplatin affects the cell cycle distribution and apoptotic endpoints. OAW42 cell line was treated for 24, 48 and 72 hours with Nutlin-3 or cisplatin alone and at constant 1:1 ratios of 1/2x and 1x their respective GI_{50} concentrations. Combination of Nutlin-3 with cisplatin led to a decreased proportion of cells in G2/M phase (A) and SubG1 events (B) compared to cisplatin alone. Nut-3, Nutlin-3; CDDP, Cisplatin. Data are shown as the average of at least 3 independent experiments and error bars represent SEM.

7.4.3.2 The effect of RG7388 in combination with cisplatin on cell cycle distribution and SubG1 events in wild-type *TP53* ovarian cancer cell lines

RG7388 alone after 24 hours treatment led to a higher increase in the proportion of cells in the G0/G1 phase of the cell cycle across all cell lines compared to Nutlin-3 at the same GI_{50} doses (Figure 7-8A, Figure 7-9A & Figure 7-10A). RG7388 induced SubG1 events in all cell lines in a concentration and time-dependent manner (Figure 7-8B, Figure 7-9B & Figure 7-10B). The IGROV-1 cell line showed a higher basal level of SubG1 events on Flow cytometry compared to the other cell lines, which was further increased by MDM2 inhibitor or cisplatin treatment.

In terms of the proportional distribution of cells in G0/G1 or G2/M, the effect of RG7388 combination with cisplatin was time dependent. Combined treatment for 24 hours led to proportionally more cells in the G0/G1 cell cycle phase compared to the effect of cisplatin on its own and a higher proportion of cells in the G2/M phase compared to the effect of RG7388 alone across all 3 cell lines. After 48 and 72 hours treatment, the combination of RG7388 with cisplatin led to a greater proportional increase in G2/M phase compared to either agent alone for A2780 and IGROV-1, whereas for OAW42 there was a reduction in the proportion of cells in G2/M phase (Figure 7-8A, Figure 7-9A & Figure 7-10A). Combined treatment of RG7388 with cisplatin resulted in increased SubG1 events in A2780 and IGROV-1 cells compared to cisplatin on its own, which was treatment time and dose-dependent (Figure 7-8B & Figure 7-9B). Interestingly, combined treatment of RG7388 with cisplatin at 1x GI_{50} significantly increased SubG1 events compared to cisplatin on its own even at 2x GI_{50} concentration in A2780 (after 48 hours) and IGROV-1 (after 24 hours). In contrast, combination treatments resulted in decreased SubG1 events after 48 and 72 hours post-treatment for OAW42 compared to cisplatin on its own, demonstrating a protective effect of RG7388 against cisplatin (Figure 7-10B).

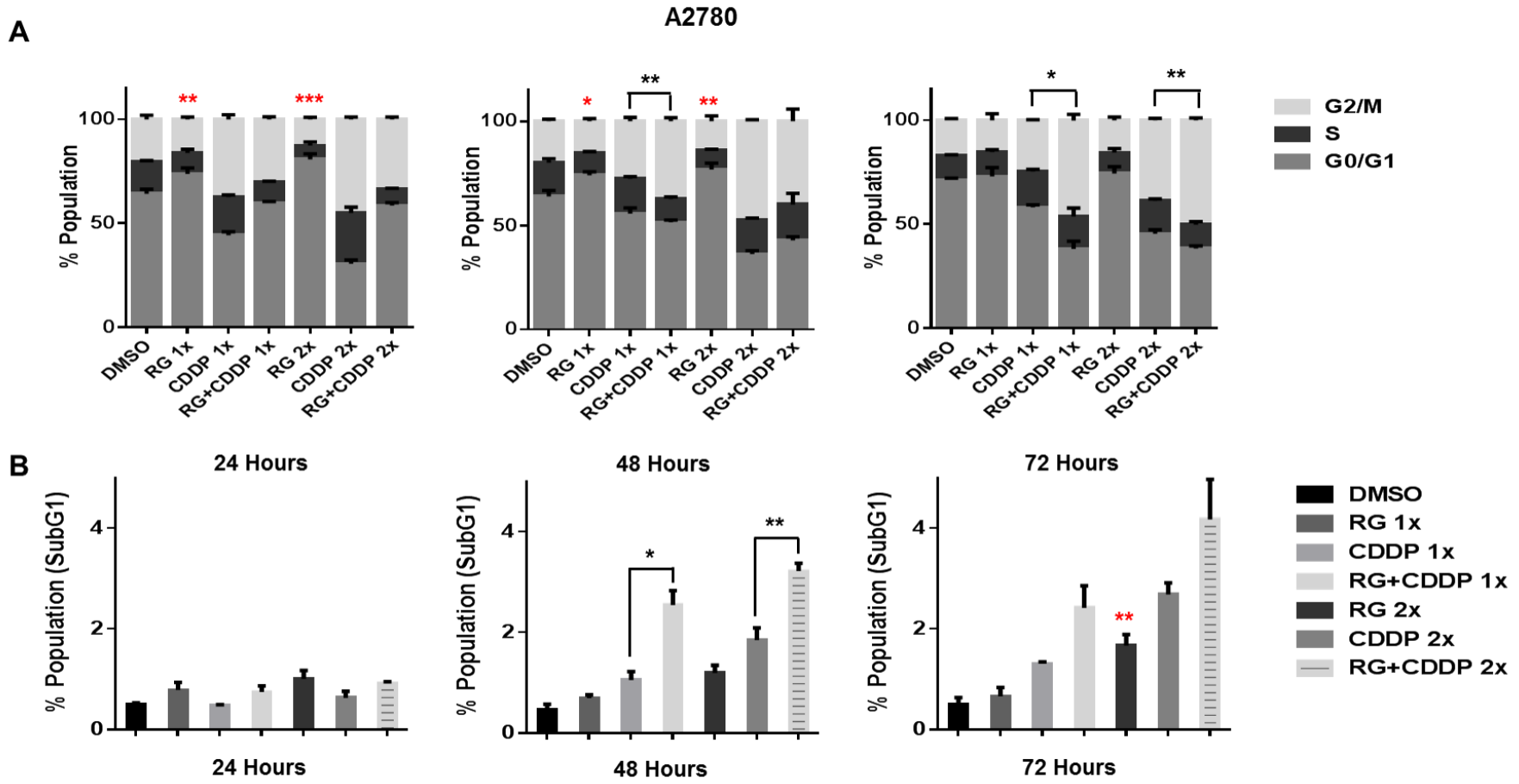

252

Figure 7-8: Combination of RG7388 with cisplatin affects the cell cycle distribution and apoptotic endpoints. A2780 cell line was treated for 24, 48 and 72 hours with RG7388 or cisplatin alone and at constant 1:1 ratios of 1x and 2x their respective GI_{50} concentrations. Combination of RG7388 with cisplatin led to an increased proportion of cells in G2/M phase (A) and SubG1 events (B) after 48 and 72 hours post-treatment compared to either agent alone in a time and concentration-dependent manner. RG, RG7388; CDDP, Cisplatin; *, *p<0.05*; **, *p<0.01*; *, *p<0.001*. The red stars represent significant increase in G0/G1 or SubG1 events compared to DMSO control. Data are shown as the average of at least 3 independent experiments and error bars represent SEM.**

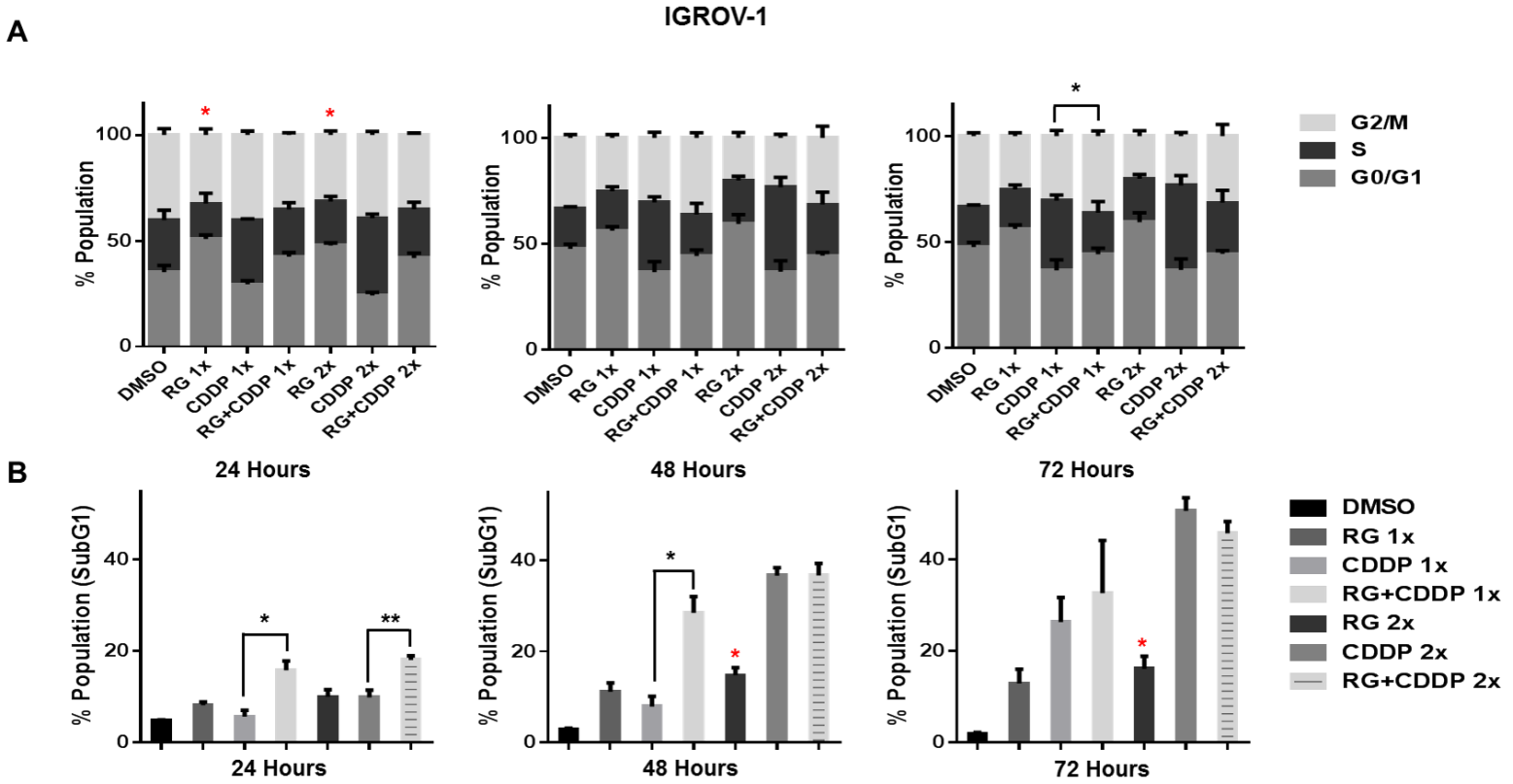

253

Figure 7-9: Combination of RG7388 with cisplatin affects the cell cycle distribution and apoptotic endpoints. IGROV-1 cell line was treated for 24, 48 and 72 hours with RG7388 or cisplatin alone and at constant 1:1 ratios of 1x and 2x their respective GI_{50} concentrations. Combination of RG7388 with cisplatin led to an increased proportion of cells in G2/M phase after 48 and 72 hours post-treatment (A) and SubG1 events after 24 and 48 hours post-treatment (B) compared to either agent alone in a time and concentration-dependent manner. RG, RG7388; CDDP, Cisplatin; *, *p<0.05*; **, *p<0.01*. The red stars represent significant increase in G0/G1 or SubG1 events compared to DMSO control. Data are shown as the average of at least 3 independent experiments and error bars represent SEM.

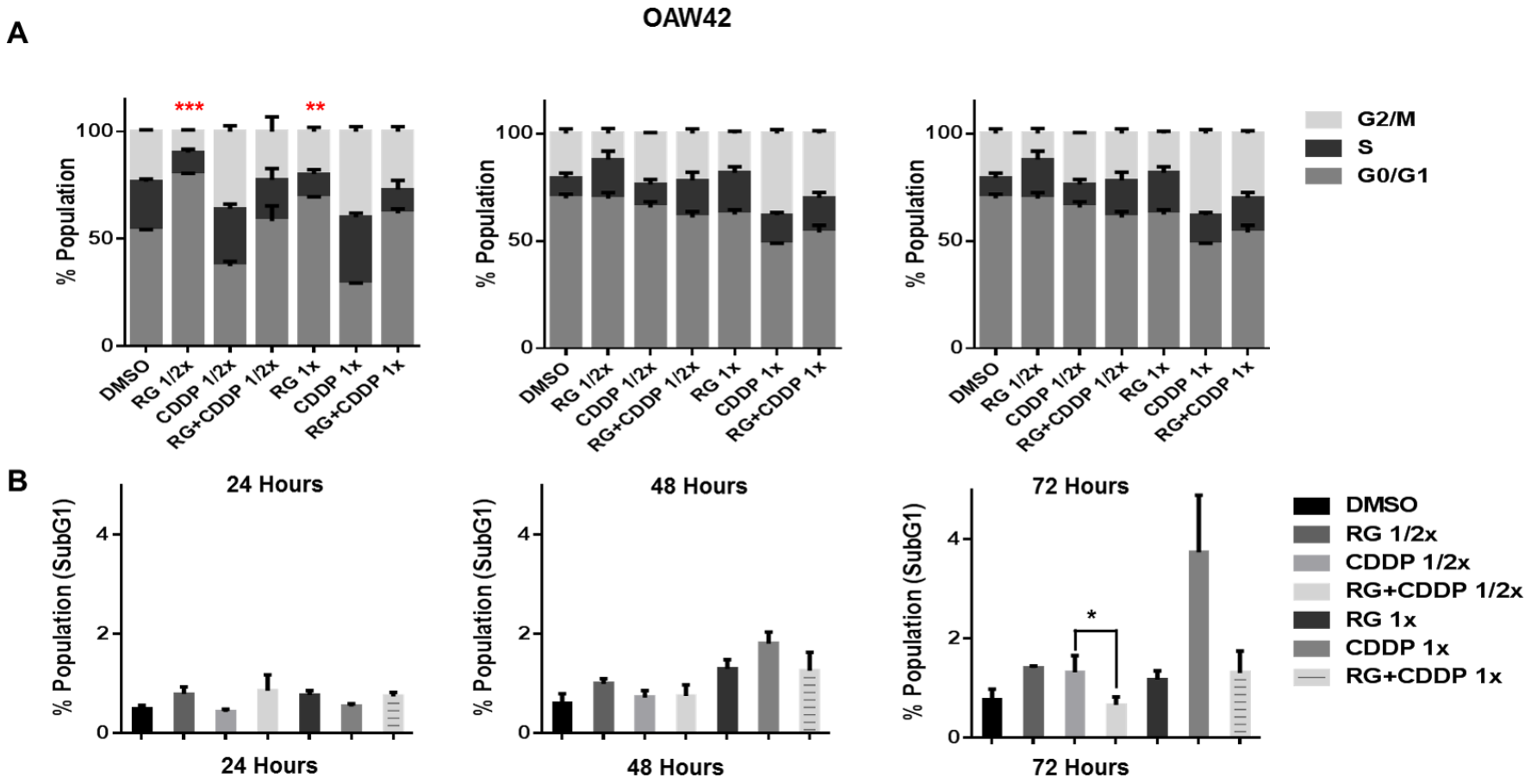

254

Figure 7-10: Combination of RG7388 with cisplatin affects the cell cycle distribution and apoptotic endpoints. OAW42 cell line was treated for 24, 48 and 72 hours with RG7388 or cisplatin alone and at constant 1:1 ratios of 1/2x and 1x their respective GI_{50} concentrations. Combination of RG7388 with cisplatin led to no increased proportion of cells in G2/M phase compared to cisplatin on its own (A) and a significant decrease in SubG1 events 72 hours post-treatment compared to cisplatin alone (B). RG, RG7388; CDDP, Cisplatin; *, *p<0.05*; **, *p<0.01*; *, *p<0.001*. The red stars represent significant increase in G0/G1 events compared to DMSO control. Data are shown as the average of at least 3 independent experiments and error bars represent SEM.**

7.4.4 The effect of Nutlin-3/RG7388 in combination with cisplatin on the caspase 3/7 activity in wild –type *TP53* ovarian cancer cell lines

The induction of apoptosis was also evaluated by caspase 3/7 enzymatic assay, which is a sensitive and specific indicator of apoptosis (Chen *et al.*, 2015). Wild-type *TP53* ovarian cancer cell lines were treated for 24 and 48 hours with 1x and 2x their respective Nutlin-3/RG7388 GI_{50} concentrations as a single agent and in combination with cisplatin. In general, across the cell lines there was a positive correlation between the caspase 3/7 activity and accumulation of SubG1 events. With IGROV-1, a concentration-dependent increase in the caspase 3/7 activity in response to Nutlin-3/RG7388 compared to DMSO control was observed. Furthermore, the combination of Nutlin-3/RG7388 with cisplatin led to more caspase 3/7 activity in IGROV-1 compared to either agent alone with the exception of combination of RG7388 with cisplatin at 2x GI_{50} values after 48 hours post-treatment (Figure 7-11 & Figure 7-12). Also no significant increase was observed for the combination of Nutlin-3/RG7388 with cisplatin compared with the effect of cisplatin alone in the A2780 cells (Figure 7-11 & Figure 7-12). Combination treatments led to a decrease in the caspase 3/7 activity in the OAW42 cells, indicating a protective effect of Nutlin-3/RG7388 against cisplatin in this cell line (Figure 7-11 & Figure 7-12). Taken together, these results demonstrated that the effect of Nutlin-3/RG7388 in combination with cisplatin on caspase 3/7 activity is cell type, compound and time dependent.

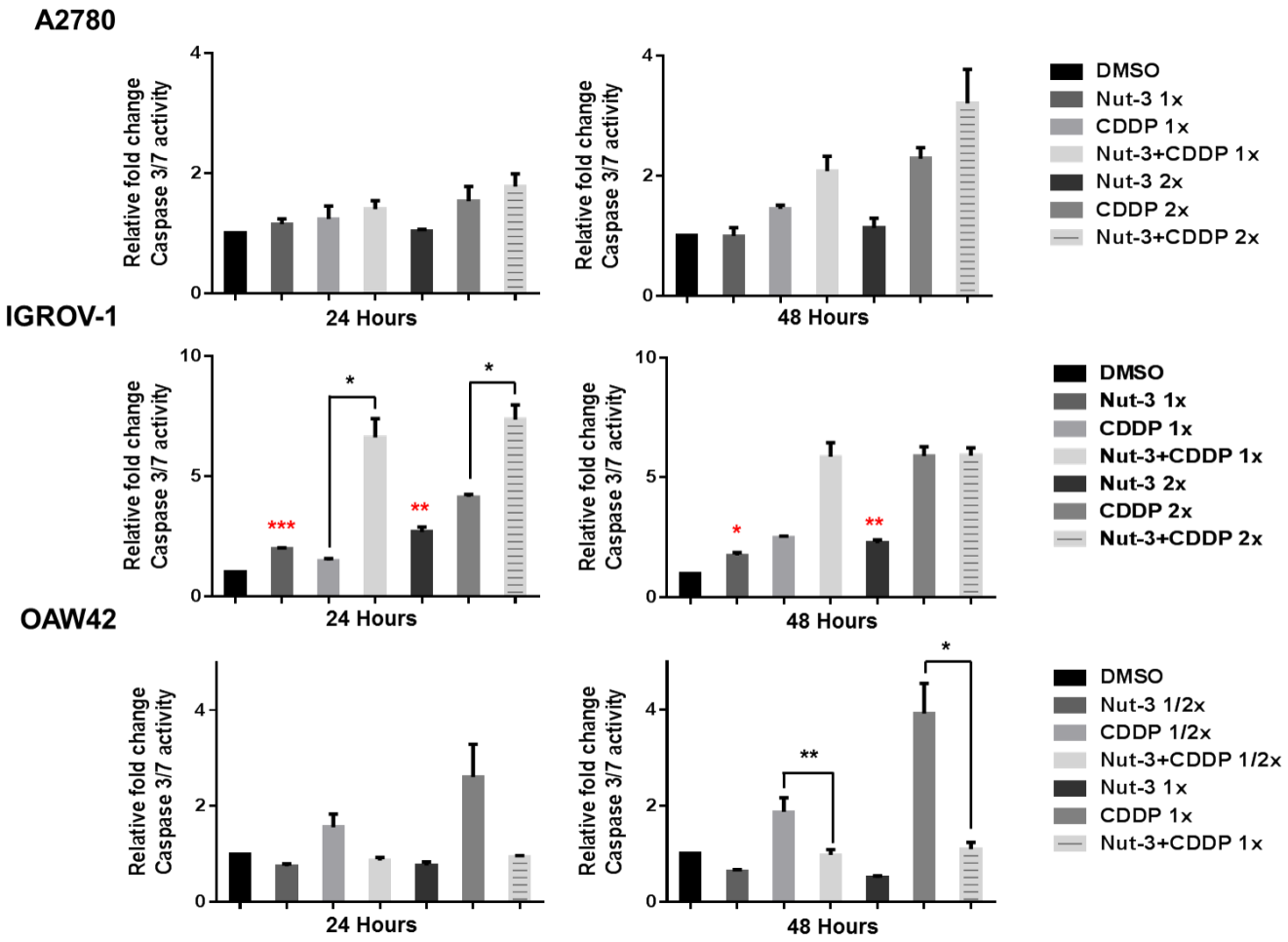

Figure 7-11: Combinations of Nutlin-3 with cisplatin affects caspase3/7 activity. The wild-type *TP53* ovarian cancer cells treated at constant 1:1 ratios of 1x and 1/2x or 2x their respective GI_{50} concentrations of Nutlin-3 and cisplatin alone, and in combination for 24 and 48 hours. Caspase 3/7 activity is represented as fold change relative to DMSO solvent control. Nut-3, Nutlin-3; CDDP, Cisplatin; *, *p<0.05*; **, *p<0.01*; *, *p<0.001*. The red stars represent a significant increase in the caspase3/7 activity compared to DMSO control.**

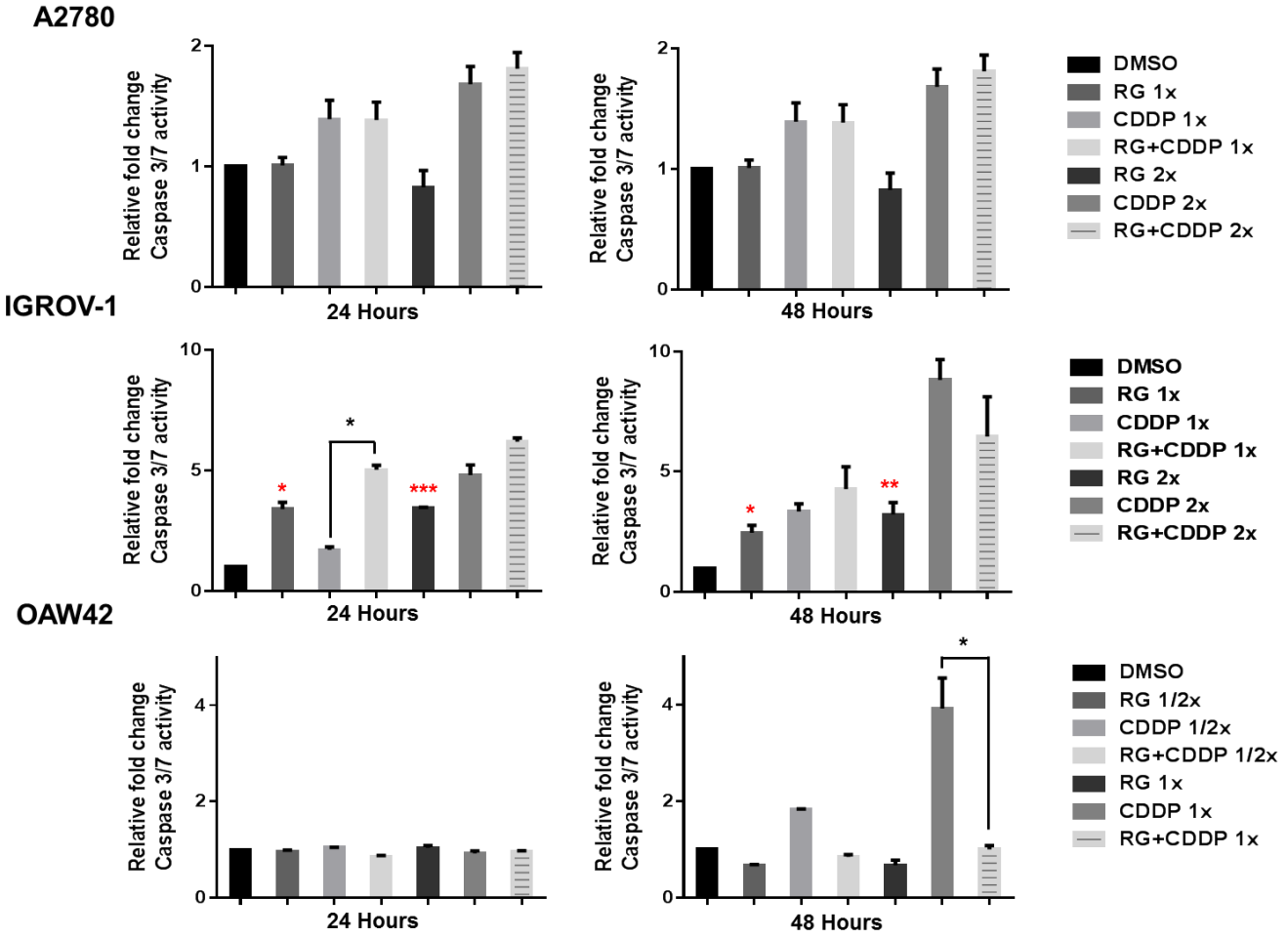

Figure 7-12: Combinations of RG7388 with cisplatin affects caspase3/7 activity. The wild-type *TP53* ovarian cancer cells treated at constant 1:1 ratios of 1x and 1/2x or 2x their respective GI_{50} concentrations of RG7388 and cisplatin alone, and in combination for 24 and 48 hours. Caspase 3/7 activity is represented as fold change relative to DMSO solvent control. RG, RGB7388; CDDP, Cisplatin; *, p<0.05; **, p<0.01; ***, p<0.001. The red stars represent a significant increase in the caspase3/7 activity compared to DMSO control.

7.4.5 Nutlin-3/RG7388 synergises with cisplatin for clonogenic cell killing of wild-type *TP53* ovarian cancer cell lines

The reduction in clonogenic survival in response to 48 hours exposure to Nutlin-3, RG7388 and cisplatin, both as single agents and in combination at 5 equipotent concentrations between 0.25× and 4× their respective LC_{50} concentrations was determined for the three wild-type *TP53* cell lines and evaluated by median-effect analysis. Due to the high LC_{50} for IGROV-1 and OAW42 in response to Nutlin-3, 3 equipotent concentrations between 0.25× and 1x their respective LC_{50} concentrations were used to assess the combination effect of Nutlin-3 with cisplatin.

The effect of combined treatment was cell type and compound-dependent (Figure 7-13 & Figure 7-14). The combination of Nutlin-3 with cisplatin led to a further decrease in colony formation compared to treatment with either agent alone for all three cell lines and was particularly marked for IGROV1 (Figure 7-13). Although the combination of Nutlin-3 with cisplatin significantly decreased the clonogenic survival of IGROV-1 and A2780 compared to either agent alone, the combined treatment of RG7388 with cisplatin at the same LC_{50} ratios only moderately reduced colony formation (Figure 7-14). For the OAW42 cell line, the combination treatment of Nutlin-3 with cisplatin reduced the ability of the OAW42 cell line to form colonies to a greater extent than either agent on its own. In contrast, there was no significant reduction in the clonogenic cell survival of OAW42 following combination treatment with RG7388 and cisplatin compared to either agent alone (Figure 7-13 & Figure 7-14).

The data were analysed using median-effect analysis and CI values calculated to evaluate whether the observed differences in clonogenic cell survival were synergistic, additive or antagonistic. CI values for each constant ratio combination at estimated effect levels of ED_{50}, ED_{75} and ED_{90} were individually computed, and the average of CI values was also determined. Across all three wild-type *TP53* cell lines, the effect of combination treatment of Nutlin-3 with cisplatin ranged from additive to strongly synergistic (Figure 7-15 & Table 7-3). In addition, for combination treatments, both Nutlin-3 and cisplatin had a favourable DRI ranging from 1.3-fold to 10.9-fold dose reduction (Table 7-4).

For A2780 and IGROV-1 cell lines a synergistic effect was observed for combination treatment with Nutlin-3 and cisplatin, whereas for RG7388 and cisplatin combinations the effect was additive to antagonistic. For the OAW42 cell line the combination of RG7388 and cisplatin

was antagonistic, suggesting RG7388 had a protective effect against cisplatin (Figure 7-15). Although the combined effect of RG7388 with cisplatin ranged from additive to antagonistic, there was nevertheless a favourable DRI for the same level of clonogenic cell killing when treatments are combined for all RG7388 concentrations and most concentrations of cisplatin (Table 7-4).

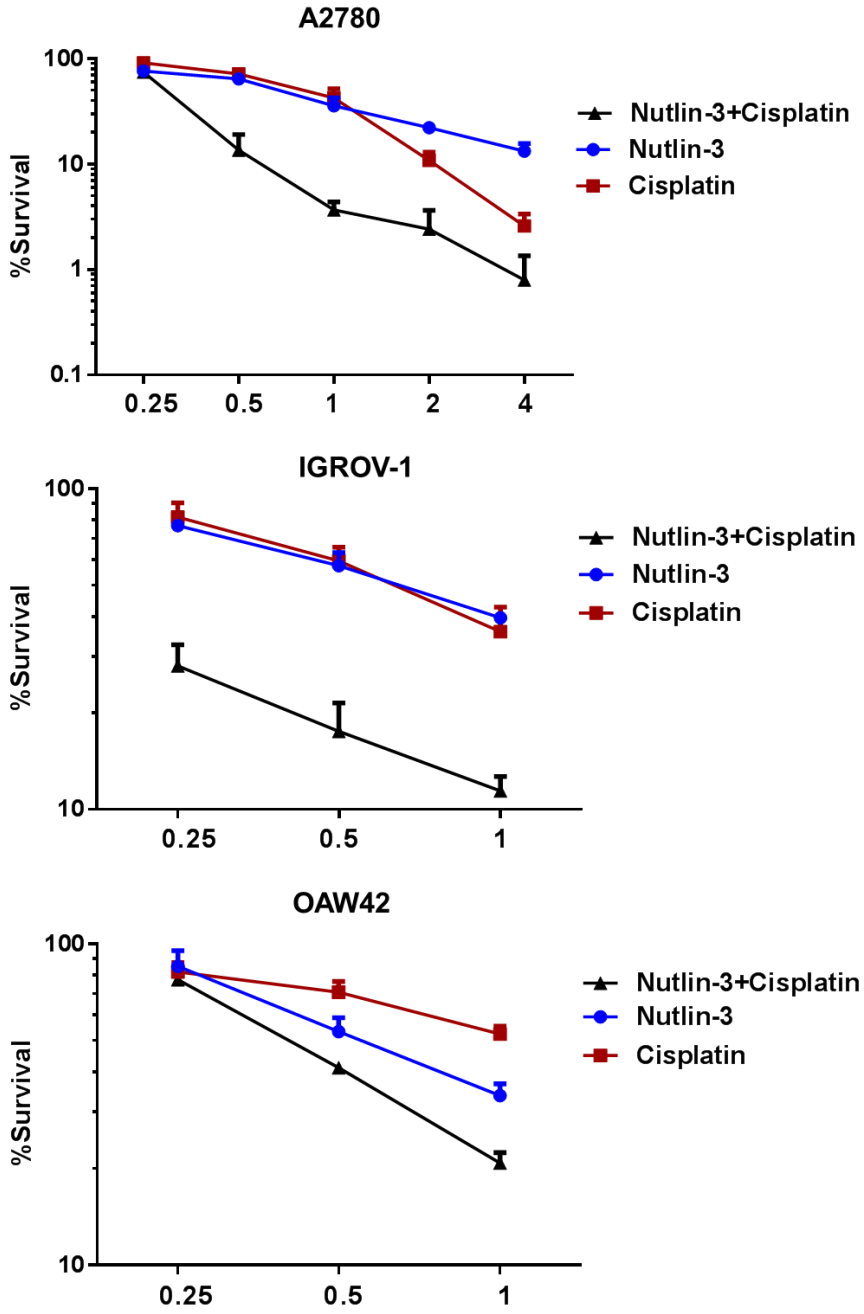

Figure 7-13: Nutlin-3 has a synergistic or additive effect with cisplatin in clonogenic survival assays in wild-type *TP53* ovarian cancer cells. Clonogenic survival for three wild-type *TP53* cell lines exposed to Nutlin-3 and cisplatin alone, and in combination at constant 1:1 ratios of 0.25x, 0.5x, 1x, 2x and 4x (A2780) and 0.25x, 0.5x, 1x (IGROV-1 & OAW42) their respective LC_{50} concentrations for 48 hours.

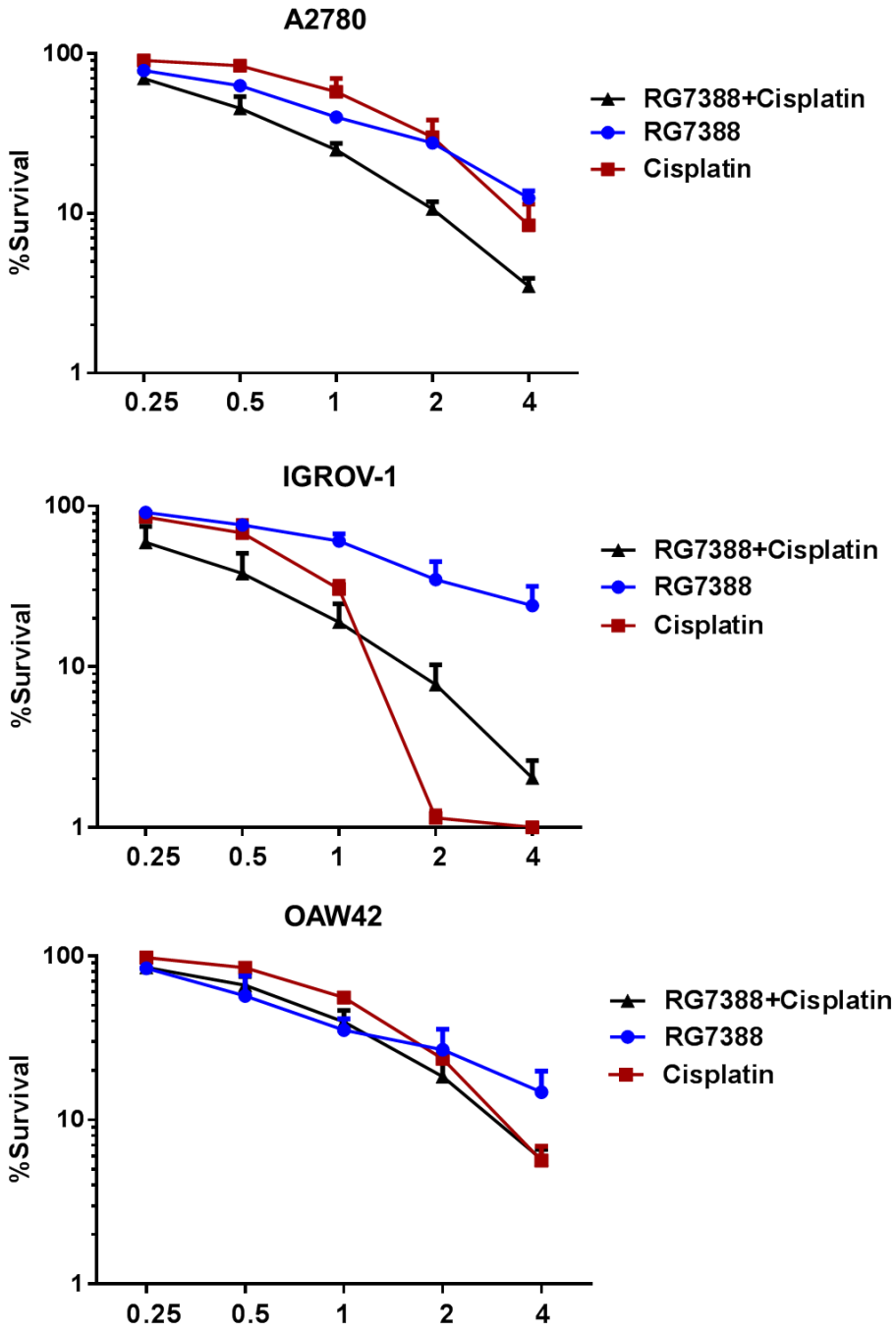

Figure 7-14: RG7388 has an additive or antagonistic effect with cisplatin in clonogenic survival assays in wild-type *TP53* ovarian cancer cells. Clonogenic survival for three wild-type *TP53* cell lines exposed to RG7388 and cisplatin alone, and in combination at constant 1:1 ratios of 0.25x, 0.5x, 1x, 2x and 4x their respective LC_{50} concentrations for 48 hours.

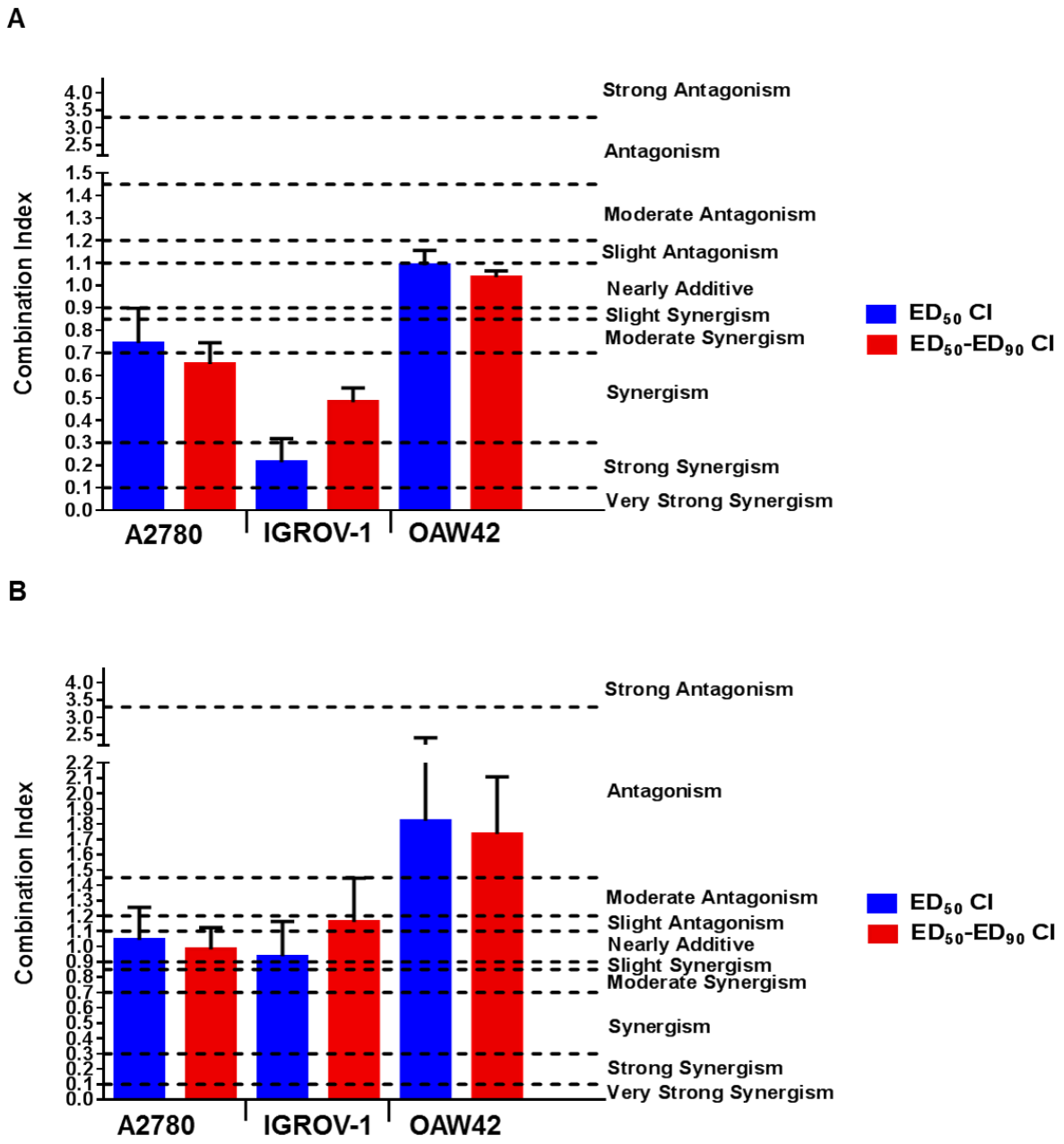

Figure 7-15: The clonogenic survival combination index (CI) values for Nutlin-3 (A) and RG7388 (B) in combination with cisplatin at ED_{50} and, the average of CI values at effect levels ED_{50}, ED_{75} and ED_{90} in three wild-type *TP53* ovarian cancer cell lines. Data are shown as the average of at least 3 independent experiments and error bars represent SEM. CI, Combination Index; ED, Effective dose.

Cell Line	Combination	CI					CI ED_{50}	CI ED_{75}	CI ED_{90}	CI Average ED_{50-90}
		XLC_{50}								
		0.25	0.5	1	2	4				
A2780	Nutlin-3+Cisplatin	1.9	**0.4**	**0.4**	**0.6**	**0.6**	**0.7**	**0.6**	**0.6**	**0.7**
	RG7388+Cisplatin	1.2	1.0	1.0	1.0	**0.9**	1.0	1.0	**0.9**	1.0
IGROV-1	Nutlin-3+Cisplatin	**0.4**	**0.5**	**0.7**	ND	ND	**0.2**	**0.4**	**0.9**	**0.5**
	RG7388+Cisplatin	**0.8**	1.0	1.4	1.9	1.9	**0.9**	1.1	1.4	1.1
OAW42	Nutlin-3+Cisplatin	1.8	1.0	1.0	ND	ND	1.1	1.0	1.0	1.0
	RG7388+Cisplatin	1.2	1.9	1.7	1.7	1.7	1.8	1.7	1.7	1.7

262

Table 7-3: Clonogenic survival CI values for RG7388/Nutlin-3 in combination with cisplatin for the wild-type *TP53* ovarian cancer cell lines. The combined treatment was performed at the indicated fixed 1:1 ratios relative to their respective GI_{50} concentrations. CI values were calculated for each constant ratio combination and at effect levels ED_{50}, ED_{75} and ED_{90} from the average of at least three independent experiments. CI Ave ED_{50-90} represents the average of CI values at effect levels of ED_{50}, ED_{75} and ED_{90}. CI range: < 0.1 very strong synergism; 0.1-0.3 strong synergism; 0.3-0.7 synergism; 0.7-0.85 moderate synergism; 0.85-0.9 slight synergism; 0.9-1.1 nearly additive; 1.1-1.2 slight antagonism; 1.2-1.45 moderate antagonism; 1.45-3.3 antagonism; 3.3-10 strong antagonism; > 10 very strong antagonism. Synergistic combinations are highlighted in bold font. CI, Combination Index; ED, Effective dose; ND; Not determined.

Cell Line	Combination	Compound	DRI				
			XLC_{50}				
			0.25	0.5	1	2	4
A2780	Nutlin-3+Cisplatin	Nutlin-3	**1.3**	**8.1**	**10.7**	**9.3**	**14.7**
		Cisplatin	**2.1**	**4.0**	**3.4**	**2.2**	**2.0**
	RG7388+Cisplatin	RG7388	**1.6**	**1.9**	**2.0**	**2.5**	**3.5**
		Cisplatin	**3.2**	**2.6**	**2.1**	**1.8**	**1.7**
IGROV-1	Nutlin-3+Cisplatin	Nutlin-3	**6.4**	**5.4**	**4.1**	ND	ND
		Cisplatin	**5.1**	**3.7**	**2.2**	ND	ND
	RG7388+Cisplatin	RG7388	**4.3**	**4.3**	**4.3**	**4.5**	**11.0**
		Cisplatin	**2.1**	**1.4**	0.9	0.6	0.6
OAW42	Nutlin-3+Cisplatin	Nutlin-3	**1.6**	**1.5**	**1.3**	ND	ND
		Cisplatin	**1.8**	**3.2**	**5.0**	ND	ND
	RG7388+Cisplatin	RG7388	1.0	**1.1**	**1.2**	**1.4**	**2.0**
		Cisplatin	**2.1**	**1.7**	**1.4**	**1.1**	0.9

Table 7-4: DRI values for clonogenic cell killing by RG7388/Nutlin-3 in combination with cisplatin in wild-type *TP53* ovarian cancer cell lines. The combined treatment was performed at the indicated fixed 1:1 ratios relative to their respective LC_{50} concentrations. DRI values were calculated for each constant ratio combination from the average of at least three independent experiments. DRI, Dose reduction index; ND; Not determined. Favourable DRI values are highlighted in bold font.

7.4.6 Nutlin-3/RG7388 induces expression of cell cycle arrest/apoptosis-related genes and those implicated in DNA repair in response to cisplatin

To investigate the mechanistic basis for the observed combination effects, the effect of MDM2 inhibitor treatment on mRNA expression of candidate genes with potential for influencing the response to cisplatin was analysed by qRT-PCR. Changes in the expression of cell cycle/apoptosis-related genes as well as those involved in nucleotide excision repair (NER) and mismatch repair (MMR) for the three wild-type *TP53* cell lines in response to Nutlin-3 and RG7388 are shown in Figure 7-16. The cells were treated with 5 (μM) Nutlin-3 and 0.5 (μM) RG7388, and total RNA was extracted 6 hours after the commencement of treatment.

Overall, the fold changes in expression in response to MDM2 inhibitors were less in A2780 cells than IGROV-1 and OAW42 (Figure 7-16 & Figure 7-17). In the case of the genes involved in cell cycle arrest and growth inhibition, Nutlin-3 and RG7388 treatment significantly induced *CDKN1A*, *SESN1* and *GADD45A* gene expression in all three cell lines, with *CDKN1A* consistently showing the highest level of induction ($p<0.05$) (Figure 7-16). Both treatments showed a significant increase in the expression of the pro-apoptotic *TNFRSF10B* and *PUMA* genes in all three cell lines, with increases of *PUMA* mRNA being highest in the IGROV-1 cell line ($p<0.05$) (Figure 7-16). The Nutlin-3/RG7388 treatment also increased expression of the pro-apoptotic gene *TP53INP1* in A2780 and OAW42 cells; however, there was no significant induction in IGROV-1. No significant increase was observed for the pro-apoptotic gene *BAX* in any of the cell lines. Although Nutlin-3/RG7388 treatment led to significantly increased expression of *AEN* in IGROV-1, the induction of *AEN* was not statistically significant for A2780 (Figure 7-16). Furthermore, both Nutlin-3 and RG7388 treatments significantly increased the expression of the *MDM2* gene, the negative regulator of p53, across all three cell lines. The treatments led to a statistically significant decrease in the expression of *BCL-2* for A2780 and IGROV-1 cell lines although the changes were small and unlikely to be biologically significant. Also, no significant changes were observed in the expression levels of the anti-apoptotic *BIRC5* and *MCL-1* genes (Figure 7-16).

To study the effect of Nutlin-3 and RG7388 on the expression of genes implicated in the response to DNA repair induced by cisplatin, the expression of *TP53BP1*, *DDB2*, *ERCC1*, *XPC*, *MLH1*, *MSH2*, *RAD51* and *RRM2B* genes in response to Nutlin-3 and RG7388 was investigated. A significant increase was measured in the expression of *DDB2* in response to Nutlin-3 and *XPC* in response to both Nutlin-3 and RG7388 for A2780 cells ($p<0.05$). In the

case of IGROV-1, *XPC* and *MSH2* gene expression levels were significantly induced in response to Nutlin-3 and reduced in response to RG7388 respectively ($p<0.05$). For OAW42 cells, there was a significant increase in the expression of *DDB2* gene and a significant decrease in the *MLH1* and *MSH2* expression levels in response to Nutlin-3 treatment ($p<0.05$). With Nutlin-3 treatment, the *TP53BP1* gene expression decreased in all three cell lines, although statistically this trend was not significant ($p>0.05$) (Figure 7-16).

The mRNA profile found for *CDKN1A* and *BAX* genes was consistent with the western blot analysis for $p21^{WAF1}$ and BAX proteins (Figure 7-4). The increased *CDKN1A* and *SESN1* gene expression is also in agreement with induced cell cycle arrest and growth inhibition across the three cell lines. Furthermore, induction of *PUMA* and *TNFRSF10B* is in accordance with the induction of apoptosis, SubG1 events and caspase 3/7 activity, in A2780 and IGROV-1 (Figure 7-5B, Figure 7-6B, Figure 7-8B, Figure 7-9B, Figure 7-11A & Figure 7-12). However, in spite of significantly increased *PUMA* and *TNFRSF10B* gene expression levels in OAW42, no induction of apoptosis was observed in this cell line (Figure 7-7B, Figure 7-10B, Figure 7-11 & Figure 7-12).

The increased sensitivity to MDM2 inhibitors and their synergy with cisplatin observed with the A2780 cells was not obviously attributable to any individual change in candidate gene expression. However, as can be seen in Figure 7-17, the balance of expression between the growth arrest genes and the autoregulatory negative feedback MDM2 gene on the one hand and the pro-apoptotic and DNA repair genes on the other hand, was somewhat less with the A2780 cells (Figure 7-18).

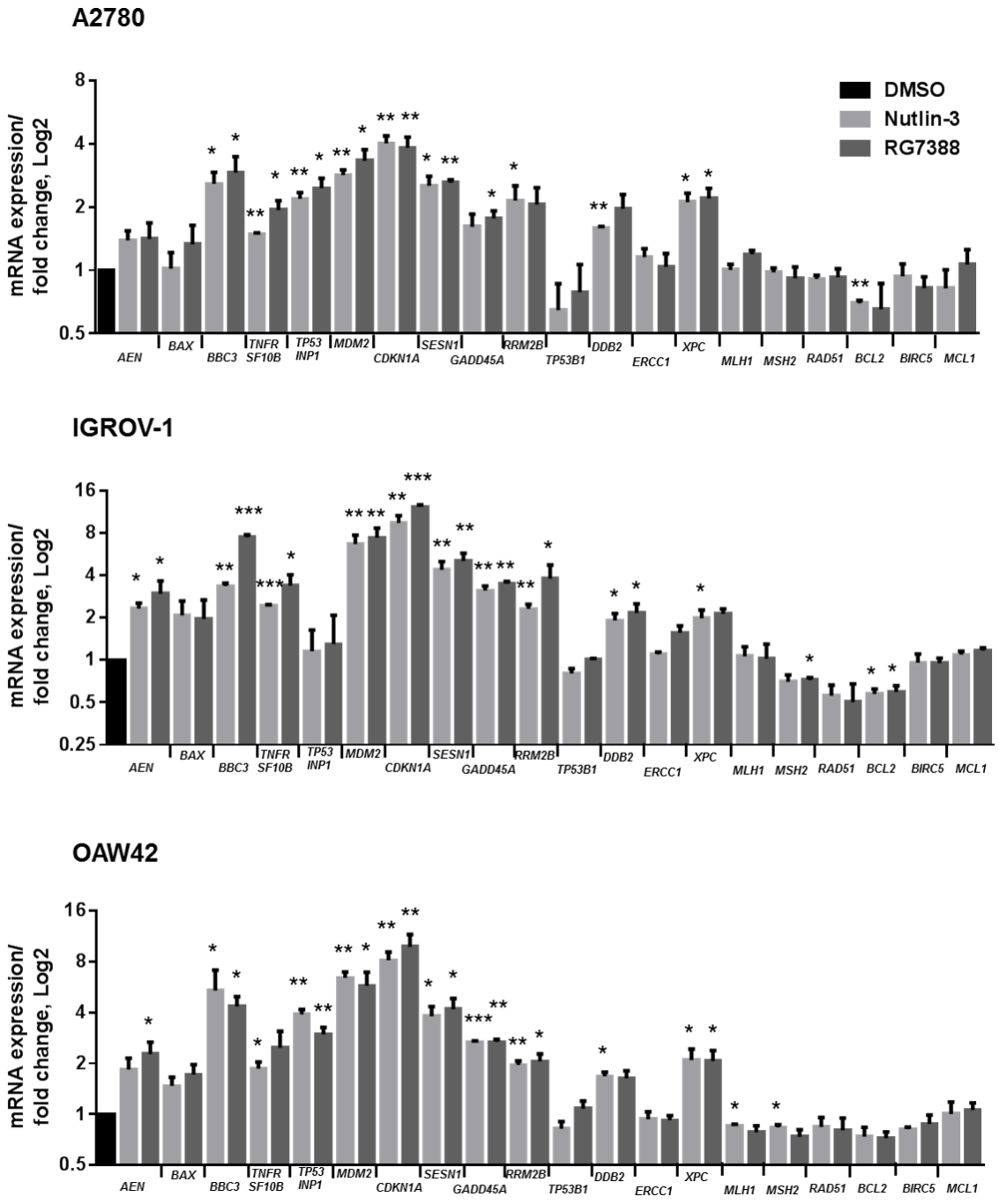

Figure 7-16: mRNA expression of genes relating to apoptosis, cell cycle arrest, nucleotide excision repair (NER) and DNA mismatch repair (MMR) in response to 5 µM Nutlin-3 or 0.5 µM RG7388 for 6 hours relative to DMSO solvent control. *, *p<0.05*; **, *P<0.01*; *, *P<0.001*. Data are presented as mean ± standard error of mean (SEM) of three independent repeats.**

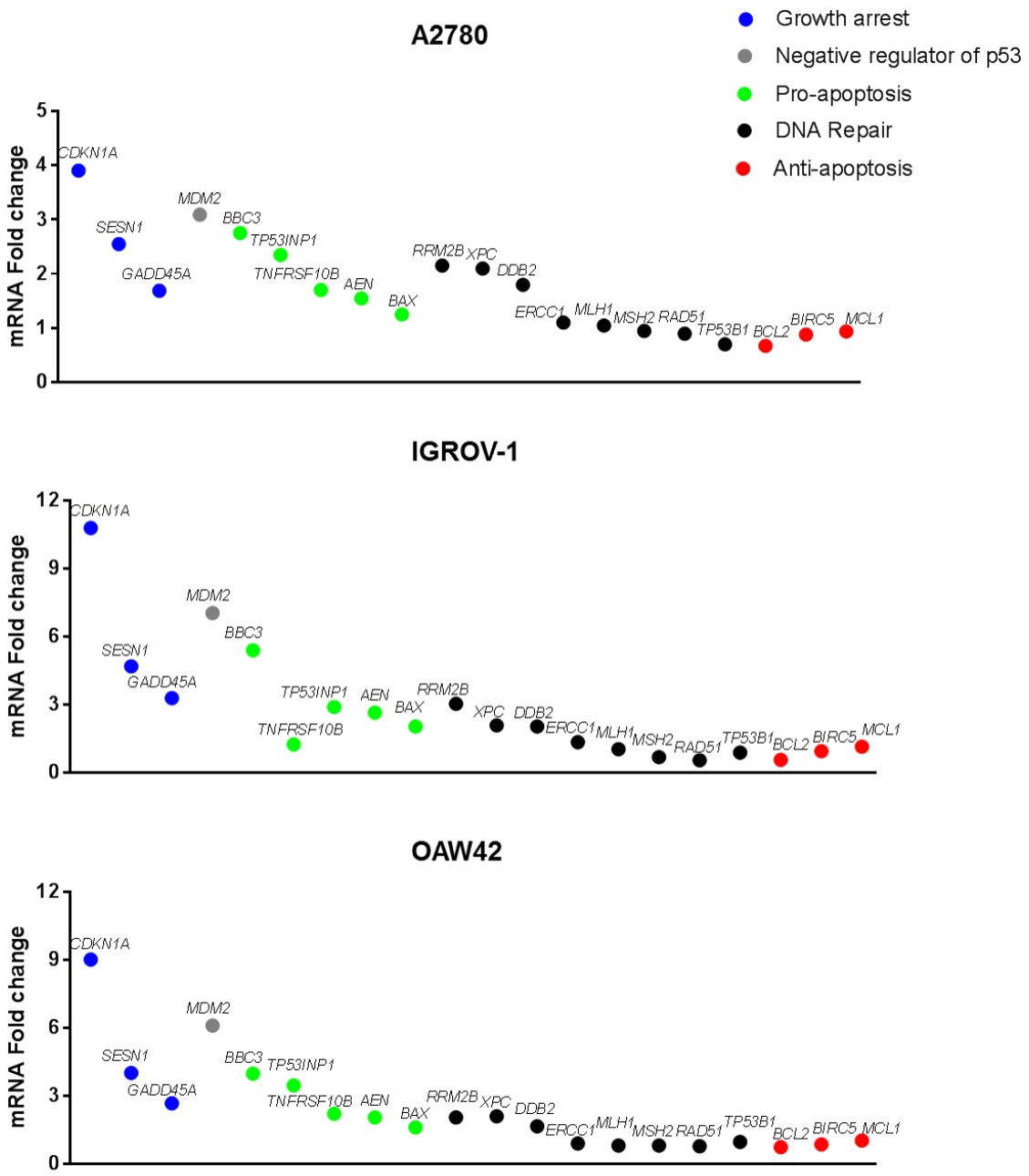

Figure 7-17: Growth arrest, pro-apoptotic, anti-apoptotic and DNA repair-related gene expression changes induced by 5 µM Nutlin-3 or 0.5 µM RG7388 for 6 hours relative to DMSO solvent control. Summary data are presented as a combination of three independent repeats for Nutlin-3 and three for RG7388.

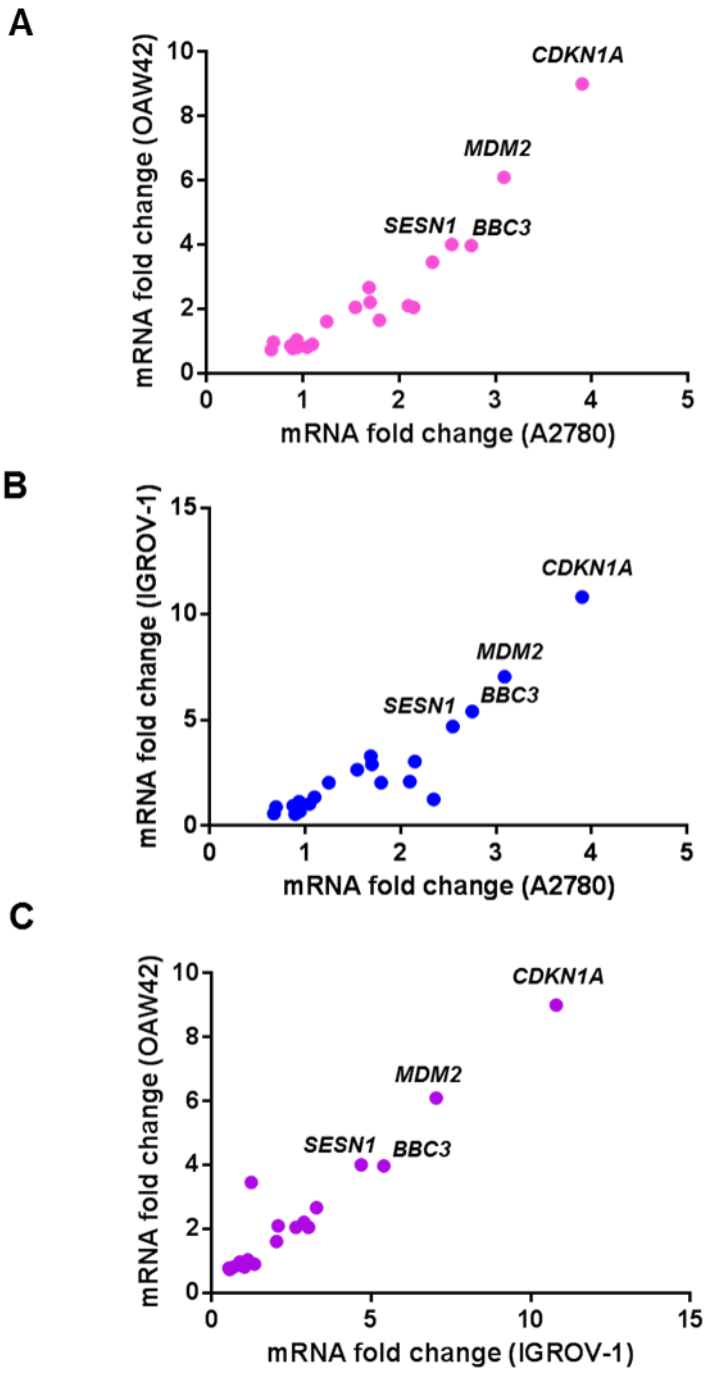

Figure 7-18: Gene expression changes (*CDKN1A, MDM2, PUMA* and *SESN1*) induced by 5 µM Nutlin-3 or 0.5 µM RG7388 for 6 hours relative to DMSO solvent control in one cell line against another cell line (three pairwise comparisons). Summary data are presented as a combination of three independent repeats for Nutlin-3 and three for RG7388. (A) A2780 versus OAW42 (*$p<0.05$*), (B) A2780 versus IGROV-1 (*$p<0.05$*) and (C) IGROV-1 versus OAW42 (*$p>0.05$*).

7.5 Discussion

Advanced ovarian cancer treatment usually involves debulking surgery followed by platinum based chemotherapy, alone or with the addition of paclitaxel. Although chemotherapy prolongs survival, most patients with advanced disease die from treatment resistant progressive disease (Kim *et al.*, 2012; Ledermann *et al.*, 2013). Cancer therapy has recently been improving with the introduction of targeted therapies to achieve greater specificity and less cytotoxicity (Munagala *et al.*, 2011; Yuan *et al.*, 2011; Nicolas Andre *et al.*, 2012). When new agents are evaluated against particular cancers they are compared against established treatments and also in combination with established treatments, particularly when there is a mechanistic rationale to suggest that there may be an additive or synergistic effect of the combination. Platinum agents are the standard treatment used for ovarian cancer which induces cell cycle arrest and apoptosis through both p53-dependent and p53-independent pathways. Therefore in addition to the effect of MDM2-p53 binding antagonists alone, it is of interest to investigate the combined effect of these novel agents with cisplatin.

7.5.1 Nutlin-3/RG7388 synergises with cisplatin for growth inhibition of wild-type *TP53* ovarian cancer cell lines

Resistance to MDM2-p53 binding antagonists has been suggested to be acquired by prolonged exposure of cells to sub-lethal doses through *de novo* inactivating *TP53* mutations or selection of pre-existing subclones of *TP53* mutant cells that might be present as a result of cancer cell instability and tumour heterogeneity (Shen *et al.*, 2008; Aziz *et al.*, 2011). For this reason, it is suggested that MDM2-p53 antagonists are likely be most effective in combination with standard existing chemotherapeutic agents or agents that target or limit the potential outgrowth of *TP53* mutated cells. Platinum agents used to treat ovarian cancer have major adverse side effects including nephrotoxicity, ototoxicity, myelosuppression and gastrointestinal disorders (Florea and Büsselberg, 2011; Pabla and Dong, 2012). This study set out with the aim of assessing the effect combination treatment of Nutlin-3 and RG7388 with cisplatin in a panel of ovarian cancer cell lines of known *TP53* status.

Overall, the combination effect of Nutlin-3 and RG7388 with cisplatin varied with synergism in A2780 and moderate synergism to antagonism in IGROV-1 and OAW42 cell lines, depending on drug concentration. A single limited previous study examined the combination of Nutlin-3a with cisplatin in A2780p, A2780cis and the OV90 cell lines. The results showed a synergistic effect in A2780p and A2780cis, consistent with our study (Mir *et al.*, 2013). Based

on the CI values at the average of ED_{50}-ED_{90} and ED_{50} (Chou, 2006), the combination effect of Nutlin-3 and RG7388 with cisplatin ranged from synergism to moderate synergism in A2780 and moderate synergism to antagonism in IGROV-1 and OAW42 cell lines. Unexpectedly, combination of RG7388 with cisplatin resulted in less synergistic or additive effect compared to combined treatment of Nutlin-3 with cisplatin across all three cell lines. The reason for this is not clear but it may be related to the induction of G0/G1 cell cycle arrest following exposure to RG7388 which leads to protection of the cells against cisplatin, since cisplatin is preferentially cytotoxic against S-phase cells. Chen *et al*. (2015) obtained the least degree of synergy for cisplatin with RG7388 in neuroblastoma cell lines compared to synergies between RG7388 and doxorubicin, topotecan, temozolomide or busulfan.

The most important clinically relevant finding from the data is favourable DRI values in both combination treatment of Nutlin-3 and RG7388 with cisplatin. DRI values represent the magnitude (fold) of dose reduction that is achievable in combination for a given degree of effect compared with the dose of each drug alone (Chou, 2006; Zhang *et al.*, 2009; Chou, 2010). Even in the absence of synergy, combined treatment can nevertheless be of potential clinical use, because in most cases a favourable dose reduction for each agent may still be achievable for a given level of effect compared with each agent alone (Table 7-2). This is of particular potential benefit when the agents in question, in this case MDM2 inhibitors and cisplatin, have different dose limiting toxicities. Overall, the effects observed were compound and cell type dependent.

7.5.2 Combination of Nutlin-3/RG7388 with cisplatin induces functional activation of the p53 pathway in *TP53* wild-type ovarian cancer cell lines

The combination treatments increased stabilization of p53 and upregulation of $p21^{WAF1}$ and MDM2 compared to either agent alone, particularly compared to cisplatin in A2780 and IGROV-1, which is in agreement with data obtained by Mir *et al*. (2013) in the A2780p cell line, Barbieri *et al*. (2006) and Koster *et al*. (2011) in testicular carcinoma cells and Voon *et al*. (2015) in nasopharyngeal carcinoma. However, there was no significant increase in p53 stabilization and $p21^{WAF1}$ upregulation with combined treatment of OAW42 cells compared to Nutlin-3 and RG7388 as single treatments. These results help to explain the observed differences in the effect of combined treatment on growth inhibition between these cell lines. These findings are in keeping with functional activation of p53 as a driver of the synergistic effects in combination treatment. For growth inhibition the increased upregulation of $p21^{WAF1}$

is consistent with its role in cell cycle arrest (Giono and Manfredi, 2007; Abbas and Dutta, 2009; Cazzalini *et al.*, 2010). Nutlin-3 and RG7388 led to little change of BAX compared to DMSO control and combination of Nutlin-3 with cisplatin at 1x GI_{50} showed a slight increase in the expression of BAX in A2780 and IGROV-1 cell lines compared to cisplatin on its own. These results differ from Mir *et al*. (2013) who found induction of BAX following combined treatment of Nutlin-3a with cisplatin compared to cisplatin on its own. A possible explanation for this inconsistency might be the high concentration of Nutlin-3a (5 µM) and cisplatin (3.5 µM) used compared to what has been used in this study.

7.5.3 Nutlin-3/RG7388 synergises with cisplatin for cell cycle arrest and/or apoptosis in wild-type *TP53* ovarian cancer cell lines

Individually, Nutlin-3 and RG7388 induced cell cycle arrest and/or apoptosis in wild-type *TP53* ovarian cancer cell lines in a time and dose-dependent manner. Combination treatment with Nutlin-3 or RG7388 and cisplatin led to greater G2/M and/or G0/G1 cell cycle phase accumulation, more SubG1 events and/or higher levels of caspase 3/7 activity compared to either agent alone in a cell type and time-dependent manner. These results are consistent with those of Mir *et al*. (2013) who found more accumulation of cells in G2/M phase in wild-type *TP53* ovarian cancer cell lines, A2780p and A2780cis, treated with a combination of Nutlin-3a and cisplatin compared to either agent alone.

Overall, there was a positive correlation between the detection of SubG1 events on Flow cytometry and caspase 3/7 activity; however, cell cycle arrest is not always accompanied by the induction of apoptosis (Weng *et al.*, 2001; Simone Fulda *et al.*, 2010) as seen for OAW42 cells in this study. The apparent protective effect of Nutlin-3/RG7388 against cisplatin in OAW42, indicated by the antagonistic effect of combination, was reflected by fewer SubG1 events and Caspase 3/7 activity compared to cisplatin on its own (Figure 7-7B, Figure 7-10B, Figure 7-11C Figure 7-12C). In terms of A2780 cells, there was a significant increase in SubG1 events following combination of Nutlin-3/RG7388 with cisplatin even though no significant increased caspase 3/7 activity was observed, indicating the involvement of alternative pathways implicated in cell death, rather than caspase 3/7 activation.

7.5.4 Nutlin-3/RG7388 affects the response to cisplatin for clonogenic cell killing of *TP53* wild-type ovarian cancer cell lines

Combined treatment with Nutlin-3 and cisplatin significantly decreased the clonogenic survival of wild-type *TP53* ovarian cancer cells compared with either agent alone, and the combination effect ranged from additive to strong synergy. Nutlin-3 may sensitize wild-type *TP53* ovarian cancer cell lines to cisplatin via multiple factors including increased p53-dependent apoptosis (Arya *et al.*, 2010; Voon *et al.*, 2015). Surprisingly, the combination of RG7388 with cisplatin showed no evidence of synergy for reduction of colony forming ability. The clonogenic assay results for combination of RG7388 with cisplatin ranged from antagonism for OAW42, indicating a protective effect of RG7388 against cisplatin, to additive for A2780 and IGROV-1. The difference between the results for combination of cisplatin with Nutlin-3 compared to the combination with RG7388 may in part be due to different p53-dependent off-target effects of these MDM2 inhibitors (Contractor and Harris, 2012; Khoo *et al.*, 2014). A contributory factor may be differences in G0/G1 cell cycle arrest with MDM2 inhibitors, since an increased G0/G1 cell cycle arrest may protect against agents such as cisplatin which are preferentially cytotoxic against S-phase cells (Wagner and Karnitz, 2009).

7.5.5 Nutlin-3/RG7388 affects expression of cell cycle arrest/ apoptosis-related genes and those involved in response to DNA repair

Across the three cell lines, Nutlin-3/RG7388 increased *CDKN1A* and *SESN1* expression consistent with their essential role in cell cycle arrest and growth inhibition (Budanov and Karin, 2008; Abbas and Dutta, 2009). Both Nutlin-3 and RG7388 treatment significantly induced the expression of the pro-apoptotic *TNFRSF10B* and *PUMA* genes in all three cell lines. TNFRSF10B and its ligand, TRAIL, have been reported to preferentially induce apoptosis in transformed and tumour cells even though TNFRSF10B is expressed at a significant level in most normal tissues (Ashkenazi and Herbst, 2008; Bossi *et al.*, 2015). This may contribute to the generally greater toxicity of MDM2 inhibitors for cancer cells compared to normal cells, although some haematopoietic cell lineages also appear to be sensitive, as evidenced by the dose limiting thrombocytopenia seen in the early phase clinical trials of MDM2 inhibitors (Jiang *et al.*, 2007). There was a positive concordance between the expression of these pro-apoptotic genes and the apoptotic endpoints shown by ubG1 signals on Flow cytometry and caspase 3/7 activity in A2780 and IGROV-1 cell lines. However, this relationship did not extend to the OAW42 cell line, for which increased pro-apoptotic

TNFRSF10B, *TP53INP1* and *PUMA* gene expression was not in keeping with low caspase 3/7 activity and SubG1 FACS signals. Failure to undergo apoptosis in OAW42 cells in response to C1311, a new class of imidazoacridinones, has been reported, consistent with our observation (Zaffaroni *et al.*, 2001). A possible explanation for the lack of evidence of apoptosis in OAW42 might be high levels of anti-apoptotic proteins such as BCL-2, BCL-X and MCL-1 or deficiency in downstream factors involved in the apoptosis cascade (Haupt *et al.*, 2003; Jeffers *et al.*, 2003). This would imply that OAW42 would be responsive to inhibitors of these anti-apoptotic proteins and they would potentiate the effect of MDM2 inhibitors in OAW42 in particular. Although BAX is reported to be required for PUMA-induced apoptosis, there was no significant increase in BAX expression, either at the mRNA or protein level in response to Nutlin-3/RG7388 treatment in any of the cell lines.

Significantly increased expression of several p53-regulated genes involved in the repair of DNA lesions induced by cisplatin, including *DDB2*, *XPC* and *RRM2B*, lead us to reject the hypothesis that reduced capacity for repair of cisplatin induced DNA damage leads to a synergistic effect in combined treatment with Nutlin-3/RG7388 and cisplatin. Although there was some evidence of a reduced expression of the DNA mismatch repair genes, *MLH1* and *MSH2*, the changes were very small and unlikely to be biologically significant.

7.5.6 Conclusion and further work

In conclusion, the present study demonstrates that combination treatment with MDM2 inhibitors and cisplatin has synergistic and/or dose reduction potential dependent on cell genotype and compound and merits further investigation. Our study clearly indicates that the presence of wild-type *TP53* remains the main predictive biomarker of response to MDM2 inhibitors. However, an additional determinant of response involves the balance of activity between growth inhibitory/pro-survival and pro-apoptotic genes and our results indicate that this dominates the small changes in the expression of DNA repair genes as an explanation for the synergy observed for treatment with cisplatin and MDM2 inhibitors.

Due to the effectiveness of MDM2-p53 antagonists as single agents in wild-type *TP53* ovarian cancer cell lines, it was of interest to study the effect of combination of MDM2-p53 antagonists with the PARP inhibitor, rucaparib, in ovarian cancer cell lines. Inhibition of PARP might promote DNA damage related signalling to the p53 pathway.

Chapter 8: An investigation of the combination effect of MDM2-p53 antagonists Nutlin-3/RG7388 or cisplatin with PARP inhibitor rucaparib on ovarian cancer cell lines

8.1 Introduction

This chapter focuses on the effect of combination treatment of MDM2-p53 antagonists Nutlin-3/RG7388 or cisplatin with rucaparib, a PARP-1 inhibitor also known as AG014699 or PF-01367338 (McCrudden *et al.*, 2015), in a panel of ovarian cancer cell lines. Due to the high rate of *BRCA1*, *BRCA2* mutations and BRCAness, ovarian cancer sensitivity to PARP inhibitors has been explored and clinical trials are ongoing (Rigakos and Razis, 2012; Stordal *et al.*, 2013; O'Sullivan *et al.*, 2014). Data presented in chapter 6 confirmed the sensitivity of wild-type *TP53* ovarian cancer cell lines to Nutlin-3/RG7388 as a single agent.

Mechanistically, rucaparib inhibits the Base Excision Repair pathway (BER) as a result of PARP inhibition. Unrepaired single-strand DNA breaks are converted to double-strand breaks at fork replication, which do not get repaired accurately in deficient-HRR (Homologous Recombination Repair) cells (Underhill *et al.*, 2011; Bai *et al.*, 2015). These unrepaired double strand breaks lead to increased levels of p53 due to persistence of unpaired DNA.

Findings about the interplay between p53 and PARP are controversial (Valenzuela *et al.*, 2002; Jelinic and Levine, 2014; Bai *et al.*, 2015). It was hypothesized that following combination treatment of Nutlin-3/RG7388 with rucaparib the p53 pathway is activated by inhibition of PARP and further induction and stabilisation of p53 via Nutlin-3/RG7388 treatment would result in more growth arrest and/or apoptosis in wild-type *TP53* ovarian cancer cell lines.

This chapter set out to evaluate the effect of combined treatment of Nutlin-3/RG7388 or cisplatin with rucaparib in a panel of ovarian cancer cell lines in regard to the effect on growth arrest, p53 downstream pathway activation and cell cycle progression.

8.1.1 Rucaparib (AG014699, PF-01367338)

Rucaparib is one of a series of tricyclic benzimidazole carboxamide PARP inhibitors with a Ki of 1.4 nM for PARP1 in a cell-free assay. It was the first PARP inhibitor to enter into clinical trials as a chemopotentiator (Figure 8-1) (Thomas *et al.*, 2007; McCrudden *et al.*, 2015). It was successfully granted a license by the FDA in 2015 for use as a monotherapy for patients with *BRCA1/2* mutant advanced ovarian cancer after at least two prior lines of platinum-based chemotherapy. It inhibits DNA BER via both inhibition of PARP enzyme activity and formation of trapped PARP-DNA complexes (Brown *et al.*, 2016). It has off-target effects for 9 protein kinases in the 1.2-18 micromolar range, demonstrating less selectivity compared to olaparib as a PARP inhibitor (Antolín and Mestres, 2014).

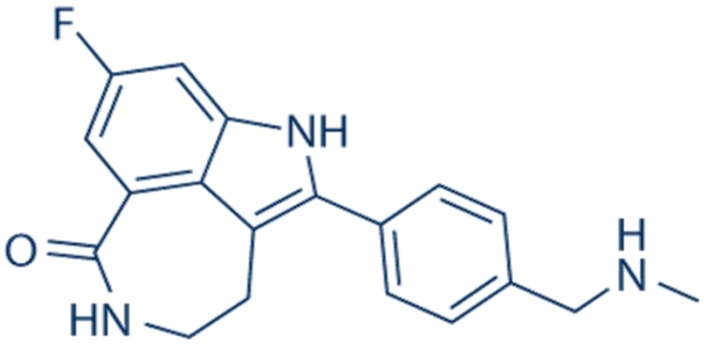

Figure 8-1: Chemical structure of rucaparib.

8.2 Hypothesis and Objectives

Hypothesis:

1. Combined treatment of MDM2-p53 antagonists Nutlin-3/ RG7388 or cisplatin with rucaparib increases growth inhibition and/or apoptosis in ovarian cancer cell lines compared to either agent alone.

Objectives:

1. To test a panel of established wild-type *TP53* ovarian carcinoma cell lines for their response to combination treatment of Nutlin-3/RG7388 with rucaparib and determine the synergistic, additive or antagonistic effect of combination.
2. To investigate the effect of combined treatment of cisplatin with rucaparib on a panel of wild-type *TP53* ovarian cancer cell lines and determine the synergistic, additive or antagonistic effect of combination.

8.3 Specific Materials and Methods

8.3.1 Cell lines

The same panel of cell lines described in chapter 6.3.1 was used for the experiments in this chapter.

8.3.2 Growth inhibition assay and combined treatments

Growth inhibition curves for 72 hours were constructed using SRB assay and GI_{50} values were calculated as described in general Materials and Methods (2.8). Based on the growth curves, the appropriate cell densities were chosen when cells were in exponential phase of growth and treated with different concentrations of rucaparib (0.4-25 μM).

Combination treatment of Nutlin-3/RG7388 or cisplatin with rucaparib was performed as described in chapter 7.3.2.

8.3.3 Western blot

2 x 10^5 cells were seeded in a small dish T25 for western blot analysis and left for 48 hours to adhere and grow. To investigate the effect of combined treatment of Nutlin-3/RG7388 or cisplatin with rucaparib on the p53 pathway, cells were treated with each agent alone and in simultaneous combination at constant 1:1 ratios of 1/2x and 1x their respective GI_{50} concentrations. The lysates were extracted following 4 hours treatment. The antibodies used and their details are found in chapter 2.11.7.

8.3.4 Flow cytometry

Flow cytometry was performed to analyse cell cycle distribution changes and induced apoptosis over 24, 48 and 72 hours after treatment as described in general Materials and Methods (2.14.3 & 2.14.4) and chapter 7.3.4.

8.3.5 Clonogenic cell survival assay

Clonogenic survival assays were performed for the panel of 6 ovarian cancer cell lines as described in section 2.9.

8.3.6 Statistical analysis

The statistical paired t-test or Mann-Whitney test was used to compare the mean of 3 or more paired biological repeats and the p-value <0.05 were considered statistically significant.

8.4 Results

8.4.1 The growth inhibitory response of ovarian cancer cell lines to rucaparib

The cells were treated with a wide range of rucaparib concentrations (0.4-25 µM) for 72 hours to construct growth inhibition curves and calculate the GI_{50} values. The GI_{50} values significantly varied showing a range of responses, with A2780 (3.26±0.47 µM) and SKOV-3 (> 25 µM) as the most sensitive and resistant cell lines respectively (Figure 8-2). Across mutant *TP53* cell lines, there was a direct correlation between cisplatin sensitivity and response to rucaparib (Table 8-1). The results of this study showed no relationship between the status of *TP53* and response to rucaparib (Mann-Whitney, $p>0.05$) (Figure 8-3).

Cell line	*TP53* Status	Rucaparib (µM)	Cisplatin (µM)
A2780	Wild-type	3.26 ± 0.47	0.82 ± 0.17
IGROV-1	Wild-type	11.34 ± 0.05	0.85 ± 0.04
OAW42	Wild-type	19.00 ± 0.58	0.73 ± 0.02
CP70	Mutant	17.00 ± 0.64	5.8 ± 1.1
***MLH1*-corrected CP70+**	Mutant	14.00 ± 2.84	2.4 ± 0.25
MDAH-2774	Mutant	6.92 ± 1.48	1.11± 0.14
SKOV-3	Mutant	>25	8.8 ± 0.49

Table 8-1: GI_{50} concentrations of rucaparib and cisplatin for the panel of ovarian cancer cell lines of varying *TP53* status. Data represent the mean of at least three independent experiments ± SEM.

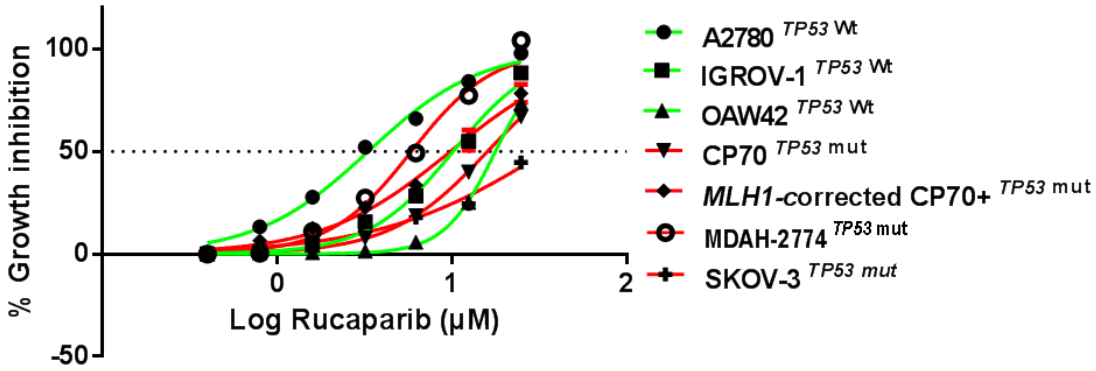

Figure 8-2: Growth inhibition curves demonstrating the effect of rucaparib for a panel of ovarian cancer cell lines. Data represent the mean of at least three independent experiments. Wt, Wild-type; mut, Mutant.

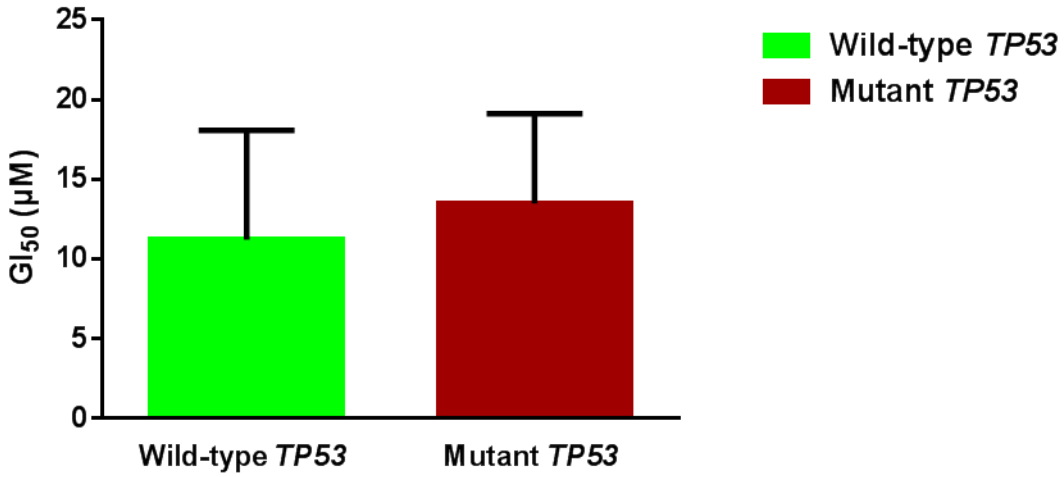

Figure 8-3: The sensitivity to rucaparib in a panel of wild-type and mutant *TP53* ovarian cancer cell lines. The *TP53* status has no effect on the sensitivity of cell lines in response to rucaparib (Mann-Whitney, *p>0.05*). Data shown are the average of at least three independent experiments and error bars represent SEM.

8.4.2 Rucaparib synergises with Nutlin-3/RG7388 and cisplatin for growth inhibition of wild-type *TP53* ovarian cancer cell lines

The effect of rucaparib in combination with Nutlin-3/RG7388 or cisplatin was investigated for three wild-type *TP53* ovarian cancer cell lines using median-effect analysis. The sensitivity of the wild-type *TP53* cell lines to growth inhibition during 72 hours exposure to rucaparib, Nutlin-3/RG7388 and cisplatin was determined as single agents, and in combination at 5 equipotent concentrations between 0.25× and 4× their respective GI_{50} concentrations for the A2780 cell line. Owing to the high GI_{50} for IGROV-1 and OAW42 in response to rucaparib, 3 equipotent concentrations between 0.25× and 1x their respective GI_{50} concentrations were used to evaluate the combination effect of rucaparib with cisplatin or Nutlin-3/RG7388. The effect of combined treatment was cell type and compound dependent. Overall, greater synergy was observed with the combination of rucaparib and Nutlin-3/RG7388 compared to the combination of rucaparib with cisplatin. The combination of rucaparib with Nutlin-3/RG7388 or cisplatin at all concentrations led to greater growth inhibition compared to either agent alone for the A2780 and IGROV-1 cell lines (Figure 8-4 & Figure 8-5). As shown in Figure 8-4, combination treatment of rucaparib with cisplatin or with Nutlin-3/RG7388 at concentrations equal and lower than the individual 1x GI_{50} dose resulted in more growth arrest compared to doses higher than 1x GI_{50} for the A2780 cell line. For the OAW42 cell line, there was little change in the growth inhibitory effect of rucaparib combination with cisplatin compared to either agent alone while the combination of rucaparib with RG7388/Nutlin-3 resulted in more growth inhibition compared to either agent alone (Figure 8-6).

To determine whether the observed differences in growth inhibition were additive, synergistic or antagonistic, the data were analysed using median-effect analysis and CI values calculated. CI values for each constant ratio combination and at effect levels of ED_{50}, ED_{75} and ED_{90} were computed and the average of CI values at ED_{50}, ED_{75} and ED_{90} was also determined (Figure 8-7 & Table 8-2). Combined treatment of rucaparib with Nutlin-3/RG7388 ranged from additive to strong synergism based on the CI at ED_{50} and overall CI for A2780 and IGROV-1 cell lines, whereas only slight synergism to antagonism was observed for the OAW42 cell line (Figure 8-7 & Table 8-2). Although the effect of combination treatment of rucaparib with cisplatin based on the CI at ED_{50} was antagonist, additive and synergistic for OAW42, IGROV-1 and A2780 respectively, it was antagonistic based on overall CI across all three cell lines. Interestingly, rucaparib, Nutlin-3, RG7388 and cisplatin had favourable DRI values for combined treatment

with all experimental values, aside from two cases, ranging from 1.2-fold to 7.8-fold dose reduction (Table 8-3).

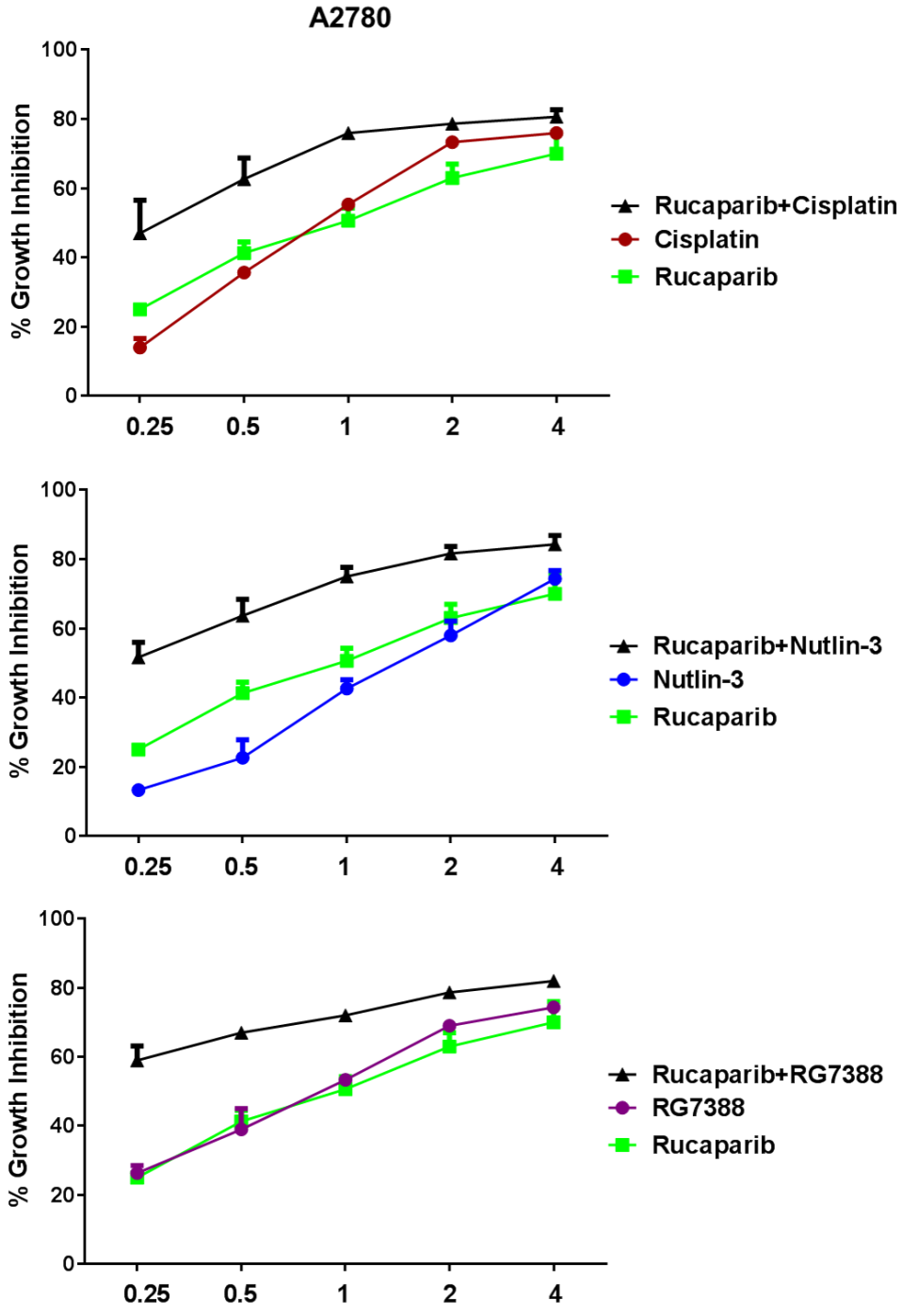

Figure 8-4: Growth inhibition curves for the A2780 cell line exposed to rucaparib, Nutlin-3/RG7388 or cisplatin alone, and in combination at constant 1:1 ratios of 0.25x, 0.5x, 1x, 2x and 4x their respective GI_{50} concentrations for 72 hours. Data are shown as the average of at least three independent experiments and error bars represent SEM.

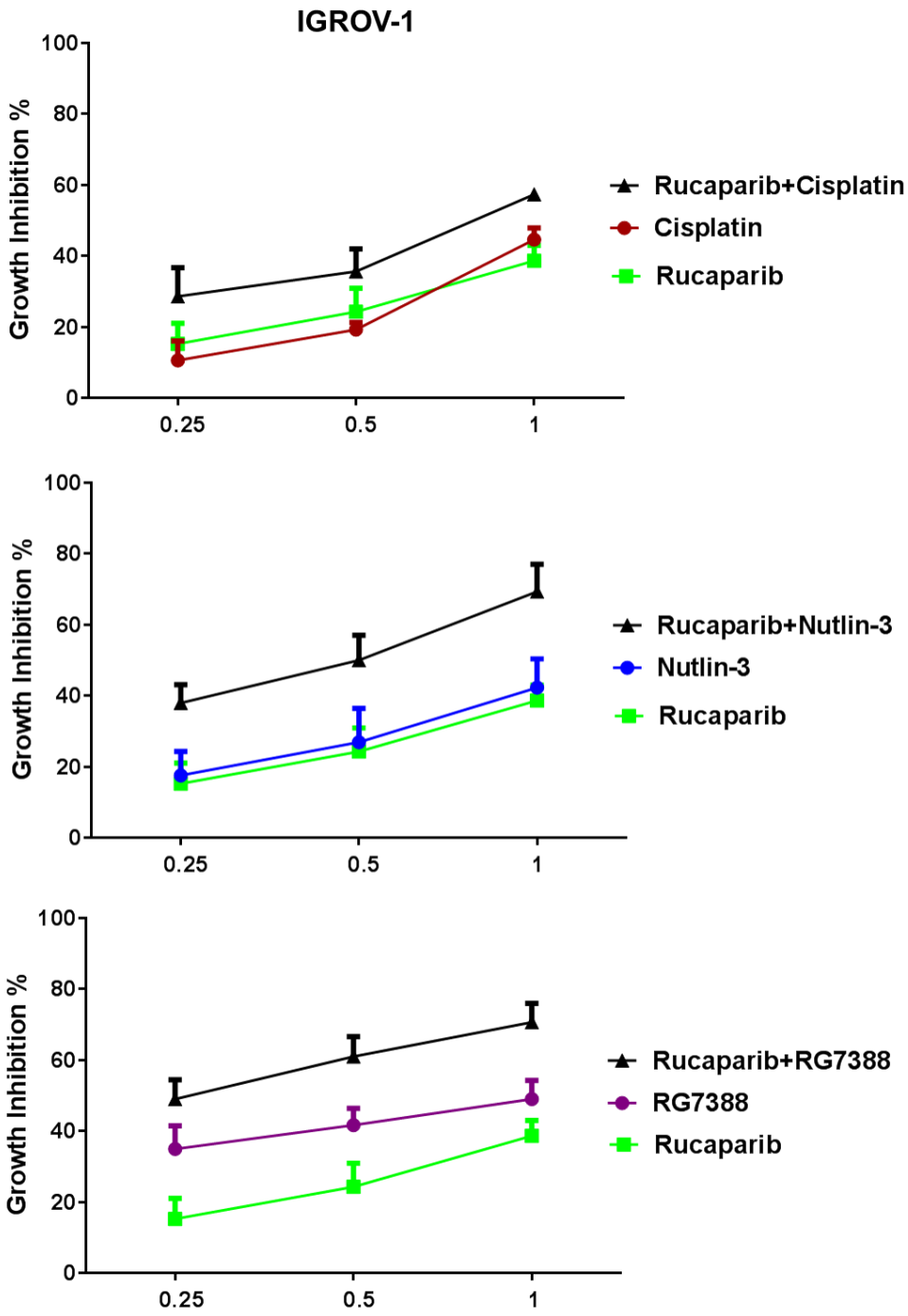

Figure 8-5: Growth inhibition curves for the IGROV-1 cell line exposed to rucaparib, Nutlin-3/RG7388 or cisplatin alone, and in combination at constant 1:1 ratios of 0.25x, 0.5x and 1x their respective GI_{50} concentrations for 72 hours. Data are shown as the average of at least three independent experiments and error bars represent SEM.

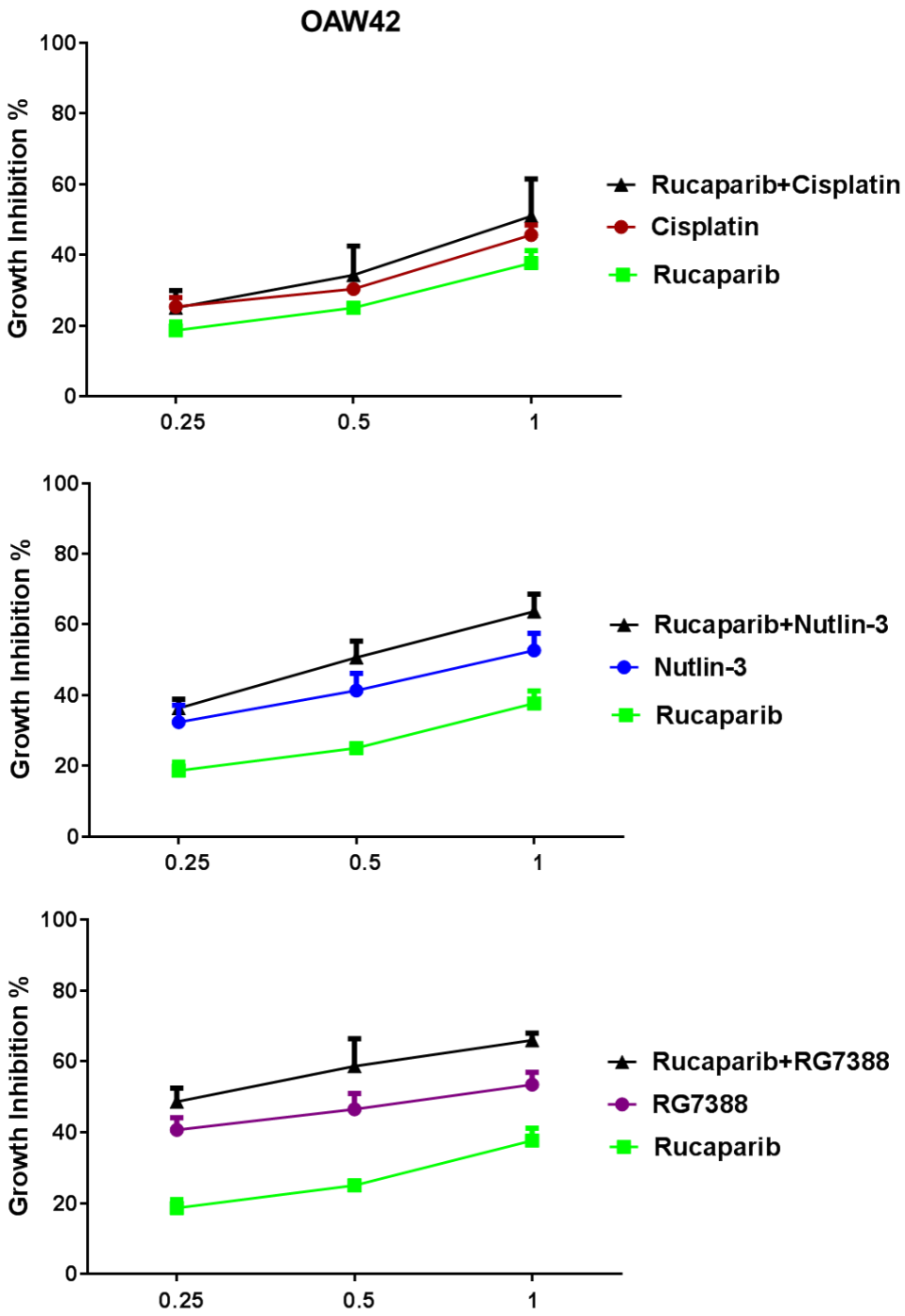

Figure 8-6: Growth inhibition curves for the OAW42 cell line exposed to rucaparib, Nutlin-3/RG7388 or cisplatin alone, and in combination at constant 1:1 ratios of 0.25x, 0.5x and 1x their respective GI_{50} concentrations for 72 hours. Data are shown as the average of at least three independent experiments and error bars represent SEM.

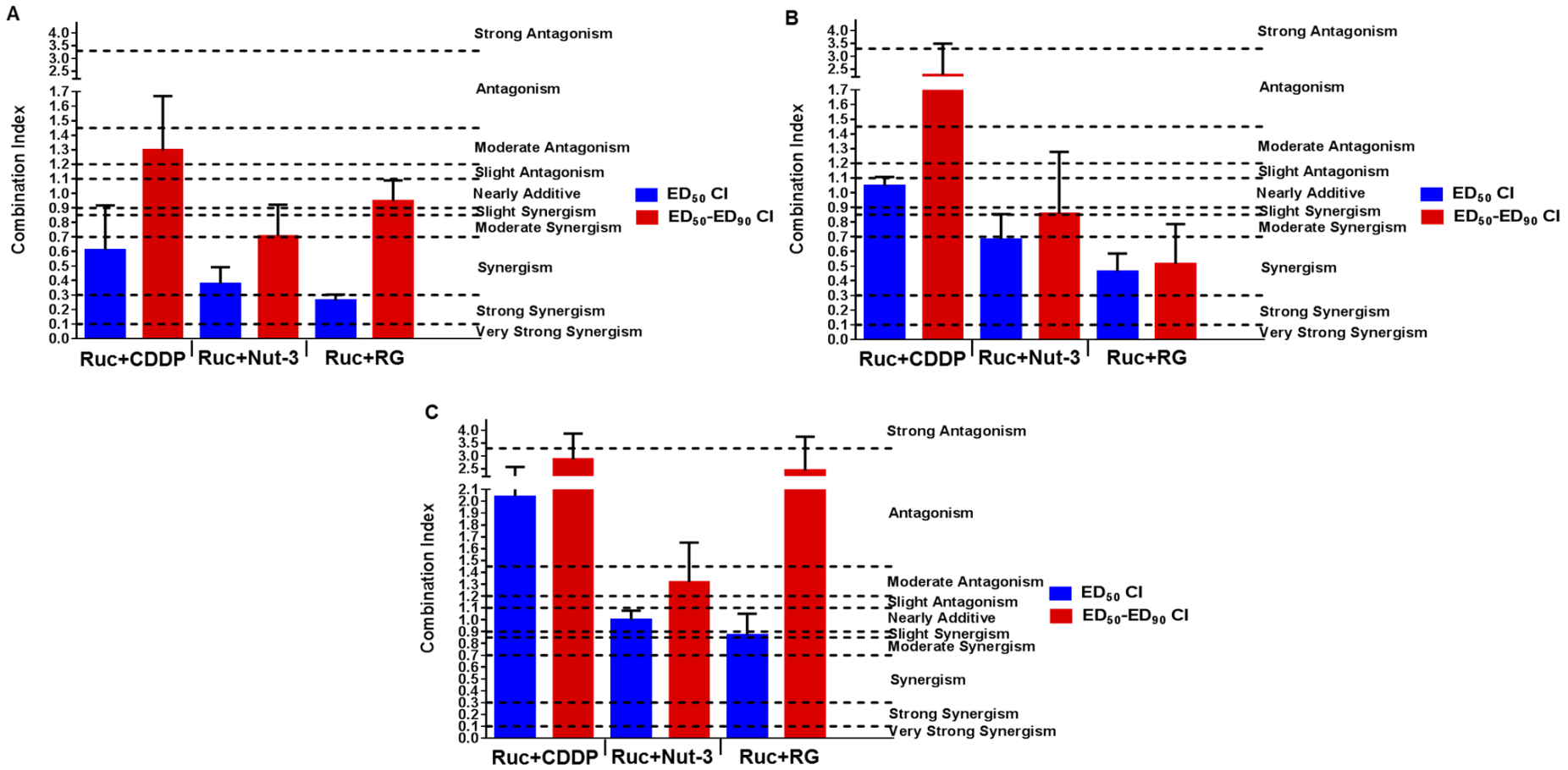

285

Figure 8-7: The growth inhibition combination index (CI) values for rucaparib in combination with cisplatin or Nutlin-3/RG7388 at the ED_{50} and the average of CI values at effect levels ED_{50}, ED_{75} and ED_{90} for three wild-type *TP53* ovarian cancer cell lines. (A) A2780, (B) IGROV-1 and (C) OAW42. Data are shown as the average of at least three independent experiments and error bars represent SEM. CI, Combination index; Ruc, Rucaparib; Nut-3, Nutlin-3; RG, RG7388; CDDP, Cisplatin; ED, Effective dose.

Cell Line	Combination	CI XGI_{50} 0.25	0.5	1	2	4	CI ED_{50}	CI ED_{75}	CI ED_{90}	CI Average ED_{50-90}
A2780	Rucaparib+Cisplatin	**0.6**	**0.6**	**0.6**	1.0	1.7	**0.5**	**0.9**	2.0	1.1
	Rucaparib+Nutlin-3	**0.4**	**0.5**	**0.5**	**0.6**	1.0	**0.4**	**0.6**	1.1	**0.7**
	Rucaparib+RG7388	**0.4**	**0.4**	**0.6**	**0.7**	1.2	**0.3**	**0.7**	1.9	**0.9**
IGROV-1	Rucaparib+Cisplatin	**0.8**	1.0	1.1	ND	ND	1.0	3.1	2.7	2.3
	Rucaparib+Nutlin-3	**0.6**	**0.7**	**0.6**	ND	ND	**0.7**	**0.8**	1.1	**0.9**
	Rucaparib+RG7388	**0.4**	**0.4**	**0.3**	ND	ND	**0.5**	**0.4**	**0.7**	**0.5**
OAW42	Rucaparib+Cisplatin	1.2	1.8	1.5	ND	ND	2.0	2.7	3.8	2.9
	Rucaparib+Nutlin-3	**0.9**	**0.7**	**0.9**	ND	ND	1.0	1.3	1.7	1.3
	Rucaparib+RG7388	**0.9**	**0.8**	**0.9**	ND	ND	**0.9**	2.8	3.6	2.4

Table 8-2: Growth inhibition CI values for rucaparib in combination with cisplatin or Nutlin-3/RG7388 for the wild-type *TP53* ovarian cancer cell lines. The combined treatment was performed at the indicated fixed 1:1 ratios relative to their respective GI_{50} concentrations. CI values were calculated for each constant ratio combination and at effect levels ED_{50}, ED_{75} and ED_{90} from the average of at least three independent experiments. CI Average ED_{50-90} represents the average of CI values at effect levels of ED_{50}, ED_{75} and ED_{90}. CI range: < 0.1 very strong synergism; 0.1-0.3 strong synergism; 0.3-0.7 synergism; 0.7-0.85 moderate synergism; 0.85-0.9 slight synergism; 0.9-1.1 nearly additive; 1.1-1.2 slight antagonism; 1.2-1.45 moderate antagonism; 1.45-3.3 antagonism; 3.3-10 strong antagonism; > 10 very strong antagonism. Synergistic combinations are highlighted in bold font. CI, Combination index; ED, Effective dose.

Cell Line	Combination	Compound	DRI				
			XGI_{50}				
			0.25	0.5	1	2	4
A2780	Rucaparib+Cisplatin	Rucaparib	**1.9**	**2.5**	**3.4**	**2.0**	**1.2**
		Cisplatin	**4.2**	**3.6**	**2.9**	**1.7**	1.0
	Rucaparib+Nutlin-3	Rucaparib	**3.1**	**2.7**	**3.0**	**2.5**	**1.6**
		Nutlin-3	**5.00**	**3.9**	**3.6**	**2.6**	**1.6**
	Rucaparib+RG7388	Rucaparib	**5.4**	**4.0**	**3.1**	**2.5**	**1.4**
		RG7388	**5.1**	**4.4**	**3.0**	**2.4**	**1.6**
IGROV-1	Rucaparib+Cisplatin	Rucaparib	**2.5**	**1.7**	**2.1**	ND	ND
		Cisplatin	**3.7**	**2.4**	**2.8**	ND	ND
	Rucaparib+Nutlin-3	Rucaparib	**3.5**	**3.0**	**3.9**	ND	ND
		Nutlin-3	**3.5**	**2.8**	**3.3**	ND	ND
	Rucaparib+RG7388	Rucaparib	**5.7**	**5.0**	**3.7**	ND	ND
		RG7388	**2.7**	**3.9**	**7.8**	ND	ND
OAW42	Rucaparib+Cisplatin	Rucaparib	**2.3**	**1.6**	**1.9**	ND	ND
		Cisplatin	**1.9**	**1.2**	**1.2**	ND	ND
	Rucaparib+Nutlin-3	Rucaparib	**4.3**	**4.0**	**3.0**	ND	ND
		Nutlin-3	**2.0**	**2.1**	**1.8**	ND	ND
	Rucaparib+RG7388	Rucaparib	**5.8**	**5.2**	**3.3**	ND	ND
		RG7388	**1.3**	**1.6**	0.9	ND	ND

Table 8-3: DRI values for growth inhibition by rucaparib in combination with cisplatin or RG7388/Nutlin-3 for the wild-type *TP53* ovarian cancer cell lines. The combined treatment was performed at the indicated fixed 1:1 ratios relative to their respective GI_{50} concentrations. DRI values were calculated for each constant ratio combination from the average of at least three independent experiments. Favourable DRI values are highlighted in bold font. DRI, Dose reduction index.

8.4.3 The effect of combination treatment with rucaparib and Nutlin-3/RG7388 or cisplatin on activation of the p53 pathway

Western blotting was used to investigate the effect of combination treatment on the p53 molecular pathway. Wild-type *TP53* cell lines were treated with rucaparib, Nutlin-3/RG7388 or cisplatin alone, and in combination at constant 1:1 ratios of 1/2x and 1x their respective GI_{50} concentrations for 4 hours. Western blot analysis showed that rucaparib treatment as a single agent had no effect on p53 stabilisation, upregulation of $p21^{WAF1}$or MDM2 compared to DMSO control (Figure 8-8 & Figure 8-9). Combination treatment of rucaparib with Nutlin-3/RG7388 in all cases led to greater levels of p53 stabilization, together with $p21^{WAF1}$ and MDM2 upregulation only compared to rucaparib on its own. However, rucaparib caused no increase in the effect of MDM2 inhibitors on the p53 pathway. Rucaparib in combination with Nutlin-3/RG7388 seems to increase stabilisation of p53 and its downstream transcriptional targets in some cases in IGROV-1, but otherwise there are no convincing differences. No evidence of synergy was observed at the molecular level to indicate that the mechanism of synergy involved enhancement of the p53 pathway activation by MDM2 inhibitors (Figure 8-8).

In contrast, combination of rucaparib with cisplatin had no effect on p53 stabilisation and upregulation of $p21^{WAF1}$ and MDM2 compared to either agent alone with the exception of A2780 and IGROV-1 cells treated with combination of rucaparib and cisplatin at constant 1:1 ratio of their respective GI_{50} concentrations. Under these conditions there was a slight increase and decrease in upregulation of $p21^{WAF1}$ compared to either agent alone respectively (Figure 8-9).

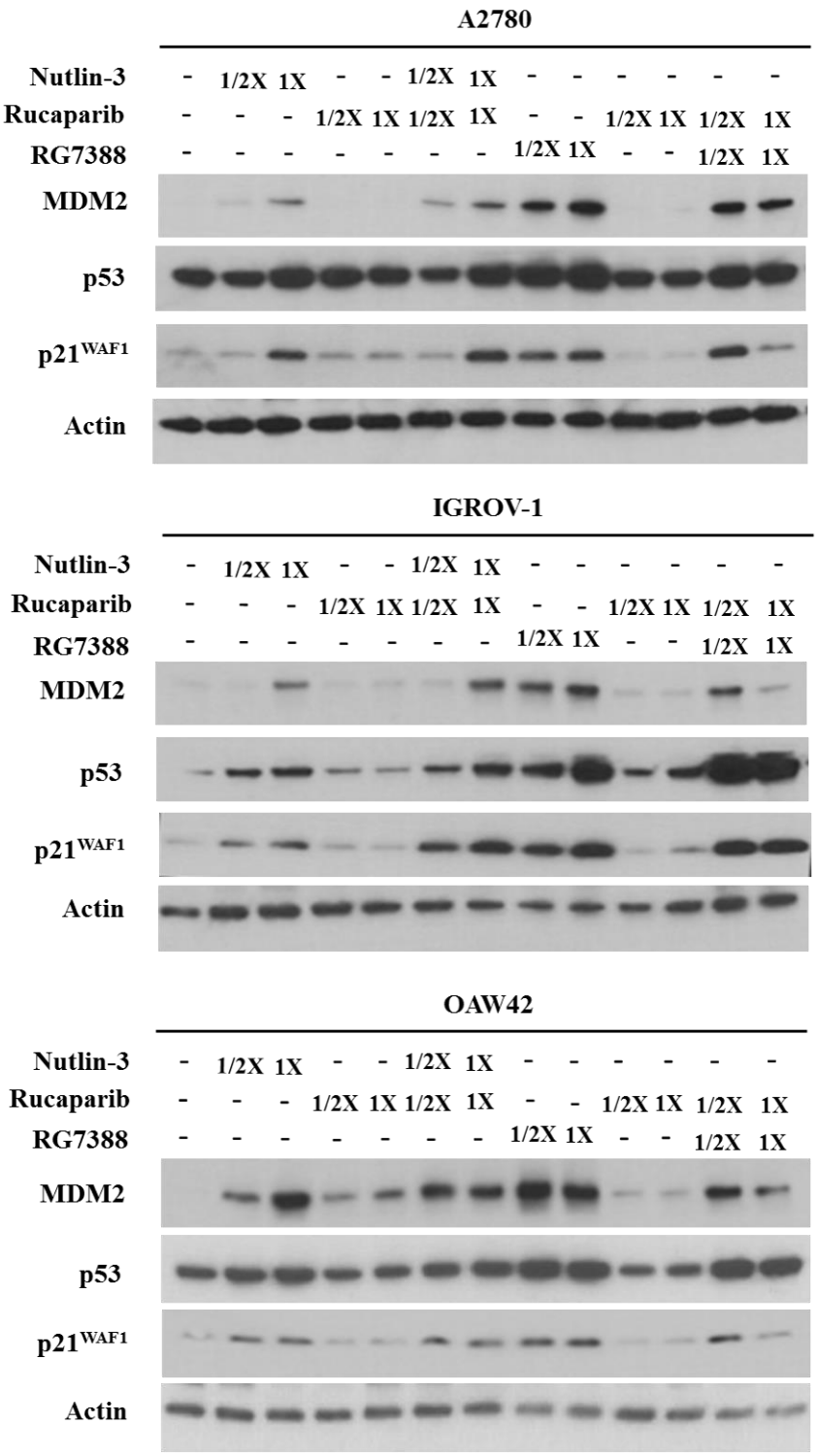

Figure 8-8: Combination of rucaparib with Nutlin-3/RG7388 increased stabilization of p53 and upregulation of its downstream targets, MDM2 and $p21^{WAF1}$ compared to rucaparib on its own but not compared to Nutlin-3/RG7388. Total levels of p53, $p21^{WAF1}$, MDM2 4 hours after the commencement of treatment with rucaparib alone and in combination with Nutlin-3/RG7388 at constant 1:1 ratios of 1/2x and 1x their respective GI_{50} concentrations analysed by western blot in three wild-type *TP53* ovarian cancer cell lines.

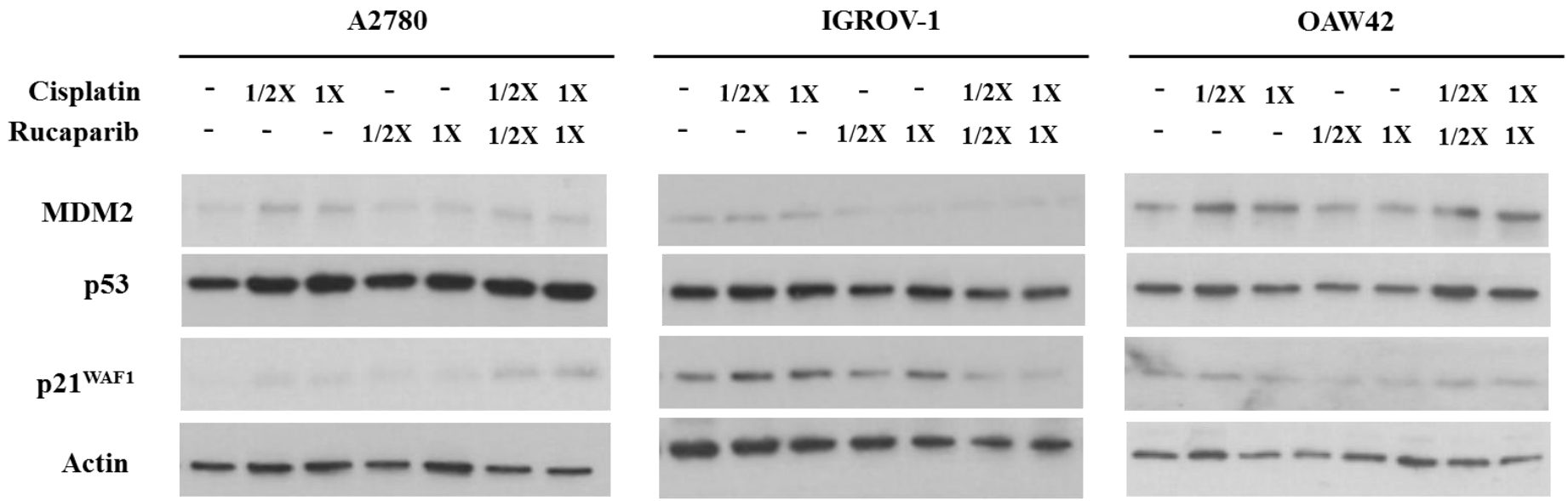

290

Figure 8-9: Combination of rucaparib with cisplatin had little or no effect on the stabilization of p53 and upregulation of its downstream targets, MDM2 and $p21^{WAF1}$ compared to either agent alone. Total levels of p53, $p21^{WAF1}$,and MDM2 4 hours after the commencement of treatment with rucaparib alone and in combination with cisplatin at constant 1:1 ratios of 1/2x and 1x their respective GI_{50} concentrations analysed by western blot in three wild-type *TP53* ovarian cancer cell lines.

8.4.4 Rucaparib in combination with Nutlin-3/RG7388 or cisplatin induces cell cycle distribution changes and/or apoptosis in wild-type *TP53* ovarian cancer cell lines

Wild-type *TP53* cell lines were treated with rucaparib and Nutlin-3/RG7388 or cisplatin, alone and in simultaneous combination at constant 1:1 ratios of 1/2x and 1x their respective GI_{50} concentrations for 24, 48 and 72 hours. Then, they were analysed by flow cytometry for cell cycle phase distribution changes and evidence of apoptosis in response to treatment.

8.4.4.1 The effect of rucaparib in combination with Nutlin-3 on cell cycle distribution and SubG1 events in wild-type *TP53* ovarian cancer cell lines

Rucaparib slightly increased the proportion of cells in G2/M phase and the number of SubG1 events in a dose and time-dependent manner. Combination treatment of rucaparib with Nutlin-3 resulted in an increased percentage of cells in the G2/M cell cycle phase compared to either agent alone, in a treatment time and dose-dependent manner for A2780 and IGROV-1 cell lines (Figure 8-10 & Figure 8-11). For the OAW42 cell line after 24 hours, it led to an increased proportion of the cell population in the G2/M phase of the cell cycle compared to Nutlin-3 as a single agent. After 48 and 72 hours, there was little change in the cell cycle distribution following combination of rucaparib with Nutlin-3 compared to either agent alone (Figure 8-12). Across all 3 cell lines, in most cases combination treatments also induced SubG1 events in a concentration and time-dependent manner (Figure 8-10, Figure 8-11 & Figure 8-12).

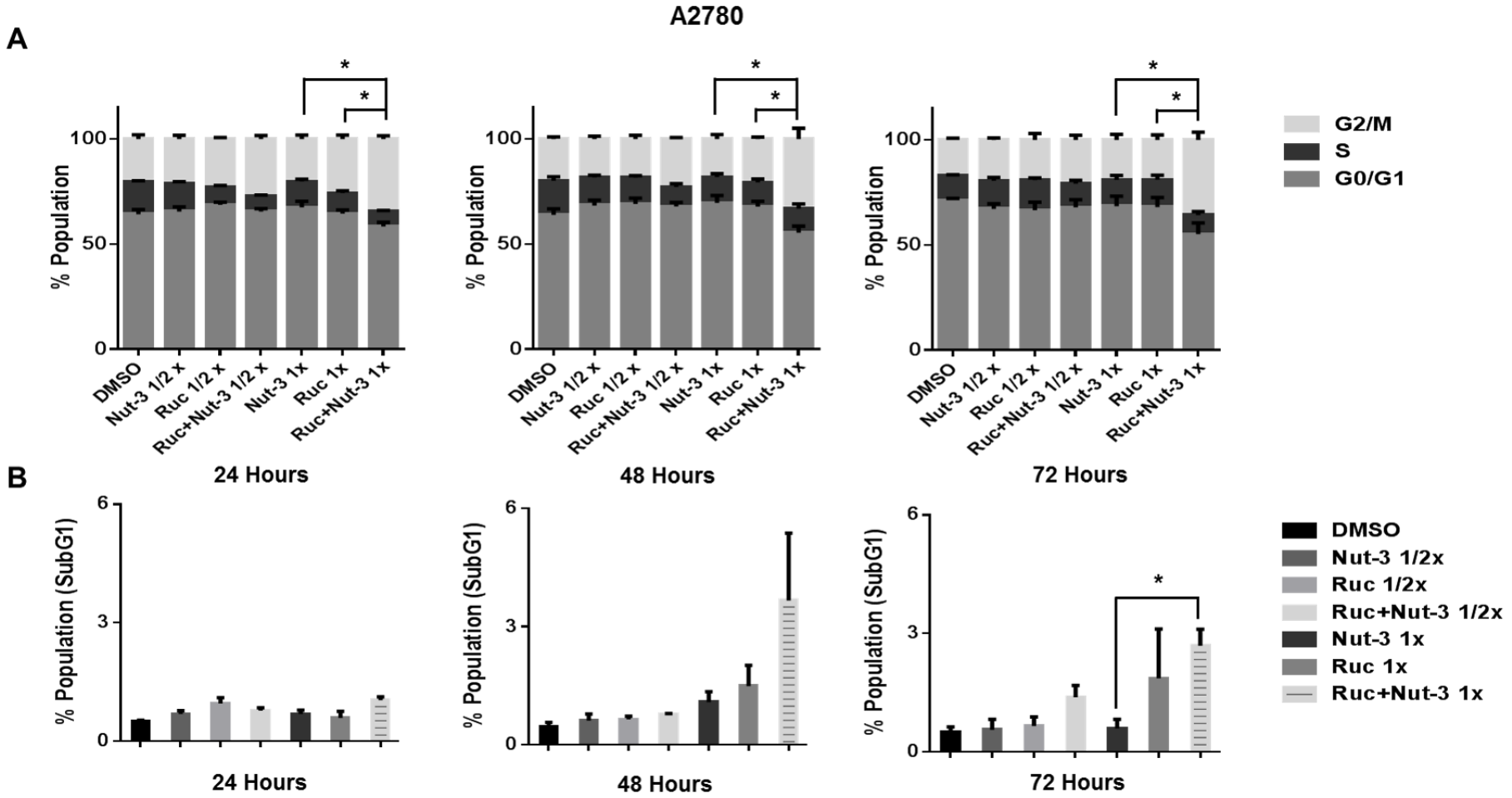

292

Figure 8-10: Combination of rucaparib with Nutlin-3 affects the cell cycle distribution and apoptotic endpoints. A2780 cells were treated for 24, 48 and 72 hours with rucaparib or Nutlin-3 alone and at constant 1:1 ratios of 1/2x and 1x their respective GI_{50} concentrations. Combination of rucaparib with Nutlin-3 led to an increased proportion of cells in G2/M phase (A) and an increased % of SubG1 signals (B) compared to Nutlin-3 and/or rucaparib alone in a time and dose-dependent manner. Nut-3, Nutlin-3; Ruc, Rucaparib; *, *$p<0.05$*. Data are shown as the average of at least three independent experiments and error bars represent SEM.

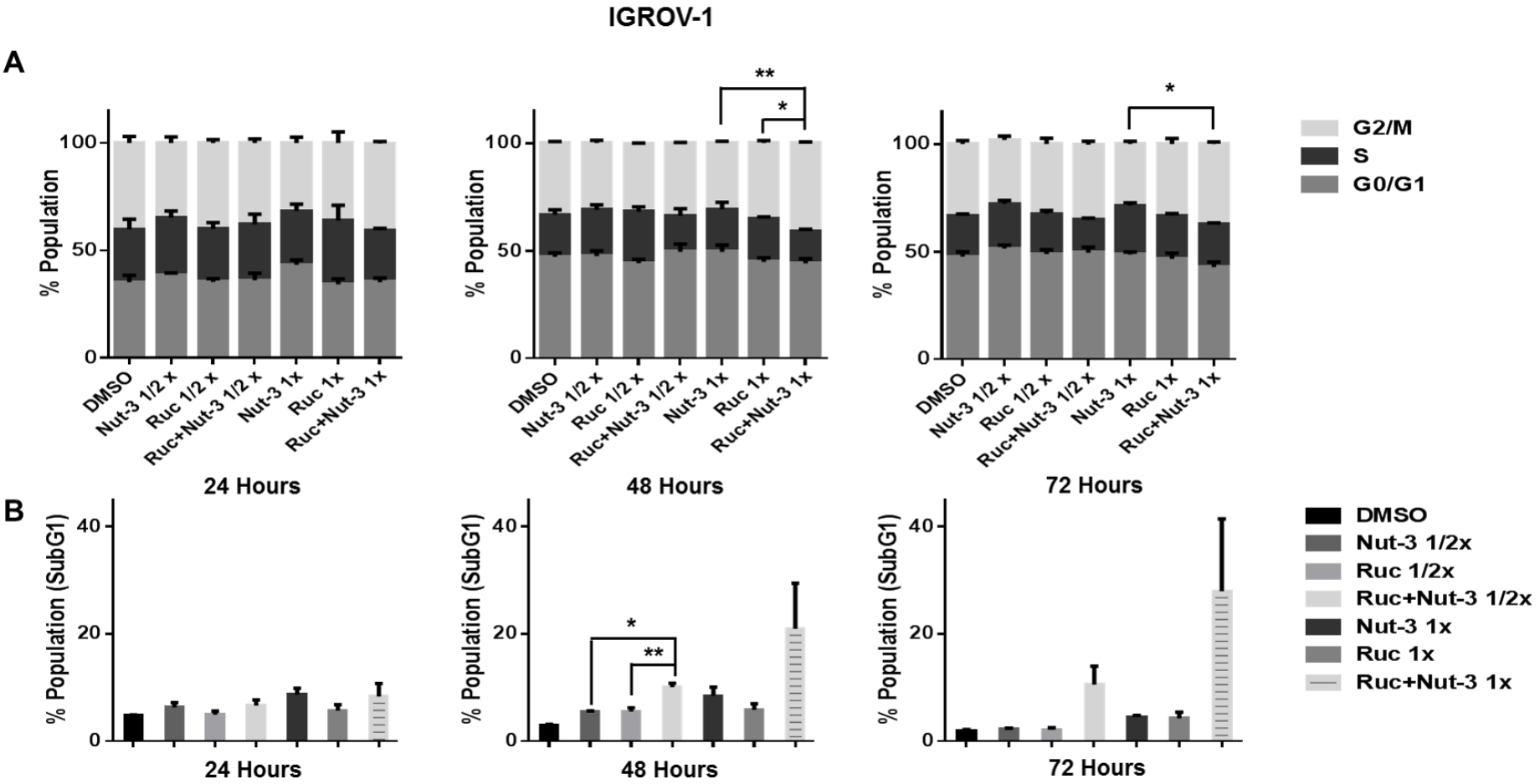

293

Figure 8-11: Combination of rucaparib with Nutlin-3 affects the cell cycle distribution and apoptotic endpoints. IGROV-1 cells were treated for 24, 48 and 72 hours with rucaparib or Nutlin-3 alone and at constant 1:1 ratios of 1/2x and 1x their respective GI_{50} concentrations. Combination of rucaparib with Nutlin-3 led to an increased proportion of cells in G2/M phase (A) and % of SubG1 signals (B) compared to rucaparib and/or Nutlin-3 alone in a time and dose-dependent manner. Nut-3, Nutlin-3; Ruc, Rucaparib; *, *p<0.05*; **, *p<0.01*. Data are shown as the average of at least three independent experiments and error bars represent SEM.

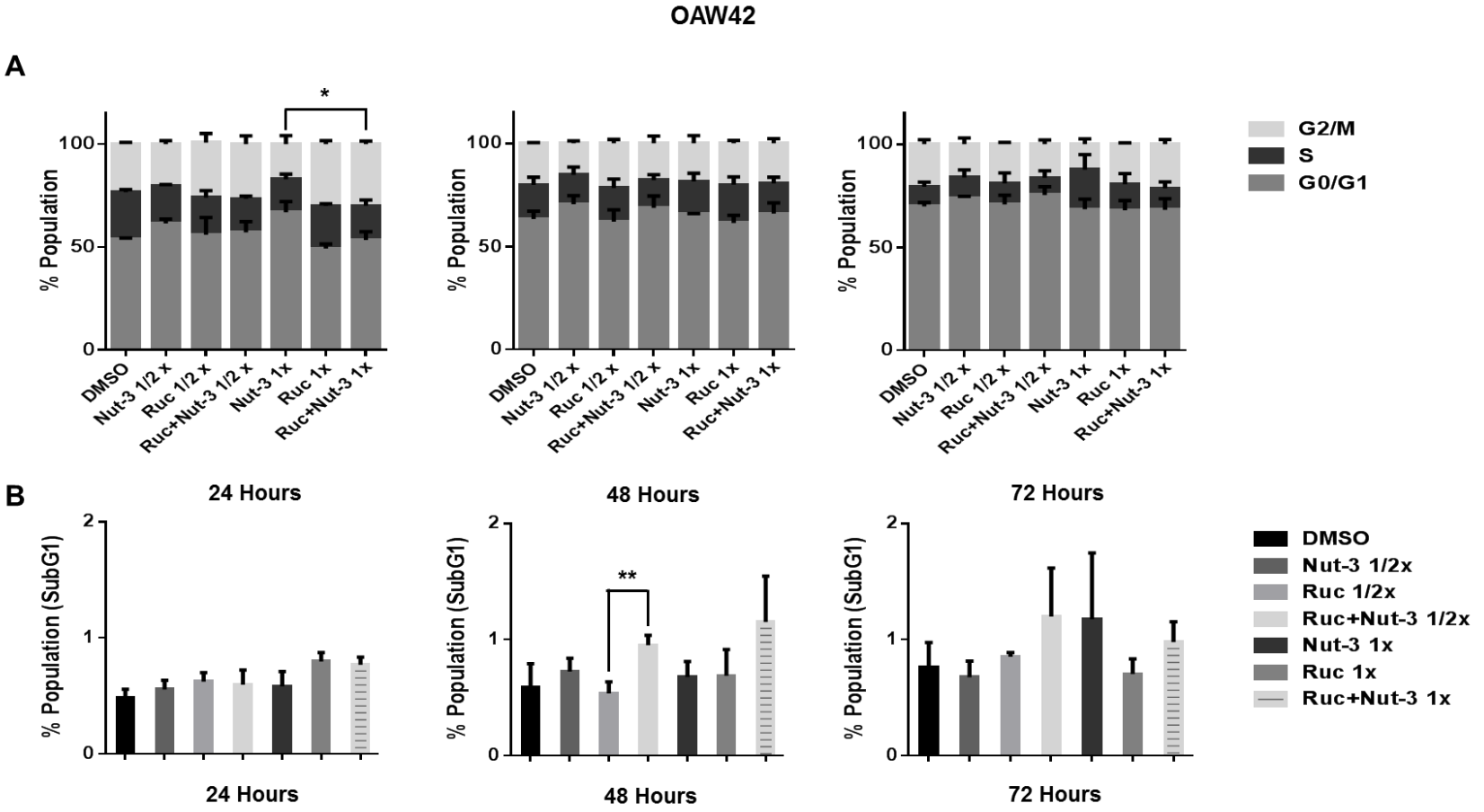

294

Figure 8-12: Combination of rucaparib with Nutlin-3 affects the cell cycle distribution and apoptotic endpoints. OAW42 cells were treated for 24, 48 and 72 hours with rucaparib or Nutlin-3 alone and at constant 1:1 ratios of 1/2x and 1x their respective GI_{50} concentrations. Combination of rucaparib with Nutlin-3 led to an increased proportion of cells in G2/M phase after 24 hours (A) and % SubG1 signals in most cases (B) compared to rucaparib and/or Nutlin-3 alone in a time and dose-dependent manner. Nut-3, Nutlin-3; Ruc, Rucaparib; *, *$p<0.05$*; **, *$p<0.01$*. Data are shown as the average of at least three independent experiments and error bars represent SEM.

8.4.4.2 The effect of Rucaparib in combination with RG7388 on cell cycle distribution and SubG1 events in wild-type *TP53* ovarian cancer cell lines

For A2780 cells, the combination of rucaparib with RG7388 increased the proportion of cells in G2/M phase and SubG1 signals compared to either agent alone, in a treatment time and dose-dependent manner, with the exception of SubG1 events after 24 hours. It also decreased the proportion of cells in S-phase compared to either agent alone (Figure 8-13). In terms of the proportional distribution of IGROV-1 cells in G0/G1 or G2/M, the effect of rucaparib combination with RG7388 was time dependent. Combined treatment for 24 and 48 hours led to proportionally more cells in G0/G1 compared to the effect of rucaparib on its own and a higher proportion of cells in G2/M compared to the effect of RG7388 alone. After 72 hours treatment, the combination of rucaparib with RG7388 resulted in increased G2/M cell cycle arrest compared to RG7388 on its own, with little change in the percentage of cells in G0/G1 cell cycle compared to rucaparib alone. Combined treatments also increased the percentage of SubG1 signals compared to either agent alone, in a time and dose-dependent manner (Figure 8-14). The effect of rucaparib combination with RG7388 for OAW42 cells is shown in Figure 8-15. Combination of rucaparib with RG7388 led to proportionally more G2/M cells and SubG1 signals compared to either agent alone. It also decreased the percentage of cells in S-phase compared to either agent alone after 24 and 48 hours.

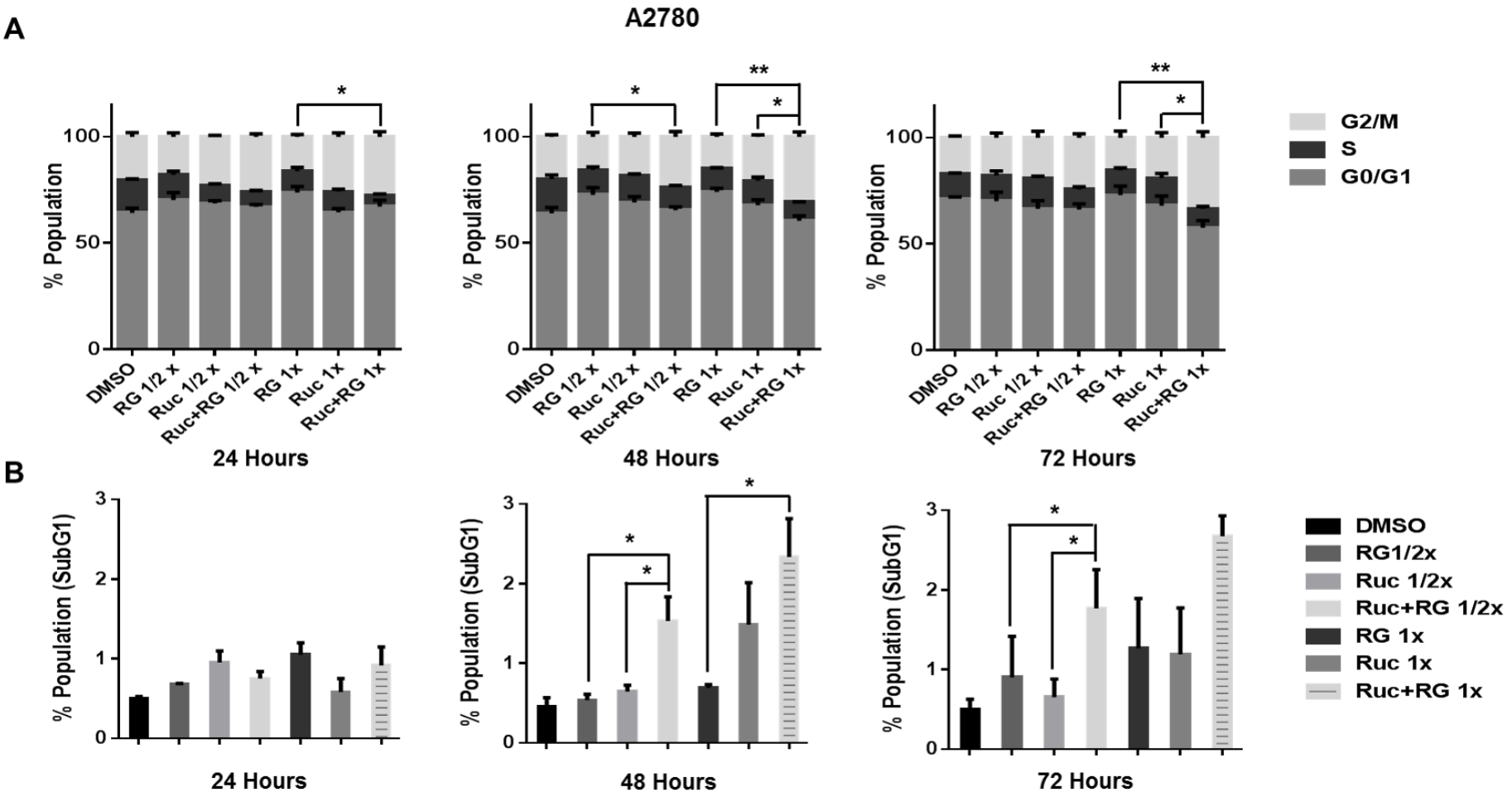

296

Figure 8-13: Combination of rucaparib with RG7388 affects the cell cycle distribution and apoptotic endpoints. A2780 cells were treated for 24, 48 and 72 hours with rucaparib or RG7388 alone and at constant 1:1 ratios of 1/2x and 1x their respective GI_{50} concentrations. Combination of rucaparib with RG7388 led to an increased proportion of cells in G2/M phase (A) and SubG1 signals (B) compared to either agent alone in most cases. RG, RG7388; Ruc, Rucaparib; *, *p<0.05*; **, *p<0.01*. Data are shown as the average of at least three independent experiments and error bars represent SEM.

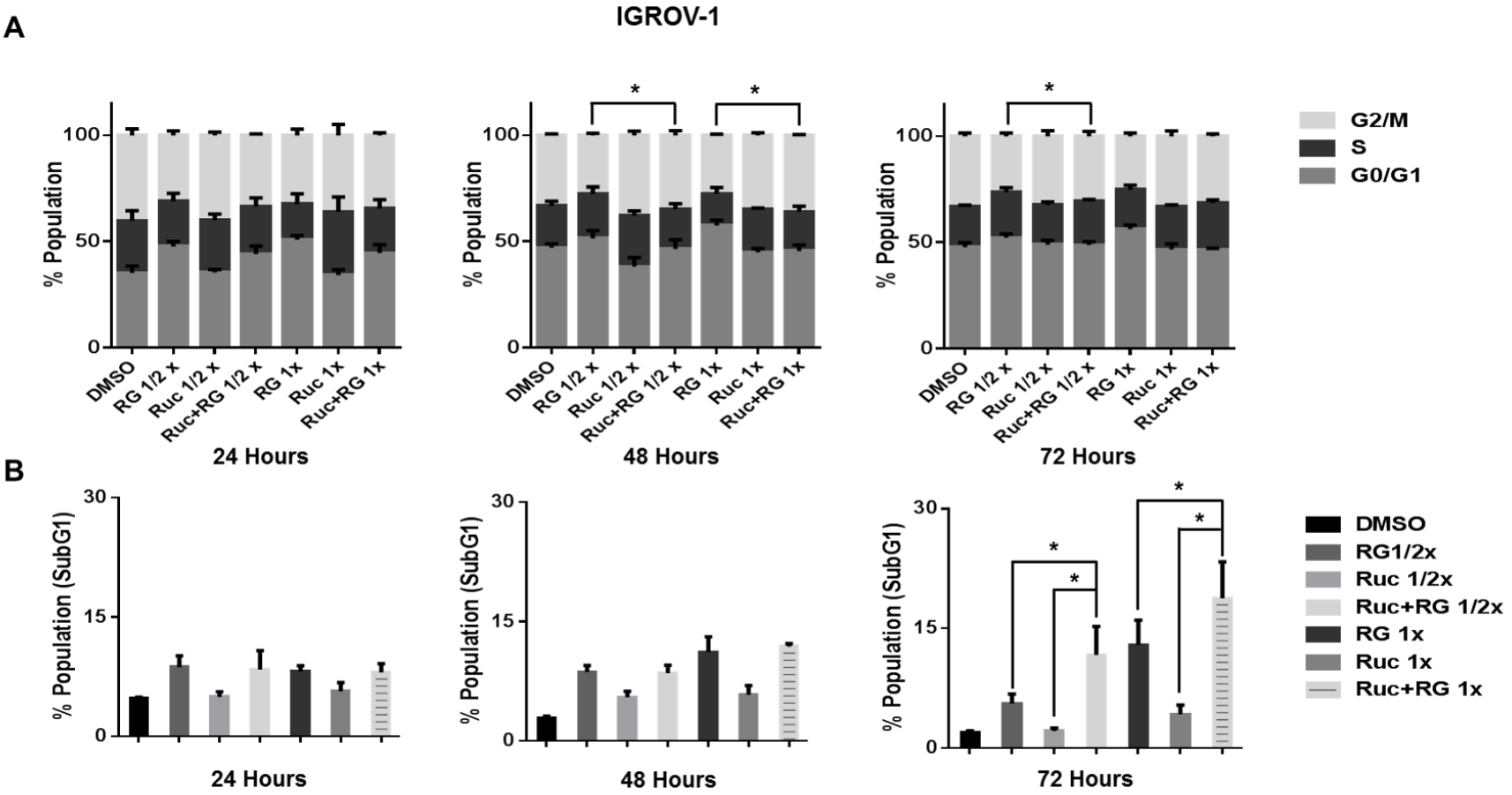

297

Figure 8-14: Combination of rucaparib with RG7388 affects the cell cycle distribution and apoptotic endpoints. IGROV-1 cells were treated for 24, 48 and 72 hours with rucaparib or RG7388 alone and at constant 1:1 ratios of 1/2x and 1x their respective GI_{50} concentrations. Combination of rucaparib with RG7388 led to an increased proportion of cells in G2/M phase compared to RG7388 on its own (A) and SubG1 signals compared to either agent alone (B). RG, RG7388; Ruc, Rucaparib; *, $p<0.05$. Data are shown as the average of at least three independent experiments and error bars represent SEM.

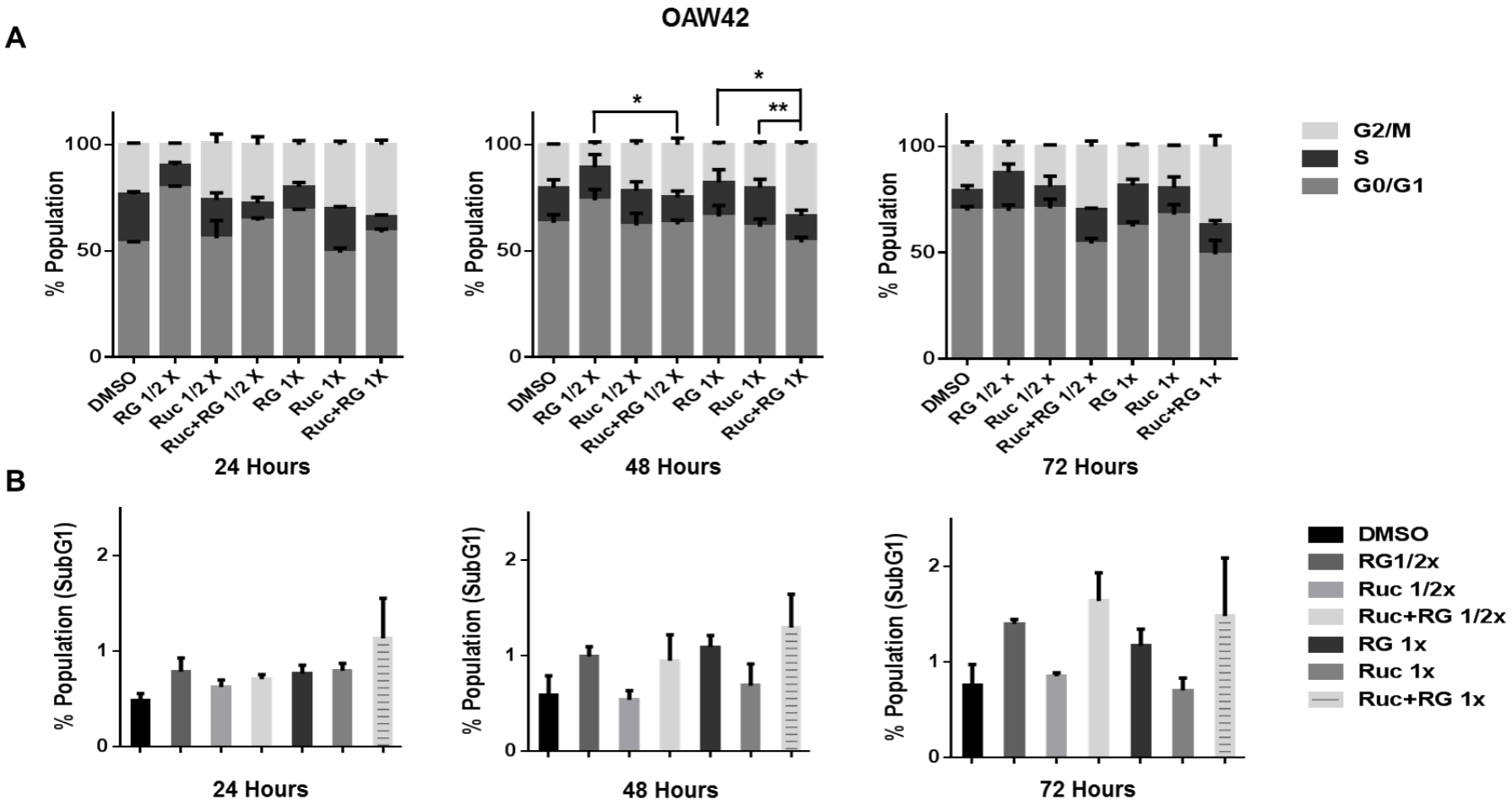

Figure 8-15: Combination of rucaparib with RG7388 affects the cell cycle distribution and apoptotic endpoints. OAW42 cells were treated for 24, 48 and 72 hours with rucaparib or RG7388 alone and at constant 1:1 ratios of 1/2x and 1x their respective GI_{50} concentrations. Combination of rucaparib with RG7388 led to an increased proportion of cells in G2/M phase (A) and SubG1 signals (B) compared to rucaparib and RG7388 as single agents in most cases. RG, RG7388; Ruc, Rucaparib; *, *p<0.05*; **, *p<0.01*. Data are shown as the average of at least three independent experiments and error bars represent SEM.

8.4.4.3 The effect of rucaparib in combination with cisplatin on cell cycle distribution andSubG1 events in wild-type *TP53* ovarian cancer cell lines

Combination treatment of rucaparib with cisplatin for A2780 cells led to an increase in the proportion of cells in G2/M phase compared to either agent alone after 24 hours, whereas it had little effect on the cell cycle distribution after 48 and 72 hours post-treatment (Figure 8-16A). In most cases, it also resulted in a higher increase in the proportion of SubG1 signals compared to either agent alone (Figure 8-16B). For IGROV-1 cells, there was little change in the proportion of cells in G2/M phase following combination treatment of rucaparib with cisplatin compared to either agent alone. The effect of combined treatments on SubG1 signals was time and dose-dependent manner although the differences were not statistically significant (Figure 8-17). For OAW42 cells, combination of rucaparib with cisplatin significantly decreased the proportion of cells in G2/M compared to cisplatin alone after 48 and 72 hours post-treatment at 1x GI_{50} dose. Furthermore, the combined treatments led to a decrease in SubG1 signals after 48 and 72 hours post-treatment compared to cisplatin on its own indicating a protective effect of rucaparib against cisplatin in this cell line (Figure 8-18).

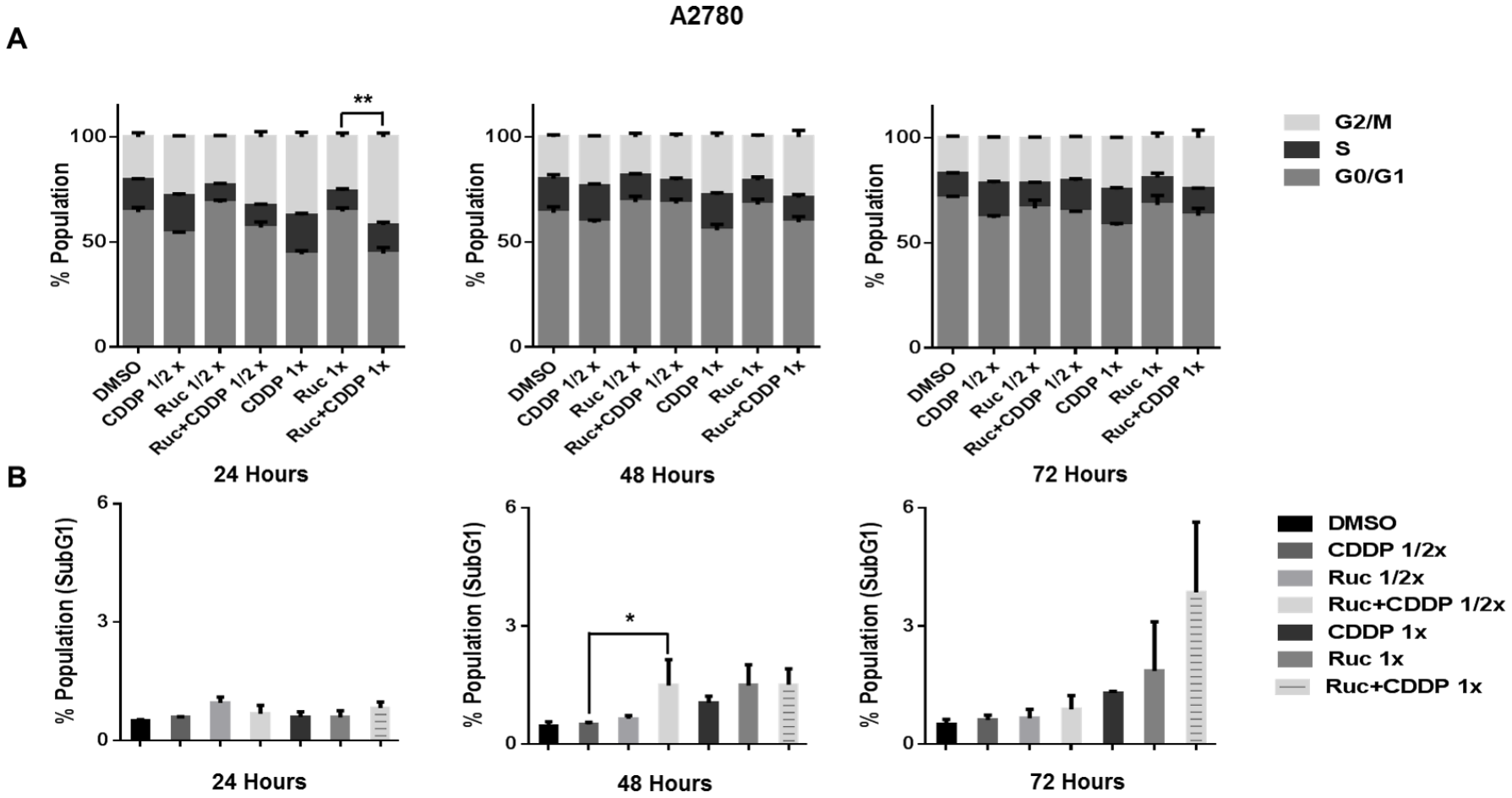

300

Figure 8-16: Combination of rucaparib with cisplatin affects the cell cycle distribution and apoptotic endpoints. A2780 cells were treated for 24, 48 and 72 hours with rucaparib or cisplatin alone and at constant 1:1 ratios of 1/2x and 1x their respective GI_{50} concentrations. Combination of rucaparib with cisplatin led to an increased proportion of cells in G2/M phase (A) and SubG1 signals (B) compared to either agent alone in most cases. CDDP, cisplatin; Ruc, Rucaparib; *, *p<0.05*; **, *p<0.01*. Data are shown as the average of at least three independent experiments and error bars represent SEM.

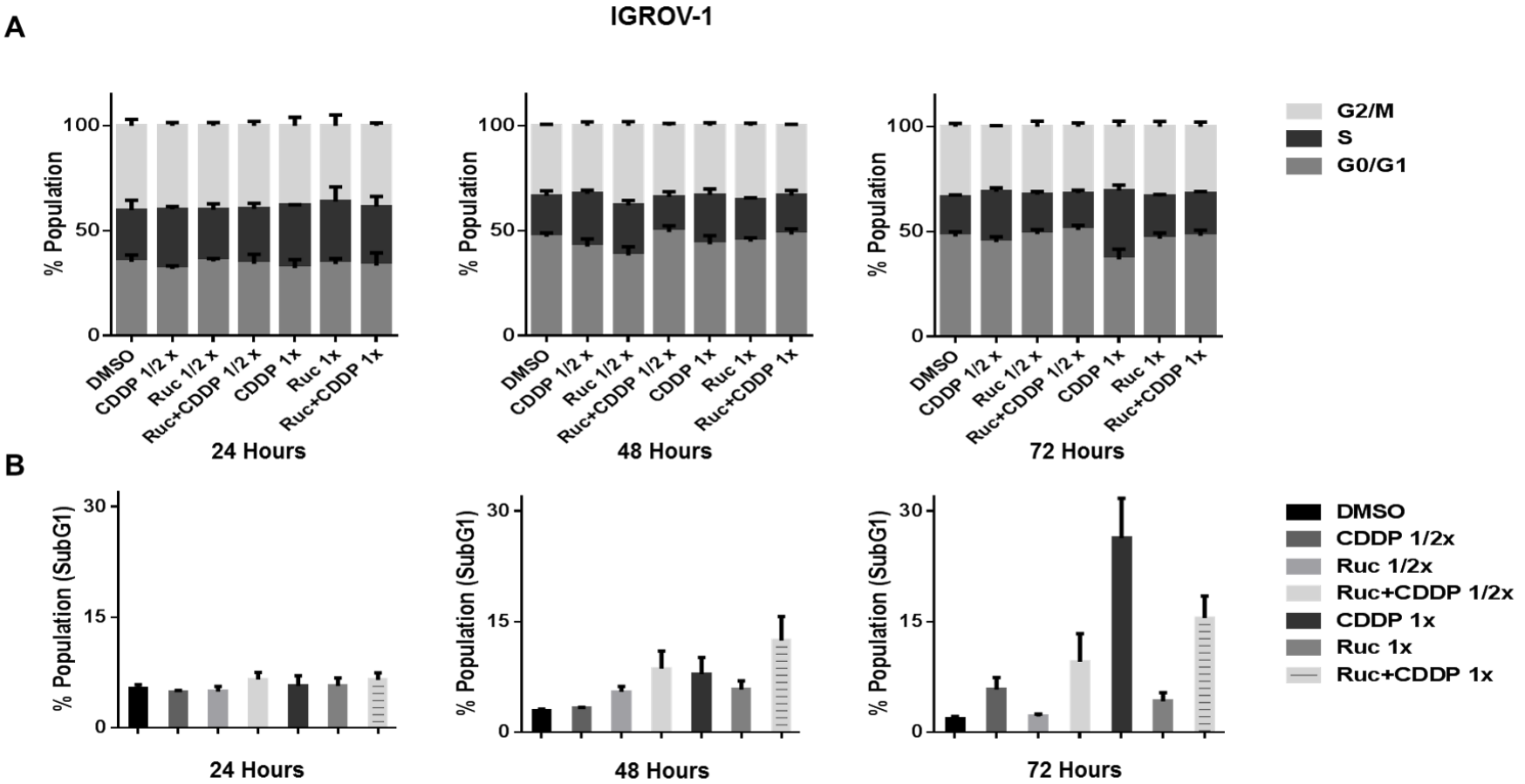

301

Figure 8-17: Combination of rucaparib with cisplatin affects the cell cycle distribution and apoptotic endpoints. IGROV-1 cells were treated for 24, 48 and 72 hours with rucaparib or cisplatin alone and at constant 1:1 ratios of 1/2x and 1x their respective GI_{50} concentrations. Combination of rucaparib with cisplatin led to little change in G2/M phase (A) and increased SubG1 signals with the exception of 72 hours' time point at GI_{50} value (B) compared to either agent alone. CDDP, cisplatin; Ruc, Rucaparib. Data are shown as the average of at least three independent experiments and error bars represent SEM.

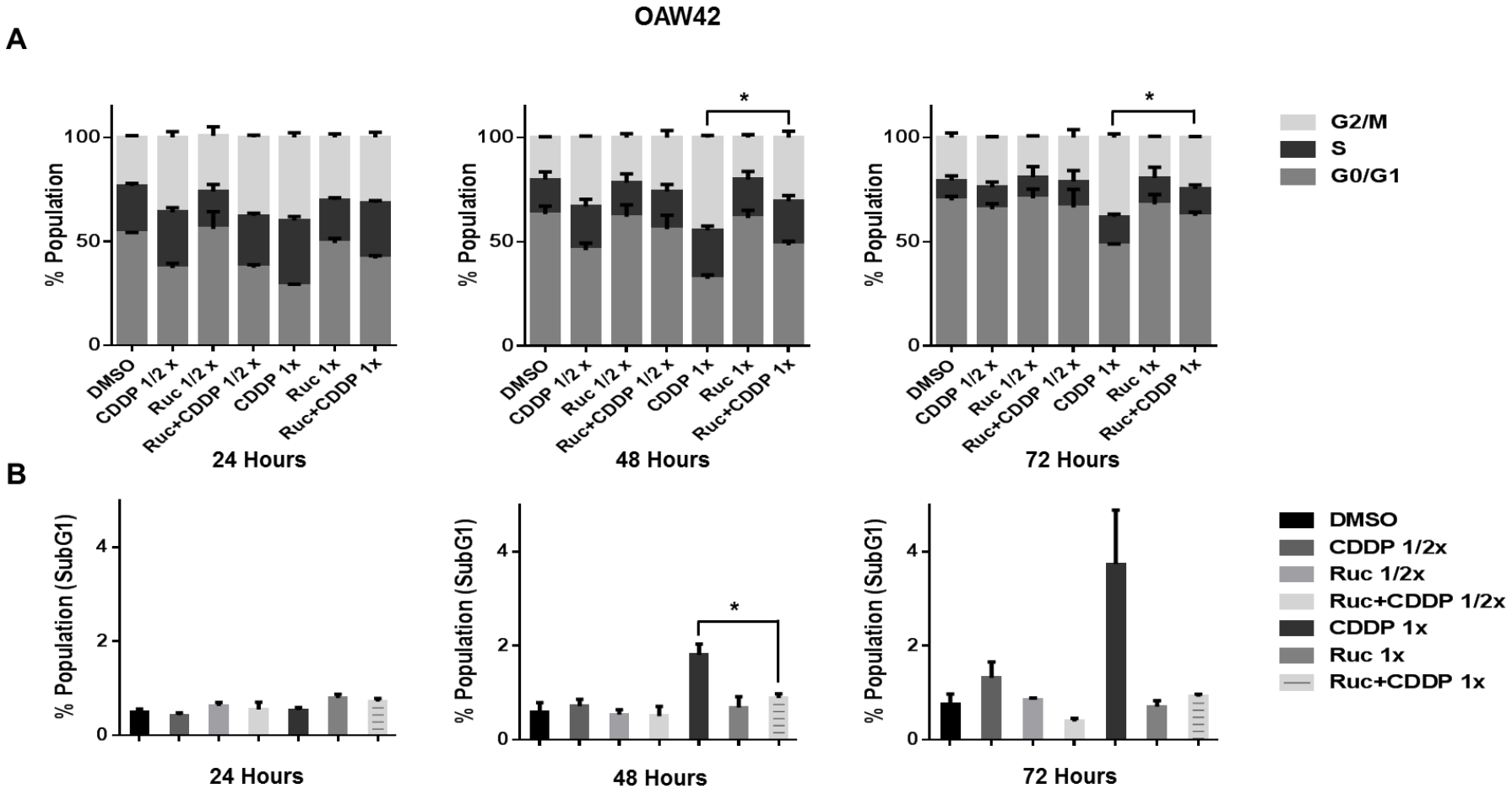

302

Figure 8-18: Combination of rucaparib with cisplatin affects the cell cycle distribution and apoptotic endpoints. OAW42 cells were treated for 24, 48 and 72 hours with rucaparib or cisplatin alone and at constant 1:1 ratios of 1/2x and 1x their respective GI_{50} concentrations. Combination of rucaparib with cisplatin led to a decreased proportion of cells in G2/M phase (A) and decreased SubG1 signals (B) after 48 and 72 hours compared to cisplatin on its own. CDDP, cisplatin; Ruc, Rucaparib; *, *$p<0.05$*. Data are shown as the average of at least three independent experiments and error bars represent SEM.

8.4.5 Rucaparib results in clonogenic cell death of ovarian cancer cells in a p53-independent manner

To perform clonogenic survival assays for the panel of six ovarian cancer cell lines, logarithmically growing cells were counted and seeded at appropriate densities for colony formation and treated with different concentrations of rucaparib (0-16 μM) for 48 hours. Then, the media including drug were replaced with drug-free media and cells were allowed to form colonies. Overall, all cell lines were more sensitive to clonogenic cell killing by rucaparib than its effect on cell growth arrest. The results demonstrated a variety of responses for different cell lines, ranging from A2780 as the most sensitive cell line (LC_{50}=1.1±0.2 μM) and OAW42 as the most resistant cell line (LC_{50}=12.1±2.3 μM). Rucaparib significantly decreased the clonogenic survival of A2780 cells and moderately reduced the colony formation of MDAH-2774; however, other cell lines were resistant to the effect of rucaparib (Table 8-4 & Figure 8-19).

Cell line	*TP53* Status	Rucaparib (μM)
A2780	Wild-type	1.1 ± 0.2
IGROV-1	Wild-type	10.8 ± 2.9
OAW42	Wild-type	12.1 ± 2.3
CP70	Mutant	9.3 ± 2.7
MDAH-2774	Mutant	4.2 ± 0.24
SKOV-3	Mutant	10.1 ± 1.6

Table 8-4: LC_{50} concentrations for rucaparib for the panel of ovarian cancer cell lines of varying *TP53* status. Data represent the mean of at least three independent experiments ± SEM.

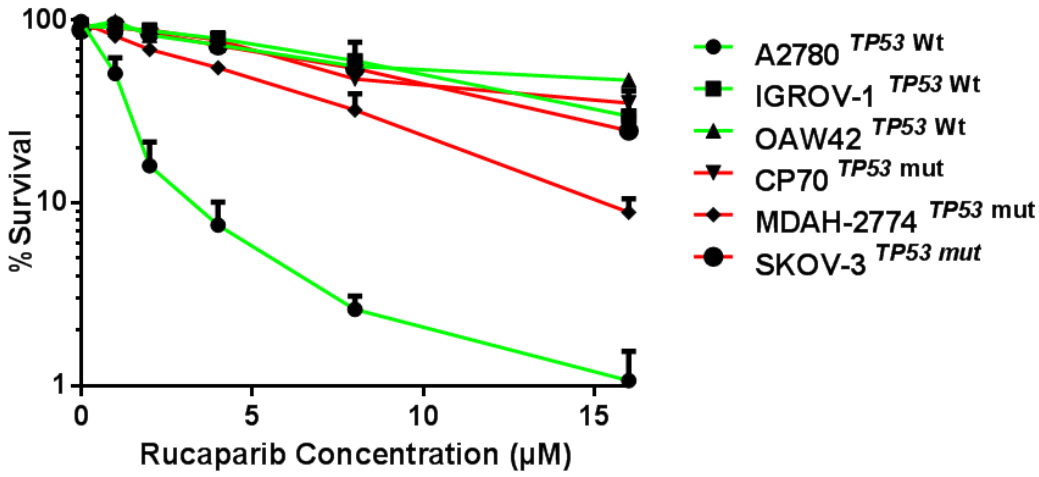

Figure 8-19: Clonogenic survival curves for the panel of ovarian cancer cell lines treated with rucaparib. Data are shown as the average of at least three independent experiments and error bars represent SEM. Wt, Wild-type; mut, Mutant.

8.5 Discussion

PARP inhibitors, have been developed over a number of decades to potentiate DNA damage and in more recent years have been shown to have efficacy as single agents against tumour cells with intrinsic deficiencies in DNA repair. They currently have been undergoing clinical trials in different types of cancers including ovarian cancer (Anwar *et al.*, 2015; Benafif and Hall, 2015; Frey and Pothuri, 2015). As mentioned in the Introduction (1.9.3), the efficacy of these drugs depends on defects in HRR (Rigakos and Razis, 2012; Ihnen *et al.*, 2013; Anwar *et al.*, 2015; Bowtell *et al.*, 2015). They have also been shown to potentiate the effect of cytotoxic radiotherapy and chemotherapy agents (Weil and Chen, 2011; Ihnen *et al.*, 2013; O'Sullivan *et al.*, 2014). Encouraging clinical trial results for the use of PARP inhibitors have been reported for ovarian cancer (Brown *et al.*, 2016; Drew *et al.*, 2016). The promising results showing activity of MDM2-p53 antagonists against wild-type *TP53* ovarian cancer cell lines (described in chapter 6) have prompted an investigation of combination treatment with rucaparib and Nutlin-3/RG7388 in a panel of wild-type *TP53* ovarian cancer cell lines. Mechanistically it was of interest to investigate the combined effect of PARP inhibition and MDM2-p53 binding antagonists on the p53 pathway activation.

8.5.1 The growth inhibitory effect of rucaparib on ovarian cancer cell lines

Growth inhibition assays were carried out to evaluate the effect of rucaparib in a panel of 7 established ovarian cancer cell lines. Among the individual cell lines, A2780 and MDAH-2774 were sensitive (GI_{50} < 10 µM) and other cell lines (IGROV-1, OAW42, CP70, *MLH1*-corrected CP70+ and SKOV-3) were resistant (GI_{50} > 10 µM). No relationship was found between the *TP53* status of cells and response to rucaparib, which is consistent with other research (Daemen *et al.*, 2012). Following the scheme suggested by Mukhopadhyay, the 10 µM cut-off value was used to categorise cell lines into sensitive and resistant to PARP inhibitor (Mukhopadhyay *et al.*, 2012). These results are in line with those of previous studies demonstrating sensitivity of A2780 and resistance of OAW42, IGROV-1, CP70 and SKOV-3 in response to rucaparib (Ihnen *et al.*, 2013; McCormick *et al.*, 2013).

Overall, the GI_{50} values for rucaparib across all cell lines were much higher than the concentration needed to reduce the enzymatic activity by half, Ki=1.4 nM (Thomas *et al.*, 2007). However, they were in the range of rucaparib concentrations achievable *in vivo* and used in clinical trials (Javle and Curtin, 2011; Weil and Chen, 2011; Brown *et al.*, 2016; Drew *et al.*, 2016).

To explore the potential mechanism involved in the sensitivity of A2780 and MDAH-2774 and resistance of other cell lines to rucaparib, the status of genes implicated as biomarkers in response to PARP inhibitors were studied (Table 8-5). The most interesting finding is that A2780 cell line was the most sensitive cell line even though among the relevant genes previously implicated in the sensitivity to rucaparib (see Introduction, section 1.9.3) it has only a heterozygous mutation in *PTEN* (Deletion-In frame, heterozygous, (c.380_388delGAAAGGGAC) (89682879_89682887delAGGGACGAA) (Ihnen *et al.*, 2013) (Table 8-5). MDAH-2774 is an ovarian endometrioid tumour with mutant *TP53* and *KRAS* (Gilloteaux *et al.*, 2015).

The IGROV-1 cell line has a number of heterozygous mutations in *BRCA1* (a.2080delA, Deletion-Frameshift and c.1961delA, Deletion-Frameshift), *ATM* (c.743G>A, Substitution-Missense) and *PTEN* (c.950-953delTACT, Deletion-Frameshift and c.464A>G, Substitution-Missense) genes . There are controversial results about the *BRCA2* gene status of the IGROV-1 cells. Sanger Institute reported a mutation in *BRCA2* (c.9448C>A, Substitution-Missense) while Stordal *et al*. (2013) reported no mutation in *BRCA2* gene in IGROV-1 cell line. Furthermore, there is a heterozygous mutation in *RAD51C* gene nonetheless it is silent mutation (c.765G>A, Substitution-Coding silent) (Table 8-5).

The OAW42 cells were resistant to rucaparib, despite amplification of the *AURKA* gene, (Ihnen *et al.*, 2013) and methylation of the *FANCF* gene (Taniguchi *et al.*, 2003) , both of which have been suggested to be associated with sensitivity to rucaparib. A possible explanation for this is that the amplification level of the *AURKA* gene. Amplification is not over-expression but it might cause it. The mutation in the *ATR* gene in OAW42 is a silent mutation with no effect on the ATR function (c.4323A>G, Substitution, Coding-silent) (Table 8-5).

The growth inhibitory effect of rucaparib on the SKOV-3 cell line is in agreement with Ihnen *et al*. (2013who reported the SKOV-3 cell line to be resistant to rucaparib. This result is consistent with the lack of mutations in the genes involved in the HRR pathway, aside from an unknown heterozygous mutation in the *ATM* gene (c.4237-2A>G, Unknown) . Another study also found a significant association between deficiency in *CDK12* and olaparib sensitivity in HGSC cell lines such as SKOV-3 cells, indicating resistance to PARP inhibitor for SKOV-3 cells which is consistent with the result of this study (Bajrami *et al.*, 2014).

For CP70 and *MLH1*-corrected CP70+ cell lines which are resistant to rucaparib more research is needed to check the status of genes implicated in response to PARP inhibitors (Table 8-5). No mutation in *MRE11, XRCC3* and *AURKA* genes are reported across all cell lines .

Overall, the reasons for the greater sensitivity of A2780 and MDAH-2774 to rucaparib are not clear. These differences may be explained by the potential involvement of off-target affinities for proteins other than PARPs including PIM1 and other kinases (Antolín and Mestres, 2014). However, further research is needed to identify reliable biomarkers to stratify patients who will benefit from treatment with PARP inhibitors.

Gene / Cell Line	Mutation								Amplification		Methylation		
	BRCA1	*BRCA2*	*ATM*	*ATR*	*CHK2*	*RAD50*	*RAD51*	*PTEN*	*AURKA*	*EMCY*	*BRCA1*	*BRCA2*	*FANCF*
A2780	- (2)	- (2)	- (1)	- (1)	- (1)	- (1)	- (1)	+ (1 & 3)	- (3)	- (3)	- (2)	- (2 & 3)	- (4 & 5)
IGROV-1	+ (1 & 3)	- (2), + (1)	+ (1)	- (1)	- (1)	- (1)	+ (1)	+ (1)	ND	ND	- (2)	- (2)	- (5)
OAW42	- (2)	- (2)	- (1)	+ (1)	- (1)	- (1)	- (1)	- (1)	+ (3)	- (3)	- (2)	- (2 & 3)	+(5 & 6)
CP70	ND	ND	ND	ND	ND	ND	ND	ND	ND	ND	ND	ND	ND
***MLH1*-corrected CP70+**	ND	ND	ND	ND	ND	ND	ND	ND	ND	ND	ND	ND	ND
MDAH-2774	ND	ND	ND	ND	ND	ND	ND	ND	ND	ND	ND	ND	ND
SKOV-3	- (2)	-(2)	+ (1)	- (1)	- (1)	- (1)	- (1)	- (1)	- (3)	- (3)	- (2)	- (2 & 3)	- (4 & 5)

308

Table 8-5: *BRCA1/2* gene status and BRCAness in a panel of ovarian cancer cell lines used in this study. (1) ,(*cancer.sanger.ac.uk*); (2), (Stordal *et al.*, 2013); (3), (Ihnen *et al.*, 2013); (4), (Lim *et al.*, 2008); (5), (Taniguchi *et al.*, 2003); (6), (Olopade and Wei, 2003); ND, Not determined.

8.5.2 Nutlin-3/RG7388 or cisplatin synergise with rucaparib for growth inhibition of wild-type *TP53* ovarian cancer cell lines in a compound and cell type-dependent manner

Combination treatment with drugs which have different mechanisms of action minimizes resistance to treatment (Kummar *et al.*, 2010; Al-Lazikani *et al.*, 2012; Yardley, 2013), a major obstacle for cancer therapy. Both MDM2-p53 antagonists and PARP inhibitors have been undergoing clinical trial as novel targeted therapeutics as single agents and/or in combination with conventional chemotherapy agents (Weil and Chen, 2011; Ding *et al.*, 2013; Anwar *et al.*, 2015; Lakoma *et al.*, 2015). This study set out to investigate the combined treatment effect of Nutlin-3/RG7388 or cisplatin with rucaparib as combined targeted therapeutics or combination of targeted therapy with conventional chemotherapy agent respectively.

Overall, the effect of combined treatment was cell type and compound dependent, with a higher synergistic effect for the combination of Nutlin-3/RG7388 with rucaparib for A2780 and IGROV-1 cell lines. Interestingly, although both IGROV-1 and OAW42 were resistant to rucaparib, there was nevertheless a synergistic effect for the combination of Nutlin-3/RG7388 with rucaparib. A possible explanation for this is that the defects conferring sensitivity to PARP inhibitors as single agents may be different from those which play an important role in the response to the combination treatment. For example, serious deficiencies in HRR may affect the sensitivity to PARP inhibitors as single agents, while mild defects in HRR may have no effect on response to PARP inhibitors alone but may nevertheless influence the effect of combination treatments (Turner and Ashworth, 2011; Ihnen *et al.*, 2013). Another possibility is that off-target effects of rucaparib with respect to PARP1 and PARP2 may influence the growth inhibitory effect of rucaparib as a single agent compared to combined treatment (Murai *et al.*, 2014).

The effect of combination treatment of rucaparib with cisplatin, based on the CI at $ED_{50,}$ was synergism, additivity and antagonism for A2780, IGROV-1 and OAW42 respectively, and was antagonism based on the overall CI across three cell lines. A number of studies have investigated combination treatment of PARP inhibitors with cytotoxic therapeutic agents including cisplatin, carboplatin and oxaliplatin, showing a range of additive to synergistic effects of combination therapy (Ihnen *et al.*, 2013; O'Sullivan *et al.*, 2014; Benafif and Hall, 2015; Livraghi and Garber, 2015). Ihnen *et al*. (2013) reported additive and synergistic interactions for the combination treatment of rucaparib with carboplatin in a panel of ovarian

cancer cell lines with differing sensitivity in response to rucaparib on its own. They observed a higher synergistic effect with A2780, the most sensitive cell line to rucaparib, which is in line with data obtained in this study. Michels *et al*. (2014) reported an additive effect of combination treatment between PARP inhibitors and cisplatin on cervical cancer and testicular germ cell tumour cell lines.

The most important clinically relevant finding from the data is the favourable DRI values in both combination treatment of Nutlin-3/RG7388 or cisplatin with rucaparib. As mentioned in the literature review and chapter 7.4.1, additive and even mildly antagonistic results of combined treatment can nevertheless be of potential clinical use due to favourable DRI values (Ohnstad *et al.*, 2011; Meng *et al.*, 2015). These favourable DRI values demonstrate that combination of Nutlin-3/RG7388 or cisplatin with rucaparib has the potential to reduce the dose of drugs in most cases, indicating a potential clinical benefit of combining these therapeutic agents.

8.5.3 The effect of combination of Nutlin-3/RG7388 or cisplatin with rucaparib on functional activation of the p53 pathway in *TP53* wild-type ovarian cancer cell lines

Rucaparib on its own had no effect on p53 stabilisation and upregulation of its downstream targets $p21^{WAF1}$ and MDM2 across all three cell lines. Combination treatment of Nutlin-3/RG7388 with rucaparib induced stabilisation of p53 and upregulation of $p21^{WAF1}$ and MDM2 compared to rucaparib on its own, whereas rucaparib caused no enhancement of the p53 activation by MDM2 inhibitors alone. These results demonstrate that the synergistic effect observed in the combination between rucaparib and Nutlin-3/RG7388 is not related to the p53 molecular pathway. Combination of cisplatin with rucaparib caused little change on the functional activation of the p53 pathway with the exception of a little change in the expression of $p21^{WAF1}$ at constant 1:1 ratios of GI_{50} values for A2780 and IGROV-1 cell lines.

The interplay between PARP and p53 is controversial. Bai *et al*. (2015) showed that PARP inhibition by the small molecule PJ-34 caused an increased p53 stabilisation for MT2, MT4, C91PL T-cell leukemia cells, and induced p53 phosphorylation and $p21^{WAF1}$ upregulation in MT4 cells. Another study performed by Valenzuela *et al*. (2002) used parental *PARP-1 +/+* and deficient *PARP-1 -/-* primary mouse embryonic fibroblasts and determined the nuclear accumulation of p53 protein following ionising radiation (IR), ultraviolet light (UV) and alkylating agent N-methyl-N-nitrosourea (MNU) treatment. There was a very rapid accumulation of p53 for

PARP-1 parental cells after IR treatment which remained at high levels for 24 hours while PARP-1 deficient cells showed little change. In contrast, p53 accumulation happened earlier and at higher levels in PARP-1 deficient cells following MNU treatment compared to parental cells. In terms of UV treatment, the p53 accumulation levels were similar for both parental and PARP-1 deficient cell lines. The authors suggested that the interplay between PARP-1 and p53 depends on the type of DNA damage. A further study investigated the effect of olaparib and veliparib on cell cycle arrest and the p53 pathway for a panel of cancer cell lines (Jelinic and Levine, 2014). These results indicated a robust increase in p53 stabilisation, $p21^{WAF1}$ upregulation and CHK1 phosphorylation in $U2OS^{DR\text{-}GFP}$ and HCT116 cells treated with olaparib but the effect on p53 accumulation and $p21^{WAF1}$ upregulation in veliparib-treatment cells was weak with no CHK1 activation. Jelinic *et al*. (2014) proposed that olaparib treatment led to strong replicative stress compared to veliparib, and its effect on cell cycle arrest and growth inhibition is p53-dependent. However, the effect of veliparib on growth inhibition and cell cycle arrest is p53-independent.

8.5.4 Combination of rucaparib with Nutlin-3/RG7388 or cisplatin affects cell cycle arrest and/or apoptosis in wild-type *TP53* ovarian cancer cell lines

Rucaparib had little effect on the cell cycle distribution of IGROV-1 and OAW42 cell lines, which is in agreement with the results obtained by Porcelli *et al*. (2013) that indicated no effect of rucaparib on the cell cycle progression of pancreatic cancer cells. However, in the current study rucaparib significantly decreased the proportion of cells in S-phase in A2780 cells, consistent with a recent study indicating a robust decrease in the percentage of cells in S-phase following treatment of $U2OS^{DR\text{-}GFP}$ cells with olaparib (Jelinic and Levine, 2014). Furthermore, there was only a slight increase in the SubG1 cell subpopulation across all cell lines treated with rucaparib compared to DMSO control, suggesting that cells are not undergoing apoptosis. These results are in line with those of Jelinic and Levine (2014) who observed low SubG1 events in the cancer cells treated with olaparib or veliparib.

Across all three cell lines, combined treatment of Nutlin-3/RG7388 with rucaparib increased the proportion of cells in the G2/M phase of the cell cycle, which was marked for A2780 and IGROV-1. Combination of rucaparib with cisplatin increased the proportion of cells in G2/M for A2780 cells, whereas there was little change in the percentage of cells in G2/M phase and a decrease in the proportion of SubG1 events for the OAW42 cell line.

The increased proportion of cells in G2/M phase following PARP inhibitor treatments may reflect their potency to trap PARP-1 and -2 to DNA and induce replicative stress response (Jelinic and Levine, 2014). Reported off-target effects of rucaparib include inhibition of nine different kinases (Antolín and Mestres, 2014); and this may contribute to the effect of rucaparib on cell cycle progression (Jelinic and Levine, 2014). For example, rucaparib presents micromolar IC_{50} values for PIM1 (1.2 µM), CDK1 (1.4 µM), and CDK9 (2.7 µM) proteins, which are known as cell cycle regulators (Antolín and Mestres, 2014).

8.5.5 Rucaparib results in clonogenic cell death in ovarian cancer cell lines

Overall, the results of clonogenic survival assays were similar to the growth inhibition assays with A2780 as the most sensitive, and OAW42 as the most resistant cell lines. As explained in chapter 8.5.1, the reason for this difference between various cell lines in regard to response to rucaparib is not clear and it is difficult to explain this result. Drew *et al*. (2011) studied the effect of rucaparib on the clonogenic cell survival for a panel of cancer cell lines with different *BRCA1/2* status. They used a 10 µM rucaparib as the cut-off value to categorise cell lines into sensitive and resistant based on the correlation of cytotoxicity with the HRR status determined by RAD51 foci in primary cultures. The results demonstrated a marked difference in the LC_{50} data in relation to HRR functionality, with less toxicity to cell lines with functional HRR (LC_{50}=20.2-50.7 µM) than those with mutant *BRCA1/2* or *XRCC3* (LC_{50}=1.3-5.5 µM). The LC_{50} for our sensitive cell lines (LC_{50}=1.1-4.4 µM) was in the same range defined by Drew *et* al (2011); however, we found no evidence of HRR deficiency in these cell lines. Therefore more research is clearly needed to identify reliable biomarkers for identifying patients likely to respond to PARP inhibitors.

8.5.6 Conclusion and further work

Monitoring cell cycle markers and PARP expression and PARP activity in addition to HRR status is likely to be additional useful information to assess the effectiveness of PARP inhibitors. This information may be helpful to better clarify and stratify the patients who might benefit from PARP inhibitors. Using preclinical xenograft models is required to confirm evidence of synergy *in vivo*.

Chapter 9: General Discussion

9 *TP53* and ovarian cancer

The studies and research presented in this thesis have focused on the genomic and functional status of *TP53* as prognostic and predictive biomarkers in ovarian cancer patients, and targeting p53 by using a small molecule inhibitor of MDM2-p53 interaction for treatment of ovarian cancer. For the study of *TP53* mutational status as prognostic and predictive biomarkers, a set of TMAs constructed from tumour samples collected from the ICON3 multicentre clinical trial was used. For the immunohistochemical prognostic biomarker studies, two sets of TMAs were used; the OVCA1-4 set representing a cohort of patients from which samples had been collected locally, and the same set of TMAs from the ICON3 clinical trial used for sequencing.

For the preclinical evaluation of MDM2 inhibitors, a panel of 7 ovarian cancer cell lines with varying status of *TP53* was studied to investigate their growth inhibitory and apoptotic response to three different MDM2-p53 binding antagonists, Nutlin-3, RG7112 and RG7388 as single agents. The growth inhibitory effect and induced apoptosis with a combination of Nutlin-3 or RG7388 with cisplatin or rucaparib were also investigated in the same panel of cell lines.

9.1 Analysis of the prognostic and predictive value of mutational status of *TP53* and TP53 expression in ovarian cancer

In spite of numerous studies which have investigated the role of genomic and/or functional status of *TP53* as prognostic and predictive biomarkers in ovarian cancer, the results are inconsistent (Shahin *et al.*, 2000; Fallows *et al.*, 2001; Reles *et al.*, 2001; Schuyer *et al.*, 2001; Havrilesky *et al.*, 2003; Nakayama *et al.*, 2003; Canevari *et al.*, 2006; Gadducci *et al.*, 2006; Bartel *et al.*, 2008; de Graeff *et al.*, 2009; Ahmed *et al.*, 2010; Bauerschlag *et al.*, 2010; Nadkarni *et al.*, 2013; Rechsteiner *et al.*, 2013; Brachova *et al.*, 2015; Seagle *et al.*, 2015).

Meta-analyses of p53 studies have been performed to increase power over individual studies, improve the estimates of the effect and resolve uncertainty amongst inconsistent results, but nevertheless methodological variability and publication bias are considerable problems (Crijns *et al*., 2003; de Graeff *et al.*, 2009). Crijns *et al*. (2003) found fifty-three studies that investigated the prognostic impact of p53 status in ovarian cancer, among which thirty-two studies were appropriate for meta-analysis. The results confirmed that ovarian cancer patients harbouring tumour with overexpressed p53 had significantly worse probabilities of survival at five years (p=*0.0006*) and concluded that p53 targeted therapy may have therapeutic potential. De Graeff *et al*. (2009) included sixty-two studies in the meta-analysis and indicated that p53

protein expression had a modest effect on prognosis and overall survival despite the presence of heterogeneity between studies. They suggested that p53 immunostaining is unlikely to be useful as a predictive biomarker in clinical practice in a manner comparable to well-known clinicopathological predictive biomarkers such as tumour stage and residual disease. They also found the mutational status of *TP53* had prognostic value in the meta-analysis even though it was of borderline significance. In addition to methodological variability and publication bias, the meta-regression analysis showed FIGO stage distribution has impact on the outcome of meta-analysis and p53 status was no longer of predictive value when the meta-analysis was restricted to studies reporting results for patients with stage III/IV tumours (de Graeff *et al.*, 2009; Levidou., 2011). In contrast, when p53 meta-analysis was performed in the studies evaluating the predictive value of p53 in patients with serous tumours, p53 retained its significance as a predictor of survival (Graeff *et al.*, 2009). Overall, the results are highly influenced by a variety of methodological variables including fixation method of paraffin-embedded tissues and storage time, type of primary antibody and IHC staining protocol, cut-off values for protein expression, size of sample and diverse chemotherapy options (Levesque *et al.*, 2000; Crijns *et al*., 2003; Graeff1, 2006; de Graeff *et al.*, 2009; Rechsteiner *et al.*, 2013) . In terms of mutational status of *TP53*, different techniques used for mutational analysis, the analysis of different exons and classification of mutations in addition to factors illustrated above effect the outcome of analysis (Shahin *et al.*, 2000; Rose *et al.*, 2003a; Canevari *et al.*, 2006; Liu *et al.*, 2010; Nadkarni *et al.*, 2013; Brachova *et al.*, 2015; Seagle *et al.*, 2015).

In conclusion, standard guidelines for use of FFPE tissue sections, standardised laboratory protocol and data collection (Graeff1, 2006), and analysis in homogeneous subgroups of patients such as those with a particular tumour type, stage or grade (de Graeff *et al.*, 2009) can be helpful to achieve comparable results among studies related to prognostic and predictive value of p53 in ovarian cancer.

9.2 A comparison between two independent cohorts in relation to the TP53 expression and its correlation with overall survival

In this study two independent cohorts were used to investigate the correlation between TP53 expression and overall survival. One cohort named OVCA1-4 included 167 ovarian cancer samples from northern England and the other cohort consisted of 260 ovarian cancer samples from the ICON3 international multicentre trial. Based on the results of the OVCA1-4 cohort, TP53 expression levels was found to have prognostic significance for overall survival ($p=0.003$). However, the results of ICON3 clinical trial indicated that the observed difference in overall survival between patients in relation to TP53 expression levels was only marginally significant ($p=0.06$).

Clinicopathological data from both cohorts had been recorded for histological subtype, stage, residual disease and grade (Table 9-1). In terms of histology, the proportion of HGSC in the ICON3 cohort is considerably higher than for OVCA1-4 and the reverse is true for endometrioid and mucinous histological subtypes. A higher proportion of patients in the ICON3 cohort was categorised in stages III/IV than for the OVCA1-4 cohort. There is also a greater percentage of patients with optimal or suboptimal cytoreductive surgery for patients from ICON3 compared to those from the OVCA1-4 cohort. Moreover, a lower frequency of well differentiated and a higher frequency of poorly differentiated tumours was observed for the ICON3 TMA sample set. Overall, a higher proportion of patients from the ICON3 cohort has aggressive ovarian cancer compared to those from OVCA1-4. The results suggest that stage of disease, grade of differentiation and histology may impact on the prognostic value of p53. Amongst the studies which have investigated the prognostic and predictive values of p53 in ovarian cancer, most of those with advanced stages and invasive ovarian cancer showed no or marginally significant association between TP53 expression levels and overall survival (Sagarra *et al.*, 2002; Havrilesky *et al.*, 2003; Gadducci *et al.*, 2006; Green *et al.*, 2006; Darcy *et al.*, 2008; Rechsteiner *et al.*, 2013).

Variable	ICON3 (Proportion)	OVCA1-4 (Proportion)
Histological Subtype		
Adenocarcinoma	**0**	2
Clear Cell	10	10
Endometrioid	8	30
High Grade Serous	63	39
Low Grade Serous	10	8
Mucinous	2	11
Undifferentiated	7	0
Stage		
I/II	**17**	25
III	66	54
IV	17	11
Lost	0	10
Residual Disease		
Complete Cytoreduction (none)	24	32
Optimal Cytoreduction	20 (<2 cm)	18 (≤1 cm)
Suboptimal Cytoreduction	56 (≥2 cm)	39 (>1 cm)
Lost	0	11
Grade		
Poorly Differentiated	61	48
Moderately Differentiated	30	27
Well Differentiated	8	25
Lost	2	0

Table 9-1: Clinicopathological data for 167 samples of the OVCA1-4 and 260 samples of the ICON3 cohorts.

9.3 The effect of the genomic status of *TP53* on survival following platinum-based chemotherapy in ovarian cancer

Cells respond to platinum-based chemotherapy agents in both p53-dependent and p53-independent manners, although which mechanism dominates is context dependent. Evidence suggests that wild-type *TP53* tumours may be more sensitive to platinum-based chemotherapy than those with mutant *TP53* and the tumours less aggressive, combining to result in longer patient survival. A number of studies have investigated the role of *TP53* status in response to platinum-based chemotherapy, among which several indicated a significantly better overall survival for the patients with wild-type *TP53* tumours compared to those with mutant *TP53* tumours (Kigawa *et al.*, 2001; Reles *et al.*, 2001; Canevari *et al.*, 2006; Gadducci *et al.*, 2009). In contrast, others found no statistically significant correlation between the genomic status of *TP53* and overall survival in ovarian cancer patients (Fallows *et al.*, 2001; Wang *et al.*, 2004; Bauerschlag *et al.*, 2010).

Overall in this study, patients whose tumours have wild-type *TP53* and who were treated with only single agent carboplatin had better overall survival than those with tumours harbouring mutant *TP53*, regardless of the sequencing method used. When the analysis is limited to patients treated with carboplatin alone and having serous histology tumours, *TP53* status retained its predictive value based on the Sanger sequencing while it lost its significance based on the NGS. For patients treated with carboplatin or CAP, only analysis of data based on the Sanger sequencing or both sequencing methods showed significant predictive value of *TP53* status in response to single agent carboplatin or CAP. Adding paclitaxel to carboplatin led to loss of the significant effect of *TP53* status on overall survival irrespective of sequencing methods used. However, a number of studies reported that patients with mutant *TP53* tumours gain benefit from adding paclitaxel to platinum drugs (Lavarino *et al.*, 2000; Ueno *et al.*, 2006; Wong *et al.*, 2013). The results from this study clearly show that sequencing methods and treatment types influence the prognostic value of *TP53* for patients with ovarian cancer, and explain somewhat the observed discrepancies between various studies.

9.4 The limitation of the IHC approach as a biomarker assay

Although IHC staining has wildly being used as a biomarker validation, it may present significant bias which is divided into reaction bias and interpretation bias. The former includes tissue handling, specimen fixation, tissue processing, antigen retrial and detection system, and the latter includes selection of antibody types, sensitivity of the chosen panel, results and literature interpretation. Therefore, the IHC results must be interpreted with caution (de Matos *et al.*, 2010; O'Hurley *et al.*, 2014).

The antigenicity of an antigen may significantly be lost if fresh specimens are submitted to long periods of fixation. Formaldehyde fixation, the most used histological processing procedure, is a major cause of masking or damaging some antibody binding sites which results in a variably reversible loss of immunoreactivity (de Matos *et al.*, 2010; O'Hurley *et al.*, 2014). The thickness of slices has an impact on the IHC results. For example, slices less than 3 µm could result in less intensity and very weak immunostaining. Antigen retrieval and its different variables including heating, the type of solution and its pH and molarity are major variables that can affect IHC staining. Hence, using appropriate antigen retrieval which is dependent on both the target protein and chosen antibody is very important, and requires to be optimised for every antibody (O'Hurley *et al.*, 2014).

Appropriate choice of antibody and its validation is another major challenge in IHC staining which is a time consuming process. The portal Antibodypedia, (http://www.antibodypedia.com), is a suitable tool to search and find appropriate antibodies proper for IHC staining. However, antibody validation is a mandatory step before performing IHC staining because of not providing the sequence of the antigen which the antibody was raised against by many companies that produce the antibodies (de Matos *et al.*, 2010).

Interpretation and scoring of IHC data can be performed via manual and automated approaches. The manual scoring can be an inherently subjective and semi-quantitative process which is time intensive and laborious. To overcome these problems, use of image analysis systems has been proposed which decrease workload and outperform manual scoring by more reproducibility, accuracy and less subjectivity. In spite of having these advantages, automated image analysis is a semi-automated approach highly influenced by the quality of sections/TMAs due to inability of the system to identify the artefacts, edge effect staining and folding of tissue (de Matos *et al.*, 2010).

A limitation of our study is how the used antibodies were validated for their specificity as described in section 3.3.2. In addition, the same antibodies were used for western blotting and confirmed antibody specificity by the presence of a single band corresponding to the predicted molecular weight of the target proteins including p53, p21 and MDM2. However, a band of the correct size is not complete evidence for targeting the expected protein due to some proteins with a similar molecular weight. Therefore, use of more appropriate positive and negative FFPE control cell lines known to express or not express the target protein will be needed to confirm the specificity of the antibodies used for MDM2 and WIP1 proteins in this study.

Another limitation of this study is the modified H-score applied for immunoscoring, in which there was a possibility of obtaining scores more than 18. For example, the final score of a core is 20 if the intensity of 50% of the core is intermediate (4 * 2=8) and 50% of that is strong (4 * 3=12). To overcome this possible challenge, all patient samples of OVCA1-4 were scored for p53 as follows: 0 = no staining, 1 = weak staining, 2 = intermediate, 3 = strong, and the percentage of each group was estimated (0-100%). H-score was calculated by multiplying the proportion of staining and intensity of staining ranged from 0 to 300. The results were compared to those of modified H-score, and the ROC curve analysis was used to examine the relationship between sensitivity and specificity for immunohistochemical staining scores and categorise the samples into low and high p53 expression (Appendix II). The Interclass Correlation Coefficient test was used to estimate the concordance in two different scoring systems, and the ICC value was 0.97 describing how strongly immunoscoring units in the same patient sample resemble each other (Appendix III). Also, the statistical significance of observed differences in patient survival was analysed (Appendix IV). As can be seen in Appendix II, III and IV, the results were very similar to those achieved by analysing the data based on the modified H-score.

One more limitation is the single observer manual scoring was applied for immunoscoring of p53, p21 and MDM2 proteins (For WIP1 protein, the cores were scored by both the manual and the automated Aperio system, ICC=0.84) (Appendix V). This type of analysis has limitations because of being subjective and arbitrary. To avoid the bias, two independent observers must score each core, and reproducibility between the two scores should be measured using an appropriate statistical test.

9.5 The issues arisen from inclusion of different subtypes of ovarian cancer in a single cohort

Ovarian cancer is a heterogeneous disease including different histological subtypes, which are considered as distinct diseases. There are dramatically different in frequency, response to current chemotherapy, genetic abnormalities and molecular events, and survival. Therefore, there is a possibility of misleading when association of biomarker expression with survival is analysed in whole cohort. There is a substantial difference in the correlation between biomarker expression and survival across different subtypes which is likely to be overlooked in the analyses of whole cohort (Köbel *et al.*, 2008).

Most prognostic and predictive biomarker studies are not subtype specific for ovarian cancer patients. Kobel *et al*. (2008) investigated prognostic significance of twenty one candidate tissue-based biomarkers including p53 and p21 in a whole cohort of 500 ovarian carcinoma and within each specific subtype. Twenty of twenty one biomarkers had significantly different expression levels between different subtypes and only one biomarker showed a similar expression frequency across all subtypes which was EPCam. The survival analysis indicated nine of the twenty one biomarkers as prognostic biomarkers in the entire cohort while only three of the nine retained their prognostic significance in the HGSC subtype and one in the endometrioid subtype. Ki-67 was an unfavourable prognostic factor in the whole cohort; however, it did not remain its prognostic significance within any subtype. In some prognostic associations, there was an inverse correlation within entire cohort compared to a specific subtype. For example, WT1 was a favourable prognostic biomarker within the HGSC subtype while it was an unfavourable prognostic factor within the whole cohort. Furthermore, biomarker expression was studied within the entire cohort and compared to one specific subtype across FIGO stages. Ten of the twenty one biomarkers including p53 and p21 had significantly different expression levels, which suggest differences between early (I & II) and late (III & IV) stage disease. However, no biomarker retained its prognostic significance by stage when biomarker expression was compared within one specific subtype across FIGO stages. The results of biomarker expression levels in the entire cohort across subtypes generally showed smaller p-values than across stages, demonstrating a stronger relationship between survival and different subtypes than stages.

Although a multivariate analysis was performed, a limitation of our study is that the biomarker studies was performed in the whole cohort. To avoid confounding the association between

biomarker expression and prognosis, different histological subtypes should be considered as distinct diseases in biomarker studies (Köbel *et al.*, 2008).

9.6 Targeting p53 using MDM2-p53 binding antagonists in ovarian cancer

Use of MDM2-p53 inhibitors would be suitable for cancer types in which p53 mutations are rare or low including neuroblastoma (Chen *et al.*, 2015), primary leukemia, sarcoma, testicular cancer, malignant melanoma and cervical cancer (Olivier *et al.*, 2010). The rate of *TP53* mutations varies considerably in epithelial ovarian cancer according to histological subtype being less common in type I compared to type II (Koshiyama *et al.*, 2014; Cobb *et al.*, 2015; Skirnisdottir *et al.*, 2015).

The frequency of *TP53* mutation reported in the literature is particularly high for HGSC ranging from 51% (Singer *et al.*, 2005) to 97% (The Cancer Genome Atlas Research, 2011). In the current study 63% of patient samples were classified as HGSC, of which 62% were *TP53* mutant by Sanger sequencing and 71% by NGS (Table 9-2). As HGSC represents about 70% of all epithelial ovarian cancer (Kurman, 2013), the other 30% of histological subtypes in which *TP53* mutation is less frequent, and the small percentage of HGSC harbouring wild-type *TP53* would gain benefit from MDM2-p53 inhibitors on their own or in combination with other therapeutic agents such as cisplatin or rucaparib. This may be particularly worth exploring with mucinous and clear cell histological subtypes which do not respond well to current chemotherapy strategies and are clinically challenging to treat.

Mutation Analysis/Exons	Reference	Clear Cell		Mucinous		Endometrioid		Undifferentiated		LGSC		HGSC	
		WT N (%)	Mut N (%)	WT N (%)	Mut N (%)	WT N (%)	Mut N (%)	WT N (%)	Mut N (%)	WT N (%)	Mut N (%)	WT N (%)	Mut N (%)
Sanger/2-11	This study	15 (60)	10 (40)	3 (60)	2 (40)	12 (57)	9 (43)	7 (41)	10 (49)	16 (62)	10 (38)	60 (38)	99 (62)
NGS/2-11	This study	18 (72)	7 (28)	3 (60)	2 (40)	11 (52)	10 (48)	3 (18)	14 (82)	9 (35)	17 (65)	45 (29)	112 (71)
Sanger/5-9	(Singer et al., 2005)	-	-	-	-	-	-	-	-	11 (92)	1 (12)	29 (49)	30 (51)
Sanger/4-9	(Salani R et al., 2008)	-	-	-	-	-	-	-	-	12 (92)	1 (8)	14 (20)	57 (80)
NGS/2-11	(Ahmed et al., 2010)	-	-	-	-	-	-	-	-	-	-	4 (3)	119 (97)
NGS/5-8	(Rechsteiner et al., 2013)	12 (48)	13 (52)	6 (43)	8 (57)	21 (72)	8 (28)	-	-	-	-	26 (41)	37 (59)
NGS/2-11	(The Cancer Genome Atlas Research, 2011)	-	-	-	-	-	-	-	-	-	-	14 (4)	302 (96)
Total		-	-	-	-	-	-	-	-	48 (62)	29 (38)	192 (20)	756 (80)
Sanger/5-8	(Fallows et al., 2001)	-	-	5 (56)	4 (44)	-	-	3 (38)	5 (62)	Serous: WT, 18 (58); Mut, 13 (42)			
Sanger/2-11	(Reles et al., 2001)	5 (83)	1 (17)	6 (75)	2 (25)	12 (40)	18 (60)	2 (20)	8 (80)	Serous: WT, 51 (46); Mut, 60 (54)			
Sanger/2-11	(Havrilesky et al., 2003)	-	-	-	-	-	-	-	-	Serous: WT, 18 (24); Mut, 56 (76)			
Sanger/2-11	(Leitao et al., 2004)	15 (88)	2 (12)	4 (80)	1 (20)	16 (80)	4 (20)	-	-	Serous: WT, 7 (33); Mut, 14 (67)			
Sanger/5-9	(Gadducci et al., 2006)	-	-	-	-	-	-	-	-	Serous: WT, 23 (50); Mut, 23 (50)			
Sanger/5-8	(Bauerschlag et al., 2010)	1 (33)	3 (67)	4 (57)	3 (43)	5 (45)	6 (55)	-	-	Serous: WT, 21 (40); Mut, 31 (60)			
NGS/2-11	(Bernardini et al., 2010)	-	-	-	-	-	-	-	-	Serous: WT, 30 (34); Mut, 59 (66)			
Total		66 (65)	36 (35)	31 (58)	22 (42)	77 (58)	55 (42)	15 (29)	37 (71)	Serous WT: 168 (40)		Serous Mut: 256 (60)	

Table 9-2: The frequency of *TP53* mutation for different histological subtypes of epithelial ovarian cancer reported in different studies. WT, Wild type; Mut, Mutant; LGSC, Low-grade serous carcinoma; HGSC, High-grade serous carcinoma; NGS, Next generation sequencing.

9.7 Nutlin-3 and RG7388 induce apoptosis in ovarian cancer

A number of studies have reported that Nutlin-3 induces apoptosis in leukemia cells while only reversible cell cycle (quiescence) arrest in solid tumours (Huang *et al.*, 2009; Demidenko *et al.*, 2010; Hoe *et al.*, 2014). Our study and two limited previous reports showed that wild-type *TP53* ovarian cancer cells undergo both growth arrest and apoptosis following exposure to Nutlin-3 and some cell lines are more sensitive than others. The previous studies indicated that Nutlin-3a treatment induced both cell cycle arrest and apoptosis in sensitive cell lines (Crane *et al.*, 2015) and potentiated apoptotic cell death in chemoresistant ovarian cancer cells to cisplatin (Mir *et al.*, 2013). In our study, all wild-type *TP53* cell lines were sensitive to Nutlin-3 and the more potent clinical candidate RG7388. Both MDM2-p53 antagonists induced cell cycle arrest and apoptosis with RG7388 showing greater potency. In terms of apoptosis endpoints, treatment with both inhibitors resulted in increased SubG1 events in Flow cytometry and caspase3/7 activity, in a cell type, time and compound-dependent manner (Zanjirband *et al.*, 2016).

The mRNA levels of p53 transcriptional target genes implicated in apoptotic pathways increased in response to treatment with the MDM2 inhibitors, including *AEN*, *PUMA*, *TNFRSF10B* and *TP53INP1*. The highest fold change was seen for *PUMA* in IGROV-1 cells. However, for the OAW42 cell line no significant changes were observed in SubG1 events and caspase3/7 activity, in spite of increased expression levels of genes involved in apoptosis, suggesting apoptotic pathway deficiencies in this cell line.

A number of studies indicated that the cyclin-dependent kinase inhibitor $p21^{WAF1}$ plays a dual role and may exert an anti-oncogenic or oncogenic role (Abbas and Dutta, 2009; Maria Teresa Piccolo1, 2012; Lu, 2016) which is dependent on the cancer type and drug treatment (Maria Teresa Piccolo1, 2012). However, a recent study indicated that removal of $p21^{WAF1}$ had no effect on Nutlin-3a induced apoptosis, and induction of $p21^{WAF1}$ did not protect cancer cells against apoptosis induced by nongenotoxic p53 activation (Xia *et al.*, 2011). In the current study, *CDKN1A* ($p21^{WAF1}$) and a number of pro-apoptotic genes were induced upon treatment with both Nutlin-3 and RG7388 across all three wild-type *TP53* cell lines, and two out of the three cell lines underwent apoptosis. The data extracted from this study suggest that Nutlin-3 or RG7388-induced $p21^{WAF1}$ levels do not prevent induction of apoptosis in ovarian cancer cells.

9.8 Mutant *TP53* cells selected for resistance to treatment from parental wild-type *TP53* cell lines may retain their sensitivity to alternative therapies

A major challenge in drug development and cancer therapy is acquired resistance of tumour cells to therapeutic agents. Due to the effect of MDM2-p53 antagonists only on the wild-type *TP53* cells, they are likely to select the mutant *TP53* cells that are present in the original populations at low frequencies, leading to resistance to other p53-dependent therapeutic agents (Aziz *et al.*, 2011; Zhao *et al.*, 2015; Burgess *et al.*, 2016). In the current study, the mutant *TP53* cell lines were sensitive to cisplatin in spite of being resistant to Nutlin-3 and RG7388. For example, there was a difference in the GI_{50} values in response to cisplatin between the *MLH1*-corrected CP70+ cell line with mutant *TP53* and its parental cell line A2780. However, there is a very noticeable difference in GI_{50} values in response to Nutlin-3 and RG7388. The cell lines that were found to be resistant to cisplatin have a deletion in *TP53*, SKOV-3, or a mutation in *MLH-1* in addition to *TP53* mutation, CP70. A number of studies investigated the role of *TP53* in response to cisplatin demonstrating increased sensitivity to cisplatin for head and neck squamous cell carcinoma lines with mutant *TP53* (Bradford *et al.*, 2003) or showing a marked response to cisplatin through both p53-dependent and p53-independent mechanisms for human ovarian xenografts (Clarke *et al.*, 2004). Another study also indicated a relatively modest role of *TP53*-dependent apoptosis in response to ionising radiation (Gudkov and Komarova, 2003). Furthermore, a recent study indicated that both NGP and SJSA-1 Nutlin-3/MI63 resistant *TP53* mutant cell lines have a response to ionising radiation which is similar to that of parental *TP53* wild-type NGP and SJSA-1 cell lines (Drummond *et al.*, 2016). The results from our study and those obtained by Drummond et al. are in accord with the data on the Sanger Genomics of Drug Sensitivity database, showing no marked difference in response to DNA damaging agents for the cell lines with wild-type *TP53* compared to those with mutant *TP53*, in spite of indicating a very significant difference in sensitivity to Nutlin-3 (http://www.cancerrxgene.org). Overall, these results demonstrate that selected mutant *TP53* cells following treatment with MDM2-p53 antagonists may retain their sensitivity to alternative therapies including platinum-based chemotherapy and ionising radiation. In addition, use of MDM2-p53 inhibitors in combination with chemotherapeutic agents or other targeted cancer treatments which act in a p53-independent manner may be a useful strategy.

9.9 MDM2-p53 antagonists in combination with other therapeutic agents in ovarian cancer

Previous studies have indicated synergistic effects between chemotherapeutic drugs and MDM2-p53 inhibitors in different types of cancer, including two limited studies with ovarian cancer cell lines demonstrating that Nutlin-3a synergises with cisplatin (Mir *et al.*, 2013) or resveratrol (Marimuthu *et al.*, 2011). The results of the present study demonstrated a significant reduction of cell growth and induction of apoptosis when the cells were treated with a combination of Nutlin-3 or RG7388 with cisplatin or rucaparib, compared to the effects of cisplatin or rucaparib alone in a cell type, compound and time-dependent manner. The response to cisplatin or rucaparib was significantly enhanced upon disruption of the MDM2-p53 interaction, with additive or synergistic effects and favourable DRI values in most cases. In terms of combined treatment between Nutlin-3 or RG7388 and cisplatin, the presence of wild-type *TP53* was the main predictive biomarker of response to MDM2-p53 antagonists. Nevertheless, an additional potential determinant of response in the current study involved the balance of expression between growth inhibitory/pro-survival and pro-apoptotic genes. Our results indicate that this dominates the small changes in the expression of DNA repair genes and provides a potential explanation for some differences in sensitivity between the *TP53* wild-type cell lines and for the synergy observed for treatment with cisplatin and MDM2-p53 inhibitors.

The use of much lower doses of genotoxic drugs may be possible by combining established chemotherapy agents with non-genotoxic MDM2-p53 inhibitors. Furthermore, combination of other targeted therapies such as RG7388 with rucaparib is a potential strategy to overcome intrinsic resistance and delay acquired resistance to either agent alone.

9.10 Conclusion remarks and future work

This study set out to investigate the prognostic and predictive value of genomic and functional status of *TP53* in ovarian cancer, and to investigate the effect of MDM2-p53 antagonists, Nutlin-3 and RG7388, as single agents or in combination with the chemotherapeutic agent cisplatin or another targeted therapy agent, rucaparib, in ovarian cancer. The present study indicates that *TP53* genomic status can be considered to be a predictive biomarker of overall survival in response to single agent carboplatin for ovarian cancer patients. It also demonstrates that MDM2-p53 antagonists have activity as a single agent against wild-type *TP53* ovarian cancer cells, leading to cell cycle arrest and/or apoptosis. In addition, combination treatment with MDM2 inhibitors and cisplatin has synergistic and/or dose reduction potential, dependent on cell genotype and compound, and merits further investigation. Our study clearly indicates that the presence of wild-type *TP53* remains the main predictive biomarker of response to MDM2 inhibitors, and the balance of activity between growth inhibitory/pro-survival and pro-apoptotic genes dominates the small changes in the expression of DNA repair genes as an explanation for the synergy observed for treatment with cisplatin and MDM2 inhibitors. Furthermore, combination treatment with MDM2 inhibitors and rucaparib has synergistic and dose reduction potential. However, more research is needed to clarify the interplay between p53 and PARP and confirmation of synergy with *ex-vivo* primary ovarian cancer cells and *in vivo* preclinical xenograft models.

References

Abbas, T. and Dutta, A. (2009a) 'p21 in cancer: intricate networks and multiple activities', *Nature reviews. Cancer*, 9(6), pp. 400-414.

Agarwal, R. and Kaye, S.B. (2003) 'Ovarian cancer: strategies for overcoming resistance to chemotherapy', *Nat Rev Cancer*, 3(7), pp. 502-516.

Ahmed, A.A., Etemadmoghadam, D., Temple, J., Lynch, A.G., Riad, M., Sharma, R., Stewart, C., Fereday, S., Caldas, C., deFazio, A., Bowtell, D. and Brenton, J.D. (2010) 'Driver mutations in TP53 are ubiquitous in high grade serous carcinoma of the ovary', *The Journal of Pathology*, 221(1), pp. 49-56.

Al-Lazikani, B., Banerji, U. and Workman, P. (2012) 'Combinatorial drug therapy for cancer in the post-genomic era', *Nat Biotech*, 30(7), pp. 679-692.

Ali, A.Y., Abedini, M.R. and Tsang, B.K. (2012a) 'The oncogenic phosphatase PPM1D confers cisplatin resistance in ovarian carcinoma cells by attenuating checkpoint kinase 1 and p53 activation', *Oncogene*, 31(17), pp. 2175-86.

Ali, A.Y., Farrand, L., Kim, J.Y., Byun, S., Suh, J.-Y., Lee, H.J. and Tsang, B.K. (2012b) 'Molecular determinants of ovarian cancer chemoresistance: new insights into an old conundrum', *Annals of the New York Academy of Sciences*, 1271(1), pp. 58-67.

Almazov, V.P., Kochetkov, D.V. and Chumakov, P.M. (2007) 'Use of p53 for Therapy of Human Cancer', *Molekuliarnaia biologiia*, 41(6), pp. 947-963.

Amikura, T., Sekine, M., Hirai, Y., Fujimoto, S., Hatae, M., Kobayashi, I., Fujii, T., Nagata, I., Ushijima, K., Obata, K., Suzuki, M., Yoshinaga, M., Umesaki, N., Satoh, S., Enomoto, T., Motoyama, S., Nishino, K., Haino, K. and Tanaka, K. (2006) 'Mutational analysis of TP53 and p21 in familial and sporadic ovarian cancer in Japan', *Gynecologic Oncology*, 100(2), pp. 365-371.

Andreeff, M., Kelly, K.R., Yee, K., Assouline, S., Strair, R., Popplewell, L., Bowen, D., Martinelli, G., Drummond, M.W., Vyas, P., Kirschbaum, M., Iyer, S.P., Ruvolo, V., Gonzalez, G.M., Huang, X., Chen, G., Graves, B., Blotner, S., Bridge, P., Jukofsky, L., Middleton, S., Reckner, M., Rueger, R., Zhi, J., Nichols, G. and Kojima, K. (2016a) 'Results of the Phase I Trial of RG7112, a Small-Molecule MDM2 Antagonist in Leukemia', *Clin Cancer Res*, 22(4), pp. 868-76.

Anglesio, M.S., Wiegand, K.C., Melnyk, N., Chow, C., Salamanca, C., Prentice, L.M., Senz, J., Yang, W., Spillman, M.A., Cochrane, D.R., Shumansky, K., Shah, S.P., Kalloger, S.E. and Huntsman, D.G. (2013) 'Type-Specific Cell Line Models for Type-Specific Ovarian Cancer Research', *PLOS ONE*, 8(9), pp.72162-75.

Anil, B., Riedinger, C., Endicott, J.A. and Noble, M.E. (2013) 'The structure of an MDM2-Nutlin-3a complex solved by the use of a validated MDM2 surface-entropy reduction mutant', *Acta Crystallogr D Biol Crystallogr*, 69(Pt 8), pp. 1358-66.

Antolín, A.A. and Mestres, J. (2014) *Linking off-target kinase pharmacology to the differential cellular effects observed among PARP inhibitors*, Oncotarget, 5(10), pp. 3023-3028.

Anttila, M.A., Kosma, V.M., Hongxiu, J., Puolakka, J., Juhola, M., Saarikoski, S. and Syrjänen, K. (1999) 'p21/WAF1 expression as related to p53, cell proliferation and prognosis in epithelial ovarian cancer', *British Journal of Cancer*, 79(11-12), pp. 1870-1878.

Anwar, M., Aslam, H. and Anwar, S. (2015) 'PARP inhibitors', *Hereditary Cancer in Clinical Practice*, 13(1), pp. 4-8.

Arkin, Michelle R., Tang, Y. and Wells, James A. (2014) 'Small-Molecule Inhibitors of Protein-Protein Interactions: Progressing toward the Reality', *Chemistry & Biology*, 21(9), pp. 1102-1114.

Arreaza, G., Qiu, P., Pang, L., Albright, A., Hong, Z.L., Marton, J.M. and Levitan, D. (2016) 'Pre-Analytical Considerations for Successful Next-Generation Sequencing (NGS): Challenges and Opportunities for Formalin-Fixed and Paraffin-Embedded Tumor Tissue (FFPE) Samples', *International Journal of Molecular Sciences*, 17(9), pp. 1579-87.
Arya, A.K., El-Fert, A., Devling, T., Eccles, R.M., Aslam, M.A., Rubbi, C.P., Vlatković, N., Fenwick, J., Lloyd, B.H., Sibson, D.R., Jones, T.M. and Boyd, M.T. (2010) 'Nutlin-3, the small-molecule inhibitor of MDM2, promotes senescence and radiosensitises laryngeal carcinoma cells harbouring wild-type p53', *British Journal of Cancer*, 103(2), pp. 186-195.
Ashkenazi, A. and Herbst, R.S. (2008) 'To kill a tumor cell: the potential of proapoptotic receptor agonists', *The Journal of Clinical Investigation*, 118(6), pp. 1979-1990.
Ataian, Y. and Krebs, J.E. (2006) 'Five repair pathways in one context: chromatin modification during DNA repair, *Biochemistry and Cell Biology*, 84(4), pp. 490-494.
Aziz, M.H., Shen, H. and Maki, C.G. (2011a) 'Acquisition of p53 mutations in response to the non-genotoxic p53 activator Nutlin-3', *Oncogene*, 30(46), pp. 4678-86.
Baekelandt, M., Kristensen, G.B., Nesland, J.M., Tropé, C.G. and Holm, R. (1999) 'Clinical Significance of Apoptosis-Related Factors p53, Mdm2, and Bcl-2 in Advanced Ovarian Cancer', *Journal of Clinical Oncology*, 17(7), p. 2061-2068.
Bai, X.T., Moles, R., Chaib-Mezrag, H. and Nicot, C. (2015) 'Small PARP inhibitor PJ-34 induces cell cycle arrest and apoptosis of adult T-cell leukemia cells', *Journal of Hematology & Oncology*, 8, p. 117-128.
Bajrami, I., Frankum, J.R., Konde, A., Miller, R.E., Rehman, F.L., Brough, R., Campbell, J., Sims, D., Rafiq, R., Hooper, S., Chen, L., Kozarewa, I., Assiotis, I., Fenwick, K., Natrajan, R., Lord, C.J. and Ashworth, A. (2014) 'Genome-wide profiling of genetic synthetic lethality identifies CDK12 as a novel determinant of PARP1/2 inhibitor sensitivity', *Cancer Res*, 74(1), pp. 287-97.
Bali, A., O'Brien, P.M., Edwards, L.S., Sutherland, R.L., Hacker, N.F. and Henshall, S.M. (2004) 'Cyclin D1, p53, and p21Waf1/Cip1 expression is predictive of poor clinical outcome in serous epithelial ovarian cancer', *Clin Cancer Res*, 10(15), pp. 5168-77.
Bamias, A., Sotiropoulou, M., Zagouri, F., Trachana, P., Sakellariou, K., Kostouros, E., Kakoyianni, K., Rodolakis, A., Vlahos, G., Haidopoulos, D., Thomakos, N., Antsaklis, A. and Dimopoulos, M.A. (2012) 'Prognostic evaluation of tumour type and other histopathological characteristics in advanced epithelial ovarian cancer, treated with surgery and paclitaxel/carboplatin chemotherapy: Cell type is the most useful prognostic factor', *European Journal of Cancer*, 48(10), pp. 1476-1483.
Banerjee, S. and Kaye, S.B. (2013) 'New strategies in the treatment of ovarian cancer: current clinical perspectives and future potential', *Clin Cancer Res*, 19(5), pp. 961-8.
Bao, L., Jaramillo, M.C., Zhang, Z., Zheng, Y., Yao, M., Zhang, D.D. and Yi, X. (2015) 'Induction of autophagy contributes to cisplatin resistance in human ovarian cancer cells', *Molecular Medicine Reports*, 11(1), pp. 91-98.
Barrette, K., van den Oord, J.J. and Garmyn, M. (2014) 'Tissue microarray', *J Invest Dermatol*, 134(9), p. 1-4.
Bartel, F., Jung, J., Bohnke, A., Gradhand, E., Zeng, K., Thomssen, C. and Hauptmann, S. (2008) 'Both germ line and somatic genetics of the p53 pathway affect ovarian cancer incidence and survival', *Clin Cancer Res*, 14(1), pp. 89-96.
Bartlett, J.M.S., D. (2003) 'A short history of the polymerase chain reaction', *Methods Mol Biol*, 226, pp. 3-6.
Bast, R.C., Hennessy, B. and Mills, G.B. (2009b) 'The biology of ovarian cancer: new opportunities for translation', *Nat Rev Cancer*, 9(6), pp. 415-428.
Bauerschlag, D.O., Schem, C., Weigel, M.T., von Kaisenberg, C., Strauss, A., Bauknecht, T., Maass, N. and Meinhold-Heerlein, I. (2010c) 'The role of p53 as a surrogate marker for

chemotherapeutical responsiveness in ovarian cancer', *Journal of Cancer Research and Clinical Oncology*, 136(1), pp. 79-88.
Benafif, S. and Hall, M. (2015) 'An update on PARP inhibitors for the treatment of cancer', *OncoTargets and therapy*, 8, pp. 519-528.
Bénard, J., Da Silva, J., De Blois, M.-C., Boyer, P., Duvillard, P., Chiric, E. and Riou, G. (1985) 'Characterization of a Human Ovarian Adenocarcinoma Line, IGROV1, in Tissue Culture and in Nude Mice', *Cancer Research*, 45(10), pp. 4970-4979.
Bernardini, M.Q., Baba, T., Lee, P.S., Barnett, J.C., Sfakianos, G.P., Secord, A.A., Murphy, S.K., Iversen, E., Marks, J.R. and Berchuck, A. (2010) 'Expression signatures of TP53 mutations in serous ovarian cancers', *BMC Cancer*, 10, pp. 237-237.
Bewick, V., Cheek, L. and Ball, J. (2004) 'Statistics review 12: Survival analysis', *Critical Care*, 8(5), pp. 1-6.
Bjørnslett, M., Knappskog, S., Lønning, P.E. and Dørum, A. (2012) 'Effect of the MDM2 promoter polymorphisms SNP309T>G and SNP285G>C on the risk of ovarian cancer in BRCA1 mutation carriers', *BMC Cancer*, 12(1), pp. 1-6.
Bo, H., Heuvel, A.P.J.v.d., Varun, V.P., Shengliang, Z. and Wafik, S.E.-D. (2014) 'Targeting Tumor Suppressor p53 for Cancer Therapy: Strategies, Challenges and Opportunities', *Current Drug Targets*, 15(1), pp. 80-89.
Bossi, F., Bernardi, S., Zauli, G., Secchiero, P. and Fabris, B. (2015) 'TRAIL Modulates the Immune System and Protects against the Development of Diabetes', *Journal of Immunology Research*, 2015, p. 680749-680760.
Bowtell, D. (2003) 'Molecular prognosis of epithelial ovarian cancer: Observations from current literature', *Cancer Forum*, 27(3), PP.157-159.
Bowtell, D.D., Böhm, S., Ahmed, A.A., Aspuria, P.-J., Bast, R.C., Beral, V., Berek, J.S., Birrer, M.J., Blagden, S., Bookman, M.A., Brenton, J., Chiappinelli, K.B., Martins, F.C., Coukos, G., Drapkin, R., Edmondson, R., Fotopoulou, C., Gabra, H., Galon, J., Gourley, C., Heong, V., Huntsman, D.G., Iwanicki, M., Karlan, B.Y., Kaye, A., Lengyel, E., Levine, D.A., Lu, K.H., McNeish, I.A., Menon, U., Narod, S.A., Nelson, B.H., Nephew, K.P., Pharoah, P., Powell, D.J., Ramos, P., Romero, I.L., Scott, C.L., Sood, A.K., Stronach, E.A. and Balkwill, F.R. (2015) 'Rethinking ovarian cancer II: reducing mortality from high-grade serous ovarian cancer', *Nature reviews. Cancer*, 15(11), pp. 668-679.
Brachova, P., Mueting, S.R., Carlson, M.J., Goodheart, M.J., Button, A.M., Mott, S.L., Dai, D., Thiel, K.W., Devor, E.J. and Leslie, K.K. (2015) 'TP53 oncomorphic mutations predict resistance to platinum- and taxane-based standard chemotherapy in patients diagnosed with advanced serous ovarian carcinoma', *International Journal of Oncology*, 46(2), pp. 607-618.
Bradford, C.R., Zhu, S., Ogawa, H., Ogawa, T., Ubell, M., Narayan, A., Johnson, G., Wolf, G.T., Fisher, S.G. and Carey, T.E. (2003) 'P53 mutation correlates with cisplatin sensitivity in head and neck squamous cell carcinoma lines', *Head Neck*, 25(8), pp. 654-61.
Braicu, E.I., Sehouli, J., Richter, R., Pietzner, K., Denkert, C. and Fotopoulou, C. (2011) 'Role of histological type on surgical outcome and survival following radical primary tumour debulking of epithelial ovarian, fallopian tube and peritoneal cancers', *British Journal of Cancer*, 105(12), pp. 1818-1824.
Brown, J.S., Kaye, S.B. and Yap, T.A. (2016) 'PARP inhibitors: the race is on', *Br J Cancer*, 114(7), pp. 713-715.
Budanov, A.V. and Karin, M. (2008) 'The p53-regulated Sestrin gene products inhibit mTOR signaling', *Cell*, 134(3), pp. 451-460.
Burgess, A., Chia, K.M., Haupt, S., Thomas, D., Haupt, Y. and Lim, E. (2016) 'Clinical Overview of MDM2/X-Targeted Therapies', *Frontiers in Oncology*, 6, p. 3389-3396.
Burry, R.W. (2011) 'Controls for Immunocytochemistry: An Update', *Journal of Histochemistry and Cytochemistry*, 59(1), pp. 6-12.

Camp, R.L., Charette, L.A. and Rimm, D.L. (2000) 'Validation of Tissue Microarray Technology in Breast Carcinoma', *Lab Invest*, 80(12), pp. 1943-1949.
Cancer Research UK, http://www.cancerresearchuk.org/about-cancer/ovarian-cancer/risks-causes, (June) (2016).
cancer.sanger.ac.uk. www.sanger.ac.uk/, COSMIC: exploring the world's knowledge of somatic mutations in human cancer (Forbes et al. 2014).
Canevari, S., Gariboldi, M., Reid, J.F., Bongarzone, I. and Pierotti, M.A. (2006) 'Molecular predictors of response and outcome in ovarian cancer', *Critical Reviews in Oncology/Hematology*, 60(1), pp. 19-37.
Cao, J., Cai, J., Huang, D., Han, Q., Chen, Y., Yang, Q., Yang, C., Kuang, Y., Li, D. and Wang, Z. (2014) 'miR-335 Represents an Independent Prognostic Marker in Epithelial Ovarian Cancer', *American Journal of Clinical Pathology*, 141(3), pp. 437-442.
Carlos J. A. Ribeiro, C.M.P.R., Rui Moreira and Maria M. M. Santos (2016) 'Chemical Variations on the p53 Reactivation Theme', *Pharmaceuticals*, 9(2).pp. 25-58.
Carol, H., Reynolds, C.P., Kang, M.H., Keir, S.T., Maris, J.M., Gorlick, R., Kolb, E.A., Billups, C.A., Geier, B., Kurmasheva, R.T., Houghton, P.J., Smith, M.A. and Lock, R.B. (2013) 'Initial testing of the MDM2 inhibitor RG7112 by the Pediatric Preclinical Testing Program', *Pediatr Blood Cancer*, 60(4), pp. 633-41.
Cazzalini, O., Scovassi, A.I., Savio, M., Stivala, L.A. and Prosperi, E. (2010) 'Multiple roles of the cell cycle inhibitor p21CDKN1A in the DNA damage response', *Mutation Research/Reviews in Mutation Research*, 704(1–3), pp. 12-20.
Chen, L., Rousseau, R.F., Middleton, S.A., Nichols, G.L., Newell, D.R., Lunec, J. and Tweddle, D.A. (2015a) 'Pre-clinical evaluation of the MDM2-p53 antagonist RG7388 alone and in combination with chemotherapy in neuroblastoma', *Oncotarget*, 6(12), pp. 10207-21.
Chen, L., Zhao, Y., Halliday, G.C., Berry, P., Rousseau, R.F., Middleton, S.A., Nichols, G.L., Del Bello, F., Piergentili, A., Newell, D.R., Lunec, J. and Tweddle, D.A. (2014) 'Structurally diverse MDM2–p53 antagonists act as modulators of MDR-1 function in neuroblastoma', *British Journal of Cancer*, 111(4), pp. 716-725.
Chene, P. (2003) 'Inhibiting the p53-MDM2 interaction: an important target for cancer therapy', *Nat Rev Cancer*, 3(2), pp. 102-9.
Cho, K.R. and Shih, I.-M. (2009) 'Ovarian cancer', *Annual review of pathology*, 4, pp. 287-313.
Chou, T.-C. (2006) 'Theoretical Basis, Experimental Design, and Computerized Simulation of Synergism and Antagonism in Drug Combination Studies', *Pharmacological Reviews*, 58(3), pp. 621-681.
Chou, T.-C. (2010) 'Drug Combination Studies and Their Synergy Quantification Using the Chou-Talalay Method', *Cancer Research*, 70(2), pp. 440-446.
Chris M.J. Conklin, M.C.B.G., MD, FRCPC (2013) 'LGSCs are uncommon, accounting for approximately 3% of ovarian surface epithelial carcinomas', *EXPERT REVIEWS*, 8(1), PP.67-82.
Christian Tovar, B.G., Kathryn Packman, Zoran Filipovic, Brian Higgins Mingxuan Xia,Christine Tardell, Rosario Garrido, Edmund Lee, Kenneth Kolinsky, Kwong-Him To, Michael Linn,Frank Podlaski, Peter Wovkulich, Binh Vu, and Lyubomir T. Vassilev (2013) 'MDM2 Small-Molecule Antagonist RG7112 Activates p53 Signaling and Regresses Human Tumors in Preclinical Cancer Models', *Therapeutics, Targets, and Chemical Biology*, 73(8), PP. 2587-2597.
Clarke, P.A., Pestell, K.E., Di Stefano, F., Workman, P. and Walton, M.I. (2004) 'Characterisation of molecular events following cisplatin treatment of two curable ovarian cancer models: contrasting role for p53 induction and apoptosis in vivo', *Br J Cancer*, 91(8), pp. 1614-23.

Cobb, L.P., Gaillard, S., Wang, Y., Shih, I.-M. and Secord, A.A. (2015) 'Adenocarcinoma of Mullerian origin: review of pathogenesis, molecular biology, and emerging treatment paradigms', *Gynecologic Oncology Research and Practice*, 2(1), pp. 1-16.
Coleman, R.L. (2016) 'Ovarian cancer in 2015: Insights into strategies for optimizing ovarian cancer care', *Nat Rev Clin Oncol*, 13(2), pp. 71-72.
Collavin, L., Lunardi, A. and Del Sal, G. (2010) 'p53-family proteins and their regulators: hubs and spokes in tumor suppression', *Cell Death Differ*, 17(6), pp. 901-911.
Colombo, N., Peiretti, M., Parma, G., Lapresa, M., Mancari, R., Carinelli, S., Sessa, C., Castiglione, M. and On behalf of the, E.G.W.G. (2010b) 'Newly diagnosed and relapsed epithelial ovarian carcinoma: ESMO Clinical Practice Guidelines for diagnosis, treatment and follow-up', *Annals of Oncology*, 21(suppl 5), pp. v23-v30.
Contractor, T. and Harris, C.R. (2012) 'p53 Negatively Regulates Transcription of the Pyruvate Dehydrogenase Kinase Pdk2', *Cancer Research*, 72(2), pp. 560-567.
Corbi-Verge, C. and Kim, P.M. (2016) 'Motif mediated protein-protein interactions as drug targets', *Cell Communication and Signaling*, 14(1), pp. 1-12.
Corney, D.C., Flesken-Nikitin, A., Choi, J. and Nikitin, A.Y. (2008) 'Role of p53 and Rb in Ovarian Cancer', *Advances in experimental medicine and biology*, 622, pp. 99-117.
Coward, J.I.G., Middleton, K. and Murphy, F. (2015) 'New perspectives on targeted therapy in ovarian cancer', *International Journal of Women's Health*, 7, pp. 189-203.
Crane, E.K., Kwan, S.-Y., Izaguirre, D.I., Tsang, Y.T.M., Mullany, L.K., Zu, Z., Richards, J.S., Gershenson, D.M. and Wong, K.-K. (2015) 'Nutlin-3a: A Potential Therapeutic Opportunity for TP53 Wild-Type Ovarian Carcinomas', *PLoS ONE*, 10(8), p. e0135101.
Creighton, C.J., Fountain, M.D., Yu, Z., Nagaraja, A.K., Zhu, H., Khan, M., Olokpa, E., Zariff, A., Gunaratne, P.H., Matzuk, M.M. and Anderson, M.L. (2010) 'Molecular profiling uncovers a p53-associated role for microRNA-31 in inhibiting the proliferation of serous ovarian carcinomas and other cancers', *Cancer Res*, 70(5), pp. 1906-15.
Crijns, A.P.G., Schouten, J.P., Arts, H.J.G., Hofstra, R.M.W., Willemse, P.H.B., Vries, E.G.E. and Zee, A.G.J. (2003) 'Prognostic factors in ovarian cancer: current evidence and future prospects', *EJC Supplements*, 1(6), PP.127-145.
Cristiana, L.N. (2014) 'New Insights into P53 Signalling and Cancer: Implications for Cancer Therapy', *Journal OF Tumor*, 2(1), PP. 73-82.
Curtin, N.J. (2013) 'Inhibiting the DNA damage response as a therapeutic manoeuvre in cancer', *British Journal of Pharmacology*, 169(8), pp. 1745-1765.
Curtin, N.J., Wang, L.-Z., Yiakouvaki, A., Kyle, S., Arris, C.A., Canan-Koch, S., Webber, S.E., Durkacz, B.W., Calvert, H.A., Hostomsky, Z. and Newell, D.R. (2004a) 'Novel Poly(ADP-ribose) Polymerase-1 Inhibitor, AG14361, Restores Sensitivity to Temozolomide in Mismatch Repair-Deficient Cells', *Clinical Cancer Research*, 10(3), pp. 881-889.
Daemen, A., Wolf, D.M., Korkola, J.E., Griffith, O.L., Frankum, J.R., Brough, R., Jakkula, L.R., Wang, N.J., Natrajan, R., Reis-Filho, J.S., Lord, C.J., Ashworth, A., Spellman, P.T., Gray, J.W. and van't Veer, L.J. (2012) 'Cross-platform pathway-based analysis identifies markers of response to the PARP inhibitor olaparib', *Breast Cancer Res Treat*, 135(2), pp. 505-17.
Dai, C. and Gu, W. (2010) 'p53 post-translational modification: deregulated in tumorigenesis', *Trends in Molecular Medicine*, 16(11), pp. 528-536.
Dai, L., Li, C., Shedden, K.A., Misek, D.E. and Lubman, D.M. (2009) 'Comparative Proteomic Study of Two Closely Related Ovarian Endometrioid Adenocarcinoma Cell Lines Using cIEF Fractionation and Pathway Analysis', *Electrophoresis*, 30(7), pp. 1119-1131.
Darcy, K.M., Brady, W.E., McBroom, J.W., Bell, J.G., Young, R.C., McGuire, W.P., Linnoila, R.I., Hendricks, D., Bonome, T. and Farley, J.H. (2008) 'Association between p53 overexpression and multiple measures of clinical outcome in high-risk, early stage or

suboptimally- resected, advanced stage epitilial ovarian cancers: A Gynecologic Oncology Group Study', *Gynecologic oncology*, 111(3), pp. 487-495.
Dasari, S. and Tchounwou, P.B. (2014) 'Cisplatin in cancer therapy: molecular mechanisms of action', *European journal of pharmacology*, 5(1), pp. 364-378.
de Graeff, P., Crijns, A.P.G., de Jong, S., Boezen, M., Post, W.J., de Vries, E.G.E., van der Zee, A.G.J. and de Bock, G.H. (2009) 'Modest effect of p53, EGFR and HER-2/neu on prognosis in epithelial ovarian cancer: a meta-analysis', *British Journal of Cancer*, 101(1), pp. 149-159.
de Matos, L.L., Trufelli, D.C., de Matos, M.G.L. and da Silva Pinhal, M.A. (2010) 'Immunohistochemistry as an Important Tool in Biomarkers Detection and Clinical Practice', *Biomarker Insights*, 5, pp. 9-20.
Deben, C., Wouters, A., Beeck, K.O.d., Bossche, J.v.D., Jacobs, J., Zwaenepoel, K., Peeters, M., Meerbeeck, J.V., Lardon, F., Rolfo, C., Deschoolmeester, V. and Pauwels, P. (2015) *The MDM2-inhibitor Nutlin-3 synergizes with cisplatin to induce p53 dependent tumor cell apoptosis in non-small cell lung cancer*, Oncotarget, 6(26), pp. 22666-79.
Demidenko, Z.N., Korotchkina, L.G., Gudkov, A.V. and Blagosklonny, M.V. (2010) 'Paradoxical suppression of cellular senescence by p53', *Proceedings of the National Academy of Sciences of the United States of America*, 107(21), pp. 9660-9664.
Devouassoux-Shisheboran, M. and Genestie, C. (2015) 'Pathobiology of ovarian carcinomas', *Chinese Journal of Cancer*, 34(1), pp. 50-55.
di Iasio, M.G. and Zauli, G. (2013) 'The non-genotoxic activator of the p53 pathway Nutlin-3 shifts the balance between E2F7 and E2F1 transcription factors in leukemic cells', *Invest New Drugs*, 31(2), pp. 458-60.
Di Leva, G. and Croce, C.M. (2013) 'The Role of microRNAs in the Tumorigenesis of Ovarian Cancer', *Frontiers in Oncology*, 3, p. 153.
Ding, Q., Zhang, Z., Liu, J.-J., Jiang, N., Zhang, J., Ross, T.M., Chu, X.-J., Bartkovitz, D., Podlaski, F., Janson, C., Tovar, C., Filipovic, Z.M., Higgins, B., Glenn, K., Packman, K., Vassilev, L.T. and Graves, B. (2013) 'Discovery of RG7388, a Potent and Selective p53–MDM2 Inhibitor in Clinical Development', *Journal of Medicinal Chemistry*, 56(14), pp. 5979-5983.
Do, H. and Dobrovic, A. (2015) 'Sequence artifacts in DNA from formalin-fixed tissues: causes and strategies for minimization', *Clin Chem*, 61(1), pp. 64-71.
Dogan, E., Saygili, U., Tuna, B., Gol, M., Gurel, D., Acar, B. and Koyuncuoglu, M. (2005a) 'p53 and mdm2 as prognostic indicators in patients with epithelial ovarian cancer: a multivariate analysis', *Gynecol Oncol*, 97(1), pp. 46-52.
Drew, Y., Ledermann, J., Hall, G., Rea, D., Glasspool, R., Highley, M., Jayson, G., Sludden, J., Murray, J., Jamieson, D., Halford, S., Acton, G., Backholer, Z., Mangano, R., Boddy, A., Curtin, N. and Plummer, R. (2016) 'Phase 2 multicentre trial investigating intermittent and continuous dosing schedules of the poly(ADP-ribose) polymerase inhibitor rucaparib in germline BRCA mutation carriers with advanced ovarian and breast cancer', *Br J Cancer*, 114(7), pp. 723-730.
Drummond, C.J., Esfandiari, A., Liu, J., Lu, X., Hutton, C., Jackson, J., Bennaceur, K., Xu, Q., Rao Makimanejavali, A., Del Bello, F., Piergentili, A., Newell, D.R., Hardcastle, I.R., Griffin, R.J. and Lunec, J. (2016) *TP53 mutant MDM2 -amplified cell lines selected for resistance to MDM2-p53 binding antagonists retain sensitivity to ionizing radiation*, Oncotarget, 7(29), pp. 46203-46218.
Eckel-Passow, J.E., Lohse, C.M., Sheinin, Y., Crispen, P.L., Krco, C.J. and Kwon, E.D. (2010) 'Tissue microarrays: one size does not fit all', *Diagnostic Pathology*, 5, pp. 48-48.
Emelyanov, A. and Bulavin, D.V. (2015) 'Wip1 phosphatase in breast cancer', *Oncogene*, 34(34), pp. 4429-4438.

Erin K. Crane , S.-Y.K., Daisy I. Izaguirre , Yvonne T. M. Tsang , Lisa K. Mullany , Zhifei Zu , JoAnne S. Richards , David M. Gershenson , Kwong-Kwok Wong (2015) 'Nutlin-3a: A Potential Therapeutic Opportunity for TP53 Wild-Type Ovarian Carcinomas', *Plos One*, 10(8), pp. 135101-135114.
Esfandiari, A., Hawthorne, T.A., Nakjang, S. and Lunec, J. (2016) 'Chemical inhibition of wild-type p53 induced phosphatase 1 (WIP1/PPM1D) by GSK2830371 potentiates the sensitivity to MDM2 inhibitors in a p53-dependent manner', *Molecular Cancer Therapeutics*, 15(3), pp. 379-391.
Espinosa, J.M. and Sullivan, K.D. (2015) 'A signature for success', *eLife*, 4, p. e08773.
Fallows, S., Price, J., Atkinson, R.J., Johnston, P.G., Hickey, I. and Russell, S.E. (2001) 'P53 mutation does not affect prognosis in ovarian epithelial malignancies', *J Pathol*, 194(1), 68-75.
Ferlay J, S.I., Ervik M, et al. (2013) 'Cancer Incidence and Mortality Worldwide: IARC CancerBase No. 11 [Internet]. Lyon, France: International Agency for Research on Cancer. Avaiable from http://globocan.iarc.fr '. Available at: http://globocan.iarc.fr.
Florea, A.-M. and Büsselberg, D. (2011) 'Cisplatin as an Anti-Tumor Drug: Cellular Mechanisms of Activity, Drug Resistance and Induced Side Effects', *Cancers*, 3(1), p. 1351.
Forslund, A., Zeng, Z., Qin, L.-X., Rosenberg, S., Ndubuisi, M., Pincas, H., Gerald, W., Notterman, D.A., Barany, F. and Paty, P.B. (2008) 'MDM2 Gene Amplification Is Correlated to Tumor Progression but not to the Presence of SNP309 or TP53 Mutational Status in Primary Colorectal Cancers', *Molecular Cancer Research*, 6(2), pp. 205-211.
Foucquier, J. and Guedj, M. (2015) 'Analysis of drug combinations: current methodological landscape', *Pharmacology Research & Perspectives*, 3(3), p. e00149.
Foulkes, W.D., Stamp, G.W., Afzal, S., Lalani, N., McFarlane, C.P., Trowsdale, J. and Campbell, I.G. (1995) 'MDM2 overexpression is rare in ovarian carcinoma irrespective of TP53 mutation status', *British Journal of Cancer*, 72(4), pp. 883-888.
Frey, M.K. and Pothuri, B. (2015) 'Targeting DNA repair: poly (ADP-ribose) polymerase inhibitors', *Translational Cancer Research*, 4(1), pp. 84-96.
Fu, T., Min, H., Xu, Y., Chen, J. and Li, G. (2012) 'Molecular Dynamic Simulation Insights into the Normal State and Restoration of p53 Function', *International Journal of Molecular Sciences*, 13(8), pp. 9709-9740.
Gadducci, A., Cosio, S., Tana, R. and Genazzani, A.R. (2009) 'Serum and tissue biomarkers as predictive and prognostic variables in epithelial ovarian cancer', *Critical Reviews in Oncology/Hematology*, 69(1), pp. 12-27.
Gadducci, A., Di Cristofano, C., Zavaglia, M., Giusti, L., Menicagli, M., Cosio, S., Naccarato, A.G., Genazzani, A.R., Bevilacqua, G. and Cavazzana, A.O. (2006) 'P53 Gene Status in Patients with Advanced Serous Epithelial Ovarian Cancer in Relation to Response to Paclitaxel- plus Platinum-based Chemotherapy and Long-term Clinical Outcome', *Anticancer Research*, 26(1B), pp. 687-693.
Gagan, J. and Van Allen, E. (2015) 'Next-generation sequencing to guide cancer therapy', *Genome Medicine*, 7(1), p. 80.
Galluzzi, L., Senovilla, L., Vitale, I., Michels, J., Martins, I., Kepp, O., Castedo, M. and Kroemer, G. (2012) 'Molecular mechanisms of cisplatin resistance', *Oncogene*, 31(15), pp. 1869-1883.
Gately, K., Kerr, K. and O'Byrne, K. (2011) 'Design, construction, and analysis of cell line arrays and tissue microarrays for gene expression analysis', *Methods Mol Biol*, 784, pp. 139-53.
Geisler, H.E., Geisler, J.P., Miller, G.A., Geisler, M.J., Wiemann, M.C., Zhou, Z. and Crabtree, W. (2001) 'p21 and p53 in ovarian carcinoma', *Cancer*, 92(4), pp. 781-786.

Georgia Levidou*, P.F., Efstratios Patsouris and Penelope Korkolopoulou (2011) 'Meta-analysis of the prognostic role of p53: Playground for solution or source of confusion?', *Journal of Public Health and Epidemiology*, 3(3), pp. 83-89.
Gilloteaux, J., Lau, H.L., Gourari, I., Neal, D., Jamison, J.M. and Summers, J.L. (2015) 'Apatone® induces endometrioid ovarian carcinoma (MDAH 2774) cells to undergo karyolysis and cell death by autoschizis: A potent and safe anticancer treatment', *Translational Research in Anatomy*, 1, pp. 25-39.
Giono, L.E. and Manfredi, J.J. (2007) 'Mdm2 Is Required for Inhibition of Cdk2 Activity by p21, Thereby Contributing to p53-Dependent Cell Cycle Arrest', *Molecular and Cellular Biology*, 27(11), pp. 4166-4178.
Green, J.A., Berns, E.M.J.J., Coens, C., van Luijk, I., Thompson-Hehir, J., van Diest, P., Verheijen, R.H.M., van de Vijver, M., van Dam, P., Kenter, G.G., Tjalma, W., Ewing, P.C., Teodorovic, I., Vergote, I. and van der Burg, M.E.L. (2006) 'Alterations in the p53 pathway and prognosis in advanced ovarian cancer: A multi-factorial analysis of the EORTC Gynaecological Cancer group (study 55865)', *European Journal of Cancer*, 42(15), pp. 2539-2548.
Groenendijk, F.H. and Bernards, R. (2014) 'Drug resistance to targeted therapies: Déjà vu all over again', *Molecular Oncology*, 8(6), pp. 1067-1083.
Gudkov, A.V. and Komarova, E.A. (2003) 'The role of p53 in determining sensitivity to radiotherapy', *Nat Rev Cancer*, 3(2), pp. 117-29.
Han, H.S., Yu, E., Song, J.Y., Park, J.Y., Jang, S.J. and Choi, J. (2009) 'The estrogen receptor alpha pathway induces oncogenic Wip1 phosphatase gene expression', *Mol Cancer Res*, 7(5), pp. 713-23.
Hanahan, D. and Weinberg, R.A. (2011) 'Hallmarks of cancer: the next generation', *Cell*, 144(5), pp. 646-74.
Harlozinska, A., Bar, J.K., Montenarh, M. and Kartarius, S. (2002) 'Relations between immunologically different p53 forms, p21WAF1 and PCNA expression in ovarian carcinomas', *Oncology Reports*, 9(6), pp. 1173-1179.
Haupt, S., Berger, M., Goldberg, Z. and Haupt, Y. (2003) 'Apoptosis - the p53 network', *Journal of Cell Science*, 116(20), pp. 4077-4085.
Havrilesky, L., Darcy, K.M., Hamdan, H., Priore, R.L., Leon, J., Bell, J. and Berchuck, A. (2003) 'Prognostic Significance of p53 Mutation and p53 Overexpression in Advanced Epithelial Ovarian Cancer: A Gynecologic Oncology Group Study', *Journal of Clinical Oncology*, 21(20), pp. 3814-3825.
Hecht, J.L., Kotsopoulos, J., Gates, M.A., Hankinson, S.E. and Tworoger, S.S. (2008) 'Validation of tissue microarray technology in ovarian cancer: results from the Nurses' Health Study', *Cancer Epidemiol Biomarkers Prev*, 17(11), pp. 3043-50.
Hennessy, B.T., Coleman, R.L. and Markman, M. (2009) 'Ovarian cancer', *Lancet*, 374(9698), pp. 1371-82.
Hills, C.A., Kelland, L.R., Abel, G., Siracky, J., Wilson, A.P. and Harrap, K.R. (1989) 'Biological properties of ten human ovarian carcinoma cell lines: calibration in vitro against four platinum complexes', *British Journal of Cancer*, 59(4), pp. 527-534.
Hirasawa, A., Saito-Ohara, F., Inoue, J., Aoki, D., Susumu, N., Yokoyama, T., Nozawa, S., Inazawa, J. and Imoto, I. (2003) 'Association of 17q21-q24 Gain in Ovarian Clear Cell Adenocarcinomas with Poor Prognosis and Identification of PPM1D and APPBP2 as Likely Amplification Targets', *Clinical Cancer Research*, 9(6), pp. 1995-2004.
Ho, S.-M. (2003) 'Estrogen, Progesterone and Epithelial Ovarian Cancer', *Reproductive biology and endocrinology : RB&E*, 1, pp. 73-73.
Hoe, K.K., Verma, C.S. and Lane, D.P. (2014) 'Drugging the p53 pathway: understanding the route to clinical efficacy', *Nat Rev Drug Discov*, 13(3), pp. 217-236.

Hong B, van den Heuvel AP, Prabhu VV, Zhang S and WS, E.-D. (2014) 'Targeting Tumor Suppressor p53 for Cancer Therapy: Strategies, Challenges and Opportunities', *Curr Drug Targets*, 15(1), pp. 80-9.
http://www.cancerrxgene.org *Analysis of drug sensitivity data*. Available at: http://www.cancerrxgene.org.
Hu, B., Gilkes, D.M., Farooqi, B., Sebti, S.M. and Chen, J. (2006) 'MDMX Overexpression Prevents p53 Activation by the MDM2 Inhibitor Nutlin', *Journal of Biological Chemistry*, 281(44), pp. 33030-33035.
Hua, G., Lv, X., He, C., Remmenga, S.W., Rodabough, K.J., Dong, J., Yang, L., Lele, S.M., Yang, P., Zhou, J., Karst, A., Drapkin, R.I., Davis, J.S. and Wang, C. (2016) 'YAP Induces High-Grade Serous Carcinoma in Fallopian Tube Secretory Epithelial Cells', *Oncogene*, 35(17), pp. 2247-2265.
Huang, B., Deo, D., Xia, M. and Vassilev, L.T. (2009) 'Pharmacologic p53 activation blocks cell cycle progression but fails to induce senescence in epithelial cancer cells', *Mol Cancer Res*, 7(9), pp. 1497-509.
Huang, J., Hu, W. and Sood, A.K. (2010) 'Prognostic Biomarkers in Ovarian Cancer', *Cancer biomarkers : section A of Disease markers*, 8(0), pp. 231-251.
Huang, M., Shen, A., Ding, J. and Geng, M. (2014) 'Molecularly targeted cancer therapy: some lessons from the past decade', *Trends in Pharmacological Sciences*, 35(1), pp. 41-50.
Hutchison, C.A. (2007) 'DNA sequencing: bench to bedside and beyond', *Nucleic Acids Research*, 35(18), pp. 6227-6237.
Ihnen, M., zu Eulenburg, C., Kolarova, T., Qi, J.W., Manivong, K., Chalukya, M., Dering, J., Anderson, L., Ginther, C., Meuter, A., Winterhoff, B., Jones, S., Velculescu, V.E., Venkatesan, N., Rong, H.-M., Dandekar, S., Udar, N., Jänicke, F., Los, G., Slamon, D.J. and Konecny, G.E. (2013) 'Therapeutic Potential of the Poly(ADP-ribose) Polymerase Inhibitor Rucaparib for the Treatment of Sporadic Human Ovarian Cancer', *Molecular cancer therapeutics*, 12(6), pp. 1002-1015.
Javle, M. and Curtin, N.J. (2011) 'The potential for poly (ADP-ribose) polymerase inhibitors in cancer therapy', *Therapeutic Advances in Medical Oncology*, 3(6), pp. 257-267.
Jawhar, N.M.T. (2009) 'Tissue Microarray: A rapidly evolving diagnostic and research tool', *Annals of Saudi Medicine*, 29(2), pp. 123-127.
Jeay, S., Gaulis, S., Ferretti, S., Bitter, H., Ito, M., Valat, T., Murakami, M., Ruetz, S., Guthy, D.A., Rynn, C., Jensen, M.R., Wiesmann, M., Kallen, J., Furet, P., Gessier, F., Holzer, P., Masuya, K., Wurthner, J., Halilovic, E., Hofmann, F., Sellers, W.R. and Graus Porta, D. (2015) 'A distinct p53 target gene set predicts for response to the selective p53-HDM2 inhibitor NVP-CGM097', *Elife*, 4.
Jeffers, J.R., Parganas, E., Lee, Y., Yang, C., Wang, J., Brennan, J., MacLean, K.H., Han, J., Chittenden, T., Ihle, J.N., McKinnon, P.J., Cleveland, J.L. and Zambetti, G.P. (2003) 'Puma is an essential mediator of p53-dependent and -independent apoptotic pathways', *Cancer Cell*, 4(4), pp. 321-328.
Jelinic, P. and Levine, D.A. (2014) 'New Insights into PARP Inhibitors' Effect on Cell Cycle and Homology-Directed DNA Damage Repair', *Molecular Cancer Therapeutics*, 13(6), pp. 1645-1654.
Jelovac, D. and Armstrong, D.K. (2011) 'Recent Progress in the Diagnosis and Treatment of Ovarian Cancer', *CA: a cancer journal for clinicians*, 61(3), pp. 183-203.
Jiang, L., Kon, N., Li, T., Wang, S.J., Su, T., Hibshoosh, H., Baer, R. and Gu, W. (2015) 'Ferroptosis as a p53-mediated activity during tumour suppression', *Nature*, 520(7545), pp. 57-62.

Jiang, M., Pabla, N., Murphy, R.F., Yang, T., Yin, X.-M., Degenhardt, K., White, E. and Dong, Z. (2007) 'Nutlin-3 Protects Kidney Cells during Cisplatin Therapy by Suppressing Bax/Bak Activation', *The Journal of biological chemistry*, 282(4), pp. 2636-2645.
Joana D, A.J.M., Xavier. Clifford J, Steer. Cecilia M, Rodrigues. (2010) 'The role of p53 in apoptosis.', *DISCOVERY MEDICINE*, 9(45), pp. 145-152.
Johnstone, T.C., Park, G.Y. and Lippard, S.J. (2014) 'Understanding and Improving Platinum Anticancer Drugs – Phenanthriplatin', *Anticancer research*, 34(1), pp. 471-476.
Kamada, R., Toguchi, Y., Nomura, T., Imagawa, T. and Sakaguchi, K. (2015) 'Tetramer formation of tumor suppressor protein p53: Structure, function, and applications', *Biopolymers*, 106(4), pp. 598-612.
Karantza, V. (2011) 'Keratins in health and cancer: more than mere epithelial cell markers', *Oncogene*, 30(2), pp. 127-138.
Khoo, K.H., Verma, C.S. and Lane, D.P. (2014) 'Drugging the p53 pathway: understanding the route to clinical efficacy', *Nat Rev Drug Discov*, 13(4), pp. 314-314.
Kigawa, J., Sato, S., Shimada, M., Takahashi, M., Itamochi, H., Kanamori, Y. and Terakawa, N. (2001) 'p53 gene status and chemosensitivity in ovarian cancer', *Hum Cell*, 14(3), pp. 165-71.
Kim, A., Ueda, Y., Naka, T. and Enomoto, T. (2012) 'Therapeutic strategies in epithelial ovarian cancer', *Journal of Experimental & Clinical Cancer Research : CR*, 31(1), pp. 14-14.
Kim, K.H., Choi, S.J., Choi, Y.I., Kim, L., Park, I.S., Han, J.Y., Kim, J.M. and Chu, Y.C. (2013) 'In-house Manual Construction of High-Density and High-Quality Tissue Microarrays by Using Homemade Recipient Agarose-Paraffin Blocks', *Korean Journal of Pathology*, 47(3), pp. 238-244.
Kim, Y.-M., Lee, S.-W., Chun, S.-M., Kim, D.-Y., Kim, J.-H., Kim, K.-R., Kim, Y.-T., Nam, J.-H., van Hummelen, P., MacConaill, L.E., Hahn, W.C. and Jang, S.J. (2014) 'Analysis and Comparison of Somatic Mutations in Paired Primary and Recurrent Epithelial Ovarian Cancer Samples', *PLoS ONE*, 9(6), p. e99451.
Kitayner, M., Rozenberg, H., Kessler, N., Rabinovich, D., Shaulov, L., Haran, T.E. and Shakked, Z. (2006) 'Structural basis of DNA recognition by p53 tetramers', *Mol Cell*, 22(6), pp. 741-53.
Kmet, L.M., Cook, L.S. and Magliocco, A.M. (2003) 'A review of p53 expression and mutation in human benign, low malignant potential, and invasive epithelial ovarian tumors', *Cancer*, 97(2), pp. 389-404.
Köbel, M., Kalloger, S.E., Boyd, N., McKinney, S., Mehl, E., Palmer, C., Leung, S., Bowen, N.J., Ionescu, D.N., Rajput, A., Prentice, L.M., Miller, D., Santos, J., Swenerton, K., Gilks, C.B. and Huntsman, D. (2008) 'Ovarian Carcinoma Subtypes Are Different Diseases: Implications for Biomarker Studies', *PLOS Medicine*, 5(12), p. e232.
Kobel, M., Piskorz, A.M., Lee, S., Lui, S., LePage, C., Marass, F., Rosenfeld, N., Mes Masson, A.M. and Brenton, J.D. (2016) 'Optimized p53 immunohistochemistry is an accurate predictor of TP53 mutation in ovarian carcinoma', *J Pathol Clin Res*, 2(4), pp. 247-258.
Konstantinopoulos, P.A., Spentzos, D., Karlan, B.Y., Taniguchi, T., Fountzilas, E., Francoeur, N., Levine, D.A. and Cannistra, S.A. (2010) 'Gene Expression Profile of BRCAness That Correlates With Responsiveness to Chemotherapy and With Outcome in Patients With Epithelial Ovarian Cancer', *Journal of Clinical Oncology*, 28(22), pp. 3555-3561.
Koshiyama, M., Matsumura, N. and Konishi, I. (2014) 'Recent Concepts of Ovarian Carcinogenesis: Type I and Type II', *BioMed Research International*, 2014, p. 11.
Kruse, J.-P. and Gu, W. (2009) 'Modes of p53 Regulation', *Cell*, 137(4), pp. 609-622.
Krimmel, JD., Schmitt, MW., Harrell, MI., Agnew, KJ., Kennedy, SR., Emond, MJ., Loeb, LA. and Risques, RA. (2016) Ultra-deep sequencing detects ovarian cancer cells in peritoneal

fluid and reveals somatic TP53 mutations in noncancerous tissues, Proc Natl Acad Sci U S A, 113(21), PP. 1073-79.
Kummar, S., Chen, H.X., Wright, J., Holbeck, S., Millin, M.D., Tomaszewski, J., Zweibel, J., Collins, J. and Doroshow, J.H. (2010) 'Utilizing targeted cancer therapeutic agents in combination: novel approaches and urgent requirements', *Nat Rev Drug Discov*, 9(11), pp. 843-856.
Kupryjanczyk, J., Kraszewska, E., Ziolkowska-Seta, I., Madry, R., Timorek, A., Markowska, J., Stelmachow, J. and Bidzinski, M. (2008) 'TP53 status and taxane-platinum versus platinum-based therapy in ovarian cancer patients: A non-randomized retrospective study', *BMC Cancer*, 8(1), pp. 1-13.
Kurman, R.J. (2013b) 'Origin and molecular pathogenesis of ovarian high-grade serous carcinoma', *Ann Oncol*, 24 Suppl 10, pp. x16-21.
Kurman, R.J. and Shih, I.-M. (2011) 'Molecular Pathogenesis and Extraovarian Origin of Epithelial Ovarian Cancer. Shifting the Paradigm', *Human pathology*, 42(7), pp. 918-931.
Laframboise S, C.W., McLaughlin J, Andrulis IL (2000) 'p53 mutations in epithelial ovarian cancers: possible role in predicting chemoresistance.', *Cancer. J.* 6(5), PP. 302-8.
Lai, P.B., Chi, T.Y. and Chen, G.G. (2007) 'Different levels of p53 induced either apoptosis or cell cycle arrest in a doxycycline-regulated hepatocellular carcinoma cell line in vitro', *Apoptosis*, 12(2), pp. 387-93.
Lakoma, A., Barbieri, E., Agarwal, S., Jackson, J., Chen, Z., Kim, Y., McVay, M., Shohet, J.M. and Kim, E.S. (2015) 'The MDM2 small-molecule inhibitor RG7388 leads to potent tumor inhibition in p53 wild-type neuroblastoma', *Cell Death Discovery*, 1, p. 15026-15035.
Lane, D.P., Cheok, C.F. and Lain, S. (2010) 'p53-based cancer therapy', *Cold Spring Harb Perspect Biol*, 2(9), p. a001222.
Lavarino, C., Pilotti, S., Oggionni, M., Gatti, L., Perego, P., Bresciani, G., Pierotti, M.A., Scambia, G., Ferrandina, G., Fagotti, A., Mangioni, C., Lucchini, V., Vecchione, F., Bolis, G., Scarfone, G. and Zunino, F. (2000) 'p53 Gene Status and Response to Platinum/Paclitaxel-Based Chemotherapy in Advanced Ovarian Carcinoma', *Journal of Clinical Oncology*, 18(23), pp. 3936-3945.
Le Guezennec, X. and Bulavin, D.V. (2010) 'WIP1 phosphatase at the crossroads of cancer and aging', *Trends Biochem Sci*, 35(2), pp. 109-14.
Le Moguen, K., Lincet, H., Deslandes, E., Hubert-Roux, M., Lange, C., Poulain, L., Gauduchon, P. and Baudin, B. (2006) 'Comparative proteomic analysis of cisplatin sensitive IGROV1 ovarian carcinoma cell line and its resistant counterpart IGROV1-R10', *Proteomics*, 6(19), pp. 5183-92.
Le Page, C., Huntsman, D.G., Provencher, D.M. and Mes-Masson, A.-M. (2010) 'Predictive and Prognostic Protein Biomarkers in Epithelial Ovarian Cancer: Recommendation for Future Studies', *Cancers*, 2(2), pp. 913-954.
Ledergerber, C. and Dessimoz, C. (2011) 'Base-calling for next-generation sequencing platforms', *Briefings in Bioinformatics*, 12(5), PP. 489-97.
Ledermann, J.A., Raja, F.A., Fotopoulou, C., Gonzalez-Martin, A., Colombo, N., Sessa, C. and on behalf of the, E.G.W.G. (2013) 'Newly diagnosed and relapsed epithelial ovarian carcinoma: ESMO Clinical Practice Guidelines for diagnosis, treatment and follow-up', *Annals of Oncology*, 24(suppl 6), pp. vi24-vi32.
Leffers, N., Lambeck, A.J., de Graeff, P., Bijlsma, A.Y., Daemen, T., van der Zee, A.G. and Nijman, H.W. (2008) 'Survival of ovarian cancer patients overexpressing the tumour antigen p53 is diminished in case of MHC class I down-regulation', *Gynecol Oncol*, 110(3), pp. 365-73.

Leitao, M.M., Soslow, R.A., Baergen, R.N., Olvera, N., Arroyo, C. and Boyd, J. (2004) 'Mutation and expression of the TP53 gene in early stage epithelial ovarian carcinoma', *Gynecol Oncol*, 93(2), PP. 301-6.
Levesque, M.A., Katsaros, D., Massobrio, M., Genta, F., Yu, H., Richiardi, G., Fracchioli, S., Durando, A., Arisio, R. and Diamandis, E.P. (2000) 'Evidence for a Dose-Response Effect between p53 (but not p21WAF1/Cip1) Protein Concentrations, Survival, and Responsiveness in Patients with Epithelial Ovarian Cancer Treated with Platinum-based Chemotherapy', *Clinical Cancer Research*, 6(8), pp. 3260-3270.
Levine, A.J. and Oren, M. (2009) 'The first 30 years of p53: growing ever more complex', *Nat Rev Cancer*, 9(10), pp. 749-758.
Levitan, D. (2016) 'Ovarian Cancer Risk Factors Show Substantial Heterogeneity Across Histologic Subtypes.', *Cancer Network*.
Li, J., Fadare, O., Xiang, L., Kong, B. and Zheng, W. (2012) 'Ovarian serous carcinoma: recent concepts on its origin and carcinogenesis', *Journal of Hematology & Oncology*, 5(1), pp. 1-11.
Li, Y., Guessous, F., Kwon, S., Kumar, M., Ibidapo, O., Fuller, L., Johnson, E., Lal, B., Hussaini, I., Bao, Y., Laterra, J., Schiff, D. and Abounader, R. (2008) 'PTEN has tumor-promoting properties in the setting of gain-of-function p53 mutations', *Cancer Res*, 68(6), pp. 1723-31.
Lim, S.L., Smith, P., Syed, N., Coens, C., Wong, H., van der Burg, M., Szlosarek, P., Crook, T. and Green, J.A. (2008) 'Promoter hypermethylation of FANCF and outcome in advanced ovarian cancer', *British Journal of Cancer*, 98(8), pp. 1452-1456.
Ling, B. and Wei-Guo, Z. (2006) 'p53: Structure, Function and Therapeutic Applications', *Journal of Cancer Molecules*, 2(4), PP. 141-153.
Lioubov G. Korotchkina, O.V.L., Elena I. Bukreeva, Zoya N. Demidenko, Andrei V. Gudkov and Mikhail V. Blagosklonny (2010) 'The choice between p53-induced senescence and quiescence is determined in part by the mTOR pathway.', *AGING*, 2(6), PP. 344-352.
Liu, D.-p., Song, H. and Xu, Y. (2010) 'A common Gain of function of p53 cancer mutants in inducing genetic instability', *Oncogene*, 29(7), pp. 949-956.
Livraghi, L. and Garber, J. (2015a) 'PARP inhibitors in the management of breast cancer: current data and future prospects', *BMC Medicine*, 13(1), p. 188-204.
Long, J., Parkin, B., Ouillette, P., Bixby, D., Shedden, K., Erba, H., Wang, S. and Malek, S.N. (2010) 'Multiple distinct molecular mechanisms influence sensitivity and resistance to MDM2 inhibitors in adult acute myelogenous leukemia', *Blood*, 116(1), pp. 71-80.
Lu, H.S., Chaoyang; Zhou, Ting; Zhou, Bo; Guo, Ensong; Shan, Wanying; Xia, Meng; Li, Kezhen; Weng, Danhui; Meng, Li; Xu, Xiaoyan; Hu, Junbo; Ma, Ding; Chen, Gang (2016) 'HSP27 Knockdown Increases Cytoplasmic p21 and Cisplatin Sensitivity in Ovarian Carcinoma Cells', *Oncology Research*, 23(3), PP. 119-128.
Lu, M., Xia, L., Li, Y., Wang, X. and Hoffman, R. (2014) 'The orally bioavailable MDM2 antagonist RG7112 and pegylated interferon alpha 2a target JAK2V617F-positive progenitor and stem cells', *Blood*, 124(5), pp. 771-9.
Lu, X., Errington, J., Curtin, N.J., Lunec, J. and Newell, D.R. (2001) 'The Impact of p53 Status on Cellular Sensitivity to Antifolate Drugs', *Clinical Cancer Research*, 7(7), pp. 2114-2123.
Lui, K., An, J., Montalbano, J., Shi, J., Corcoran, C., He, Q., Sun, H., Sheikh, M.S. and Huang, Y. (2013) 'Negative regulation of p53 by Ras superfamily protein RBEL1A', *J Cell Sci*, 126(Pt 11), pp. 2436-45.
Lupo, B. and Trusolino, L. (2014) 'Inhibition of poly(ADP-ribosyl)ation in cancer: Old and new paradigms revisited', *Biochimica et Biophysica Acta (BBA) - Reviews on Cancer*, 1846(1), pp. 201-215.

Luvero, D., Milani, A. and Ledermann, J.A. (2014) 'Treatment options in recurrent ovarian cancer: latest evidence and clinical potential', *Therapeutic Advances in Medical Oncology*, 6(5), pp. 229-239.
M. Sharon Stack, D.A.F. (2009) *Ovarian Cancer*. Available at: https://books.google.co.uk/books?isbn=0387980946.
Maddocks, O.D.K., Berkers, C.R., Mason, S.M., Zheng, L., Blyth, K., Gottlieb, E. and Vousden, K.H. (2013) 'Serine starvation induces stress and p53-dependent metabolic remodelling in cancer cells', *Nature*, 493(7433), pp. 542-546.
Madjd, Z., Karimi, A., Molanae, S. and Asadi-Lari, M. (2011) 'BRCA1 Protein Expression Level and CD44(+)Phenotype in Breast Cancer Patients', *Cell Journal (Yakhteh)*, 13(3), pp. 155-162.
Mahdieh, N. and Rabbani, B. (2013) 'An Overview of Mutation Detection Methods in Genetic Disorders', *Iranian Journal of Pediatrics*, 23(4), pp. 375-388.
Mancini, F.M.a.F. (2012) ' P53 Network in Ovarian Cancer, Ovarian Cancer - Basic Science Perspective', in Farghaly, D.S. (ed.) *Ovarian Cancer - Basic Science Perspective*.
Mandinova, A. and Lee, S.W. (2011) 'The p53 Pathway as a Target in Cancer Therapeutics: Obstacles and Promise', *Science translational medicine*, 3(64), pp. 64rv1-64rv1.
Maria Teresa Piccolo1, a.S.C. (2012) 'The Dual Role Played by p21 May Influence the Apoptotic or Anti-Apoptotic Fate in Cancer ', *Journal of Cancer Researc*, 1(2), pp. 189-202.
Marimuthu, P., Kaur, K., Kandalam, U., Jasani, V., Bukhari, N., Nguyen, M., Abdul, A., Pervez, F.F. and Rathinavelu, A. (2011) 'Treatment of ovarian cancer cells with nutlin-3 and resveratrol combination leads to apoptosis via caspase activation', *J Med Food*, 14(1-2), pp. 46-52.
McCluggage, W.G., Judge, M.J., Clarke, B.A., Davidson, B., Gilks, C.B., Hollema, H., Ledermann, J.A., Matias-Guiu, X., Mikami, Y., Stewart, C.J.R., Vang, R. and Hirschowitz, L. (2015) 'Data set for reporting of ovary, fallopian tube and primary peritoneal carcinoma: recommendations from the International Collaboration on Cancer Reporting (ICCR)', *Mod Pathol*, 28(8), pp. 1101-1122.
McCormick, A., Dixon, M., Odonnell, R., Curtin, N.J. and Edmondson, R.J. (2013) 'Abstract PR06: Ovarian cancers harbor defects in nonhomologous end joining resulting in error prone repair and resistance to rucaparib', *Clinical Cancer Research*, 19(19 Supplement), p. PR06.
McCrudden, C.M., O'Rourke, M.G., Cherry, K.E., Yuen, H.-F., O'Rourke, D., Babur, M., Telfer, B.A., Thomas, H.D., Keane, P., Nambirajan, T., Hagan, C., O'Sullivan, J.M., Shaw, C., Williams, K.J., Curtin, N.J., Hirst, D.G. and Robson, T. (2015) 'Vasoactivity of Rucaparib, a PARP-1 Inhibitor, is a Complex Process that Involves Myosin Light Chain Kinase, P2 Receptors, and PARP Itself', *PLoS ONE*, 10(2), p. e0118187.
McLaren, R.S., Reid, Y. and Storts, D.R. (2013) 'Human cell line authentication: the critical first step in any project using human cell lines', *Methods Mol Biol*, 963, pp. 341-53.
Meek, D.W. (2004) 'The p53 response to DNA damage', *DNA Repair*, 3(8–9), pp. 1049-1056.
Mendes-Pereira, A.M., Martin, S.A., Brough, R., McCarthy, A., Taylor, J.R., Kim, J.-S., Waldman, T., Lord, C.J. and Ashworth, A. (2009) 'Synthetic lethal targeting of PTEN mutant cells with PARP inhibitors', *EMBO Molecular Medicine*, 1(6-7), pp. 315-322.
Meng, G., Wang, W.E.I., Chai, K., Yang, S., Li, F. and Jiang, K.A.I. (2015) 'Combination treatment with triptolide and hydroxycamptothecin synergistically enhances apoptosis in A549 lung adenocarcinoma cells through PP2A-regulated ERK, p38 MAPKs and Akt signaling pathways', *International Journal of Oncology*, 46(3), pp. 1007-1017.
Mestan, K.K., Ilkhanoff, L., Mouli, S. and Lin, S. (2011) 'Genomic sequencing in clinical trials', *Journal of Translational Medicine*, 9, pp. 222-222.

Metindir, J., Dilek, G.B. and Pak, I. (2008) 'Staining characterization by immunohistochemistry of tumor cancer antigen in patients with endometrial cancer', *Eur J Gynaecol Oncol*, 29(5), pp. 489-92.
Michels, J., Vitale, I., Saparbaev, M., Castedo, M. and Kroemer, G. (2014) 'Predictive biomarkers for cancer therapy with PARP inhibitors', *Oncogene*, 33(30), pp. 3894-3907.
Michelsen, K., Jordan, J.B., Lewis, J., Long, A.M., Yang, E., Rew, Y., Zhou, J., Yakowec, P., Schnier, P.D., Huang, X. and Poppe, L. (2012) 'Ordering of the N-terminus of human MDM2 by small molecule inhibitors', *J Am Chem Soc*, 134(41), pp. 17059-67.
Mir, R., Tortosa, A., Martinez-Soler, F., Vidal, A., Condom, E., Perez-Perarnau, A., Ruiz-Larroya, T., Gil, J. and Gimenez-Bonafe, P. (2013a) 'Mdm2 antagonists induce apoptosis and synergize with cisplatin overcoming chemoresistance in TP53 wild-type ovarian cancer cells', *Int J Cancer*, 132(7), pp. 1525-36.
Mir, R., Tortosa, A., Martinez-Soler, F., Vidal, A., Condom, E., Pérez-Perarnau, A., Ruiz-Larroya, T., Gil, J. and Giménez-Bonafé, P. (2013b) 'Mdm2 antagonists induce apoptosis and synergize with cisplatin overcoming chemoresistance in TP53 wild-type ovarian cancer cells', *International Journal of Cancer*, 132(7), pp. 1525-1536.
Modugno, F., Laskey, R., Smith, A.L., Andersen, C.L., Haluska, P. and Oesterreich, S. (2012) 'Hormone response in ovarian cancer: time to reconsider as a clinical target?', *Endocrine-related cancer*, 19(6), pp. R255-R279.
Mukhopadhyay, A., Plummer, E.R., Elattar, A., Soohoo, S., Uzir, B., Quinn, J.E., McCluggage, W.G., Maxwell, P., Aneke, H., Curtin, N.J. and Edmondson, R.J. (2012) 'Clinicopathological Features of Homologous Recombination–Deficient Epithelial Ovarian Cancers: Sensitivity to PARP Inhibitors, Platinum, and Survival', *Cancer Research*, 72(22), pp. 5675-5682.
Mullany, L.K., Wong, K.-K., Marciano, D.C., Katsonis, P., King-Crane, E.R., Ren, Y.A., Lichtarge, O. and Richards, J.S. (2015) 'Specific TP53 Mutants Overrepresented in Ovarian Cancer Impact CNV, TP53 Activity, Responses to Nutlin-3a, and Cell Survival()', *Neoplasia (New York, N.Y.)*, 17(10), pp. 789-803.
Munagala, R., Aqil, F. and Gupta, R.C. (2011) 'Promising molecular targeted therapies in breast cancer', *Indian Journal of Pharmacology*, 43(3), pp. 236-245.
Munchel, S., Hoang, Y., Zhao, Y., Cottrell, J., Klotzle, B., Godwin, A.K., Koestler, D., Beyerlein, P., Fan, J.-B., Bibikova, M. and Chien, J. (2015) 'Targeted or whole genome sequencing of formalin fixed tissue samples: potential applications in cancer genomics', *Oncotarget*, 6(28), pp. 25943-25961.
Murai, J., Huang, S.-y.N., Das, B.B., Renaud, A., Zhang, Y., Doroshow, J.H., Ji, J., Takeda, S. and Pommier, Y. (2012) 'Differential trapping of PARP1 and PARP2 by clinical PARP inhibitors', *Cancer research*, 72(21), pp. 5588-5599.
Murai, J., Huang, S.-y.N., Renaud, A., Zhang, Y., Ji, J., Takeda, S., Morris, J., Teicher, B., Doroshow, J.H. and Pommier, Y. (2014) 'Stereospecific PARP trapping by BMN 673 and comparison with olaparib and rucaparib', *Molecular cancer therapeutics*, 13(2), pp. 433-443.
Murray-Zmijewski, F., Slee, E.A. and Lu, X. (2008) 'A complex barcode underlies the heterogeneous response of p53 to stress', *Nat Rev Mol Cell Biol*, 9(9), pp. 702-12.
Nadkarni, N.J., Geest, K.D., Neff, T., Young, B.D., Bender, D.P., Ahmed, A., Smith, B.J., Button, A. and Goodheart, M.J. (2013) 'Microvessel density and p53 mutations in advanced-stage epithelial ovarian cancer', *Cancer Letters*, 331(1), pp. 99-104.
Nag, S., Qin, J., Srivenugopal, K.S., Wang, M. and Zhang, R. (2013) 'The MDM2-p53 pathway revisited', *Journal of Biomedical Research*, 27(4), pp. 254-271.
Nakayama, K., Takebayashi, Y., Nakayama, S., Hata, K., Fujiwaki, R., Fukumoto, M. and Miyazaki, K. (2003) 'Prognostic value of overexpression of p53 in human ovarian carcinoma patients receiving cisplatin', *Cancer Letters*, 192(2), pp. 227-235.

Nam, E.J. and Kim, Y.T. (2008) 'Alteration of cell-cycle regulation in epithelial ovarian cancer', *Int J Gynecol Cancer*, 18(6), pp. 1169-82.
Narod, S. (2016) 'Can advanced-stage ovarian cancer be cured?', *Nat Rev Clin Oncol*, 13(4), pp. 255-261.
Nasma D. Eljack, H.-Y.M.M., Janine Drucker, Clara Shen,Trevor W. Hambley, Elizabeth J. New, Thomas Friedrich and Ronald J. Clarke (2014) 'Mechanisms of cell uptake and toxicity of the anticancer drug cisplatin', *Metallomics*, 6(11), pp. 2126-33.
NCBI, R. (2010) *TNFSF10* tumor necrosis factor superfamily member 10 [Homo sapiens (human)].
Nicolas Andre, Pasquier, E. and Kamen, a.B. (2012) 'Can Targeted Therapy be Successful without Metronomic Scheduling ?, *Curr Top Med Chem*, 12(16), pp. 266-270.
O'Connor, P.M., Jackman, J., Bae, I., Myers, T.G., Fan, S., Mutoh, M., Scudiero, D.A., Monks, A., Sausville, E.A., Weinstein, J.N., Friend, S., Fornace, A.J., Jr. and Kohn, K.W. (1997) 'Characterization of the p53 tumor suppressor pathway in cell lines of the National Cancer Institute anticancer drug screen and correlations with the growth-inhibitory potency of 123 anticancer agents', *Cancer Res*, 57(19), pp. 4285-300.
O'Hurley, G., Sjostedt, E., Rahman, A., Li, B., Kampf, C., Ponten, F., Gallagher, W.M. and Lindskog, C. (2014) 'Garbage in, garbage out: a critical evaluation of strategies used for validation of immunohistochemical biomarkers', *Mol Oncol*, 8(4), pp. 783-98.
O'Sullivan, C.C., Moon, D.H., Kohn, E. and Lee, J.-M. (2014) 'Beyond breast and ovarian cancers: PARP inhibitors for BRCA mutation-associated and BRCA-like solid tumors', *Frontiers in Oncology*, 4(42), pp. 3389-3402.
Ohnstad, H.O., Paulsen, E.B., Noordhuis, P., Berg, M., Lothe, R.A., Vassilev, L.T. and Myklebost, O. (2011) 'MDM2 antagonist Nutlin-3a potentiates antitumour activity of cytotoxic drugs in sarcoma cell lines', *BMC Cancer*, 11, pp. 211-211.
Olivier, M., Hollstein, M. and Hainaut, P. (2010) 'TP53 Mutations in Human Cancers: Origins, Consequences, and Clinical Use', *Cold Spring Harbor Perspectives in Biology*, 2(1), p. a001008.
Olopade, O.I. and Wei, M. (2003) 'FANCF methylation contributes to chemoselectivity in ovarian cancer', *Cancer Cell*, 3(5), pp. 417-420.
Oren, M. and Rotter, V. (2010) 'Mutant p53 Gain-of-Function in Cancer', *Cold Spring Harbor Perspectives in Biology*, 2(2), p. a001107.
Graeff1, P., Hall. J., Crijns, APG ., Bock, GH., Paul, J., Oien, KA., Hoor, KA., Jong, S., Hollema, H., Bartlett, JMS., Brown, R. and Zee1, AGJ. (2006) 'Factors influencing p53 expression in ovarian cancer as a biomarker of clinical outcome in multicentre studies', *British Journal of Cancer*, 95, PP. 627-633.
Pabla, N. and Dong, Z. (2012) 'Curtailing side effects in chemotherapy: a tale of PKCδ in cisplatin treatment', *Oncotarget*, 3(1), pp. 107-111.
Pant, V., Xiong, S., Iwakuma, T., Quintás-Cardama, A. and Lozano, G. (2011) 'Heterodimerization of Mdm2 and Mdm4 is critical for regulating p53 activity during embryogenesis but dispensable for p53 and Mdm2 stability', *Proceedings of the National Academy of Sciences*, 180(29), PP. 11995-12000.
Parmar, M.K., Ledermann, J.A., Colombo, N., du Bois, A., Delaloye, J.F., Kristensen, G.B., Wheeler, S., Swart, A.M., Qian, W., Torri, V., Floriani, I., Jayson, G., Lamont, A. and Trope, C. (2003) 'Paclitaxel plus platinum-based chemotherapy versus conventional platinum-based chemotherapy in women with relapsed ovarian cancer: the ICON4/AGO-OVAR-2.2 trial', *Lancet*, 361(9375), pp. 2099-106.
Parssinen, J., Alarmo, E.L., Karhu, R. and Kallioniemi, A. (2008) 'PPM1D silencing by RNA interference inhibits proliferation and induces apoptosis in breast cancer cell lines with wild-type p53', *Cancer Genet Cytogenet*, 182(1), pp. 33-9.

Pei, D., Zhang, Y. and Zheng, J. (2012) 'Regulation of p53: a collaboration between Mdm2 and MdmX', *Oncotarget*, 3(3), pp. 228-235.
Phalke, S., Mzoughi, S., Bezzi, M., Jennifer, N., Mok, W.C., Low, D.H., Thike, A.A., Kuznetsov, V.A., Tan, P.H., Voorhoeve, P.M. and Guccione, E. (2012) 'p53-Independent regulation of p21Waf1/Cip1 expression and senescence by PRMT6', *Nucleic Acids Res*, 40(19), pp. 9534-42.
Pizao, P.E., Lyaruu, D.M., Peters, G.J., van Ark-Otte, J., Winograd, B., Giaccone, G. and Pinedo, H.M. (1992) 'Growth, morphology and chemosensitivity studies on postconfluent cells cultured in 'V'-bottomed microtiter plates', *British Journal of Cancer*, 66(4), pp. 660-665.
Prat, J. (2012) 'New insights into ovarian cancer pathology', *Annals of Oncology*, 23(suppl 10), pp. x111-x117.
Psyrri, A., Kountourakis, P., Yu, Z., Papadimitriou, C., Markakis, S., Camp, R.L., Economopoulos, T. and Dimopoulos, M.A. (2007) 'Analysis of p53 protein expression levels on ovarian cancer tissue microarray using automated quantitative analysis elucidates prognostic patient subsets', *Annals of Oncology*, 18(4), pp. 709-715.
Qian, Y. and Chen, X. (2010) 'Tumor suppression by p53: making cells senescent', *Histology and histopathology*, 25(4), pp. 515-526.
Zhan, Q.,Wang, C. and Ngai, a.S. (2013) 'Ovarian Cancer Stem Cells: A New Target for Cancer Therapy', *BioMed Research International*, 2013, PP. 916819-916830.
Rachel N. Grisham, M. (2016) 'Low-Grade Serous Carcinoma of the Ovary.', *Oncology Journal*, 30(7), PP. 650-652.
Rajitha Lokadasan, F.V.J., Geetha Narayanan and Pranab K Prabhakaran (2016) 'Targeted agents in epithelial ovarian cancer: review on emerging therapies and future developments', *ecancermedicalscience*, 10, 626-46.
Ray-Coquard, I., Blay, J.Y., Italiano, A., Le Cesne, A., Penel, N., Zhi, J., Heil, F., Rueger, R., Graves, B., Ding, M., Geho, D., Middleton, S.A., Vassilev, L.T., Nichols, G.L. and Bui, B.N. (2012) 'Effect of the MDM2 antagonist RG7112 on the P53 pathway in patients with MDM2-amplified, well-differentiated or dedifferentiated liposarcoma: an exploratory proof-of-mechanism study', *Lancet Oncol*, 13(11), pp. 1133-40.
Rechsteiner, M., Zimmermann, A.-K., Wild, P.J., Caduff, R., von Teichman, A., Fink, D., Moch, H. and Noske, A. (2013) 'TP53 mutations are common in all subtypes of epithelial ovarian cancer and occur concomitantly with KRAS mutations in the mucinous type', *Experimental and Molecular Pathology*, 95(2), pp. 235-241.
Reles, A., Wen, W.H., Schmider, A., Gee, C., Runnebaum, I.B., Kilian, U., Jones, L.A., El-Naggar, A., Minguillon, C., Schönborn, I., Reich, O., Kreienberg, R., Lichtenegger, W. and Press, M.F. (2001) 'Correlation of p53 Mutations with Resistance to Platinum-based Chemotherapy and Shortened Survival in Ovarian Cancer', *Clinical Cancer Research*, 7(10), pp. 2984-2997.
Rew, Y. and Sun, D. (2014) 'Discovery of a Small Molecule MDM2 Inhibitor (AMG 232) for Treating Cancer', *Journal of Medicinal Chemistry*, 57(15), pp. 6332-6341.
Rew, Y., Sun, D., Gonzalez-Lopez De Turiso, F., Bartberger, M.D., Beck, H.P., Canon, J., Chen, A., Chow, D., Deignan, J., Fox, B.M., Gustin, D., Huang, X., Jiang, M., Jiao, X., Jin, L., Kayser, F., Kopecky, D.J., Li, Y., Lo, M.C., Long, A.M., Michelsen, K., Oliner, J.D., Osgood, T., Ragains, M., Saiki, A.Y., Schneider, S., Toteva, M., Yakowec, P., Yan, X., Ye, Q., Yu, D., Zhao, X., Zhou, J., Medina, J.C. and Olson, S.H. (2012) 'Structure-based design of novel inhibitors of the MDM2-p53 interaction', *J Med Chem*, 55(11), pp. 4936-54.
Ribeiro, C., Rodrigues, C., Moreira, R. and Santos, M. (2016) 'Chemical Variations on the p53 Reactivation Theme', *Pharmaceuticals*, 9(2), p. 25.
Rich, J.T., Neely, J.G., Paniello, R.C., Voelker, C.C.J., Nussenbaum, B. and Wang, E.W. (2010) 'A practical guide to understanding Kaplan-Meier curves', Otolaryngology--head and

neck surgery : official journal of American Academy of Otolaryngology-Head and Neck Surgery, 143(3), pp. 331-336.
Richter, M., Dayaram, T., Gilmartin, A.G., Ganji, G., Pemmasani, S.K., Van Der Key, H., Shohet, J.M., Donehower, L.A. and Kumar, R. (2015) 'WIP1 phosphatase as a potential therapeutic target in neuroblastoma', *PLoS One*, 10(2), p. e0115635.
Rigakos, G. and Razis, E. (2012) 'BRCAness: Finding the Achilles Heel in Ovarian Cancer', *The Oncologist*, 17(7), pp. 956-962.
Kurman, RG. and Shih, L. (2010) 'The Origin and Pathogenesis of Epithelial Ovarian Cancer:A Proposed Unifying Theory', *Am J Surg Pathol*, 34(3), PP. 433-43.
Rose, S.L., Goodheart, M.J., DeYoung, B.R., Smith, B.J. and Buller, R.E. (2003a) 'p21 expression predicts outcome in p53-null ovarian carcinoma', *Clin Cancer Res*, 9(3), pp. 1028-32.
Rose, S.L., Robertson, A.D., Goodheart, M.J., Smith, B.J., DeYoung, B.R. and Buller, R.E. (2003b) 'The Impact of p53 Protein Core Domain Structural Alteration on Ovarian Cancer Survival', *Clinical Cancer Research*, 9(11), pp. 4139-4144.
Rosen, D.G., Huang, X., Deavers, M.T., Malpica, A., Silva, E.G. and Liu, J. (2004) 'Validation of tissue microarray technology in ovarian carcinoma', *Mod Pathol*, 17(7), pp. 790-7.
Rosenfeldt, M.T., O'Prey, J., Morton, J.P., Nixon, C., MacKay, G., Mrowinska, A., Au, A., Rai, T.S., Zheng, L., Ridgway, R., Adams, P.D., Anderson, K.I., Gottlieb, E., Sansom, O.J. and Ryan, K.M. (2013) 'p53 status determines the role of autophagy in pancreatic tumour development', *Nature*, 504(7479), pp. 296-300.
Sagarra, R.A., Andrade, L.A., Martinez, E.Z., Pinto, G.A., Syrjanen, K.J. and Derchain, S.F. (2002) 'P53 and Bcl-2 as prognostic predictors in epithelial ovarian cancer', *Int J Gynecol Cancer*, 12(6), pp. 720-7.
Schmider, A., Gee, C., Friedmann, W., Lukas, J.J., Press, M.F., Lichtenegger, W. and Reles, A. (2000) 'p21 (WAF1/CIP1) Protein Expression Is Associated with Prolonged Survival but Not with p53 Expression in Epithelial Ovarian Carcinoma', *Gynecologic Oncology*, 77(2), pp. 237-242.
Schuyer, M., Burg, M.E.L.v.d., Henzen-Logmans, S.C., Fieret, J.H., Klijn, J.G.M., Look, M.P., Foekens, J.A., Stoter, G. and Berns, E.M.J.J. (2001) 'Reduced expression of BAX is associated with poor prognosis in patients with epithelial ovarian cancer: a multifactorial analysis of TP53, p21, BAX and BCL-2', *British Journal of Cancer*, 85(9), pp. 1359-1367.
Seagle, B.-L.L., Eng, K.H., Dandapani, M., Yeh, J.Y., Odunsi, K. and Shahabi, S. (2015) 'Survival of patients with structurally-grouped TP53 mutations in ovarian and breast cancers', *Oncotarget*, 6(21), pp. 18641-18652.
SenGupta, D.J. and Cookson, B.T. (2010) 'SeqSharp: A General Approach for Improving Cycle-Sequencing That Facilitates a Robust One-Step Combined Amplification and Sequencing Method', *The Journal of Molecular Diagnostics : JMD*, 12(3), pp. 272-277.
Sengupta, P.S., McGown, A.T., Bajaj, V., Blackhall, F., Swindell, R., Bromley, M., Shanks, J.H., Ward, T., Buckley, C.H., Reynolds, K., Slade, R.J. and Jayson, G.C. (2000) 'p53 And related proteins in epithelial ovarian cancer', *European Journal of Cancer*, 36(18), pp. 2317-2328.
Shahin, M.S., Hughes, J.H., Sood, A.K. and Buller, R.E. (2000) 'The prognostic significance of p53 tumor suppressor gene alterations in ovarian carcinoma', *Cancer*, 89(9), pp. 2006-17.
Shangary, S. and Wang, S. (2009) 'Small-Molecule Inhibitors of the MDM2-p53 Protein-Protein Interaction to Reactivate p53 Function: A Novel Approach for Cancer Therapy', *Annual review of pharmacology and toxicology*, 49, pp. 223-241.
Wang, S., Denzil Bernard, Y.Z., Aguilar, A. and Sanjeev Kumar (2012) 'Targeting the MDM2-p53 Protein-Protein Interaction for New Cancer Therapeutics ', *Top Med Chem*, 8, PP. 57-80.

Shen, H. and Maki, C.G. (2011) 'Pharmacologic activation of p53 by small-molecule MDM2 antagonists', *Current pharmaceutical design*, 17(6), pp. 560-568.
Shen, H., Moran, D.M. and Maki, C.G. (2008) 'Transient Nutlin-3a treatment promotes endoreduplication and the generation of therapy-resistant tetraploid cells', *Cancer research*, 68(20), pp. 8260-8268.
Shih-Chu Ho, E., Lai, C.-R., Hsieh, Y.-T., Chen, J.-T., Lin, A.-J., Hung, M.-J. and Liu, F.-S. (2001) 'p53 Mutation Is Infrequent in Clear Cell Carcinoma of the Ovary', *Gynecologic Oncology*, 80(2), pp. 189-193.
Wang, S. and El-Deiry, W.S. (2007) 'P53, Cell Cycle Arrest and Apoptosis', in Pierre Hainaut, K.G.W. (ed.) *25 years of p53 Research*, Chapter 6, pp. 141-163.
Fulda, S., Gorman, A.A., Hori, O. and Samali, A. (2010) 'Cellular Stress Responses: Cell Survival and Cell Death', *International Journal of Cell Biology*, 2010, PP. 214074-97.
Singer, G., Stohr, R., Cope, L., Dehari, R., Hartmann, A., Cao, D.F., Wang, T.L., Kurman, R.J. and Shih Ie, M. (2005) 'Patterns of p53 mutations separate ovarian serous borderline tumors and low- and high-grade carcinomas and provide support for a new model of ovarian carcinogenesis: a mutational analysis with immunohistochemical correlation', *Am J Surg Pathol*, 29(2), pp. 218-24.
Skehan, P., Storeng, R., Scudiero, D., Monks, A., McMahon, J., Vistica, D., Warren, J.T., Bokesch, H., Kenney, S. and Boyd, M.R. (1990) 'New colorimetric cytotoxicity assay for anticancer-drug screening', *J Natl Cancer Inst*, 82(13), pp. 1107-12.
Skirnisdottir, I. and Seidal, T. (2013) 'Association of p21, p21 p27 and p21 p53 status to histological subtypes and prognosis in low-stage epithelial ovarian cancer', *Cancer Genomics Proteomics*, 10(1), pp. 27-34.
Skirnisdottir, I., Seidal, T. and Åkerud, H. (2015) 'Differences in Clinical and Biological Features Between Type I and Type II Tumors in FIGO Stages I-II Epithelial Ovarian Carcinoma', *International Journal of Gynecological Cancer*, 25(7), pp. 1239-1247.
Smith-Sørensen, B., Kaern, J., Holm, R., Dørum, A., Tropé, C. and Børresen-Dale, A.L. (1998) 'Therapy effect of either paclitaxel or cyclophosphamide combination treatment in patients with epithelial ovarian cancer and relation to TP53 gene status', *British Journal of Cancer*, 78(3), pp. 375-381.
Sonego, M., Schiappacassi, M., Lovisa, S., Dall'Acqua, A., Bagnoli, M., Lovat, F., Libra, M., D'Andrea, S., Canzonieri, V., Militello, L., Napoli, M., Giorda, G., Pivetta, B., Mezzanzanica, D., Barbareschi, M., Valeri, B., Canevari, S., Colombatti, A., Belletti, B., Del Sal, G. and Baldassarre, G. (2013) 'Stathmin regulates mutant p53 stability and transcriptional activity in ovarian cancer', *EMBO Mol Med*, 5(5), pp. 707-22.
Sonkin, D. (2015) 'Expression signature based on TP53 target genes doesn't predict response to TP53-MDM2 inhibitor in wild type TP53 tumors', *Elife*, 4, PP. 10279-85.
Sourisseau, T., Maniotis, D., McCarthy, A., Tang, C., Lord, C.J., Ashworth, A. and Linardopoulos, S. (2010) 'Aurora-A expressing tumour cells are deficient for homology-directed DNA double strand-break repair and sensitive to PARP inhibition', *EMBO Molecular Medicine*, 2(4), pp. 130-142.
Soussi, T. (2012) '"THE p53 WEB SITE ". from <http://p53.free.fr/>'.
Stegh, A.H. (2012) 'Targeting the p53 signaling pathway in cancer therapy - The promises, challenges, and perils', *Expert Opinion on Therapeutic Targets*, 16(1), pp. 67-83.
Stordal, B., Timms, K., Farrelly, A., Gallagher, D., Busschots, S., Renaud, M., Thery, J., Williams, D., Potter, J., Tran, T., Korpanty, G., Cremona, M., Carey, M., Li, J., Li, Y., Aslan, O., O'Leary, J.J., Mills, G.B. and Hennessy, B.T. (2013) '*BRCA1/2* mutation analysis in 41 ovarian cell lines reveals only one functionally deleterious *BRCA1* mutation', *Molecular oncology*, 7(3), pp. 567-579.

Su, Z., Yang, Z., Xu, Y., Chen, Y. and Yu, Q. (2015) 'Apoptosis, autophagy, necroptosis, and cancer metastasis', *Molecular Cancer*, 14(1), pp. 1-14.
Sung, P.L., Chang, Y.H., Chao, K.C. and Chuang, C.M. (2014) 'Global distribution pattern of histological subtypes of epithelial ovarian cancer: a database analysis and systematic review', *Gynecol Oncol*, 133(2), pp. 147-54.
Tagawa, T., Morgan, R., Yen, Y. and Mortimer, J. (2012) 'Ovarian Cancer: Opportunity for Targeted Therapy', *Journal of Oncology*, 2012, p. 9.
Tan, B.X., Khoo, K.H., Lim, T.M. and Lane, D.P. (2014) 'High Mdm4 levels suppress p53 activity and enhance its half-life in acute myeloid leukaemia', *Oncotarget*, 5(4), pp. 933-943.
Tan, D.S.P., Lambros, M.B.K., Rayter, S., Natrajan, R., Vatcheva, R., Gao, Q., Marchiò, C., Geyer, F.C., Savage, K., Parry, S., Fenwick, K., Tamber, N., Mackay, A., Dexter, T., Jameson, C., McCluggage, W.G., Williams, A., Graham, A., Faratian, D., El-Bahrawy, M., Paige, A.J., Gabra, H., Gore, M.E., Zvelebil, M., Lord, C.J., Kaye, S.B., Ashworth, A. and Reis-Filho, J.S. (2009b) 'PPM1D Is a Potential Therapeutic Target in Ovarian Clear Cell Carcinomas', *American Association for Cancer Research*, 15(7), pp. 2269-2280.
Tanida, S., Mizoshita, T., Ozeki, K., Tsukamoto, H., Kamiya, T., Kataoka, H., Sakamuro, D. and Joh, T. (2012) 'Mechanisms of Cisplatin-Induced Apoptosis and of Cisplatin Sensitivity: Potential of BIN1 to Act as a Potent Predictor of Cisplatin Sensitivity in Gastric Cancer Treatment', *International Journal of Surgical Oncology*, 2012, pp. 862879-87.
Taniguchi, T., Tischkowitz, M., Ameziane, N., Hodgson, S.V., Mathew, C.G., Joenje, H., Mok, S.C. and D'Andrea, A.D. (2003) 'Disruption of the Fanconi anemia-BRCA pathway in cisplatin-sensitive ovarian tumors', *Nat Med*, 9(5), pp. 568-574.
Telfer, M.B.B.K.P. (2015) 'MDM2 antagonist clinical response association with a gene expression signature in acute myeloid leukaemia', *British Journal of Haematology*,171, 424-439.
Teoh, P.J. and Chng, W.J. (2014) 'p53 Abnormalities and Potential Therapeutic Targeting in Multiple Myeloma', *BioMed Research International*, 2014, pp. 717919-28.
Terauchi, F., Okamoto, A., Nagashima, T., Kobayashi, Y., Moritake, T., Yamamoto, Y., Takakura, S., Iwaki, S. and Ogura, H. (2005) 'Clinical significance of p21(WAF1/CIP1) and p53 expression in serous cystadenocarcinoma of the ovary', *Oncol Rep*, 14(2), pp. 363-8.
The Cancer Genome Atlas Research, N. (2011) 'Integrated Genomic Analyses of Ovarian Carcinoma', *Nature*, 474(7353), pp. 609-615.
Thomas, H.D., Calabrese, C.R., Batey, M.A., Canan, S., Hostomsky, Z., Kyle, S., Maegley, K.A., Newell, D.R., Skalitzky, D., Wang, L.-Z., Webber, S.E. and Curtin, N.J. (2007) 'Preclinical selection of a novel poly(ADP-ribose) polymerase inhibitor for clinical trial', *Molecular Cancer Therapeutics*, 6(3), pp. 945-956.
Tollini, L.A. and Zhang, Y. (2012) 'p53 Regulation Goes Live—Mdm2 and MdmX Co-Star: Lessons Learned from Mouse Modeling', *Genes & Cancer*, 3(3-4), pp. 219-225.
Tomsova, M., Melichar, B., Sedlakova, I. and Steiner, I. (2008) 'Prognostic significance of CD3+ tumor-infiltrating lymphocytes in ovarian carcinoma', *Gynecol Oncol*, 108(2), pp. 415-20.
Turner, N. and Ashworth, A. (2011) 'Biomarkers of PARP inhibitor sensitivity', *Breast Cancer Research and Treatment*, 127(1), pp. 283-286.
Ueno, Y., Enomoto, T., Otsuki, Y., Sugita, N., Nakashima, R., Yoshino, K., Kuragaki, C., Ueda, Y., Aki, T., Ikegami, H., Yamazaki, M., Ito, K., Nagamatsu, M., Nishizaki, T., Asada, M., Kameda, T., Wakimoto, A., Mizutani, T., Yamada, T. and Murata, Y. (2006) 'Prognostic significance of p53 mutation in suboptimally resected advanced ovarian carcinoma treated with the combination chemotherapy of paclitaxel and carboplatin', *Cancer Letters*, 241(2), pp. 289-300.

Underhill, C., Toulmonde, M. and Bonnefoi, H. (2011) 'A review of PARP inhibitors: from bench to bedside', *Annals of Oncology*, 22(2), pp. 268-279.
Valente, L. and Strasser, A. (2013) 'Distinct target genes and effector processes appear to be critical for p53-activated responses to acute DNA damage versus p53-mediated tumour suppression.', *BIODISCOVERY*, 8(3), PP. 3052-3068.
Valenzuela, M.T., Guerrero, R., Nunez, M.I., Ruiz De Almodovar, J.M., Sarker, M., de Murcia, G. and Oliver, F.J. (2002) 'PARP-1 modifies the effectiveness of p53-mediated DNA damage response', *Oncogene*, 21(7), pp. 1108-16.
van Niekerk, C.C., Bulten, J., van Dijck, J.A.A.M. and Verbeek, A.L.M. (2011) 'Epithelial Ovarian Carcinoma Types and the Coexistence of Ovarian Tumor Conditions', *ISRN Obstetrics and Gynecology*, 2011, pp. 784919-24.
Vartiainen, J., Lassus, H., Lehtovirta, P., Finne, P., Alfthan, H., Butzow, R. and Stenman, U.H. (2008) 'Combination of serum hCG beta and p53 tissue expression defines distinct subgroups of serous ovarian carcinoma', *Int J Cancer*, 122(9), pp. 2125-9.
Vassilev, L.T. (2007) 'MDM2 inhibitors for cancer therapy', *Trends in Molecular Medicine*, 13(1), pp. 23-31.
Vlachostergios, P.J., Voutsadakis, I.A. and Papandreou, C.N. (2012) 'The ubiquitin-proteasome system in glioma cell cycle control', *Cell Division*, 7, pp. 18-18.
Voon, Y.-L., Ahmad, M., Wong, P.-F., Husaini, R., Ng, W.T.-W., Leong, C.-O., Lane, D.P. and Khoo, A.S.-B. (2015) 'Nutlin-3 sensitizes nasopharyngeal carcinoma cells to cisplatin-induced cytotoxicity', *Oncology Reports*, 34(4), pp. 1692-1700.
Vousden, K.H. and Lu, X. (2002) 'Live or let die: the cell's response to p53', *Nat Rev Cancer*, 2(8), pp. 594-604.
Vu, B., Wovkulich, P., Pizzolato, G., Lovey, A., Ding, Q., Jiang, N., Liu, J.-J., Zhao, C., Glenn, K., Wen, Y., Tovar, C., Packman, K., Vassilev, L. and Graves, B. (2013) 'Discovery of RG7112: A Small-Molecule MDM2 Inhibitor in Clinical Development', *ACS Medicinal Chemistry Letters*, 4(5), pp. 466-469.
W. Edward Highsmthh, J. (2006) 'Electrophoretic Methods for Mutation Detection and DNA Sequencing', in Tsongalis, W.B.C.a.G.J. (ed.) *Molecular Diagnosis: Fior the Clinival Laboratarian*. Second edn., pp. 85-109.
Wade, M., Li, Y.-C. and Wahl, G.M. (2013) 'MDM2, MDMX and p53 in oncogenesis and cancer therapy', *Nat Rev Cancer*, 13(2), pp. 83-96.
Wade, M., Wang, Y.V. and Wahl, G.M. (2010) 'The p53 orchestra: Mdm2 and Mdmx set the tone', *Trends in Cell Biology*, 20(5), pp. 299-309.
Wagner, J.M. and Karnitz, L.M. (2009) 'Cisplatin-Induced DNA Damage Activates Replication Checkpoint Signaling Components that Differentially Affect Tumor Cell Survival', *Molecular Pharmacology*, 76(1), pp. 208-214.
Walton, J., Blagih, J., Ennis, D., Leung, E., Dowson, S., Farquharson, M., Tookman, L.A., Orange, C., Athineos, D., Mason, S., Stevenson, D., Blyth, K., Strathdee, D., Balkwill, F.R., Vousden, K., Lockley, M. and McNeish, I.A. (2016) 'CRISPR/Cas9-Mediated Trp53 and Brca2 Knockout to Generate Improved Murine Models of Ovarian High-Grade Serous Carcinoma', *Cancer Res*, 76(20), 6118-6129.
Wang, Q.-E. (2015) 'DNA damage responses in cancer stem cells: Implications for cancer therapeutic strategies', *World Journal of Biological Chemistry*, 6(3), pp. 57-64.
Wang, Q.E., Milum, K., Han, C., Huang, Y.W., Wani, G., Thomale, J. and Wani, A.A. (2011) 'Differential contributory roles of nucleotide excision and homologous recombination repair for enhancing cisplatin sensitivity in human ovarian cancer cells', *Mol Cancer*, 10(24), pp. 4598-4600.

Wang, Y., Helland, Å., Holm, R., Skomedal, H., Abeler, V.M., Danielsen, H.E., Tropé, C.G., Børresen-Dale, A.L. and Kristensen, G.B. (2004) 'TP53 mutations in early-stage ovarian carcinoma, relation to long-term survival', *British Journal of Cancer*, 90(3), pp. 678-685.
Wang, Y.C., Lin, R.K., Tan, Y.H., Chen, J.T., Chen, C.Y. and Wang, Y.C. (2005) 'Wild-type p53 overexpression and its correlation with MDM2 and p14ARF alterations: an alternative pathway to non-small-cell lung cancer', *J Clin Oncol*, 23(1), pp. 154-64.
Wang, Z. and Sun, Y. (2010) 'Targeting p53 for Novel Anticancer Therapy', *Translational Oncology*, 3(1), pp. 1-12.
Wang, Z.C., Birkbak, N.J., Culhane, A.C., Drapkin, R., Fatima, A., Tian, R., Schwede, M., Alsop, K., Daniels, K.E., Piao, H., Liu, J., Etemadmoghadam, D., Miron, A., Salvesen, H.B., Mitchell, G., DeFazio, A., Quackenbush, J., Berkowitz, R.S., Iglehart, J.D., Bowtell, D.D.L., for the Australian Ovarian Cancer Study, G. and Matulonis, U.A. (2012) 'Profiles of Genomic Instability in High-Grade Serous Ovarian Cancer Predict Treatment Outcome', *Clinical cancer research : an official journal of the American Association for Cancer Research*, 18(20), pp. 5806-5815.
Wei, S.J., Joseph, T., Sim, A.Y.L., Yurlova, L., Zolghadr, K., Lane, D., Verma, C. and Ghadessy, F. (2013) 'In Vitro Selection of Mutant HDM2 Resistant to Nutlin Inhibition', *PLoS ONE*, 8(4), p. e62564.
Weil, M.K. and Chen, A. (2011) 'PARP Inhibitor Treatment in Ovarian and Breast Cancer', *Current problems in cancer*, 35(1), pp. 7-50.
Wen, W.H., Reles, A., Runnebaum, I.B., Sullivan-Halley, J., Bernstein, L., Jones, L.A., Felix, J.C., Kreienberg, R., el-Naggar, A. and Press, M.F. (1999) 'p53 mutations and expression in ovarian cancers: correlation with overall survival', *Int J Gynecol Pathol*, 18(1), pp. 29-41.
Weng, L.-P., Brown, J.L. and Eng, C. (2001) 'PTEN induces apoptosis and cell cycle arrest through phosphoinositol-3-kinase/Akt-dependent and -independent pathways', *Human Molecular Genetics*, 10(3), pp. 237-242.
Wilson, A.P., Dent, M., Pejovic, T., Hubbold, L. and Radford, H. (1996) 'Characterisation of seven human ovarian tumour cell lines', *British Journal of Cancer*, 74(5), pp. 722-727.
Wiman, G.S.a.K. (2007) 'Reactivation of mutant p53: molecular mechanisms and therapeutic potential', *Oncogene*, 26, pp. 2243-2254.
Witham, J., Valenti, M.R., De-Haven-Brandon, A.K., Vidot, S., Eccles, S.A., Kaye, S.B. and Richardson, A. (2007) 'The Bcl-2/Bcl-XL family inhibitor ABT-737 sensitizes ovarian cancer cells to carboplatin', *Clin Cancer Res*, 13(23), pp. 7191-8.
Wong, K.-K., Izaguirre, D.I., Kwan, S., King, E.R., Deavers, M.T., Sood, A.K., Mok, S.C. and Gershenson, D.M. (2013) 'Poor survival with wild-type TP53 ovarian cancer?', *Gynecologic oncology*, 130(3), pp. 565-569.
www.abcam.com/MDM2-antibody-SMP-14-ab3110 *Anti-MDM2 antibody [SMP 14] ab3110*.
www.emdmillipore.com/.../Anti-MDM2-Antibody, -.c.-S., MM 'MAB3776 | Anti-MDM2 Antibody, clone SMP14 - EMD Millipore'.
Xia, M., Knezevic, D. and Vassilev, L.T. (2011a) 'p21 does not protect cancer cells from apoptosis induced by nongenotoxic p53 activation', *Oncogene*, 30(3), pp. 346-355.
Xia, X., Ma, Q., Li, X., Ji, T., Chen, P., Xu, H., Li, K., Fang, Y., Weng, D., Weng, Y., Liao, S., Han, Z., Liu, R., Zhu, T., Wang, S., Xu, G., Meng, L., Zhou, J. and Ma, D. (2011b) 'Cytoplasmic p21 is a potential predictor for cisplatin sensitivity in ovarian cancer', *BMC Cancer*, 11, pp. 399-399.
Yang-Hartwich, Y., Soteras, M.G., Lin, Z.P., Holmberg, J., Sumi, N., Craveiro, V., Liang, M., Romanoff, E., Bingham, J., Garofalo, F., Alvero, A. and Mor, G. (2015) 'p53 protein aggregation promotes platinum resistance in ovarian cancer', *Oncogene*, 34(27), pp. 3605-3616.

Yardley, D.A. (2013) 'Drug Resistance and the Role of Combination Chemotherapy in Improving Patient Outcomes', *International Journal of Breast Cancer*, 2013, p. 15.
Yasmeen, A., Beauchamp, M.-C., Piura, E., Segal, E., Pollak, M. and Gotlieb, W.H. (2011) 'Induction of apoptosis by metformin in epithelial ovarian cancer: Involvement of the Bcl-2 family proteins', *Gynecologic Oncology*, 121(3), pp. 492-498.
Yemelyanova, A., Vang, R., Kshirsagar, M., Lu, D., Marks, M.A., Shih, I.M. and Kurman, R.J. (2011) 'Immunohistochemical staining patterns of p53 can serve as a surrogate marker for TP53 mutations in ovarian carcinoma: an immunohistochemical and nucleotide sequencing analysis', *Mod Pathol*, 24(9), pp. 1248-1253.
Yin, S., Wang, P., Yang, L., Liu, Y., Wang, Y., Liu, M., Qi, Z., Meng, J., Shi, T.Y., Yang, G. and Zang, R. (2016) 'Wip1 suppresses ovarian cancer metastasis through the ATM/AKT/Snail mediated signaling', *Oncotarget*, 7(20), pp. 29359-29370.
Yuan, Y., Liao, Y.-M., Hsueh, C.-T. and Mirshahidi, H.R. (2011) 'Novel targeted therapeutics: inhibitors of MDM2, ALK and PARP', *Journal of Hematology & Oncology*, 4(1), pp. 1-14.
Zhao, Y., Bernard, D. and Wang, S. (2013) 'Small Molecule Inhibitors of MDM2-p53 and MDMX-p53 Interactions as New Cancer Therapeutics', *BioDiscovery*, 8(4), PP. 7750-65.
Zaffaroni, N., De Marco, C., Villa, R., Riboldi, S., Daidone, M.G. and Double, J.A. (2001) 'Cell growth inhibition, G2M cell cycle arrest and apoptosis induced by the imidazoacridinone C1311 in human tumour cell lines', *European Journal of Cancer*, 37(15), pp. 1953-1962.
Zanjirband, M., Edmondson, R.J. and Lunec, J. (2016) *Pre-clinical efficacy and synergistic potential of the MDM2-p53 antagonists, Nutlin-3 and RG7388, as single agents and in combined treatment with cisplatin in ovarian cancer*, Oncotarget, 7(26), PP. 40115-40134.
Zeppernick, F. and Meinhold-Heerlein, I. (2014) 'The new FIGO staging system for ovarian, fallopian tube, and primary peritoneal cancer', *Archives of Gynecology and Obstetrics*, 290(5), pp. 839-842.
Zeppernick, F., Meinhold-Heerlein, I. and Shih, I.-M. (2015) 'Precursors of ovarian cancer in the fallopian tube: Serous tubal intraepithelial carcinoma – an update', *The journal of obstetrics and gynaecology research*, 41(1), pp. 6-11.
Zhan, Q., Wang, C. and Ngai, S. (2013) 'Ovarian Cancer Stem Cells: A New Target for Cancer Therapy', *BioMed Research International*, 2013, p. 10.
Zhang, N., Wu, Z.-M., McGowan, E., Shi, J., Hong, Z.-B., Ding, C.-W., Xia, P. and Di, W. (2009) 'Arsenic trioxide and cisplatin synergism increase cytotoxicity in human ovarian cancer cells: Therapeutic potential for ovarian cancer', *Cancer Science*, 100(12), pp. 2459-2464.
Zhang, Q., Zeng, S.X. and Lu, H. (2014) 'Targeting p53-MDM2-MDMX Loop for Cancer Therapy', *Sub-cellular biochemistry*, 85, pp. 281-319.
Zhao, Y., Aguilar, A., Bernard, D. and Wang, S. (2015) 'Small-molecule inhibitors of the MDM2-p53 protein-protein interaction (MDM2 Inhibitors) in clinical trials for cancer treatment', *J Med Chem*, 58(3), pp. 1038-52.
Zhu,W.G. and Bai, L. (2006) 'p53: Structure, Function and Therapeutic Applications', *Journal of Cancer Molecules*, 2(4), PP. 141-153.

Appendix I

The average depth of sequencing for each exon.

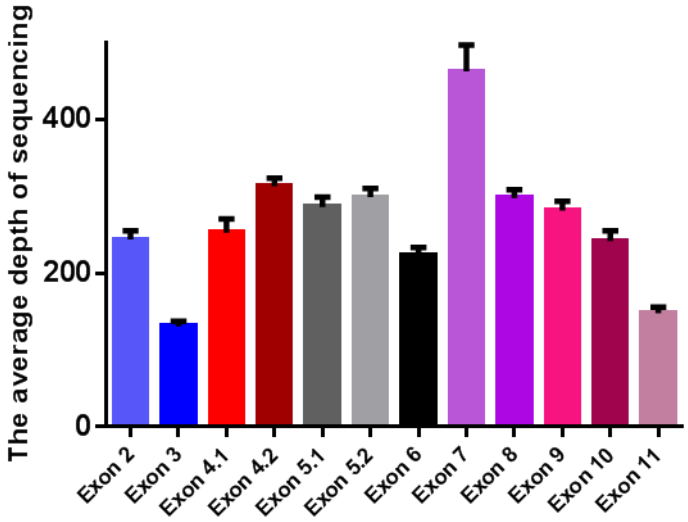

Appendix II

The ROC curve in relation to p53 expression demonstrating the area under the curve (AUC=0.66, P=0.001), and the optimal categorisation cut-off point for patient samples based on the p53 expression (H-score: 0-300).

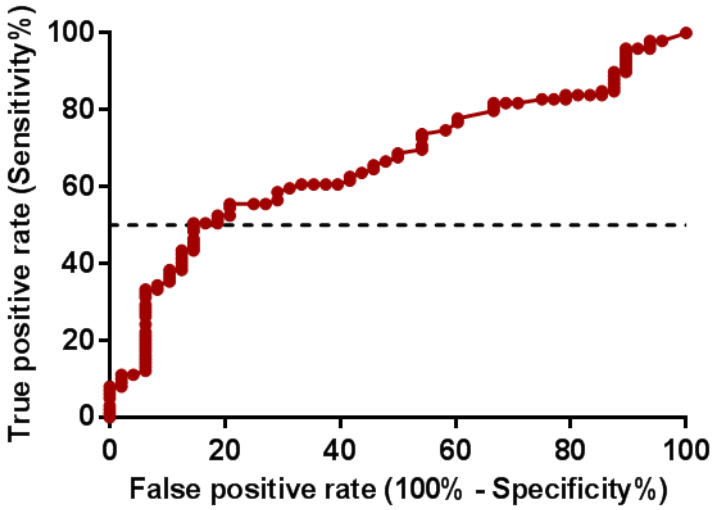

Appendix III

The concordance in two different scoring methods (modified H-score and 0-300) used to score ovarian cancer samples for p53 expression, OVCA1-4 (ICC-0.97).

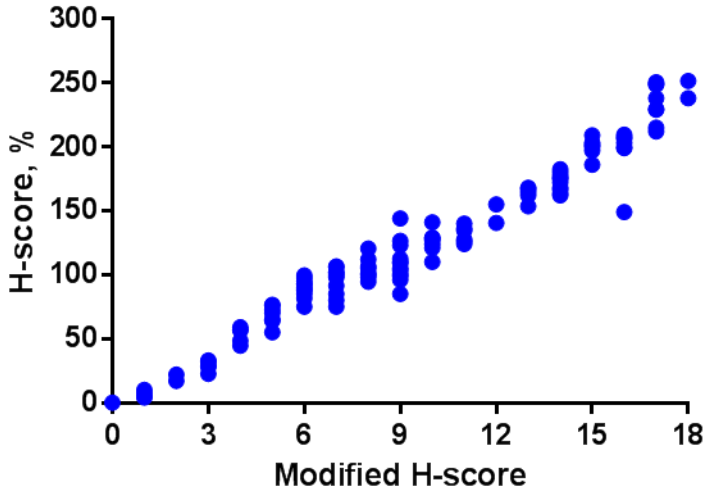

Appendix IV

The survival times in relation to low (H-Score≤123) and high (123<H-score≤300) expression of p53 (p<0.001).

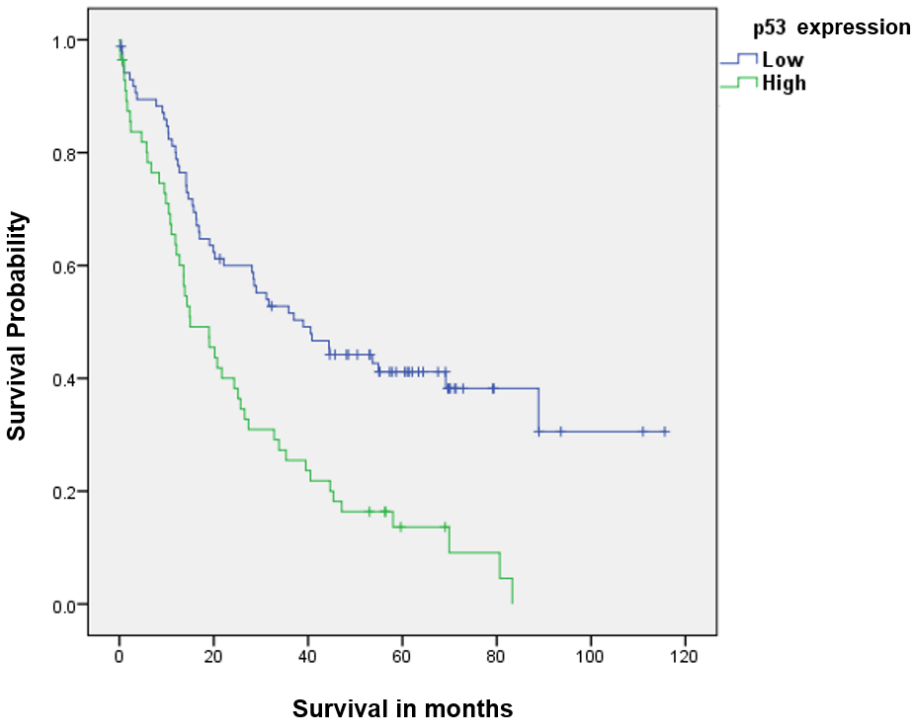

Appendix V

The concordance in two different scoring systems used to score ovarian cancer samples for WIP1 protein, OVCA3-4, (the manual and the automated Aperio system, ICC=0.84).